

**The relationship between chironomids and
climate in high latitude Eurasian lakes:
implications for reconstructing Late Quaternary
climate variability from subfossil chironomid
assemblages in lake sediments from northern
Russia.**

Angela Edith Self

Department of Geography, UCL

Thesis submitted for the degree of Doctor of Philosophy

Declaration

I, Angela Self, confirm that the work presented in this thesis is my own. Where information has been derived from other sources, I confirm that this has been indicated in the thesis.

Angela Self

January 2010

Abstract

This thesis investigates climate variability during the Late Quaternary in northern Russia by analysis of subfossil Chironomid assemblages in lake sediment cores. The modern chironomid fauna was determined in surface-sediment samples from 94 lakes, located between 61° - 72°N and 52° - 131°E. The influence of chemical and physical environmental variables on the distribution and abundance of taxa was investigated using multivariate analysis and modelling of taxon responses. Chironomid distribution showed a statistically strong relationship to mean July air temperature and continentality, and inference models were developed to reconstruct these variables. Palaeoclimate reconstructions for the past 700 years are presented from lakes on the Putoran Plateau, western Siberia (68°N, 92°E). These reconstructions show that whilst July air temperatures have remained relatively stable over the last 50 years, continentality has declined, resulting in a longer growing season. The results also enabled the models to be validated against instrumental records. Reconstructions are then presented from lakes in north-east European Russia: Lake Kharinei, (67.36°N, 62.75°E) where sedimentation started approximately 12600 cal. yrs BP, and a mid-Holocene sequence (4500 – 6500 cal. yr BP) from VORK5 (67.86°N, 59.03°E). The chironomid-inferred reconstructions suggest the early Holocene was approximately 2°C warmer than present with a more continental climate. July air temperatures then declined but remained warmer than present until 6000 yrs BP. From approximately 6000 yrs BP, July temperatures declined and the climate became more continental, indicating a shift to short cool summers. Combined use of the July air temperature and continentality inference models enhances the explanatory power of the palaeoenvironmental reconstructions and helps to reconcile apparent discrepancies with other proxy records. The results improve our understanding of the nature and timing of climate change, such as the spatial extent of the Younger Dryas, in poorly-studied regions of northern Eurasia.

Table of contents

Title	1
Declaration	2
Abstract	3
Table of contents	4
List of figures	11
List of tables	22
Glossary	28
Acknowledgements	30
Chapter 1. Introduction.....	31
1.1. Introduction.....	31
1.2. Mechanisms of climate change.....	32
1.2.1. External forcing.....	33
1.2.2. Internal forcing.....	35
1.2.3. Sensitivity of high latitude sites to climate change.....	38
1.3. Late Quaternary climate variability in the northern hemisphere.....	38
1.3.1. Late Quaternary climate variability in northern Russia.....	42
1.3.2. Recent climate variability in northern Russia.....	44
1.3.3. Issues to be addressed.....	46
1.4. Palaeoclimate reconstructions using proxy records.....	48
1.4.1. Lake sediments as archives of palaeoenvironmental records.....	49
1.4.2. The selection of chironomids for this study.....	49
1.4.3. Chironomids as a proxy in palaeoenvironmental reconstructions.....	51
1.5. Biology of chironomids.....	53
1.5.1. The chironomid life cycle and its adaptations to temperature.....	53
1.5.2. Physiological adaptation of insects to arctic environments....	56
1.5.3. Responses of insects to continentality.....	57

1.6.	Scientific issues to be addressed in this thesis.....	58
1.7.	Structure of the thesis.....	61
	Chapter 2. Description of the study areas.....	62
2.1.	Introduction.....	62
2.2.	Selection of training set lakes in arctic and subarctic Russia.....	62
2.2.1.	Pechora Basin and Komi Republic.....	64
2.2.1.1.	Previously studied sites used in thesis.....	64
2.2.1.2.	Vorkuta lakes.....	65
2.2.1.3.	Lakes from the Komi Republic.....	67
2.2.2.	Igarka and Putorana Plateau.....	68
2.2.3.	Lower Lena River and Lena delta lakes.....	71
2.2.4.	Central Yakutia, Lena River.....	72
2.3.	Physical and geological characteristics of the study areas.....	74
2.4.	Permafrost.....	77
2.5.	Weather and climate characteristics of the study areas.....	79
2.5.	Biological characteristics.....	81
2.6.	Human settlement.....	84
2.7.	Summary.....	86
	Chapter 3 Methods.....	88
3.1	Introduction.....	88
3.2	Field methods.....	88
3.2.1	Water chemistry.....	88
3.2.2	Collection of sediment cores from the study areas.....	89
3.2.3	Collection of contemporary chironomid pupae.....	92
3.2.4.	Field descriptions.....	93
3.3.	Laboratory methods.....	94
3.3.1.	Water chemistry.....	94
3.3.2.	Analysis of sediment cores.....	94
3.3.2.1.	Wet density, dry weight, loss-on-ignition and carbonate content of sediments.....	94
3.3.2.2.	Carbon and nitrogen isotopic composition.....	94
3.3.2.3.	Preparation of larval head capsules.....	95

3.3.3.	Chironomid pupae.....	97
3.3.4.	Core chronologies.....	97
3.3.4.1.	Lead-210 dating.....	97
3.3.4.2.	Radiocarbon dating.....	99
3.3.5.	Derivation of environmental variables.....	100
3.3.6.	Note on collection of primary data.....	105
3.3.7.	Secondary data.....	106
3.4.	Numerical analysis.....	107
3.4.1.	Transformation of data prior to analysis	107
3.4.2.	Exploratory data analysis.....	108
3.4.3.	Species response models.....	109
3.4.4.	Indirect and direct gradient analysis (Ordination and constrained ordination).....	112
3.4.4.1.	Principal Components Analysis (PCA).....	114
3.4.4.2.	Correspondence Analysis (CA); Detrended Correspondence Analysis (DCA).....	115
3.4.4.3.	Redundancy Analysis (RDA).....	115
3.4.4.4.	Canonical Correspondence Analysis (CCA).....	116
3.4.4.5.	Analysis and presentation of results.....	116
3.4.5.	Calibration and environmental reconstruction.....	117
3.4.5.1.	Inference models.....	119
3.4.5.2.	Analogue matching techniques.....	121
3.4.5.3.	Down-core reconstruction of environmental variables.....	122
3.4.5.4.	Down-core ordination and zonation.....	122
3.5.	Summary.....	123
Chapter 4. Factors influencing present-day chironomid distribution.....		
4.1	Introduction.....	125
4.2.	Russian surface sediment data-set.....	126
4.2.1.	Environmental data.....	126
4.2.2.	Chironomid data	137
4.2.3.	Patterns of chironomid distribution	140
4.2.4.	Species – environment relationships	142

4.3.	Norwegian surface sediment data-set.....	148
4.3.1.	Environmental data	148
4.3.2.	Chironomid data	158
4.3.3.	Patterns of chironomid distribution	162
4.3.4.	Species – environment relationships	164
4.4.	Combined Russian and Norwegian surface sediment data-sets.....	168
4.4.1.	Environmental data	168
4.4.2.	Patterns of chironomid distribution.....	176
4.4.3.	Species – environment relationships.....	179
4.5.	Norwegian and Russian surface sediments with LOI data.....	186
4.5.1.	Species – environment relationships	187
4.6.	Discussion	193
4.6.1.	Patterns of chironomid distribution	193
4.6.2.	Species - environment relationships	194
4.6.3.	Implications for development of inference models	196
	Chapter 5. Taxonomic resolution and species responses.....	198
5.1.	Introduction.....	198
5.2.	Examination of chironomid pupae.....	198
5.2.1.	Introduction	199
5.2.2.	Taxonomy.....	199
5.2.3.	Comparison with larval assemblages from the surface Sediments	203
5.2.4.	Discussion	206
5.3.	Species responses to significant environmental variables.....	208
5.3.1.	Species response to mean July air temperature	210
5.3.2.	Species response to continentality.....	225
5.3.3.	Species response to continentality and July air temperature .	239
5.4.	Implications for the development of palaeoclimatic inference models	246
	Chapter 6 Development of the inference models.....	248
6.1.	Introduction.....	248
6.2.	Russian CI-T models	249
6.2.1.	CI-T model A	250

6.2.2.	CI-T model K	254
6.3.	Norwegian CI-T model (CI-T model N)	259
6.4.	Combined Norwegian – Russian CI-T models	260
6.4.1	CI-T model C	261
6.4.2	CI-T model R	263
6.5.	Comparison with published chironomid – July air temperature inference models	268
6.6.	Summary and discussion of temperature inference models	268
6.7.	Chironomid – inferred continentality (CI-C) model	270
6.7.1.	The relationship between climate parameters and ice-free period.....	271
6.7.2.	Chironomid – continentality inference model (CI-C)	273
6.7.3.	Summary and conclusions for continentality inference model	278
	 Chapter 7. Putorana Plateau.....	280
7.1.	Introduction	280
7.2.	Selection of lakes for palaeoenvironmental analysis	280
7.3.	Descriptions of selected lakes	282
7.3.1.	Lake AFOX	282
7.3.2.	Lake PONE	283
7.3.3.	Lake PTHE	284
7.4.	Radiometric chronologies	285
7.4.1.	PONE	286
7.4.2.	PTHE	288
7.5.	Sedimentary analysis	290
7.5.1.	AFOX	291
7.5.2.	PONE	292
7.5.3.	PTHE	295
7.6.	Chironomid biostratigraphies	297
7.6.1.	AFOX	297
7.6.2.	PONE	301
7.6.3.	PTHE	306
7.7.	Chironomid-inferred temperature (CI-T) reconstructions.....	311
7.7.1.	Selection of regional training set	311

7.7.2.	Selection of statistical method	316
7.7.3.	Comparison of July air temperature reconstructions for PONE and PTHE.....	318
7.7.4.	The reliability of down-core reconstructions	321
7.8.	Chironomid-inferred continentality (CI-C) reconstruction	323
7.8.1.	Selection of the statistical technique for CI-C reconstructions	324
7.8.2.	Comparison to instrumental records	326
7.8.3.	Continentality reconstructions	327
7.9.	Palaeoenvironmental interpretation	329
7.10.	Summary	335
Chapter 8 North-east European Russia.....		338
8.1.	Introduction	338
8.2.	Description of coring sites	338
8.2.1.	Lake Kharinei, code KHAR	339
8.2.2.	Lake Nerusaveito code NERU.....	340
8.2.3.	Sandivei Lake, code SAND.....	341
8.2.4.	Unnamed tundra lake, code VORK5	342
8.3.	Selection of lakes for palaeoenvironmental analysis	343
8.4.	Chronology of Lake Kharinei	347
8.4.1.	Correlation of Russian cores	347
8.4.2.	Dating and development of age – depth model	349
8.4.2.1.	²¹⁰ Pb dating and chronology	349
8.4.2.2.	Radiocarbon dating and chronology	352
8.4.2.3.	Compiled ²¹⁰ Pb and radiocarbon chronology	356
8.5.	Chronology of VORK5	357
8.5.1.	Correlation of Russian cores	357
8.5.2.	Dating and development of age – depth model	359
8.5.2.1.	²¹⁰ Pb dating and chronology	359
8.5.2.2.	Radiocarbon dating and chronology	361
8.5.2.3.	Combined ²¹⁰ Pb and radiocarbon chronology	364
8.6.	Sedimentary analysis	365
8.6.1.	Lake Kharinei (KHAR)	365
8.6.2.	VORK5	368

8.7.	Chironomid biostratigraphy	369
8.7.1.	Lake Kharinei (KHAR)	369
8.7.2.	VORK5	374
8.8.	Chironomid-inferred temperature (CI-T) reconstructions	377
8.8.1.	Lake Kharinei (KHAR)	378
8.8.2.	VORK5	380
8.9.	Chironomid-inferred continentality (CI-C) reconstructions	381
8.9.1.	Lake Kharinei (KHAR)	382
8.9.2.	VORK5	383
8.10.	Palaeoenvironmental interpretation	384
8.11.	Summary	395
	Chapter 9 Conclusions	398
9.1.	Introduction	398
9.2.	Evaluation of the inference models.....	398
9.3.	Application of the inference models	403
9.4.	Evaluation of the Research	404
9.5.	Conclusions	406
9.6.	Suggestions for future work	408
9.6.1.	Expanding the Russian training sets	408
9.6.2.	Improving the climate reconstructions for NEER	409
9.6.3.	Testing the sensitivity of the chironomid-inferred continentality (CI-C) model	409
9.6.4.	Modelling chironomid responses to variation in the length of the ice-free period	410
9.6.5.	Integration into multiproxy studies	411
	References	408

List of figures

Figure	Caption	Page
1.1.	Schematic of the changes in Earth's orbit (the Milankovitch cycles).....	34
1.2.	a. Location of the Russian Federation within the Arctic and b. locations in northern Russia referred to in the thesis.....	43
1.3.	Colour-coded trend maps for the Arctic in (a) winter (DJF), (b) spring (MAM), (c) summer (JJA), and (d) autumn (SON) for the period August 1981 to July 2001.....	45
1.4.	Chironomid life cycle.....	54
2.1.	Map showing the locations of the training set lakes.....	63
2.2.	Topographic map of the Pechora River study area.....	64
2.3.	Location of the training set lakes within the Pechora basin and Komi Republic.....	66
2.4.	Map showing the locations of the lakes at Igarka and on the Putorana Plateau.....	68
2.5.	Topographic map of the Lena River basin indicating the two study areas.....	70
2.6.	Location of the training set lakes along the Lower Lena River and Lena delta.....	71
2.7.	Location of the training set lakes in Central Yakutia.....	73
2.8.	Geology of Russia, showing the location of the study areas...	75
2.9.	Photograph showing extensive talus slopes on the Putorana Plateau.....	77
2.10.	Permafrost regions of northern Russia.....	78
2.11.	Polygonal patterned ground at lake LS-7 in the Lena delta....	79
2.12.	Climate zones and provinces of the north European Russia and Central Siberia.....	79
2.13.	Mean monthly air temperatures and precipitation for Narjan-Mar, Turuhansk on the Yenisey River and Yakutsk.....	80
2.14.	Vegetation zones of Russia, showing the location of the study areas.....	81

Figure	Caption	Page
2.15.	Alas (treeless pastures) in Central Yakutia.....	84
3.1.	Extruding HON-Kajak core from lake PTHE.....	89
3.2.	Subsampling Renberg core from SAND in the field.....	91
3.3.	Sampling using the Russian corer at lake SAND.....	91
3.4.	Criteria for assessing human impact on the Russian lakes....	103
3.5.	The five hierarchical Huisman-Olff-Fresco (HOF) models of species response, ranked by their increasing complexity.....	110
3.6.	Diagram summarising the procedure for selection of an appropriate ordination model to explore the biological data....	114
4.1.	Box-Whisker plots for selected water chemical characteristics of the Russian lakes. Box-Whisker plots are categorized by geographical location 1: Northeast European Russia, 2: Putoran Plateau, 3: Central Yakutia and 4: Lena Delta.....	132
4.2.	Kernel-density estimates showing the distribution of un- and log-transformed major anion and cation concentrations within the Russian lakes	133
4.3.	Kernel-density estimates showing the distribution of climatic and physical variables within the Russian lakes	135
4.4.	The distribution of the 30 most abundant taxa in the Russian lakes along the mean July air temperature gradient.....	139
4.5.	Dendrogram of the Russian chironomid assemblages classified by single-link clustering	141
4.6.	DCA plot of site scores for the Russian lakes with fitted convex hulls.....	142
4.7.	CCA biplots of axis 1 and 2 illustrating the relationship between the significant environmental variables and faunal assemblage showing (a) the site scores and (b) the species scores.....	146
4.8.	CCA biplot of the 94 Russian lakes on CCA axis 3 and 4 based on the chironomid assemblages of the lakes.....	147

Figure	Caption	Page
4.9.	Kernel-density estimates showing the distribution of climatic and physical variables within the Norwegian training set.....	155
4.10.	The spatial distribution of physical and climatic variables in mainland Norway.....	156
4.11.	Dendrogram of the Norwegian chironomid assemblages classified by single-link clustering.....	161
4.12.	DCA plot of site scores for the Norwegian lakes with fitted convex hulls.....	163
4.13.	CCA biplots of axis 1 and 2 illustrating the relationship between the significant environmental variables and faunal assemblage showing (a) the site scores and (b) the species scores.....	167
4.14.	Box-Whisker plots for selected water chemical characteristics of the combined Norwegian - Russian lakes...	169
4.15.	Kernel-density estimates showing the distribution of water depth and climatic variables in the combined Norwegian – Russian trainings set.....	171
4.16.	Box-Whisker plots of geographic and climatic variables associated with TWINSPAN groups.....	174
4.17.	Box-Whisker plots of water depth and water chemistry variables associated with TWINSPAN groups.....	175
4.18.	Vegetation types of the TWINSPAN groups expressed as a percentage of the lakes in each group	177
4.19.	DCA plot of site scores for the Norwegian and Russian lakes (excluding Lake Birgervatnet) with fitted convex hulls.....	178
4.20.	DCA plot of site scores for the Norwegian and Russian lakes with fitted convex hulls based on their TWINSPAN groups....	179
4.21.	CCA biplots of axis 1 and 2 illustrating the relationship between the significant environmental variables and faunal assemblage showing (a) the site scores and (b) the species scores.....	183

Figure	Caption	Page
4.22.	CCA biplot illustrating the relationship between sites and the significant environmental variables with Yakutian lakes plotted passively.....	185
4.23.	Kernel density estimations showing the distribution of un-, log and square-root transformed loss-on-ignition data for the 134 lake subset.....	187
4.24.	DCA plot of site scores for the Norwegian and Russian lakes with loss-on-ignition data showing ‘trumpet’ configuration.....	189
4.25.	CCA biplots of axis 1 and 2 illustrating the relationship between the significant environmental variables and faunal assemblage showing (a) the site scores and (b) the species scores.....	191
4.26.	Plot of CCA axis 1 and 3 illustrating the relationship between the significant environmental variables and site scores.....	193
5.1.	Pupal anal lobes of (a) unknown Diamesinae and (b) <i>Protanypus morio</i> exuviae.....	200
5.2.	Thoracic horns from the three <i>Procladius</i> species; (a) <i>Procladius crassinervis</i> , (b) <i>Procladius</i> unknown species I and (c) <i>Procladius</i> unknown species II.....	202
5.3.	Taxon – mean July air temperature response curves for taxa common (10 or more occurrences) in the Norwegian and Russian (with Komi lakes) training sets.....	211
5.4.	Taxon – mean July air temperature response curves for species-rich taxa.....	223
5.5.	Examples of taxon – continentality response curves for taxa identified as having a statistically significant response by HOF models but not supported by GAMs.....	226
5.6.	Taxon – continentality response curves for taxa common (10 or more occurrences) in the CI-C training set.....	228
5.7.	Examples of three-dimensional response surface plots of GAM models showing least-smooth surfaces.....	240

Figure	Caption	Page
5.8.	Response surface plots produced by the GAM models for selected taxa common to the Norwegian and Russian training sets which show a unimodal response to July air temperature.....	241
5.9.	Response surface plots produced by the GAM models for <i>Cricotopus cylindraceus</i> -type showing bimodality along x-axis.....	245
6.1.	Relationship between (a) observed and estimated mean July air temperatures using a weighted averaging partial least squares (WA-PLS) 2 component CI-T model A.....	252
6.2.	Comparison of the temperature optima of common taxa derived from the Norwegian CI-T model N and CI-T model A training sets.....	253
6.3.	Frequency histogram showing the distribution of lakes along mean July air temperature gradient.....	255
6.4.	Relationship between (a) observed and estimated mean July air temperatures using a weighted averaging partial least squares (WA-PLS) 2 component CI-T model K.....	256
6.5.	Comparison of the temperature optima of common taxa derived from (a) the Russian CI-T model A and CI-T model K training sets and (b) the Norwegian CI-T model N and Russian CI-T model K.....	258
6.6.	Relationship between (a) observed and estimated mean July air temperatures using a weighted averaging partial least squares (WA-PLS) 3-component CI-T model C.....	263
6.7.	Frequency histograms showing the distribution of lakes along (a) the mean July air temperature and (b) the continentality index gradients.....	265
6.8.	Relationship between (a) observed and estimated mean July air temperatures using a weighted averaging partial least squares (WA-PLS) 3-component CI-T model R.....	266

Figure	Caption	Page
6.9.	Comparison of the temperature optima of common taxa derived from the Norwegian CI-T model N and reduced Russian – Norwegian CI-T model R training sets.....	267
6.10.	(a) Polar stereographic projection map showing the mean number of frost-free days per year in northern Eurasia and (b) equidistant cylindrical projection map showing the Gorchynski continentality indices (CI).....	270
6.11.	The relationship between the total number of days above 0°C per annum and mean May temperature, mean annual temperature (MeAT) and continentality (CI).....	273
6.12.	The distribution of lakes along the July air temperature and CI gradients.....	275
6.13.	(a) Predicted CI as a function of observed CI for 2-component WA-PLS model and (b) residuals (predicted – observed) of CI as a function of observed CI for the 2-component WA-PLS model.....	276
6.14.	Continentality optima of taxa which showed a statistically significant response to continentality.....	278
7.1.	Unnamed lake, Code AFOX. (a) photograph and (b) sketch map showing the simplified morphometry and location of the sampling site.....	283
7.2.	Unnamed lake, Code PONE. (a) photograph and (b) sketch map showing the simplified morphometry and location of the sampling site.....	284
7.3.	Unnamed lake, Code PTHE. (a) photograph and (b) sketch map showing the simplified morphometry and location of the sampling site.....	285
7.4.	Stratigraphy of (a) unsupported ²¹⁰ Pb and total ²¹⁰ Pb activity; and (b) the ¹³⁷ Cs maximum in PONE.....	287
7.5.	Age-depth model and sediment accumulation rates for core PONE.....	287

Figure	Caption	Page
7.6.	Stratigraphy of (a) unsupported ^{210}Pb and total ^{210}Pb activity; and (b) the maxima of the artificial fallout radionuclides ^{137}Cs and ^{241}Am in PTHE.....	288
7.7.	Age-depth model and sediment accumulation rates for core PTHE.....	290
7.8.	Wet density, percentage dry weight and loss-on-ignition in sediment core from AFOX.....	292
7.9.	% LOI, % dry weight, % TOC, $\delta^{13}\text{C}$ (‰) and $\delta^{15}\text{N}$ (‰) from bulk sediment analysis of core PONE with C/N mass ratio.....	294
7.10.	% LOI, % dry weight, % TOC, $\delta^{13}\text{C}$ (‰) and $\delta^{15}\text{N}$ (‰) from bulk sediment analysis of core PTHE with C/N mass ratio.....	296
7.11.	Chironomid stratigraphy, of taxa with more than 2 occurrences, from AFOX plotted against depth.....	300
7.12.	Larval mentum of (a) <i>Trichotanypus posticalis</i> and (b) unknown Diamesinae.....	301
7.13.	Chironomid stratigraphy, of taxa with greater than 4% abundance, from PONE.....	304
7.14.	CCA plot of (a) axes 1 and 2 and (b) axes 2 and 3 with samples from PONE fitted passively and joined as a time-track to show the changes in chironomid assemblages in relation to lake chemical and physical variables over the last 630 years.....	306
7.15.	Chironomid stratigraphy, of taxa with greater than 4% abundance, in PTHE.....	308
7.16.	CCA plot of (a) axes 1 and 2 and (b) axes 2 and 3 with samples from PTHE fitted passively and joined as a time-track to show the changes in chironomid assemblages in relation to lake chemical and physical variables in the last 725 years.....	310

Figure	Caption	Page
7.17.	July air temperature anomalies (a) of instrumental records from Dudinka, Turuhansk, Hatanga and Ostrov Dikson, based on deviation from a 60 year mean (1946 – 2005) fitted with LOWESS smoother.....	315
7.18.	Reconstructions of mean July air temperature (°C) for PONE based on weighted-averaging partial least squares (WA-PLS, 2 component model), weighted averaging (WA), tolerance downweighted weighted averaging (WA-TOL) and modern analogue technique (MAT) using CI-T model K.....	316
7.19.	Reconstructions of mean July air temperature (°C) for PTHE based on WA-PLS (2 component model), WA, WA-TOL and MAT using CI-T model K.....	318
7.20.	Comparison of July air temperature anomalies from CI-T WA-PLS and WA reconstructions for (a) PONE, based on 50 year mean, and (b) PTHE, based on 68 year mean with instrument record anomalies.....	319
7.21.	Reconstructions of mean July air temperature (°C) for PONE and PTHE based on weighted-averaging partial least squares (WA-PLS, 2 component model using training set K) and composite reconstruction fitted with LOWESS smoother.	320
7.22.	Reconstructions of continentality (CI) for PONE based on weighted-averaging partial least squares (WA-PLS, 2-component model, with LOWESS smoother), weighted averaging (WA) and tolerance downweighted weighted averaging (WA-TOL).....	324
7.23.	Reconstructions of continentality (CI) for PTHE based on weighted-averaging partial least squares (WA-PLS, 2-component model with LOWESS smoother), weighted averaging (WA) and tolerance downweighted weighted averaging (WA-TOL).....	325

Figure	Caption	Page
7.24.	Continental Indices anomalies (a) of instrumental records from Dudinka, Turuhansk, Hatanga and Ostrov Dikson, based on deviation from a 60 year mean (1946 – 2005).....	327
7.25.	Reconstructions of CI-C for PONE and PTHE based on weighted-averaging (WA with classical deshrinking) and composite reconstruction fitted with LOWESS smoother.....	328
7.26.	Summary diagram for PTHE showing the percentage of cool-water taxa, warm-water taxa and non training set taxa, chironomid-inferred mean July air temperature and continentality, total organic carbon of bulk sediment, sediment accumulation rate, DCCA scores, CCA axes 1 and 2 scores.....	330
7.27.	Summary diagram for PONE showing the percentage of cool-water taxa, warm-water taxa and non training set taxa, chironomid-inferred mean July air temperature and continentality, total organic carbon of bulk sediment, sediment accumulation rate, DCCA scores, CCA axes 1 and 2 scores.....	331
7.28.	Comparison of chironomid-inferred continentality from PONE and PTHE with GISP2 K ⁺ ice core record, proxy for the strength of the Siberian High.....	332
8.1.	Lake Kharinei, Code KHAR. (a) GoogleEarth™ image and (b) topographic map of Kharinei.....	340
8.2.	GoogleEarth™ image of Lake Nerusaveito.....	341
8.3.	GoogleEarth™ image of Sandivei Lake.....	341
8.4.	Unnamed lake, Code VORK5. (a) GoogleEarth™ image and (b) topographic map.....	342
8.5.	Preliminary age-depth models for the northeast European lakes based on calibrated ¹⁴ C dates (a) Lake Kharinei, (b) Lake Nerusaveito and unnamed lake VORK5.....	345

Figure	Caption	Page
8.6.	Comparison of percentage dry weight and LOI in consecutive KHAR cores (a) before and (b) after adjustment of estimated depths to correlate cores.....	348
8.7.	Stratigraphy of (a) unsupported ^{210}Pb and total ^{210}Pb activity; and (b) the ^{137}Cs maximum in Lake Kharinei.....	350
8.8.	Age-depth model and sedimentation rates for Lake Kharinei.	351
8.9.	Preliminary age – depth relationship of Lake Kharinei (KHAR) based on 14 calibrated radiocarbon dates.....	353
8.10.	Age-depth models for Lake Kharinei, (a) excluding dates at 852 and 880 cm depth; (b) excluding date at 880 cm depth only and (c) excluding date at 852cm depth only.....	355
8.11.	Age-depth models for Lake Kharinei with top of core constrained by ^{210}Pb date.....	357
8.12.	Comparison of percentage dry weight and LOI in consecutive cores (a) before and (b) after adjustment of estimated depths to correlate cores.....	358
8.13.	Stratigraphy of (a) unsupported ^{210}Pb and total ^{210}Pb activity; and (b) the ^{137}Cs and ^{241}Am maxima in VORK5.....	360
8.14.	Age-depth model and sediment accumulation rates for VORK5.....	361
8.15.	Age – depth relationship for the lake VORK5, based on 6 bulk sediment and 3 macrofossil calibrated radiocarbon dates.....	362
8.16.	Age – depth profile for VORK5 with linear regression lines fitted to ‘reliable’ dates.....	363
8.17.	% LOI, % dry weight, % carbonate, % TOC, $\delta^{13}\text{C}$ (‰) and $\delta^{15}\text{N}$ (‰) of sediments from KHAR, with C/N mass ratio.....	367
8.18.	% LOI, % dry weight and % carbonate in sediments from VORK5.....	368
8.19.	Larval mentum of unknown Chironomini.....	369
8.20.	Lake Kharinei chironomid stratigraphy.....	372

Figure	Caption	Page
8.21.	CCA plot of (a) axes 1 and 2 and (b) axes 1 and 3 with samples from Lake Kharinei fitted passively and joined as a time-track to show the changes in chironomid assemblages in relation to lake chemical and physical variables in the last 13000 years.....	373
8.22.	VORK5 chironomid stratigraphy.....	376
8.23.	CCA plot of (a) axes 1 and 2 and (b) axes 1 and 3 with samples from VORK5 fitted passively and joined as a time-track to show the changes in chironomid assemblages in relation to lake chemical and physical variables.....	377
8.24.	Reconstructions of mean July air temperature (°C) for Lake Kharinei (KHAR) based on WA-PLS (2 component model), WA with inverse deshrinking, MAT and consensus reconstruction.....	379
8.25.	Reconstructions of mean July air temperature (°C) for VORK5 based on WA-PLS (2 component model), WA with inverse deshrinking, MAT and consensus reconstruction derived by fitting LOWESS smoother (span 0.1) through all reconstructed values.....	381
8.26.	Reconstructions of CI, continentality index, for Lake Kharinei (KHAR) based on WA-PLS (2 component model) and WA with classical deshrinking.....	382
8.27.	Reconstructions of CI, continentality index, for VORK5 based on WA-PLS (2 component model) and WA with classical deshrinking with sample-specific errors.....	384
8.28.	Summary diagram for Lake Kharinei showing the percentage of cool-water taxa , warm-water taxa and non training set taxa, chironomid-inferred mean July air temperature and continentality, total organic carbon of bulk sediment, sediment accumulation rate, DCCA scores, CCA axes 1 and 2 scores.....	387

Figure	Caption	Page
8.29.	Summary diagram for VORK5 showing the percentage of cool-water taxa, warm-water taxa and non training set taxa, chironomid-inferred mean July air temperature and continentality, total organic carbon of bulk sediment, sediment accumulation rate, DCCA scores, CCA axes 1 and 2 scores.....	388
8.30.	Comparison of chironomid-inferred continentality from KHAR and VORK5 with GISP2 K ⁺ record and solar insolation at 60°N over the past 13000 years.....	394

List of Tables

No.	Caption	Page
2.1.	Location and physical characteristics of the archived material from the Pechora and Usa River basins.....	65
2.2.	Location and physical characteristics of the sites near Inta and Vorkuta sampled in April 2007.....	66
2.3.	Location and physical characteristics of the sampling sites in the southern Komi Republic.....	67
2.4.	Location and physical characteristics of the sampling sites at Igarka and on the Putorana Plateau.....	69
2.5.	Location and physical characteristics of the sampled lakes within the lower Lena River and delta study area.....	72
2.6.	Location and physical characteristics of the sampled lakes within the upper Lena River – Central Yakutia lowlands study area.....	74
3.1.	Core length and sampling resolution of the samples from the Putorana Plateau and Igarka.....	90
3.2.	Core length and sampling resolution of the samples collected in April 2007.....	92

No.	Caption	Page
3.3.	Summary of the meteorological stations and years used in the calculation of mean January and July air temperatures....	101
3.4.	Summary of the environmental parameters used in the statistical analysis.....	104
3.5.	Summary of secondary and joint primary/secondary data sources.....	106
3.6.	Ecological responses described by the HOF models.....	110
4.1.	Physical and chemical characteristics of the Russian lakes...	127
4.2.	Summary of environmental variables for the Russian lakes...	131
4.3.	Correlation matrix showing the relationship between environmental variables in the Russian lakes.....	136
4.4.	Checklist of Chironomidae taxa recorded in the Russian lakes.....	138
4.5.	Summary statistics for the first four axes of DCA.....	143
4.6.	Summary statistics for the first four axes of CCA with 94 sites, 124 chironomid taxa (a) for all environmental variables and (b) after select of seven significant environmental variables.....	144
4.7.	Physical and chemical characteristics of the Norwegian lakes	149
4.8.	Summary of environmental variables for the Norwegian lakes.....	148
4.9.	Correlation matrix showing the relationship between environmental variables in the Norwegian training set.....	156
4.10.	Checklist of Chironomidae taxa recorded in the Norwegian lakes.....	160
4.11.	Summary statistics for the first four axes of DCA (a) for all 157 Norwegian lakes and (b) excluding Lake Birgervatnet.....	162
4.12.	Summary statistics for the first four axes of CCA with 94 sites, 124 chironomid taxa (a) for all environmental variables and (b) after select of significant environmental variables.....	165
4.13.	Summary of environmental variables for the combined Norwegian - Russian datasets	168

No.	Caption	Page
4.14.	Effect on the descriptive statistics of excluding three lakes from the combined Norwegian – Russian data-set	170
4.15.	Correlation matrix showing the relationship between environmental variables in the Norwegian – Russian training set.	172
4.16.	TWINSpan classification of the combined Norwegian – Russian lakes based on the chironomid fauna	173
4.17.	Summary statistics for the first four axes of DCA (a) for all 251 Norwegian and Russian lakes and (b) excluding Lake Birgervatnet	180
4.18.	Summary statistics for the first four axes of CCA with 250 sites, 157 chironomid taxa (a) for all environmental variables and (b) after select of seven significant environmental variables	181
4.19.	Loss-on-ignition data for the subset of 133 Norwegian - Russian lakes	188
4.20.	Summary statistics for the first four DCA axes of 133 lakes with loss-on-ignition data	189
4.21.	Summary statistics for the first four axes of CCA with 133 sites, 138 chironomid taxa (a) for all environmental variables and (b) after select of significant variables	190
5.1.	Chironomid taxa from the Putorana lakes based on the pupae exuviae	199
5.2.	Distribution of chironomids in the Putorana lakes as identified from pupal exuviae and the head capsules of larvae in the surface sediments.....	204
5.3.	The five HOF models of ecological response.....	208
5.4.	Taxon responses modelled using the HOF programme for (a) 57 taxa in the Russian training set, (b) 83 taxa in the Norwegian training set and (c) 104 taxa in the combined training set.....	209

No.	Caption	Page
5.5.	Taxon responses to continentality, modelled using the HOF programme, GLM and GAMs, for species with more than 10 occurrences in the CI-C training set.....	227
6.1.	Lakes identified as outliers in the CI-T model A.....	250
6.2.	Performance of the CI-T model A applied to the 88 sample chironomid-July air temperature dataset.....	251
6.3.	Lakes identified as outliers in the CI-T model K.....	255
6.4.	The performance of the CI-T inference model K applied to the 81 sample chironomid-July air temperature dataset.....	256
6.5.	Lakes identified as outliers in the CI-T model N.....	259
6.6.	The performance of the CI-T inference model N applied to the 153 sample chironomid-July air temperature dataset.....	260
6.7.	Lakes identified as outliers in the CI-T model K.....	262
6.8.	The performance of the combined Norwegian – Russian CI-T model C, with 146 chironomid taxa in 233 lakes, based on leave-one-out cross validation.....	262
6.9.	Subset of Norwegian – Russian lakes selected for CI-T model R.....	264
6.10.	The performance of the combined Norwegian - Russian CI-T model R, with 144 chironomid taxa in 188 lakes, based on leave-one-out cross validation.....	266
6.11.	Comparison of the performance statistics of minimum adequate WA-PLS chironomid-mean July air temperature inference models from Finland (1), Finland (2), Norway, Sweden, Switzerland and this study.....	268
6.12.	Meteorological station records used in the calculation of the climate parameters.....	271
6.13.	Regression coefficients (r^2) showing the strength of the correlation between climate parameters and total days and continuous period above 0°C.....	272
6.14.	Subset of Norwegian – Russian lakes selected for CI-C training set.....	274

No.	Caption	Page
6.15.	Performance statistics of the continentality models created from subset of northern Eurasian lakes using WA and WA-PLS methods.....	275
6.16.	Comparison of the observed and estimated CI values from the independent test set.....	277
7.1.	Temperature reconstructions based on chironomid assemblages in surface and basal sediments from short cores collected in the Putorana.....	281
7.2.	Summary table showing the ^{210}Pb and ^{137}Cs activity, with respective errors, for the core PONE.....	286
7.3.	Summary table showing the ^{210}Pb and ^{137}Cs activity with respective errors, for the core PTHE.....	288
7.4.	Chironomid fauna of AFOX core, with total number of occurrences, effective number of occurrences (Hill's N2) and minimum and maximum percent abundance.....	298
7.5.	Chironomid fauna of PONE core, with total number of occurrences, effective number of occurrences (Hill's N2) and minimum and maximum percent abundance.....	302
7.6.	Chironomid fauna of PTHE core, with total number of occurrences, effective number of occurrences (Hill's N2) and minimum and maximum percent abundance.....	307
7.7.	Summary of CI-T models developed in Chapter 6.....	311
7.8.	Reconstructions of mean July air temperatures for PONE estimated from the surface chironomid assemblage (2002 – 2005) using the inference models developed in Chapter 6....	312
7.9.	Reconstructions of mean July air temperatures for PTHE estimated from the surface chironomid assemblage (1977 – 2004) using the inference models developed in Chapter 6.....	313
7.10.	Assessment of the reliability of palaeoenvironmental reconstructions from PONE.....	322
7.11.	Assessment of the reliability of palaeoenvironmental reconstructions from PTHE.....	323

No.	Caption	Page
8.1.	The abundance and diversity of the chironomid fauna in surface samples from the NEER lakes.....	344
8.2.	Radiocarbon rangefinder dates for the NEER sediment cores	346
8.3.	Summary of measured and adjusted depths for Russian cores from Lake Kharinei.....	349
8.4.	Summary table showing the ^{210}Pb and ^{137}Cs activity with respective errors, for Lake Kharinei.....	350
8.5.	Radiocarbon dates from Lake Kharinei (KHAR) sediment core.....	352
8.6.	Age and depth of samples dated by ^{210}Pb and radiocarbon determinations.....	356
8.7.	Summary of measured and adjusted depths for Russian cores from VORK5.....	358
8.8.	Summary table showing the ^{210}Pb , ^{137}Cs and ^{241}Am activity, with respective errors, for VORK5.....	359
8.9.	Radiocarbon dates from VORK5 sediment cores.....	362
8.10.	Age and depth of samples dated by ^{210}Pb and radiocarbon determinations.....	364
8.11.	Chironomid fauna of KHAR core, with total number of occurrences, effective number of occurrences (Hill's N2) and minimum and maximum percent abundance.	370
8.12.	Chironomid fauna of VORK5 core, with total number of occurrences, effective number of occurrences (Hill's N2) and minimum and maximum percent abundance.	375

Glossary

AIC	Akiake Information Criterion
BBOE	billion barrels of oil equivalent
BIC	Bayes Information Criterion
Ca ²⁺	calcium ions
CA	Correspondence Analysis
Cal yrs BP	calendar years before (1950)
CCA	Canonical Correspondence Analysis
CH ₄	methane
CI	continentality index
CIC	constant initial concentration (²¹⁰ Pb dating)
CI-C	chironomid-inferred continentality
CI-T	chironomid-inferred mean July air temperature
Cl ⁻	chloride ions
cla	classical deshrinking
CO ₂	carbon dioxide
CRS	constant rate of supply (²¹⁰ Pb dating)
DCA	Detrended Correspondence Analysis
DCCA	Detrended Canonical Correspondence Analysis
HTC	Halothermal circulation
HTM	Holocene thermal maximum
H ₂ O	water
HOF	Huisman-Olff-Fresco models
GAM	Generalised additive models
GISP2	Greenland Ice Sheet Project 2 – ice core from 72.58°N 38.46°W
GLR	Generalised linear models
inv	inverse deshrinking
kyrs	thousand years before present
LIA	Little Ice Age
m a.s.l.	metres above sea-level
MAT	modern analogue technique
MCR	Mutual Climatic Range
MeAT	mean annual temperature

Mg ²⁺	magnesium ions
MOC	Atlantic Meridional Overturning Circulation
MWP	Medieval warm period
Myrs	Million years before present
NADW	North Atlantic Deep Water
Na ⁺	sodium ions
NE	north east
NEER	north-east European Russia
NH	northern hemisphere
NHM	Natural History Museum, London
PCA	Principal Components Analysis
r ²	coefficient of determination
RDA	Redundancy Analysis
RMSE	root-mean-square-error
RMSEP	root-mean-square-error of prediction
rpm	revolutions per minute
SD	standard deviation
SO ₄ ⁻	sulphate ions
THC	thermohaline circulation
T _{july}	mean July air temperature
TOC	total organic carbon
UCL	University College London
UK	United Kingdom
USA	United States of America
VIF	variance inflation factors
WA	weighted averaging regression and calibration
WA opt	weighted averaging mean July temperature optima
WMAT	weighted averaging modern analogue techniques
WA-PLS	weighted averaging partial least squares regression – calibration
WATOL	weighted averaging regression and calibration with tolerance downweighting

Acknowledgements

I would like to thank:

- Dr Larisa Nazarova and Dr David Porinchu for providing me with data, and allowing access to slide-mounted chironomid collections, from Yakutia and the Lena Delta respectively. And to Dr Thomas Kumke and Prof John Smol for providing the associated environmental data.
- Steve Brooks and Prof John Birks for providing the unpublished Norwegian chironomid training set data.
- Dr Viv Jones, Dr Nadia Solovieva, Dr Vasily Ponomarev, Dr Mikhail Berezin, Dr Elena Tkacheva, Prof Heikki Seppä and Sebastien Seboni for help in the field.
- Prof Avrid Odland for calculating mean January and July air temperatures at the Russian lakes.
- Rachel Preedy, Felicity Muth and Malcolm Aldridge for help in the preparation and identification of chironomid pupal exuviae.
- Pat Haynes for help in preparing chironomid samples.
- Steve Brooks, Tula Maxted and Ian Patmore for help in the lab.
- Dr Andrew Polaszek for photomontage images of the chironomids
- Dr Handong Yang for providing the ^{210}Pb dating.
- Dr Charlotte Bryant and staff at the NERC Radiocarbon Facility (Environment) and SUERC AMS Laboratory, East Kilbride, UK for radiocarbon dates under allocation numbers 1243.1007 and 1289.0408.
- Prof John Birks and Dr Gavin Simpson for statistical advice.
- And NERC for studentship NER/S/A/2005/13227 which supported the research.

I also wish to thank Steve Brooks and Viv Jones for their supervision, help and advice throughout this Ph.D.

And finally, special thanks to my children, Chris and Rachel, and my husband, Nigel, for their support and encouragement.

Chapter 1

Introduction

1.1. Introduction

'Climate change affects every aspect of society, from the health of the global economy to the health of our children. It is about water in our wells. It is about food on the table. It is about energy security and international security...(It) is the defining challenge of our time.'

Ban Ki-moon, U.N. Secretary General,
at the World Business Summit on Climate Change, Copenhagen 24th May 2009

Our ability to plan action to meet the challenge of climate change, and mitigation against its potential effects on society and the environment, relies on the accuracy of climate predictions. Whilst the computer models are based on well-established physical laws and principles, confidence in the models and their projections is built on the ability of the models to predict key features of the present-day climate and to simulate past climate variations (Wood 2007a). As instrumental records rarely have comprehensive spatial coverage or extend beyond the past few hundred years, palaeoclimate reconstructions, using indirect or proxy records, play a fundamental role in verifying climate models. The palaeoclimate perspective allows the instrumental record of climate change to be put into a long baseline of natural climate variability, and also demonstrates how changes in natural climate forcing, including changes in the Earth's orbit, greenhouse gases, explosive volcanism, and the sun have driven climate change in the past (Overpeck 2007). Understanding the natural variability of the climate, and the underlying drivers of climate change, is also essential in attributing a cause to the observed recent warming and reliably predicting future trends.

The Holocene has been a period of continuous climate change in response to changes in the relative importance of climate drivers such as orbital forcing and anthropogenic emissions. Many organisms have not evolved significantly during the relatively short Holocene; proxy records provide continuity and

overlap with the present-day and contribute to our understanding of how ecosystems and environmental processes have developed (Oldfield 2003). Therefore Holocene sequences can provide high resolution data on climate variability during warm interglacial times and the physical and biotic responses to Pleistocene - early Holocene warming serve as an analogue for the possible impacts of future climate change (Oldfield 2003).

Global mean surface temperatures have increased at the rate of $0.13 \pm 0.03^{\circ}\text{C}$ decade⁻¹ over the past 50 years (Trenberth *et al.* 2007). Average arctic temperatures have increased at almost twice the rate of the rest of the world over the last 100 years (Trenberth *et al.* 2007) due to amplification from positive feedbacks (see section 1.2.3). This trend is predicted to continue as high latitudes warm by 4-7°C in the next century (ACIA 2004, 2005). Due to the paucity of observational and proxy records, northern Russia is poorly represented in the global perspective of climate trends and their affects on ecosystems (for example Smol *et al.* 2005).

The aim of this research is to examine the relationship between chironomids and climate in high latitude Eurasian lakes and, thereby, assess the sensitivity of chironomids for reconstructing Late Quaternary climate variability from sub-fossil chironomid assemblages in lake sediments from northern Russia. To provide a context for the research, this chapter reviews mechanisms of climate change and the evidence for northern hemisphere late Quaternary climate change; the rationale behind the selection of the study areas and methods used; and the adaptations (physiological and behavioural) of chironomids to cold, continental environments. This research, and the current review, covers the period of the Late Quaternary from the inception of the Younger Dryas cooling episode (ca. 12800 yrs BP) to the present-day.

1.2. Mechanisms of climate change

As discussed in section 1.1, to accurately predict future climate change we need to understand the mechanisms of climate forcing and the nature of variability they engender. The following sections (1.2.1 – 1.2.2) give an overview of the mechanisms causing climate change on decadal to millennial

time-scales. Climate change is amplified in Polar Regions due to internal feedback mechanisms; these are reviewed in section 1.2.3 to highlight the importance of high latitude regions in climate studies.

Incoming solar radiation is unevenly distributed across the Earth's surface covering only the day-side of the globe and with peaks at low latitudes. The climate system acts to eliminate the resultant energy gradients by transporting energy through atmospheric and oceanic circulation. In addition, part of the incoming radiation is reflected, scattered or absorbed on its passage through the atmosphere. All these radiative processes are dependent on the composition of the atmosphere (gases, aerosols, dust, clouds). These components are the product of chemical, thermal and dynamic processes taking place in the atmosphere over a range of time-scales and any changes in these processes can force the climate to change. The mechanisms of external (orbital and solar) and internal (volcanic and atmospheric-ocean circulation) forcing are reviewed in the following sections and their influence on Late Quaternary climate in the northern hemisphere discussed in section 1.3.

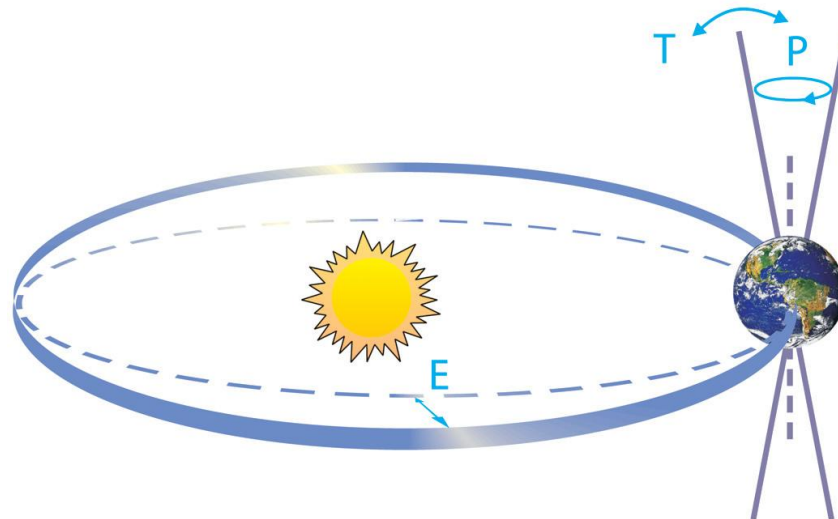
1.2.1. External forcing

The amount of solar radiation arriving at the top of the atmosphere depends on the total amount of radiation emitted by the sun (solar forcing) and the relative positions of the Sun and Earth (orbital forcing).

Orbital forcing: Orbital forcing affects three parameters, the Milankovitch cycles, (Figure 1.1) with known periodicities:

1. eccentricity (the deviation of Earth's orbit from a circle) with periods of 106 000 and 410 000 yrs,
2. obliquity (the tilt angle of the Earth's axis) with a period of 41 000 yrs and
3. precession. Precession has two components: axial precession which causes the rotational axis of the Earth to gyrate (giving precession of the equinoxes) and elliptical precession, in which the elliptical orbit of the Earth rotates about a focus (movement of the perihelion). These are modulated by eccentricity to give two periods of 19 000 and 23 000 yrs.

Figure 1.1. Schematic of the changes in Earth's orbit (the Milankovitch cycles). 'T' denotes changes in the tilt (or obliquity) of the Earth's axis, 'E' denotes changes in the eccentricity of the orbit (due to variations in the minor axis of the ellipse), and 'P' denotes precession, changes in the direction of the axis tilt at a given point of the orbit (Rahmstorf and Schellnhuber 2006 from Jansen *et al.* 2007).



Eccentricity (E) leads to changes in the mean annual distance between the Earth and the Sun and therefore the total incoming radiation, whereas the other two parameters affect the relative distribution of the solar radiation. In the northern hemisphere, 11000 yrs BP, perihelion occurred in mid-June increasing the receipt of summer solar radiation. Over the past 11000 years, at high northern latitudes, orbital forcing has caused a strong decreasing trend in June insolation (the solar radiation energy received at the Earth's surface) and an increase in December insolation from the beginning of the Holocene to a maximum between 4000 and 2000 years BP (Berger and Loutre 1991). These trends would result in a decline in continentality, the difference between mean summer and winter temperatures, over this interval.

Solar Variations: Cosmic rays bombard the upper atmosphere creating cosmogenic radionuclides such as ^{14}C and ^{10}Be . The intensity of the cosmic ray flux is influenced by the geomagnetic field of the Earth and the strength of the solar wind. In periods of more intense solar activity the solar wind intensifies deflecting the cosmic ray flux and reducing radionuclide production. Instrumental data show total solar irradiance fluctuations by approximately 0.1% over the 11-year Schwabe cycle, but reaches values of more than 100% in the

UV part of the spectrum (Beer and Van Geel 2008). These changes strongly influence the photochemistry of the upper atmosphere, particularly ozone concentration, and computer models have shown that this can cause shifts in troposphere circulation and therefore climate change (Haigh and Blackburn 2006).

Galactic variations: variations in the interstellar medium or in the gravitational torque as the Solar System orbits about the centre of the Galaxy are considered to be possible external climate forcing mechanisms (Williams 1975). However, as the galactic year is estimated at 303 million years, the influence on the Holocene climate variability is likely to be minimal.

1.2.2. Internal Forcing

Volcanic activity: Aerosols (SO_2 , CO_2 , H_2O , N_2) and dust are injected into the atmosphere during explosive volcanic eruptions which affects the Earth's radiative balance through enhanced absorption and scattering of solar radiation (Beer and Van Geel 2008). This leads to warming in the upper atmosphere and cooling in the lower atmosphere and can significantly affect the climate on an annual to decadal time-scale (Crowley 2000; Robock 2000). Deglaciation can trigger volcanic activity as ice-sheet unloading and/or sea-level rises may alter the loading on the geological structures confining the magma (Capra 2006; Self 2006).

Ocean Circulation: Due to their volume, heat-capacity and inertia the oceans store and transport an immense amount of heat energy, and consequently play a crucial role in the regulation of the global climate system. Wind-driven currents, such as the Gulf Stream, carry heat polewards in the North Atlantic. As the warm water meets cold polar air, the water cools by evaporative cooling and sinks. This process is assisted by the formation of sea ice which increases the salinity and density of the unfrozen water. The cold, dense water sinks and flows southwards forming the North Atlantic Deep Water current (NADW). The NADW flows, at depth, as part of the 'ocean conveyor belt' into the Pacific Ocean. The North Atlantic is warmer than the North Pacific. Evaporation rates, and therefore salinity, are higher relative to the North Pacific and this salinity

gradient drives global thermohaline circulation (THC). The circulation is perpetuated by the 'pull' created by the sinking of the NADW which draws surface water from the Gulf of Mexico.

Periodic changes in grain size within deep sea sediment cores, from the North Atlantic, suggest the strength of the NADW is linked to climate oscillations (Bianchi and McCave 1999). During glacial periods, formation of the NADW is reduced or, possibly, shut down by the southwards displacement of the polar front and reduced evaporation due to cooler sea surface temperatures (Broecker and Denton 1989). Broecker (1987) proposed that salinity changes between the North Atlantic and North Pacific could be sufficient to reverse the pattern of global thermohaline circulation. The change to a salinity-thermal driven halothermal circulation (HTC) mode may explain the rapid (<1,000 years) termination of the YD (Dansgaard *et al.* 1989). However empirical evidence in support of mode changes is inconclusive and reduction or shutdown of ocean heat transport would not be sufficient to initiate global temperature changes and ice sheet development without the involvement of other internal feedback mechanisms such as changes in atmospheric composition (Broecker and Denton 1989).

Atmospheric Composition: Changes in atmospheric composition, particularly of 'greenhouse gases' CO₂, CH₄ and H₂O vapour, act to amplify the effects of radiative forcing by absorbing outgoing long-wave radiation and re-radiating the energy back to the Earth's surface. In addition compositional changes impact on the formation of clouds and aviation-induced contrails and surface albedo. Changes in composition occur as a result of both natural and anthropogenic factors. Natural factors include solar changes and volcanic emissions which have been previously discussed together with processes such as biogeochemical cycles in soils and the ocean (Forster *et al.* 2007). Over geological timescales changes in atmospheric greenhouse gas composition are associated with transitions between glacial and interglacial periods. Ice-core records from Antarctica show that atmospheric greenhouse gases co-vary with temperatures over glacial-interglacial cycles, with a lag of several centuries to millennium (Mudelsee 2001). Therefore changes in atmospheric composition

act as a feedback mechanism to enhance and sustain climate change rather than as a primary forcing mechanism.

Anthropogenic change: Human activity, through forest clearance, land use, burning of fossil fuels and other industrial processes, has increased the concentration of CO₂, CH₄, N₂O and other greenhouse gases since the eighteenth century (Andres *et al.* 2000; Forster *et al.* 2007). Analysis of gases trapped in ice cores suggests recent concentrations of CO₂, CH₄ and N₂O far exceed their pre-industrial values and the average rate of increase in their radiative forcing is greater than at any time during the past 13000 years of the Late Quaternary (Jansen *et al.* 2007). Shifts in atmospheric CH₄ and CO₂ gas concentrations over the Late Quaternary, prior to the industrial period, were generally small-scale, with the exceptions of declines in CH₄ concentrations at 8200 yrs BP and CO₂ concentrations at 1200 yrs BP. Therefore Mayewski *et al.* (2004) suggested changes in greenhouse gas concentrations played a negligible forcing role and acted to amplify climate variations until approximately 250 yrs BP. Ruddiman (2003), however, argues that atmospheric CO₂ and CH₄ concentrations have diverged from trends of previous interglacial cycles and steadily increased from 8000 years BP due to the development of agriculture. However the hypothesis conflicts with evidence of high CO₂ concentrations during the interglacial MIS 11 (Siegenthaler *et al.* 2005). Atmospheric concentrations of carbon dioxide (CO₂) have increased from a pre-industrial value of 280 ppm to 385 ppm in 2008 (Keeling *et al.* 2009) and exceeds the natural range (of 180 – 300 ppm) over the past 650,000 years (EPICA community members 2004). Climate models only reproduce the observed 20th century global mean surface warming when both anthropogenic and natural forcings are included (Zwiers 2007). The evidence for warming in the Arctic over the past 150 years is reviewed in section 1.3.2.

Tectonic processes: Orogeny (the uplift of mountain ranges) influences global climate by affecting atmospheric circulation patterns and the drawdown of atmospheric CO₂ through enhanced rates of physical and chemical weathering of the rocks (Raymo and Ruddiman 1992). Epeirogeny (changes in the global arrangement of land masses) influences surface albedo, oceanic circulation

patterns and increases atmospheric CO₂ during periods of intense sea-floor surface spreading. However these mechanisms operate over timescales of tens to hundreds of millions of years so their influence on variability in the Late Quaternary - Holocene climate is likely to be minimal.

1.2.3. Sensitivity of high latitude sites to climate change

The effects of global warming are especially pronounced at high latitudes due to amplification by positive feedbacks. Poleward migration of boreal forests (Chapin *et al.* 2005; Soja *et al.* 2007) and decreasing sea-ice in the Arctic Ocean (Comiso 2001) reduce the albedo and contribute to warming trends. The changes in vegetation, and climate, also increase the frequency of wild fires; the black carbon emitted enhances heat absorption and melting of the snow pack (Flanner *et al.* 2007; Generoso *et al.* 2007; Groisman *et al.* 2007). Enhanced snow pack and permafrost melting increases freshwater discharge from Eurasian rivers and hence heat advection from low latitudes (Peterson *et al.* 2002; McClelland *et al.* 2004). Melting permafrost releases organic matter which is susceptible to biodegradation; the methane released is also a potent greenhouse gas and further amplifies global warming (Walter *et al.* 2006). The enhanced freshwater discharge alters the salinity of the Arctic Ocean with important ramifications for regional and global ocean circulation and climate (Arnell 2005; Serreze *et al.* 2007). The sensitivity of the Arctic climate system to perturbations has resulted in the highest observed and predicted rates of warming (IPCC 2007), therefore studies of high latitude regions are important for understanding the impacts of climate change and the mechanisms underlying those changes.

1.3. Late Quaternary climate variability in the northern hemisphere

After the climate oscillations of the preceding glacial cycles, the climate over the past 11 550 years of the Holocene was traditionally viewed as a period of climate stability (for example Dansgaard *et al.* 1993). A thermal optimum, in the early to mid Holocene, was followed by gradual cooling in the late Holocene. However measurements of chemical ions in the Greenland ice cores (O'Brien *et al.* 1996) demonstrated that the Holocene was punctuated by a series of

millennial- to decadal-scale shifts in climate, the evidence and mechanisms for which were recently reviewed in Battarbee and Binney (2008).

The warming trend of the Pleistocene – Holocene transition was triggered by orbitally driven changes in the latitudinal and seasonal distribution of insolation. Changes in insolation were relatively gradual and continued throughout the early Holocene. Solar insolation has only been broadly comparable to the present-day for the past 6000 years. At the start of the Holocene the effects of smoothly changing external forcing were mediated by internal dynamics to generate abrupt and synchronous climate changes in many parts of the world (Oldfield 2003). Retreat of continental ice sheets, formed during the last glacial period, and the associated changes in ice-albedo feedback are thought to have locally influenced the regional climate responses to orbital forcing (Jansen *et al.* 2007).

Although the amplitude and occurrence of volcanic forcing have varied significantly during the Holocene (Zielinski 2000; Castellano *et al.* 2005). Magma unloading, due to ice sheet melting, resulted in increased volcanism in the early Holocene, with three times the volcanic activity between 11,500 and 9,500 cal yr BP compared with the last 2000 years, which may have contributed to regional cooling (Zielinski *et al.* 1994). However there are considerable uncertainties in the estimates of volcanic forcing due to assumptions made in the analysis of ice cores and inclusion of aerosols in model simulations (Jansen *et al.* 2007).

The general warming trend from the last glacial period was interrupted by cold intervals including the Younger Dryas (YD, 12800-11550 yrs BP, immediately preceding the Holocene) and at 8200 yrs BP. These cold intervals are associated with changes in vegetation (Tinner and Lotter 2001; Veski *et al.* 2004) and the southwards shift of the treeline (Peteeet 1995; Shuman *et al.* 2002). During the YD, mean annual temperatures, in Europe, declined by 5–15°C (Severinghaus *et al.* 1998; Alley 2000) whereas summer temperatures decreased by only 2–10°C (Birks and Ammann 2000; Marshall *et al.* 2002; Peyron *et al.* 2005). This suggests winter temperatures were primarily affected

and Giesecke *et al.* (2008) suggested the continental climate of the YD became more maritime in the early Holocene. However the severity and duration of YD cooling shows considerable heterogeneity and the climate may have been warmer-than-present through most of Central Alaska, North-east Siberia and the Russian Far East (Kokorowski *et al.* 2008). By comparison, an abrupt, transient cold event at *c.* 8200 cal yr BP appears to have a global signature (Stager *et al.* 1997; Neff *et al.* 2001; Staubwasser *et al.* 2002). Although the timing of the onset and its duration are contentious (Alley *et al.* 1997; Johnsen *et al.* 2001; McDermott *et al.* 2001; Spurk *et al.* 2002).

Freshwater influxes into the Arctic – Atlantic Oceans, due to the inflow of melt water from ice melting in the warming climate at the time, are believed to be the cause of the Younger Dryas (YD) and 8200 yrs BP cold events (Jansen *et al.* 2007). During the YD, freshwater discharge into the Arctic may have disrupted Meridional Overturning Circulation (MOC) and heat transport in the Atlantic (Tarasov and Peltier 2005) while the 8200 year event was probably triggered by catastrophic release from pro-glacial Lake Agassiz (Clarke *et al.* 2004). Both events would have disrupted ocean circulation and the poleward distribution of heat.

A number of the other Holocene climate oscillations, such as the Holocene Thermal Maximum (HTM) also show considerable spatial and temporal complexity. At high latitudes, in areas adjacent to the North Pacific and Arctic Oceans, the maxima usually occurred in the early Holocene (10 – 8 kyrs BP), reflecting to the direct influence of the summer insolation maxima on sea ice extent (Kim *et al.* 2004; Kaplan and Wolfe 2006). Near decaying ice sheets, in northern Europe and North America, the maxima was locally delayed, due to the influx of meltwater weakening the poleward heat transport by the ocean and the high albedo of the ice (Renssen *et al.* 2009) or an interplay between ice elevation, albedo, atmospheric and oceanic circulation and orbital forcing (MacDonald *et al.* 2000; Kaufman *et al.* 2004). For example, the Holocene Thermal Maximum (HTM) occurred between 11000–9000 yrs BP in Alaska and northwest Canada, but was delayed in northeast Canada until 7000–6000 yrs BP due to the cooling effect of the Laurentide Ice-Sheet (Kaufman *et al.* 2004).

In Europe, proxy-based reconstructions suggest the early Holocene (before 8000 – 7500 yrs BP) was relatively cool and the HTM occurred between ca. 8000 – 5000 yrs BP (Renssen *et al.* 2009). The differences in the timing of the HTM appear related to the distance from the Atlantic coast and the latitudinal position (Renssen *et al.* 2009). Proxy records, from northern Russia, suggest the period from c. 10500–9000 yrs BP was the warmest interval of the Holocene (MacDonald *et al.* 2000; Pisaric *et al.* 2001a; Andreev *et al.* 2005).

Reconstructions of sea surface temperatures (SST) in mid-northern latitudes show a continuous decline from the warm early Holocene to the cooler late Holocene (Kim *et al.* 2004; Kaplan and Wolfe 2006). From ca. 6 kyrs BP, summer temperatures appear to have cooled across the northern hemisphere over a period of approximately 4000 years (Jones and Mann 2004). This cooling is evident in periodic glacial advances in, for example, Scandinavia (Lie *et al.* 2004; Bakke *et al.* 2005) and the Brooks Range, Alaska (Ellis and Calkin 1984). Between 5 – 4 kyrs BP northern sea ice increased (Jennings *et al.* 2002) and pollen records indicate abrupt cooling events in northern Europe (Seppä and Birks 2001). The cooling trend is probably a response to changes in orbital forcing and annual mean and summer insolation (Renssen *et al.* 2005) which also influenced large-scale features of atmospheric circulation such as monsoonal and El Niño Southern Oscillation circulation (Clement *et al.* 2000)

Global and northern hemisphere climate variability over the past two thousand years has been comprehensively reviewed by Jones and Mann (2004) and Jansen *et al.* (2007). Instrumental and proxy records, and climate simulations, show close agreement regarding the major features. Conditions were relatively cool during the 17th and early 19th century and warm in the 11th and early 15th century, with a sharp rise to unprecedented levels of warmth at the end of the 20th century (Jansen *et al.* 2007). The Maunder Minimum, a period of reduced solar activity identified by a reduction in sunspots, coincides with the cool interval in the 17th – 18th centuries (Grove 1988). The cooling due to reduce irradiance (Camp and Tung 2007) would be insufficient to account for the estimated 0.5 - 1.5°C cooling (Rind and Overpeck 1993). Stuiver and Braziunas (1993) suggested the initial temperature decline was accompanied

by increased precipitation which led to reduced salinity and changes in the THC so amplifying the solar-induced climate signal. Major differences exist between the proxy records as to the magnitude and spatial extent of cool fluctuations during the 12th to 14th, 18th and 19th centuries. The warm and cool intervals, ca. the 11th and 17th – 19th centuries respectively are often referred to as the 'Medieval Warm Period (MWP)' and 'Little Ice Age (LIA)' (for example Solomina 2000; Pavlov *et al.* 2002; Solomina and Alverson 2004). However Jones and Mann (2004) argue use of the terms 'Little Ice Age (LIA)' and 'Medieval Warm Period (MWP)' are inappropriate as discernible warm or cold periods occur during the LIA and MWP respectively, and in more southerly locations these intervals are characterised by wetter or drier conditions rather than changes in temperature

1.3.1. Late Quaternary climate variability in northern Russia

Pollen and plant macrofossil records from the Taymyr Peninsula and Polar Urals indicate that the Pleistocene-Holocene transition was characterised by changes from sparse steppe-like communities to shrub tundra (Andreev *et al.* 2002; Andreev *et al.* 2004a; Andreev *et al.* 2005). The skeletal remains of large herbivores including the woolly mammoth (*Mammuthus primigenius*) and musk-ox (*Ovibus moschatus*), in the permafrost of the Taymyr Peninsula, are dated from ca. 55800 yrs BP – ca. 13000 yrs BP. The collapse of the Pleistocene megafauna is primarily attributed to increased temperature and precipitation, with resulting succession from dry steppe to moist tundra vegetation (Mol *et al.* 2006). Across the Siberian Arctic there was also a cultural transition as the Paleolithic Dyuktai culture was replaced by the Sumnagin tradition. Stone, bone and ivory artefacts indicative of dependence on mammoth hunting were superseded by reindeer hunting in the tundra and elk hunting in forested areas (Pitul'ko 2001)

Chironomids, pollen and plant macrofossil records, from northern Russia, suggest the period from c. 10500–9000 yrs BP was the warmest interval of the Holocene, with mean July temperatures 2 - 3°C warmer than present at 11 – 13°C (MacDonald *et al.* 2000; Pisaric *et al.* 2001a; Andreev *et al.* 2005). The tree-line extended approximately 200 – 300 km north of the present limit and

reached the present day shore-lines of the Barents, Kara and Laptev Seas and 72°N on the Taymyr Peninsula (Kremenetski et al. 1998) (see Figure 1.2).

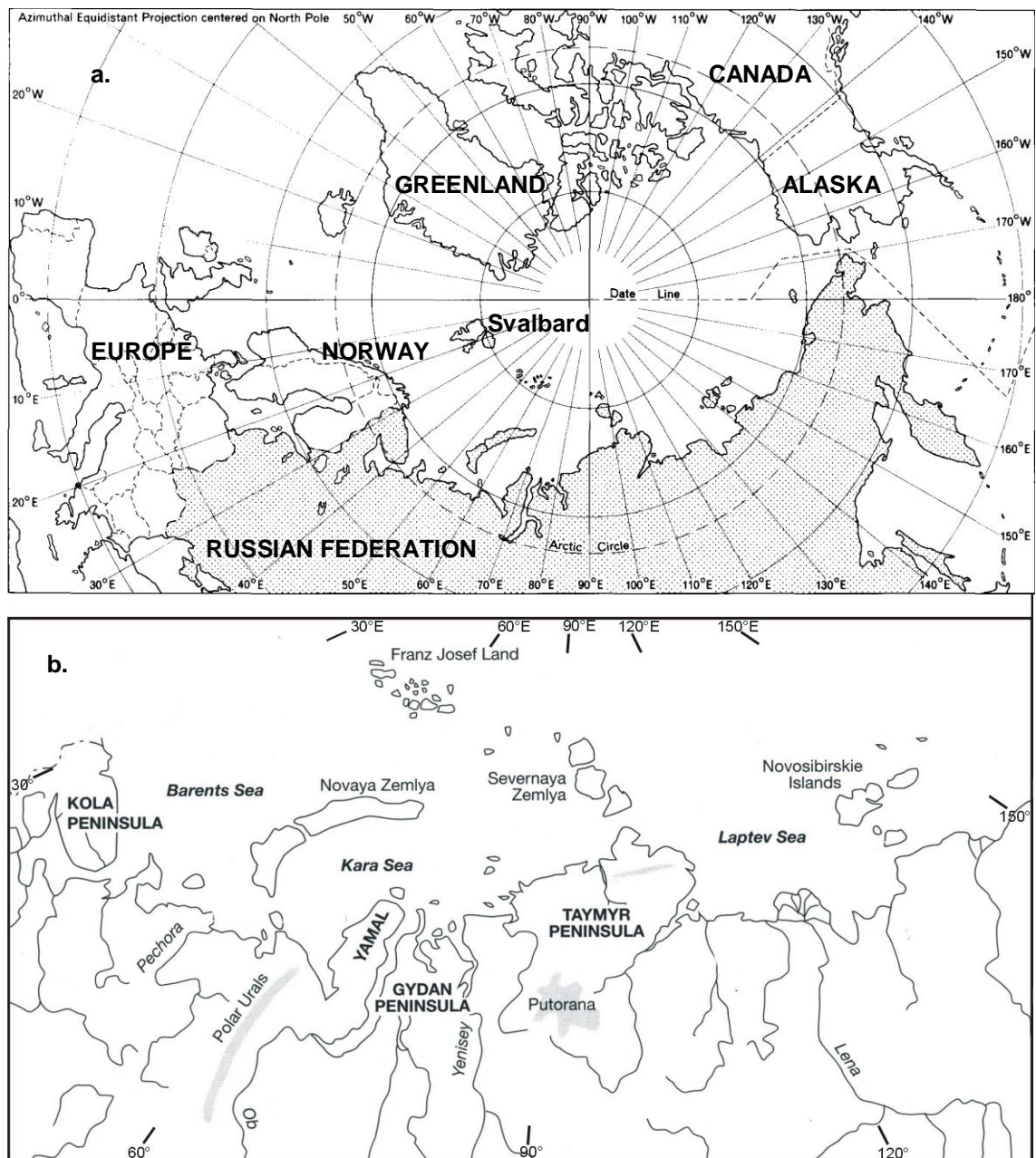


Figure 1.2. a. Location of the Russian Federation (referred to as Russia in the thesis) within the Arctic (Dewdney 1982) and b. locations in northern Russia referred to in the thesis (Shahgedanova and Kuznetsov 2002). Mountainous areas are shown in grey in map b, the Novosibirskie Islands are also referred to as the New Siberian Islands.

In Northern Russia, the climate cooled gradually from 8800 – 5500 yrs BP but remained relatively warm. The onset of the cooling shows regional

discrepancies; cool-water taxa appear in the chironomid record at c. 9200 yrs BP in the Lena River Delta (Porinchu and Cwynar 2002; Andreev *et al.* 2004b) and c. 8800 yrs BP in the Polar Urals (Andreev *et al.* 2005). Radiocarbon dating of Mesolithic artefacts at Zhokhov, on the Novosibirskie or New Siberian Islands (76°N), suggests occupancy was established approximately 8480-8175 yrs BP (Pitul'ko 2001). Subsistence was based on the hunting of polar bears and reindeer; the occurrence of these species suggests the presence of sea ice and thick snow cover in winter. Cooling intensified between c. 5500 – 2500 yrs BP leading to the establishment of the modern day tree-line (Kremenetski *et al.* 1998). Diatom assemblages from the Polar Urals suggest the longer persistence of lake-ice with pollen-based climate reconstructions indicating mean July temperatures of 8 – 10°C (Andreev *et al.* 2005).

Tree-ring chronologies from the Yamal (Hantemirov and Shiyatov 2002) and the Taymyr Peninsulas (Jacoby *et al.* 2000; Naurzbaev *et al.* 2002; Sidorova *et al.* 2007) show anomalous warming between c. 1800-1700 and 1100-800 yrs BP and over the last 100 years. The records also indicate cold periods persisted from 500-300 yrs BP and c. 200 yrs BP, which is consistent with ice-core data from Severnaya Zemlya and Franz Josef Land (Henderson 2002) and glacier advances on Novaya Zemlya (Murdmaa *et al.* 2003).

1.3.2. Recent climate variability in northern Russia

Instrumental and proxy records suggest mean arctic temperatures have increased at almost twice the rate of the rest of the world over the past 100 years with greatest warming occurring in winter (DJF) and spring (MAM) (Solomon *et al.* 2007). Annual and summer arctic sea ice extent have decreased since 1978 (Lemke *et al.* 2007). The extent of snow cover and seasonal river and lake ice duration over the past 150 years has decreased; freeze-up of rivers has, typically, been delayed by a rate 5.8 ± 1.6 days per century, while the breakup date occurs earlier at a rate of 6.5 ± 1.2 days per century (Magnuson *et al.* 2000). Analysis of Russian river data showed a trend towards earlier freeze-up in Western Russia and later freeze-up in Eastern Siberia (Smith 2000). In the Arctic temperatures at the top of the permafrost layer have increased by up to 3°C since the 1980s (Pavlov 1996; Oberman and

Mazhitova 2001; Walsh *et al.* 2005). The maximum extent of seasonally frozen ground has decreased by about 7% since 1900 (Zhang *et al.* 2003) and its maximum depth has decreased by about 0.3 m in Eurasia since 1956 (Frauenfeld *et al.* 2004).

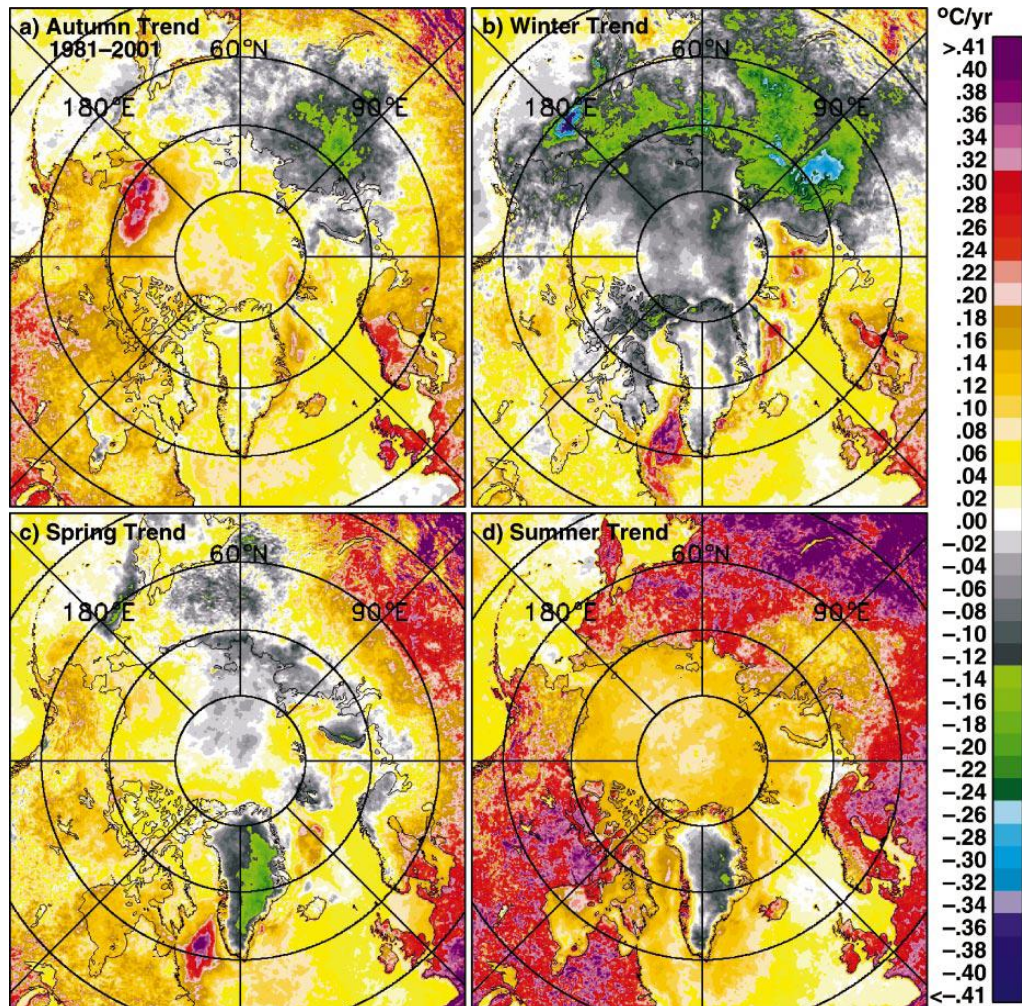


Figure 1.3. Colour-coded trend maps for the Arctic in (a) winter (DJF), (b) spring (MAM), (c) summer (JJA), and (d) autumn (SON) for the period August 1981 to July 2001 (reproduced from Comiso, 2003) Trends are derived by linear regression of seasonal anomalies from 1981 to 2001. The anomalies were calculated by subtracting the mean of the 20 years of data from the observed values.

However the trends show considerable spatial and seasonal heterogeneity. Satellite thermal infrared data (Comiso 2003) suggest mean annual temperatures have increased since 1981 in the northern Urals, southern Yamal and Lena River delta, whereas the Taymyr Peninsula has cooled. These trends

also vary throughout the year (Figure 1.3). The Taymyr Peninsula and western Siberia plain, between 85° and 100°E, cooled by 0.05 – 0.1 °C yr⁻¹ during the autumn whereas temperatures in the Yamal Peninsula remained constant. Spring temperatures warmed in the Yamal peninsula and northern Urals, while northern Taymyr and the Lena River Delta have cooled. In summer most areas of northern Russia appears to be warming and wide areas of Siberia and the Arctic basin show cooling winter trends. Therefore the annual trends reflect the balance of seasonal changes; in Taymyr, for example, the magnitude of winter cooling is greater than summer warming resulting in an annual cooling trend.

Over the longer term (1954 – 2003) instrumental data indicates increasing annual and winter air temperatures over both the Yamal and Taymyr Peninsulas and cooling in the Lena River delta (ACIA 2004, 2005). The discrepancy in observed trends partially reflects the sparseness of meteorological data and the short duration of remote-sensed records in northern Russia. From 1989–1995 the AO (Arctic Oscillation) was strongly positive; this is associated with temperature maxima in northern Europe and north-central Asia and could partially account for the warming trend. However this warming has continued into the early 21st century while the behaviour of the AO has been more episodic with near-neutral or negative phases (Richter-Menge et al. 2006). This suggests that internal processes in the western Arctic, such as reduced sea-ice and vegetation changes, may play an important role in maintaining the current trends (Overland and Wang 2005).

1.3.3. Issues to be addressed

The preceding review of climate variability during the late Quaternary highlighted the spatial and temporal heterogeneity in palaeoclimate reconstructions across the northern hemisphere, even at times of major climate change such the Younger Dryas. In comparison to western Europe and North America, there are few continuous, well-dated, high resolution palaeoclimate records from northern Russia. For example, the spatial extent, magnitude and duration of the YD and HTM are poorly studied and uncertain in north east European Russia, Siberia and the far East. The lack of high quality climate data extends to recent meteorological records. Instrumental records are sparse, of

short duration and often intermittent (Rigor *et al.* 2000). Meteorological stations are often located in the most benign habitats, for example at lower, warmer elevations, unrepresentative of the regional climate (Rawlins and Willmott 2003). Satellite data suggest mean annual temperatures have increased since 1981 in some areas of northern Russia whereas other regions have cooled (Comiso 2003). The paucity of palaeoclimate records mean it is not possible to determine whether these regional responses are a persistent feature of Holocene climate change across northern Russia or a short-term non-equilibrium response to present climate forcing.

Many of the existing quantitative records, based on biological proxies, are reconstructed using modern data that may not be appropriate for biological assemblages from northern Russia. For example, climate variables from Nikolay Lake, in the Lena Delta, were reconstructed using a training set of 800 pollen spectra from across Russia, however arctic sites were poorly represented in the dataset (Andreev *et al.* 2004b). Similarly, there is, currently, no Russian chironomid-temperature training set and reconstructions from northern Russia are based either on a Swedish (Larocque *et al.* 2001) or Norwegian (Brooks and Birks 2001) datasets. These may not be applicable as a number of common taxa in the Russian subfossil assemblages, such as *Constempellina* and *Mesocricotopus* (Andreev *et al.* 2005), are absent or poorly represented in the European datasets. Many chironomids are identified to morphotypes (Brooks *et al.* 2007), and species composition of a morphotype, and therefore possibly their response to environmental variables, may vary between the geographical locations. The climate regimes of western Europe and continental Russia vary considerably, the cooler, briefer summers in central Russia may result in different selective pressures and physiological or behavioural response to the climate (see section 1.5). Therefore, for most biological proxies, the development of Russian datasets with high taxonomic resolution and consistent, high quality environmental data is a priority for palaeoclimatic studies in northern Russia.

The remoteness of many areas and the lack of long-term studies or reliable palaeoenvironments records, based on biological proxies such as diatoms,

chironomids and cladocera, mean little is known about the biology of organisms or ecosystems in arctic Russia, or their response to recent environmental change such as increased atmospheric pollution or climate change. This has resulted in northern Russia, particularly to the east of the Urals, being poorly represented in global assessments of the impact of recent climate change on phenology (Walther *et al.* 2002; Hoyer *et al.* 2007) or individual organisms and ecosystems (for example Smol *et al.* 2005).

Due to the spatial and temporal heterogeneity of past and present climate responses in northern Russia, study areas were selected from two regions showing contrasting responses to recent climate change; the Putorana Plateau and northeast European Russia (Figure 1.3) (Comiso 2003). The rationale for the selection of study areas is discussed in Chapter 2; sites were selected to enable past trends in the regional expression of climate change to be examined.

1.4. Palaeoclimate reconstructions using proxy records

This section examines the criteria for the selection of record and proxy type for the study. Their strengths and weaknesses in palaeoenvironmental and palaeoclimate reconstructions are then discussed. Instrumental records in northern Russia, typically, extend back less than a hundred years and even the longest European temperature record only covers the past 350 years (Manley 1974). Their short duration mean they provide an inadequate perspective on climatic variation where forcing mechanisms act on centennial to millennial time-scales. Many natural systems, biological and physical, are climate-dependent and therefore provide an indirect record of palaeoclimatic conditions. However the climatic signal may be weak and embedded in random (climatic or environmental) noise. Interpretation of these proxy records can be challenging and a multi-proxy approach, using mutually independent records, is often used to reinforce inferences (Lotter 2003; Birks and Birks 2006). The choice of proxy depends on the research question to be answered and study location; the strengths and weaknesses of proxy records have been reviewed by Elias (2006).

1.4.1. Lake sediments as archives of palaeoenvironmental records

In continental regions the palaeoenvironment can be reconstructed from records preserved in specific depositional environments; for example, glaciers (Nesje and Dahl 2003), peatlands (Barber and Charman 2003) or speleothems (Lauritzen 2003). The choice is determined by the environments available within the selected study area and the proxy under consideration. The semi-terrestrial nature of peatlands, for example, would affect the composition of the chironomid fauna. As the composition and ecology of these assemblages are poorly known, and peatlands respond primarily to changes in hydrology (Barber and Charman 2003), this environment would not be suitable for chironomid-based palaeoclimatic reconstructions.

Lake deposits are one of the best archives of continental climate and its environmental impact (Fritz 2003). Sedimentary sequences are often continuous and may span thousands of years. Even in environments with low sediment accumulation rates, such as tundra lakes, sediment cores can give records with multiannual or decadal temporal resolution. As lakes are widespread throughout the study area lake sediment cores were selected as the most appropriate archive. A lake's response to regional climate is mediated by site-specific catchment and basin characteristics including the presence of inflows and outflows, soils, vegetation, topography and lake morphometry (Fritz 2003). Therefore sediment cores were collected from 2-3 lakes to discern the regional climate response.

1.4.2. The selection of chironomids for this study

To minimise the response of the biota to environmental parameters other than temperature, lakes were selected above the present-day tree line. In these tundra areas, with low local pollen production, pollen records may be compromised by long-distance or extra-regional pollen transport (Birks and Birks 2003). Although plant macrofossil data can be used to valid pollen-based climate reconstruction (Birks and Birks 2003) arctic and sub-arctic vegetation is dominated by slow-growing species which may dampen observed climate responses (Birks 1981). The location above the tree-line also precludes the use of dendrochronology. There has also been a loss of thermal response in tree

ring width since the 1960s (Vaganov *et al.* 1999; Jacoby *et al.* 2000; Briffa *et al.* 2002b) which has reduced the sensitivity of this technique for reconstructing recent climatic change.

Diatom-inferred temperature reconstructions show close correspondence to instrumental data, in most cases, but correlated poorly when changes in the pH of the lake water occurred (Bigler and Hall 2003). However their sensitivity to pH means changes in the diatom assemblages can give an indication of changes in pH or trophic conditions which can help in the interpretation of the chironomid response (Battarbee *et al.* 2001).

Coleopteran assemblages have been used to reconstruct palaeotemperatures (Coope *et al.* 1998; Lemdahl 2000). However the large volumes of material required for analysis, typically 0.5-1kg would require the export of large quantities of sediment which would be logistically difficult. In comparison, the larval head capsules of Chironomidae (Insecta, Diptera) are abundant, diverse, well-preserved and ubiquitous in lake sediment samples (Brooks *et al.* 2007). A minimum of fifty head capsules are required for estimating past temperatures using a chironomid-based inference model (Heiri and Lotter 2001; Larocque 2001; Quinlan and Smol 2001). Therefore, even from arctic lakes with low productivity, less than two grams of sediment are required for analysis so cores can be finely sliced and analysed at high temporal resolution (Brooks and Birks 2004).

Chironomids are sensitive indicators of past climates. Many taxa are stenothermic and the winged adults disperse readily across the landscape which means they effectively respond instantaneously to changes in the climate. European chironomid-mean July air temperature inference models have prediction errors of about $\pm 1.0^{\circ}\text{C}$ (Lotter *et al.* 1997; Brooks and Birks 2000a; Larocque *et al.* 2001; Luoto 2008) and show close agreement with instrumental records over the past 100 years (Larocque and Hall 2003).

Although chironomid-inferred temperature reconstructions for the Lateglacial show good agreement with other proxy records, Holocene reconstructions are

less consistent (Brooks 2006b). Chironomid distributions are influenced by many environmental factors and changes in these may invoke a stronger response in the chironomid fauna than temperature alone (Brooks *et al.* 2007). Re-forestation of northern Eurasia during the Holocene would have enhanced soil development, which in turn, would alter the pH, DOC and chemical characteristics of lakes within the catchment. Chironomids responding to these localised parameters may give anomalous temperature reconstructions.

1.4.3. Chironomids as a proxy in palaeoenvironmental reconstructions

Chironomids have been used in palaeoenvironmental studies in Eurasia since the 1920s (Brooks 2006b). In early work chironomids were used as qualitative indicators of trophic change (reviewed by Lindegaard 1995). Changes in faunal assemblages over the Holocene were interpreted as classical lake succession from oligotrophic to eutrophic status (for example Bryce 1962; Goulden 1964). Andersen (1938) published a Lateglacial stratigraphy from Denmark in which he suggested shifts in the faunal composition between the Older Dryas and the Allerød and again in the Younger Dryas were climate-driven. However the concept that chironomids were influenced by changing climate as well as changes in lake productivity was seldom considered until the 1980s (Brodin 1986; Hofmann 1988).

Walker and Mathewes (1987; 1989) demonstrated that chironomids were sensitive to Lateglacial and Holocene climate change and, in a pioneering step, developed chironomid-temperature inference models to quantify the climate change (Walker *et al.* 1991; Walker *et al.* 1997). The encouraging results led to the development of chironomid-inferred temperature (CI-T) models in several European countries; Finland (Olander *et al.* 1999), Norway (Brooks and Birks 2000a, 2001) and Sweden (Larocque *et al.* 2001). Initially the inference models focused on reconstructing surface-water temperature; since the majority of the chironomid life cycle (section 1.5) is aquatic, water temperature would have a significant impact on the distribution and abundance of species (Brooks 2006b). However prediction errors were relatively high. Water temperatures show wide day-to-day fluctuations and the use of 30-year mean July air temperatures, based on meteorological data corrected for altitude and distance from the coast,

improved the performance of the models (Lotter *et al.* 1997; Olander *et al.* 1999; Brooks and Birks 2001; Larocque *et al.* 2001). Air temperature influences the dispersal of the terrestrial adult stage and is usually closely correlated with surface-water temperature (Livingstone and Lotter 1998; Livingstone *et al.* 1999). However air temperatures are consistently underestimated if the lake receives substantial influxes of melt-water from glaciers or snow-beds (Brooks and Birks 2001).

The chironomid larvae are identified from characteristic features of the heavily chitinised head capsules. In most specimens these are only identifiable to a generic or morphological type level. This limits the applicability of a training set to the biogeographical region in which it was assembled as species within the same genus, which are indistinguishable as subfossils, may have different temperature optima (Brooks *et al.* 2007). Therefore one of the aims of the research (section 1.6) is determine whether a regional training set compiled from Russian assemblages is more appropriate for palaeoclimate reconstructions in northern Russia than either the Norwegian dataset (Brooks and Birks 2001 and unpublished data) currently used (for example Solovieva *et al.* 2005) or a combined Norwegian – Russian training set. Combining the datasets would greatly increase the number of samples and give a more even distribution along the environmental gradients but can only be justified if the faunal composition, selective pressures and taxon-responses are similar in the two geographical areas.

The relationship between chironomids and environmental variables, other than temperature, has been used to quantitatively reconstruct past total phosphorus (Lotter *et al.* 1998; Brooks *et al.* 2001), chlorophyll-a (Brodersen and Lindegaard 1999a), salinity (Walker *et al.* 1995; Verschuren *et al.* 2004; Eggermont *et al.* 2006; Zhang *et al.* 2007), hypolimnetic oxygen conditions (Quinlan *et al.* 1998) and water depth (Korhola *et al.* 2000). Birks and Birks (2006) argued that the emphasis on palaeoenvironmental reconstructions has led to a neglect of the study and understanding of lake biotic responses to changing internal or external factors, of lake dynamics and processes, and of the underlying biology and ecology of the organisms preserved in lake

sediments. These factors need to be considered in data interpretation. Multiproxy studies are often used to study these ecosystem-scale processes, with their complex networks of interactions, in order to gain a wider overview of the situations than could be acquired from a single proxy (Birks and Birks 2006). Therefore dry weight, loss-on-ignition (LOI) and stable isotopes ($\delta^{15}\text{N}$ and $\delta^{13}\text{C}$) concentrations were determined in the sediment cores to facilitate the interpretation of changes in subfossil chironomid assemblages.

1.5. Biology of chironomids

The Chironomidae is a family of two-winged flies (Insecta: Diptera); with an estimated 15,000 species worldwide (Cranston 1995). This section examines the biology and ecology of chironomids, with special emphasis on their adaptations to arctic environments. Survival, in these environments is challenged by the severity of the climate (cold temperatures, limited heat accumulation for growth), its continentality or seasonality (wide differences between summer and winter temperatures), short term unpredictability (such as the potential for sudden changes in temperature or freezing events) and the wide interannual variability (year-to-year variations in the climate which govern development and survival) (Danks 2004).

1.5.1 The chironomid life cycle and its adaptations to temperature

The life cycle is illustrated in Figure 1.4. Voltinism (the number of generation per year) is negatively correlated to latitude (Tokeshi 1985) and extended life cycles of 2-3 years are common in many species at high latitude, for example *Sergentia coracina* (Aagaard 1982) and *Paracladius quadrinodosus* (Welch 1976). The longest recorded life cycles are two *Chironomus* species in arctic tundra lakes in Alaska which need seven years to complete development (Butler 1982). Arctic species are capable of overwintering in any developmental stage and may remain in diapause or overwintering state for several years if conditions are unfavourable for development (Danks 2004).

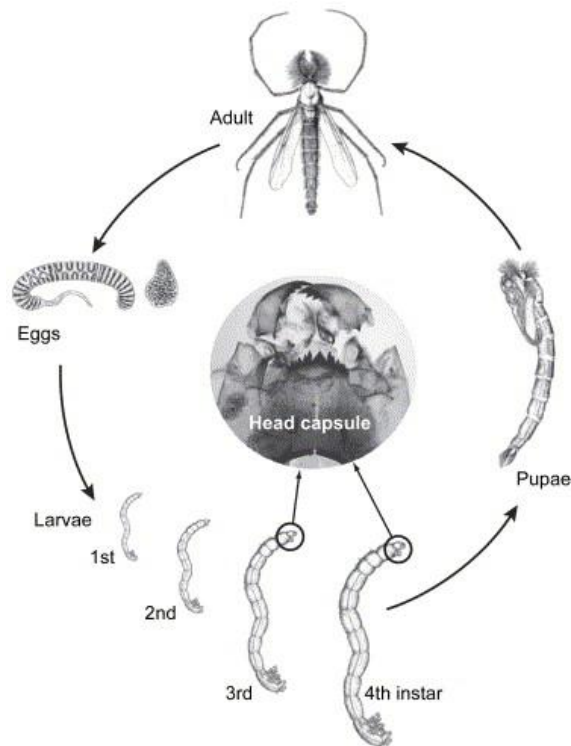


Figure 1.4. Chironomid life cycle (adapted from Brodersen and Anderson 2000; by Ruiz *et al.* 2006)

Eggs are laid in a hydrophilic jelly mass either in the water or attached to a substrate. Many arctic insects, such as *Aedes* mosquitoes, lay overwintering eggs in south-facing pond margins which thaw earliest (Corbet and Danks 1975), although habitat selection has not been observed in Chironomids. Hatching rate and survival are temperature dependent. In *Chironomus plumosus* the rate of egg development is positively correlated with temperature within the range of 5-30°C but declines above the temperature optimum so that eggs fail to hatch at 35°C (Iwakuma 1986).

Chironomids pass through four larval stages; duration of the instars varies with species but most species pass through the early stages within a few months and spend longer, overwintering, in the fourth instar (Carter 1980; Rasmussen 1984). Development time of the larvae is dependent on temperature and food availability (Johannsson 1980). Developmental rate is positively related to temperature (Mackey 1977; Edwards 1986) whereas daily growth rate appears to reach a maxima at a temperature optimum (Storey 1987; Hauer and Benke 1991). This ensures that larvae mature and pupate in as shorter time as possible regardless of size.

In arctic environments all individuals which emerge in a given season overwinter as larvae which pupate in the spring without further feeding (mature larvae) (Danks and Oliver 1972a, b). Immature larvae, which require feeding after winter, do not metamorphose until the following year (Danks and Oliver 1972a). This facilitates the synchronised emergence of adults and maximises the likelihood the offspring will reach the overwintering stage before winter returns (Danks 2004). The pupal stage usually lasts 3-4 days; in some chironomid species, if conditions cool during the prepupal stage, development is arrested until the following year (Oliver 1968).

In temperate species the timing of emergence of the adults is dependent on water temperature and light intensity (Kureck 1979; 1980). However the continuous daylight of the polar summer precludes initiation of activity by light intensity, day-length or daily alterations of light and dark. Emergence of adults in the Arctic, for example, appears to be governed by water temperature with thresholds of 4-5°C for pupation and 7°C for pupal ecdysis, the physiological changes associated with moulting of the pupa (Danks and Oliver 1972b). The pharate adult swims to the water surface, breaks through the meniscus and emerges directly into the air leaving the discarded pupal case on the surface.

Adults of most species live for a few days; many arctic species swarm and mate on the ground as conditions are frequently too cold or windy for flight (see section 1.5.2). Parthenogenesis, development of larvae from unfertilised eggs, is also more common in arctic insects, including chironomids, than faunas at lower latitudes (Danks 1981). Parthenogenesis removes the necessity for mating when summer conditions are cool and unpredictable and also buffers the population from responding to short-term environmental change. For example, selection after recombination may remove genotypes well adapted to cold conditions during a series of warm summers in favour of individuals who might be vulnerable when more typical severe conditions return (Downes 1965). The prevalence of parthenogenesis in arctic chironomid species implies that they may respond to temperature change by distributional changes rather than the selection for different genotypes, as seen in *Drosophila subobscura* (van

Heerwaarden and Hoffmann 2006). This makes arctic chironomid assemblages particularly sensitive to climate change.

1.5.2 Physiological adaptations of insects to arctic environments

The adaptations of insects to arctic environments is comprehensively reviewed by Lee and Denlinger (1991). Arctic insects are typically smaller in size, with more compact bodies, than lower latitude species (for example Danks 1981). This may be an adaptation to reduced food resources and enhance the conservation of moisture or ability to shelter in small microhabitats (Sømme and Block 1991). Brachypterous (small or rudimentary) wings or complete loss of wings occurs in many Arctic insects and many adult chironomids aggregate and mate on the ground (Danks 1981; Butler 2000; Danks 2004). Correlated with this behaviour the eyes and antennae are often reduced and the genitalia enlarged. Melanistic colours and hairiness are also common in many arctic insects. Melanin pigments absorb solar radiation more effectively for thermoregulation and hairs allow a warm boundary layer of air to be retained next to the cuticle (Danks 2004).

Many arctic insects overwinter in diapause, a programmed suppression of development, to conserve energy and prevent unseasonable warm spells from restarting development (Danks 2004). In chironomids diapause is restricted to the egg, larval and pupal stages (Tokeshi 1985). Arctic, and temperate, chironomids build special winter cocoons for protection against mechanical damage caused by the expansion of water as it freezes (Danks 1971). Larvae also become dehydrated to enhance cold hardiness; *Polypedilum halterale* and *Einfeldia pagana* larvae collected in winter have 5% lower water content than those collected in summer (Danks 1971). Chironomidae are considered to be cold-adapted (Oliver 1971; Danks 1981) but the ability to withstand freezing varies between taxa (Tokeshi 1985). After freezing at -4°C for 24 hours, over 80% of *Stictochironomus*, *Chironomus* and *Procladius* survived while only 67% of *Tanytarsus* spp. were alive (Danks 1971).

1.5.3 Responses of insects to continentality

In comparison to temperature, there has been little work on the effects of continentality, independent of temperature, on insect populations or their physiology. Zaitsev and Wolters (2006) found a gradual faunistic shift in the structure and diversity of oribatid mite communities along a longitudinal transect from western Europe to Moscow. Soil-dwelling species increased and litter-dwellers decreased with increased continentality. Outbreaks of forest defoliating insects are, also, more frequent and intensive in eastern than western Ukraine (Meshkova 2002); the greater continentality results in more rapid increases in spring air temperature which accelerate larval development.

A number of insects show physiological responses to seasonality in the induction, progression and termination of diapause in populations across their geographic range. The critical photoperiod of the pitcher plant mosquito, *Wyeomyia smithii*, is longer in areas with a shorter growing season to enable the mosquito to synchronise its life cycle with the growing season of its plant breeding site (Bradshaw 1976). With increasing temperatures over the past 30 years the photoperiodic response of *W. smithii*, has shifted toward shorter day lengths as the growing seasons has become longer (Bradshaw and Holzapfel 2001). Similar changes in photoperiod response are reported for the burnet moth, *Zygaena trifolii* (Wipking and Neumann 1986). Diapause in the Colorado beetle, *Leptinotarsa decemlineata*, is less intense (shorter) and a lower thermal time required to initiate oviposition in areas where environmental conditions result in earlier spring growth of the beetle's host plant (Tauber *et al.* 1988b, a).

The majority of these studies are restricted to terrestrial insects, however a number of aquatic arthropods, such as freshwater copepods, show the temperature-related modification of photoperiod in response to length of the growing season (Marcus 1982; Hairston and Kearns 1995). The dependence on water temperature to determine the initiation and subsequent rate of development of chironomids (section 1.5.1) suggests that increased continentality may delay initiation but enhance the rate of development. This would help to ensure that development to an overwintering stage was completed within the short continental summer.

1.6. Scientific issues to be addressed in this thesis

The **aims** of the research are:

- To investigate the environmental variables influencing the modern distribution of chironomids in lakes from high northern latitudes of Russia and Norway.
- To examine species responses to the key environmental variables and assess the suitability of the selected environmental variables for the development of inference models for palaeoenvironmental reconstructions.
- To determine whether a regional Russian training set or a combined Russian-Norwegian training set would be more accurate for palaeoenvironmental reconstructions in northern Russia.
- To provide high resolution, low error quantitative reconstructions of climate, over the Holocene, from two sites in northern Russia showing differing trends in recent warming.
- To examine the biotic response of chironomids to environmental change over the Holocene, in terms of the ecology of individual taxa, changes in faunal composition and rates of change.
- To assess the relative influence of climate and other environmental variables on the observed chironomid faunal changes.
- And to examine the relative influence of hemispheric versus local climate drivers.

The preceding review of the literature has identified a number of **research questions** that need to be addressed in this thesis, namely:

- What is the present-day distribution of Chironomidae taxa in northern Russia and which environmental variables influence these distributions?
- Can chironomids be used to quantify changes in palaeoclimate, in particular past July air temperatures and continentality, in northern Russia?
- How have chironomid faunal assemblages changed at specific Russian sites over the Holocene?

- What is the sensitivity of the chironomid response to recent 20th century climate change?
- How do chironomid-inferred climate reconstructions compare with instrumental records and climate variability inferred from other proxy records and climate model stimulations?
- Are the major late Quaternary climate fluctuations (e.g. the HTM and 'Medieval Warm' periods and the YD, 8.2 ka BP, 2.7 ka BP and 'LIA' cold oscillations), which are apparent in the climate records from the North Atlantic region, also recorded in continental northern Eurasia?
- Are there significant differences in the magnitude, timing or duration of these oscillations between these regions indicating the differences in the relative influence of atmospheric and oceanic climate forcing?
- Is there evidence for the role of internal climate forcing and feedback amplification over the Holocene, i.e. does the general climate trend, disregarding short-term oscillations, solely reflect solar radiation?
- Are there significant spatial differences within northern Russia in the magnitude and timing of recent (past 700 years) climate fluctuations?
- Are the palaeoenvironmental reconstructions in agreement with current research, do they contribute to our understanding of late Quaternary climate change in northern Russia and/or do they address current controversies within the field?

These are summarised as the following **Hypotheses**:

- The distribution and abundance of chironomids in high-latitude lakes in Russia is primarily determined by July air temperature, but is also strongly influenced by continentality.
- Climate fluctuations in continental northern Russia, such as the YD, differ in timing and intensity from the North Atlantic region due to internal forcing (atmospheric – oceanic circulation) and feedback amplification (for example from ice-sheet and sea-ice dynamics).
- The YD – early Holocene transition in northern Russia marked a shift from a continental climate to a more oceanic climate due to impact of the

decaying Fennoscandian ice-sheet on atmospheric and oceanic circulation.

- Changes in continentality results in changes in faunal composition and/or physiological (e.g. temperature optima) responses in chironomids.
- Biotic changes over recent decades in regions showing a negative or neutral trend in summer temperature are, primarily, a response to decreased continentality (longer growing season).

To answer these questions the following **objectives** were undertaken to:

- Compile a dataset of chironomid faunas (the training set) from the surface sediment samples of Russian lakes with a range of known or derived standardised environmental variables.
- Standardise the taxonomy of the chironomid assemblages from Norway and different regions of Russia in line with recent advances in chironomid taxonomy (Brooks *et al.* 2007).
- Examine the species composition of generic morphotypes, using pupae exuviae, to identify speciose taxa which may vary in composition, and therefore in their response to climate, over the geographical regions.
- Examine the influence of chemical – physical variables on the distribution of chironomids in the Russian lakes and in lakes from Norway (Brooks and Birks 2001, and unpublished data).
- Identify climate variables which have the potential for palaeoenvironmental reconstructions.
- Model species response to the selected climate variable to assess their sensitivity, in terms of optima, tolerances and type of ecological response.
- Compare species responses, in terms of faunal composition, the environmental variables driving chironomid distribution and their climate optima, between the Russian and Norwegian training sets to whether a regional or Palaeoartic training set would be more appropriate for palaeoenvironmental reconstructions in northern Russia.
- Develop inference models to reconstruct the selected climate variable.

- Obtain representative Holocene sequences from regions of northern Russia showing differing trends to recent, late 20th century, warming.
- Date and develop age-depth models for the sediment cores.
- Analyse dry weight, loss-on-ignition, stable isotope concentrations and subfossil chironomid assemblages in subsamples from the sediment cores.
- Use generated inference models to reconstruct appropriate climate variables from the subfossil chironomid assemblages.
- Use reconstructed climate variables and modern ecology to interpret the faunal changes.
- Compare reconstructed climate variables to climate models, instrumental and other proxy records to assess the reliability of the reconstructions.
- Evaluate the performance of the inference models.

1.7. Structure of the thesis

Chapter 2 describes the physical and biological characteristics of the study area of the lakes used to compile the training set and in the collection of sediment cores. **Chapter 3** describes the methods, analytical and statistical techniques used in the research. This chapter also details the sources of secondary data used in the analysis. **Chapter 4** examines the factors influencing the distribution of chironomids in northern Russia, Norway and northern Eurasia. **Chapter 5** investigates the response of chironomid taxa to mean July air temperature and continentality. **Chapter 6** describes the development of the chironomid-inferred mean July air temperature and continentality models, including the identification of outliers and performance statistics. **Chapter 7** and **Chapter 8** describe the selection of coring sites on the Putorana Plateau and north-east European Russia respectively and analysis of the sediment cores. The results of sedimentary and isotopic analyses are presented together with the CI-T and CI-C reconstructions. These are then compared to instrumental and other proxy records to assess the reliability of the reconstruction. **Chapter 9** provides a synthesis of the results to answer the above research questions, review the contribution of this study to current palaeolimnological research and suggests future work.

Chapter 2

Description of the study areas

2.1. Introduction

As discussed in Chapter 1 observational evidence suggests that some areas of Arctic Russia, such as the northern Urals and Yamal Peninsula, warmed during the period from 1981 to 2001 whereas other regions including northwest Siberia cooled (Comiso 2003, figure 1.3). One aim of the project (section 1.6) is to examine the extent and persistence of this regional expression of climate change over longer time-scales. Therefore coring sites were selected within these two regions; 9 lakes were cored from the Putorana Plateau in northwest Siberia, a region of cooling surface temperatures and 4 lakes from the Pechora Basin, an area of NE European Russia showing a warming trend (Figure 2.1).

Present-day July air temperatures at the cored lakes range from 10.5-13.3°C (section 4.2); to reconstruct the past climate at these sites a training set was compiled using surface sediments from lakes within arctic and sub-arctic Russia with contemporary July air temperatures of 8.8-19.0°C. This chapter describes the rationale for the selection of the training set lakes (section 2.2). Methods for the collection and analysis of the sediment and water samples are described in Chapter 3. The coring and training set lakes are located in 5 geographical distinct study areas. The physical, biological and geographical characteristics of these study areas are then described in sections 2.3 – 2.6. The rationale for selection of coring sites for detailed palaeolimnological analyses is discussed in Chapter 7 for the Putorana lakes and Chapter 8 for the north-east European Russia.

2.2. Selection of training set lakes in arctic and subarctic Russia

The 100 lakes of the training set are located in northern Russia between 50 to 132°E and 61 to 72°N (Figure 2.1). Their locations cross major ecotones such as the latitudinal tree-lines and the boundaries of permanent and discontinuous permafrost. Surface sediments were collected from lakes within the watersheds of three major north-draining Eurasian river systems; the Pechora, Yenisey and

Lena Rivers. The locations of the study areas, the Pechora, Komi Republic, Igarka-Putorana, Lena Delta and Central Yakutia, are shown in Figure 2.1. Due to the logistical difficulties and expense of working in northern Russia, not all the surface sediments included in this study were collected or analysed, solely, by the author. The provenance of the samples is detailed in section 3.3, Table 3.5. Where possible, sites were selected in order to minimise the impact of direct anthropogenic disturbance to both the catchments and the lakes, in terms of agricultural land-use and habitation. However some lakes sampled by other workers, particularly in Central Yakutia, are close to major towns and have been shown to be eutrophic (Kumke *et al.* 2007). The location of the training set lakes are detailed in sections 2.2.1 to 2.2.4.



Figure 2.1. Map showing the locations of the training set lakes in:

- the Pechora River basin,
- Komi Republic,
- Igarka and the Putorana Plateau
- Lena River Delta, and
- Central Yakutia.

(Map created using Online Map Creation <http://www.aquarius.ifm-geomar.de/>)

2.2.1. Pechora Basin and Komi Republic

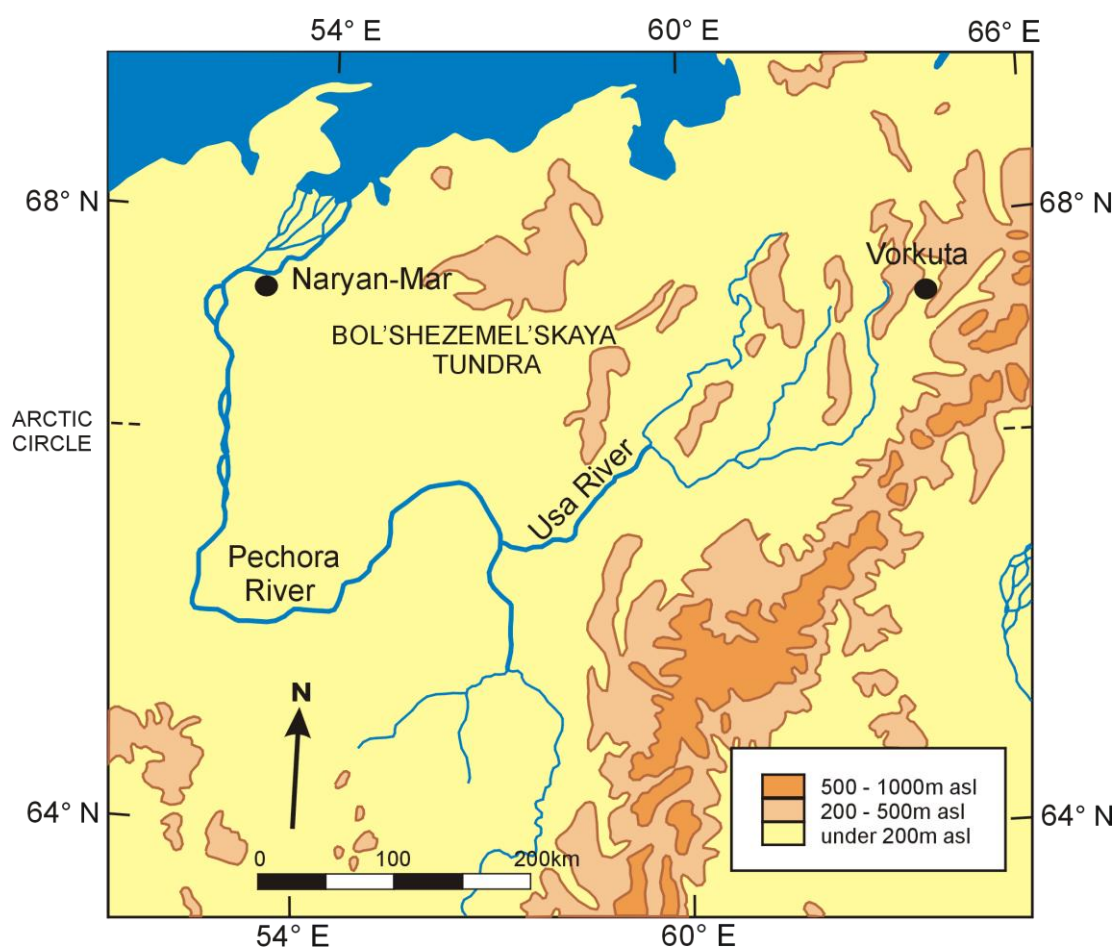


Figure 2.2. Topographic map of the Pechora River study area (based on map G.S.G.S. 4625 produced by the Geographical section, the War Office, 1948, U.S.S.R. and adjacent areas)

2.2.1.1. Previously studied sites used in thesis

Surface sediments had previously been collected from tundra and forest-tundra lakes in the watershed of the Pechora River and its major tributary, the Usa River, in NE European Russia, between 1998 and 2001 (Figure 2.2). Figure 2.3 shows the location of the sampling sites; their co-ordinates and physical characteristics are given in Table 2.1. Details of the collection and storage of the sediments are given in Chapter 3. Although the Usa basin includes highly industrialised towns, such as the coal mining area of Vorkuta, previous studies suggest the lakes show little impact from human activity or atmospheric pollution due to their high buffering capacity (Solovieva *et al.* 2002).

Table 2.1. Location and physical characteristics of the archived material from the Pechora and Usa River basins. (ND = not determined; lake area was calculated from GoogleEarth image and could not be calculated if the lake could not be identified or was obscured by clouds).

Site	Sampling date	Name	Latitude	Longitude	Altitude (m ASL)	Area of lake (ha)	Max lake depth (m)
F3-2	1.7 - 7.7.2000		067° 56' N	054° 02' E	13	11	4.3
F3-3	1.7 - 7.7.2000		067° 56' N	054° 03' E	20	26	1.5
F3-5	1.7 - 7.7.2000		067° 55' N	054° 02' E	17	12	3.3
F3-6	1.7 - 7.7.2000		067° 56' N	054° 00' E	18	28	1.3
F3-12	1.7 - 7.7.2000		067° 57' N	053° 56' E	13	ND	2.8
F4-2	7.7 - 13.7.2000		068° 00' N	052° 23' E	5	40	6
F4-4	7.7 - 13.7.2000		068° 00' N	052° 27' E	72	38	1.1
F4-5	7.7 - 13.7.2000		068° 00' N	052° 24' E	72	45	1.1
F6-2	23.6 - 29.6.2001		064° 19' N	059° 05' E	225	ND	15
F7-3	30.6 - 7.7.2001		067° 07' N	056° 41' E	75	ND	0.7
F7-4	30.6 - 7.7.2001		067° 07' N	056° 43' E	78	ND	1
F7-5	30.6 - 7.7.2001		067° 08' N	056° 41' E	82	ND	2.5
F8-2	7.7 -12.7.2001		067° 52' N	059° 43' E	23	ND	3.5
F8-4	7.7 -12.7.2001		067° 53' N	059° 40' E	15	ND	6
TDRA	27.03.1998	Vankavad	065° 59' N	060° 01' E	59	36	6.6
TDRC	29.03.1998	Swan	066° 06' N	060° 15' E	50	135	1.7
TDRD	30.03.1998	Malinkaya tumbolovat	067° 07' N	059° 34' E	110	42	5.2
TDRE	31.03.1998	Mezhgornoe	065° 15' N	059° 40' E	514	6	17
TDRU11a	21.05.1999	Podvaty	067° 27' N	063° 05' E	60	43	1.7
TDRU42a	21.05.1999		065° 58' N	057° 16' E	116	44	8.7
MITRO	06.06.2001	Mitrofanovskoe	067° 51' N	058° 59' E	132	31	20
VANUK-TY	01.04.2001	Vanuk-ty	068° 00' N	062° 45' E	124	830	25

2.2.1.2. Vorkuta lakes

Five surface sediments and four lake sediment cores were collected, in April 2007, from a latitudinal transect across the tundra-taiga ecotone near Vorkuta as part of the CARBO-North Project; '*Quantifying the carbon budget in Northern Russia: past, present and future*'. The project, funded under the 6th framework programme of the EU, started in November 2006 and examines spatial and temporal variation in the carbon budget in Northern Russia. Lake Nerusaveito (NERU), Lake Kharinei (KHAR), VORK3 and VORK5 are tundra lakes and Sandivei Lake (SAND) is a forest lake (Figure 2.3). The location of VORK5 was selected as it lies close to Lake Mitrofanovskoe which has shown major compositional changes in diatom and chironomid assemblages in the 20th

century (Solovieva *et al.* 2005). The location and physical characteristics of the lakes are given in Table 2.2.

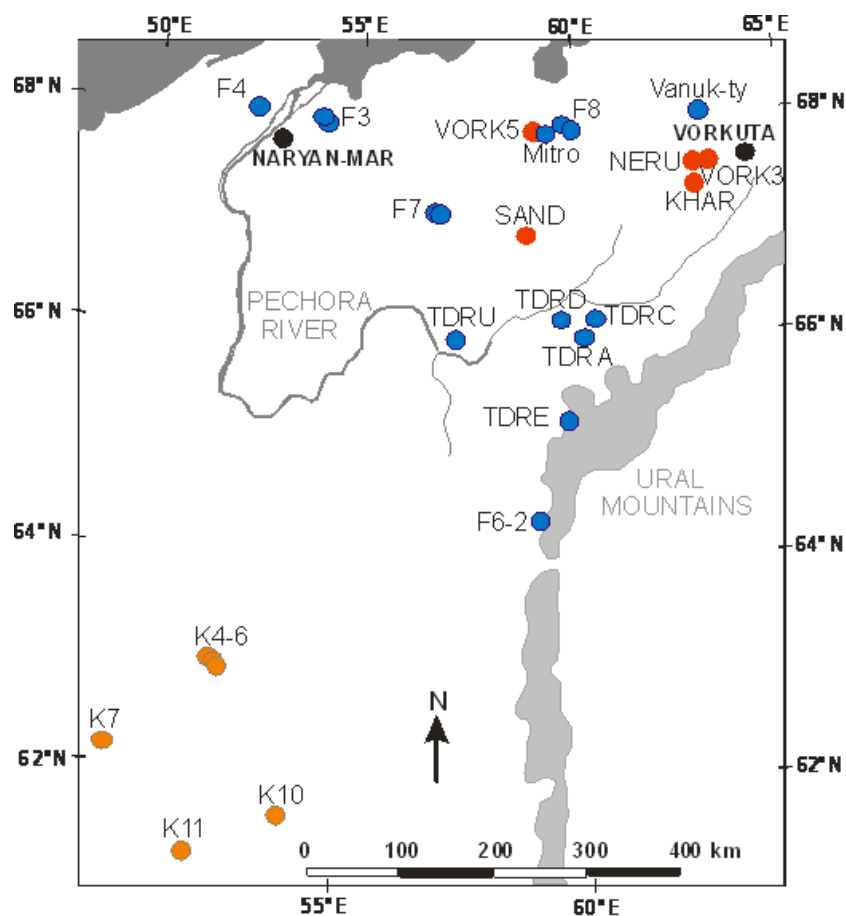


Figure 2.3. Location of the training set lakes within the Pechora basin and Komi Republic. Blue circles represent lakes from which archived material was used, red circles lakes, in the Pechora basin, sampled in April 2007 and orange circles lakes in the Komi Republic sampled in August 2007. The circles labelled F 3, F 4, F 7 and F 8 represent more than one lake in close proximity. (Map based on GoogleEarth™ image, accessed 05.11.2008)

Table 2.2. Location and physical characteristics of the sites near Inta and Vorkuta sampled in April 2007.

Site	Sampling date	Name	Latitude	Longitude	Altitude (m ASL)	Area of lake (ha)	Area of catchment (ha)
NERU	20.04.2007	Nerusaveito	067° 31' 31.8" N	062° 45' 27.4" E	121	95	1500
KHAR	21.04.2007	Kharinei	067° 21' 46.1" N	062° 45' 02.6" E	108	50	510
VORK 3	22.04.2007		067° 30' 54.7" N	062° 59' 35.0" E	122	20	120
SAND	24.04.2007	Sandivei	066° 55' 18.6" N	058° 46' 45.3" E	86	52	600
VORK5	26.04.2007		067° 51' 25.1" N	059° 01' 32.6" E	123	42	110

2.2.1.3. Lakes from the Komi Republic

Eleven surface sediments were collected by Heikki Seppä and Sebastien Seboni, of the University of Helsinki, in August 2007 from forested lakes in the southern region of the Komi Republic. Preliminary analysis showed the concentrations of chironomid head capsules were extremely low in five sediments and these lakes were not included in the training set. The location and physical characteristics of the 6 lakes included in the study are given in Table 2.3.

Table 2.3. Location and physical characteristics of the sampling sites in the southern Komi Republic. (ND = not determined; see note on Table 2.1).

Site	Sampling date	Latitude	Longitude	Altitude (m ASL)	Area of lake (ha)	Area of catchment (ha)
K4	14.08.2007	062 59' 31.8" N	052 26' 19.6" E	125	14	160
K5	15.08.2007	062 58' 43" N	052 23' 19.8" E	130	29	180
K6	15.08.2007	062 55' 33.4" N	052 29' 50.8" E	145	88	80
K7	16.08.2007	062 09' 19.1" N	050 30' 10.6" E	65	18	150
K10	18.08.2007	061 37' 21.2" N	053 55' 22" E	102	196	9500
K11	18.08.2007	061 12' 50.3" N	052 12' 50.3" E	95	ND	ND

2.2.2. Igarka and Putorana Plateau

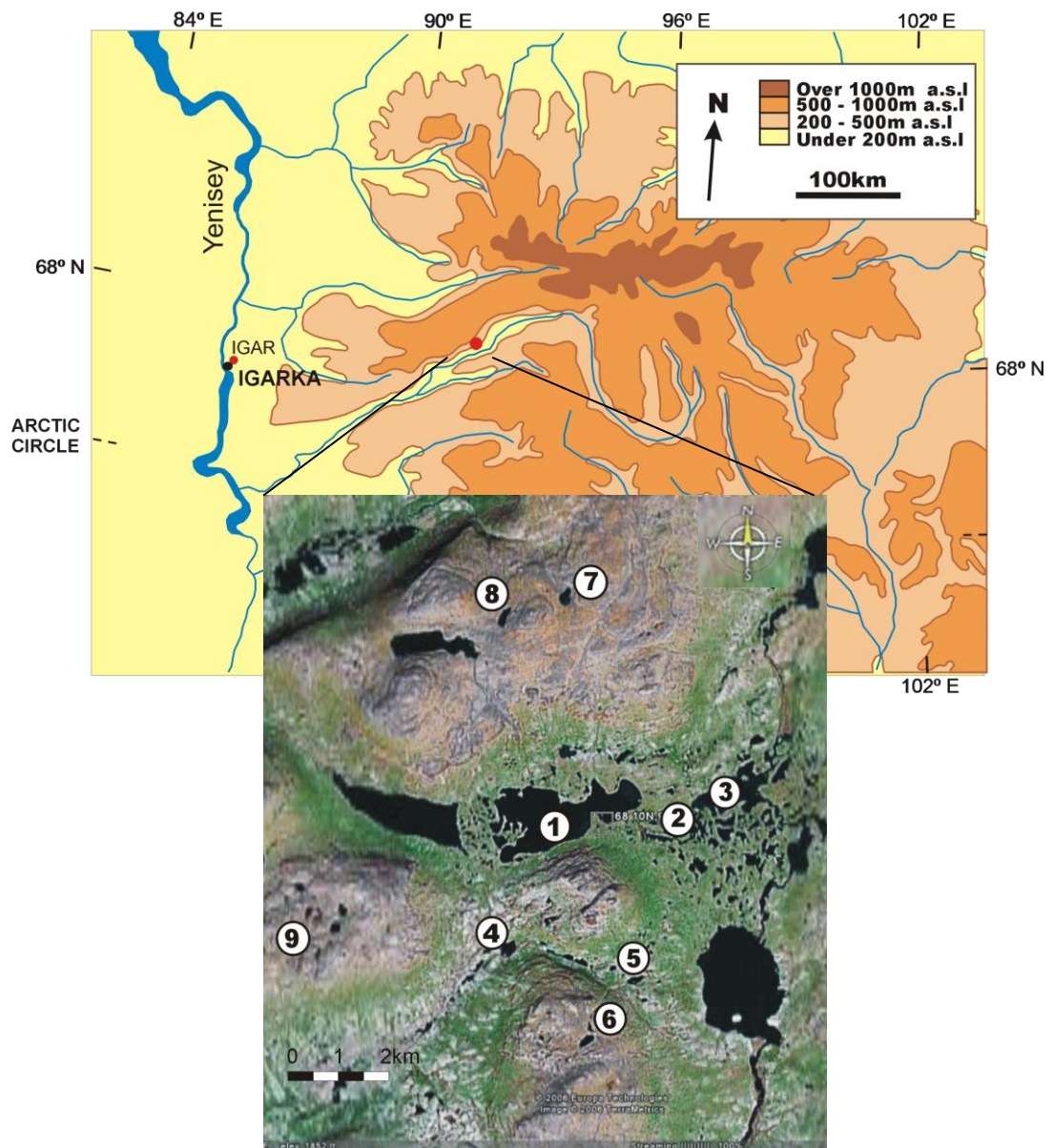


Figure 2.4. Map showing the locations of the lakes at Igarka and on the Putorana Plateau. Identity of numbered lakes 1 – GYXO, 2 – AFOX, 3 – WILD, 4 – ARTE, 5 – PONE, 6 – PTWO, 7 – PTHE, 8 – PFOR and 9 – PFIV. (Topographic map based on map G.S.G.S. 4625 produced by the Geographical section, the War Office, 1948, 'U.S.S.R. and adjacent areas' and inset map of Putorana study area on GoogleEarth™ image, accessed 20.08.2006).

Nine lakes on the Putorana Plateau and one lake at Igarka, near the Yenisey River, were sampled in July 2006. The locations of the lakes are shown in

Figure 2.4; the Putorana lakes were selected to represent the different habitat types on the plateau distinguished by the physical and vegetation characteristics of their catchments. GYXO, AFOX and WILD were located at lower altitudes within the valley floor - wetlands complex. PTWO, PTHE and PFOR were perched in cwms or hollows on the mountain plateau at higher altitudes and ARTE, PONE and PFIV at mid-altitudes close to the tree line. The location and physical characteristics of the lakes are given in Table 2.4. The sampling site at Igarka (67.47°N, 86.50°E) lies 6 km north of the Yenisey river and 4.5 km north of a former large-scale timber processing factory.

Table 2.4. Location and physical characteristics of the sampling sites at Igarka and on the Putorana Plateau.

Site	Sampling date	Latitude	Longitude	Altitude (m ASL)	Area of lake (ha)	Area of catchment (ha)	Max lake depth (m)
GYXO	01.07.2006	068° 10' 14" N	092° 12' 12" E	569	230	2000	10.5
AFOX	03.07.2006	068° 09' 59" N	092° 13' 41" E	573	1.5	4	4.9
WILD	03.07.2006	068° 10' 12" N	092° 14' 26" E	557	67	72	3.8
ARTE	04.07.2006	068° 09' 03" N	092° 10' 28" E	631	2.3	15	3.5
PONE	05.07.2006	068° 08' 33" N	092° 12' 11" E	596	0.9	16	5
PTWO	05.07.2006	068° 07' 59" N	092° 11' 41" E	740	0.8	5	3.7
PTHE	07.07.2006	068° 12' 12" N	092° 10' 44" E	805	6.3	71	3.9
PFOR	07.07.2006	068° 12' 08" N	092° 09' 26" E	780	4.8	140	4.9
PFIV	09.07.2006	068° 09' 37" N	092° 02' 46" E	668	0.8	6	6.2
IGAR	12.07.2006	067° 30' 32" N	086° 33' 27" E	36	0.4	0.6	12.5

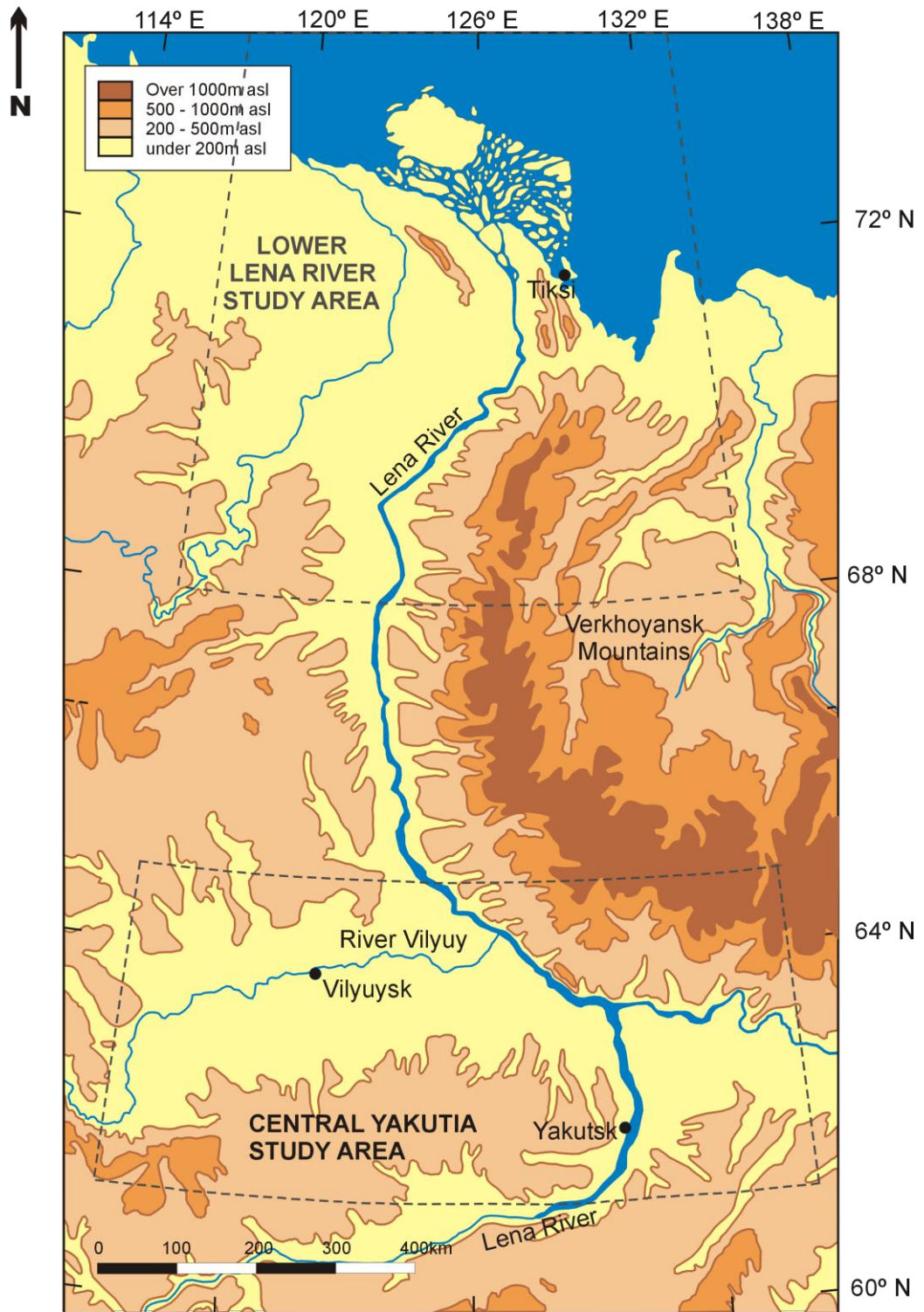


Figure 2.5. Topographic map of the Lena River basin indicating the two study areas. (based on map G.S.G.S. 4625 produced by the Geographical section, the War Office, 1948, U.S.S.R. and adjacent areas)

2.2.3. Lower Lena River and Lena delta lakes

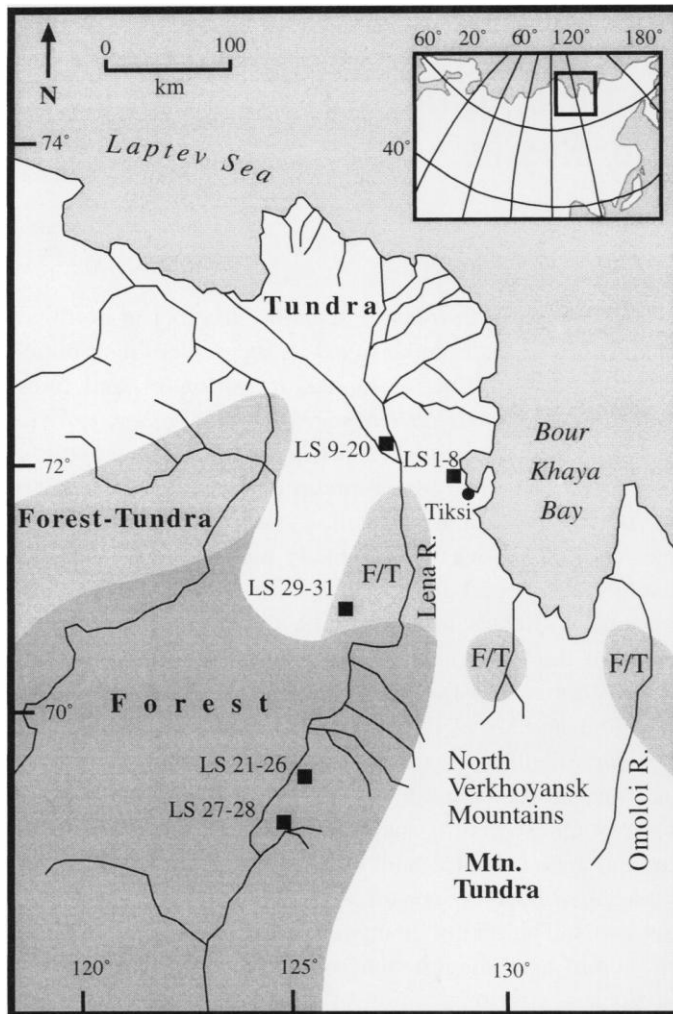


Figure 2.6. Location of the training set lakes along the Lower Lena River and Lena delta (map: Porinchu and Cwynar 2000).

The Lena River is the second largest river in northern Eurasia, after the Yenisey, in terms of its discharge, and drains northwards into the Laptev Sea (Koronkevich 2002). There were two distinct study areas within its catchment; the lower Lena river and central Yakutia (Figure 2.5). The lower Lena River – Lena delta study area comprises the more northerly locations.

Thirty-one lakes along the lower Lena River and the river delta were sampled in July and August 1994 (Figure 2.6). Details of the collection and sampling procedures are described in Duff *et al.* (1998). Preliminary analysis (Porinchu, pers. com. 2007) indicated chironomid abundances were extremely low in a number of lakes and sufficient head capsules (greater than 50) could only be isolated from twenty-one lakes for inclusion in the training set. The location and physical characteristics of these lakes are given in Table 2.5. There was no evidence of permanent human activity, from mining, farming or housing, within the catchment of the lower Lena River lakes (Duff *et al.* 1998).

Table 2.5. Location and physical characteristics of the sampled lakes within the lower Lena River and delta study area. (ND = not determined; see note on Table 2.1)

Site	Sampling date	Latitude	Longitude	Altitude (m ASL)	Area of lake (ha)	Lake depth (m)
LS-1	23.07.1994	071° 30' 38" N	128° 52' 25" E	42	2	2.0
LS-2	23.07.1994	071° 30' 38" N	128° 52' 17" E	42	ND	1.2
LS-3	23.07.1994	071° 30' 00" N	128° 52' 22" E	67	0.1	1.0
LS-4	23.07.1994	071° 30' 57" N	128° 51' 44" E	20	665	2.6
LS-5	24.07.1994	071° 30' 06" N	128° 53' 57" E	88	4	2.2
LS-6	24.07.1994	071° 29' 55" N	128° 53' 43" E	76	6	2.2
LS-7	24.07.1994	071° 29' 55" N	128° 52' 46" E	69	8	2.2
LS-8	24.07.1994	071° 30' 00" N	128° 51' 25" E	68	9	2.2
LS-10	28.07.1994	071° 52' 39" N	127° 03' 44" E	9	41	3.0
LS-11	28.07.1994	071° 53' 27" N	128° 02' 40" E	3	11	3.0
LS-12	28.07.1994	071° 54' 05" N	128° 02' 09" E	2	6	1.7
LS-13	28.07.1994	071° 54' 05" N	127° 01' 11" E	3	94	3.4
LS-15	28.07.1994	071° 52' 03" N	127° 02' 21" E	22	11	2.0
LS-16	29.07.1994	071° 52' 01" N	127° 02' 20" E	22	11	2.2
LS-17	29.07.1994	071° 52' 10" N	127° 03' 26" E	17	4	1.0
LS-19	29.07.1994	071° 52' 26" N	127° 05' 07" E	8	5	2.2
LS-24	03.08.1994	069° 23' 49" N	125° 07' 15" E	57	43	1.9
LS-25	03.08.1994	069° 24' 02" N	125° 07' 47" E	56	128	8.0
LS-27	05.08.1994	069° 02' 37" N	124° 12' 30" E	101	ND	3.1
LS-28	05.08.1994	069° 02' 34" N	125° 13' 10" E	104	ND	4.5
LS-30	06.08.1994	070° 40' 43" N	125° 52' 03" E	175	6	2.0

2.2.4. Central Yakutia, Lena River

The more southerly study area of the Lena River basin encompasses the Central Yakutian lowlands (Figure 2.5). During July 2003, 30 lakes (PG1700 to PG1729) were sampled near the town of Vilyuysk and the river Vilyui. An additional 17 lakes (PG1730 to PG1746) were sampled during July 2004 from lakes to the west and northeast of the city of Yakutsk on the Lena River (Figure 2.7).

Surface sediment and water samples were collected from the deepest part of each lake (Kumke *et al.* 2007). After preliminary analysis, by Larisa Nazarova of the Alfred Wegener Institute, the numbers of head capsules isolated were sufficient (greater than 50) in 36 lakes for inclusion in the training set. The location and physical characteristics of these lakes are given in Table 2.6.

Figure 2.7. Location of the training set lakes in Central Yakutia (based on GoogleEarth™ image, accessed 04.09.2008)

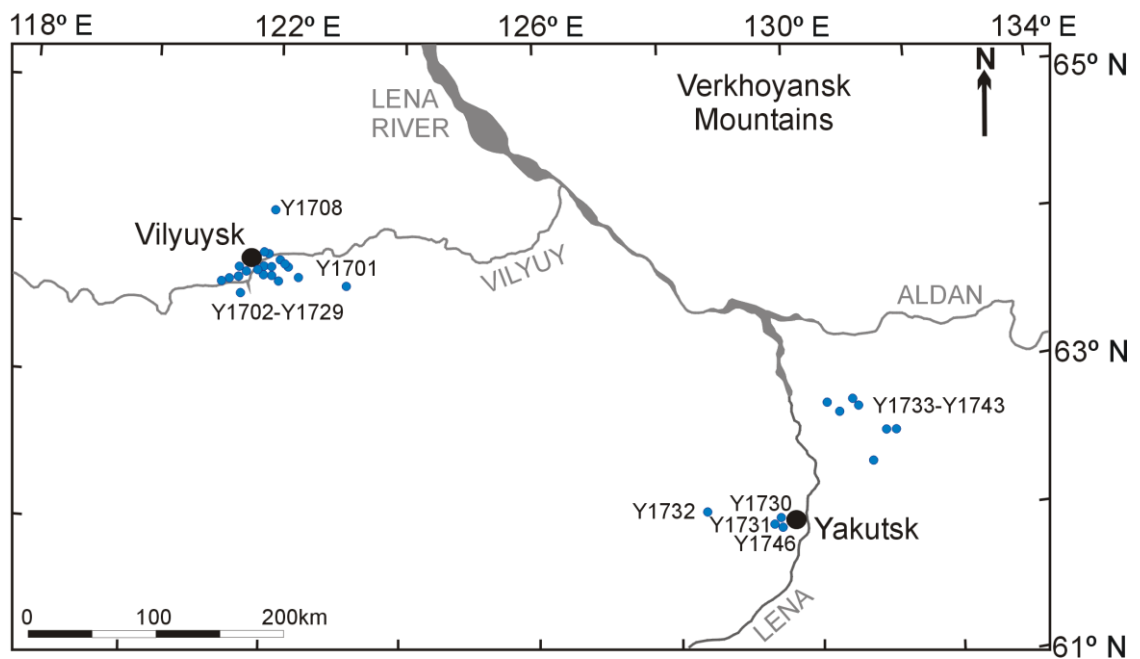


Table 2.6. Location and physical characteristics of the sampled lakes within the upper Lena River – Central Yakutia lowlands study area

Site	Sampling date	Name	Latitude	Longitude	Altitude (m ASL)	Area of lake (ha)	Lake depth (m)
Y1700	22.07.2003	Orukhtaakh	63° 44' 10" N	121° 38' 01" E	110	127	2.0
Y1701	24.07.2003	Meekingde	63° 40' 23" N	123° 07' 34" E	119	160	1.0
Y1703	26.07.2003	Uolba-Beti	64° 29' 59" N	122° 43' 03" E	179	9	0.8
Y1704	26.07.2003	Kybytyky	64° 30' 37" N	122° 43' 01" E	174	1	1.6
Y1705	27.07.2003	Beti	64° 29' 36" N	122° 43' 15" E	177	91	0.9
Y1706	27.07.2003	Satagay	64° 28' 28" N	122° 43' 502 E	178	0.2	1.1
Y1707	27.07.2003	Kjulelyakh	64° 27' 23" N	122° 23' 52" E	180	32	1.6
Y1708	28.07.2003	Njurgyn	64° 09' 45" N	121° 59' 24" E	165	9	1.8
Y1709	30.07.2003	Khodusalaakh	63° 43' 31" N	121° 57' 32" E	115	1	1.8
Y1711	31.07.2003	Mundyua	63° 41' 18" N	122° 04' 17" E	131	38	2.0
Y1712	31.07.2003	Khorulaakh	63° 42' 37" N	122° 01' 11" E	125	104	1.2
Y1713	01.08.2003	Chondulu	63° 42' 25" N	121° 53' 49" E	116	93	1.9
Y1716	03.08.2003	Buukaan	63° 43' 08" N	122° 22' 38" E	130	17	1.1
Y1717	03.08.2003	Khatyr	63° 47' 13" N	122° 11' 51" E	99	23	2.7
Y1718	04.08.2003	Ketekh	63° 44' 53" N	121° 40' 31" E	105	43	0.9
Y1719	04.08.2003	Negros	63° 45' 42" N	121° 44' 56" E	103	9	3.0
Y1720	04.08.2003	Muorkhan	63° 45' 32" N	121° 45' 03" E	104	32	3.8
Y1721	05.08.2003	Mejik	63° 48' 05" N	122° 11' 21" E	112	37	2.6
Y1722	05.08.2003	Kytalyk	63° 48' 17" N	122° 09' 56" E	105	10	1.2
Y1723	05.08.2003	Kustaakh	63° 43' 35" N	121° 32' 05" E	96	28	4.0
Y1724	06.08.2003	Bergemde	63° 39' 49" N	121° 15' 50" E	112	88	2.0
Y1725	06.08.2003	Kjubeeji	63° 40' 13" N	121° 18' 30" E	118	63	1.9
Y1726	06.08.2003	Chemekh	63° 40' 29" N	121° 18' 01" E	117	66	2.0
Y1727	07.08.2003	Sydybyl	63° 35' 23" N	121° 29' 55" E	127	35	1.4
Y1729	07.08.2003	Siebit	63° 37' 30" N	121° 29' 46" E	125	6	1.7
Y1730	02.07.2004	Malaya Khabyda	61° 57' 37" N	129° 24' 31" E	188	22	1.4
Y1731	03.07.2004	Bolshaya Khabyda	61° 58' 06" N	129° 22' 47" E	204	121	0.7
Y1732	06.07.2004	Akhigui Kariyalak	62° 07' 29" N	128° 24' 12" E	208	29	1.5
Y1733	09.07.2004	Beydine	62° 23' 20" N	130° 51' 57" E	130	414	2.3
Y1735	10.07.2004	Turgaayu	62° 35' 07" N	131° 06' 36" E	139	41	3.7
Y1737	11.07.2004	Uhun Kuel	62° 35' 05" N	131° 13' 38" E	144	86	1.5
Y1739	12.07.2004		62° 47' 07" N	130° 43' 47" E	123	24	1.8
Y1740	13.07.2004	Taastaakh	62° 48' 21" N	130° 38' 56" E	122	6	17.1
Y1741	14.07.2004	Orgennekh	62° 48' 54" N	130° 15' 41" E	111	187	4.1
Y1743	15.07.2004	Tuumpu	62° 44' 13" N	130° 26' 34" E	135	2	3.7
Y1746	18.07.2004	Temiyе	62° 03' 02" N	129° 29' 02" E	208	52	0.9

2.3. Physical and geological characteristics of the study areas

The sampled lakes from the catchment of the Pechora River, near Yakutsk in central Yakutia, the northern Lena Delta and at Igarka formed on Quaternary sediments (Figure 2.8). In the Pechora River basin (location 2, Figure 2.8), the Quaternary cover of lacustrine, fluvio-glacial and fluvial deposits varies in

thickness from a few metres to approximately 200-300m depending on the underlying topography (Nalvikin 1973). The Pechora lakes, with the exception of F6 and TDRE, are located on the Bol'shezemel'skaya Tundra between the Pechora River and the Urals (Figure 2.2). This extensive undulating lowland plain, incised by deep river valleys, varies in altitude between 80 and 150 m a.s.l. The remaining lakes, F6 and TDRE, are located in the foothills of the Ural Mountains.

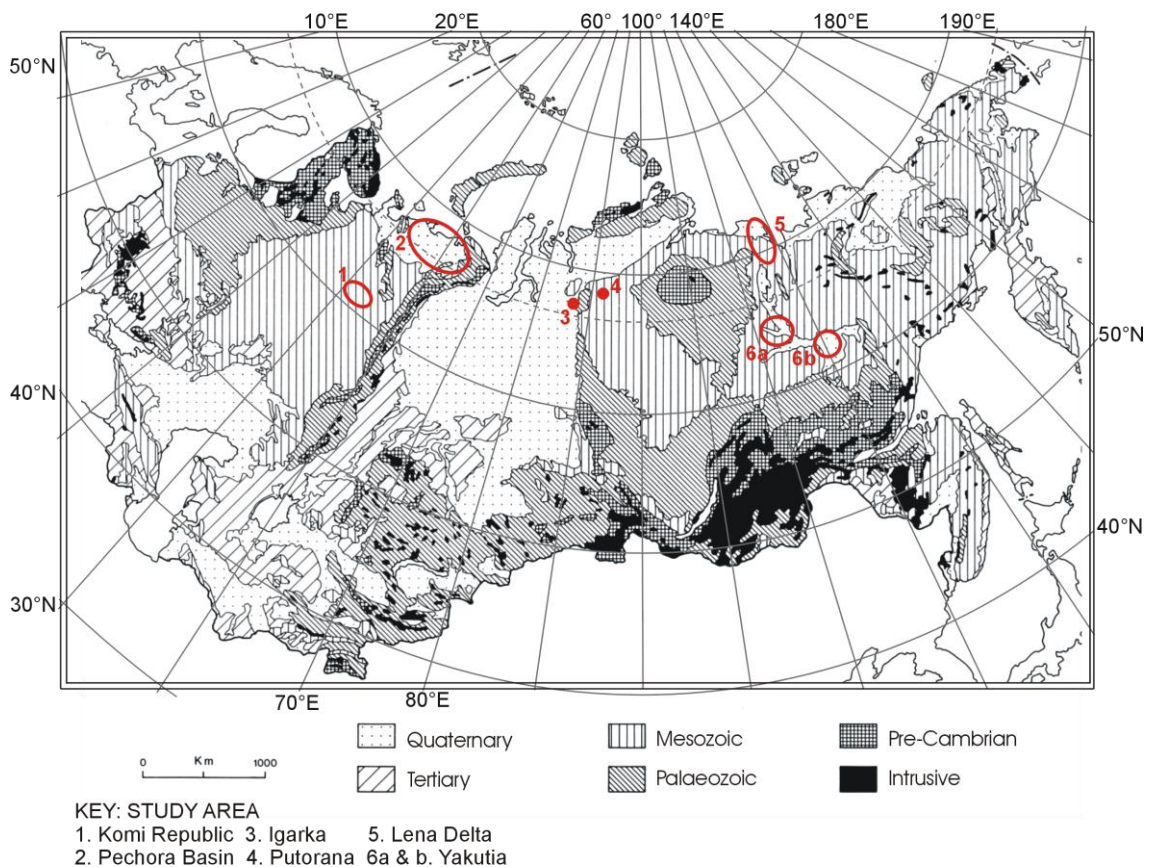


Figure 2.8. Geology of Russia, categorised by geological age of the rock and intrusive material, showing the location of the study areas (adapted from Dewdney 1982).

Quaternary deposits are widely distributed throughout low-lying areas and the Ob, Lena and Yenisey river valleys. Glacial sediments are more prevalent in the north-west giving way to periglacial and lacustrine-alluvial sediments further south (Koronovsky 2002). These deposits are particularly extensive in central Yakutia, near Yakutsk, and the Lena River valley (locations 6a and b, Figure 2.8). Interglacial marine deposits occur intermittently throughout the southern Taymyr lowlands and along the Yenisey valley as far as Turukhansk. The town

and lake at Igarka (location 3, Figure 2.8) lies on outcrops of Precambrian and Ordovician sedimentary rocks surrounded by Quaternary glacial and fluvio-glacial deposits (Nalvikin 1973).

The Lena River Delta is the largest in the Arctic and occupies an area of 32 000 km² (Mikhailov 1997). Formation of the modern delta began in the mid-Holocene inside an archipelago of islands created by vertical tectonic block movements. The islands are composed of Devonian rocks and remnants of a pre-Holocene plain composed of perennially frozen fine-grained Quaternary sediments with large ice-wedges and a high ice content (Are and Reimnitz 2000). Lakes LS 1-19 (section 2.2.3) are located within the delta; LS 1-8 near Tiksi lie on the Kharaulakh Ridge which forms the southeast boundary of the delta and LS 10-19 on islands between major drainage channels (Pisaric *et al.* 2001a).

The lakes in the Komi Republic (location 1, Figure 2.8) formed on a sedimentary sequence of Palaeozoic carbonates and deep marine shales (Lindquist 1999). The remaining lakes from the Putorana Plateau, the southern Lena Delta (location 5, Figure 2.8) and near Vilyuysk, in central Yakutia, (location 6a, Figure 2.8) lie on an extensive plateau known as the Siberian Traps. This is a large igneous province extruded in the late Permian ca. 240 – 220 Myrs (Zolotukhin and Almukhamedov 1988). The Putorana Plateau, in the north-west, is the highest part of the plateau with heights of 1500 – 2000m (Nalvikin 1973). The flat summits and mountain terraces of the plateau are remnants of the ancient volcanic peneplain, which is dissected by faults leading to the formation of the major valleys (Shahgedanova *et al.* 2002). The Putorana lakes (GYXO – PFIV) were selected to reflect the differing altitudes and physical environments on the Plateau. The volcanic rocks consist of thick horizontal basaltic lava flows interbedded with tuffs and traps (enclosed sedimentary rocks) and quartz-rich pegmatite veins. The trap and basalt have a pronounced tendency to disintegrate by frost weathering. This susceptibility, together with low temperatures and cryogenic processes such as solifluction, has resulted in the formation of extensive areas of block fields and talus slopes (Webber and Klein 1977) (figure 2.9). Soil cover is thin and rocky with a thin layer of organic

material near the surface. Repeated cryogenic mixing of the soil has prevented the development of a differentiated soil profile.



Figure 2.9. Photograph showing extensive talus slopes on the Putorana Plateau. (Photograph taken by N. Solovieva, 2006)

2.4. Permafrost

The study sites cross the major ecotonal boundary from continuous – discontinuous permafrost zones (Figure 2.10). Discontinuous permafrost occurs in the mires of the central Pechora basin. Sites further north in the tundra, at Igarka-Putorana and along the Lena River lie in the >90% continuous permafrost zone (Kotlyakov and Khromova 2001). The permafrost is composed of two distinct permafrost layers; the upper layer formed during the late Holocene and is between 50-100m thick. In the Museum of the Permafrost, Igarka, tree macrofossils deposited in fluvial sediments at 9m depth have been dated to 46 kyrs. The upper permafrost layer is underlain by an unfrozen layer of melt water from the early Holocene. The lower permafrost layer originates from the early Weichselian glaciation, 90-80 000 yrs BP, (Rozenbaum and Shpolyanskaya 1998). Many of the lakes in northern Russia are thermokarst lakes, formed by melting permafrost which causes the ground to subside and

releases meltwater. Formation of thermokarst lakes occurs predominately during periods of warming temperatures, the initiation of many lakes in northern Russia is linked to climate warming and gradual melting of the permafrost from ca. 13000 yrs BP (Sidorchuk *et al.* 2001). Lake number and lake area has also increased over the past 30 years in the continuous permafrost zone of Siberia in response to recent warming (Smith *et al.* 2005).

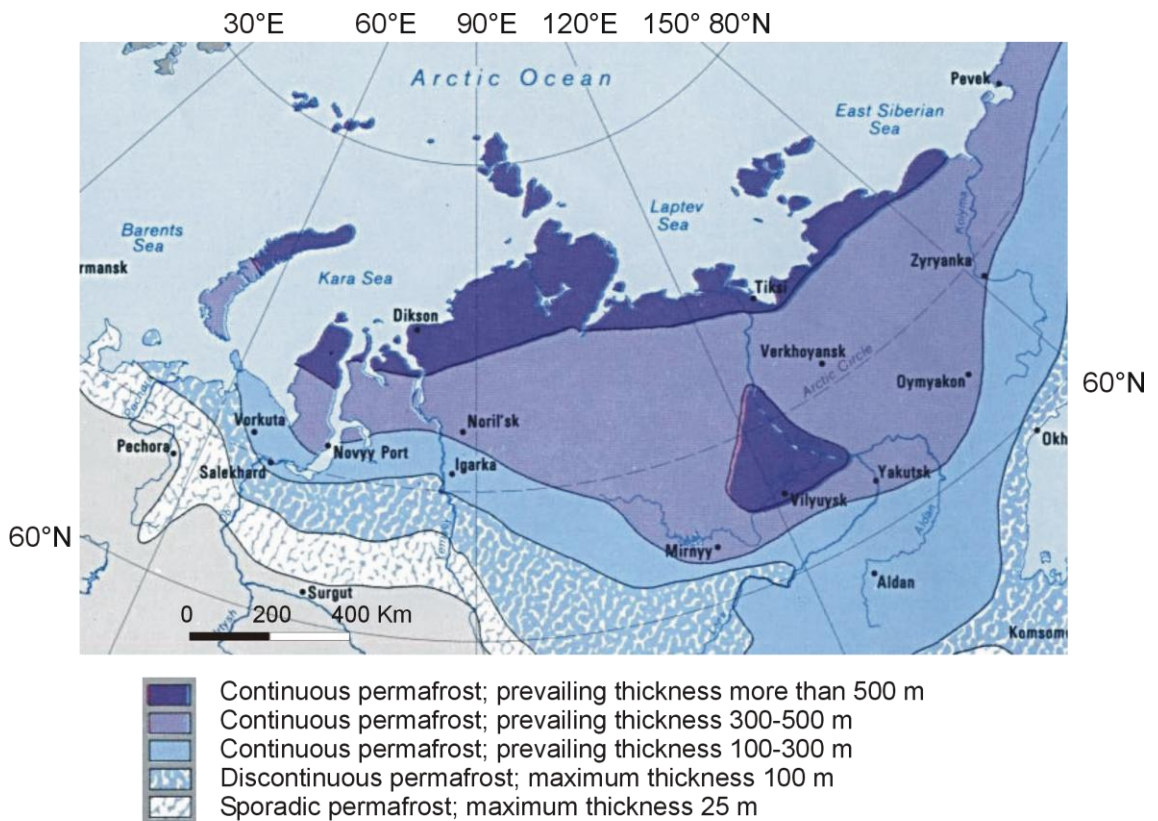


Figure 2.10. Permafrost regions of northern Russia (adapted from US Government - C.I.A 1984).

Many of the present landforms result from the cryogenic environment. Seasonal melting of frozen ground and ice destabilises sediments leading to solifluction, sediment collapse and mud flows. Alternate freezing and thawing of the ground results in frost heaving bring stones to the surface and creating structures such as patterned ground. These periglacial features are particularly well developed in the Lena delta (Figure 2.11).



Figure 2.11. Polygonal patterned ground at lake LS-7 in the Lena delta (GoogleEarth™ image, accessed 14.09.2008).

2.5. Weather and climate characteristics of the study areas

Alisov (1956) classified the climate of Northern Eurasia based on the radiation regime and atmospheric circulation, drawing climatic boundaries to reflect the distribution of soil and vegetation type (Shahgedanova 2002). On the basis of this model (Figure 2.12.) the Lena delta lakes lie within the Arctic, the lakes on the Putorana, at Igarka and in the north of the Pechora basin in the subarctic and the lakes in southern Pechora and Central Yakutia in the temperate zone.

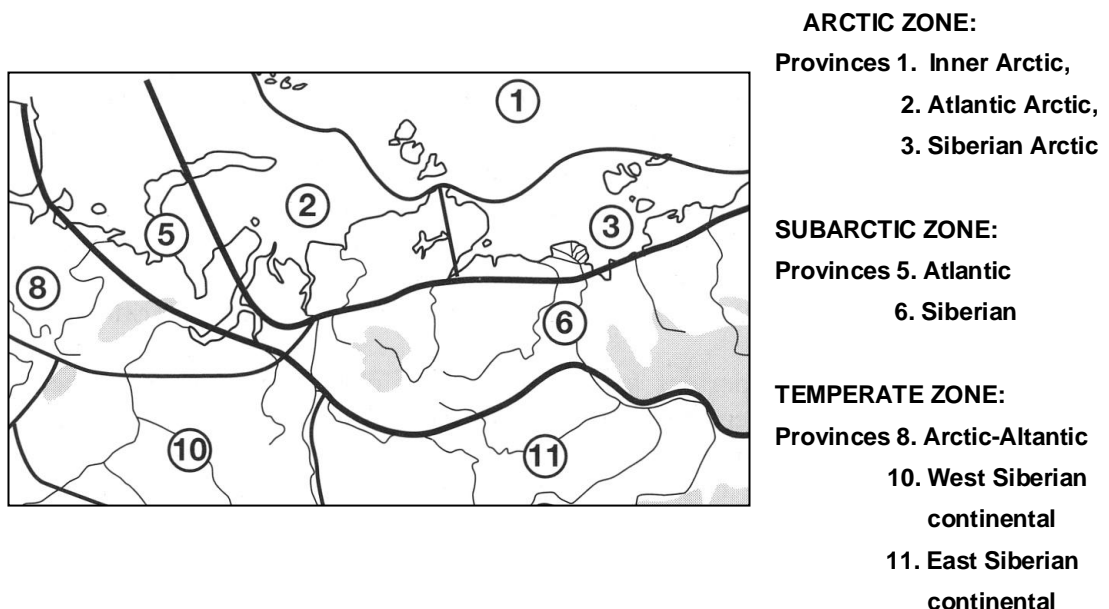


Figure 2.12. Climate zones and provinces of the north European Russia and Central Siberia (Shahgedanova 2002).

The climatic zones are subdivided into climatic provinces based on the prevalence of air masses. The northern Pechora lakes lies within the Atlantic subarctic as defined by Alisov (1956) whereas the Putorana lakes are in the Siberian subarctic. The climate of the Atlantic subarctic is ameliorated by cyclonic activity and warm oceanic currents from the Atlantic, although their influence is greatly reduced in areas east of Novaya Zemlya. The Atlantic provinces are also characterised by reduced climate continentality compared to any given latitude further east. Mean monthly temperatures at Yakutsk (62.02°N, 129.72°E) show a range of approximately 60°C between the coldest and warmest months compared with 44°C in Turuhansk (65.78°N, 87.93°E) and 32°C in Narjan-Mar (67.63°N, 53.02°E) (Figure 2.13). The climate of Central Siberia is characterised by extreme continental climates and aridity. Winter temperatures are dominated by the Siberian high; air temperatures decline rapidly in towards the centre of the high, near Oimekon (63°28'N, 142°49'E). The lowest temperatures in the Northern Hemisphere were recorded at Verkhoyansk (67°34'N, 133°51'E) (Przybylak 2003). The boundary of the Atlantic and continental provinces occurs on the Putorana Plateau at approximately 94°E (Shahgedanova *et al.* 2002) the Putorana lakes are therefore affected by both climate regimes depending on their relative strengths.

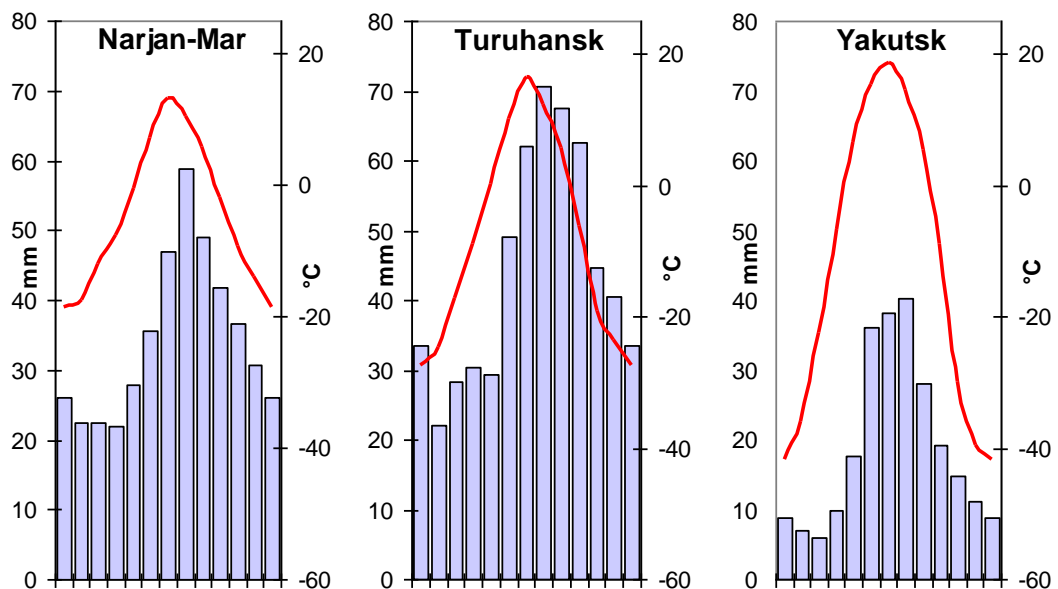


Figure 2.13. Mean monthly air temperatures and precipitation for Narjan-Mar (Pechora basin; 67.63°N, 53.02°E), Turuhansk (65.78°N, 87.93°E) on the Yenisey River and Yakutsk (62.02°N, 129.72°E). Monthly mean 2m air temperature and mean monthly precipitation calculated using CHCN v2 (adjusted) database for the period 1960-89.

The dominance of the continental Siberian high pressure system results in low winter precipitation in Central Siberia. In the summer, winds from the north or east are more prevalent resulting in higher rainfall (Figure 2.13). However precipitation throughout the year is significantly less in the Siberian area than the Atlantic climate provinces where intense cyclonic activity results in heavy precipitation (Figure 2.13). In Central Yakutsk annual evaporation of approximately 350 – 400 mm exceeds annual precipitation (243 mm and 203 mm in Vilyuysk and Yakutsk, respectively) leading to a moisture deficit and the development of saline conditions in some of the lakes (Kumke *et al.* 2007). With little winter precipitation the depth of snow, and its insulating capacity, is reduced favouring the growth of cold-resistant plants (section 2.6).

2.5. Biological characteristics

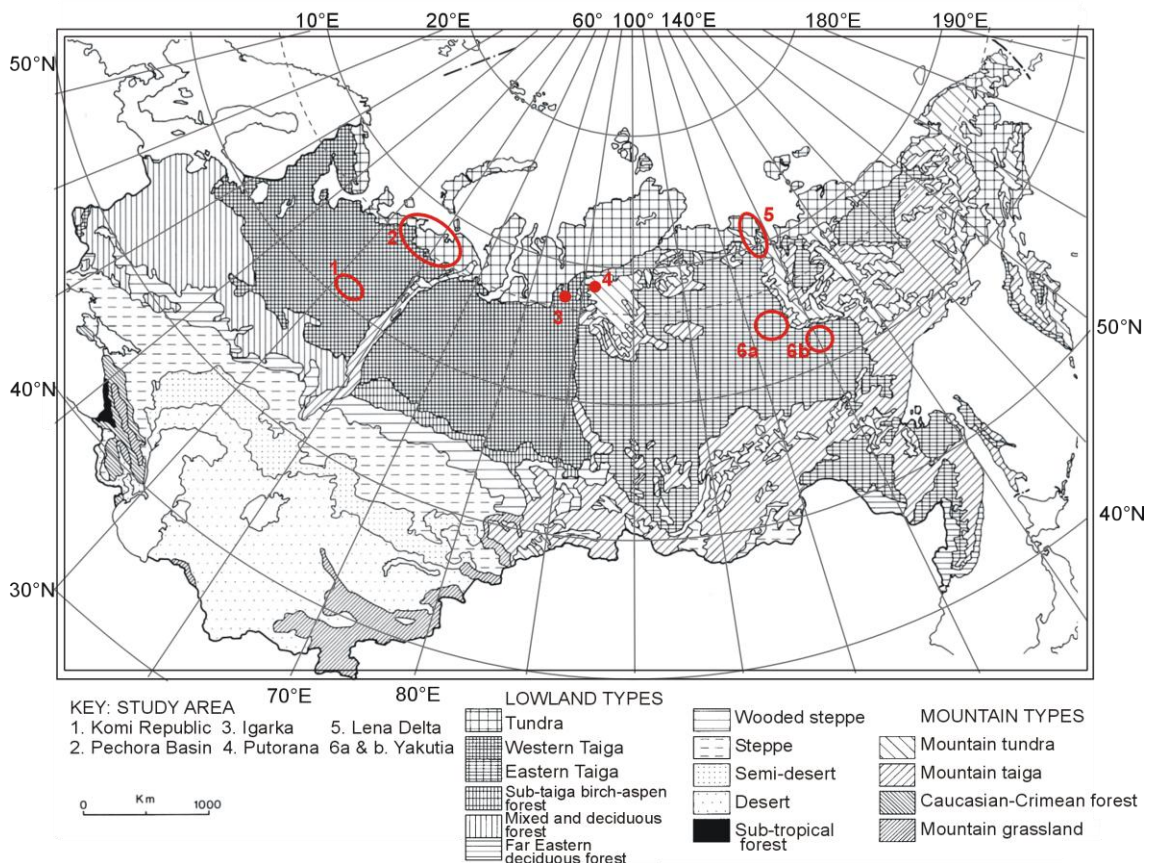


Figure 2.14. Vegetation zones of Russia, showing the location of the study areas (adapted from Dewdney 1982).

The sampling sites cross major ecotones such as the altitudinal and latitudinal tree lines. The development of biomes is dependent on climatic factors, principally thermal thresholds and annual precipitation, and the latitudinal tree line approximates to the mean July temperature isotherm of 10°C (Zlotin 2002). The forested taiga is subdivided into western and eastern subzones based on species composition, physical and environmental characteristics (Figure 2.14). The western taiga is dominated by spruce, *Picea*, species and the eastern taiga by the larch, *Larix* spp., which is able to tolerate the extremely low temperatures, aridity and poor soils of Central Siberia (Shahgedanova *et al.* 2002).

In the Komi Republic (location 1, Figure 2.14) *Picea obovata* forms a dense forest with a relatively poor understorey. Further northern in the southern Pechora basin (location 2, Figure 2.14) the short cold summers result in sparse and stunted tree growth. The more open forest allows the development of understorey of *Betula* and mosses such as *Hylocomium splendens*, *Pleurozium schreberi* and *Polystichum commune* (Tishkov 2002). The transition from taiga to tundra vegetation is usually gradual reflecting microclimates in the environment. In the Pechora study area the tundra is dominated by *Betula nana*, up to 1 m tall, with thickets of mixed *Salix* species, thick moss swards and dwarf shrubs (Aleksandrova 1980).

The Putorana Plateau (location 4, Figure 2.14) marks the longitudinal boundary of many plant species; 15% of the plant species, including *Larix gmelinii* have their western limit and 18%, including *L. sibirica*, their eastern limit on the Plateau (Ivanova 1976; Major 1980). The Odonata fauna at Igarka, approximately 100km to the west of the Plateau, included *Coenagrion glaciale* and *Leucorrhinia orientalis* with east Eurasia distribution, and *C. hastulatum*, and *C. johanssoni* typical of boreal regions in western Eurasia (Brooks, 2006, pers. comm.). The taiga at Igarka (location 3, Figure 2.14) is dominated by *Picea obovata* and *Larix sibirica* with an understorey of *Alnus fruticosa* and *Betula nana* shrubs. Further east, for example in the southern Lena Delta (location 5, Figure 2.14), the tree species are replaced by *Larix gmelinii* (synonym *L. dahurica*) (Pisaric *et al.* 2001b) Further south in the drier areas of

Sakha-Yakutia (locations 6a and 6b, Figure 2.14) floristic diversity is poor; *Larix gmelinii* dominates with a shrub tier of *Betula exilis*, *Salix pyrolifolia* and the dwarf shrub *Vaccinium vitis-idaea*. The *Larix-Vaccinium* xerophilous forests occupy approximately 75% of all forested land in Central Siberia (Tishkov 2002).

The Putorana Plateau has a sub-arctic alpine flora comprising mountainous open *Larix* woodland, alpine tundra and polar desert. Sparse forest and forest tundra extend to 300-400 m above sea level in the north and 700-800 m in the south and alpine tundra to 1200-1400 m (Shahgedanova *et al.* 2002). In the study area the tree line occurred at approximately 500-600 m a.s.l. resulting in sparse *Larix* growth in the valleys and alpine tundra on the higher slopes. The alpine tundra is composed of dwarf shrub, moss and lichen communities. In certain areas, for example between PONE and PTWO, a narrow belt of shrubs including *A. fruticosa*, *Salix* spp. and *B. nana* separated the forested and alpine tundra zones. The remoteness of the plateau has probably contributed to the survival of a number of rare and endemic animal species such as snow-sheep (*Ovis nivicola*), alpine pikas (*Ochotona alpina*) and northern pikas (*O. hyperborea*) (Webber and Klein 1977; Formozov and Yakhontov 2003).

Treeless pasture areas, known as alases, are a characteristic feature of the forested areas around Yakutia and Vilyuysk (locations 6a and b, Figure 2.14). Alases form as a result of permafrost degradation; melting permafrost causes the soil to collapse which kills the trees. The centre of the alas is usually filled with water bordered by a band of meadow vegetation, typically less than 500m wide, and enclosed by forest (Figure 2.15). About 40-50% of the land surface in Central Yakutia is affected by alases (Tishkov 2002). They are used as pasture for cattle; previous studies have shown that the chironomid assemblages are indistinguishable from those in the forested lakes due to the proximity of the forest (Nazarova *et al.* 2008).



Figure 2.15. Alas (treeless pastures) in Central Yakutia (photograph by Makharov Alexander, GoogleEarth™ gallery, 2007)

2.6. Human settlement

Paleolithic and Mesolithic sites have been found across Arctic Siberia, extending as far north as the Taymyr Peninsula and the New Siberian Islands (76°N). At Zhokhov, in the New Siberian Islands, dating of bone and wooden artefacts suggest occupancy was established approximately 8480-8175 cal yr BP with subsistence based on the hunting of polar bears and reindeer (Pitul'ko 2001). The Siberian Islands were abandoned approximately 4500 yr BP, when rising sea levels inundated the land connection to the continent (Pitul'ko 2001).

The European Russian Arctic was partially colonised by Russians from the city republic of Novgorod in the twelfth to fifteenth centuries. Novgorod was annexed by the Russian principality, based in Moscow, in 1478 and a small army dispatched to the region which built a fort at Pustozersk on the Pechora. Campaigns by the army and the steady northwards migration of colonists, many of them peasants, brought the whole of European Russia from the Kola Peninsula to the Gulf of the Ob' under the control of the Tsars by about 1600. Russia's eastward expansion continued and conquest of the entire tract from the Urals to the Sea of Okhotsk was completed by 1697 (Vaughan 1994). Their hold was consolidated by the building of fortified towns at strategic points such as Salekhard and Yakutsk. Siberia was governed by Cossacks who collected taxes, paid in furs and ivory; the availability of ivory from walrus and fossil

mammoths tusks led to increased exploration of arctic Siberia. However settlements remained widely dispersed and sparsely populated until the twentieth century.

Following the 1917 revolution, the rate of development, for both settlements in the arctic and the Northern Sea Route, increased greatly (Vaughan 1994). Foreign hostility meant the Bolsheviks needed to fully exploit domestic resources, many of which occurred in the Arctic. There was a new emphasis on northern development to strengthen the economy and raise living standards. Committees were set up to administer the Northern Sea Route and the economic development of Siberia. Navigation of the sea route was greatly facilitated by the construction of lighthouses, ports and polar stations. Many of the important ports, including Igarka and Dudinka on the Yenisey, Dikson on the Taymyr Peninsula and Tiksi on the Lena delta, were built between 1929 and 1946. Igarka, which was used as the base for the fieldwork in 2006, was founded in 1929 as a Gulag-run lumber mill and timber-exporting port. Although Igarka is 673km from the Kara Sea, the river, at this point, is navigable by ocean-going vessels. In winter, when sea ice blocks the river further north, the port at Igarka remains ice-free and goods are transported overland to northern towns and industrial complexes. Timber production at the lumber mill peaked in the late 1980s; the mill closed in 2005 due to the poor quality of the timber and the loss of government subsidies following the breakup of the Soviet Union. The factory supported a population of 18 820 (1989 Census) which has fallen to 8,627 inhabitants (2002 Census) since its closure.

Vorkuta, which was used as a base for the fieldwork in 2007, is a coal mining town in the Komi Republic which was established in 1932 as a forced labour camp. After the Nazi invasion of the Donbas coal mines in 1942, a rail link was constructed linking the camps at Inta and Vorkuta with Moscow and coal mining started. At its peak, in the 1940s to early 50s, there were 40 pitheads serviced by the Vorkuta camps with an estimated population of 235 000 guards, officials and prisoners (Anon 1955). Although many Gulag camps closed in the 1950s some in Vorkuta continued to operate until the 1980s. High operation costs and the loss of government subsidies during the 1990s led to closure of the majority

of the mines. In 2007 only 6 remained operational and Vorkuta's population had declined to 84 917 (2002 census).

Substantial gas and oil reserves occur throughout the Russian Arctic; the West Siberian Basin is the richest petroleum province in Russia and known reserves are estimated at 335.6 billion barrels of oil equivalent (BBOE) (Ulmishek 2003). The first commercial oil field, at Chib'yū, was discovered in 1930, followed by the first commercial gas field (Sed'yal) in 1935 (Lindquist 1999). By the mid-1970s pipelines had been constructed to take oil from wells on the Bol'shezemel'skaya tundra to the port of Nar'yan-Mar on the Pechora. In 1978 the Urengog gas field in north-western Siberia, possibly the world's largest field (Vaughan 1994) became the centre of a gas pipeline network which distributes gas throughout the Russian Federation and Europe. However exploration and exploitation of the petroleum reserves has led to severe environmental degradation (Leonova 2004; Stenina *et al.* 2004; Dzyuba 2006). Therefore the Gydan Peninsula and the area between the Ob and Yenisey Rivers (Figure 1.2) were excluded from the study.

From fieldwork observations, the Putorana Plateau and Lena Delta are considered pristine. Although resources in the Pechora and Komi areas are frequently used, i.e. for fishing and hunting, and these areas are crossed by ice-roads, previous analysis suggested the lakes are not impacted (Solovieva *et al.* 2002). By comparison, a number of the lakes in central Yakutia are adjacent to towns or agricultural lands which, in some instances, has resulted in eutrophic conditions within the lake (Kumke *et al.* 2007).

2.7. Summary

This chapter has described the locations for the 100 lakes of the training set and the provenance of the material analysed from each site. The training set lakes cluster into 5 geographically distinct regions; the Pechora Basin, Komi Republic, Putorana Plateau, Lower Lena River and Central Yakutia. As sections 2.3 – 2.6, describing the physical and biological characteristics of these regions, show the lakes cross major ecotones and cover wide environmental gradient such as:

- the boundaries between continuous and discontinuous permafrost,
- the latitudinal-dependent temperature gradient,
- a continentality gradient influencing temperature range, length of the ice-free season and aridity,
- the latitudinal tree-line and
- from pristine condition to severe anthropogenic impact.

In addition, the underlying geology varies from carbonates, to clay-rich glacial deposits and extrusive lava flows. Catchment geology can influence the water chemistry and buffering capacity of lakes (Moss 1998). Many of these environmental variables, such as temperature and water chemistry, are known to influence chironomid distribution (see section 1.4). Therefore the influence of these variables on chironomid distribution is examined in Chapter 4, either directly as in vegetation type or indirectly as in pH, to assess the potential of the variables as quantitative palaeoenvironmental indicators in northern Eurasia.

Descriptions of the coring sites and the criteria for the selection of sediment cores for detailed palaeolimnological study are given in Chapter 7 for lakes from the Putorana Plateau and in Chapter 8 for lakes in north-east European Russia.

Chapter 3

Methods

3.1 Introduction

This chapter describes the sampling and analytical methods used in this study. The first section details the field methods including collection of sediment cores and water samples from study sites on the Putorana Plateau and north-east European Russia. The sampling of chironomid pupal exuviae during summer fieldwork is also described. The second section focuses on laboratory analyses to determine the contemporary and fossil chironomid assemblages in sediment cores from the study areas and training-set sites. This section also describes the analysis and compilation of physico-chemical parameters for the training set lakes and the isotopic and sedimentary analysis of the sediment core samples. The final section describes the numerical analyses, in particular, the use of multivariate techniques including ordination, classification and clustering. Numerical analyses, other than multivariate analysis, are described in the relevant chapters.

3.2 Field methods

3.2.1 Water chemistry

The chemical composition of lake water is determined by the initial composition and amount of precipitation. This is subsequently modified by dissolved substances derived from the local geology, soils, vegetation and human activities (Moss 1998). The pH, conductivity and concentrations of major ions were determined to examine the influence of these environmental variables on the present-day distribution of chironomids.

The conductivity and pH of the lakes were measured in the field using a combined pH/EC/TDS/temperature meter (model HI 991300) from Hanna Instruments. At each location 250ml unfiltered water samples were collected in acid-washed polyethylene bottles for analysis of major cations and anions. Where possible the water samples were stored at 4°C prior to analysis. During the summer fieldwork samples were kept wrapped in dark plastic and immersed

in the lake water to prevent microbial degradation. On return to the laboratory they were transferred to a coldroom at 4°C for storage.

3.2.2 Collection of sediment cores from the study areas

This section describes the procedure for collecting surface and core samples from the Igarka – Putorana, July 2006, and an area near Vorkuta in April 2007. Not all the surface sediments used in the calibration set were collected or analysed, solely, by the author. Details of the samples' provenance, the researchers and organisations involved and their contributions are detailed in Chapter 2 and Table 3.5, in this Chapter. Sampling methods for the archived Pechora sites (section 2.2.1.1) are described by Solovieva *et al.* (2002; 2005) and Sarmaja-Korjonen (2003), the Lower Lena River (section 2.2.3) by Porinchi and Cywnar (2000) and Central Yakutia (section 2.2.4) by Kumke *et al.* (2007). The sampling methods from all the locations are comparable and broadly similar to the methods described below.



Figure 3.1. Extruding HON-Kajak core from lake PTHE (left – right V. Jones and N. Solovieva)

The bathymetry of the Putorana lakes was initially assessed by making transects of the lakes and measuring the water depth, at timed intervals, using a hand-held echo sounder. Sediment cores were then collected from the deepest point of each lake using an 80mm diameter HON-Kajak corer (Renberg 1991) with a 0.5m Perspex coring tube. The cores were extruded in the field (Figure

3.1); samples were stored in whirl-paks and kept cool and dark in the field. On return to the UK they were transferred to a coldroom at 4°C for storage. Sampling resolution of the cores is shown in Table 3.1. The location and altitude of the lakes was recorded using Garmin™ GPS devices based on the WGS84 datum; water depth at the sampling location was also noted.

Core	Sampling date	Approx length (cm)	Resolution
GYXO 1	01.07.2006	27.5	0-27.5cm depth = 0.25cm intervals
GYXO 2	01.07.2006	surface	0-1, 1-2 cm
GYXO 3	01.07.2006	31	0-31cm = 0.25cm intervals
AFOX	03.07.2006	28	0-24cm = 0.25cm intervals
WILD 1	03.07.2006	34	0-1, 1-2 cm + 33-34cm
ARTE 1	04.07.2006	40	0-20cm = 0.25cm intervals; 20-35.5cm = 0.5cm intervals; 35.5-40cm combined, 40-42cm = 0.5cm intervals
ARTE 2	04.07.2006	surface	0-1 cm
PONE 1	05.07.2006	28	0-20cm = 0.25cm intervals; 20-28cm = 0.5cm intervals
PONE 2	05.07.2006	surface	0-1, 1-2cm
PTWO	05.07.2006	36	0-16cm = 0.25cm intervals; 16-36cm = 1cm intervals
PTHE	07.07.2006	35	0-20cm = 0.25cm intervals; 20-34cm = 0.5cm intervals
PFOR 1	07.07.2006	34	0-5cm = 0.25cm intervals + 33-34cm at 1cm interval
PFOR 2	07.07.2006	surface	0-1cm
PFIV	09.07.2006	38	0-2cm = 0.25cm intervals; 2-26cm = 0.5cm intervals; 26-35cm = 1cm intervals
IGAR 1	12.07.2006	34	0-20cm = 0.25cm intervals; 20-34cm = 0.5cm intervals
IGAR 2	12.07.2006	44	0-1, 1-2cm

Table 3.1. Core length and sampling resolution of the samples from the Putorana Plateau and Igarka.

The lakes near Vorkuta (NERU, KHAR, VORK3, SAND and VORK5) were sampled in April 2007 whilst ice-covered. Prior to sampling, a hole, approximately 25cm in diameter, was drilled through the ice; therefore it was impossible to assess the lake bathymetry in detail. The maximum working depth of the Russian corer and rods was 13m so sampling sites were selected with a water depth less than 8m. This water depth would still potentially allow 4m of sediment to be collected. Surface sediments and short cores, up to

19cm, were collected from all 5 lakes using a 80mm diameter Renburg gravity corer (Renberg 1991) (Figure 3.2). Renburg cores were subsampled in the field as previously described for the HON-Kajak corer.



Figure 3.2. Subsampling Renburg core from SAND in the field (left – right V. Jones, V. Ponomarev and A. Self

Long cores, 1.85 – 3.2m, were collected from NERU, KHAR and VORK5 using a Jowsey Russian corer (Jowsey 1966) (Figure 3.3). The Russian corer extracts a semi-cylindrical sample 50 or 100cm in length. The long cores were therefore collected from 2 adjacent ice holes, approximately 1m apart, with consecutive samples taken from alternate holes to ensure the sampled sediment had not been disturbed. The depths sampled were overlapped by 10-40cm to ensure a contiguous sequence was obtained. Cores were taken until a firm basal sand layer was reached. The retrieved cores were wrapped in polythene, in the field, and placed onto a firm board for transporting. Due to the logistical problems of transporting intact cores by air, the Russian cores were sectioned later in the trip into 1cm slices, placed in whirl-pak bags and stored at 4°C. Sampling resolution of the cores is shown in Table 3.2.



Figure 3.3. Sampling using the Russian corer at lake SAND (left – right H. Seppä and S. Seboni)

Location	Core code	Core type	Sampling date	Water depth (m)	Core depth from water surface (m)	Approx length (cm)	Sampling resolution
NERU	NERU 0	Renberg	20.04.2007	5.85	7.60 - 7.80	20	0-20cm depth = 1cm intervals
	NERU 1	Renberg			5.85 - 5.99	14	0-14cm = 1cm intervals
	NERU 2	Russian			5.80 - 6.50	100	1 cm intervals
	NERU 3	Russian			6.40 - 7.40	100	1 cm intervals
	NERU 4	Russian			6.75 - 7.75	100	1 cm intervals
	NERU 5	Russian			7.25 - 7.75	50	1 cm intervals
	NERU 6	Russian			7.75 - 8.25	50	1 cm intervals
KHAR	KHAR1	Russian	21.04.2007	7.80	7.80 - 8.50	70	1 cm intervals
	KHAR2	Russian			8.40 - 9.40	100	1 cm intervals
	KHAR3	Russian			9.30 - 10.30	100	1 cm intervals
	KHAR4	Russian			10.30 - 10.80	50	1 cm intervals
	KHAR5	Russian			10.48 - 10.98	50	1 cm intervals
	KHARa	Renberg			7.80 - 7.82	2	0-1, 1-2cm intervals
	KHARb	Renberg			7.80 - 7.95	15	0-5cm = 0.5cm intervals, 5-15cm = 1cm intervals
	KHARc	Renberg			7.80 - 7.83	3	0-1, 1-3cm intervals
VORK3	VORK3a	Renberg	22.04.2007	2.60	2.60 - 2.77	17	0-17cm = 1cm intervals
	VORK3b	Renberg			2.60 - 2.61	1	0-1cm
SAND	SAND1	Russian	24.04.2007	6.60	6.60 - 7.30	70	1cm intervals
	SAND2	Russian			7.20 - 8.20	100	1cm intervals
	SAND3	Russian			11.80 - 12.30	50	1cm intervals
	SANDa	Renberg			6.60 - 6.79	19	0-5cm = 0.5cm intervals, 5-19cm = 1cm intervals
	SANDb	Renberg			6.60 - 6.61	1	0-1cm
VORK5	VORK51	Russian	26.04.2007	2.00	2.05 - 2.70	65	1cm intervals
	VORK52	Russian			2.58 - 3.58	100	1cm intervals
	VORK53	Russian			2.60 - 3.60	100	1cm intervals
	VORK54	Russian			2.05 - 2.70	65	1cm intervals
	VORK55	Russian			2.85 - 3.85	100	1cm intervals
	VORK5a	Renberg			2.05 - 2.24	19	0-5cm = 0.5cm intervals, 5-19cm = 1cm intervals
	VORK5b	Renberg			2.05 - 2.06	1	0-1cm

Table 3.2. Core length and sampling resolution of the samples collected in April 2007

3.2.3 Collection of contemporary chironomid pupae

As described in Chapter 1, Chironomidae develop through a pupal stage before emerging as an adult. The pupal cuticle is shed when the adult chironomid ecloses at the water surface; the shed pupal exuviae float on the water surface and are moved by wind and water currents to accumulate along the leeward shore or against obstructions such as emergent vegetation or amongst rocks.

The exuviae survive intact for approximately 48 hours before decomposing (Coffman 1973; McGill 1980) so a sample represents only recently eclosed species. Whereas many chironomid larvae can only be identified to generic or species morphotypes, pupal exuviae can frequently be identified to species (Langton 1991; Langton and Visser 2003). Therefore pupal exuviae were collected to improve the taxonomic resolution of the contemporary fauna. As the adults emerge during ice-free conditions pupal exuviae were collected only during summer fieldwork on the Putorana Plateau.

Pupal exuviae were collected from the leeward shores of seven of the nine Putorana lakes from 1st to 9th July 2006. Potential sites for the accumulation of exuviae were inaccessible at WILD and PFOR due to the prevailing wind direction. Flotsam samples were collected by skimming the water surface with a 250µm mesh pond-net (Wilson and Ruse 2005) between emergent plants and rocks. Large debris such as leaves and twigs were removed; the retained material was transferred to a sterile universal bottle and preserved in 40% alcohol.

3.2.4. Field descriptions

During the fieldwork on the Putorana Plateau the land cover (proportion of snow beds, rock or vegetation) surrounding the sampled lakes was recorded and photographed. The vegetation was described and sketch maps drawn to show the lake bathymetry and precise location of the sampling sites. Distance to the coast, lake and catchment areas were measured from Google Earth™ images (Google-Earth™ v4.2 2007). The catchments of lakes sampled in April 2007 were snow covered; only mature trees were visible. Vegetation descriptions are, therefore, based on descriptions from previous studies (Solovieva *et al.* 2002; Sarmaja-Korjonen *et al.* 2003; Solovieva *et al.* 2005), Vasily Ponomarev of the Komi Science Centre, Syktyvkar (pers.comm. 2007) and Google Earth™ images. These also formed the basis for maps of the sampled lakes (Chapter 7 and 8) and estimations of lake and catchment areas, given in Chapter 2.

3.3. Laboratory methods

3.3.1. Water chemistry

Major anions and cations, in the water samples, were analysed at the Komi Science Centre, Syktyvkar, Russia. Sodium (Na^+) and potassium (K^+) were determined by flame emission and magnesium (Mg^{2+}) and calcium (Ca^{2+}) by atomic absorption spectroscopy. Nitrate (NO_3^-) concentrations were determined colorimetrically by cadmium reduction. Sulphate (SO_4^{2-}) was analysed photometrically and chloride (Cl^-) determined by potentiometric titration. Analysis of total phosphorus (P_{tot}) in unfiltered water followed Murphy and Riley (1962).

3.3.2. Analysis of sediment cores

3.3.2.1. Wet density, dry weight, loss-on-ignition and carbonate content of sediments

The wet density was calculated from the weight of a known volume of sediment. Dry weight, loss-on-ignition and carbonate content were determined after combustion at 105, 550 and 925°C respectively as described by Heiri *et al.* (2001).

3.3.2.2. Carbon and nitrogen isotopic composition

The isotopes ^{13}C and ^{15}N were analysed in bulk sediment samples from the PONE, PTHE and KHAR cores at the UC Davis Stable Isotope Facility, California, USA. C/N ratios were calculated to examine the relative importance of autochthonous and allochthonous sources of organic material in the lake sediments, whilst $^{13}\text{C}/^{12}\text{C}$ analyses is used to determine the dominant source of carbon in the lake (Talbot and Laerdal 2000).

Samples for bulk organic matter ($\delta^{13}\text{C}$) analysis were prepared by adding 5ml of 10% hydrochloric acid to 0.5g of wet sediment to remove carbonates. Once the reaction had ceased, approximately 2 hours, the samples were centrifuged at 1500 rpm for 4 minutes and the supernatant decanted. Samples were washed, three times, with deionised water and air dried at 40°C. Additional 0.5g samples of wet sediment were air dried, untreated, for $\delta^{15}\text{N}$ analysis. Dried samples were ball milled and 8-19mg subsamples encapsulated in tin capsules. Samples were analysed from Lake Kharinei (KHAR) at 1cm intervals for the first

10cm depth then at 2-4cm intervals to the base of the core. PONE and PTHE were analysed at 0.5cm intervals to 17cm depth, then 1cm intervals.

The samples were analyzed using a PDZ Europa ANCA-GSL elemental analyzer interfaced to a PDZ Europa 20-20 isotope ratio mass spectrometer (Sercon Ltd., Cheshire, UK). Samples were combusted at 1020°C in a reactor packed with chromium oxide and silvered cobaltous/cobaltic oxide. Following combustion, oxides were removed in a reduction reactor (reduced copper at 650°C). Nitrogen and CO₂ were separated on a Carbosieve GC column (65°C, 65 mL/min) before entering the IRMS. During analysis, samples are interspersed with laboratory standards, which have been previously calibrated against NIST Standard Reference Materials (IAEA-N1, IAEA-N2, IAEA-N3, IAEA-CH7, and NBS-22). The results were expressed relative to the international standards PDB (PeeDee Belemnite) and Air for carbon and nitrogen, respectively (Sharp 2005).

3.3.2.3. Preparation of larval head capsules

The modern chironomid distribution and abundance in the study sites was investigated by analysing the uppermost 0 – 1 cm of the sediment core. For downcore samples between 0.5 and 2 g sediment were analysed. Wet sediments were deflocculated in 10% potassium hydroxide (KOH) at 70°C for 5 minutes then left to stand in hot water for 20 minutes (Brooks and Birks 2000a; Brooks *et al.* 2005) . Samples were washed through 90 and 212 µm sieves and the re-suspended sediment sorted in a grooved Bogorov tray using a dissecting microscope at 25 – 50 times magnification. A minimum of 50 head capsules per sample is considered sufficient for reliable temperature reconstructions (Heiri and Lotter 2001; Larocque 2001; Quinlan and Smol 2001). Therefore if less than 50 head capsules were isolated additional sediment was prepared until between 50 and 300 head capsules were separated from each sample. Isolated head capsules were stored in 80% ethanol. Prior to mounting, the head capsules were progressively dehydrated by transferring to 100% ethanol, then Euparal essence, for approximately 5 minutes in each. The head capsules were mounted, 2 per 6mm coverslip, with the ventral side up, in Euparal.

Identifications were primarily based on mentum and, where present, mandible characteristics with reference to Wiederholm (1983), Schmid (1993), Makarchenko and Makarchenko (1999), Brooks *et al.* (2007) and the national Chironomidae collection at the Natural History Museum, London, UK. Tanypodinae head capsules were identified using the morphology of the paraligula for *Procladius* or ventral and dorsal pore arrangement as described in Rieradevall and Brooks (2001). Chironomid head capsules that retained the entire mentum or greater than half were counted as one head capsule, and those with half a mentum as half a head capsule. Head capsules comprising less than half the mentum were not counted.

Not all the chironomid larval assemblages included in this study were prepared or identified, solely, by the author. The researchers and organisations involved in the collection of the surface sediments are detailed in sections 2.2.1 to 2.2.4. Samples from northeast European Russia (Lake Vanuk-ty, Lake Mitrofanovskoe and lakes prefixed F- or TDR) were collected between 1995 and 2001 as part of the EU-funded SPICE (ICA2-CT2000-10018) and TUNDRA (ENV4-CT97-0522) projects. Although chironomids had been prepared and identified from these lakes by L. Nazarova, Alfred Wegener Institute, Potsdam, additional material was prepared and identified by the author to ensure over 100 head capsules were identified for each lake. This higher number should ensure the sub-sampled assemblage more accurately reflects the population (Heiri and Lotter 2001). From Nazarova's original material, taxa which were identified at higher resolution in Brooks *et al.* (2007) (i.e. Tanytarsini, Tanypodinae, *Cricotopus/Orthocladius* spp. and *Chironomus* morphotypes) were re-examined to ensure consistent taxonomy. These taxa were also re-examined in material from Central Yakutia (prefixed Y-) prepared and identified by Larisa Nazarova. For the remaining taxa, head capsules were selected at random to check for taxonomic consistency between Larisa Nazarova and the author. As identifications appeared consistent Nazarova's identifications and counts were used for taxa not specified above. Material from the Lower Lena River (prefixed LS-) was collected by John Smol of Queen's University, Kingston and prepared by David Porinchu of Ohio State University. Due to differences in taxonomic resolution and the method of preparation; with multiple head capsules (5-150)

under each coverslip, all head capsules on these slides were re-identified and counted by the author.

3.3.3. Chironomid pupae

In the laboratory a subsample of the collected flotsam material was removed, using forceps, and dispersed in a shallow tray containing 80% ethanol. All pupal exuviae were picked out and sorted into similar morphotypes using a low-powered dissecting microscope. Between 4 and 6 exuviae of each morphotype were dehydrated in 100% ethanol for 5 minutes then mounted, dorsal side up, in Euparal. Pupal exuviae were identified on the basis of size, colour and morphology with reference to Wilson and Ruse (2005), Langton (1991) and Langton and Visser (2003). Taxonomic resolution varied between genera, subgenera, species group and species.

3.3.4. Core chronologies

The top 8 – 12cm of sediment from cores PONE, PTHE, KHAR and VORK5 were dated by measurement of Lead-210 (^{210}Pb) as detailed in section 3.3.4.1. Due to the half-life of ^{210}Pb this technique is only applicable to samples less than 150 years old. Therefore samples deeper than 20cm below the sediment-water interface in the cores KHAR, NERU and VORK5 were dated by radiocarbon analysis as described in section 3.3.4.2.

3.3.4.1 Lead-210 dating

Lead-210 (^{210}Pb) is a naturally occurring radionuclide produced by the decay of radon gas (^{222}Rn) in the atmosphere, as part of the uranium-series decay chain. Deposited in sediments, it decays to stable ^{206}Pb over an interval of approximately 150 years (half-life 22.3 yrs). By determining the ratio of ^{210}Pb to ^{206}Pb in the sediment in relation to its depth, the time elapsed since the sediment was deposited can be estimated (Olsson 1986). The method has proved reliable in stable environments, with uniform and continuous sedimentation rates, where the dating calculations are unambiguous (Appleby 2001). In these circumstance dates are calculated using the CRS (constant rate of ^{210}Pb supply) model. However in areas with non-uniform accumulation, such as sites where environmental conditions have varied over the last 100-150

years (Appleby 2004), it may be necessary to select an alternative dating model. The most widely used alternative is the CIC (constant initial concentration) model which assumes that sediments have a constant initial ^{210}Pb concentration regardless of accumulation rates (Appleby 2001). Caesium-137 (^{137}Cs , half-life 30 years) and Americium-241 (^{241}Am , half-life 432.2 years) are artificially produced radionuclides introduced by atmospheric fallout from nuclear weapons testing and the Chernobyl reactor accidents. These radionuclides produce well-defined peaks of known age and are used as an independent dating technique to verify the ^{210}Pb chronology.

Sediments from the cores PONE, PTHE, KHAR and VORK5 were sub-sampled at 1 – 2 cm intervals for the top 12 – 19 cm of each core and the sub-samples freeze-dried to give approximately 1g dry weight of sediment. Although the Putorana cores had been sectioned at 0.25cm intervals it was necessary to amalgamate samples to provide sufficient material for analysis due to the high water content of surface samples. Sediment accumulation rates are generally low in arctic lakes, therefore amalgamation will increase the age range of the sample and so decrease precision but could not be avoided. Freeze-dried samples were analysed for ^{210}Pb , ^{226}Ra , ^{137}Cs and ^{241}Am by Handong Yang in the Bloomsbury Environmental Isotope Facility (BEIF) at University College London. The concentrations were determined by direct gamma assay, using an ORTEC HPGe GWL series well-type coaxial low background intrinsic germanium detector. Lead-210 was determined via its gamma emissions at 46.5keV, and ^{226}Ra by the 295keV and 352keV gamma rays emitted by its daughter isotope ^{214}Pb following 3 weeks storage in sealed containers to allow radioactive equilibration. ^{137}Cs and ^{241}Am were measured by their emissions at 662keV and 59.5keV respectively. The absolute efficiencies of the detector were determined using calibrated sources and sediment samples of known activity. Corrections were made for the effect of self absorption of low energy gamma rays within the sample.

Radiometric dates were calculated using the CRS (constant rate of ^{210}Pb supply) and CIC (constant initial ^{210}Pb concentration) dating models and compared to the 1963 depths determined from the $^{137}\text{Cs}/^{241}\text{Am}$ stratigraphic

records to determine which model was most appropriate (Appleby 2001; Appleby 2004). Mean sedimentation rates were calculated in cm/y and ^{210}Pb dates calculated using the appropriate model (Appleby and Oldfield 1978; Appleby 2001). The sediment accumulation rate was extrapolated down core, for the Putorana cores PONE and PTHE, to provide an age estimate of sediment age beyond the ^{210}Pb record. Older sediments, below 20cm depth, from the Vorkuta cores were radiocarbon dated as described below, section 3.3.4.2. Dates from both procedures were combined to form an age-depth model for these lakes. Details of the models used and the age-depth chronologies are described in chapter 7 for the Putorana samples and chapter 8 for the North-east European Russia sites.

3.3.4.2. Radiocarbon dating

Radiocarbon dating was one of earliest radiometric methods to be developed and is still one of the most widely used dating techniques for material less than 50 kyrs old. ^{14}C is formed when free neutrons, formed by cosmic radiation, interact with atmospheric nitrogen in the upper atmosphere. The isotope is fixed through photosynthesis in equilibrium with the atmospheric concentration. On death the organism no longer incorporates ^{14}C and decays with a half life of 5735 yr. The samples were converted to graphite at the NERC Radiocarbon Laboratory, East Kilbride by digesting approximately 2 – 3 g of wet sediment in 2M hydrochloric acid for 8 hours at 80°C. The residual was washed free from acid with deionised water then dried on filter paper in a vacuum oven and homogenised. The total carbon in a known weight (approximately 10 mg) of pre-treated sample was recovered as CO_2 by heating with CuO in a sealed quartz tube and the gas converted to graphite by Fe/Zn reduction (Bryant, pers. comm., 2008). ^{14}C was analysed at the SUERC AMS laboratory (under radiocarbon dating allocation numbers 1243.1007 and 1289.0408) and expressed as conventional radiocarbon years BP (relative to AD 1950) and % modern ^{14}C , both expressed at + 1 σ confidence level. Radiocarbon determinations were converted to calibrated dates using the OxCal v4 program (Bronk Ramsey 1995, 2001, 2008).

3.3.5. Derivation of environmental variables

The environmental variables latitude, longitude, altitude, water depth, pH and conductivity were determined in the field as described in sections 3.2.1 and 3.2.2. and the major anion and cation composition was determined as described in section 3.3.1. In addition to these variables, other variables were determined which were expected to influence the distribution of chironomids. The rationale for their inclusion and their derivation are detailed below:

Air temperatures: Temperature influences every stage of the chironomid life cycle, governing the rate of development of eggs, larvae and pupae (Pinder 1986, also see Chapter 1). This behaviour is particularly marked in the arctic where changes in light intensity do not reliably indicate temperatures (Danks and Oliver 1972b; Danks 1992). Air temperatures were used in the numerical analysis as they give a more robust approximation of water temperatures than isolated measurements taken during fieldwork, and improve the performance of temperature inference models (Brooks and Birks 2001). The mean January and July air temperatures were calculated for each lake by Arvid Odland of Telemark College, Bø, Norway. Mean July and January temperatures were calculated from the meteorological stations close to the sampled lakes for the 30 years prior to sampling (Table 3.3). All values were corrected for altitude assuming an environmental lapse rate of $0.57\text{ }^{\circ}\text{C }100\text{m}^{-1}$ for July and $0.44\text{ }^{\circ}\text{C }100\text{m}^{-1}$ for January (Laaksonen 1976). For each study area the spatial relationships between distance to coast-latitude and temperature were examined. The meteorological stations close to the Putorana Plateau and in Central Yakutia did not show a strong spatial gradient and mean values were based on the closest three and two stations, respectively, corrected for altitude. In the Lena delta there was a strong linear coast-inland temperature gradient (R^2 for the linear relationship between distance from the coast and mean July temperature was 0.9893 and 0.9451 for mean January temperature). Temperatures were estimated for the sampled lakes based on these relationships and corrected for altitude. Similarly there was a linear latitude – temperature gradient in the Pechora basin ($R^2 = 0.725$ for mean July temperature and 0.595 for mean January temperature) and mean temperature data for the lakes were calculated on the basis of these relationships.

Sampling region	Transliterated name of meteorological station	Dates
Pechora: Archived material from sites prefixed TDR- or F, Vanuk-ty and Mitro Lakes sampled in 2007	Narjan-Mar Berezovo Vorkuta Kamennyj Khosed-hard Pecora (Pechora)	1971 - 2000 1977 - 2006
Putorana: GYXO, WILD, ARTE, AFOX, IGAR or prefixed P	Dudinka Turuhansk Essej	1976 - 2005
Lena delta: prefixed LS-	Dzardzan Salaurova Olenek Ostrovkotel Zhigansk	1964 - 1993
Yakutia: prefixed Y-	Jakutsk (Yakutsk) Vilyuysk Isit Aldan Ust-Maja	1974 - 2003

Table 3.3. Summary of the meteorological stations and years used in the calculation of mean January and July air temperatures. Historical records are available online from Royal Dutch Meteorological Institute (<http://climexp.knmi.nl/>)

Gorczynski Continentality Index: The commencement of pupal development and the timing of the emergence of adult chironomids is governed by temperature thresholds in the Arctic (Danks and Oliver 1972a). Developmental rates of eggs and larvae are also temperature-dependent (Edwards 1986; Iwakuma 1986), therefore it was hypothesised in Chapter 1 that continentality would influence the population structure and/or physiological response of the chironomids. Gorczynski Continentality Indices (Gorczynski 1920) were calculated, for each lake, based on the equation:

$$K_G = 1.7 \frac{A}{\sin \varphi} - 20.4$$

where A, the annual temperature amplitude, equals the difference in monthly mean temperatures of warmest and coldest months and φ the latitude.

Mean annual and summer precipitation for the Russian lakes was estimated, for the 30-year period prior to sampling, from monthly observations in the Global Precipitation Climatology Centre (GPCC) database version 3, based on 0.5° grid intervals (Rudolf *et al.* 1994; Rudolf *et al.* 2003). The geography of lakes in northern Eurasia is controlled by water availability and topography (Koronkevich 2002). Many arctic lakes are fed primarily by melting permafrost or snow melt and summer precipitation rather than surface flow. Annual precipitation, therefore, influences the occurrence, abundance and depth of water bodies. Water depth exhibits a strong influence on the distribution of chironomids and their species richness (Pinder 1995). Many species show depth preferences (Petridis and Sinis 1993; Brodersen *et al.* 2004) reflecting the availability of suitable habitats and light or oxygen limitations at depth. Water depth determined in the field, at the point of sampling, is included as a separate environmental variable. For some lakes, for example on the Putorana Plateau, the sampling point was the deepest part of the lake. But for other sites, such as the ice-covered lakes near Vorkuta, the sampling depth was constrained by the working depth of the equipment (section 3.2.2) and the maximum lake depth is unknown. Therefore annual and summer precipitation was included to quantify water availability on a more generalised, landscape scale.

Vegetation type: Although taxa such as *Polypedilum* and *Glyptotendipes* are commonly associated with plant macrophytes (Brodersen *et al.* 2001), the vegetation surrounding lakes also influences the chironomid assemblage by determining the openness of the landscape and the lateral dispersion of adult chironomids (Delettre and Morvan 2000; Meltser *et al.* 2008). Vegetation type is directly related to climate. The latitudinal tree-line coincides approximately with the mean July temperature isotherm of 10°C (Zlotin 2002) and several studies have shown significant changes in chironomid composition across the tree-line (Walker and MacDonald 1995; Porinchu and Cwynar 2000; Larocque *et al.* 2001; Walker *et al.* 2003). The presence of forests enhances soil development which in turn affects the pH, DOC and chemical characteristics of lakes within the catchment and their faunal composition. Vegetation was categorised as polar desert, tundra, mire or wetlands or forest/alas pasture. Sites close to ecotonal boundaries with mixed vegetation were included in both categories, for

example areas of tundra, near the tree-line, with scattered trees were categorised as forest-tundra. In the ordination techniques vegetation was recorded as a nominal variable (presence or absence) of each vegetation type. Assessments were based on field observations, photographs, previous studies and Google Earth™ images.

Human impact: Human activity, through agriculture and settlement, has a major effect on key nutrient concentrations in freshwater ecosystems, while atmospheric pollution and industry increasingly influence those of trace elements (Moss 1998). Increased nutrient input from sewage or farm run-off can lead to eutrophication and increased hypoxia or anoxia. Lake trophic status and levels of dissolved oxygen have a major impact on the chironomid assemblage and abundance. Chironomids have been used to assess the trophic status of lakes (Brundin 1958; Sæther 1979; Wiederholm 1984) and indicate past changes in lake productivity and dissolved oxygen (Brodersen and Quinlan 2006). Human impact was recorded on an ordinal scale (0, 1 or 2) based on no, little or heavy impact respectively. Assessments were based on field observations, photographs, previous studies and Google Earth™ images. Examples are shown in Figure 3.4.




<p>Putorana, near GYXO</p> 	<p>Ice fishing at Kharinei Lake (KHAR)</p> 	<p>Lake (Y1718) in Vilyuysk, Central Yakutia</p> 
<p>0 : No human impact No signs of human habitation, no tracks or roads</p>	<p>1 : Little human impact No permanent habitation, some evidence of human activity; such as fishing, tracks, rubbish</p>	<p>2 : Heavy human impact Close to (<5 km) permanent occupation, connected by road or tracks, frequent or heavy use</p>

Figure 3.4. Criteria for assessing human impact on the Russian lakes

Proximity to other lakes: Landscape connectivity is an important factor in the population dynamics of aquatic insects such as chironomids (Delettre and Morvan 2000). Chironomids are poor fliers and in densely vegetated landscapes the adults are generally confined to the water bodies in which they emerge. In more open landscape the adults disperse over short distances of less than 500m (Delettre and Morvan 2000), although passive dispersal by the wind (Armitage *et al.* 1995) or in the guts of migratory waterbirds (Green and Sánchez 2006) may facilitate dispersal over a wider area. This variable was recorded as a nominal variable based on the presence or absence of 3 or more lakes within 500m in Google Earth™ images.

The environmental variables used in the statistical analysis (Chapter 4) to determine the factors influencing the modern distribution are summarised in Table 3.4. Water chemistry, water depth, mean January air temperature (T_{jan}) and continentality indices were not available for the Komi lakes, therefore these were excluded from the analysis in Chapter 4 but included in the development of the inference models (Chapter 6).

Table 3.4. Summary of the environmental parameters used in the statistical analysis

Environmental parameter	Units	Description of source
Russian lakes excluding Komi lakes:		
Latitude	Decimal degree N	Section 3.2.2
Longitude	Decimal degree E	“
Altitude	m above sea level	“
Water depth	m	“
pH		Section 3.2.1
conductivity	$\mu\text{S cm}^{-1}$	“
Distance from coast	km	Section 3.2.4
Mean July air temperature	$^{\circ}\text{C}$	Section 3.3.5
Mean January air temperature	$^{\circ}\text{C}$	“
Continental index		“
Mean annual precipitation	mm yr^{-1}	“
Summer precipitation	mm Jun, July & Aug	“
Water chemistry:		
Chloride (Cl)	$\mu\text{eq l}^{-1}$	section 3.3.1
Sodium (Na)	$\mu\text{eq l}^{-1}$	“
Sulphate (SO_4)	$\mu\text{eq l}^{-1}$	“
Calcium (Ca)	$\mu\text{eq l}^{-1}$	“
Magnesium (Mg)	$\mu\text{eq l}^{-1}$	“
Vegetation type:		
Tundra/forest/mire/polar desert	presence/absence	Section 3.3.5
Proximity to other lakes	presence/absence	“
Human influence	scale 0, 1 or 2	“
Norwegian lakes: Above parameters excluding summer precipitation		
Subset of Norwegian and Russian lakes: Above parameters plus LOI	%	Section 3.2.2.1

3.3.6. Note on collection of primary data

Not all the surface sediments included in this study were collected or analysed, solely, by the author. Surface sediments from the Putorana Plateau and Vorkuta area (NERU, KHAR, VORK3, SAND and VORK5) were collected and analysed by the author. The researchers and organisations involved in the collection of the remaining surface sediments are detailed in Table 3.5. The preparation and identification of the chironomid larval head capsules from these surface sediments is discussed in section 3.3.2.3 and also summarised in Table 3.5. Chironomid assemblages from surface sediments in the Pechora Basin (NE European Russia) and Central Yakutia were initially prepared and identified by L. Nazarova, selected taxa were then re-examined by the author to ensure consistent taxonomy. Additional material from NE European Russia was also prepared and identified by the author to increase the number of head capsules identified from each lake so that the sampled assemblage more accurately reflects the composition of the population.

Chemical analysis of the water samples from the Putorana Plateau and lakes near Vorkuta was carried out at the Komi Science Centre, Syktyvkar, Komi Republic. Details of the organisations responsible for water chemistry analysis of the remaining lakes are shown in Table 3.5. Sediment cores were ^{210}Pb and radiocarbon dated (section 3.3.4), however analysis of the radiocarbon results to give calibrated dates and the development of age-depth models was the responsibility of the author.

Pupal exuviae were prepared with help from Natural History Museum volunteers Rachel Preedy, Felicity Muth and Malcolm Aldridge and identified by F. Muth and the author. Identifications by F. Muth were confirmed by re-examining selected examples of each taxon to ensure consistent taxonomy. Material from KHAR (cores 2 – 5) was prepared and mounted by Pat Haynes, NHM, and identified by the author. Continentality indices, precipitation, proximity to other lakes and human impact were derived for the Norwegian calibration set (Brooks and Birks 2000b; 2001 and unpublished data) by the author. All other environmental variables for the Norwegian calibration set, including vegetation, were recorded by H.J.B. Birks and S. Brooks. All other primary data presented

in this thesis, including laboratory measurements, preparation, experimental work and taxonomic analyses are the result of work carried out by the author.

3.3.7. Secondary data

In addition to primary data, this thesis uses secondary data from a variety of sources. These are acknowledged within the thesis and summarised in Table 3.5.

Table 3.5. Summary of secondary and joint primary/secondary data sources.

(*Chironomid assemblages prepared and identified by L. Nazarova; selected taxa re-examined by author to ensure consistent taxonomy)

Data	Collected by	Source
Surface Sediments		
Norwegian training set		
Field observations Chironomid assemblages Environmental data	H.J.B. Birks	H.J.B. Birks, University of Bergen, Norway S. J. Brooks, NHM, London H.J.B. Birks, University of Bergen – excluding CI, precipitation, proximity to lakes and human impact
Russian training set:		
NE European Russia		
Field observations Chironomid assemblages* Water chemistry	SPICE and TUNDRA projects	Prefixed F-, TDR, Vanuk-ty or Mitro P. Noon/V Jones, UCL; TUNDRA and SPICE: http://www.ulapland.fi/home/arktinen/tundra/tundra.htm http://www.ulapland.fi/home/arktinen/spice/spice.htm L. Nazarova, Alfred Wegener Inst.* and author Komi Science Centre, Syktyvkar, Russia
Putorana samples		
Water chemistry	Author	Komi Science Centre, Syktyvkar, Russia
Yakutia: Prefixed Y-		
Field observations Chironomid assemblages* Water chemistry	Kazan State University	L. Pestryakova, Kazan State University L. Nazarova, Alfred Wegener Inst., Potsdam* Water System Lab, Yakutsk State University
Lena delta: Prefixed LS-		
Field observations Chironomid assemblages Water chemistry	PACT programme	J. P. Smol, Queen's University, Kingston, Canada (Duff et al. 1998; Porinchi and Cwynar 2000) Prepared D. F. Porinchi, Ohio State University, identified by author National Water Research Inst., Ontario, Canada

Table 3.5. Summary of secondary data sources continued.

Data	Compiled by	Source
Environmental data		
Meteorological data for European Russia, western and central Siberia 30-year mean January and July air temperatures	GHCN, Global Historical Climatological Network	The Royal Netherlands Meteorological Institute Climate Explorer http://climexp.knmi.nl/ Arvid Odland, Telemark College, Bø, Norway
Precipitation: monthly data for European Russia, western and central Siberia	GPCC, Offenbach, Germany	Global Precipitation Climatology Centre (GPCC) database v 3, based on 0.5° x 0.5° grid intervals http://www.dwd.de/en/FundE/Klima/KLIS/int/GPCC/GPCC.htm
GISP2: Potassium ion concentrations from GISP2 ice core	P.Mayewski	(Analysed by Mayewski <i>et al.</i> 1997). Data available at: ftp://ftp.ncdc.noaa.gov/pub/data/paleo/icecore/greenland/summit/gisp2/chem/ionb.txt
Solar insolation: June and January insolation for past 800,000 years	A. Berger	Calculated by A. Berger of the Catholic University of Louvain, Belgium (Berger and Loutre 1991): ftp://ftp.ncdc.noaa.gov/pub/data/paleo/insolation/

3.4. Numerical analysis

A number of statistical techniques are used within this thesis to explore variation in the biological data and its relationship to the environmental variables determined. The techniques and programmes used, together with their theoretical basis, are briefly described below.

3.4.1. Transformation of data prior to analysis

Raw chironomid counts were stored and converted to percentage abundances in Microsoft Excel, version 2003. The total abundance of head capsules per gram was calculated as the total number of head capsules per dry weight of sediment analysed in grams. Percentage chironomid data from the surface samples and the core samples were square-root transformed to stabilise variance within the data. Rare taxa were down-weighted in ordination analyses in direct proportion to their abundance.

Many environmental variables display a right-skewed distribution with numerous low values and a few extreme values resulting in large variance relative to the mean (for example the water chemistry data for both the Russian and Norwegian lakes, chapter 4). In these cases the variables were log transformed, or $\log(x + 1)$ transformed for those variables with many zero values. These transformations prevent the few extreme values from unduly influencing the regression analysis. Transformations of the environmental data are discussed further in chapter 4.

3.4.2. Exploratory data analysis

The aim of the initial data exploration was to examine the relationships between the environmental variables. Quantitative environmental variables often show linear relationships and a high degree of correlation between variables (Birks 2003). The preliminary analysis highlighted data redundancy so that when the relationship between the species and their environment was examined, by ordination, redundant variables could be removed without significantly reducing the explanatory power of the model.

The distributions of the environmental variables were visualised by kernel-density estimation. This is a nonparametric density estimation which is used as an alternative to frequency histograms. The distribution is broken into a number of sections or bins, the relative number of observations per bin width is calculated and a smoothed line overlain. The distributions of environmental variables, visualised by kernel-density estimates, are shown in Chapter 4. Statistical analyses, unless specified otherwise, were performed using the R computer software (R Development Core Team, 2004) and kernel-density estimates produced using the MASS package for R (Venables and Ripley 2003). Relationships between environmental variables were examined by multiple linear regression. Scatter-plot and correlation matrices were generated using the R function `corProb()`; Pearson product-moment correlation coefficients, and associated p-values, were calculated to determine the strength and direction of the relationships.

Cluster analysis was used to identify structure within the chironomid abundance data. Lake assemblages were partitioned into groups using hierarchical agglomerative and divisive techniques. In agglomerative hierarchical cluster analysis a matrix of proximity is calculated for all pairs of samples and objects fused into groups according to stated statistical criteria. For example, single-link clustering finds and fuses groups with the shortest chord or Euclidean distance (Gordon 1999). In minimum variance, groups are fused if neither produce a lower sum-of-squares with any other groups (Orloci 1967). Cluster analysis was performed using R-hclust function in the package mva; the clustering strategy and underlying algorithm are detailed with the output in chapter 4. In agglomerative techniques the individual samples are progressively fused to produce clusters; in divisive clustering, such as TWINSpan (Hill 1979) are successively split into groups with common differential variables on either side of the dichotomy. In TWINSpan the samples are ordinated along Correspondence Analysis (CA) axis 1 and split into groups where the largest taxonomic differences occur. The chironomid assemblages were classified using TWINSpan for Windows (WinTWINS), version 2.3 (Hill and Šmilauer 2005). Cut levels for pseudo-species were set at 1, 2, 5, 10, 20 and 40%. Composite taxonomic groupings such as Tanytarsini indeterminate were identified as non-diagnostic species so were not considered in the determination of indicator species.

3.4.3. Species response models

The response of individual species to specific environmental variables was evaluated using HOF models, generalised linear models (GLM) and generalised additive models (GAM). The HOF programme (Oksanen and Minchin 2002) was used to fit the models of Huisman-Olff-Fresco (Huisman *et al.* 1993) to the chironomid percentage abundance data. These are a series of hierarchical models which model species responses to environmental variables (Figure 3.5, Table 3.6). The most complex model V is fitted first by maximum likelihood estimation with Poisson error function. Parameters are then removed from the regression model one at a time, fitting models IV, then III and II, until the removal of a parameter resulted in a statistically significant ($p < 0.05$) change in the model's deviance. The simplest model with the minimum number of significant

parameters is adopted to describe a species response. Model III (plateau) has the same number of parameters as model IV and is not routinely fitted. If model IV is rejected in favour of model V, the latter is compared to model III and model simplification continued (Huisman *et al.* 1993). HOF models were fitted to taxa with 10 or more occurrences in the training set lakes.

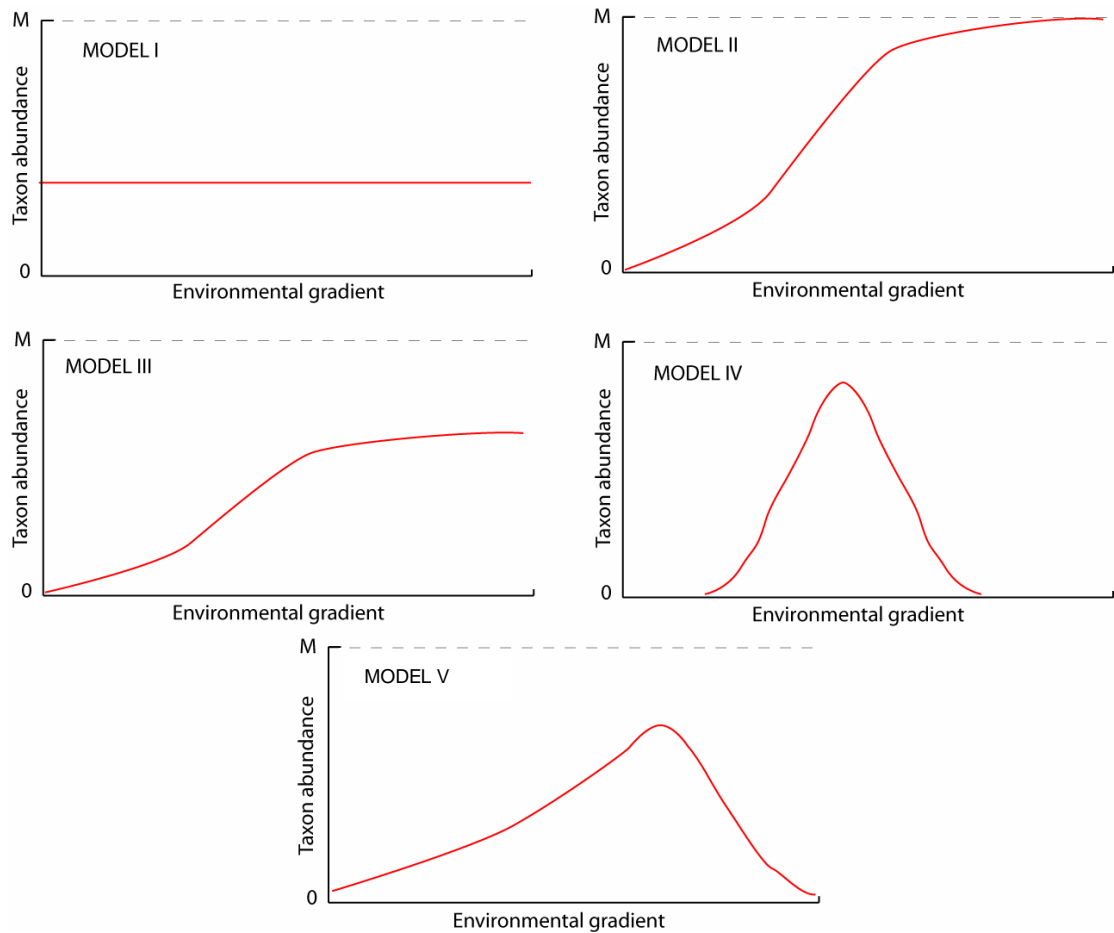


Figure 3.5. The five hierarchical Huisman-Olff-Fresco (HOF) models of species response, ranked by their increasing complexity (Holmes 2006 modified from Huisman *et al.* 1993).

Model	Ecological response described
Model I	No significant trend
Model II	Increasing or decreasing monotonic sigmoidal trend
Model III	Increasing or decreasing trend bounded below the maximum attainable response
Model IV	Symmetric unimodal response curve
Model V	Asymmetric/skewed unimodal response curve

Table 3.6. Ecological responses described by the HOF models (Huisman *et al.* 1993).

To generate generalised linear models (GLM) linear combinations of predictor variables are evaluated to find which best predicts the response variable. For example, the response of a species is first modelled as a function of pH and then modelled as a response to $(\text{pH} + \text{pH}^2)$. The additional parameters in the extended model are significant when the drop in residual deviance is larger than the critical value of a chi-squared distribution with k degrees of freedom, where k = number of additional parameters. The minimum adequate model has the fewest number of statistically significant parameters. The linear model consists of a link function and an error component. The link function is a non-linear intermediary function used to predict the response (y) from linear combinations of the predictor variable (x). The error and link functions used depend on the data type used (for example count, category, continuous interval or continuous ratio) and the probability distribution of the error (Poisson, binomial, gamma or exponential) (Birks and Simpson 2006). For taxon-response models a binomial error distribution and logit link function were used. For logit link functions the linear predictor operates on the log scale of the species abundance (Simpson, pers. comm. 2009).

Generalised additive models (GAMs) are generalised from GLM; the linear function of the predictor variables are replaced by an unspecified (non-parametric) smoothing function. The unspecified smoothing function is obtained by an iterative process of applying smoothers to the data to find the smoothing function that best represents the relationship between the variable and the partial residues (the residuals after removing the effect of all other predictor variables). The data therefore determine the shape of the response curve rather than being limited to the shapes available in parametric GLM (Birks and Simpson 2006). In 3D response surface plots GAM models are fitted for each variable (T_{july} and Cl) separately and thin-plate splines applied to produce a smoothed surface. The splines are applied in all directions with no attempt to make the responses parallel to the axes (Birks and Simpson 2006). Species abundance is plotted as the linear predictor which equates to the fitted log abundance of the species for values of the two covariates (Simpson, pers. comm. 2009). GLMs, GAMs and 3D response surface plots were produced using the R computer software (R Development Core Team, 2004);

GAMs were fitted using mgcv package for R, version 1.3 – 24 (Wood 2007b). HOF models are derived from percentage abundance data whereas GLMs and GAMs are based on presence or absence data. Presence-absence data are more reliable over long environmental gradients where total abundance and total number of taxa differ widely.

Models were assessed using Akaike Information Criterion (AIC) and Bayes Information Criterion (BIC), these are indices of fit which penalises for the number of parameters in the model. Including more parameters in a model improves the fit, but reduces the explanatory power. Therefore a trade-off is required, by parsimony, between the goodness of fit and the number of parameters. AIC penalises any superfluous parameters in the model by adding $(2 \times \text{number of parameters} + 1)$ to the variance and BIC by adding $\log_e n(\text{parameters} + 1)$. Therefore given alternative models involving different numbers of parameters the model with the lowest AIC and/or BIC is selected to give the minimum adequate model (Birks and Simpson 2006).

3.4.4. Indirect and direct gradient analysis (Ordination and constrained ordination)

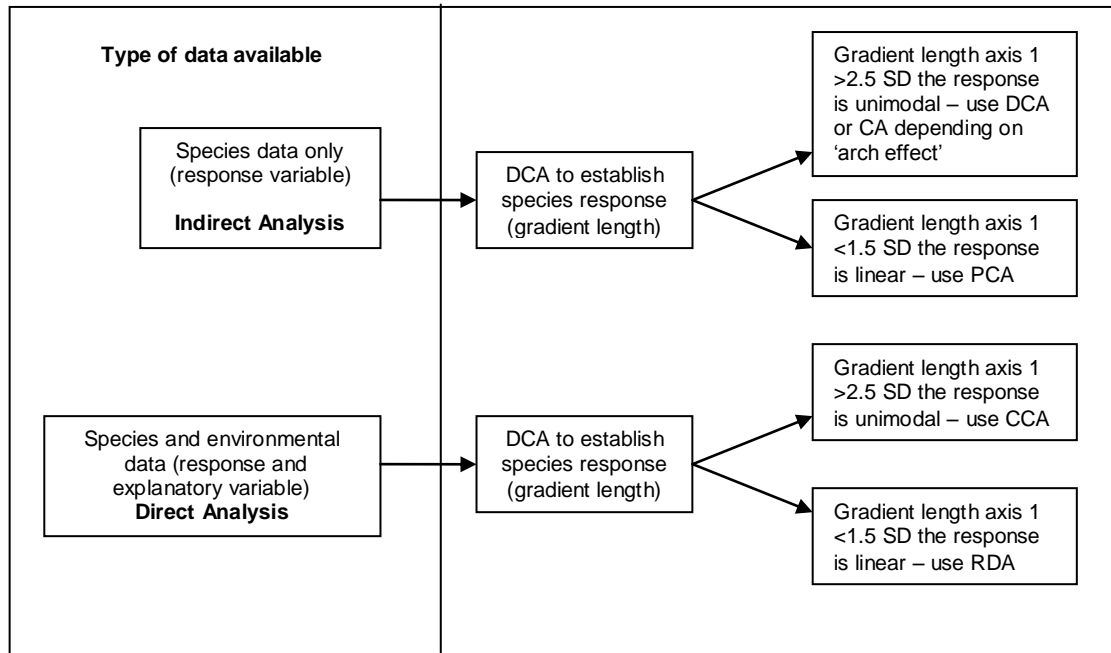
Gradient analysis is used to investigate variation and relationships within datasets by relating the ‘response variable’, for example species composition, to measured or hypothetical ‘explanatory variables’ such as environmental gradients (ter Braak and Prentice 1988). Ordination techniques are a type of gradient analysis where the explanatory variables are theoretical composite latent variables rather than known environmental variables measured in the field and are constructed so they ‘best’ explain the species data.

Indirect gradient analysis explores species composition or environmental variables without reference to the explanatory variables; for example, variability in species composition might be explored independently of any environmental data such as water temperature or depth. It summarises multivariate data in a low-dimensional space and uncovers any underlying latent structure in the data. In indirect gradient analysis, variability in species composition is explained by a *posteriori* knowledge of species ecology and distribution.

In direct gradient analysis the response variables and explanatory variables are analysed at the same time (ter Braak 1987). This is known as constrained ordination as the response variables are constrained by the use of the explanatory variables. Patterns within the response variable are interpreted in relation to the explanatory variables. For example, the chironomid data are analysed in conjunction with the environmental data; the location of the species within the ordination space is linked to, and partially explained by, the environmental gradients within the dataset.

There are two basic types of ordination techniques depending on whether the species abundances show a linear or unimodal response to the latent environmental variables. The species responses are usually dependent on the length of the environmental gradient. Over short gradients, gradient length <1.5 Standard Deviations (SD), the response is assumed to be linear and linear methods are appropriate whereas over longer gradients (>2.5 SD) the response is unimodal (ter Braak 1987; Birks 1995). For gradient lengths between 1.5 and 2.5 SD either linear or unimodal techniques may be appropriate and generally both methods are applied. The choice of techniques, therefore, depends on whether only the 'response variable' or 'response and explanatory variables' are available for indirect or direct gradient analysis respectively and secondly on the amount of variation within the response variable (low variation - linear methods, high variation - unimodal methods). To assess the most appropriate method the data is first examined by Detrended Correspondence Analysis (DCA). This determines the gradient length of the data, in relation to the underlying environmental variables, and is used to inform the choice of statistical techniques as shown in figure 3.6. The individual techniques are then described in sections 3.4.4.1 – 3.4.4.4. These ordination techniques were applied to the modern chironomid data and environmental data (Chapter 4) to determine the factors which influence their distribution and in the interpretation of biostratigraphic data in Chapters 7 and 8.

Figure 3.6. Diagram summarising the procedure for selection of an appropriate ordination model to explore the biological data. See text for explanation of ‘arch effect’.



3.4.4.1. Principal Components Analysis (PCA)

PCA is a method of indirect gradient analysis, based on linear responses, which is used to visualise structure and relationships in the biological or environmental data independently. If a multivariate dataset is visualised as a set of coordinates in a high-dimensional data space with one axis per variable, PCA fits a straight line through these points to minimise the sum of the squared vertical distances between the points and the line (the residual sum of squares). The line represents the first ordination axis, subsequent lines or axes are constructed, orthogonally, to minimise the sum of squared distances along these axes. These ordination axes represent hypothetical latent variables. The goodness of fit of the ordination axis, known as the eigenvalue, is expressed as a percentage of the total variance in the data. The first axis explains most of the variance in the data and has the highest eigenvalue, the amount of variance explained and the eigenvalues decline for subsequent axes.

3.4.4.2. Correspondence Analysis (CA); Detrended Correspondence Analysis (DCA)

CA and DCA are indirect (response variable only) gradient analysis techniques used when response curves are unimodal (Figure 3.6). Correspondence analysis is conceptually similar to PCA but simultaneously ordines both species and samples. The process is iterative; new species scores are calculated by weighted averaging of the site scores and new site scores by weighted averaging of the species scores. The site scores are standardised and the process repeated until convergence i.e. the new site scores are sufficiently close to the previous iteration (Birks and Simpson 2006). Dispersion of the species scores increases steadily and stabilises at a maximum value, this maximum dispersion equates to CA axis 1. The second and higher axes are extracted in a similar way but the trial scores for the new axis are made uncorrelated to previous axes.

DCA is used when an 'arch' (curvature in the ordination) is present in the CA plot. This arises when there is a single strong gradient in the data, the second axis is the first axis folded (Oksanen and Minchin 2002). Detrending methods remove the arch effect by reducing variation along the second axis. The data may be detrended by segments or polynomials although detrending-by-segments consistently performs best (Birks and Simpson 2006) and was used in this study. In detrending-by-segments the first axis is divided into segments, the mean of the trial scores of the second axis are subtracted from the site scores in each segment and the residuals taken as the new second axis.

3.4.4.3. Redundancy Analysis (RDA)

RDA is used to model species-environment relationships where the variation within the species response is linear (van den Wollenberg 1977). It is a constrained form of PCA but whereas in PCA the axes represent hypothetical latent variables which give the smallest total residual sum of squares RDA selects linear combinations of environmental variables that give the smallest total residual sum of squares (ter Braak 1994). Redundancy analysis expresses how much of the variance in the dependent variable, the species data, can be explained by the independent variable, the environmental variable.

The method is based on ordination and multiple regression. Ordination models the species data (abundances or presence/absence data) as a function of the ordination axis and multiple regression models the ordination axis as a function of the environmental variables, so linking the environmental data to the species data in one technique.

3.4.4.4. Canonical Correspondence Analysis (CCA)

CCA is a direct gradient analysis technique used where the response variable is unimodal (Figure 3.6). The species and environmental data are analysed simultaneously to identify the main relationships between species and each environmental variable. The procedure is similar to the iterative process described for Correspondence Analysis (section 3.4.4.2) with an additional step: multiple regression of the calculated site scores on the environmental variables. The fitted values of this regression are then taken as the new site scores (Birks and Simpson 2006). CCA selects linear combinations of environmental variables that maximise dispersion of species scores. Each ordination axis is independent so that an axis is selected to maximise dispersal along this axis, unrelated to previous axes.

3.4.4.5. Analysis and presentation of results

Gradient and ordination analyses were performed using Canoco for Windows version 4.5, software for canonical community ordination, and ordinations plotted using CanoDraw (ter Braak and Smilauer 2002). The taxonomic groupings Tanytarsini, Pentaneurini, Tanypodinae and *Corynoneura* undifferentiated were treated as supplementary. In ordination biplots species and site scores are typically represented by points and environmental variables by arrows, with the variable increasing in the direction of the arrow. The angle between vector arrows approximates to their correlations; environmental variables with strong positive correlations have small angles between their biplot arrows. The origin represents the average and the distance from the origin the magnitude of change, so longer arrows represent a greater increase in that variable. The relative importance of each axis, in explaining the variance within the data, is expressed by the eigenvalue and the total variance by the total inertia. Taxa are positioned in the ordination space on the weighted

average of their site scores which approximates to Gaussian optima along individual environmental gradients. The lakes are located by their site scores which are generally linear combinations of the environmental variables. In indirect gradient analysis (PCA, DCA or CA) samples close together, in ordination space, are inferred to resemble one another in species composition and there is a tacit assumption that samples with similar species composition represent similar environments (Oksanen and Minchin 2002). The relationship between taxon and specific environmental variables is not statistically established but can be achieved by analysis of the known ecological preferences of the species.

Within the ordinations some environmental parameters are included which do not explain any statistically significant proportion of the variance. The significant variables were identified using the 'forward selection' function within Canoco. This is a model building approach; environmental variables are added to the model one at a time. At each step, each variable that is not already in the model is tested for inclusion in the model and the most significant of these variables is added to the model. The procedure is repeated until no other variables significantly explain the remaining variation and these remaining variables can be omitted from the model.

3.4.5. Calibration and environmental reconstruction

There are three main approaches to quantitative palaeoenvironmental reconstruction: (1) indicator species approach, (2) assemblage approach and (3) multivariate indicator species approach involving a mathematical transfer function (Birks 1981, 1995, 2003). These approaches are based on the principle of uniformitarianism i.e. that the present day distribution of organisms and their relationship to environmental variables can be used as a model to infer past environmental conditions. This tacitly assumes that organism – environment relationships have not changed over the time-scale of the study (Birks and Birks 2004).

Of these approaches indicator species have not been widely used for environmental reconstructions using chironomid subfossils. Specific taxa are

qualitatively interpreted as warm- or cool-adapted indicators (Brooks and Birks 2000a; Porinchu and Cwynar 2002; Andreev *et al.* 2004b) but for most chironomid species their precise distributions and ecological requirements are too poorly known for causal relationships to be established. Dimitriadis and Cranston (2001) used modern presence/absence data to map the distribution of 25 chironomid taxa in Australia, infer their climatic envelopes and reconstruct palaeoenvironmental conditions by the mutual climatic range (MCR) method. The MCR technique has been criticised for not taking into account the relative frequencies of taxa in assemblages or the probability of occurrence of an individual taxon (Birks 1995). This approach was not used in this study due to the lack of comprehensive modern chironomid surveys in Arctic Russia.

The modern analogue technique (MAT) is based on the assemblage approach; the fossil assemblage and proportions of the different taxa are compared with the modern assemblages using a dissimilarity measure such as squared chord distance. Having found the modern sample or samples most similar to the fossil sample, the environment at the time the fossil sample was deposited is inferred from the analogous modern sample(s) (Birks 2003). MAT was used in this study to reconstruct July temperatures and continentality. The software used is detailed in section 3.4.5.2 and the results presented in Chapters 7 and 8.

Multivariate transfer functions derive estimates of the taxon optima for an environmental variable from a modern training or calibration set rather than the modern autecological observations used in MCR methods. The modern chironomid assemblages in the surface sediments and environmental variables are determined in the calibration set lakes. The modern relationship between taxon and a selected environmental variable can then be modelled numerically, by regression, from the calibration set data. The resulting transfer function is then applied to the down-core fossil assemblages to give quantitative estimates of the past environmental variable (Birks 2003). As with ordination techniques, section 3.5.3, whether the use of linear or unimodal techniques is generally dictated by the length of the gradient of variation within the biological data, measured in standard deviations. With longer gradient lengths >1.5 SD unimodal methods (weighted averaging (WA) and weighted averaging partial

least squares (WA-PLS)) are more appropriate (Birks 1995) and these were used in this study. The numerical techniques used in this study to generate the transfer function are described in section 3.4.5.1. Detailed descriptions of the methods used for quantitative palaeoenvironmental reconstructions from biological data, their assumptions and limitations can be found in Birks (1995; 2003) and Birks and Birks (2004).

3.4.5.1 Inference models

Several numerical techniques have been developed for deriving transfer functions (Birks 1995). Two-way weighted averaging (WA) and weighted averaging partial least squares (WA-PLS) were used in this study as they perform consistently well with a range of data, do not involve an excessive number of parameters to be estimated and fitted, are statistically robust and computationally economical (Birks 2003). Weighted averaging assumes that taxa will be most abundant close to their optima for a particular environmental variable. The estimated species temperature optima, for example, is therefore the average of all the temperature values of sites at which the taxon occurs weighted by the taxon's relative abundance (Birks 2003). Indicator taxa with narrow tolerances can be given greater weighting, in tolerance downweighting, but reliable tolerances are difficult to derive. In weighted averaging the predictive power is reduced if the species optimum lies outside the observed environmental gradient.

Weighted averaging also calculates the 'average of averages' so the environmental range is effectively compressed. The full range of the data is restored by deriving regression coefficients and applying them to the reconstructed values (deshrinking regression). Therefore, in WA regression and calibration, species optima are calculated by weighted averaging of sample scores (WA regression), new sample scores calculated by weighted averaging of the species optima (WA calibration) and the environmental variable regressed on the preliminary new sample scores (deshrinking regression) and the fitted values taken as an estimate of the environmental variable. Two approaches, classical or inverse regression, can be used in deshrinking regression. Classical regression regresses the weighted averaging of species

scores on the environmental variable and inverse regression the environmental variable on the weighted averaging species scores. Weighted averaging partial least squares (WA-PLS) regression refines the WA model by taking into account variations (scatter) in the original species abundance data to improve the estimate of species optima (ter Braak and Juggins 1993).

The following transfer functions were generated, in C2 (Juggins 2005) using the Russian, Norwegian and combined species and environmental datasets: weighted-averaging (WA) and weighted averaging with tolerance down-weighting (WATOL) with inverse and classical regression coefficients and weighted averaging partial least squares (WA-PLS) regression. The performance of the models was evaluated by correlating the observed and estimated July air temperature for the training set (r^2) and calculating the root mean square error (RMSE) i.e. the amount the estimated temperature varies from the observed value. For comparison with published models, the performance of the model was evaluated by leave-one-out or jack-knifed cross validation. In leave-one-out cross validation the model is repeatedly run leaving out each sample in turn, the transfer function is applied to the omitted sample to give a predicted value for that sample. This is subtracted from the known value to give a prediction error; prediction errors are accumulated to give a 'leave-one-out' root mean square error of prediction (RMSEP) (Birks 2003). In down-core reconstructions the data was resampled by bootstrapping to obtain a sample specific error of prediction and bootstrapped RMSEP. In bootstrap error estimation, samples are selected at random from the training set to form a subset the same size as the training set. Samples are replaced after selection so that a sample may appear more than once in the training set to mimic sampling variation. Any samples not selected form a bootstrap test set. The bootstrapped training set is then used to estimate the environmental variable for the bootstrapped test set. This is repeated for 1000 cycles, Monte Carlo simulation, and the standard deviation of the inferred values calculated to give the estimation error. A second error component is derived from the root mean square of the difference between observed temperatures and mean bootstrap estimates of temperature when the modern sample is in the bootstrap test set.

The estimated RMSEP for a fossil sample is the square root of the sum of squares of these two components (Birks 2003).

The final model used in reconstructions was selected on the basis of lowest RMSEP, highest r^2 and lowest mean and maximum bias with the smallest number of useful components (ter Braak and Juggins 1993; Birks 2003). A component was considered useful if it gave a RMSEP reduction of $\geq 5\%$ of the one-component model (Birks 1995). The development and selection of the inference models used in this study are discussed in Chapter 6. These models were then applied to the fossil assemblages from the selected cores to reconstruct July air temperature and continentality.

3.4.5.2. Analogue matching techniques

The computer programme MAT (modern analogue technique) in C2 (Juggins 2005) was used (1) to perform an 'analogue' match between the modern and fossil (down-core) chironomid data to evaluate the reliability of the reconstruction and (2) to produce a July air temperature reconstruction independent of regression analysis. The optimal number of analogues and the cut-off value of the squared chord distance dissimilarity used to define a 'good' analogue were determined using the MAT function in R (R Development Core Team, 2004). The optimum number of analogues (n), based on the lowest RMSE, was then applied to the MAT programme in C2 (Juggins 2005) to reconstruct July air temperatures and continentality for the fossil samples using MAT and weighted modern analogue (WMAT) techniques. In MAT the reconstructed value is the mean of the variable from each of the n -closest analogues. In WMAT the reconstructed value is the mean of the variable from each of the n -closest analogues weighted by the reciprocal of the dissimilarity between the fossil sample and the modern analogue. Therefore the environmental variable from a lake with a similar faunal composition to the fossil sample is given a higher weighting than the variable with a more dissimilar fauna in the reconstruction. The temperatures and continentality reconstructions for the cores from the Putorana Plateau and Pechora basin, and their comparisons with other reconstruction techniques, are presented in Chapters 7 and 8 respectively.

3.4.5.3. Down-core reconstruction of environmental variables

Environmental reconstructions, inferred from down-core chironomid assemblages, were performed on cores from PONE, PTHE, AFOX, KHAR and VORK5 (see Chapters 7 and 8) to assess changes in July air temperature and continentality. The development of the July temperature and continentality transfer functions are discussed in Chapter 6, using the WA, tolerance-downweighted WA and WA-PLS methods described in section 3.4.5.1. These variables were also constructed using MAT and WMAT as detailed in section 3.4.5.2. The reconstructions for the Putorana cores (PONE and PTHE) are presented in Chapter 7 and from the North-east European Russia cores (KHAR and VORK5) in Chapter 8. Before reconstruction the chironomid counts were converted to percentages and square-root transformed as described in section 3.4.1.

3.4.5.4. Down-core ordination and zonation

Ordination techniques described in section 3.4.3 and applied to the calibration set data in Chapter 4 were also used in the interpretation of the fossil chironomid assemblages from the sediment cores (see Chapters 7 and 8). Changes in the chironomid assemblages in the down-core samples were compared with the modern environmental data using CCA with the modern species active and the fossil species added as supplementary passive samples. A time track was applied by joining the samples stratigraphically from the core bottom to the core top to show the trajectory of the fossil samples against the direction of influence of the environmental variables selected as significant by forward selection (section 3.4.4.4). CCA axis 1 and axis 2 sample scores, derived from the chironomid assemblages, were extracted and plotted stratigraphically with the chironomid data to provide a time-series record of compositional changes. Shifts in sample score down the core helps to identify major changes in chironomid composition which can then be related to environmental change. Variations in the rate of compositional change of the chironomid fauna were estimated from the DCCA scores following ordination with age as the sole constraint environmental variable (Birks 2007). Ordinations were performed using Canoco for Windows, version 4.5 (ter Braak and Smilauer 2002).

Chironomid assemblages from the cores taken from Lake Kharinei (KHAR), VORK5, PONE and PTHE were zoned by constrained optimal partitioning using the ZONE program, version 1.2 (Juggins 1991), with untransformed species percentage data (Birks and Gordon 1985). Zonation identifies sections of the sediment core with broadly similar faunal composition that differ from underlying or overlying sediments and is useful in the description and interpretation of stratigraphic data. A constrained ordination of the stratigraphically ordered chironomid assemblages is performed and the data classified into zones with similar faunal composition. In optimal partitioning, unlike other zonation procedures such as CONSLINK, CONISS, SPLITLSQ and SPLITINF, the zones are not nested within previous divisions and are decided afresh for each successive number of zones. The location of the zone boundaries is determined to minimise the within-group sum-of-squares. The number of significant zones was determined using the broken-stick method (Bennett 1996). The proportion of the variance explained by addition of another zone in a randomised dataset, the 'broken stick model', is compared with the proportion from the original dataset. The maximum number of zones occurs where additional zones do not explain more of the variance in the original data than the randomised data. Stratigraphic diagrams and zones showing the significant change in faunal composition were drawn using C2 version 1.4.3 software (Juggins 2005).

3.5. Summary

This chapter has described the field and laboratory methods involved in this study and justified their suitability for this investigation. Where samples or data have been used, which were not derived by the author, the researchers and organisations involved have been identified. As discussed in Chapter 1, the study comprises two main aims: (1) an exploration of the relationships between the present-day fauna and environmental variables and (2) the reconstruction of palaeoenvironmental records from lake sediment cores. The methods described in this chapter enabled the compilation of datasets of the modern chironomid fauna from lakes with known physical, chemical and biological characteristics. Use of the statistical methods outlined allowed robust, quantitative inferences to be made about the relationships between the fauna and the environmental variables which provided the framework for

reconstructing the past environment. The down-core palaeoenvironmental records were complemented by isotopic and sedimentary analysis to facilitate their interpretation. The application of ^{210}Pb and ^{14}C dating provided a chronology for the sediment records to enable comparisons with instrumental and other palaeoclimatic records.

Chapter 4

Factors influencing present-day chironomid distribution

4.1 Introduction

This chapter investigates the relationships between the chironomid faunal assemblages and environmental variables for the Russian lakes, the Norwegian lakes and the regions combined. As discussed in Chapter 1, one of the aims of the research was to determine whether a regional Russian training set and inference model would be more accurate at reconstructing past climatic variables in northern Russia than a combined Norwegian-Russian training set which would have a greater number of lakes and a more even distribution of lakes along the environmental gradients. To combine the datasets from two geographical regions:

1. the physical and environmental variables of the lakes,
2. the faunal compositions of the surface assemblages,
3. the environmental variables driving chironomid distribution and abundance,
4. the species composition of morphotypes, and
5. the responses of individual taxa to environmental variables, such as their July air temperature optima,

need to be broadly similar. In this chapter the similarity between the Russian, Norwegian and combined datasets for the first three criteria are examined, the later two criteria are examined in Chapters 5 and 6.

In this chapter the factors influencing the distribution of the present-day fauna are also examined to determine whether the link between the climatic variables and taxonomic distribution is strong enough to allow the development of a palaeoclimatic transfer function. The results of the following analyses form the basis for subsequent palaeo-environmental interpretations.

4.2. Russian surface sediment data-set

In total, 100 lakes were sampled from 5 distinct geographic regions within the Russian Federation. These consisted of 27 lakes from north-east European Russia, 6 lakes from the Komi Republic, 10 from the Putorana Plateau, 21 from the Lena River delta and 36 lakes from Central Yakutia (Figures 2.1-2.7). The biological and physical characteristics of the study areas, and location of the lakes, are described in Chapter 2 and the provenance of the samples of the samples detailed in Table 3.5. The physical and environmental characteristics recorded in each region varied; this chapter considered only those variables common to all locations. A more even geographical distribution of lakes, although desirable, was not possible due to economic and logistic constraints.

4.2.1. Environmental data

The locations of the lakes sampled, together with their associated environmental variables and water chemistry data are shown in Table 4.1. Variable specific minima, maxima, means, medians and standard deviations are summarised in Table 4.2.

Lake code	Latitude (N)	Longitude (E)	Altitude (m ASL)	Coast (km)	pH	Cond (uS/cm)	Water depth (m)	Tjuly (°C)	Tjan (°C)	Cl	MAP (mm)	SP (mm)	Cl ueq/l	SO4 ueq/l	Ca ueq/l	Mg ueq/l	Na ueq/l	Veg. type	Other lakes	Human impact
F3-2	67.93	54.03	13	34	6.9	16.1	4.3	13.2	-15.9	33	423	139	41	20	90	35	40	T	Y	0
F3-3	67.93	54.05	20	34	6.79	20.5	1.5	13.2	-15.9	33	423	139	47	15	95	41	64	T	Y	0
F3-5	67.92	54.03	17	36	6.58	17.3	3.3	12.3	-15.9	31	423	139	37	13	78	41	41	T	Y	0
F3-6	67.93	54.00	18	35	6.97	32.7	1.3	13.2	-15.9	33	423	139	89	10	152	92	101	T	Y	1
F3-12	67.95	53.93	13	35	6.63	16.8	2.8	13.2	-15.9	33	422	140	36	13	65	36	47	T	Y	1
F4-2	68.00	52.38	4.8	43	7.07	42.7	6	13	-16	33	418	136	123	16	176	87	148	T	Y	0
F4-4	68.00	52.45	72	42	6.98	42.9	1.1	12.5	-15.7	31	418	136	104	14	238	87	108	T	Y	0
F4-5	68.00	52.40	72	43	7.24	78.7	1.1	12.5	-15.7	31	418	136	190	32	405	196	207	T	Y	0
F6-2	64.32	59.08	225	471	6.22	10	15	15.1	-19	44	637	212	6	43	47	15	17	F	Y	0
F7-3	67.12	56.68	75	140	5.73	18	0.7	13.5	-18.7	39	465	157	30	28	100	39	21	T/M	Y	1
F7-4	67.12	56.72	78	140	5.14	15	1	13.5	-18.7	39	465	157	37	23	55	24	13	T/M	Y	1
F7-5	67.13	56.68	82	139	7.4	116	2.5	13.5	-18.6	39	465	157	51	87	778	345	84	F/T	Y	1
F8-2	67.87	59.72	23	52	6.36	16	3.5	13.3	-19.9	41	445	153	51	12	59	37	47	T	Y	0
F8-4	67.88	59.67	15	50	6.71	30	6	13.2	-19.9	40	445	153	46	14	1497	76	48	T	Y	0
TDRA 2	65.98	60.02	59	262	7.08	4.4	6.6	14.6	-18.9	42	512	170	51	20	135	61	122	F	Y	1
TDRC 2	66.10	60.25	50	252	7.44	3.25	1.7	14.5	-19	42	488	162	68	83	813	266	152	F	N	1
TDRD 2	67.12	59.57	110	135	6.82	2.4	5.2	13.3	-19.5	40	445	155	65	30	344	109	70	T	N	1
TDRE 1	65.25	59.67	514	343	6.92	2.7	17	12.6	-17.7	36	555	187	76	76	279	121	96	F/T	N	0
TDRU11a	67.45	63.08	60	266	7.6	41.4	1.7	13	-18.2	37	531	175	34	29	250	113	90	F	N	1
TDRU 42a	65.97	57.27	116	170	7.29	60.2	8.7	14.6	-19	42	490	167	71	5	284	183	82	T	N	0
Mitro	67.85	58.98	132	141	6.8	67.2	20	12.6	-19.5	39	447	155	124	26	419	141	120	T	Y	0
Vanuk-ty	68.00	62.75	123.9	121	6.77	70.9	25	12	-18.9	36	439	148	56	21	429	158	100	T	Y	0
GYXO	68.165	92.173056	569	543	7.28	22	13	11.8	-29.4	55	500	174	4	39	144	57	30	T	Y	0
AFOX	68.166389	92.228056	573	548	7.28	39	4.9	11.8	-29.4	55	500	174	3	19	62	44	10	T	Y	0
WILD	68.17	92.240556	557	544	7.28	26	3.8	11.9	-29.4	55	500	174	5	30	143	59	29	T/M	Y	0
ARTE	68.150833	92.174444	631	541	8.05	17	3.5	11.5	-29.4	55	500	174	5	39	118	41	28	T	Y	0
PONE	68.1425	92.203056	596	546	7.7	27	5	11.7	-29.4	55	500	174	4	30	170	80	33	T	Y	0
PTWO	68.133056	92.194722	740	546	7.74	39	3.7	10.9	-29.4	53	500	174	3	35	191	105	34	T	N	0

Table 4.1. Physical and chemical characteristics of the Russian lakes

(Abbreviations: Coast: shortest distance to coast, Cond: conductivity, Tjuly: mean July air temperature, Tjan: mean January air temperature, Cl: continentality index, MAP: mean annual precipitation, SP: mean summer (June-August) precipitation, Veg type: vegetation type, Other lakes: proximity of other lakes, Concentrations of ions in lake water; Cl: chloride, SO4: sulphate, Ca: calcium, Mg: magnesium, Na: sodium)

Table 4.1. continued

Lake code	Latitude (N)	Longitude (E)	Altitude (m ASL)	Coast (km)	pH	Cond (uS/cm)	Water depth (m)	Tjuly (°C)	Tjan (°C)	Cl	MAP (mm)	SP (mm)	Cl ueq/l	SO4 ueq/l	Ca ueq/l	Mg ueq/l	Na ueq/l	Veg. type	Other lakes	Human impact
PTHE	68.203333	92.178889	805	536	7.28	19	3.9	10.5	-29.4	53	500	174	2	27	127	69	32	T	N	0
PFOR	68.202222	92.157222	780	535	7.27	9	4.9	10.6	-29.4	53	500	174	2	28	72	33	22	T	N	0
PFIV	68.160278	92.046111	668	536	7.28	7	6.2	11.3	-29.4	54	500	174	10	24	70	32	13	T	N	0
IGAR	67.508889	86.5575	36	362	7.31	38	12.5	15.3	-28.6	60	511	165	10	77	243	132	20	F	Y	1
NERU	67.5255	62.757611	121	155	7.25	34	5.85	13.2	-19.5	40	481	162	23	38	256	123	53	T	Y	1
KHAR	67.362806	62.750722	108	166	7.25	64	7.8	13.3	-19	39	490	164	17	31	554	165	41	T	Y	0
VORK3	67.515194	62.993056	122	162	7.25	73	2.6	13.2	-19	39	481	162	23	38	329	86	29	T	Y	1
SAND	66.921833	58.77925	86	160	7.25	30	6.6	12.1	-19.6	38	460	157	27	23	205	76	55	F	N	1
VORK5	67.856972	59.025722	123	55	7.16	20	2	11.9	-19.5	37	445	153	102	54	165	74	84	T	Y	0
Y1700	63.736167	121.63367	110	876	8.55	177	2	18.4	-37	85	261	117	37	6	629	441	159	F	Y	2
Y1701	63.673167	123.12617	119	860	8.84	109	1	18.3	-37	84	263	117	22	1	434	271	102	F	Y	0
Y1703	64.499833	122.7175	179	777	9.92	257	0.75	18	-37.3	84	261	115	109	65	753	1390	526	F/P	N	1
Y1704	64.510333	122.717	174	776	8.06	177	1.6	18	-37.3	84	267	113	28	1	853	629	126	F	N	0
Y1705	64.493333	122.72083	177	777	9.01	284	0.9	18	-37.3	84	261	115	128	33	1238	1283	264	F/P	N	1
Y1706	64.4745	122.73067	178	779	8.97	270	1.1	18	-37.3	84	261	115	54	46	1427	970	177	F/P	N	1
Y1707	64.4565	122.39767	180	787	9.57	305	1.6	18	-37.3	84	263	115	185	49	838	1776	496	F/P	Y	1
Y1708	64.1625	121.99	165	826	7.7	304	1.8	18.1	-37.2	84	262	116	9	6	26	24	23	F	Y	1
Y1709	63.725333	121.959	115	871	8.37	340	1.8	18.3	-37	84	261	117	288	18	1208	1513	813	F/P	Y	2
Y1711	63.688333	122.07133	131	872	8.6	368	2	18.3	-37.1	85	261	116	202	5	773	2681	1122	F/P	N	1
Y1712	63.710167	122.01983	125	878	8.66	146	1.2	18.3	-37.1	85	261	116	8	1	734	738	258	F/P	N	2
Y1713	63.706833	121.89433	116	879	7.95	341	1.9	18.3	-37	84	261	117	99	15	1657	1612	618	F/M	Y	2
Y1716	63.718833	122.37717	130	869	8.73	208	1.12	18.3	-37.1	85	261	116	14	38	933	761	448	F/P	Y	2
Y1717	63.786833	122.1975	99	865	7.97	391	2.7	18.4	-36.9	84	261	116	68	2	1462	1957	648	F/P	N	1
Y1718	63.748	121.67533	105	879	9.47	92	0.9	18.4	-37	85	261	117	21	1	412	341	165	F	N	2
Y1719	63.761667	121.74883	103	879	7.94	70	3	18.4	-37	85	261	117	31	1	313	247	106	F	Y	2
Y1720	63.759	121.75083	104	877	8.83	113	3.8	18.4	-37	85	261	117	28	1	564	445	215	F	Y	1
Y1721	63.801333	122.18917	112	864	7.96	277	2.6	18.4	-37	85	261	116	64	1	1257	1250	492	F/P	Y	1
Y1722	63.804667	122.16567	105	864	7.88	256	1.2	18.4	-37	85	261	116	32	1	1362	888	492	F	Y	1
Y1723	63.726667	121.53467	96	884	8.02	100	4	18.5	-36.9	85	261	117	16	1	524	374	133	F	N	2
Y1724	63.663667	121.264	112	896	7.85	151	2	18.4	-37	85	262	117	23	1	798	561	313	F	Y	0
Y1725	63.670333	121.30833	118	895	7.78	118	1.9	18.3	-37	84	262	117	141	98	589	418	304	F	Y	0

Table 4.1. continued

Lake code	Latitude (N)	Longitude (E)	Altitude (m ASL)	Coast (km)	pH	Cond (uS/cm)	Water depth (m)	Tjuly (°C)	Tjan (°C)	Cl	MAP (mm)	SP (mm)	Cl ueq/l	SO4 ueq/l	Ca ueq/l	Mg ueq/l	Na ueq/l	Veg. type	Other lakes	Human impact
Y1726	63.674833	121.30017	117	894	7.79	115	2	18.3	-37	84	262	117	23	1	519	409	265	F	Y	0
Y1727	63.589833	121.4985	127	899	8.46	476	1.35	18.3	-37.1	85	262	117	648	29	1013	2451	2344	F/P	Y	2
Y1729	63.625	121.49617	125	896	7.98	321	1.7	18.3	-37.1	85	262	117	139	1	1213	1727	531	F/P	N	1
Y1730	61.960167	129.4085	188	748	8.6	89.1	1.4	18.5	-39.3	91	242	113	29	79	325	238	304	F	N	1
Y1731	61.968333	129.37967	204	751	8.48	448	0.7	18.4	-39.4	91	242	113	186	199	1552	1694	2518	F	N	1
Y1732	62.124833	128.403	208	805	8.96	213	1.5	18.4	-39.4	91	244	115	72	55	1277	855	509	F	N	0
Y1733	62.388833	130.86583	130	709	9.15	637	2.3	18.9	-39.1	91	241	114	389	17	1078	5839	2627	F/P	Y	2
Y1735	62.5855	131.11017	139	712	8.8	507	3.7	18.8	-39.1	90	254	120	202	3	1572	3906	957	F	N	0
Y1737	62.584833	131.22733	144	707	8.74	336	1.5	18.8	-39.1	90	254	120	60	2	1208	2262	457	F	N	1
Y1739	62.785333	130.72933	123	741	8.16	356	1.8	18.9	-39	90	250	118	168	1	1587	1382	779	F/P	N	2
Y1740	62.805833	130.64883	122	746	9.06	1802	17.1	18.9	-39	90	250	118	2039	1	239	16776	8873	F	Y	2
Y1741	62.815	130.261	111	762	9.03	2980	4.1	19	-39	90	248	117	5896	1	329	17270	25141	F/P	N	1
Y1743	62.736833	130.44283	135	749	8.23	110.3	3.7	18.8	-39.1	90	248	117	51	1	336	317	344	F	N	1
Y1746	62.050333	129.48367	208	752	8.22	269	0.9	18.4	-39.4	91	239	112	276	38	1921	1012	535	F/P	N	2
LS-1	71.510667	128.87367	42	16	7.7	58	2	9.1	-34.3	57	269	114	28	138	344	173	48	T	Y	0
LS-2	71.510667	128.8715	42	16	7.2	143	1.2	9.1	-34.3	57	269	114	27	760	998	609	52	T	Y	0
LS-3	71.5	128.87267	67	17	7.4	58	0.95	8.9	-34.2	57	269	114	12	219	419	197	35	T	N	0
LS-4	71.516	128.86217	20	17	7.4	70	2.6	9.2	-34.4	58	269	114	23	292	439	214	43	T	Y	0
LS-5	71.501667	128.89917	88	16	7.3	53	2.2	8.8	-34.1	57	269	114	22	235	369	140	43	T	N	0
LS-6	71.498667	128.89433	76	16	7.2	41	2.2	8.9	-34.1	57	290	120	16	135	264	132	35	T	N	0
LS-7	71.498667	128.8795	69	17	7.3	28	2.2	8.9	-34.2	57	290	120	14	38	165	99	26	T	N	0
LS-8	71.5	128.857	68	18	7.4	51	2.2	8.9	-34.2	57	269	114	20	227	314	156	30	T	N	0
LS-10	71.8775	127.06217	9	77	7.4	20	3	9.7	-34.7	59	276	112	13	19	130	49	17	T	N	0
LS-11	71.890833	127.04467	3	80	7.5	39	3	9.8	-34.7	59	276	112	17	23	274	123	30	T	Y	0
LS-12	71.9015	127.03583	2	80	7.4	38	1.7	9.8	-34.7	59	276	112	26	33	245	132	39	T	Y	0
LS-13	71.9015	127.017	3	80	7.5	56	3.4	9.8	-34.7	59	276	112	133	58	299	156	135	T	Y	0
LS-15	71.8675	127.03917	22	83	7.3	30	2	9.8	-34.7	59	276	112	16	44	190	115	30	T	Y	0
LS-16	71.866833	127.039	22	83	7.4	29	2.2	9.7	-34.6	59	276	112	18	48	185	107	26	T/M	Y	0
LS-17	71.8695	127.05733	17	83	7.5	53	1	9.7	-34.7	59	276	112	34	42	439	132	48	T/M	Y	0
LS-19	71.874	127.08583	8	80	7.7	101	2.2	9.7	-34.7	59	276	112	47	38	554	502	117	T/M	Y	0
LS-24	69.397	125.121	57	259	9.1	68	1.9	12.5	-36.2	68	312	122	12	10	479	280	52	F/M	Y	0

Table 4.1. continued

Lake code	Latitude (N)	Longitude (E)	Altitude (m ASL)	Coast (km)	pH	Cond (uS/cm)	Water depth (m)	Tjuly (°C)	Tjan (°C)	Cl	MAP (mm)	SP (mm)	Cl ueq/l	SO4 ueq/l	Ca ueq/l	Mg ueq/l	Na ueq/l	Veg. type	Other lakes	Human impact
LS-25	69.400667	125.12983	56	259	7.9	66	8	12.5	-36.2	68	312	122	19	19	459	271	57	F	Y	0
LS-27	69.043667	124.20833	101	312	7.4	23	3.1	13	-36.5	70	307	121	12	33	170	90	17	F	Y	0
LS-28	69.042833	124.2195	104	313	7.5	31	4.5	13	-36.4	70	307	121	13	40	210	123	26	F	Y	0
LS-30	70.678667	125.8675	175	153	7.0	10	2	10.1	-34.7	60	331	127	5	15	55	16	17	T/M	N	0
K4	62.99217	52.43978	125	500	9.2	40	-	16.4	-	-	610	209	-	-	-	-	-	F	Y	1
K5	62.97861	52.38883	130	5000	6.2	20	-	16.3	-	-	610	209	-	-	-	-	-	F	Y	0
K6	62.92594	52.49744	145	505	5.6	10	-	16.3	-	-	610	209	-	-	-	-	-	F	N	0
K7	62.15531	50.50294	65	545	8.0	90	-	17.2	-	-	567	204	-	-	-	-	-	F	N	1
K10	61.62256	53.92278	102	670	9.5	40	-	17.3	-	-	640	199	-	-	-	-	-	F	N	2
K11	61.21397	52.21372	95	675	7.2	40	-	17.2	-	-	607	204	-	-	-	-	-	F	N	1

	RUSSIAN LAKES (94 lakes)				
	Minimum	Mean	Median	Maximum	Std dev
Latitude (N)	61.21397	66.495119	67.116667	71.9015	
Longitude (E)	50.50294	99.482238	121.6545	131.22733	
Altitude (m ASL)	2.0	150.5	110.5	805.0	175.9
Distance to coast (km)	16	485	503	5000	566
pH	5.14	7.70	7.50	9.92	0.89
Conductivity (uS/cm)	2.4	160.1	58.0	2980.0	356.4
Water depth (m)	0.7	3.8	2.2	25.0	4.3
T _{july} (°C)	8.8	14.5	13.4	19.0	3.5
T _{jan} (°C)	-39.4	-30.5	-34.7	-15.7	8.4
Continentality Index	31	63	59	91	21
Mean annual precipitation (mm)	239	349	276	637	107
Summer (JJA) precipitation (mm)	112	134	118	212	24
Cl (ueq/l)	2	149	33	5896	639
SO ₄ (ueq/l)	1	47	26	760	92
Ca (ueq/l)	26	528	340	1921	470
Mg (ueq/l)	15	894	162	17270	2551
Na (ueq/l)	10	611	87	25141	2747

Table 4.2. Summary of environmental variables for the Russian lakes

Many of the environmental variables, particularly conductivity and water chemistry, show wide variability in the Russian lakes (Table 4.2). For example, magnesium ion concentrations vary from 15 to 17270 $\mu\text{eq/l}$ and sodium ion concentrations from 10 to 25140 $\mu\text{eq/l}$. Analysis of the chemical characteristics of the lakes by geographical region (Figure 4.1) indicated that, with the exception of calcium ions concentrations, the measured variables vary to a greater degree in the Yakutia area. This is particularly evident in the ranges of electrical conductivity, chloride and sodium ions and results primarily from extreme values in two lakes (Y1740 and Y1741). The Yakutian lakes also experience a more continental climate with higher July air temperatures (T_{july}), lower January air temperatures (T_{jan}) and lower precipitation than lakes from other regions in the Russian training set (Table 4.1). The high concentrations of major anions and cations, and related variables, are strongly affected by the negative hydrological balance in Central Yakutia and land use intensity in the lakes' catchments (Kumke *et al.* 2007). The wide differences between the mean and median values (Table 4.1) suggest the water chemistry variables have skewed distributions. This was confirmed by kernel density plots and variables were normalised by log transformation prior to further analysis (Figure 4.2).

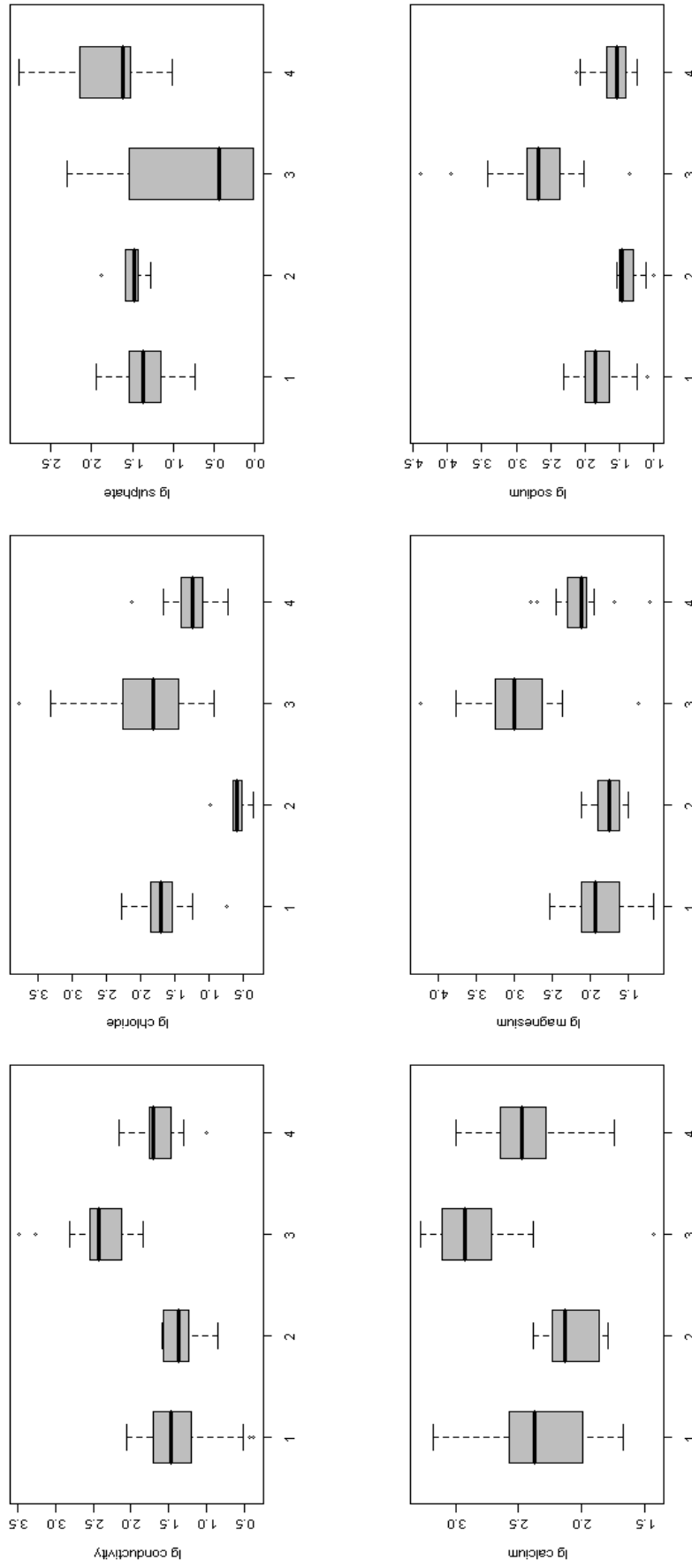


Figure 4.1. Box-Whisker plots for selected water chemistry characteristics of the Russian lakes. The Box-Whisker plots are categorised by geographical location. 1: North-east European Russia, 2: Putorana Plateau, 3: Centra, Yakutia and 4: Lena Delta. The box is drawn between the 1st and 3rd quartile with the median represented by the black horizontal line; the vertical lines or whiskers represent the maximum and minimum values unless outliers are present (represented by circles) when whiskers are drawn at 1.5 times the inter-quartile range.

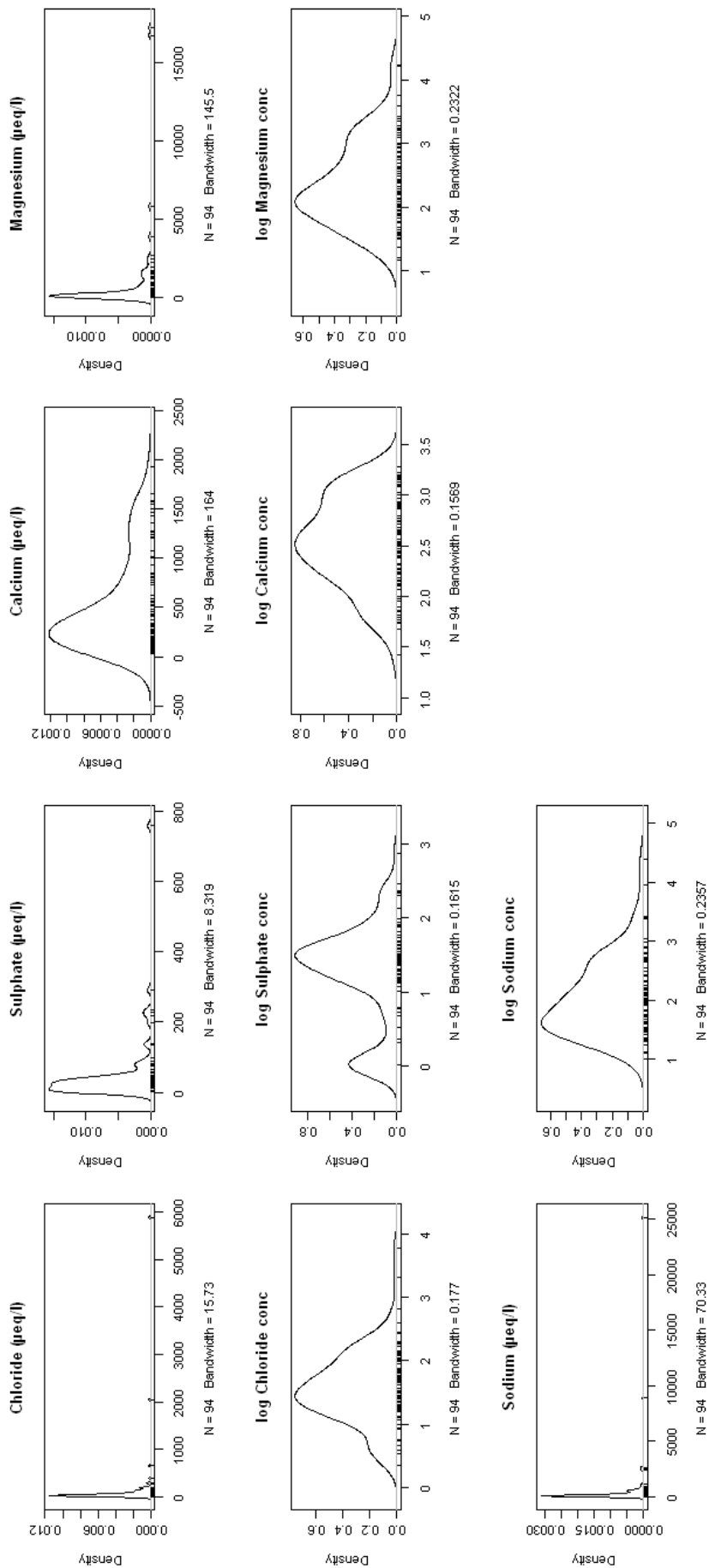


Figure 4.2. Kernel-density estimates showing the distribution of un- and log-transformed major anion and cation concentrations within the Russian lakes

The distributions of the climatic variables; temperature, continentality index and precipitation, visualised by kernel-density estimations, appear bimodal due to discontinuous climate gradients (Figure 4.3). For example there is an absence in the dataset of lakes with mean July air temperatures (T_{july}) between 15.3°C (IGAR) and 18°C (Y1703). The Komi lakes, with T_{july} 16.3 – 17.3°C, are used in the development of the inference models specifically to give a more even distribution along the temperature gradient (see Chapter 6) but were not included in the analysis of factors influencing the modern chironomid distribution (this Chapter) as water chemistry data were unavailable. Lakes with intermediate summer temperatures are located further north in central Siberia, near Olenek and Zhigansk or further south in European Russia, but material from these areas was not available. The distributions of climate variables are also distorted by the high proportion of lakes from Yakutia (36 out of a total of 94 lakes) with high T_{july} , high continentality indices and low T_{jan} , located more than 700km from the coast (Table 4.1).

Multiple regression analysis of the quantitative environmental and log transformed water chemistry variables indicated there are strong correlations between several of the variables (Table 4.3). Latitude is strongly negatively correlated to July air temperature ($r^2 = -0.96$) and longitude to January air temperatures, continentality index and annual and summer precipitation ($r^2 > -0.77$). Annual precipitation showed strong positive correlation with summer precipitation ($r^2 = 0.98$). Conductivity, Mg and Na were also positively correlated ($r^2 > 0.78$). The results suggest there is considerable redundancy within the environmental variables and that variables could be removed to produce the minimal adequate model whilst retaining the goodness of fit. This procedure is described later, in section 4.2.4.

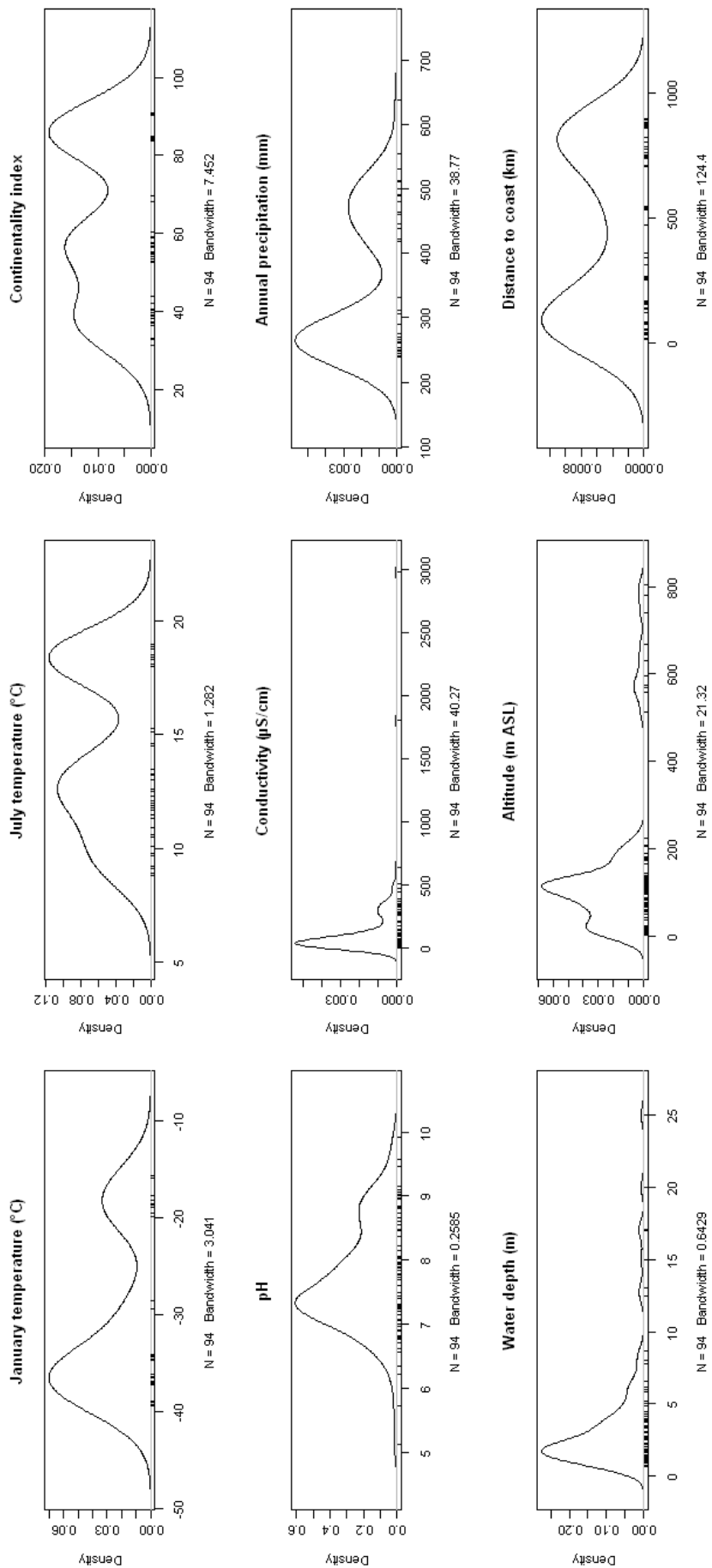


Figure 4.3. Kernel-density estimates showing the distribution of climate and physical variables within the Russian lakes

	Latitude (N)	Longitude (E)	Altitude (m ASL)	Distance to coast (km)	pH	Ig Conductivity (uS/cm)	Water depth (m)	July air temp (°C)	Jan air temp (°C)	Continental Index	Annual precipitation (mm)	Summer (JJA) precipitation (mm)	Ig Cl (ueq/l)	Ig SO4 (ueq/l)	Ig Ca (ueq/l)	Ig Mg (ueq/l)
Longitude (E)	-0.1329															
Altitude (m ASL)	-0.0835	-0.0617														
Distance to coast (km)	-0.8454	0.4915	0.2883													
pH	-0.5485	0.6643	0.0331	0.7085												
Ig Conductivity (uS/cm)	-0.5557	0.5920	-0.2044	0.6172	0.7183											
Water depth (m)	0.0381	-0.3562	0.1903	-0.1457	-0.2636	-0.1990										
July air temp (°C)	-0.9598	0.2643	-0.0860	0.8610	0.6248	0.6548	-0.1216									
Jan air temp (°C)	0.2865	-0.9798	-0.0298	-0.6382	-0.7295	-0.6408	0.3373	-0.4044								
Continental Index	-0.6249	0.8480	0.0002	0.8454	0.8127	0.7569	-0.3034	0.7243	-0.9229							
Annual precipitation (mm)	0.2386	-0.8662	0.4193	-0.4263	-0.6427	-0.7026	0.4636	-0.4069	0.8349	-0.7966						
Summer (JJA) precipitation (mm)	0.1188	-0.7781	0.5413	-0.2724	-0.5458	-0.6329	0.4870	-0.3073	0.7232	-0.6680	0.9763					
Ig Cl (ueq/l)	-0.4442	0.0654	-0.4419	0.1876	0.3290	0.5680	-0.0033	0.4830	-0.0807	0.2628	-0.3649	-0.3747				
Ig SO4 (ueq/l)	0.5578	-0.1525	0.0694	-0.5592	-0.3127	-0.3743	0.0196	-0.6238	0.2385	-0.4365	0.2590	0.2070	-0.1891			
Ig Ca (ueq/l)	-0.4555	0.4486	-0.2441	0.4636	0.6110	0.6561	-0.2027	0.5236	-0.4821	0.5830	-0.5680	-0.5161	0.4824	-0.1542		
Ig Mg (ueq/l)	-0.5943	0.5650	-0.1867	0.6154	0.7705	0.8638	-0.1436	0.6687	-0.6143	0.7439	-0.6597	-0.5783	0.6891	-0.3374	0.8131	
Ig Na (ueq/l)	-0.7195	0.3561	-0.1813	0.6135	0.6722	0.7832	-0.0867	0.7449	-0.4251	0.6369	-0.5310	-0.4605	0.8139	-0.4067	0.6693	0.9043

Table 4.3. Correlation matrix showing the relationship between environmental variables in the Russian lakes. The strength of the relationship was expressed using Pearson product-moment correlation coefficients, figures highlighted in yellow showed strong correlation (r squared equal to or greater than 0.6) which were highly significant (p-values < 0.05).

4.2.2. Chironomid data

A total of 119 different chironomid taxa or morphotypes were identified from surface sediments from the 94 Russian lakes (Table 4.4). In addition there were 6 composite taxonomic groupings (Unidentified Tanypodinae, unidentified Tanytarsini and unidentified Pentaneurini and undifferentiated *Corynoneura* spp., *Tanytarsus* spp. and *Cricotopus/Orthocladius*). Of the 119 taxa, 37 occurred in 3 or fewer lakes. These rare occurrences included rarely recorded taxa such as *Acalcarella* (Wiederholm 1983) and non-lacustrine taxa such as *Parachaetocladius* which is associated with shallow spring-fed streams (Lindegaard 1995).

There are few independent descriptions of the distribution of chironomids in northern Russia in the widely available, English-based literature. Published faunal descriptions from the Lena River delta (Porinchu and Cwynar 2000) and central Yakutia (Nazarova *et al.* 2008) are based on material included in this study. The fauna is taxonomically more diverse than the fauna recorded for Barnaulka and Bolshaya Cheremshanka rivers, in the Upper Ob river basin (Bezmaternyh 2001). However Bezmaternyh does not record the surveying technique or sampling frequency. The apparent lower diversity may result from analysis of a single or limited number of collections of larvae, pupae or adults whereas palaelimnological techniques amalgamated larvae from habitats throughout the lake and over a longer time.

The majority of common morphotypes, such as *Psectrocladius sordidellus*-type *Tanytarsus lugens*-type, *Procladius* and *Chironomus anthracinus*-type, are widespread throughout the Arctic and Subarctic; in Norway (Brooks and Birks 2000a and unpublished data), Sweden (Larocque *et al.* 2001), Iceland (Holmes 2006; Langdon *et al.* 2008) and Canada (Porinchu *et al.* 2009). Morphotypes may be composed of a number of different, but morphologically similar species. However species composition, and therefore environmental optima, of the morphotypes or species-group may vary between the different regions. Of the more abundant taxa ($n \geq 10$) only *Einfeldia* was restricted to Yakutia, although this genus has been recorded in eutrophic lakes throughout temperate regions of the Holarctic (Sæther 1979; Pinder and Reiss 1983; Brooks and Birks 2001)

and in relatively cool lakes in the alpine region of Switzerland (Heiri 2001). *Constempellina-Thienemanniola* was not recorded in the Norwegian lakes used in the training set but is present in Norway (Sæther *et al.* 2007). *Propsilocerus jacuticus* was only recorded in a single lake in Yakutia. This species was thought to occur in eastern and central Europe (Wang and Sæther 2001) so its range is either more extensive than believed or the larvae belongs to a morphologically similar taxa.

Table 4.4. Checklist of Chironomidae taxa recorded in the Russian lakes

Taxon or morphotype name	Taxon or morphotype name	Taxon or morphotype name
TANYPODINAE:	ORTHOCLADIINAE:	3 or less occurrences
<i>Ablabesmyia</i>	<i>Abiskomyia</i>	TANYPODINAE:
<i>Procladius</i>	<i>Chaetocladius</i>	<i>Macropelopia</i>
<i>Tanypus</i>	<i>Corynoneura arctica</i> -type	<i>Paramerina</i>
CHIRONOMINI:	<i>Corynoneura edwardi</i> -type	<i>Thienemannimyia</i> -group
Chironomini 1st instar larvula	<i>Corynoneura lobata</i> -type	CHIRONOMINI:
<i>Chironomus anthracinus</i> -type	<i>Cricotopus cylindraceus</i> -type	<i>Acalcarella</i>
<i>Chironomus plumosus</i> -type	<i>Cricotopus intersectus</i> -type	<i>Glyptotendipes barbipes</i> -type
<i>Cladopelma lateralis</i> -type	<i>Cricotopus laricomalis</i> -type	<i>Lauterborniella</i>
<i>Cryptochironomus</i>	<i>Cricotopus sylvestris</i> -type	<i>Lipiniella</i>
<i>Dicrotendipes</i>	<i>Cricotopus</i> type C	<i>Microtendipes rydalisensis</i> -type
<i>Einfeldia</i>	<i>Cricotopus</i> type P	<i>Paracladopelma</i>
<i>Endochironomus albipennis</i> -type	<i>Eukiefferiella claripennis</i> -type	<i>Paratendipes nudisquama</i> -type
<i>Endochironomus impar</i> -type	<i>Heterotrissocladius grimshawi</i> -type	<i>Stenochironomus</i>
<i>Endochironomus tendens</i> -type	<i>Heterotrissocladius maeaeri</i> -type	<i>Zavreliella</i>
<i>Glyptotendipes pallens</i> -type	<i>Hydrobaenus conformis</i> -type	ORTHOCLADIINAE:
<i>Glyptotendipes severini</i> -type	<i>Hydrobaenus lugubris</i> -type	<i>Acamptocladius</i>
<i>Microchironomus</i>	<i>Limnophyes</i> - <i>Paralimnophyes</i>	<i>Brillia</i>
<i>Microtendipes pedellus</i> -type	<i>Mesocricotopus</i>	<i>Cricotopus obnixus</i> -type
<i>Pagastiella</i>	<i>Metricnemus eurynotus</i> -type	<i>Cricotopus trifasciatus</i> -type
<i>Parachironomus varus</i> -type	<i>Metricnemus fuscipes</i> -type	<i>Diplocladius</i>
<i>Phaenopsectra flavipes</i> -type	<i>Nanocladius branchicolus</i> -type	<i>Georthocladius</i>
<i>Phaenopsectra</i> type A	<i>Nanocladius rectinervis</i> -type	<i>Heterotanytarsus apicalis</i> -type
<i>Polypedilum nubeculosum</i> -type	<i>Orthocladius oliveri</i> -type	<i>Heterotrissocladius marcidus</i> -type
<i>Polypedilum sordens</i> -type	<i>Orthocladius</i> type S	<i>Heterotrissocladius subpilosus</i> -type
<i>Sergentia coracina</i> -type	<i>Paracladius</i>	<i>Hydrobaenus johannseni</i> -type
<i>Stictochironomus rosenschoeldi</i> -type	<i>Parakiefferiella bathophila</i> -type	<i>Orthocladius consobrinus</i> -type
TANYTARSINI:	<i>Parakiefferiella nigra</i> -type	<i>Orthocladius trigonolabis</i> -type
<i>Cladotanytarsus mancus</i> -type	<i>Parakiefferiella triquetra</i> -type	<i>Orthocladius</i> type I
<i>Constempellina</i> - <i>Thienemanniola</i>	<i>Parakiefferiella</i> type A	<i>Parachaetocladius</i>
<i>Corynocera ambigua</i>	<i>Paraphaenocladius</i>	<i>Propsilocerus lacustris</i> -type
<i>Corynocera oliveri</i> -type	<i>Psectrocladius barbatipes</i> -type	<i>Propsilocerus lusatensis</i>
<i>Micropsectra insignilobus</i> -type	<i>Psectrocladius septentrionalis</i> -type	<i>Propsilocerus jacuticus</i>
<i>Micropsectra radialis</i>	<i>Psectrocladius sordidellus</i> -type	<i>Psectrocladius psilopterus</i> -type
<i>Paratanytarsus</i>	<i>Pseudosmittia</i>	<i>Psectrocladius barbimanus</i> -type
<i>Paratanytarsus austriacus</i> -type	<i>Smittia</i> - <i>Parasmittia</i>	<i>Pseudorthocladius</i>
<i>Paratanytarsus penicillatus</i> -type	<i>Trissocladius</i>	<i>Rheocricotopus chalybaetus</i> -type
<i>Stempellina</i>	<i>Zalutschia mucronata</i> -type	<i>Synorthocladius</i>
<i>Tanytarsus chinyensis</i> -type	<i>Zalutschia</i> type B	<i>Thienemanniella clavicornis</i> -type
<i>Tanytarsus glabrescens</i> -type	<i>Zalutschia zalutschicola</i>	<i>Zalutschia</i> type A
<i>Tanytarsus lugens</i> -type	DIAMESINAE:	PODONOMINAE:
<i>Tanytarsus mendax</i> -type	<i>Protanypus</i>	<i>Lasiodiamesa</i>
<i>Tanytarsus pallidicornis</i> -type	PRODIAMESINAE:	
<i>Zavrelia</i> - <i>Stempellinella</i>	<i>Monodiamesa</i>	
PSEUDOCHIRONOMINI:		
<i>Pseudochironomus</i>		

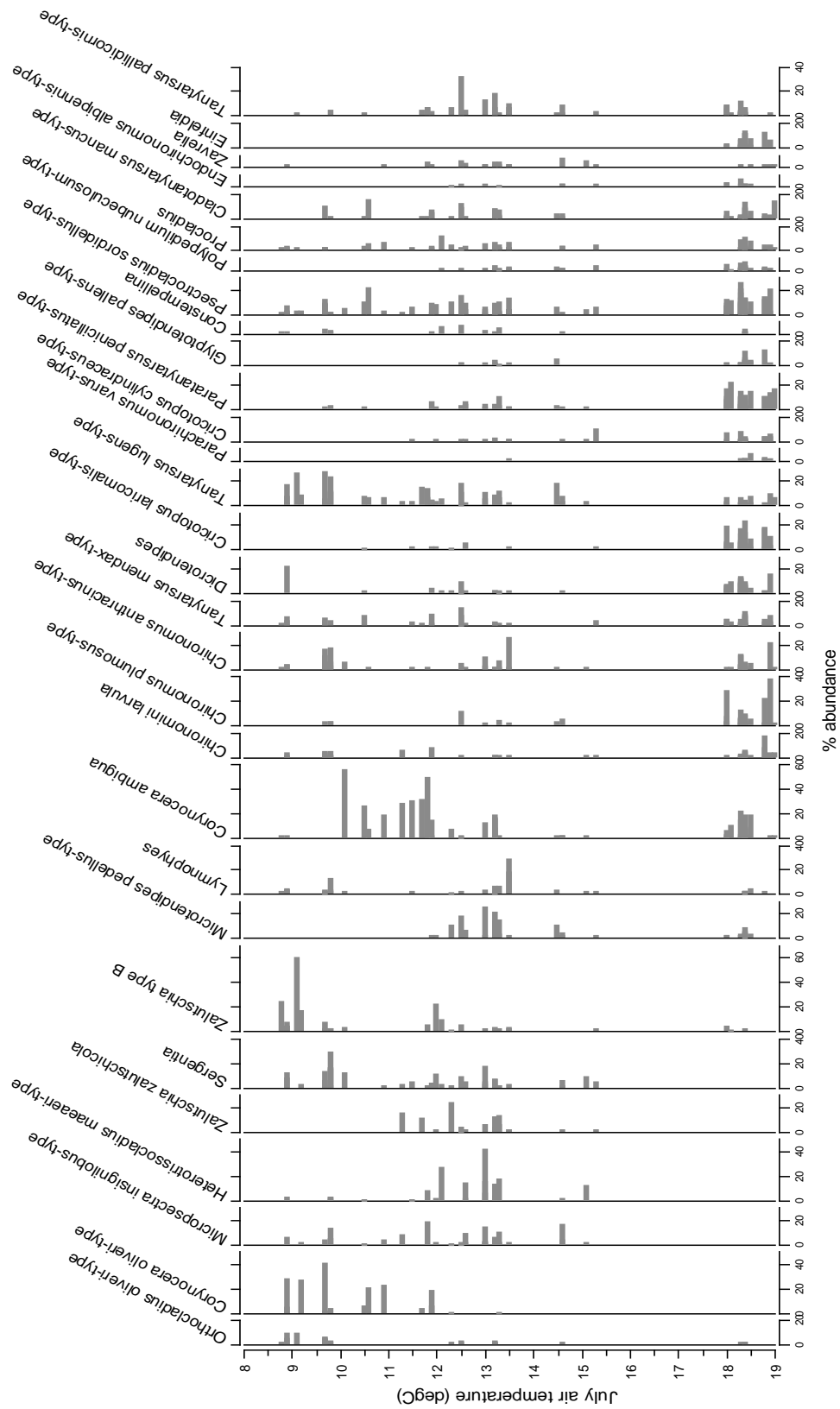


Figure 4.4. The distribution of the 30 most abundant taxa in the Russian lakes along the mean July air temperature gradient.

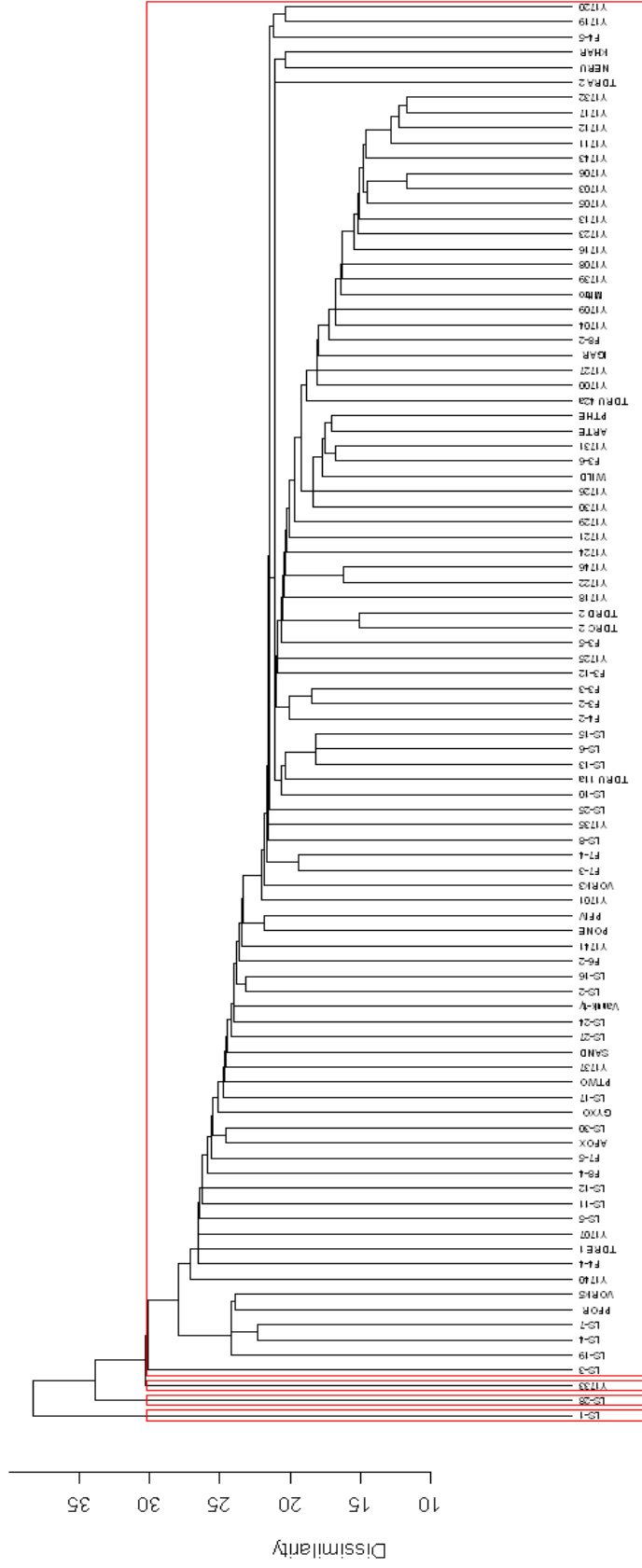
The assemblages show distinct changes in relation to July air temperature (Figure 4.4). Taxa such as *Corynocera oliveri*-type, *Orthocladius oliveri*-type and *Zalutschia* type B are more prevalent in the colder lakes whereas Chironomini such as *Chironomus* spp., *Glyptotendipes pallens*-type, *Dicrotendipes* and *Einfeldia* together with *Cricotopus laricomalis*-type and *Paratanytarsus penicillatus*-type dominate the warmer lakes. No species were recorded in all 94 lakes, although *Psectrocladius sordidellus*-type, *Tanytarsus lugens*-type and *Procladius* occurred in greater than 75%. The absence of lakes with July air temperatures between 15.3 - 18°C is apparent in the distribution data and may adversely affect the estimation of temperature optima for species whose optima lie within or near this range.

4.2.3. Patterns of chironomid distribution

Lakes with anomalous faunas were identified by single-link or nearest neighbour cluster analysis (section 3.4.2). In this technique, the similarity between all pairs of samples is calculated and the closest pairs, based on the Euclidean distance, are fused to identify discontinuities or anomalies within the data (Olafsson et al. 2002). The analysis suggested the assemblages from the lakes LS-1, LS-28 and Y1733 are distinct from the other assemblages (Figure 4.6). These three lakes are dominated by single taxon; LS-1 has 61% *Zalutschia* type B, LS-28 42% *Heterotrissocladius maeaeri*-type and Y1733 39% *Chironomus plumosus*-type. In general, the 'nearest neighbour' i.e. the lake with the most similar assemblage is geographically close but at the level of fourth or fifth closest neighbours the lakes are spatial heterogeneous with the exception of clusters of Yakutian lakes.

The patterns in chironomid diversity, between the geographical regions, are confirmed by detrended correspondence analysis (DCA) with fitted convex hulls (Figure 4.6) which show considerable overlap in the assemblages from north-east European Russia, the Putorana Plateau and Lena Delta, along a longitudinal gradient from 52.38°E to 128.87°E. The faunal similarity suggests many taxa have a cosmopolitan distribution within arctic Russia. The Yakutian assemblages occupy a distinct position in the ordination space and do not

Russia species data



Single Link

Figure 4.5. Dendrogram of the Russian chironomid assemblages classified by single-link clustering. Rectangles delineate the dendrogram into 4 clusters to highlight the 3 most distinct faunal assemblages from lakes LS-1, LS-34 and Y1733.

overlap with other sites. This is probably due to the abundance of Chironomini species such as *Microchironomus* and *Glyptotendipes* which are typically found in warmer mesotrophic to eutrophic lakes (Brodin 1986; Brooks *et al.* 2001) and reflects the more southerly and warmer location of this region. The DCA also confirms the distinctiveness of LS-28 from other lakes in the Lena Delta. LS-28 is the most southerly lake from the Lena Delta region and, although geographically closer, it also appears more dissimilar to lakes from Central Yakutia than other delta lakes. Therefore its distinctiveness is unlikely to result from latitude or temperature alone.

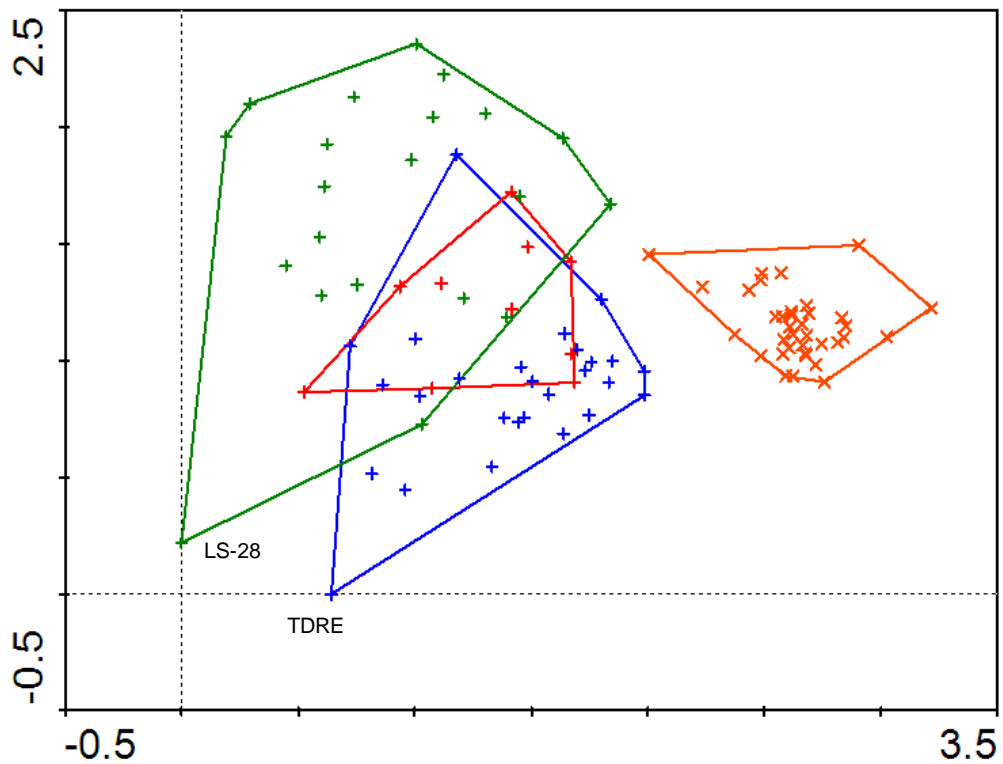


Figure 4.6. DCA plot of site scores for the Russian lakes with fitted convex hulls. Sites classified by geographic region; blue – north-east European Russia, red – Putorana, orange – Yakutia and green – Lena Delta. Rare taxa downweighted.

4.2.4. Species – environment relationships

To determine the most appropriate statistical methods for exploring taxa – environment relationships the modern chironomid and environmental data were first analysed by Detrended Correspondence Analysis (DCA) (see section

3.4.4). The gradient length of the first DCA axis (3.2 SD units) indicates that unimodal-based numerical methods are appropriate for data analysis (Table 4.5). The eigenvalues of the first two axes of the DCA accounts for 21.3% of the variance in the species. This low percentage of variance explained is typical of 'noisy' datasets with a large number of taxa and many zero values (e.g. Bennion 1994). The eigenvalue of the first axis ($\lambda_1 = 0.392$) is more than twice the eigenvalue of the second ($\lambda_2 = 0.157$) indicating the DCA results are stable (Oksanen and Minchin 1997).

Axes	1	2	3	4	Total inertia
Eigenvalues	: 0.392	0.157	0.118	0.072	2.580
Lengths of gradient	: 3.217	2.356	1.952	1.525	
Cumulative percentage variance of species data	: 15.2	21.3	25.8	28.7	
Sum of all eigenvalues					2.580

Table 4.5. Summary statistics for the first four axes of DCA

As the gradient length of the first DCA axis is greater than 2.5 SD the environmental and chironomid assemblages were analysed by CCA - canonical correspondence analysis (section 3.4.4.4). CCA was initially performed with longitude, latitude and altitude as passive environmental variables. The eigenvalues for CCA axis 1 ($\lambda_1 = 0.344$) and axis 2 ($\lambda_2 = 0.133$) explain 13.4% of the variance in the chironomid taxa (Table 4.6). The species-environment correlations for CCA axis 1 (0.947) and axis 2 (0.905) are high indicating a strong relationship between the measured environmental variables and chironomid distribution. January and July air temperatures, continentality index, summer precipitation, distance to the coast and calcium and magnesium concentrations have high variance inflation factors (VIF) showing high levels of inter-correlations. These variables were eliminated one by one, based on the correlations identified in section 4.4.1, and the remaining subset of variables tested until all VIFs were less than 20. Forward selection of the remaining variables indicates seven environmental variables make independent and significant contributions ($p \leq 0.05$) to explaining the variance in the chironomid data.

(a)

Axes		1	2	3	4	Total inertia
Eigenvalues	:	0.344	0.133	0.069	0.064	2.563
Species-environment correlations	:	0.947	0.905	0.757	0.806	
Cumulative percentage variance						
of species data	:	13.4	18.6	21.3	23.8	
of species-environment relation:		38.8	53.8	61.6	68.8	
Sum of all eigenvalues						2.563
Sum of all canonical eigenvalues						0.887

(b)

Axes		1	2	3	4	Total inertia
Eigenvalues	:	0.341	0.127	0.063	0.057	2.563
Species-environment correlations	:	0.943	0.894	0.732	0.792	
Cumulative percentage variance						
of species data	:	13.3	18.3	20.7	22.9	
of species-environment relation:		51.0	70.0	79.5	87.9	
Sum of all eigenvalues						2.563
Sum of all canonical eigenvalues						0.669

Table 4.6. Summary statistics for the first four axes of CCA of the Russian lakes based on 94 sites, 124 chironomid taxa (a) for all environmental variables and (b) with seven significant environmental variables

The most significant of the selected variables is July air temperature which explains 41.8% of the total variance explained by all the measured environmental variables, followed by continentality (15.2%) annual precipitation (7.5%), forest vegetation (6.3%), water depth (5.1%), Na⁺ concentration (5.1%) and pH (3.8%). The results of the CCA showing the significant variables are given in Table 4.6 and illustrated in Figure 4.7. The eigenvalues of CCA axis 1 ($\lambda_1 = 0.341$) and axis 2 ($\lambda_2 = 0.130$), constrained to the seven significant variables, capture 18.3% of the cumulative variance in the species data. The species-environment correlations of CCA axis 1 (0.943) and axis 2 (0.894) are high and the first two axes account for 70% of the variance in the chironomid-environment relationship.

Axis 1 of the CCA constrained to the significant variables (Figure 4.7) separates the warm lakes with meso- to eutrophic, thermophilic assemblages from cooler

lakes with assemblages dominated by cold stenothermic taxa. For example the Yakutia lakes (orange rings) which experience the warmest July air temperatures are dominated by *Einfeldia*, *Pseudochironomus*, *Chironomus plumosus*-type and *Dicrotendipes*-type whereas the cooler lakes have assemblages typified by cold stenotherms such as *Sergentia coracina*-type, *Micropsectra insignilobus*-type and *Hydrobaenus conformis*-type. The first axis is also related to sodium (Na⁺) ion concentrations; the association of increasing Na⁺ with increasing July temperatures suggests the Yakutia lakes are subject to negative water balance resulting in salinization of the lakes. Salinization of the soil has been recorded from Central Yakutia (Lopez et al. 2007) due to permafrost degradation and summer evaporation, however the study did not extend to lakes.

The second axis reflects water depth and annual precipitation. Profundal species such as *Heterotrissocladius maeaeri*-type and *Zalutschia zalutschicola*-type are associated with the deeper lakes. However littoral species including *Microtendipes pedellus*-type and *Psectrocladius septentrionalis*-type and stream taxa such as *Zavrelia-Stempellina* are also associated with increasing water depth and annual precipitation. High precipitation may result in flooding which washes stream and littoral taxa into deep lakes, where they are unable to survive, so that the subfossil assemblage comprises a number of allochthonous taxa.

Key to abbreviations used in Figure 4.7: tjul – July air temperature, wdepth – water depth (m), precA – annual precipitation (mm), ci – continentality index and vforest – forest vegetation. (b) Species with species weight >10% included, points scaled relative to Hill's N2 value for each species. Taxa abbreviations: Abla – *Ablabesmyia*, Ca – *Corynocera ambigua*, Car – *Corynoneura arctica* type, Cha – *Chironomus anthracinus* type, Chl – Chironomini larvula, Chp – *Chironomus plumosus* type, Clm – *Cladotanytarsus mancus* type, Co – *Corynocera oliveri* type, Cpel – *Cladopelma lateralis* type, Crcy – *Cricotopus cylindraceus* type, Crl – *Cricotopus laricomalis* type, CrP – *Cricotopus* type P, Cstem – *Constempellina*, Dict – *Dicrotendipes* type, Ea – *Endochironomus albipennis* type, Ein – *Einfeldia* type, Gp – *Glyptotendipes pallens* type, Hcon – *Hydrobaenus conformis* type, Hbr – *Heterotrissocladius maeaeri* type, Lm – *Limnophyes*, Min – *Micropsectra insignilobus* type, Mped – *Microtendipes pedellus* type, Oo – *Orthocladius oliveri* type, Para – *Paratanytarsus* type, Pb – *Parakiefferiella bathophila* type, Pn – *Paratendipes nudisquama* type, Pp – *Paratanytarsus penicillatus* type, Proc – *Procladius*, Ps – *Psectrocladius sordidellus* type, Psep – *Psectrocladius septentrionalis* type, Pt – *Protanypus*, Pv – *Parachironomus varus* type, Ser – *Sergentia* type, Stic – *Stictochironomus* type, Tm – *Tanytarsus mendax* type, Tl – *Tanytarsus lugens* type, Tp – *Tanytarsus pallidicornis* type, Zav – *Zavrelia*, ZB – *Zalutschia* type B and Zz – *Zalutschia zalutschicola*.

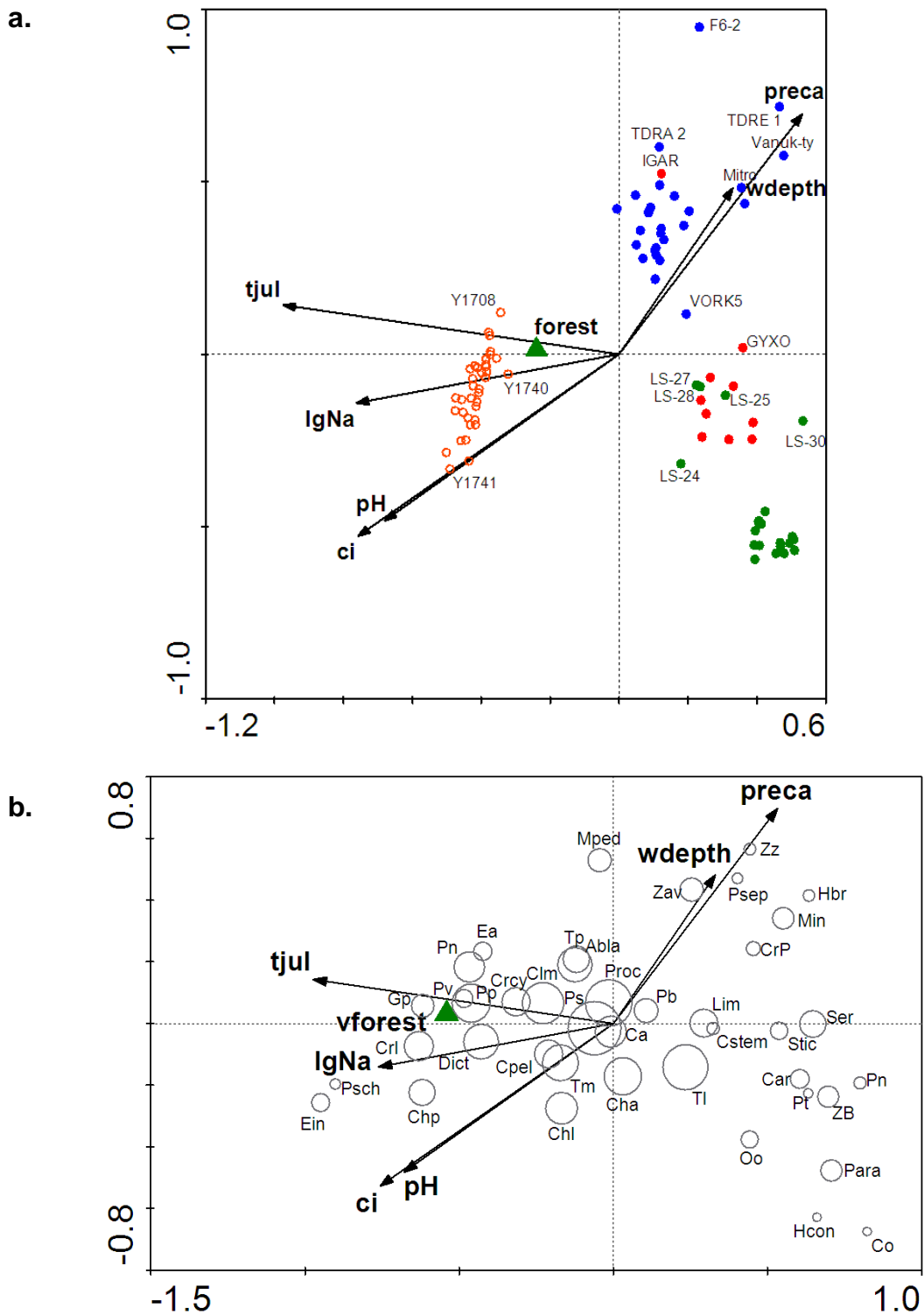


Figure 4.7. CCA biplots of axis 1 and 2 illustrating the relationship between the significant environmental variables and faunal assemblage in the Russian lakes showing (a) the site scores and (b) the species scores. Quantitative environmental variables, chosen by forward selection, are shown as arrows and the nominal variable (forest) as centroid. (a) Sites classified by geographic region blue dot: European Russia, red: Putorana, orange open circle: Yakutia and green dot: Lena Delta.

The Yakutia lakes constitute the highest proportion of lakes (36 lakes from a total of 94 lakes) within the Russian data set and their characteristics, in terms of extreme continentality, higher July temperatures, pH and sodium ion concentrations, appear to drive the ordination. Although temperature along the first axis results in some separation of the other regions, pH, water depth and annual precipitation appear to be the main factors influencing chironomid distribution in these lakes (Figure 4.8). The lake at Igarka (IGAR) is deeper and experiences warmer July temperature than the lakes on the Putorana Plateau; it consistently plots within the northeast European lakes. Lake F6-2 appears an outlier in plots of axis 1 and 2 (Figure 4.7) and axis 3 and 4 (Figure 4.8).

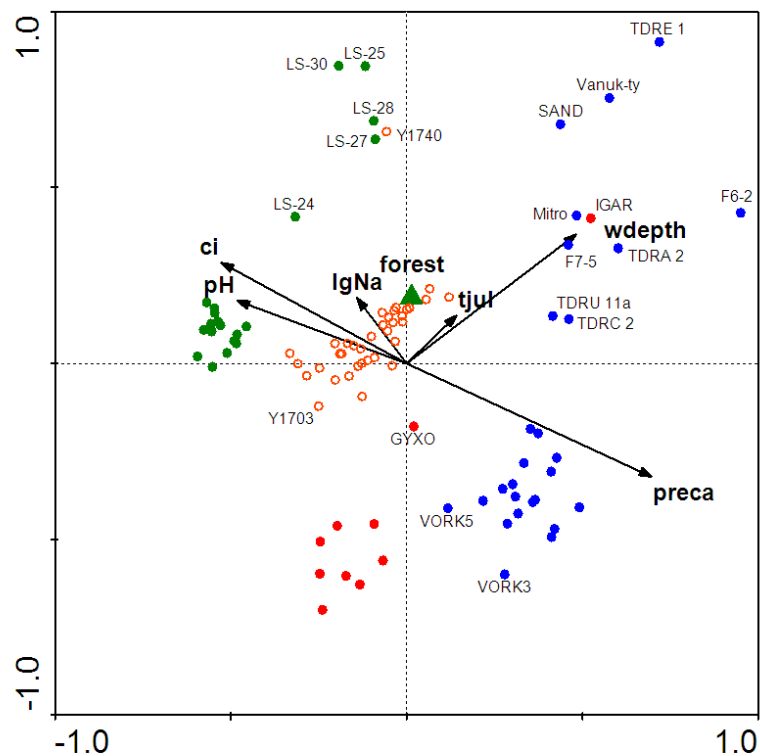


Figure 4.8. CCA biplot of the 94 Russian lakes on CCA axis 3 and 4 based on the chironomid assemblages of the lakes. Quantitative environmental variables, chosen in forward selection, are shown as arrows and the nominal variable (forest) as centroid. Abbreviations as in Figure 4.9 for predictor variables. Sites classified by geographic region blue dot: European Russia, red: Putorana, orange, open circle: Yakutia and green dot: Lena Delta.

4.3. Norwegian surface sediment data-set

Surface sediments were collected from lakes along altitudinal transects on mainland Norway, off-shore islands and Svalbard between 1995 and 1999 by S.J. Brooks and H.J.H. Birks (Figure 1.2). Surface sediments (0–1 cm) were collected from the deepest point in each lake for chironomid analyses. Chironomid assemblages in the surface sediments were prepared and identified by S. Brooks (Brooks and Birks 2000a). The provenance of environmental data is detailed in Table 3.5.

4.3.1. Environmental data

The physical and environmental characteristics of the Svalbard lakes (A – Lake Birgervatnet, Bir, in Table 4.7) are described in Birks *et al.* (2004). Chironomid abundance for all the Norwegian lakes and environmental data for the remaining lakes from the ‘Brooks-Birks’ Norwegian training set (lakes 96-1 – 99-50 in Table 4.7) are unpublished and reproduced in this thesis with permission. However the statistical analyses, and comparisons with the Russian data, made in this study, have not been previously performed. The locations of the Norwegian lakes, with associated environmental variables and water chemistry data are given in Table 4.7 and summarised in Table 4.8.

Table 4.8. Summary of environmental variables for the Norwegian lakes.

	NORWEGIAN LAKES (157 lakes)				
	Minimum	Median	Mean	Maximum	Std dev
Latitude (N)	58.0800	61.5400	64.7100	79.8000	
Longitude (E)	5.0050	8.8620	11.2700	31.0380	
Altitude (m ASL)	5	260	484	1594	473
Distance to coast (km)	0.1	42.0	70.1	250.0	71.5
pH	4.66	6.37	6.40	8.40	0.70
Conductivity (uS/cm)	4	33	51	367	55
Water depth (m)	0.5	7.0	8.1	29.0	5.9
July air temp (°C)	3.5	10.5	10.3	16.0	3.5
Jan air temp (°C)	-15.6	-7.6	-7.5	2.6	4.8
Continentality Index	-1	12	13.7	29	7
Annual precipitation (mm)	390	796	995	2700	631
Cl (ueq/l)	2.0	67.0	147.2	2342.0	253.6
SO ₄ (ueq/l)	7.0	46.0	72.3	1226.0	111.6
Ca (ueq/l)	20.0	99.0	232.6	3004.0	355.2
Mg (ueq/l)	7.0	44.0	94.6	930.0	140.0
Na (ueq/l)	7.0	78.0	150.8	2127.0	223.8

Lake code	Latitude (N)	Longitude (E)	Altitude (m ASL)	Distance to coast (km)	pH	Cond (uS/cm)	Water depth (m)	Tjuly (°C)	Tjan (°C)	Cl	MAP (mm)	Cl ueq/l	SO4 ueq/l	Ca ueq/l	Mg ueq/l	Na ueq/l	Veg. type	Other lakes	Human impact
A	78.2500	12.9167	20	0.1	8.19	169	0.9	6.0	-13.9	14	397	342	42	853	411	278	T	N	0
B	78.3167	12.8333	20	0.3	8.40	189	2.2	6.0	-13.9	14	397	227	42	863	466	357	T	N	0
C	78.9500	12.4667	60	1.2	7.99	153	26.0	4.7	-13.9	12	396	77	51	1043	439	109	T	N	0
D	78.8667	10.9000	20	0.4	6.78	44	1.3	4.5	-13.9	11	400	88	19	145	84	113	T	N	0
E	78.7500	11.1000	30	1	7.05	28	1.4	4.5	-13.9	11	399	151	46	240	171	152	T	N	0
F	79.1833	11.6500	45	1.6	6.62	133	1.5	4.5	-13.9	11	395	69	25	50	30	44	T	N	0
G	79.2500	11.5333	30	0.6	6.53	33	5.1	4.5	-13.9	11	395	64	20	45	39	61	T	N	0
H	79.2500	11.5500	35	0.5	6.61	26	11.5	4.5	-13.9	11	395	66	22	50	39	61	T	N	0
I	79.6667	10.8000	70	0.6	5.57	22	6.8	3.5	-13.9	10	390	90	17	20	36	122	T	N	0
J	79.6833	10.8000	10	0.3	6.06	69	6.7	3.5	-13.9	10	390	241	26	25	84	300	T	N	0
K	79.6833	10.9000	50	1.7	6.35	76	12.5	3.5	-13.9	10	390	36	7	50	22	57	PD	N	0
M	79.7667	10.7500	10	0.2	5.85	34	5.1	3.5	-13.9	10	390	142	27	25	33	104	T	N	0
N	79.7500	10.7167	10	0.5	6.06	12	2.1	3.5	-13.9	10	390	50	12	20	24	70	T	N	0
O	79.8000	11.5500	20	0.4	7.60	129	2.0	3.5	-13.9	10	390	65	15	434	160	235	T	N	0
P	78.9500	12.5000	50	1	8.05	367	6.7	4.7	-13.9	12	396	67	1226	3004	930	178	T	N	0
Q	78.2167	12.9333	20	0.4	7.92	153	2.6	6.0	-13.9	14	397	190	74	649	348	204	T	N	0
R	78.2167	13.3333	20	1	7.66	120	1.2	6.3	-13.9	15	396	228	144	853	183	191	T	N	0
S	77.7500	13.9500	15	1.9	8.17	243	1.3	5.5	-13.9	13	405	656	308	1652	900	518	T	N	0
T	77.5500	14.2167	55	1	8.11	129	10.5	5.0	-13.9	13	402	149	32	913	405	126	T	N	0
U	78.1000	10.0333	5	1	7.07	323	2.5	6.5	-13.9	15	401	2342	327	339	563	2127	T	N	1
Scur	79.7333	12.3000	15	0.3	6.86	39	0.5	3.5	-13.9	10	396	203	30	35	56	183	T	N	0
Arsj	79.6667	10.8500	15	0.5	6.20	25	29.0	3.5	-13.9	10	390	96	19	65	31	65	T	N	0
Bir	79.7333	11.6167	10	0.5	6.50	27	15.0	3.5	-13.9	10	390	73	15	115	61	96	PD	N	0
96-1	61.548333	8.975000	990	188	7.01	35	5.0	10.3	-9.6	18	540	18	87	195	70	34	F	N	0
96-2	61.815000	9.028333	822	162	7.50	91	7.0	11.2	-10.3	21	495	23	216	658	224	44	F	N	0
96-7	61.330000	7.283333	463	143	6.54	27	12.5	12.4	-4.8	13	700	48	42	124	46	55	F	N	0
96-10	61.540000	8.250000	1440	160	5.82	4	3.5	5.7	-11.0	12	600	8	9	33	7	7	T	N	0
96-11	61.258333	8.828333	934	200	6.13	13	3.7	10.9	-9.8	20	1022	15	45	83	18	21	F	N	0

Table 4.7. Physical and chemical characteristics of the Norwegian lakes

For key to abbreviations see Table 4.1.

Table 4.7. continued

Lake code	Latitude (N)	Longitude (E)	Altitude (m ASL)	Distance to coast (km)	pH	Cond (uS/cm)	Water depth (m)	Tjuly (°C)	Tjan (°C)	Cl	MAP (mm)	Cl ueq/l	SO4 ueq/l	Ca ueq/l	Mg ueq/l	Na ueq/l	Veg. type	Other lakes	Human impact
96-12	61.701667	8.861667	1298	172	6.73	18	2.1	8.4	-12.4	20	540	14	36	101	56	27	T	N	0
96-13	61.758333	9.121667	900	172	6.90	28	14.5	10.7	-10.7	21	495	32	62	143	77	42	F	N	0
96-14	61.006667	7.331667	1205	144	6.27	9	2.6	8.1	-8.5	12	700	12	24	58	16	16	T	Y	0
96-15	61.976667	6.113333	163	50	5.91	12	15.5	13.4	-1.2	8	2000	40	20	38	19	62	F	N	0
96-20	61.870000	5.076667	110	1	6.33	28	6.5	13.2	0.8	4	2000	128	44	59	44	155	F	N	0
96-21	61.831667	5.448333	382	7	6.46	24	26.0	11.8	-1.0	4	1500	121	27	77	35	117	F	Y	0
96-24	61.570000	5.611667	147	24	5.90	19	12.0	13.3	-0.4	6	2500	75	33	57	34	95	F	N	0
96-25	61.821667	6.040000	416	42	5.95	13	8.5	11.9	-2.2	7	1800	53	22	35	23	64	F	N	0
96-26	61.693333	5.805000	222	37	6.02	13	13.5	12.9	-1.0	6	2700	38	28	48	22	59	F	Y	0
96-28	61.480000	6.053333	200	45	6.03	21	13.0	13.2	-1.5	8	2200	72	31	63	30	77	F	N	0
96-29	61.411667	5.885000	356	37	5.31	18	9.5	12.3	-1.9	7	2500	73	16	39	32	78	F	Y	0
96-31	61.495000	5.538333	25	6	6.18	23	14.5	14.0	0.2	6	2500	65	41	62	34	96	F	N	0
96-32	61.345000	6.186667	561	60	5.56	14	8.5	11.2	-3.3	8	2300	50	19	43	27	66	F	N	0
96-35	61.393333	5.741667	297	31	5.87	17	11.5	12.5	-1.4	7	2200	39	22	38	30	77	F	Y	0
96-36	59.848333	6.938333	1020	97	6.43	19	6.6	9.0	-6.5	10	1360	25	39	95	15	26	T	N	0
96-37	59.841667	6.730000	1052	86	5.47	9	12.5	8.6	-6.1	9	2000	10	19	38	9	18	T	Y	0
96-38	59.911667	6.586667	555	85	5.71	15	9.0	11.4	-3.8	9	2000	45	23	41	21	59	F/M	N	0
96-39	59.893333	6.661667	656	88	6.15	23	6.1	10.9	-4.3	9	2000	41	35	79	31	67	F/M	N	0
96-44	59.761667	7.651667	955	138	6.86	21	15.0	10.2	-7.9	15	900	24	31	146	17	32	F	N	0
96-45	59.743333	6.676667	870	64	5.70	14	19.5	9.6	-5.2	9	2500	24	19	54	14	30	T	N	0
96-47	59.731667	6.645000	828	66	5.74	12	6.5	9.9	-4.9	9	2500	18	25	55	12	28	T	N	0
96-49	59.611667	6.348333	340	42	5.30	24	6.2	12.5	-2.2	9	2200	34	33	35	22	53	F	Y	0
96-51	59.705000	6.546667	580	59	6.16	16	18.5	11.2	-3.7	9	2500	32	28	65	19	47	F/M	Y	0
96-52	59.723333	6.563333	670	58	6.18	22	7.8	10.7	-4.1	9	2500	34	29	60	23	51	F	Y	0
96-53	59.728333	6.731667	712	65	5.23	20	18.0	10.4	-4.4	9	2500	23	27	42	18	33	F	Y	0
96-54	59.808333	7.253333	1107	95	6.23	14	5.0	8.6	-7.4	11	900	17	54	81	19	22	T	Y	0
96-56	59.643333	5.588333	47	18	5.61	47	16.0	13.7	0.5	6	1750	214	74	53	54	227	F	Y	0
96-58	59.531667	5.658333	125	23	6.23	37	7.5	13.3	0.0	6	2000	142	70	68	56	171	F	N	0
96-60	59.526667	5.691667	22	24	6.61	58	13.5	13.9	0.5	6	2000	215	102	159	81	231	F	Y	0

Table 4.7. continued

Lake code	Latitude (N)	Longitude (E)	Altitude (m ASL)	Distance to coast (km)	pH	Cond (uS/cm)	Water depth (m)	Tjuly (°C)	Tjan (°C)	Cl	MAP (mm)	Cl ueq/l	SO4 ueq/l	Ca ueq/l	Mg ueq/l	Na ueq/l	Veg. type	Other lakes	Human impact
96-61	59.731667	6.055000	221	46	6.46	38	15.0	13.0	-1.3	8	2300	169	53	97	41	187	F	N	0
96-63	59.913333	6.556667	426	78	6.01	17	10.2	12.1	-3.3	10	2400	47	39	54	27	62	F	N	0
96-65	59.956667	6.566667	460	85	6.01	18	13.0	11.9	-3.3	9	2300	37	35	61	23	63	F/M	Y	0
96-67	59.670000	7.541667	890	110	6.15	18	8.1	10.4	-7.6	15	990	38	26	74	22	50	F	Y	0
96-70	59.816667	7.210000	980	103	6.96	40	10.5	9.3	-6.7	11	980	104	49	250	25	94	F	Y	0
96-71	59.843333	6.993333	1144	97	5.55	8	8.2	8.2	-7.1	10	900	13	16	24	16	18	T	Y	0
96-72	59.766667	7.436667	783	110	6.40	29	11.5	10.5	-6.2	12	800	94	46	126	27	105	F	N	0
96-74	59.320000	7.343333	500	89	5.67	19	18.5	13.0	-5.0	15	900	72	45	43	24	93	F	N	0
96-77	59.173333	7.528333	300	100	6.17	20	12.0	14.1	-4.1	16	1000	52	57	76	30	65	F	N	0
96-78	59.851667	7.021667	1318	98	5.42	6	15.5	7.1	-8.0	9	900	9	12	32	12	12	T	N	0
97-35	62.028333	5.005000	38	0.3	6.70	209	2.4	12.6	2.6	-1	1280	1412	158	235	394	1192	F	N	0
97-8	58.666667	7.820000	203	59	5.83	16	2.5	15.2	-5.0	20	1270	50	42	58	23	57	F	N	1
97-10	58.540000	7.736667	180	75	5.18	25	9.5	15.2	-3.5	17	1430	95	56	42	28	101	F/M	N	0
97-12	58.361667	7.798333	242	29	5.18	40	10.0	14.3	-3.2	15	1310	221	64	48	38	205	F	Y	0
97-13	58.763333	7.815000	274	67	5.13	22	3.3	15.2	-5.0	20	1270	71	58	26	22	87	F/M	Y	0
97-15	58.326667	7.785000	245	25	6.34	40	9.2	14.3	-3.2	15	1310	166	79	136	53	154	F	N	0
97-16	58.300000	7.748333	295	25	5.48	32	9.5	14.1	-3.4	15	1310	137	75	70	44	136	F/M	N	0
97-17	58.273333	7.740000	165	24	5.78	36	6.3	14.8	-2.7	15	1310	173	68	99	50	163	F	N	0
97-18	58.261667	7.785000	195	19	4.98	40	7.0	14.6	-2.8	14	1310	192	82	59	42	170	F	Y	0
97-19	58.296667	7.848333	180	21	6.45	54	17.0	14.7	-2.8	15	1310	262	77	170	68	238	F	N	1
97-21	58.245000	7.006667	40	21	6.97	100	5.2	14.9	-1.5	12	1380	492	117	366	100	431	F	Y	0
97-23	58.185000	7.870000	123	11	6.47	77	11.0	14.3	-1.9	12	1380	446	94	231	90	322	F	N	0
97-24	58.145000	7.913333	80	6	7.19	155	7.8	14.5	-1.7	12	1380	677	235	634	137	654	F	Y	0
97-25	58.076667	7.743333	17	2	6.43	110	13.0	14.9	-1.5	12	1380	631	170	298	131	515	F	N	0
97-26	58.336667	7.785000	315	28	6.04	30	17.0	14.1	-3.4	15	1310	124	70	109	43	126	F	Y	0
97-27	58.271667	8.053333	135	15	6.09	42	8.7	15.0	-2.4	14	1310	193	97	124	67	168	F	Y	0
97-28	58.325000	8.003333	70	22	6.47	55	12.0	15.2	-2.1	14	1310	269	106	168	75	242	F	N	0
97-31	58.246667	8.288333	30	6	6.41	70	19.5	15.6	-1.2	13	1230	256	121	333	91	221	F	Y	0
97-32	58.188333	8.241667	10	3	5.99	110	4.7	15.6	-1.2	13	1230	636	145	250	132	578	F	Y	0

Table 4.7. continued

Lake code	Latitude (N)	Longitude (E)	Altitude (m ASL)	Distance to coast (km)	pH	Cond (uS/cm)	Water depth (m)	Tjuly (°C)	Tjan (°C)	CI	MAP (mm)	Cl ueq/l	SO4 ueq/l	Ca ueq/l	Mg ueq/l	Na ueq/l	Veg. type	Other lakes	Human impact
B97-33	58.173333	8.196667	35	5	6.14	75	10.0	15.6	-1.2	13	1230	425	108	186	121	348	F	Y	0
B98-1	60.925000	7.315000	1290	139	6.27	9	3.0	7.6	-8.0	10	700	7	35	68	21	12	T	Y	0
B98-2	60.960000	7.363333	1289	157	6.15	7	12.5	7.6	-8.0	10	700	8	17	52	13	14	T	N	0
B98-3	60.926667	7.328333	1240	140	6.22	8	4.8	7.8	-7.8	10	700	6	28	54	24	15	T	N	0
B98-4	60.810000	7.633333	1420	159	5.74	6	13.5	5.9	-11.0	13	1030	7	20	39	10	13	T	Y	0
B98-5	60.741667	7.533333	1400	152	6.40	8	10.5	5.9	-11.0	13	1039	6	22	57	24	12	T	N	0
B98-6	61.546667	8.258333	1401	166	6.01	6	15.0	7.4	-12.5	18	600	4	19	41	11	12	T	Y	0
B98-7	61.590000	7.948333	1221	145	5.88	5	18.0	6.8	-9.9	12	860	4	15	38	7	10	T	Y	0
B98-8	61.578333	7.948333	1371	144	5.79	5	11.0	5.9	-10.5	11	860	5	14	34	7	12	T	Y	0
B98-9	61.550000	7.948333	1391	146	5.69	4	16.0	5.8	-10.6	11	860	5	10	25	7	9	T	Y	0
B98-10	61.538333	7.848333	1301	143	5.76	5	14.0	6.3	-10.2	12	860	4	18	33	8	13	T	Y	0
B98-11	61.660000	8.146667	994	150	7.52	80	4.0	9.7	-10.7	19	530	15	42	798	62	33	F	Y	0
B98-12	61.660000	8.156667	1000	148	6.71	14	8.5	9.6	-10.7	19	530	6	25	116	28	28	F/T	Y	0
B98-13	62.026667	8.963333	1194	140	7.53	113	2.0	8.9	-11.5	19	430	26	376	977	167	39	T	N	0
B98-14	62.066667	8.943333	1080	133	7.22	50	1.6	9.5	-11.0	19	430	10	105	425	75	39	T	N	0
B98-15	62.268333	9.836667	1169	142	7.17	49	6.0	8.6	-14.4	24	450	7	187	399	54	34	T	Y	0
B98-16	62.321667	9.870000	1075	138	7.57	90	1.1	9.1	-14.0	24	450	23	270	786	92	44	F/T	Y	0
B98-17	61.500000	9.448333	1114	202	7.41	58	2.8	9.3	-11.2	19	500	6	89	572	42	25	T	Y	0
B98-18	61.031667	9.568333	1261	250	6.89	20	12.5	8.5	-11.8	19	500	6	41	156	35	24	T	N	0
B98-19	61.465000	8.711667	1594	183	6.38	7	13.0	7.1	-12.7	18	540	3	18	53	25	11	T	N	0
B98-20	61.390000	8.763333	1461	190	6.15	8	4.5	7.9	-12.2	19	540	4	24	50	14	18	T	N	0
B98-21	61.393333	8.795000	1377	192	6.62	11	3.0	8.3	-11.8	19	540	3	28	74	34	22	T	Y	0
B98-22	61.376667	8.841667	1329	192	6.64	12	1.9	8.6	-11.6	19	540	2	27	72	43	22	T	Y	0
B98-23	61.318333	8.820000	1055	199	6.41	10	6.5	10.2	-10.4	20	540	7	22	67	23	24	F/T	Y	0
N98-1	61.675000	7.236667	285	109	6.96	11	12.2	13.6	-4.7	15	1380	17	40	77	11	31	F	N	0
99-1	69.945000	19.268333	185	22	7.53	76	6.8	10.2	-3.3	4	1020	156	65	481	80	210	F	Y	0
99-2	69.921667	18.850000	128	6	6.68	19	2.0	10.6	-3.1	4	1030	77	28	57	28	111	F/M	Y	0
99-3	69.893333	18.871667	109	1	6.61	34	4.8	10.7	-3.0	4	1030	95	24	50	31	104	F	N	0
99-4	70.216667	19.698333	85	1.3	7.25	101	1.1	10.8	-1.2	1	900	281	47	482	304	295	F	Y	0

Table 4.7. continued

Lake code	Latitude (N)	Longitude (E)	Altitude (m ASL)	Distance to coast (km)	pH	Cond (uS/cm)	Water depth (m)	Tjuly (°C)	Tjan (°C)	Cl	MAP (mm)	Cl ueq/l	SO4 ueq/l	Ca ueq/l	Mg ueq/l	Na ueq/l	Veg. type	Other lakes	Human impact
99-5	70.005000	19.423333	206	1.7	7.81	109	6.5	10.1	-3.4	4	1020	163	55	835	130	187	F	Y	0
99-6	70.245000	24.080000	305	39	6.37	28	4.6	10.7	-9.0	15	600	145	19	87	45	143	F	Y	0
99-7	70.651667	23.671667	53	0.5	6.82	95	7.7	11.3	-5.2	9	820	561	131	179	149	537	F	N	1
99-8	70.688333	23.725000	116	3	6.82	57	1.5	10.8	-5.5	9	820	305	61	137	70	311	T	N	1
99-9	70.655000	23.715000	67	2	5.78	48	2.3	11.3	-5.2	9	820	298	70	47	75	300	T	Y	1
99-10	71.095000	25.795000	46	2	6.58	82	8.7	10.1	-3.6	4	796	542	92	116	131	488	T	Y	0
99-11	71.098333	25.778333	66	0.5	7.27	102	16.0	10.1	-3.6	4	796	515	88	328	131	494	T	Y	0
99-12	71.125000	25.718333	285	2	6.89	88	0.6	8.5	-4.9	4	796	538	101	122	127	558	T	Y	0
99-13	71.021667	24.766667	100	0.5	6.38	49	10.5	9.6	-4.0	4	796	233	75	75	69	225	T	N	0
99-14	71.036667	25.796667	267	4	7.00	58	1.5	8.6	-4.8	4	796	267	52	176	81	301	T	N	0
99-15	71.048333	25.768333	232	3	6.34	29	1.3	8.8	-4.7	4	796	181	29	56	43	176	T	N	0
99-16	70.455000	27.183333	128	4	6.71	46	18.0	11.6	-12.8	24	455	194	95	114	126	203	F	Y	0
99-17	70.590000	27.578333	345	5	5.41	26	1.0	10.3	-13.7	23	455	106	49	63	62	114	F	N	0
99-18	65.626667	11.161667	156	0.8	5.95	41	0.9	10.5	-8.7	15	550	170	55	118	160	158	F	N	0
99-19	70.318333	31.038333	110	0.8	5.35	76	0.6	8.6	-5.9	6	563	518	57	93	163	435	T	Y	0
99-20	70.436667	27.780000	155	2	6.61	95	10.0	11.4	-12.9	23	455	186	228	586	185	206	F	Y	0
99-21	70.613333	29.120000	125	12	6.70	125	2.3	10.2	-10.6	17	660	249	112	604	542	257	F	Y	0
99-22	70.476667	28.875000	320	19	5.38	34	0.5	9.0	-6.9	8	660	160	69	79	75	171	T	N	0
99-23	70.561667	29.546667	260	9	6.34	70	5.2	9.5	-7.6	10	575	171	47	181	127	168	T	Y	0
99-24	70.588333	29.603333	220	4	6.66	45	2.5	9.6	-7.5	10	575	235	44	288	226	197	T	N	0
99-25	70.540000	29.691667	211	9	6.61	98	5.7	9.7	-7.5	11	575	255	61	462	402	221	T	N	0
99-26	59.058333	11.611667	227	32	4.66	38	12.0	15.2	-4.7	19	880	123	74	51	49	136	F	Y	0
99-27	59.846667	11.431667	224	75	5.84	21	11.5	15.9	-7.5	26	830	41	60	83	45	64	F	Y	0
99-28	59.621667	11.385000	140	60	6.63	32	7.5	16.0	-5.3	22	850	116	46	125	67	133	F/M	N	0
99-29	59.641667	11.463333	141	63	6.34	77	3.0	16.0	-5.3	22	850	274	87	275	168	293	F	N	0
99-30	59.290000	11.365000	130	34	5.91	40	3.2	15.8	-4.2	19	880	119	99	161	82	145	F/M	N	0
99-31	59.366667	11.298333	118	35	6.40	72	4.7	15.9	-4.2	19	880	230	120	336	156	215	F	Y	0
99-32	60.268333	11.365000	230	114	6.56	24	18.0	14.9	-7.5	23	790	33	68	153	50	47	F	N	0
99-33	60.246667	11.446667	264	117	5.30	21	18.5	14.7	-7.7	23	790	29	37	111	37	58	F/M	N	0

Table 4.7. continued

Lake code	Latitude (N)	Longitude (E)	Altitude (m ASL)	Distance to coast (km)	pH	Cond (uS/cm)	Water depth (m)	Tjuly (°C)	Tjan (°C)	CI	MAP (mm)	Cl ueq/l	SO4 ueq/l	Ca ueq/l	Mg ueq/l	Na ueq/l	Veg. type	Other lakes	Human impact
99-34	60.268333	11.271667	216	125	6.72	40	5.8	15.0	-7.4	23	790	33	74	313	64	60	F	Y	0
99-35	60.345000	11.353333	260	130	6.16	31	14.0	14.7	-7.7	23	790	67	49	199	55	79	F	N	0
99-37	60.835000	10.875000	338	182	6.66	33	8.5	14.4	-9.1	25	570	19	66	251	108	45	F/M	N	0
99-38	61.110000	10.363333	591	212	7.15	56	4.7	12.9	-10.5	25	700	15	138	445	127	49	F	N	0
99-40	61.520000	9.700000	814	208	6.04	40	2.0	11.7	-14.0	29	430	15	89	310	86	35	F/M	N	0
99-41	61.555000	10.258333	843	218	6.62	59	2.0	11.6	-14.1	29	545	12	66	547	39	40	F	N	0
99-42	61.565000	10.271667	843	216	6.38	54	3.6	11.6	-14.1	29	545	18	53	507	34	38	F	N	0
99-43	61.698333	10.155000	1013	200	5.99	22	1.6	10.6	-14.9	29	545	8	44	201	16	30	F/T	Y	0
99-44	61.728333	10.176667	1056	199	6.36	47	1.3	10.4	-15.1	29	545	10	113	439	23	28	T	Y	0
99-45	61.850000	10.080000	915	190	6.68	48	1.3	11.2	-14.5	29	545	13	56	279	201	63	F/T	N	0
99-46	61.653333	9.865000	991	166	5.80	22	1.0	10.7	-14.8	29	430	10	52	159	47	36	F/T	N	0
99-47	61.650000	9.878333	991	200	5.89	20	9.0	10.7	-14.8	29	430	14	50	125	31	39	F/T	N	0
99-50	62.383333	10.021667	1000	135	6.78	173	2.1	9.5	-15.6	28	400	28	286	1585	197	60	F/T	Y	0

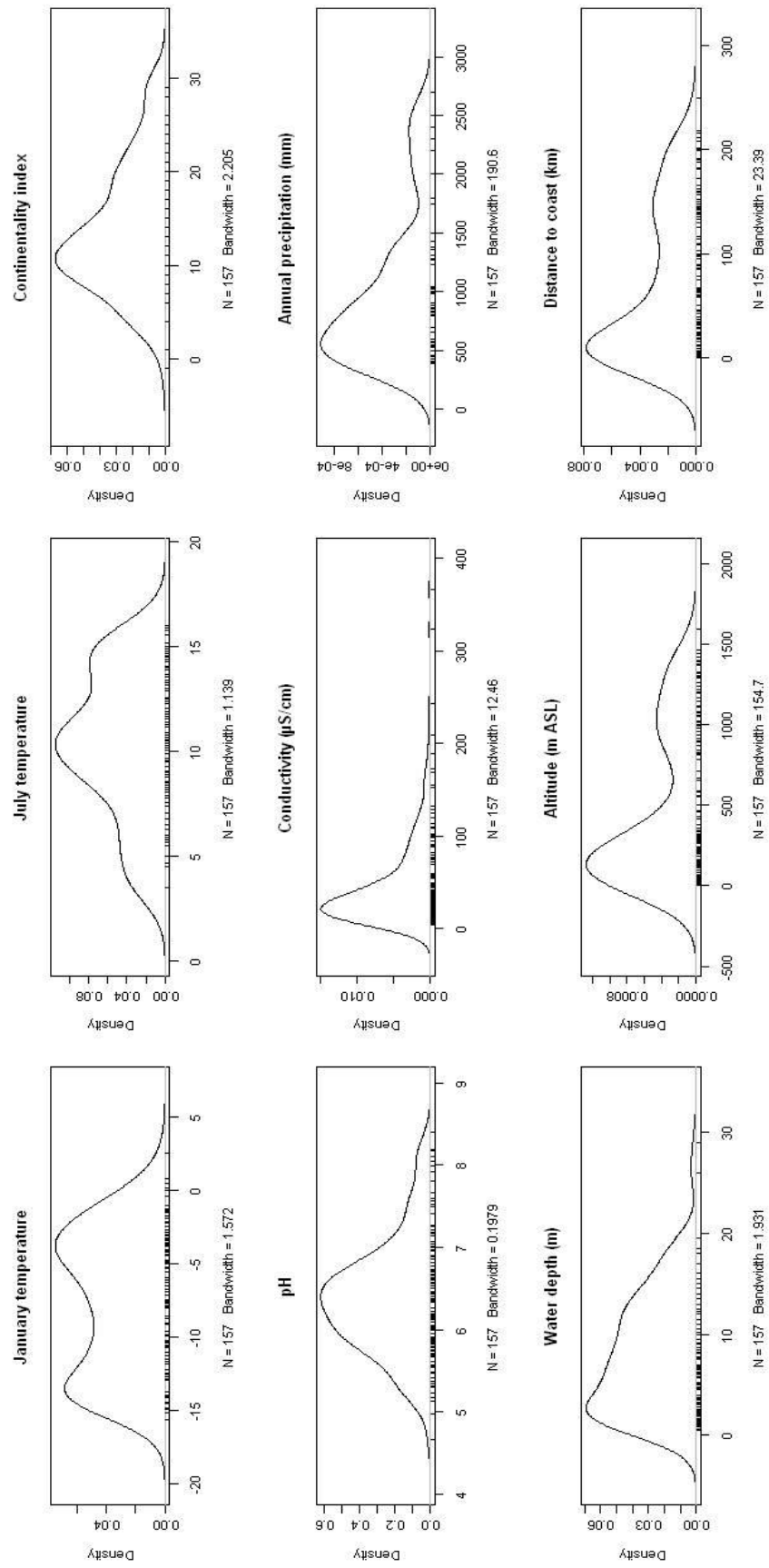


Figure 4.9. Kernel density estimates showing the distribution of climatic and physical variables within the Norwegian training set.

In construction of the Norwegian dataset lakes were selected to maximise the July temperature gradient and provide an even distribution over that gradient whilst minimising variation in the other parameters (Brooks and Birks 2000a). These selection criteria help minimise the errors associated with temperature reconstructions based on the training set (ter Braak and Looman 1986; Birks 1995; Brooks *et al.* 2001). The distribution of the climatic and physical variables (Figure 4.9), with the exception of January temperature, are essentially unimodal indicating the lakes are evenly distributed along these environmental gradients. The standard deviations of variables such as pH, conductivity and major cations are also reduced in the Norwegian dataset compared to Russian data (Table 4.8) as primarily naturally acid or circum-neutral, clear-water lakes were selected (Brooks and Birks 2000a). However the maxima and standard deviation of altitude and annual precipitation are greater in the Norwegian dataset and these variables are probably spatially correlated (Figure 4.10). A coastal mountain range runs along the west coast of Norway resulting in higher altitude lakes with greater orographic precipitation. The distribution of chironomids may therefore be influenced by the mountain topography and its more maritime climate.

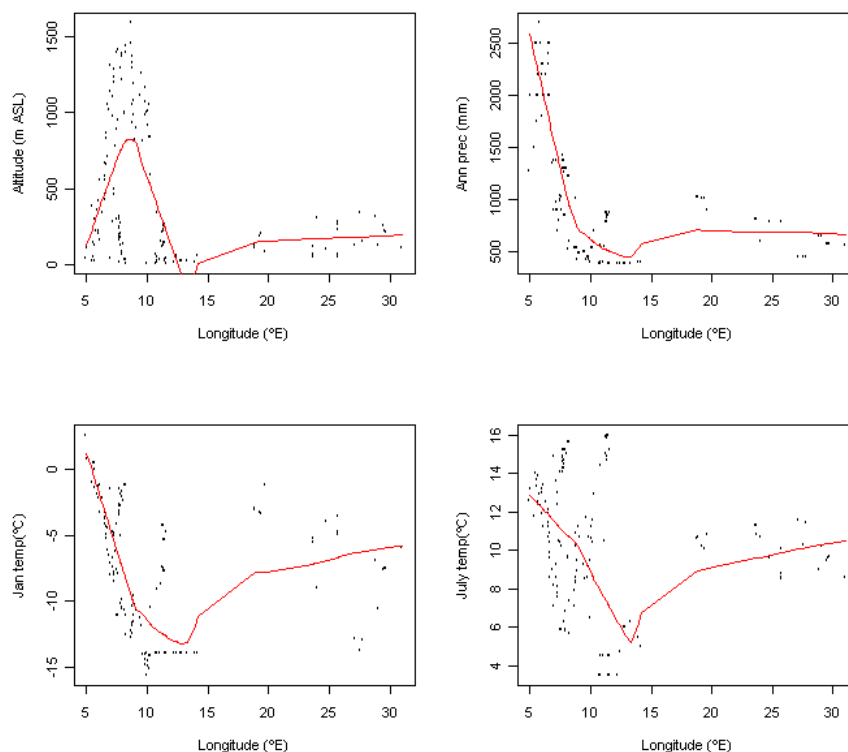


Figure 4.10.
The spatial
distribution of
physical and
climatic
variables in
mainland
Norway

	Latitude (N)	Longitude (E)	Altitude (m ASL)	Distance to coast (km)	pH	Ig Conductivity (uS/cm)	Water depth (m)	July air temp (°C)	Jan air temp (°C)	Continental Index	Annual precipitation (mm)	Ig Cl (ueq/l)	Ig SO4 (ueq/l)	Ig Ca (ueq/l)	Ig Mg (ueq/l)
Longitude (E)	0.5184														
Altitude (m ASL)	-0.4532	-0.3260													
Distance to coast (km)	-0.5057	-0.3688	0.8507												
pH	0.4408	0.2023	-0.1233	-0.0567											
Ig Conductivity (uS/cm)	0.4197	0.3790	-0.6078	-0.4755	0.6035										
Water depth (m)	-0.2336	-0.2943	-0.0120	-0.0403	-0.2307	-0.2893									
July air temp (°C)	-0.7242	-0.1540	-0.2223	0.0086	-0.3073	0.0571	0.1536								
Jan air temp (°C)	-0.5145	-0.1377	-0.3298	-0.3622	-0.3350	-0.0515	0.2783	0.7039							
Continental Index	-0.2541	-0.1071	0.3378	0.6239	0.0388	0.0200	-0.1671	0.1971	-0.5455						
Annual precipitation (mm)	-0.5016	-0.4070	-0.1194	-0.1900	-0.4203	-0.2679	0.3628	0.4867	0.7644	-0.4416					
Ig Cl (ueq/l)	0.3460	0.4125	-0.8635	-0.8387	0.1651	0.7058	-0.0761	0.2386	0.3971	-0.3931	0.0789				
Ig SO4 (ueq/l)	-0.0709	0.1919	-0.2768	-0.1208	0.3950	0.7254	-0.2323	0.3779	0.0705	0.2843	-0.1541	0.4490			
Ig Ca (ueq/l)	0.1779	0.2443	-0.1605	-0.0047	0.7794	0.7743	-0.2624	0.0434	-0.2490	0.3264	-0.3774	0.2659	0.7181		
Ig Mg (ueq/l)	0.4471	0.4581	-0.5488	-0.4306	0.6244	0.8886	-0.3148	0.0110	-0.1168	0.0524	-0.3533	0.6454	0.6878	0.7717	
Ig Na (ueq/l)	0.3518	0.4321	-0.8412	-0.7713	0.2517	0.7795	-0.1507	0.2482	0.3392	-0.3052	0.0211	0.9622	0.5323	0.3693	0.7349

Table 4.9. Correlation matrix showing the relationship between environmental variables in the Norwegian training set.

The strength of the relationship was expressed using Pearson product-moment correlation coefficients, figures highlighted in yellow showed strong correlations (r squared equal to or greater than 0.6) which were highly significant (p -values < 0.05).

Multiple regression analysis of the environmental variables with associated p-values (Table 4.9) indicates there are strong correlations between several of the variables, although fewer correlations than the Russian dataset (Table 4.2). In common with the Russian lakes conductivity is strongly correlated to the concentration of major ions ($r^2 > 0.71$) and there are significant correlations between concentrations of the major ions. This suggests there is considerable redundancy within the environmental variables and that variables could be removed to produce the minimal adequate model whilst retaining the goodness of fit. In the Norwegian lakes distance to the coast is strongly negatively correlated to Cl^- ($r^2 = -0.84$) and Na^+ ($r^2 = -0.77$) and positively correlated to continentality ($r^2 = 0.62$). This suggests the lakes are influenced by the maritime climate and sea-spray. In the Russian lakes distance to the coast was positively correlated to July air temperature, continentality, conductivity, Mg^{2+} and Na^+ which suggests the water chemistry of the Russian lakes results from the negative water balance associated with extreme continentality. In the Norwegian lakes July air temperature is negatively correlated to latitude ($r^2 = -0.72$) and positively correlated to January air temperatures ($r^2 = 0.70$).

4.3.2. Chironomid data

In total, 142 different chironomid taxa or morphotypes were identified in surface sediments from the 157 Norwegian lakes (Table 4.10). Of these, 28 taxa occur in 3 or fewer lakes. None of the identified taxa were recorded in all 157 lakes; however the most abundant, *Psectrocladius sordidellus*-type, *Sergentia coracina* and *Procladius*, occur in greater than 75% of the lakes. Comparisons with other published European records are difficult due to incompatibility in the sampling techniques or taxonomic resolution. For example, many of the common chironomid taxa from surface sediments in Sweden (Larocque *et al.* 2001) were identified to genera or genus-group only. However *Constempellina brevicosta* and *Einfeldia*, which were identified in the Russia surface-sediments, are also recorded in Sweden but are apparently absent or not found in the sampled Norwegian lakes. As discussed in section 4.2.2, the majority of common morphotypes, such as *Psectrocladius sordidellus*-type *Tanytarsus lugens*-type, *Procladius* and *Chironomus anthracinus*-type, are widespread throughout the Arctic and Subarctic. This would suggest the taxa may have a

cosmopolitan distribution due to wide environmental tolerances or the species composition, and therefore possibly the temperature optima, of the generic morphotypes may vary between geographical regions. Wide tolerances would reduce the sensitivity of the taxa in palaeoenvironmental reconstructions whereas changes in species composition may restrict application of the dataset to the region in which it was compiled.

Although the majority of taxa were common to both the Norwegian and Russian lakes, 30 taxa were recorded which were not found in the Russian lakes (highlighted in Table 4.10). Of these, *Diamesa aberrata*-type was recorded on Svalbard only. Many of these are rare in the Norwegian dataset, occurring in 3 or less lakes (Table 4.10), therefore their occurrence may reflect greater sampling effort (i.e. a greater number of lakes) in the Norwegian data compared to the Russian dataset. A number of the taxa are associated with springs, streams or running water; for example, *Krenosmittia* (Schmid 1993), *Rheotanytarsus* (Pinder and Reiss 1983), *Rheocricotopus* spp. (Cranston *et al.* 1983) and *Parochlus* (Brundin 1983). Their occurrence in the Norwegian lakes may reflect the greater importance of surface inflow into these lakes due to the high precipitation and mountainous terrain compared to the Russian lakes. Variations in the distribution of chironomid taxa may also be a response to temperature, continentality or species biogeography.

Taxon or morphotype name	Taxon or morphotype name	Taxon or morphotype name	Taxon or morphotype name
TANYPODINAE:	CHIRONOMINI cont.	ORTHOCLADIINAE cont.	3 or fewer occurrences
<i>Ablabesmyia</i>	<i>Polypedium nubeculosum</i> -type	<i>Parakiefferiella bathophila</i> -type	TANYPODINAE:
<i>Guttipelopia</i>	<i>Polypedium sordens</i> -type	<i>Parakiefferiella nigra</i> -type	<i>Labrundinia</i>
<i>Krenopelopia</i>	<i>Sergentia coracina</i> -type	<i>Parakiefferiella triquetra</i> -type	<i>Nilotanytus</i>
<i>Macropelopia</i>	<i>Stenochironomus</i>	<i>Parakiefferiella</i> type A	<i>Tanytus</i>
<i>Monopelopia</i>	<i>Stictochironomus</i>	<i>Paraphaenocladus</i> - <i>Parametriochnemus</i>	CHIRONOMINI:
<i>Natarsia</i>	PSEUDOCHIRONOMINI:	<i>Psectrocladius barbipes</i> -type	<i>Endochironomus tendens</i> -type
<i>Paramerina</i>	PSEUDOCHIRONOMINI:	<i>Psectrocladius flavus</i> -type	<i>Glyptotendipes severini</i> -type
<i>Peritaneurini</i> undiff.	TANYTARSINI:	<i>Psectrocladius septentrionalis</i> -type	<i>Microchironomus</i>
<i>Procladius</i>	<i>Cladotanytarsus mancus</i> -type	<i>Psectrocladius sordidellus</i> -type	<i>Omisis</i>
<i>Thienemannimyia</i>	<i>Cladotanytarsus mancus</i> -type 'with spur'	<i>Pseudorthocladus</i>	<i>Polypedium convictum</i> -type
<i>Zavrellimyia</i>	<i>Corynocera ambigua</i>	<i>Pseudosmittia</i>	TANYTARSINI:
CHIRONOMINI:	<i>Corynocera oliveri</i> -type	<i>Rheocricotopus effusus</i> -type	<i>Rheotanytarsus</i>
<i>Chironomus</i> 1st instar larva	<i>Microsectra insignilobus</i> -type	<i>Rheocricotopus fuscipes</i> -type	ORTHOCLADIINAE:
<i>Chironomus anthracinus</i> -type	<i>Microsectra pallidula</i> -type	<i>Smittia</i> - <i>Parasmittia</i>	<i>Brillia</i>
<i>Chironomus plumosus</i> -type	<i>Microsectra radialis</i> -type	<i>Synorthocladus</i>	<i>Cricotopus intersectus</i> -type
<i>Cladopelma</i>	<i>Paratanytarsus austriacus</i> -type	<i>Thienemanniella clavicornis</i> -type	<i>Diplocladus</i>
<i>Cryptochironomus</i>	<i>Paratanytarsus penicillatus</i> -type	<i>Zalutschia</i> type A	<i>Eukiefferiella devonica</i> -type
<i>Demicryptochironomus</i>	<i>Paratanytarsus</i> undiff.	<i>Zalutschia</i> type B	<i>Euorthocladus</i>
<i>Dicrotendipes</i>	<i>Stempellina</i>	<i>Zalutschia zalutschicola</i>	<i>Georthocladus</i>
<i>Endochironomus albipennis</i> -type	<i>Stempellinella</i> - <i>Zavrelia</i>	DIAMESINAE:	<i>Hydrobaenus johannseni</i> -type
<i>Endochironomus impar</i> -type	<i>Tanytarsini</i> undiff.	<i>Diamesa aberrata</i> -type	<i>Krenosmittia</i>
<i>Glyptotendipes pallens</i> -type	<i>Tanytarsus chrysenis</i> -type	<i>Diamesa zernyi/cinerella</i> type	<i>Metriochnemus fuscipes</i> -type
<i>Lauterborniella</i>	<i>Tanytarsus glabrescens</i> -type	<i>Protanytus</i>	<i>Nanocladus branchicolus</i> -type
<i>Microtendipes pedellus</i> -type	<i>Tanytarsus lugens</i> -type	<i>Pseudodiamesa</i>	<i>Nanocladus rectinervis</i> -type
<i>Pagastella</i>	<i>Tanytarsus mendax</i> -type	PRODIAMESINAE:	<i>Parachaetocladus</i>
<i>Parachironomus varus</i> -type	<i>Tanytarsus pallidicornis</i> -type	<i>Monodiamesa</i>	<i>Propiolocerus</i> type N
<i>Paracladopelma</i>	ORTHOCLADIINAE:	PODONIMINAE:	<i>Rheocricotopus chalybeatus</i> -type
<i>Paratendipes albianus</i> -type	<i>Abiskomyia</i>	<i>Parochilus kiefferi</i>	<i>Thienemanniella</i> type E
<i>Paratendipes nudisquama</i> -type	<i>Acamptocladus</i>	PRODIAMESINAE:	<i>Prodiamesa</i>
<i>Phaenopsectra flavipes</i> -type	<i>Bryophaenocladus</i>		
<i>Phaenopsectra</i> type A	<i>Chaetocladus</i>		

Table 4.10. Checklist of Chironomidae taxa recorded in the Norwegian lakes. Taxa highlighted in yellow were not recorded in the Russian lakes.

Norwegian species data

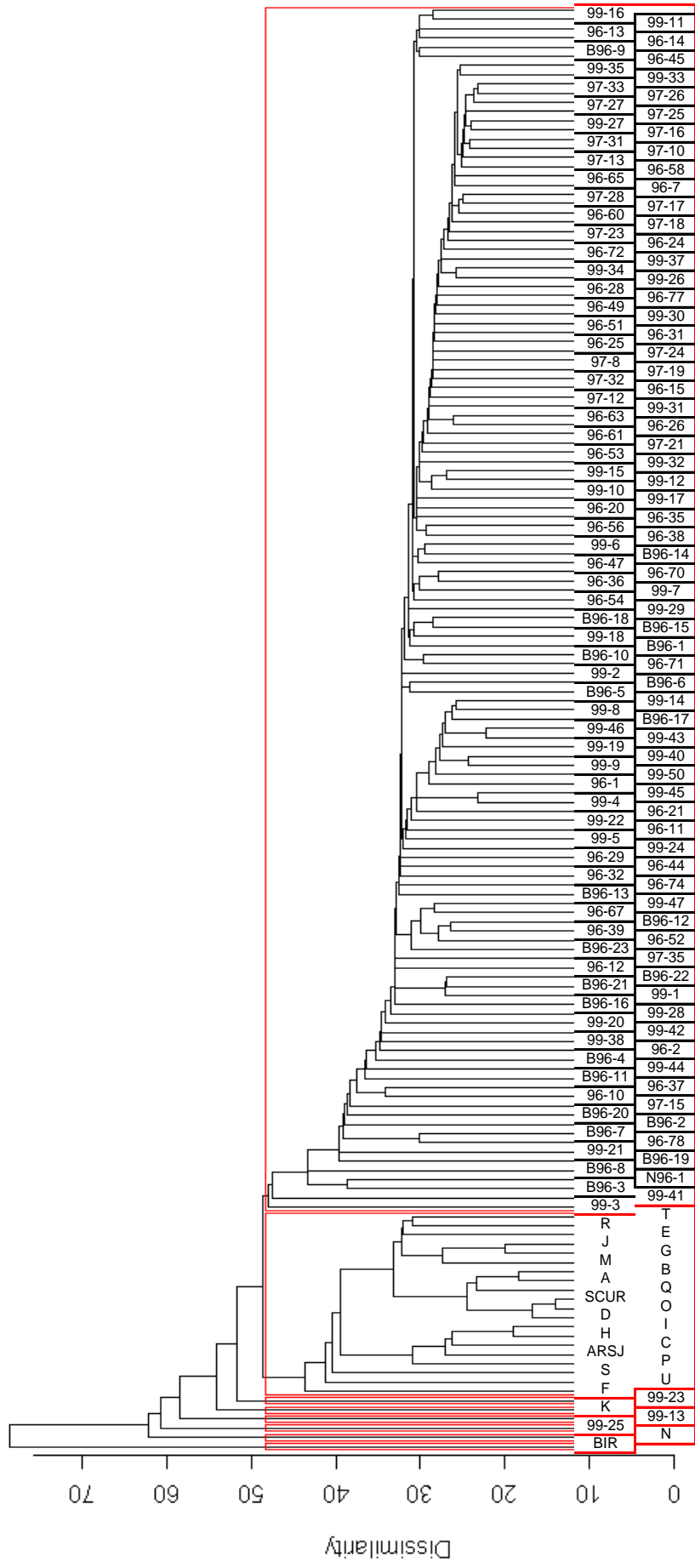


Figure 4.11. Dendrogram of the Norwegian chronomid assemblages classified by single-link clustering. Rectangles delineate the dendrogram into 8 clusters to highlight the distinct faunal assemblages of the Svalbard lat

(A – Bir in Table 4.7) and the north Norwegian lakes 99-13, 99-23 and 99-25 (Table 4.7).

4.3.3. Patterns of chironomid distribution

The assemblages from the Svalbard lakes (A – Bir in Table 4.7) and three lakes from northern Norway (99-13, 99-23 and 99-25) were highlighted as distinct from the remaining Norwegian lakes. The assemblage from lake 99-23, in particular, is more similar to the Svalbard faunas than those from mainland lakes. Single-link cluster analysis suggests the assemblage from lake Bir (Birgervatnet) is extremely distinct from the all other chironomid assemblages (dissimilarity coefficient > 70). Birgervatnet is a glacial melt-water fed lake on Spitsbergen (Birks et al. 2004) where the assemblage is composed of a single taxon, *Hydrobaenus lugubris*-type. Similarly the other lakes identified as distinct (N, 99-25, 99-13, F and 99-23) are dominated by a single taxon. Species richness is low in most of the Svalbard lakes (number of taxa = 1-10 compared to 11-43 in mainland lakes) and their faunas are typically dominated by 1 or 2 species. The remaining Svalbard lakes cluster together when the dominant species occurs in more than one lake, for example, *Micropsectra radialis*-type dominants in C, H, I and Ars and these lakes cluster together in the analysis. The chironomid assemblages from the remaining mainland lakes are generally similar (dissimilarity coefficient less than 40).

a. all lakes

Axes	1	2	3	4	Total inertia
Eigenvalues	: 0.580	0.218	0.130	0.092	3.783
Lengths of gradient	: 6.599	3.715	2.696	2.669	
Cumulative percentage variance of species data	: 15.3	21.1	24.6	27.0	
Sum of all eigenvalues					3.783

(b) minus Lake Birgervatnet (Bir)

Axes	1	2	3	4	Total inertia
Eigenvalues	: 0.576	0.210	0.156	0.101	3.526
Lengths of gradient	: 4.394	2.087	3.299	2.522	
Cumulative percentage variance of species data	: 16.4	22.3	26.7	29.6	
Sum of all eigenvalues					3.526

Table 4.11. Summary statistics for the first four axes of DCA (a) for all 157 Norwegian lakes and (b) excluding Lake Birgervatnet

A preliminary DCA based on all the Norwegian lakes had a gradient length of 6.6 SD units along the first axis (Table 4.11a). The long gradient length results primarily from the atypical fauna of the Svalbard lake Bir (Figure 4.12). This confirms the results of the cluster analysis which identified Bir as an outlier and its deletion from the dataset reduced the gradient length of the first axis to 4.4 SD units (Table 4.11b). The DCA with fitted convex hulls (Figure 4.12) shows considerable overlap between assemblages from mainland Norway. However the Svalbard assemblages occupy a distinct position in ordination space and only overlap with lake 99-23 from northern Norway. This lake (99-23) is fed by melt-water and the measured water temperature was considerably cooler than the estimated July air temperature (H.J.H. Birks, pers. comm. 2006). Like the Svalbard lakes, the assemblage has low species richness and is dominated by a single taxon, the cold-stenotherm *Pseudodiamesa*. The assemblages from southern Norway (lime green) do not overlap with those from northern Norway (brown) and the arrangement of Svalbard, northern and southern lakes along the axis suggests the first axis reflects July air temperatures and latitude.

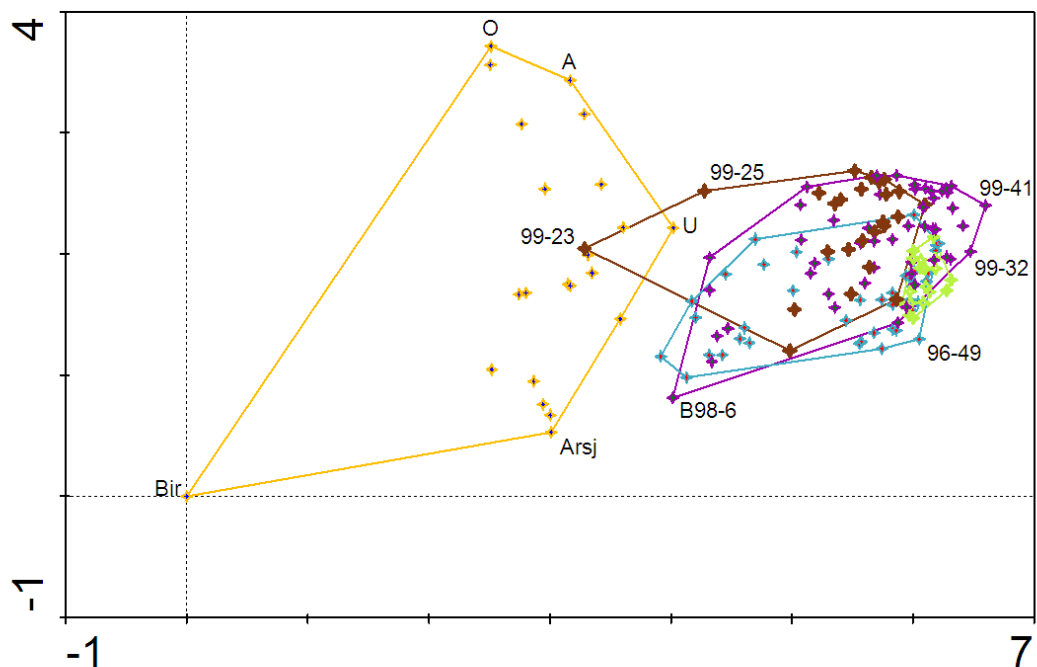


Figure 4.12. DCA plot of site scores for the Norwegian lakes with fitted convex hulls.

Sites classified by geographic region; Orange star – Svalbard, brown star – northern Norway, purple star – central and south-east Norway, lime stars – south-west Norway and light blue stars – western Norway.

4.3.4. Species – environment relationships

As the gradient length of the first DCA axis is greater than 2.5 SD units unimodal-based numerical methods were used to explore species – environment relationships. The eigenvalues of the first two DCA axes account for 22.3% of the variance in the species (Table 4.11) which is comparable to the explained variance in the Russian lakes (21.3% of species data, Table 4.5) and is typical of ‘noisy’ datasets.

Canonical correspondence analysis (CCA) was initially performed on the Norwegian environmental and species datasets with lake Bir deleted and longitude, latitude and altitude as supplementary environmental variables. The eigenvalues for CCA axis 1 ($\lambda_1 = 0.469$) and axis 2 ($\lambda_2 = 0.178$) explain 18.4% of the variance in the chironomid taxa (Table 4.12). The high species-environment correlations for CCA axis 1 (0.914) and axis 2 (0.808) suggest there is a strong relationship between the measured environmental variables and chironomid faunas. January and July air temperatures, continentality index, chloride (Cl^-) and sodium (Na^+) concentrations have high variance inflation factors (VIF) showing high levels of inter-correlations. These variables were eliminated one by one, based on the correlations identified in section 4.3.1., removing the variables with the highest VIFs. Sodium concentrations (Na^+), January temperature and conductivity were successively removed which reduced the VIFs to less than 10. Forward selection of the remaining variables indicated that eleven environmental variables make independent and significant contributions ($p \leq 0.05$) in explaining the variance in the chironomid data.

The most significant environmental variable is July air temperature which explains 37.3% of the total variance explained by all the measured environmental variables, followed by water depth (12.7%), distance to coast (9.7%) and continental index (7.8%). The remaining seven variables (annual precipitation, pH, Ca^{2+} , Cl^- , SO_4^{2-} , tundra and forest vegetation) each explain 3.9 – 4.9% of the total variance explained by all the measured environmental variables. The results of the CCA with significant variables are given in Table 4.12b and illustrated in Figure 4.13. The eigenvalues of CCA axis 1 ($\lambda_1 = 0.447$) and axis 2 ($\lambda_2 = 0.168$), constrained to the eleven significant variables, capture

17.4% of the cumulative variance in the species data. The species-environment correlations of CCA axis 1 (0.898) and axis 2 (0.806) are high and the first two axes account for 66.5% of the variance in the chironomid-environment relationship.

(a)

Axes	1	2	3	4	Total inertia
Eigenvalues	0.469	0.178	0.132	0.057	3.526
Species-environment correlations	0.914	0.808	0.784	0.661	
Cumulative percentage variance					
of species data	13.3	18.4	22.1	23.7	
of species-environment relation:	42.0	58.0	69.9	75.0	
Sum of all eigenvalues					3.526
Sum of all canonical eigenvalues					1.115

(b)

Axes	1	2	3	4	Total inertia
Eigenvalues	0.447	0.168	0.114	0.051	3.526
Species-environment correlations	0.898	0.806	0.699	0.660	
Cumulative percentage variance					
of species data	12.7	17.4	20.7	22.1	
of species-environment relation:	48.3	66.5	78.8	84.3	
Sum of all eigenvalues					3.526
Sum of all canonical eigenvalues					0.924

Table 4.12. Summary statistics for the first four axes of CCA of the Norwegian lakes, based on 157 lakes and 142 chironomid taxa (a) for all environmental variables and (b) after selection of significant environmental variables

Axis 1 of the CCA constrained to the eleven significant variables (Figure 4.13) separates lakes with low July air temperatures dominated by cold stenothermic species from warmer lakes. For example the cold Svalbard lakes (orange stars) are dominated by the cold stenotherms *Micropsectra radialis*-type, *Paratanytarsus austriacus*-type and *Orthocladius* type S whereas the warmer lakes from south-west Norway (lime-green stars) have more diverse assemblages including *Dicrotendipes*-type, *Microtendipes pedellus*-type, *Chironomus anthracinus*-type and *Paratanytarsus penicillatus*-type. The lakes

from Svalbard, north Norway and south-west Norway cover relatively short ranges along the 1st axis whereas the lakes from western Norway and central and south-east Norway show a wider scatter reflecting the greater range of latitudes and, hence, temperature in these regions. The second axis is related to water depth and calcium (Ca²⁺) concentrations. *Heterotrissocladius maeaeri*-type and *H. marcidus*-type which occur in the profundal of cold oligotrophic lakes are associated with the deeper lakes in the ordination. Lakes from western Norway generally appear to be deeper and have lower Ca²⁺ suggesting that underlying geology and tectonic history strongly influences lake characteristics.

The selection of distance to the coast, Cl⁻ concentrations and continentality as significant environmental variables suggests that the maritime environment is important in determining the climate regime and water chemistry of the lakes and, therefore, the distribution of chironomids. At a synoptic scale mean July air temperature is the most important environmental variable influencing chironomid distribution. However the site selection procedure purposely reduced the other environmental gradients in order to reduce their influence on the species data.

Key to abbreviations used in Figure 4.13: tjul – July air temperature, wdepth – water depth (m), coast – distance to coast (km), precA – annual precipitation (mm), ci – continentality index; tundra and forest – vegetation type. (b) Species with species weight >20% included, points scaled relative to Hill's N2 value for each species. Taxa abbreviations: Abla – *Ablabesmyia*, Ca – *Corynocera ambigua*, Cha – *Chironomus anthracinus* type, Dict – *Dicrotendipes* type, Hap – *Heterotanytarsus*, Hbr – *Heterotrissocladius maeaeri* type, Hma – *Heterotrissocladius marcidus*-type, Lm – *Limnophyes*, Min – *Micropsectra insignilobus* type, Mped – *Microtendipes pedellus* type, Mra – *Micropsectra radialis*-type, OS – *Orthocladius* type S, Pa – *Paratanytarsus austriacus*-type, Para – *Paratanytarsus* type, Pp – *Paratanytarsus penicillatus* type, Proc – *Procladius*, Ps – *Psectrocladius sordidellus* type, Psep – *Psectrocladius septentrionalis* type, Ser – *Sergentia* type, Tm – *Tanytarsus mendax* type, Tl – *Tanytarsus lugens* type, Tp – *Tanytarsus pallidicornis* type,

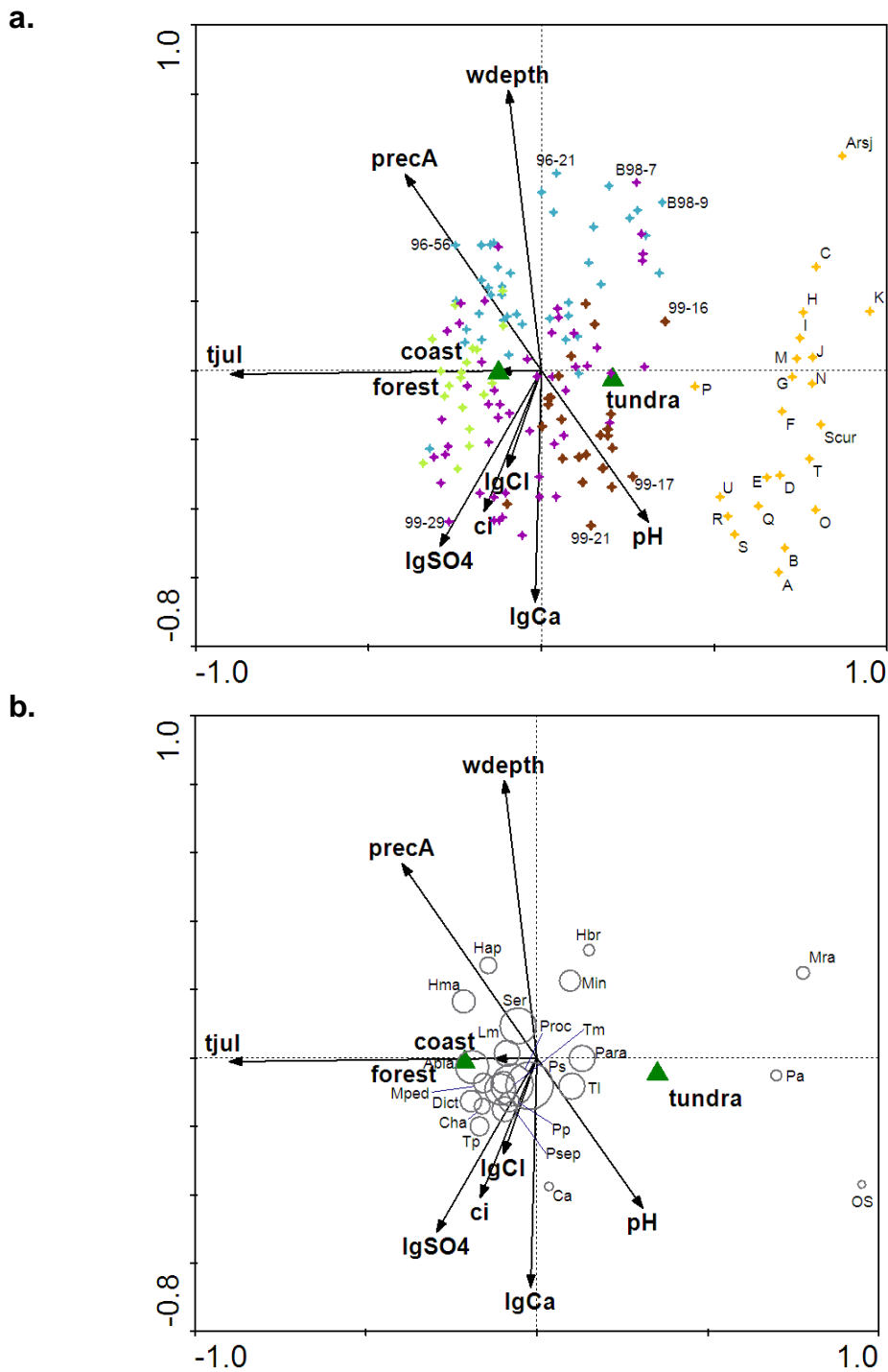


Figure 4.13. CCA biplots of axis 1 and 2 illustrating the relationship between the significant environmental variables and faunal assemblage in the Norwegian lakes, showing (a) the site scores and (b) the species scores. Quantitative environmental variables, chosen in forward selection, are shown as arrows and the nominal variables (forest and tundra vegetation) as centroids. (a) Sites classified by geographic region: Orange star – Svalbard, brown star – northern Norway, purple star – central and south-east Norway, lime stars – south-west Norway and light blue stars – western Norway.

4.4. Combined Russian and Norwegian surface sediment data-sets

The environmental data in section 4.2.1 highlighted the discontinuous and uneven distribution of lakes along environmental gradients in the Russian data-set which may cause problems with the estimation of accurate optima in derived inference models. Therefore the Russian and Norwegian datasets were combined, giving 161 taxa in 251 lakes. The aims of this section are:

1. To assess whether combining the datasets improves the distribution of lakes along the climate-based environmental gradients,
2. To assess the impact of combining the datasets on species – environment relationships, and
3. To identify outliers, in terms of species composition and/or environmental variables which should be removed from the datasets prior to development of chironomid-climate inference models.

4.4.1. Environmental data

Table 4.13. Summary of environmental variables for the combined Norwegian - Russian datasets

	COMBINED NORWEGIAN AND RUSSIAN LAKES (251 lakes)				
	Minimum	Median	Mean	Maximum	Std dev
Latitude (N)	58.0800	63.6700	65.4800	79.8000	
Longitude (E)	5.0050	12.4670	45.4330	131.2270	
Altitude (m ASL)	2	144	360	1594	421
Distance to coast (km)	0.1	86	205.6	899	278.8
pH	4.66	6.73	6.88	9.92	0.99
Conductivity (uS/cm)	2	95	40	2980	235
Water depth (m)	0.5	4.6	6.5	29.0	5.7
July air temp (°C)	3.5	11.7	11.8	19.0	4.0
Jan air temp (°C)	-39.4	-13.9	-16.2	2.6	12.8
Continental Index	-1	19	32	91	28
Annual precipitation (mm)	239	500	753	2700	592
Cl (ueq/l)	2.0	50.0	147.8	5896.0	438.4
SO4 (ueq/l)	1.0	38.0	62.0	1226.0	105.2
Ca (ueq/l)	20.0	168.0	343.1	3004.0	425.9
Mg (ueq/l)	7.0	75.0	393.8	17270.0	1607.3
Na (ueq/l)	7.0	84.0	323.2	25141.0	1699.7

Combining the training sets increased the range of the climate variables (January temperature, July temperature, continentality and annual precipitation). As maximum values for water chemistry excluding SO_4^{2-} ions

and conductivity were derived from the Russian lakes, incorporating the Norwegian lakes reduced the variance in these environmental variables in terms of standard deviation. The variability only increased in altitude, pH, water depth and SO_4^{2-} ions (Table 4.13, see Tables 4.2 and 4.8 for summaries of Russian and Norwegian environmental variables respectively).

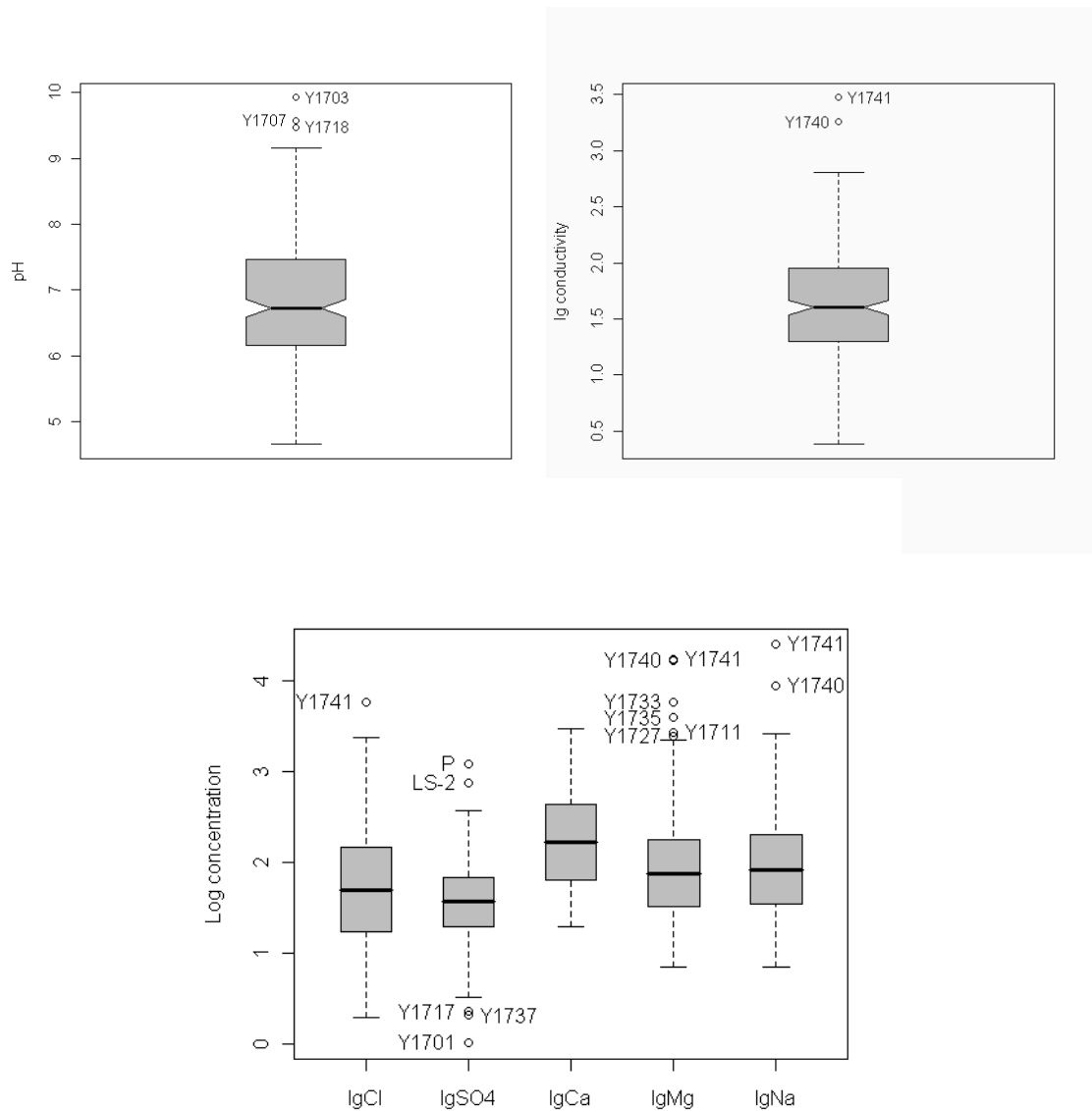


Figure 4.14. Box-Whisker plots for selected water chemical characteristics of the combined Norwegian - Russian lakes. The box is drawn between the 1st and 3rd quartile with the median represented by the black horizontal line; the vertical lines or whiskers represent the maximum and minimum values unless outliers are present (represented by circles) when whiskers are drawn at 1.5 times the inter-quartile range. See Tables 4.1 and 4.7 for lake codes.

Box and whisker plots of the water chemistry variables (Figure 4.14) indicated that the extreme values could be attributed to a small number of lakes. Exclusion of 3 lakes, Y1741, Y1740 and Y1733, removed the more extreme values and reduced the variance in the water chemistry data (Table 4.14).

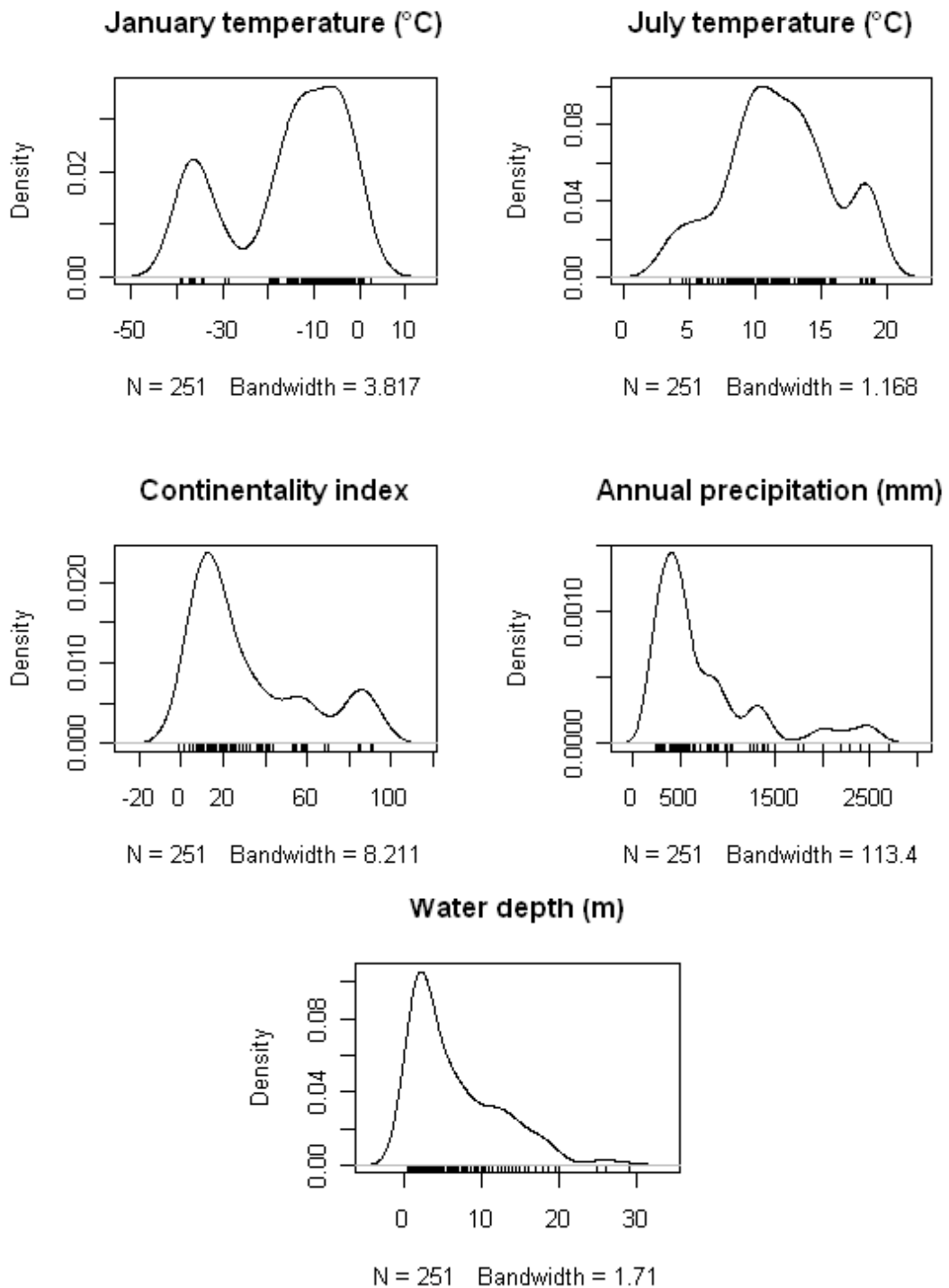
Table 4.14. Effect on the descriptive statistics of excluding three lakes from the combined Norwegian – Russian data-set

	ALL RUSSIAN AND NORWEGIAN LAKES						COMBINED LAKES MINUS Y1733, Y1740 AND Y1741					
	Minimum	Median	Mean	Maximum	Range	Std dev	Minimum	Median	Mean	Maximum	Range	Std dev
pH	4.66	6.73	6.88	9.92	5.26	0.99	4.66	6.72	6.86	9.92	5.26	0.96
Conductivity (uS/cm)	2	95	40	2980	2978	235	2	39	74	507	505	93
Cl (ueq/l)	2	50	148	5896	5894	438	2	48	116	2342	2340	212
SO4 (ueq/l)	1	38	62	1226	1225	105	1	38	64	1226	1225	106
Ca (ueq/l)	20	168	343	3004	2984	426	20	165	341	3004	2984	426
Mg (ueq/l)	7	75	394	17270	17263	1607	7	75	238	3906	3899	480
Na (ueq/l)	7	84	323	25141	25134	1700	7	81	179	2518	2511	304

Lakes in a training set should be continuously and evenly distributed over the environmental gradient of interest, with low between-lake variation in other environmental variables, to reduce prediction errors and bias in the inference model (ter Braak and Looman 1986; Birks 1995). The distributions of the many climatic variables in the Russian lakes are bimodal due to clustering of the lakes along the environmental gradients (Figure 4.3). After combining the datasets only January temperature remains bimodal due to the extreme continentality of the Lena River samples (prefixed Y- and LS-) and the absence of intermediate lakes (Figure 4.15). January temperature would be unsuitable for development of an inference model as the formation of lake ice in winter ensures the water remains at 0 – 4°C whatever the air temperature. The discontinuous July temperature gradient, with an absence of lakes with July air temperatures between 16 – 18°C, is still present but less pronounced than in the Russian dataset alone (section 4.2.1). The high kurtosis of the mean July air temperature (T_{july}) and continentality index (CI) curves suggests the dataset is dominated by Norwegian lakes (CI 0-30) and lakes with T_{july} of approximately 10°C. Reduction in the number of lakes with these characteristics would improve the evenness of the distribution along the environmental gradients. The distribution of water depth and annual precipitation curves indicates the typical

water depth is between 0-10m and annual precipitation between 0-1000mm. Minimising variation along these gradients by removing deeper lakes or those experiencing high precipitation may improve the performance of the inference model

Figure 4.15. Kernel-density estimates showing the distribution of water depth and climatic variables in the combined Norwegian – Russian trainings set



	Latitude (N)	Longitude (E)	Altitude (m ASL)	Distance to coast (km)	pH	Ig Conductivity (uS/cm)	Water depth (m)	July air temp (°C)	Jan air temp (°C)	Continental Index	Annual precipitation (mm)	Ig Cl (ueq/l)	Ig SO4 (ueq/l)	Ig Ca (ueq/l)	Ig Mg (ueq/l)	
Longitude (E)	0.1878															
Altitude (m ASL)	-0.4457	-0.3859														
Distance to coast (km)	-0.1919	0.7111	-0.0302													
pH	0.2478	0.7342	-0.3016	0.6747												
Ig Conductivity (uS/cm)	0.1742	0.4499	-0.4934	0.4474	0.6678											
Water depth (m)	-0.2321	-0.4204	0.1523	-0.2849	-0.4011	-0.3194										
July air temp (°C)	-0.5472	0.4907	-0.3332	0.6561	0.3698	0.4154	-0.1211									
Jan air temp (°C)	-0.2508	-0.9504	0.2407	-0.7589	-0.7649	-0.44	0.4432	-0.3667								
Continental Index	0.0089	0.9433	-0.273	0.8602	0.7554	0.4962	-0.4046	0.6275	-0.9531							
Annual precipitation (mm)	-0.474	-0.558	0.1245	-0.4005	-0.5756	-0.3512	0.4631	-0.0007	0.6863	-0.5715						
Ig Cl (ueq/l)	0.1523	-0.0906	-0.6231	-0.151	0.0753	0.5531	0.0049	0.2073	0.2082	-0.1244	0.1109					
Ig SO4 (ueq/l)	0.0371	-0.3921	0.0374	-0.5797	-0.2623	-0.0781	0.0522	-0.3157	0.4219	-0.4633	0.1621	0.1592				
Ig Ca (ueq/l)	0.1177	0.5079	-0.3031	0.4558	0.7667	0.7336	-0.362	0.3821	-0.5321	0.5633	-0.4947	0.2363	0.0356			
Ig Mg (ueq/l)	0.2039	0.6344	-0.5049	0.5665	0.7861	0.8671	-0.3738	0.4836	-0.6193	0.6659	-0.4869	0.4743	-0.1634	0.8196		
Ig Na (ueq/l)	0.0797	0.2279	-0.5878	0.2906	0.4176	0.7748	-0.1515	0.4577	-0.1458	0.2609	-0.0864	0.8518	-0.0795	0.4853	0.7608	

Table 4.15. Correlation matrix showing the relationship between environmental variables in the Norwegian – Russian training set.

The strength of the relationship was expressed using Pearson product-moment correlation coefficients, figures highlighted in yellow showed strong correlations (r^2 equal to or greater than 0.6) which were highly significant (p -values < 0.05).

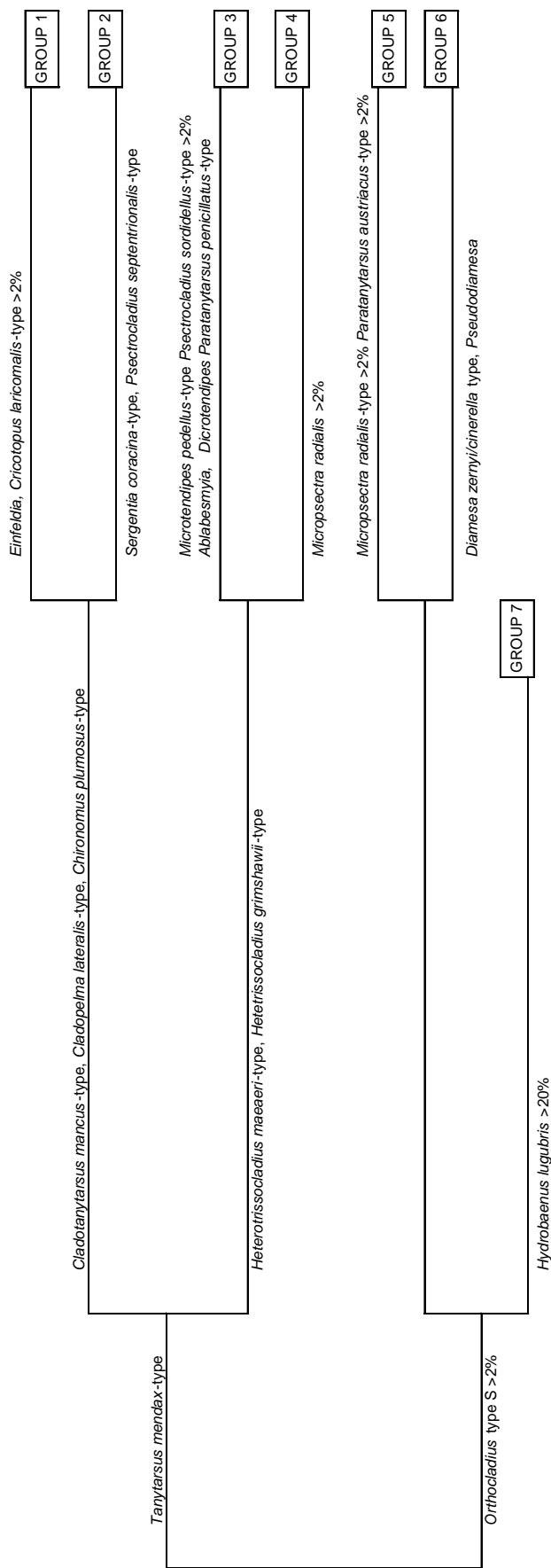


Table 4.16. TWINSpan classification of the combined Norwegian – Russian lakes based on the chironomid fauna.

GROUP 1	GROUP 2	GROUP 3	GROUP 4	GROUP 5	GR 6	GR7
Y1708	Y1740	Y1740	KHAR			
Y1731	99-44	99-44	NERU			
Y1712	99-42	99-42	LS-27			
Y1706	99-41	99-41	Vanuk-ty			
Y1705	99-40	99-40	Mitro			
Y1703	99-22	99-22	TDRU 11a			
Y1701	99-32	99-32	TDRE 1			
Y1700	99-27	99-27	TDRA 2			
Y1743	99-26	99-26	F8-4			
Y1739	97-27	97-27	F6-2			
Y1735	97-16	97-16	PFIV			
Y1732	96-39	96-39	99-47			
Y1729	96-7	96-7	99-20			
Y1727	99-37	99-37	99-11			
Y1721	99-34	99-34	99-7			
Y1717	97-32	97-32	99-6			
Y1716	96-20	96-20	99-1			
Y1711	VORK5	VORK5	B98-23			
Y1709	PFOR	PFOR	B98-18			
Y1704	PTHE	PTHE	B98-15			
Y1703	PONE	PONE	B98-12			
Y1723	AFOX	AFOX	F8-4			
Y1723	VORK3	VORK3	F6-2			
Y1713	ARTE	ARTE	PFIV			
Y1746	WILD	WILD	99-47			
Y1730	F3-12	F3-12	99-20			
Y1726	99-50	99-50	99-11			
Y1725	99-46	99-46	99-7			
Y1724	99-45	99-45	99-6			
Y1722	99-43	99-43	B98-23			
Y1718	99-38	99-38	B98-18			
Y1717	99-34	99-34	B98-15			
Y1707	99-24	99-24	B98-12			
Y1737	99-19	99-19	F8-4			
Y1733	99-17	99-17	F6-2			
Y1741	99-15	99-15	PFIV			
Y1720	99-14	99-14	99-47			
Y1719	99-9	99-9	99-20			
	99-4	99-4	99-11			
	B98-17	B98-17	99-7			
	B98-16	B98-16	99-6			
	B98-14	B98-14	B98-23			
	B98-11	B98-11	B98-18			
	96-11	96-11	B98-15			
	96-1	96-1	B98-12			
	LS-25	LS-25	F8-4			
	IGAR	IGAR	F6-2			
	TDRU 42a	TDRU 42a	PFIV			
	TDRD 2	TDRD 2	99-47			
	TDCR 2	TDCR 2	99-20			
	F8-2	F8-2	99-11			
	F7-5	F7-5	99-7			
	F7-3	F7-3	99-6			
	F4-5	F4-5	B98-23			
	F4-4	F4-4	B98-18			
	F4-2	F4-2	B98-15			
	F3-6	F3-6	B98-12			
	F3-5	F3-5	F8-4			
	F3-3	F3-3	F6-2			
	F3-2	F3-2	PFIV			
	99-31	99-31	99-47			
	97-12	97-12	99-20			
	97-35	97-35	99-11			
	LS-24	LS-24	99-7			
	LS-17	LS-17	99-6			
	LS-16	LS-16	B98-23			
	LS-12	LS-12	B98-18			
	99-30	99-30	B98-15			
	99-29	99-29	B98-12			
	99-28	99-28	F8-4			
			F6-2			
			PFIV			
			99-47			
			99-20			
			99-11			
			99-7			
			99-6			
			99-1			
			B98-23			
			B98-18			
			B98-15			
			B98-12			
			F8-4			
			F6-2			
			PFIV			
			99-47			
			99-20			
			99-11			
			99-7			
			99-6			
			99-1			
			B98-23			
			B98-18			
			B98-15			
			B98-12			
			F8-4			
			F6-2			
			PFIV			
			99-47			
			99-20			
			99-11			
			99-7			
			99-6			
			99-1			
			B98-23			
			B98-18			
			B98-15			
			B98-12			
			F8-4			
			F6-2			
			PFIV			
			99-47			
			99-20			
			99-11			
			99-7			
			99-6			
			99-1			
			B98-23			
			B98-18			
			B98-15			
			B98-12			
			F8-4			
			F6-2			
			PFIV			
			99-47			
			99-20			
			99-11			
			99-7			
			99-6			
			99-1			
			B98-23			
			B98-18			
			B98-15			
			B98-12			
			F8-4			
			F6-2			
			PFIV			
			99-47			
			99-20			
			99-11			
			99-7			
			99-6			
			99-1			
			B98-23			
			B98-18			
			B98-15			
			B98-12			
			F8-4			
			F6-2			
			PFIV			
			99-47			
			99-20			
			99-11			
			99-7			
			99-6			
			99-1			
			B98-23			
			B98-18			
			B98-15			
			B98-12			
			F8-4			
			F6-2			
			PFIV			
			99-47			
			99-20			
			99-11			
			99-7			
			99-6			
			99-1			
			B98-23			
			B98-18			
			B98-15			
			B98-12			
			F8-4			
			F6-2			
			PFIV			
			99-47			
			99-20			
			99-11			
			99-7			
			99-6			
			99-1			
			B98-23			
			B98-18			
			B98-15			
			B98-12			
			F8-4			
			F6-2			
			PFIV			
			99-47			
			99-20			
			99-11			
			99-7			
			99-6			
			99-1			
			B98-23			
			B98-18			
			B98-15			
			B98-12			
			F8-4			
			F6-2			
			PFIV			
			99-47			
			99-20			
			99-11			
			99-7			
			99-6			
			99-1			
			B98-23			
			B98-18			
			B98-15			
			B98-12			
			F8-4			
			F6-2			
			PFIV			
			99-47			
			99-20			
			99-11			
			99-7			
			99-6			
			99-1			
			B98-23			
			B98-18			
			B98-15			
			B98-12			
			F8-4			
			F6-2			

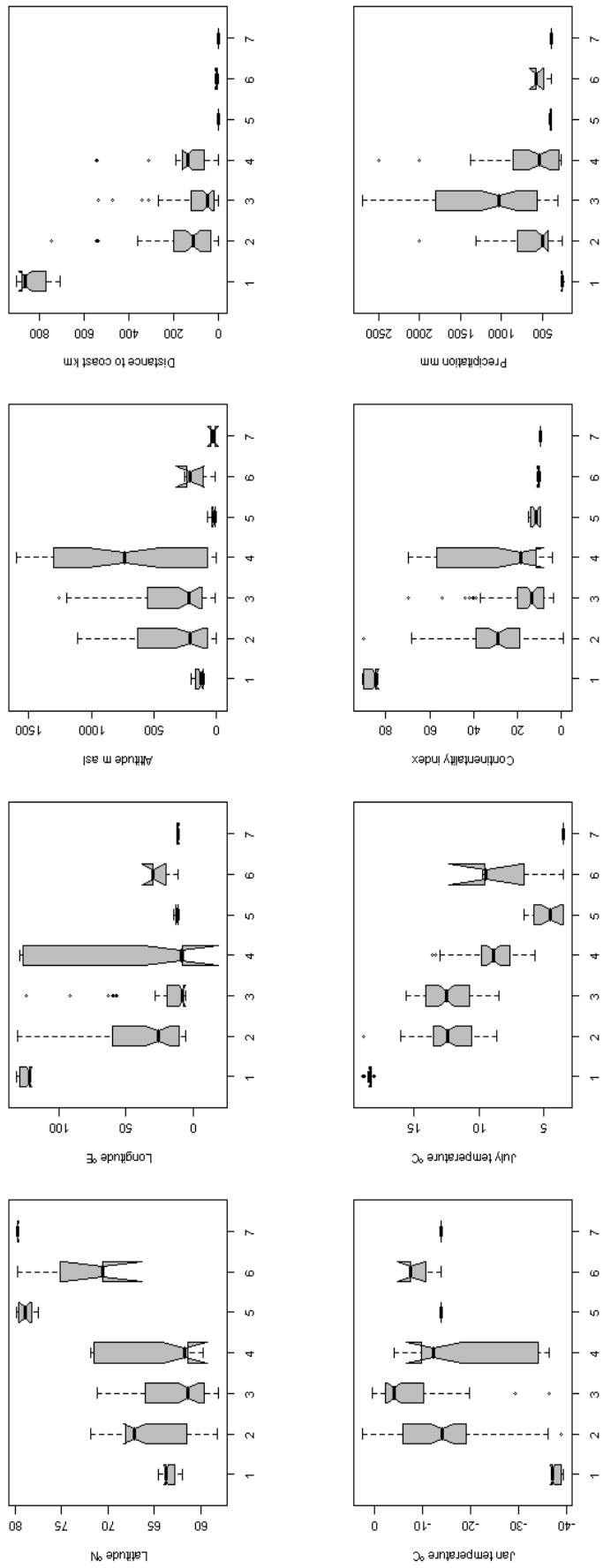


Figure 4.16 Box-Whisker plots of geographic and climatic variables associated with TWINSpan groups see Table 4.16.

The box is drawn between the 1st and 3rd quartile with the median represented by the black horizontal line; the vertical lines or whiskers represent the maximum and minimum values unless outliers are present (represented by circles) when whiskers are drawn at 1.5 times the inter-quartile range.

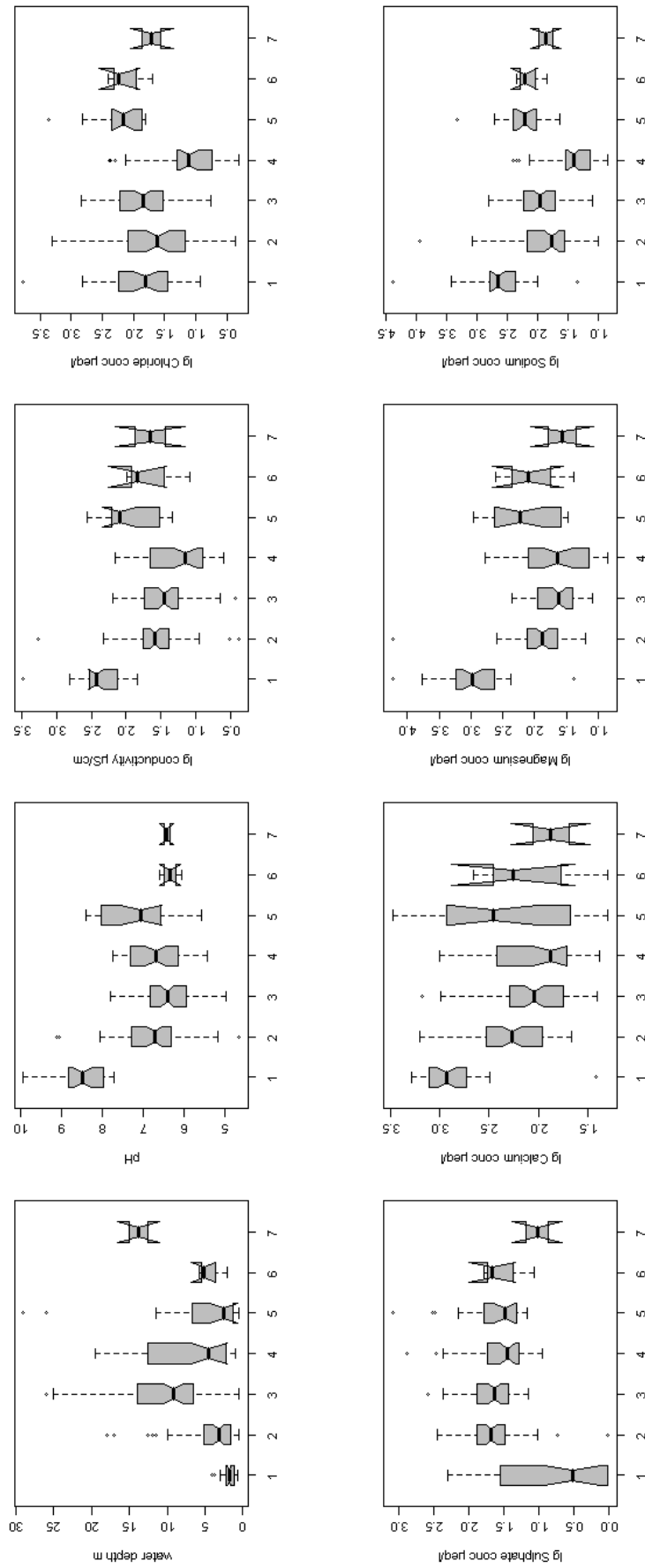


Figure 4.17 Box-Whisker plots of water depth and water chemistry variables associated with TWINSpan groups. For TWINSpan groups see Table 4.16. The box is drawn between the 1st and 3rd quartile with the median represented by the black horizontal line; the vertical lines or whiskers represent the maximum and minimum values unless outliers are present (represented by circles) when whiskers are drawn at 1.5 times the inter-quartile range.

The Norwegian and Russian training sets individually showed strong correlation between a number of the environmental variables (sections 4.2.1 and 4.3.1). These are still apparent in the combined dataset (Table 4.15); pH is correlated to conductivity and both these parameters to Ca^{2+} , Mg^{2+} and Na^+ concentrations. Continentality is strongly correlated to January and July air temperatures, which are used in the calculation of the continentality index, and longitude. The high degree of correlation suggests there is considerable redundancy within the environmental variables and that variables could be removed (as described in section 4.4.4) to produce the minimal adequate model.

4.4.2. Patterns of chironomid distribution

Single-link clustering was used in sections 4.2.3 and 4.3.3 to identify lakes with anomalous faunas in the Russian and Norwegian datasets. To examine patterns of similarity, and the environmental variables which might be driving their distribution, the chironomid assemblages of the Norwegian and Russian lakes were classified using TWINSpan (Hill 1979; Hill and Šmilauer 2005). TWINSpan analysis produced 7 groups after 3 successive divisions (Table 4.16); the environmental characteristics of the 7 groups are shown in Figures 4.16 and 4.17.

The presence of *Orthocladius* type S separates the Svalbard and 2 Norwegian lakes (99-23 and 99-25) from the remaining lakes to form groups 5, 6 and 7. Although the ranges of many environmental variables of the 7 groups overlap, lakes in groups 5, 6 and 7 generally experience cooler July temperatures than the other lakes. The Svalbard and 2 Norwegian lakes are located close to the coast with low precipitation; they also have higher conductivities than the majority of the groups with the exception of group 1 – the Yakutia lakes. The high conductivity may reflect the maritime environment as chloride and sodium ions were generally higher in groups 5 and 6; concentrations in group 7 were similar to the mainland groups but these lakes are deeper which would result in dilution of spray derived chemicals. The two lakes in group 7, K (Kobberfjorden) and Bir (Birgervatnet), are surrounded by sparse polar desert vegetation (Figure 4.18).

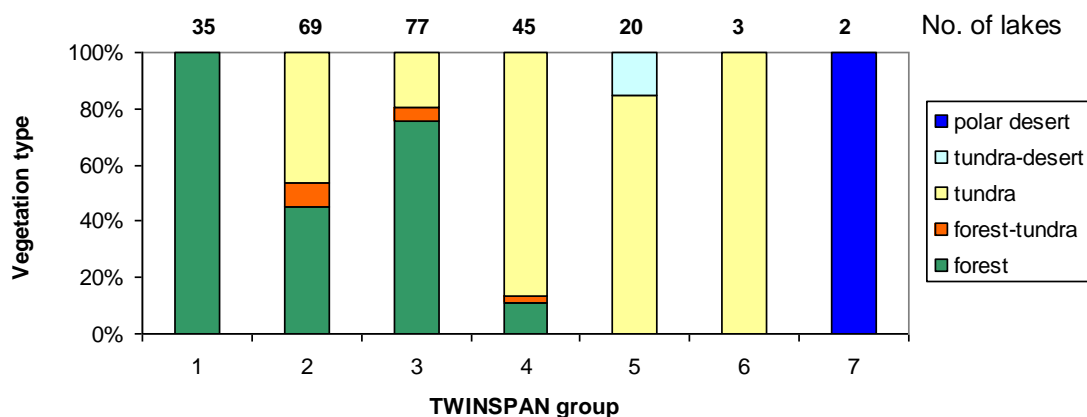


Figure 4.18. Vegetation types of the TWINSpan groups expressed as a percentage of the lakes in each group.

In the Russian and remaining Norwegian lakes, groups 1 and 2 are distinguished by the presence of *Cladotanytarsus mancus*-type, *Cladopelma lateralis*-type and *Chironomus plumosus*-type. The negative indicator species generally occur in the littoral of relatively warm lakes; Figures 4.16 and 4.17 indicate this grouping includes the warmer Yakutia lakes (group 1) and shallow lakes with relatively warm air temperatures (group 2). Groups 3 and 4 are distinguished by the presence of *Heterotrissocladius maeaeeri*-type and *H. grimshawii*-type which typically occur in the profundal of cold oligotrophic lakes, although not as cold as the lakes in groups 5, 6 and 7. The lakes in group 3 experience similar air temperatures to group 2 but are significantly deeper (Figure 4.17). Lakes in group 4 are generally, but not significantly, deeper than the group 2 lakes but experience cooler July air temperatures (Figure 4.17). July air temperatures appear to be the most important factor determining the chironomid assemblage and gives statistical significant separation of 5 of the 7 groups; water depth and water chemistry are important factors in the identification of the remaining groups.

Although the chironomid faunas from Yakutia and Svalbard appear distinct, the remaining assemblages from Russia and Norway (with the exception of lakes 99-23 and 99-25) are inter-dispersed in the TWINSpan analysis which suggests their faunal compositions are similar and independent of geographical location. These trends are also apparent in the DCA, with fitted convex hulls

based on the geographical region, (Figure 4.19) which show little commonality between assemblages from either Yakutia or Svalbard and the remaining lakes. By comparison the ordination space occupied by assemblages from lakes in northeast European Russia, the Putorana Plateau and the Lena Delta overlap and are therefore similar to the assemblages in lakes from North, West, central and southeast Norway. The compositional homogeneity between the two datasets suggests the datasets could be combined to develop a northern Eurasia chironomid inference models.

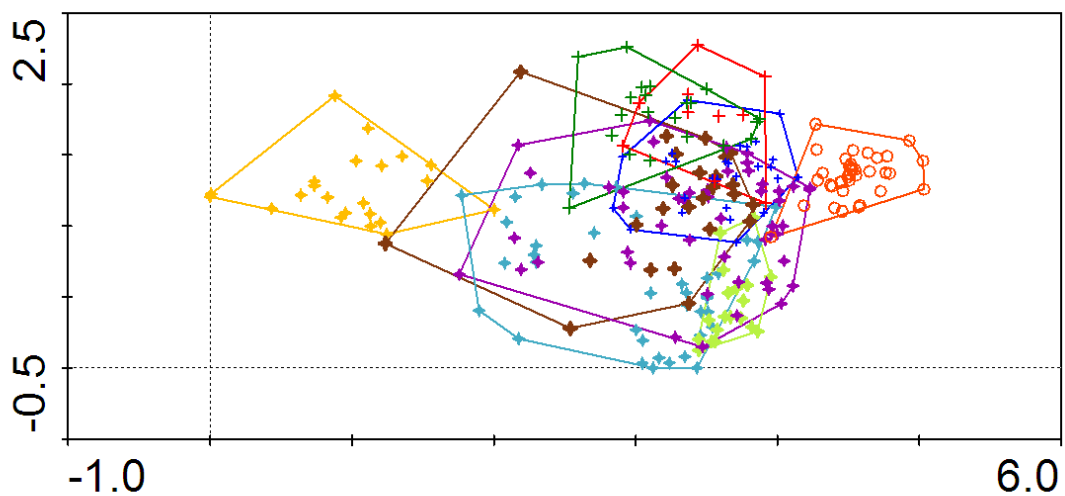


Figure 4.19. DCA plot of site scores for the combined Norwegian-Russian dataset (excluding Lake Birgervatnet) with fitted convex hulls. Sites classified by geographic region; Orange star – Svalbard, brown star – northern Norway, purple star – central and south-east Norway, lime stars – south-west Norway, cyan stars – western Norway, blue cross – north-east European Russia, red cross – Putorana, orange ring – Yakutia and green cross – Lena Delta.

Lake U, which has the warmest July air temperature of the Svalbard lakes, plots within the sample envelopes of the mainland Norwegian lakes and lake B98-2 from western Norway plots within the envelope for Svalbard. These overlaps, together with the inclusion of mainland lakes within the Svalbard lakes in the TWINSpan analysis, suggest that although the assemblages from Svalbard are distinctive they demonstrate some commonality with lakes from the mainland. The assemblages may therefore result from the low summer temperatures rather than island biogeography.

When the lakes are classified according to their TWINSPAN grouping the group envelopes cut across the geographical regions supporting the concept that many of the species are cosmopolitan (Figure 4.20). However total turnover of species occurs within a gradient length of 4SD (ter Braak 1987). The distance between the centroids of the Svalbard sample envelope and the Yakutia sample envelope (Figure 4.19) is approximately 4SD. Therefore the two locations should have few species in common and the morphotypes which occur in both (for example *Chironomus anthracinus*-type, *Procladius*, *Psectrocladius sordidellus*-type and *Tanytarsus lugens*-type) may actually represent different species. The difficulties associated with the taxonomy of these taxa will be discussed in chapter 5. The positioning of the TWINSPAN groups along the first axis (Figure 4.20), together with their characteristic environmental variables (Figures 4.16 and 4.17), suggests the first axis primarily reflects a response to July air temperatures.

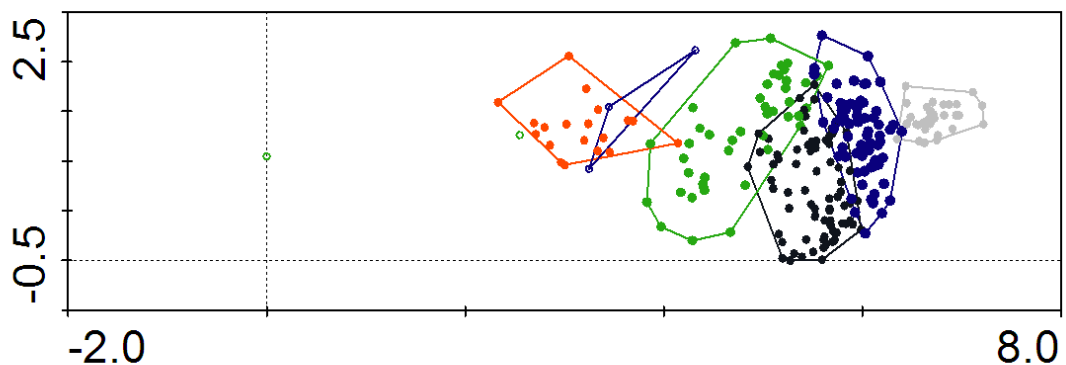


Figure 4.20. DCA plot of site scores for the combined Norwegian and Russian lakes with fitted convex hulls based on their TWINSPAN groups. Sites classified by TWINSPAN group; grey – group 1, dark blue filled circles – group 2, black – group 3, green – group 4, red – group 5, blue unfilled circles (3 lakes) – group 6 and green unfilled circles (2 lakes) group 7.

4.4.3. Species – environment relationships

The distribution of lakes in the DCA (Figure 4.20) suggested that the first axis represented T_{july} ; this was confirmed by CCA. A preliminary DCA based on all the lakes had a gradient length of 7.2 standard deviations along the first axis (Table 4.17a). The long gradient length results partially from the anomalous fauna of the Svalbard lake Bir, which had previously been identified as an

outlier (sections 4.3.3) and its exclusion from the dataset reduced the gradient length along the first axis to 5.0 SD (Table 4.17b). The eigenvalues of the first two axes of the DCA, with Bir excluded, account for 18.9% of the variance in the species data which is less than the percentages explained in each country individually (22.3% of the variance in the species data for Norway and 21.3% of species data for Russia). This suggests that combining the datasets has introduced noise by lengthening the gradients in most environmental variables (section 4.4.1).

a. all lakes

Axes	1	2	3	4	Total inertia
Eigenvalues	: 0.516	0.213	0.161	0.109	4.056
Lengths of gradient	: 7.218	2.267	3.764	2.621	
Cumulative percentage variance of species data	: 12.7	18.0	22.0	24.6	
Sum of all eigenvalues					4.056

(b) minus Lake Birgervatnet (Bir)

Axes	1	2	3	4	Total inertia
Eigenvalues	: 0.513	0.209	0.134	0.103	3.824
Lengths of gradient	: 5.031	2.272	3.458	2.225	
Cumulative percentage variance of species data	: 13.4	18.9	22.4	25.1	
Sum of all eigenvalues					3.824

Table 4.17. Summary statistics for the first four axes of DCA (a) for all 251 Norwegian and Russian lakes and (b) excluding Lake Birgervatnet

As the gradient length of the first DCA axis was greater than 2.5 SD the environmental and chironomid assemblages were analysed by CCA - canonical correspondence analysis (section 3.2.4.1) which was performed on the combined environmental and species datasets with lake Bir deleted and longitude, latitude and altitude as supplementary environmental variables. The eigenvalues for CCA axis 1 ($\lambda_1 = 0.364$) and axis 2 ($\lambda_2 = 0.246$) explain 15.9% of the variance in the chironomid taxa (Table 4.18). The species-environment

correlation for CCA axis 1 is 0.877 and 0.892 for axis 2. The correlation coefficient and the eigenvalue of axis 1 are lower than the equivalent from the Norwegian data (Table 4.12) and higher than the values from the Russian data (Table 4.6). This is probably due to the selection of the Norwegian lakes to optimise the chironomid - temperature response whereas the Russian lakes have more diverse range of environmental variables and therefore a 'noiser' temperature signal.

(a)

Axes	1	2	3	4	Total inertia
Eigenvalues	0.364	0.246	0.118	0.074	3.824
Species-environment correlations	0.877	0.892	0.742	0.623	
Cumulative percentage variance					
of species data	9.5	15.9	19.0	21.0	
of species-environment relation:	34.5	57.8	69.0	76.1	
Sum of all eigenvalues					3.824
Sum of all canonical eigenvalues					1.053

(b)

Axes	1	2	3	4	Total inertia
Eigenvalues	0.360	0.242	0.114	0.065	3.824
Species-environment correlations	0.872	0.887	0.726	0.600	
Cumulative percentage variance					
of species data	9.4	15.7	18.7	20.4	
of species-environment relation:	39.0	65.4	77.7	84.7	
Sum of all eigenvalues					3.824
Sum of all canonical eigenvalues					0.921

Table 4.18. Summary statistics for the first four axes of CCA of combined Norwegian-Russian dataset, based on 250 lakes and 157 chironomid taxa (a) for all environmental variables and (b) after selection of eleven significant environmental variables

January and July air temperatures, continentality index, magnesium (Mg^{2+}) and sodium (Na^+) concentrations had high variance inflation factors (VIF) showing high levels of inter-correlations. These variables were eliminated one by one, based on the correlations identified in section 4.4.1. January temperature and Na^+ were removed which reduced VIFs to less than 11.4. Forward selection of the remaining variables indicated eleven environmental variables make independent and significant contributions ($p \leq 0.05$) in explaining the variance in the chironomid data. The most significant of these is July air temperature which explains 31.4% of the total variance explained by all the measured

environmental variables, followed by continentality (17.6%), Cl^- (8.8%), water depth (7.8%) and distance to coast (7.8%). The remaining six variables (polar desert vegetation, annual precipitation, conductivity, pH, SO_4^{2-} and proximity to other lakes) each explain 3.9 – 2.0% of the total variance explained by all the measured environmental variables. The results of the CCA showing the significant variables are given in Table 4.18 and illustrated in Figures 4.21.

The eigenvalues of CCA axis 1 ($\lambda_1 = 0.360$) and axis 2 ($\lambda_2 = 0.242$), constrained to the eleven significant variables, capture 15.7% of the cumulative variance in the species data. The species-environment correlation for CCA axis 1 is 0.872 and 0.887 for axis 2 and these two axes account for 65.4% of the variance in the chironomid-environment relationship. Axis 1 of the CCA constrained to the eleven significant variables (Figure 4.21) reflects the influence of temperature on the chironomid assemblages. The cold Svalbard lakes and the warm Yakutia lakes are separated from the remaining Russian and Norwegian sites, although the geographic zones show more overlap than was apparent in the ordinations of the countries individually. This is probably due to the increased range in the environmental variables reducing the importance of the intra-lakes variation in the countries individually. The first axis also reflects the influence of polar desert land cover on the assemblage. Vegetation type was categorised by visual inspection (section 3.3.5), polar desert was predominantly bare rock and desert-tundra bare rock with sparse tundra vegetation. Although all vegetation types were included in the analysis only polar desert type was selected as significant. Vegetation type is temperature-dependent and the July air temperatures at the lakes with polar desert or desert-tundra vegetation range from 3.5 – 4.5°C whilst six other Svalbard lakes with July temperatures of 3.5°C have typical tundra vegetation. Therefore this variable captures some non-temperature related environmental characteristic such as exposure, aspect, soil development or geology which determine the vegetation and, hence, chironomid assemblage. The second CCA axis reflects continentality, distance to coast, water depth, annual precipitation, conductivity and pH and separates the low precipitation polar desert lakes and lakes from wetter areas of south-west and western Norway.

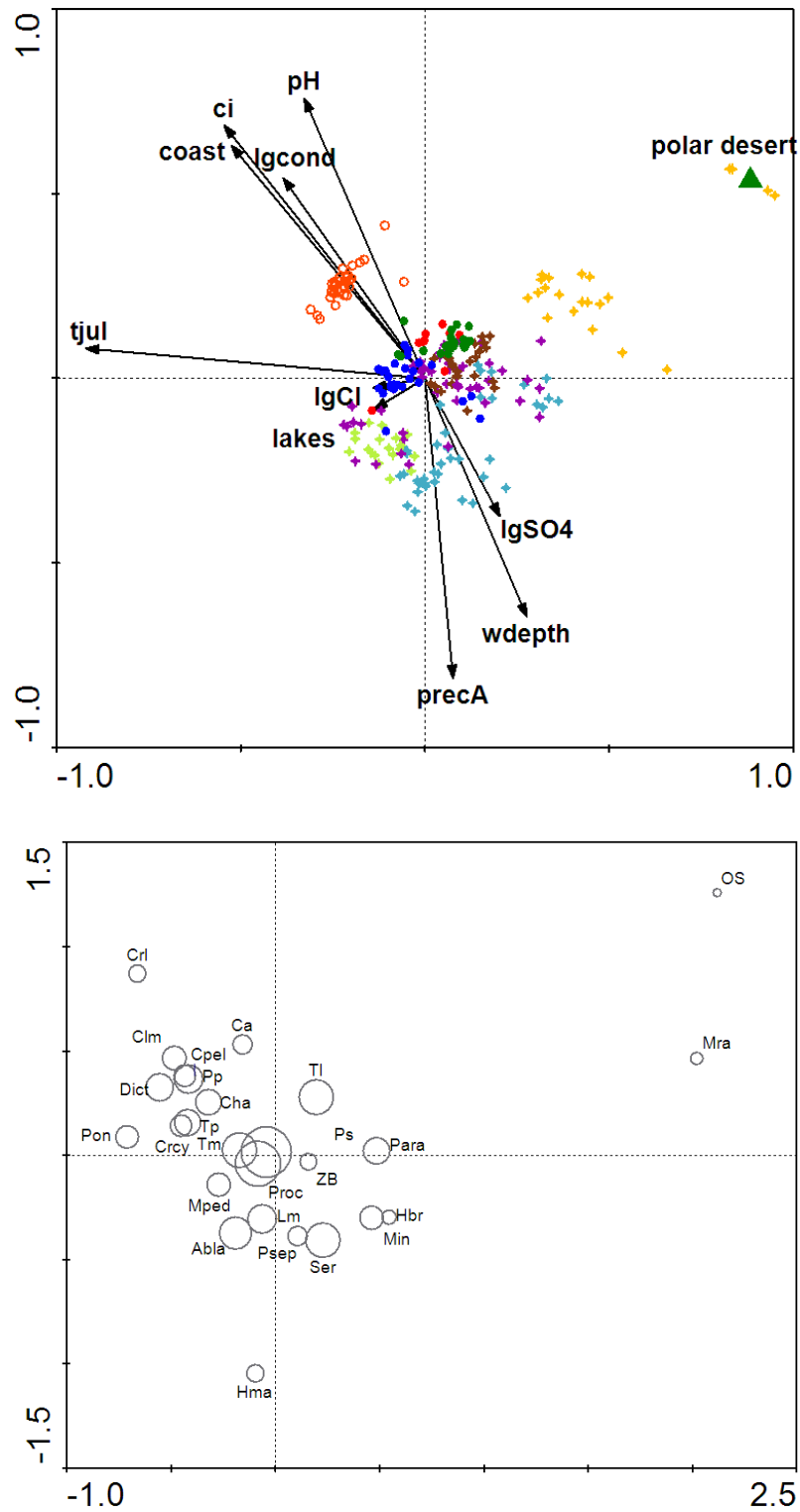


Figure 4.21. CCA biplots of axis 1 and 2 illustrating the relationship between the significant environmental variables and faunal assemblage in the combined Norwegian-Russian dataset showing (a) the site scores and (b) the species scores. Quantitative environmental variables, chosen in forward selection, are shown as arrows and the nominal variables (polar desert vegetation) as centroids. Further abbreviations overpage:

Key to abbreviations: (a) Sites classified by geographic region; Orange star – Svalbard, brown star – northern Norway, purple star – central and south-east Norway, lime stars – south-west Norway, cyan stars – western Norway, blue cross – north-east European Russia, red cross – Putorana, orange ring – Yakutia, green cross – Lena Delta. tjul – July air temperature, wdepth – water depth (m), precA – annual precipitation (mm), ci – continentality index, lgcond – log conductivity ($\mu\text{S}/\text{cm}$), lakes – proximity to other lakes, coast – distance to coast (km), and polar desert – vegetation classification. (b) Species with species weight >20% included, points scaled relative to Hill's N2 value for each species. Taxa abbreviations: Abla – *Ablabesmyia*, Ca – *Corynocera ambigua*, Cha – *Chironomus anthracinus* type, Clm – *Cladotanytarsus mancus* type, Cpel – *Cladopelma lateralis* type, Crcy – *Cricotopus cylindraceus* type, Crl – *Cricotopus laricomalis* type, Dict – *Dicrotendipes* type, Hbr – *Heterotrissocladius maeaeri* type, Lm – *Limnophyes*, Min – *Micropsectra insignilobus* type, Mra – *Micropsectra radialis*-type, Mped – *Microtendipes pedellus* type, OS – *Orthocladius* type S, Para – *Paratanytarsus* type, Pp – *Paratanytarsus penicillatus* type, Pon – *Polypedillum nubeculosum*-type, Proc – *Procladius*, Ps – *Psectrocladius sordidellus* type, Psep – *Psectrocladius septentrionalis* type, Ser – *Sergentia* type, Tm – *Tanytarsus mendax* type, Tl – *Tanytarsus lugens* type and Tp – *Tanytarsus pallidicornis* type.

The cold stenotherms *Micropsectra radialis*-type and *Orthocladius* type S are associated with the Svalbard lakes, *Heterotrissocladius marcidus*-type with the deeper lakes from wetter areas of Norway and *Cricotopus laricomalis*-type with Yakutian lakes. The Yakutian lakes occupy a distinct space in the ordination reflecting the low precipitation, extreme continentality, high pH, high conductivity and long distances from the coast. The extreme environmental variables which characterise the Yakutia lakes (section 4.2.1) were all selected as significant in this ordination and may therefore be driving the analysis. To test the influence of these lakes on the ordination the CCA was repeated with the Yakutia lakes supplementary and plotted passively (Figure 4.22).

With the Yakutian lakes passive ten of the eleven environmental variables previously selected remained significant. Na^+ was selected instead of Cl^- concentrations but these two variables are highly correlated and selection depends on which has the higher VIF in any analysis. The percentage of the total variance explained by July air temperature (32.3%), water depth (9.7%) and precipitation (5.4%) increased whilst the percentage explained by continentality (14.0%) and distance to coast (4.3%) decreased. The remaining variables remained relatively unchanged. Therefore although the extreme

continentality and distance from the coast of the Yakutian lakes are reflected in the CCA all the selected environmental variable have a significant influence on the distribution of chironomids within the study areas. From the CCA (Figure 4.22) the Yakutian lakes plot within the ordination space typified by assemblages responding to low precipitation, shallow water depth, high continentality and high conductivity. However the ordination fails to position them as the warmest lakes. This could be due to a highly endemic fauna which is not well represented in the remainder of the dataset. However of the five taxa found exclusively in the Yakutian lakes, only *Einfeldia*-type occurred in over 80% of the lakes at abundances up to 13.75%. *Prosilocerus yacuticus*-type, *Prosilocerus lacustris*-type and *Zavreliella* occurred once and *Trissocladius* in 5 lakes. The CCA shows the Yakutian lakes having a similar continentality index to the Lena Delta lakes which lack these taxa and therefore the failure to predict them as the warmest lakes suggests the assemblages are responding primarily to negative water balance caused by low precipitation and extreme continentality rather than temperature.

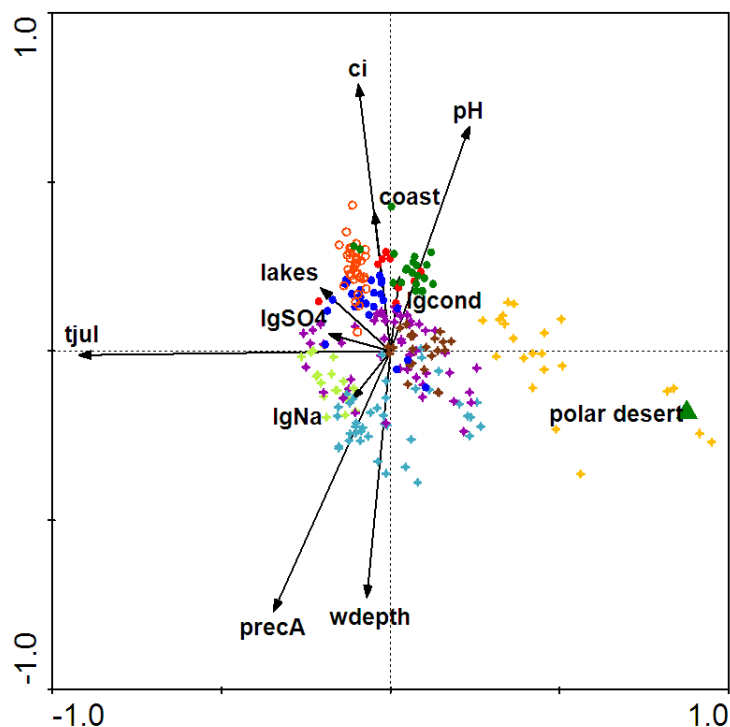


Figure 4.22. CCA biplot of the combined Norwegian-Russian dataset, illustrating the relationship between sites and the significant environmental variables with Yakutian lakes plotted passively. For key to symbols and abbreviation see Figure 4.21, lgNa – log of sodium ion concentrations.

4.5. Norwegian and Russian surface sediments with loss-on ignition data

The trophic status of lakes is known to influence the distribution, abundance and larval growth rates of chironomid fauna (Ward and Cummins 1979; Lindegaard 1995). Variations in the chironomid assemblages were used in early attempts to classify lake trophic types based on indicator species (Brundin 1958; Wiederholm 1984) and more recently in quantitative investigations of lake trophic history (Brooks *et al.* 2001; Langdon *et al.* 2006). The water chemistry of the Russian and Norwegian lakes used in the training set was primarily obtained from secondary sources (section 3.3.7) and there was no consistent method of determining key nutrients such as phosphate, nitrate and organic carbon. For example, dissolved organic carbon (DOC) was determined for the Yakutian and Putorana lakes and total organic carbon (TOC) in the mainland Norwegian lakes. Therefore the importance of these nutrients in chironomid distribution could not be assessed in the previous analyses.

Lakes with loss-on-ignition (LOI) data comprise the largest available subset of lakes with a consistent method for determining organic carbon (133 lakes). Percent weight loss-on-ignition (% LOI) during combustion at 550°C and 950°C is a widely used method for estimating the organic and carbonate content, respectively, of lake sediments (Dean 1974; Heiri *et al.* 2001). However a high sedimentary LOI does not necessarily equate to high trophic status in the lake. LOI reflects the proportion of organic carbon, carbonate and mineral matter in the sediment (Dean 1974; Boyle 2001); a high LOI may result from high organic carbon input or low minerogenic inwash. The organic and mineral components may originate in the lake and/or the catchment (Birks and Birks 2006), so that high organic inputs may be derived from bioproduction or humus development within the catchment rather than bioproductivity within the lake. The accuracy of LOI determinations, also, depends on the nature of the sediment (Boyle 2001); loss of structurally bound water from clay minerals or metal oxides, loss of volatile compounds or loss of inorganic carbon in minerals such as siderite contribute to LOI (Boyle 2001; Heiri *et al.* 2001). However LOI is a valuable summarising proxy for changes in lake ecosystems (Birks and Birks 2006). The organic content of surface sediments, determined by loss-on-ignition, has been identified as an important driver of chironomid distribution in alpine Swiss (Bigler

et al. 2006) and Icelandic (Langdon *et al.* 2008) lakes in its own right. Therefore the influence of sediment organic matter content on species-environment relationships was examined using a subset of 133 lakes, with LOI data, from Norway, north-east European Russia and the Putorana. The locations and LOI values of the lakes are given in Table 4.19; other physical and environmental characteristics are detailed in Tables 4.1 and 4.7. Untransformed and log-transformed % LOIs had a skewed distribution and the data was square-root transformed to give a Gaussian distribution (Figure 4.23).

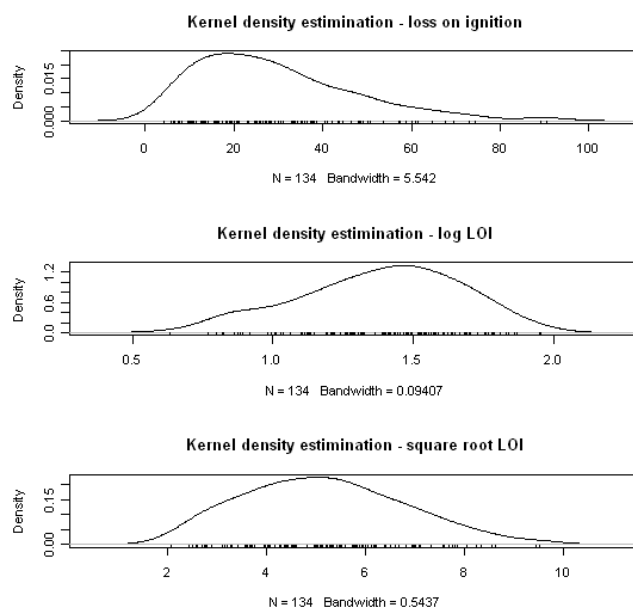


Figure 4.23. Kernel density estimations showing the distribution of un-, log and square-root transformed loss-on-ignition data for the 133 lake subset.

4.5.1. Species – environment relationships

The LOI subset comprised 142 taxa from 133 lakes; the gradient length of the first DCA axis was 4.4 SD suggesting that unimodal-based numerical methods are appropriate for data analysis (Table 4.20). Interpretation of the DCA plot is problematic. The DCA configuration is ‘trumpet’-shaped (Figure 4.24), the upper end of axis 1 has a greater range along DCA axis 2 than the lower end. This is an artefact introduced by detrending affecting the second and subsequent axes and does not mean there is greater variation at that end of the gradient (Birks and Simpson 2006).

Table 4.19. Loss-on-ignition data for the subset of 133 Norwegian - Russian lakes

Lake code	Latitude (N)	Longitude (E)	% LOI	Lake code	Latitude (N)	Longitude (E)	% LOI	
A	78.25	12.9167	73.0	99-14	71.03666667	25.79666667	13.3	
B	78.3167	12.8333	49.1	99-15	71.04833333	25.76833333	16.6	
C	78.95	12.4667	10.3	99-16	70.455	27.18333333	21.0	
D	78.8667	10.9	35.0	99-17	70.59	27.57833333	25.0	
F	79.1833	11.65	15.5	99-18	65.62666667	11.16166667	8.3	
G	79.25	11.5333	13.3	99-19	70.31833333	31.03833333	26.4	
H	79.25	11.55	12.6	99-20	70.43666667	27.78	32.9	
I	79.6667	10.8	38.2	99-21	70.61333333	29.12	25.0	
J	79.6833	10.8	48.0	99-22	70.47666667	28.875	12.8	
K	79.6833	10.9	33.8	99-23	70.56166667	29.54666667	16.3	
M	79.7667	10.75	10.9	99-24	70.58833333	29.60333333	35.9	
N	79.75	10.7167	38.7	99-25	70.54	29.69166667	7.3	
O	79.8	11.55	48.2	99-26	59.05833333	11.61166667	57.5	
P	78.95	12.5	4.3	99-27	59.84666667	11.43166667	57.1	
Q	78.2167	12.9333	35.4	99-28	59.62166667	11.385	69.5	
R	78.2167	13.3333	6.7	99-29	59.64166667	11.46333333	74.3	
S	77.75	13.95	30.5	99-30	59.29	11.365	50.1	
T	77.55	14.2167	7.7	99-33	60.24666667	11.44666667	61.6	
U	78.1	10.0333	20.8	99-34	60.26833333	11.27166667	60.8	
Scur	79.7333	12.3	40.6	99-37	60.835	10.875	42.1	
96-11	61.25833333	8.828333333	35.4	99-38	61.11	10.36333333	48.6	
96-14	61.00666667	7.331666667	7.5	99-40	61.52	9.7	33.6	
96-20	61.87	5.076666667	31.2	99-41	61.555	10.25833333	60.1	
96-21	61.83166667	5.448333333	10.2	99-42	61.565	10.27166667	48.5	
96-24	61.57	5.611666667	44.5	99-43	61.69833333	10.155	23.1	
96-25	61.82166667	6.04	58.8	99-44	61.72833333	10.17666667	29.9	
96-26	61.69333333	5.805	24.8	99-45	61.85	10.08	46.5	
96-28	61.48	6.053333333	36.6	99-46	61.65333333	9.865	25.3	
96-35	61.39333333	5.741666667	37.5	99-47	61.65	9.878333333	18.3	
96-36	59.84833333	6.938333333	25.7	99-50	62.38333333	10.02166667	28.0	
96-39	59.89333333	6.661666667	64.7	F3-2	67.93333333	54.03333333	24.6	
96-51	59.705	6.546666667	50.6	F3-3	67.93333333	54.05	37.9	
96-52	59.72333333	6.563333333	33.2	F3-5	67.91666667	54.03333333	11.6	
96-54	59.80833333	7.253333333	33.3	F3-6	67.93333333	54	25.9	
96-58	59.53166667	5.658333333	29.3	F3-12	67.95	53.93333333	10.7	
96-61	59.73166667	6.055	28.3	F4-2	68	52.38333333	9.6	
96-63	59.91333333	6.556666667	20.2	F4-4	68	52.45	6.6	
96-65	59.95666667	6.566666667	43.6	F4-5	68	52.4	18.4	
96-67	59.67	7.541666667	31.1	F6-2	64.31666667	59.08333333	26.0	
96-77	59.17333333	7.528333333	41.0	F7-3	67.11666667	56.68333333	90.5	
97-15	58.32666667	7.785	48.6	F7-4	67.11666667	56.71666667	89.1	
97-17	58.27333333	7.74	37.4	F7-5	67.13333333	56.68333333	6.3	
97-23	58.185	7.87	44.6	F8-2	67.86666667	59.71666667	21.2	
97-26	58.33666667	7.785	67.6	F8-4	67.88333333	59.66666667	26.1	
97-27	58.27166667	8.053333333	53.6	TDRA 2	65.98333333	60.01666667	18.9	
B98-1	60.925	7.315	6.6	TDRC 2	66.1	60.25	43.4	
B98-2	60.96	7.363333333	19.5	TDRE 2	67.11666667	59.56666667	21.0	
B98-3	60.92666667	7.328333333	5.9	TDRE 1	65.25	59.66666667	14.1	
B98-5	60.74166667	7.533333333	8.3	TDRU11a	65.96666667	57.26666667	10.3	
B98-6	61.54666667	8.258333333	19.2	TDRU 42a	67.45	63.08333333	16.4	
B98-18	61.03166667	9.568333333	17.4	Mitro	67.85	58.98333333	28.5	
B98-19	61.465	8.711666667	7.8	Vanuk-ty	68	62.75	13.6	
B98-20	61.39	8.763333333	13.7	GYXO	68.165	92.173056	15.7	
B98-23	61.31833333	8.82	20.2	AFOX	68.166389	92.228056	20.5	
99-1	69.945	19.26833333	29.3	WILD	68.17	92.240556	20.9	
99-2	69.92166667	18.85	16.5	ARTE	68.150833	92.174444	50.3	
99-3	69.89333333	18.87166667	29.3	PONE	68.1425	92.203056	19.3	
99-4	70.21666667	19.69833333	27.8	PTWO	68.133056	92.194722	16.5	
99-5	70.005	19.42333333	19.0	PTHE	68.203333	92.178889	27.2	
99-6	70.245	24.08	43.6	PFOR	68.202222	92.157222	25.9	
99-7	70.65166667	23.67166667	23.2	PFIV	68.160278	92.046111	27.1	
99-8	70.68833333	23.725	30.0	IGAR	67.508889	86.5575	27.2	
99-9	70.655	23.715	36.0	NERU	67.5255	62.757611	7.3	
99-10	71.095	25.795	34.4	KHAR	67.362806	62.750722	13.4	
99-11	71.09833333	25.77833333	19.6	SAND	66.921833	58.77925	9.9	
99-12	71.125	25.71833333	13.0	VORK5	67.856972	59.025722	18.2	
99-13	71.02166667	24.76666667	16.1					
Summary of LOI data				Min	Mean	Median	Max	Std dev
				4.3245	29.20749551	11.3	90.45	18.37711884

	1	2	3	4	Total inertia
Eigenvalues	: 0.565	0.219	0.148	0.115	3.489
Lengths of gradient	: 4.353	2.353	2.907	2.569	
Cumulative percentage variance of species data	: 16.2	22.5	26.7	30.0	
Sum of all eigenvalues					3.489

Table 4.20. Summary statistics for the first four DCA axes of 133 lakes with loss-on-ignition data

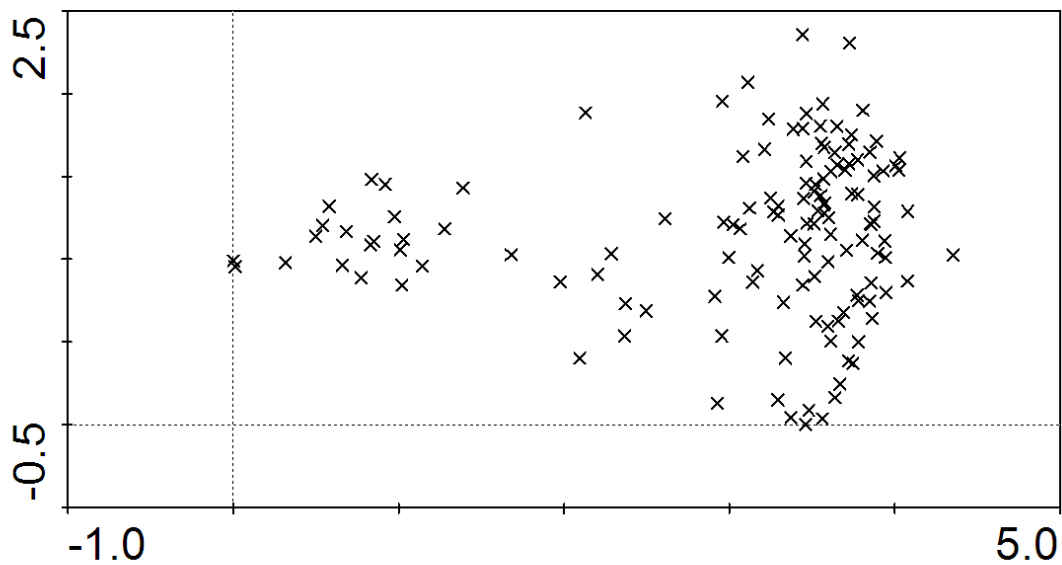


Figure 4.24. DCA plot of site scores for the Norwegian and Russian lakes with loss-on-ignition data showing 'trumpet' configuration

Canonical correspondence analysis (CCA) was initially performed on the environmental and species data for the 133 lakes with loss-on-ignition data with longitude, latitude and altitude supplementary. CCA axis 1 ($\lambda_1 = 0.442$) and axis 2 ($\lambda_2 = 0.179$) explain 17.8% of the variance in the chironomid taxa (Table 4.21a). January and July air temperatures, continentality index, chloride (Cl^-) and sodium (Na^+) concentrations had high variance inflation factors (VIF) showing high levels of inter-correlations. Cl^- then January temperature, the variables with the highest VIF, were removed which reduced all VIFs to less than 10.4. Forward selection of the remaining variables indicated nine environmental variables make independent and significant contributions ($p \leq 0.05$) in explaining the variance in the chironomid data.

(a)

Axes		1	2	3	4	Total inertia
Eigenvalues	:	0.442	0.179	0.135	0.080	3.489
Species-environment correlations	:	0.897	0.885	0.770	0.781	
Cumulative percentage variance						
of species data	:	12.7	17.8	21.7	24.0	
of species-environment relation:		37.3	52.5	63.9	70.6	
Sum of all	eigenvalues					3.489
Sum of all canonical	eigenvalues					1.184Axes

(b)

Axes		1	2	3	4	Total inertia
Eigenvalues	:	0.423	0.171	0.122	0.064	3.489
Species-environment correlations	:	0.881	0.879	0.731	0.710	
Cumulative percentage variance						
of species data	:	12.1	17.0	20.5	22.4	
of species-environment relation:		46.2	64.8	78.2	85.2	
Sum of all	eigenvalues					3.489
Sum of all canonical	eigenvalues					0.916Axes

Table 4.21. Summary statistics for the first four axes of CCA with 133 lakes from Norway and Russia with loss-on-ignition data (a) for all environmental variables and (b) after selection of nine significant environmental variables

The most significant variable is July air temperature which explains 32.5% of the total variance explained by all the measured environmental variables, followed by annual precipitation (12.3%), loss-on-ignition (7.0%) and water depth (7.0%). The remaining five variables (Mg^{2+} , continentality, distance to the coast, polar desert vegetation and proximity to other lakes) each explain 3.5 – 5.3% of the total variance explained by all the measured environmental variables. The results of the CCA showing the significant variables are given in Table 4.21b and illustrated in Figure 4.25. The eigenvalues of CCA axis 1 ($\lambda_1 = 0.423$) and axis 2 ($\lambda_2 = 0.171$), constrained to the nine significant variables, capture 17.0% of the cumulative variance in the species data. The species-environment correlations of CCA axis 1 (0.881) and axis 2 (0.879) are high and the first two axes account for 64.8% of the variance in the chironomid-environment relationship.

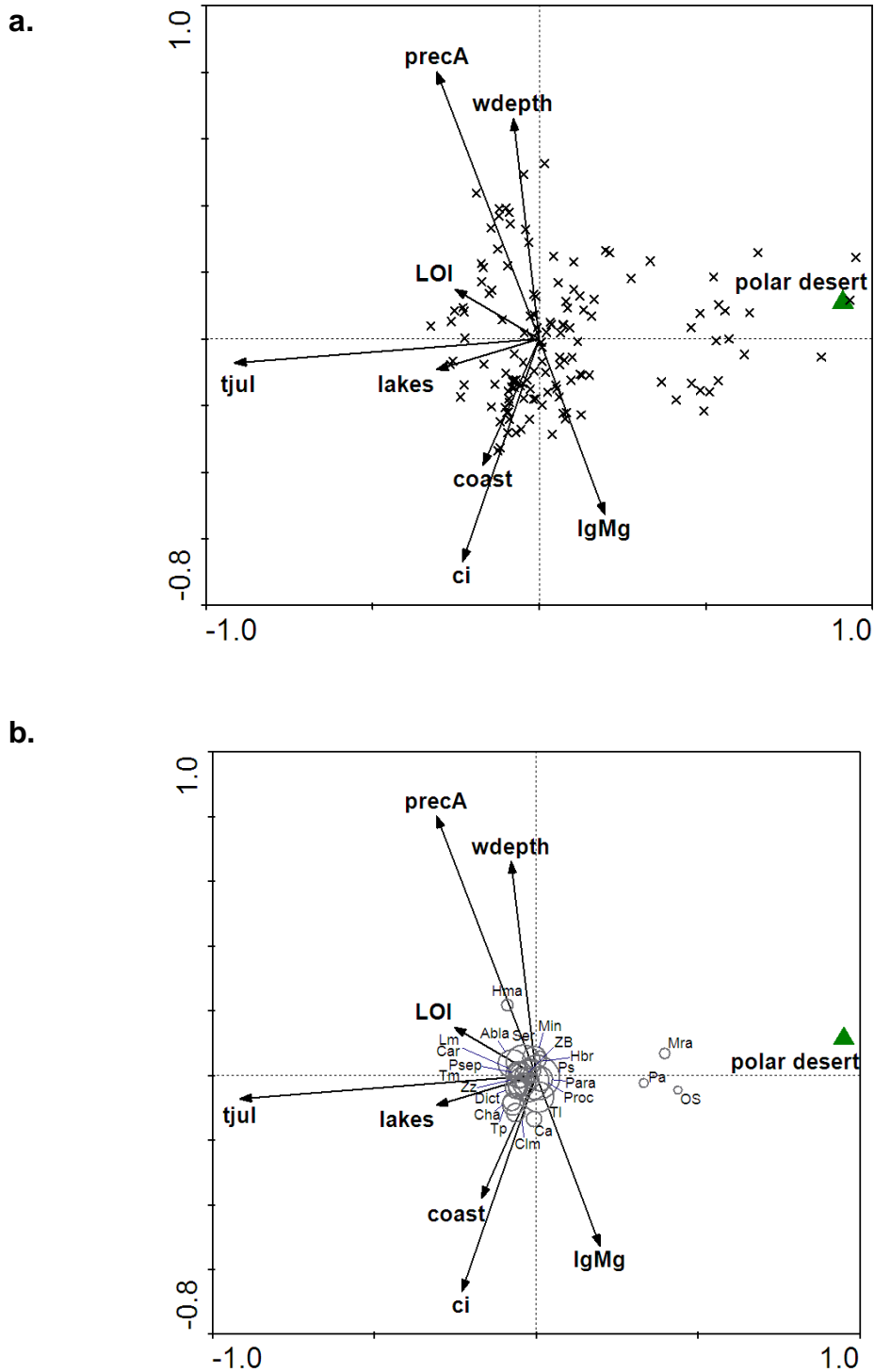


Figure 4.25. CCA biplots of axis 1 and 2 illustrating the relationship between the significant environmental variables and faunal assemblage showing (a) the site scores and (b) the species scores. (Abbreviations: tjul – July air temperature, wdepth – water depth (m), coast – distance to coast (km), precA – annual precipitation (mm), ci – continentality index; LOI – loss-on-ignition, IgMg – Mg^{2+} concentration and polar desert vegetation type. (b) Species with species weight >20% included, points scaled relative to Hill's N2 value for each species. Taxa abbreviations overpage.

Taxa abbreviations: Abla – *Ablabesmyia*, Ca – *Corynocera ambigua*, Car – *Corynoneura arctica*-type, Cha – *Chironomus anthracinus* type, Clm – *Cladotanytarsus mancus*-type, Dict – *Dicrotendipes* type, Hma – *Heterotrissocladius marcidus*-type, Lm – *Limnophyes*, Min – *Micropsectra insignilobus* type, Mra – *Micropsectra radialis*-type, OS – *Orthocladius* type S, Para – *Paratanytarsus* type, Proc – *Procladius*, Ps – *Psectrocladius sordidellus* type, Psep – *Psectrocladius septentrionalis* type, Ser – *Sergentia* type, Tm – *Tanytarsus mendax* type, Tl – *Tanytarsus lugens* type, Tp – *Tanytarsus pallidicornis* type, ZB – *Zalutschii* type B and ZZ – *Zalutschii zalutschicola*.

Axis 1 of the CCA constrained to the nine significant variables (Figure 4.25) separates lakes with low July air temperatures dominated by cold stenothermic species from warmer lakes. The coldest lakes are dominated by the cold stenotherms including *Micropsectra radialis*-type, *Paratanytarsus austriacus*-type and *Orthocladius* type S whereas the assemblages of the warmer lakes are composed of thermophilic taxa such as *Dicrotendipes* and *Chironomus anthracinus*-type. The second axis is related to water depth, annual precipitation and continentality. The distributions of these variables are skewed towards shallower lakes and relatively low precipitation, therefore the most abundant taxa plot close together near the origin. Loss-on-ignition was selected as the 3rd most important factor and axis 3 is related to LOI (Figure 4.26). The organic content of the substrate has been reported as an important explanatory variable in chironomid distribution in Fennoscandia (Larocque *et al.* 2001), Switzerland (Bigler *et al.* 2006) and Iceland (Langdon *et al.* 2008). In the European datasets LOI was positively correlated to summer temperature. Warmer lakes tend to be more productive and have more organically enriched sediments than colder lakes which are less productive and have minerogenic dominated sediments. Some chironomid larvae burrow in lake sediments and a number of taxa are detritus feeders (Pinder 1986) therefore the organic matter of lake sediments may have a direct influence on chironomid populations (Bigler *et al.* 2006). As LOI can be determined directly from sediment cores this variable would not be suitable for development of an inference model. However this analysis indicates that organic content of the substrate strongly influences chironomid distribution and its possible influence on chironomid assemblages should be considered during palaeoenvironmental reconstructions.

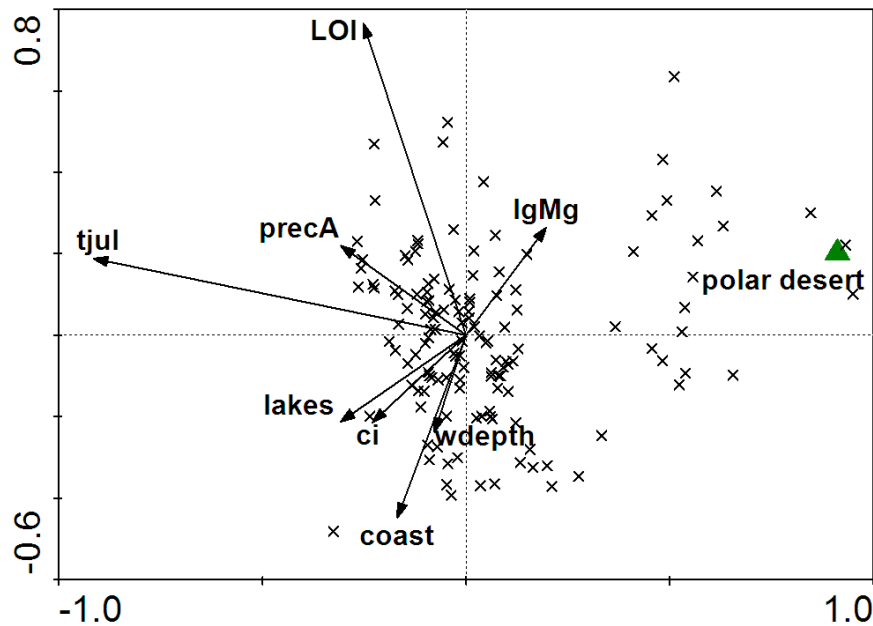


Figure 4.26. Plot of CCA axis 1 and 3 illustrating the relationship between the significant environmental variables and site scores Abbreviations as in Figure 4.25.

4.6. Discussion

4.6.1. Patterns of chironomid distribution

The majority of taxa are common to both Russia and Norway across wide environmental gradients of temperature, water depth and water chemistry. There are two possible explanations for this widespread distribution;

1. either these are cosmopolitan taxa with wide environmental tolerances or
2. the morphotypes are represented by morphologically similar but genetically distinct species across their geographical range.

The latter is supported by the ordination gradient lengths ($>4SD$) of the combined dataset (section 4.3.3) which suggest total turnover of species may have occurred (ter Braak 1987). Variability in taxon composition, the effects of geographic location on temperature optima and tolerances, and the implications for the development of inference models are examined in Chapter 5.

In the Russian dataset *Einfeldia*, *Prosilocerus jacuticus*, *P. lusatensis*, *Trissocladius* and *Zavreliella* were recorded in Yakutia only and the Yakutian chironomid fauna appeared compositionally distinct from the other Russian

faunas studied. This may reflect the environmental conditions (low precipitation, high conductivity and extreme continentality with high mean July air temperatures compared to the other lakes) or a geographically restricted fauna.

The assemblages from Svalbard were also identified as compositionally distinct. *Diamesa aberrata*-type was only recorded from Svalbard and the number of taxa in the Svalbard lakes is, generally, lower ($n = 1 - 10$) compared to the mainland faunas ($n = 11 - 42$). The Svalbard lakes are the coldest in the datasets ($3.5 - 6.0^{\circ}\text{C}$) which would influence species occurrence. However the islands are also approximately 700 km from the Norwegian mainland, therefore the restricted fauna may result from limited dispersal to the island. However many adult chironomid species are frequently found on the island (H.J.S. Birks, pers. comm., 2007) but cannot survive overwinter and TWINSPAN analysis grouped the Svalbard lakes with lakes from northern Norway. Therefore the restricted fauna probably reflects the low July air temperatures rather than island biogeography. Lake Birgervatnet, with a single taxon, distorts the statistical analyses and was removed from all subsequent analysis.

4.6.2. Species - environment relationships

Mean July air temperature, continentality, annual precipitation, maximum water depth and pH were identified as statistically significant drivers of chironomid distribution in Russia and Norway, individually, and combined. Of these, T_{july} explains the highest proportion of variance in the chironomid data. The air temperature of the warmest month has been identified as important determinants of chironomid distribution in similar studies from Europe (Lotter *et al.* 1997; Olander *et al.* 1999; Bigler *et al.* 2006; Luoto 2008), Iceland (Langdon *et al.* 2008) and Quebec in Canada (Larocque *et al.* 2006). The influence of low temperatures on the life cycle and physiology of chironomids was discussed in Chapter 1. Although continentality is temperature related, the value of the continentality index reflects the temperature range and the length of the summer or ice-free period. The relationship between continentality indices and the length of the ice-free period is examined in section 6.7.1. The effects of continentality on chironomid distribution has not been studied, its influence on other insects and invertebrates is discussed in Chapter 1.

Maximum water depth was identified as a key explanatory variable; many chironomid species show depth preferences (Petridis and Sinis 1993; Brodersen *et al.* 2004) reflecting the availability of suitable habitats or physical parameters. Macrophytes and epiphytic algae are generally restricted to the littoral zone so the fauna is dominated by Orthoclaadiinae which feed by grazing and Chironomini taxa associated with plants such as *Glyptotendipes* and *Polypedilium* (Brodersen *et al.* 2001). As water depth increases water temperature and oxygen decline so that the profundal environment is dominated by Chironomini and *Procladius* species (Brodersen *et al.* 2004). Maximum water depth has been identified as an important determinant of chironomid distribution in Switzerland (Lotter *et al.* 1997; Bigler *et al.* 2006), Fennoscandia (Olander *et al.* 1999), Iceland (Langdon *et al.* 2008) and Quebec in Canada (Larocque *et al.* 2006).

Changes in pH affect the abundance and diversity of chironomids (Schnell and Willassen 1996), many of these effects are mediated by profound changes in the biological and chemical characteristics of the lake. Acidification increases the solubility of heavy metals so increasing their bioavailability and toxicity (Wiederholm 1984). Many aquatic invertebrates are sensitive to pH, acidification results in profound changes to the biota which alter predator-prey and competitive relationships (Wiederholm 1984). Although lake acidification may result from atmospheric contamination (acid rain) the pH of lake water also reflects the regional geology, lake productivity and surrounding vegetation (Moss 1998).

Sediment organic matter determined by loss-on-ignition (LOI) was identified as an important variable influencing chironomid distribution from a reduced dataset. This was found to be influential in explaining chironomid distribution in western Finnish Lapland (Nyman *et al.* 2005) and Iceland (Langdon *et al.* 2008) and its influence on chironomid assemblages should be considered during palaeoenvironmental reconstructions.

Human impact was not selected as significant in the analyses; eutrophication from agriculture or industrial processes is likely to have a dramatic impact on individual lakes (Moss 1998). However the impacts are probably localised (for example Brooks *et al.* 2005). There may have been insufficient affected lakes in the datasets or the categories used may be too insensitive to detect a response. Inclusion of concentrations of atmospheric pollutants such as mercury or eutrophic indicators such as phosphorus or nitrogen compounds may be more appropriate.

4.6.3. Implications for development of inference models

- The Russian chironomid fauna includes a number of taxa which form frequent components of the present-day assemblages but are not present in the Norwegian fauna. Therefore either development of a Russian training set or combining the Norwegian and Russian data is necessary for palaeoenvironmental reconstructions in northern Russia.
- Of the climate variables, mean July air temperature and continentality are statistically significant drivers of chironomid distribution in both Norway and Russia which suggests there is potential for the development of chironomid-based inference models for both these variables.
- The lakes are discontinuously distributed along environmental gradients in the Russian dataset with high inter-lake variability in non-climate variables. Lakes are also unevenly distributed along climate gradients with a large proportion of lakes (36 out of 94) from Yakutia with high July temperatures, high continentality and low precipitation.
- Chironomid assemblages in Yakutia appear to be responding primarily to the negative water balance caused by low precipitation and extreme continentality rather than high July temperatures alone.
- Extreme outliers in the Russian environmental data can be attributed to a small number of Yakutian lakes, removal of some or all of the Yakutian lakes would reduce inter-lake variability, improve the evenness of lake distribution along climate gradients and strengthen species – temperature relationships.

- Removing outliers and reducing variability along environmental gradients, other than the variable of interest, improves the statistical performance of the inference model but increases the risk of non-analogue situations.
- The absence of lakes with July air temperatures between 15.3°C and 18°C will affect the accuracy of temperature optima estimations for taxa restricted to the warmer lakes. Therefore inclusion of lakes with partial environmental data may be necessary to improve model performance.
- To achieve maximum robustness with inference models the ratio of taxa:lakes must be decreased to a minimum (Racca *et al.* 2003). The ratio of the Russian taxa:lakes is 1.27; removal of all the Yakutian lakes would give a ratio of 1.97 and reducing the ratio would require exclusion of significant number of taxa from the model. Therefore a compromise between removal of outliers and retaining taxon diversity is required. Alternatively combining with the Norwegian data would increase the number of lakes so reducing the ratio of taxa:lakes to 0.64.

These considerations were used to inform the development of a number of inference models as described in Chapter 6.

Chapter 5

Taxonomic resolution and species responses

5.1. Introduction

The previous chapter examined the environmental variables influencing the modern distribution of chironomids in sub-arctic to arctic regions of Norway and Russia. In this chapter the responses of individual taxa to these variables is examined and modelled using a range of statistical techniques. Many head capsule fossils from chironomid larvae are identifiable only to genus or species-morphotype. Therefore it is useful, prior to examining their responses, to establish if these morphotypes represent more than one species and/or geographically specific taxa. For example, are the species identified as *Chironomus anthracinus*-type the same in European and Central Russia? The distribution of chironomids in northern Russia is poorly known; a number of published faunal lists are based solely on subfossil assemblages (e.g. Bezmaternyh and Nazarova 2006). To examine morphotype composition and highlight potential problems in taxonomy or taphonomy, pupal exuviae were collected and identified from lakes on the Putorana Plateau. The results are discussed in the first part of this chapter (section 5.2) and are used in the interpretation of species response to environmental variables (section 5.3).

5.2. Examination of chironomid pupae

5.2.1. Introduction

Pupal exuviae were collected from seven lakes on the Putorana Plateau between 1st and 9th July 2006. Fieldwork in north-east European Russia was completed in April when the lakes were frozen and, therefore, before chironomid pupae had emerged. Suitable collecting sites were inaccessible at two lakes on the Putorana Plateau and no exuviae were collected from these lakes. Methods for the collection and preparation of the exuviae are described in sections 3.2.3 and 3.3.3 respectively. Representative samples of the different species from each lake were slide mounted and identified to give a qualitative analysis of the fauna. The identification of the pupae is discussed in section 5.2.2. The pupal assemblage is compared to the contemporary larval

assemblage derived from surface sediments in section 5.2.3 and the implications for the examination of species responses or development of inference models discussed in section 5.3.3.

5.2.2. Taxonomy

In total, 24 taxa were identified from pupal exuviae (Table 5.1) compared with 53 from the larval head capsules in surface sediments from the same seven Putorana lakes. The majority of pupae were identified to species with the exception of two *Procladius* spp., *Corynoneura* sp. and *Tanytarsus* sp, which were identified to genera and a Diamesinae which was identified to subfamily only, based on the descriptions of Langton and Visser (2003).

Chironomini	<i>Chironomus esai</i> (Wülker 1997) <i>Stictochironomus sticticus</i> (Fabricius 1781) <i>Sergentia coracina</i> (Zetterstedt 1850)
Diamesinae	<i>Diamesa</i> species unknown <i>Protanypus morio</i> (Zetterstedt 1838)
Orthocladiinae	<i>Abiskomyia virgo</i> (Edwards 1937) <i>Corynoneura</i> species unknown <i>Cricotopus flavocinctus</i> (Kieffer 1924) <i>Cricotopus magus</i> (Hirvenoja 1973) <i>Cricotopus obnixus</i> (Walker 1856) <i>Orthocladius lignicola</i> (Kieffer 1915) <i>Prosilocerus lacustris</i> (Kieffer 1923) <i>Psectrocladius fennicus</i> (Storå 1939) <i>Psectrocladius limbatellus</i> (Holmgren 1869) <i>Zalutschia tornetraeskensis</i> (Edwards 1941)
Tanypodinae	<i>Procladius</i> unknown species I <i>Procladius</i> unknown species II <i>Procladius crassinervis</i> (Zetterstedt 1838)
Tanytarsini	<i>Corynocera ambigua/oliveri</i> <i>Neozavrelia pe1</i> (form described by Langton 1991) <i>Paratanytarsus dissimilis</i> (Johannsen 1905) <i>Paratanytarsus inopertus</i> (Walker 1856) <i>Paratanytarsus penicillatus</i> (Goetghebuer 1928) <i>Tanytarsus</i> unknown species

Table 5.1. Chironomid taxa from the Putorana lakes based on the pupae exuviae

The unknown Diamesinae was represented by a single specimen (Figure 5.1a). The tergites lacked the well-developed transverse tooth rows common in many *Diamesa* species. The anal lobes have short triangular lobes at the postero-lateral corners with three macrosetae set laterally. This suggests the specimen is a *Potthastia* or *Pseudodiamesa* species, but the shagreen patterns, armaments and lateral setae differ from described species (Langton and Visser 2003). Additional specimens would be required to determine if this is a new, undescribed species for the Palaeoarctic.

Figure 5.1. Pupal anal lobes of (a) unknown Diamesinae and (b) *Protanypus morio* exuviae. Photographs taken under phase-contrast at x100 magnification; transverse width of anal lobes in (a) 500 μ m and (b) 450 μ m

(a)



(b)



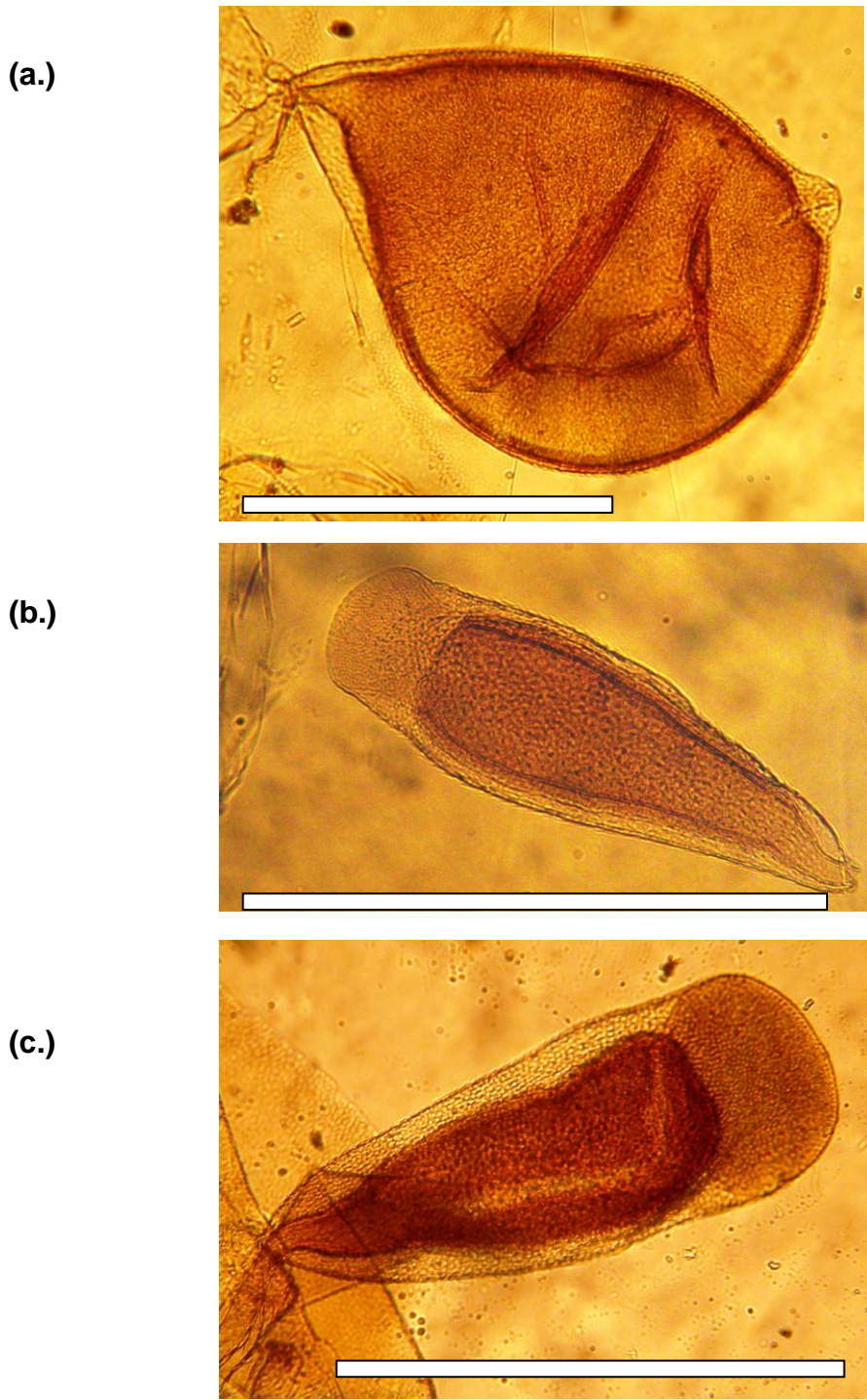
The other Diamesinae, *Protanypus morio*, has five terminal macrosetae and an anterior fringe of five marginal setae (Figure 5.1b). *P. morio* is common in northern and montane lakes within the western Palaearctic (Langton and Visser 2003) but has not been recorded in the Ob and Lena River regions (Bezmaternyh and Nazarova 2006). The larval stage found in the Putorana lakes had three outer lateral teeth instead of the two described in Brooks *et al.* (2007). Without further work it is not possible to say whether this represents natural phenotypic plasticity or a characteristic which could be used to improve the larval taxonomy. However as this species is usually a minor component of the fauna it is unlikely to affect the performance of an inference model.

The taxon *Corynocera oliveri* has been described from the morphology of the larval head capsule but the appearance of the pupal and adult stages are uncertain. The taxonomic key of Langton and Visser (2003) combines *C. oliveri* and *Corynocera ambigua* and describes the taxa as having a terminal tuft of 7-14 setae on the anal lobes. Wilson and Ruse (2005) describes *C. ambigua* as having a terminal tuft of 4-8 setae. The number of setae on the anal lobes was determined for each specimen from the Putorana. All specimens had between 6 -12 setae, the majority (82%) had 10 – 12 with a mode of 10. The number was independent of pupal size (measured from the width of the anal lobes) but as the number of setae formed a continuum the characteristic could not be used to separate morphotypes.

Many subfossil chironomid larvae, such as *Procladius*, can only be identified to genus level, whereas the pupal exuviae can frequently be identified to species or species-group (Langton 1991; Langton and Visser 2003). Three species of *Procladius* were identified from the Putorana lakes, *P. crassinervis* and two unidentified species, based on the morphology of the thoracic horns (Figure 5.2). In *P. crassinervis* the thoracic horn is sac-like. The plastron plates of both unidentified species are well-developed; in type I, *Procladius (Holotanypus)*, the respiratory atrium is expanded medially and in type II, *Procladius (Psilotanypus)*, the respiratory atrium is widest near the plastron plate, tapering to the base. On re-examination of the larval head capsules variation in the number and length of the points on the outer side of the paraligula were

apparent. However as the paraligula is frequently lost in fossil material this would be an unsuitable characteristic for improving the taxonomy. Adults of *Procladius ferrugineus* have been recorded in the Ob River basin (Bezmaternyh 2001) but the pupal form is unknown (Langton and Visser 2003).

Figure 5.2. Thoracic horns from the three *Procladius* species; (a) *Procladius crassinervis*, thoracic horn length (ThL) 750 μ m (b) *Procladius* unknown species I, ThL 500 μ m and (c) *Procladius* unknown species II, ThL 600 μ m. Photographs taken at x100 magnification, in transmitted white light. White bars represents 500 μ m.



Paratanytarsus dissimilis is distinguished from *Paratanytarsus inopertus* by the presence of lateral longitudinal spine bands, connected anteriorly to the median point patch spreading on tergite IV. However Langton and Visser (2003) suggest these taxa may be the extremes of a single variable species. Therefore only two species of *Paratanytarsus* may be present. The identification of the *Tanytarsus* species was problematic; many of the characteristics were similar to *Tanytarsus quadridentatus*, but the pattern of armaments on tergites III – VI and filaments on tergite VIII did not match any descriptions in Langton and Visser (2003).

5.2.3. Comparison with larval assemblages from the surface sediments

The majority of genera present in the pupal assemblage were also found as larval head capsules in surface sediments of the Putorana lakes. However the correlation is poor at the individual lake - species level (Table 5.2). For example pupal exuviae of *Sergentia coracina* were isolated from GYXO, PTWO and PTHE, however head capsules of the larval stage were only found in PTWO and PTHE. Conversely larval head capsules were present in surface sediments from AFOX, ARTE and PFIV although no pupal exuviae of *Sergentia* were found in these lakes. In general, individual taxa were recorded more frequently as larval subfossils than pupae. This probably reflects the temporal resolution of the surveying technique; the pupae were sampled by a single collection of exuviae when species may be emerging on different dates throughout the spring – autumn season and the shed pupal exuviae degrade in 2-3 days. By comparison the larval assemblage may represent up to 5 years accumulation of head capsules. The difficulties with the pupal survey technique are typified by the assemblage recorded for GYXO where fewer taxa were recorded than at any other lake. The lake was large and windswept so pupae may have been distributed over a wide area of rocky shoreline and so were not sampled or the lake depth may have maintained cooler water temperatures so that the species emerged later than the other sampled lakes.

In some instances species were recorded as pupae but not in the larval stage. As the chironomid has to develop through a larval stage before pupating both stages should be present. The presence of the pupal exuviae, only, may reflect

TAXA	GYXO	AFOX	ARTE	PONE	PTWO	PTHE	PFIV	TAXA	GYXO	AFOX	ARTE	PONE	PTWO	PTHE	PFIV
<i>Chironomus esai</i>								<i>Abiskomyia virgo</i>							
<i>Chironomus anthracinus</i> -type			X			X	X	<i>Abiskomyia</i>	X			X			
<i>Chironomus plumosus</i> -type		X					species unknown								
<i>Chironomus larvula</i>			X			X	<i>Corynoneura arctica</i> -type		X		X				
<i>Stictochironomus sticticus</i>							<i>Cricotopus (Isocladius) flavinocinctus</i>								
<i>Stictochironomus rosenscholdi</i> -type			X		X	X	<i>Cricotopus (Isocladius) magus</i>								
<i>Sergentia coracina</i>							<i>Cricotopus (Isocladius) obnixus</i>								
<i>Sergentia coracina</i> -type		X	X		X	X	<i>Orthocladus (Symposiocladius) lignicola</i>								
							<i>Cricotopus obnixus</i>								
<i>Corynocera ambigua/oliveri</i>							<i>Cricotopus cylindraceus</i> -type		X		X				
<i>Corynocera ambigua/oliveri</i>	X	X	X	X	X	X	<i>Cricotopus laricomalis</i> -type		X	X	X	X	X	X	X
<i>Neozavrelia</i> pe 1							<i>Cricotopus</i> -type P		X	X	X	X	X	X	X
<i>Paratanytarsus dissimilis</i>							<i>Propiloscerus lacustris</i>								
<i>Paratanytarsus penicillatus</i>							<i>Propiloscerus lacustris</i> -type					X			
<i>Paratanytarsus inopertus</i>							<i>Psectrocladius fennicus</i>								
<i>Paratanytarsus austriacus</i> -type							<i>Psectrocladius limbatellus</i>				X				
<i>Paratanytarsus penicillatus</i> -type	X					X	<i>Psectrocladius septentrionalis</i> -type			X	X	X	X	X	X
<i>Paratanytarsus</i> undifferentiated	X						<i>Psectrocladius sordidellus</i> -type		X	X	X	X	X	X	X
<i>Tanytarsus</i> species unknown							<i>Zalutschia tometraeskensis</i>								
<i>Tanytarsus lugens</i> -type	X	X	X	X	X	X	<i>Zalutschia</i> type A			X	X	X	X	X	X
<i>Tanytarsus pallicornis</i> -type	X	X	X	X	X	X	<i>Zalutschia</i> type B		X	X	X	X	X	X	X
<i>Tanytarsus mendax</i> -type															
							<i>Procladius (Holotanypus)</i> sp unknown I								
<i>Diamesinae</i> species unknown							<i>Procladius (Holotanypus)</i> sp unknown II								
<i>Protanypus morio</i>							<i>Procladius (Holotanypus) crassinervis</i>								
<i>Protanypus</i>	X		X				<i>Procladius undifferentiated</i>	X	X	X	X	X	X	X	X

Table 5.2. Distribution of chironomids in the Putorana lakes as identified from pupal exuviae and the head capsules of larvae in the surface sediment. (Names in black with blue rectangles indicates taxa present as pupae exuviae and names in blue with black X are taxa identified from larval head capsules).

differences in the sampling methods; for pupal exuviae a large amount of material was processed to maximise the number of species whereas with surface sediments the chironomid taxa are isolated from a small sub-sample. Pupae may also be washed into the lakes from adjacent lakes, rivers or streams as a buoyant, discarded exuviae or during the pupal stage.

As discussed in section 5.2.2 *Paratanytarsus dissimilis* and *P. inoperutus* may be the same species. The mandible of *P. dissimilis* larvae has two inner teeth and therefore the larvae would be identified as *Paratanytarsus penicillatus*-type or *Paratanytarsus* in the absence of the mandible. The larval mentum of *Neozavrelia* has a minute outermost lateral tooth and can be confused with worn specimens of *Paratanytarsus*. The two taxa have been combined in the training set to reduce false identifications. Therefore the three *Paratanytarsus* taxa and *Neozavrelia*, identified as pupae, would be identified as *P. penicillatus*-type in the larval stage. However, the distribution of *P. penicillatus*-type larvae shows no correlation to the occurrence of these taxa based on the pupae. Additionally *P. austriacus*-type larvae were found at three lakes. This suggests that *Paratanytarsus*, in the Putorana, includes several different species.

The morphology of the larval head capsule of some species identified from the pupae, such as *Chironomus esai*, are incompletely or un-described and need to be established. *Chironomus esai* may be identified as either the larval *C. anthracinus*- or *C. plumosus*-morphotype. The presence of both larval morphotypes suggests the *Chironomus* species are more diverse than the single species identified from the pupae. Fifteen species of *Chironomus* have been identified from central and southern Yakutia (Gruzdev 1996) and six from the Upper Ob basin (Bezmaternyh 2001).

Zalutschia tornetraeskensis is present throughout Norway, Finland, the Russian North and Novaya Zemlya (Spies and Sæther 2004). In Sæther (1976) the larvae of *Zalutschia tatica*-group, including *Zalutschia zalutschicola*, are readily distinguished by the distinctive mentum. However the *tornetraeskensis*-group is distinguished from *mucronata* group on the relative lengths of the anal tubules and posterior parapods which are generally not preserved in fossil material and,

therefore, can not be used to distinguish the taxonomic groups in *Zalutschia*. The larval head capsules of *Zalutschia* type B were relatively abundant (up to 6% of fauna) in four of the six lakes where *Z. tornetraeskensis* pupae were recorded. In the palaeolimnological literature *Zalutschia* type B has sometimes been referred to as *Z. tornetraekensis* (Ilyashuk, pers. comm. 2008). However in the absence of pharate or reared material this identification remains tentative.

Approximately 180 *Cricotopus/Orthocladius* species are recorded from the Holarctic region (Cranston et al. 1983) and the majority have not been described as larvae. In described species the mentum characteristics are often similar making reliable larval identification problematic (Brooks et al. 2007). From the pupal exuviae 4 species were recorded from 3 lakes, larval morphotypes were identified in an additional 4 lakes. The absence of pupae in these lakes may result from limited sampling or later emergence of the same taxa, as previously discussed, or later emergence of additional taxa. The results show several *Cricotopus/Orthocladius* species are present in the Putorana and the larval morphotypes probably include a number of species.

5.2.4. Discussion

The pupal cuticle is shed when the adult chironomid ecloses, the wings expand within the pupal cuticle and gases are released. This increases its buoyancy and forces the pupa to the water surface. The pupal cuticle bursts, releasing the wings which rapidly inflate and the adult flies away. Shed chironomid exuviae float on the water surface and are moved by wind and water currents to accumulate along the leeward shore or against obstructions such as emergent vegetation or amongst rocks.

The pupal exuviae survive intact for approximately 48 hours before decomposing (Coffman 1973; McGill 1980). A single sample, therefore, represents only recently eclosed species and fewer species were identified from the pupal exuviae than the larval subfossils. However many of the taxa identified from pupae were not found as larval remains in the same lake and conversely larval stage were not found of some species identified from pupae. These anomalies may reflect differing sampling strategies and sample sizes in

the two techniques as previously discussed. Identifying pupal exuviae uses a large sample to qualitatively maximise species diversity whereas the quantitative abundances of larval subfossils are determined from a small sample volume. Variations between the larval and pupal assemblages may also reflect differences in the taphonomy of the insect remains. Buoyant exuviae may be more readily transported from subsidiary habitats such as streams or adjacent wetlands than larval stages living in sediments or in cases attached to plants or rocks. Physical abrasion and rapid decomposition in aerobic environments would decrease the preservation potential of the pupal exuviae whereas rapid burial in sediment would enhance the possibility of preserving the larvae.

The poorer taxonomic resolution of the larval stage to species morphotypes rather than distinct species may broaden the apparent ecological range of the taxon and result in the calculation of erroneous optima. For example three species of *Procladius* were identified from the pupal exuviae although only a single morphotype is recognised from subfossil larvae. Similarly analysis of the pupal assemblage suggests *Paratanytarsus* and *Cricotopus/Orthocladius* larval morphotypes also include several different species. The *Procladius* species co-occur in three lakes and occur singularly in three lakes. Therefore it is impossible to determine whether the species have similar ecological tolerances. They may have different optima but would be assigned a single temperature optima based on the larval stage or the species may have similar optima so variations in morphotype composition would be unimportant. Five taxa could not be identified to species level using West Palaeoartic taxonomic keys (Langton and Visser 2003) although they appeared to be distinct species. These taxa may have localised Russian distributions or be endemic to the Putorana; a number of plant and animal species are also restricted to this region (Malyshev 1976; Formozov and Yakhontov 2003). If they are endemic species, the response to environmental variables, such as temperature, may vary from the Norwegian morphotype. More work would be required, ideally with collection throughout the life cycle, to establish the identity of these unknown taxa and their ecological requirements.

5.3. Species responses to significant environmental variables

The results in Chapter 4 showed that several variables have a significant influence on chironomid distribution within the Russian, Norwegian and combined datasets. The quantitative relationships of taxa with 10 or more occurrences to the environmental variables identified as significant (sections 4.2.4, 4.3.4 and 4.4.3) were statistically assessed by a hierarchical series of taxon - response models (Oksanen and Minchin 2002). The HOF models are sequentially fitted and the simplest significant response model generated for each species or morphotype (Table 5.3); details of the programme are given in section 3.4.3. The responses of 57 taxa from the Russian, 83 from the Norwegian and 104 for the combined Russian – Norwegian datasets were assessed.

Table 5.3. The five HOF models of ecological response (Huisman et al. 1993)

Model	Ecological response
Model I	No significant trend
Model II	Increasing or decreasing monotonic sigmoidal trend
Model III	Increasing or decreasing trend bounded below the maximum attainable response
Model IV	Symmetric unimodal response curve
Model V	Asymmetric/skewed unimodal response curve

July air temperature is the most significant environmental variable, with the highest percentage of species having a statistically significant response, in all three training sets (Table 5.4.) Over 75% of taxa tested have a significant response to continentality and pH in the Russian lakes and to conductivity, water depth, distance to the coast and annual precipitation in the Norwegian lakes. When the training sets are combined, the environmental gradients are increased, and 90% of the taxa tested showed a significant response to continentality and pH. The prime objective of this research is to reconstruct palaeoclimatic records. Therefore although these results indicate that many species respond to environmental variables, such as pH and water depth, which

are independent of or indirectly linked to climate, the remainder of the chapter will focus on species response to July temperature and continentality.

Table 5.4. Taxon responses modelled using the HOF programme for (a) 57 taxa in the Russian training set, (b) 83 taxa in the Norwegian training set and (c) 104 taxa in the combined training set.

(a) Russian training set

Taxon response model type	No. of taxa						
	July temperature	Continentality Index	Annual precipitation	Forest vegetation	Water depth	Na ⁺	pH
Null (model I)	9	10	23	20	29	15	12
Monotonic (model II)	20	24	19	37	13	25	14
Plateau (model III)	1	0	0	0	3	2	3
Symmetric Gaussian response (model IV)	23	18	10	0	11	11	20
Skewed unimodal response (model V)	4	5	5	0	1	4	8
Number of species showing a significant response (II + III + IV + V)	48	47	34	37	28	42	45
% of species showing a significant response to the variable $[(II + III + IV + V)/57] \times 100$	84	82	60	65	49	74	79
Number of species showing a unimodal response (IV + V)	27	23	15	0	12	15	28
% of species showing a unimodal response to the variable $[(IV + V)/57] \times 100$	47	40	26	0	21	26	49

(b) Norwegian training set

Taxon response model type	No. of taxa						
	July temperature	Continentality Index	Water depth	Distance to coast	pH	Conductivity	Annual precipitation
Null (model I)	5	28	21	21	26	21	18
Monotonic (model II)	15	23	18	22	22	20	24
Plateau (model III)	0	0	0	0	0	1	1
Symmetric Gaussian response (model IV)	51	18	38	35	28	31	37
Skewed unimodal response (model V)	12	14	6	5	7	10	3
Number of species showing a significant response (II + III + IV + V)	78	55	62	62	57	62	65
% of species showing a significant response to the variable $[(II + III + IV + V)/83] \times 100$	94	66	75	75	69	75	78
Number of species showing a unimodal response (IV + V)	63	32	44	40	35	41	40
% of species showing a unimodal response to the variable $[(IV + V)/83] \times 100$	76	39	53	48	42	49	48

(c.) Combined training sets

Taxon response model type	No. of taxa						
	July temperature	Continentality Index	lg Ca	Water depth	Distance to coast	pH	Annual precipitation
Null (model I)	2	10	17	22	12	10	15
Monotonic (model II)	19	32	27	25	33	30	39
Plateau (model III)	0	0	0	0	0	1	0
Symmetric Gaussian response (model IV)	56	41	39	40	42	47	39
Skewed unimodal response (model V)	27	21	21	17	17	16	11
Number of species showing a significant response (II + III + IV + V)	102	94	87	82	92	94	89
% of species showing a significant response to the variable $[(II + III + IV + V)/104] \times 100$	98	90	84	79	88	90	86
Number of species showing a unimodal response (IV + V)	83	62	60	57	59	63	50
% of species showing a unimodal response to the variable $[(IV + V)/104] \times 100$	80	60	58	55	57	61	48

5.3.1. Species response to mean July air temperature

Of the taxa in the Russian dataset 84% have a statistically significant response to mean July air temperature (Table 5.4); however only 47% have a unimodal response compared with 76% in the Norwegian and 80% for the combined datasets. When species responses were modelled the uneven distribution of Russian lakes along the temperature gradient and absence of samples with T_{july} between 15.3-18°C (section 4.2.1) resulted in an apparent bimodal response by many species. A second Russian training set was compiled which excluded 26 lakes from Yakutia with extreme environmental variables and included 6 lakes from the Komi Republic (training set detailed in section 6.2.2). Water chemistry data was unavailable for the Komi lakes so these lakes could not be included in the analysis in chapter 4 or the HOF models for water depth, continentality or Na^+ (Table 5.4), however their inclusion results in a more even and continuous distribution along the July temperature gradient which improves the modelled responses. HOF models of the 53 taxa, with 10 or more occurrences in this dataset, showed 90.6% have a statistically significant response to T_{july} and 52.8% statistically significant unimodal responses.

Taxon responses to T_{july} were examined by fitting response models to species abundance data, for taxa with 10 or more occurrences and present in both the Norwegian and Russian lakes, using GLMs and GAMs (Figures 5.3 and 5.4). The aim of this analysis was to determine whether taxa, and taxon responses, are comparable in Norway and Russia and therefore whether the training sets could be merged to develop a western Palaearctic inference model or if a localised Russian model was more appropriate, as discussed in Chapter 1. GLR sequentially fits linear and unimodal models; these are statistically evaluated, using a chi-square test, to select the minimal adequate model (see methods 3.4.3). In GAMs the linear predictors are replaced with smooth predictors, therefore the species data drives the model rather than impose a fixed structure. This allows more complex bimodal, skewed unimodal or plateau responses to be modelled; however the results are 'noisier' as they are more susceptible to variations in the probability of occurrence and sample distribution along the temperature gradient. The results are compared to the fitted HOF

model and temperature optima (WA opt) calculated using Weighted Averaging regression (see 3.4.5 for methods and Chapter 6 for model development).

Figure 5.3. Taxon – mean July air temperature response curves for taxa common (10 or more occurrences) in the Norwegian and Russian (with Komi lakes) training sets. Curves (a) and (b) are GAM smoothers on the T_{July} gradient plotted on the scale of the link function with 95% confidence limits and (c) the ‘best-fit’ minimal adequate model (either GLM or GAM) on the scale of ‘probability of occurrence’. The HOF model, WA opt and number of occurrences (n) associated with each species are also illustrated. Norwegian samples are showed in blue and Russian in red.

Species showing a unimodal response:

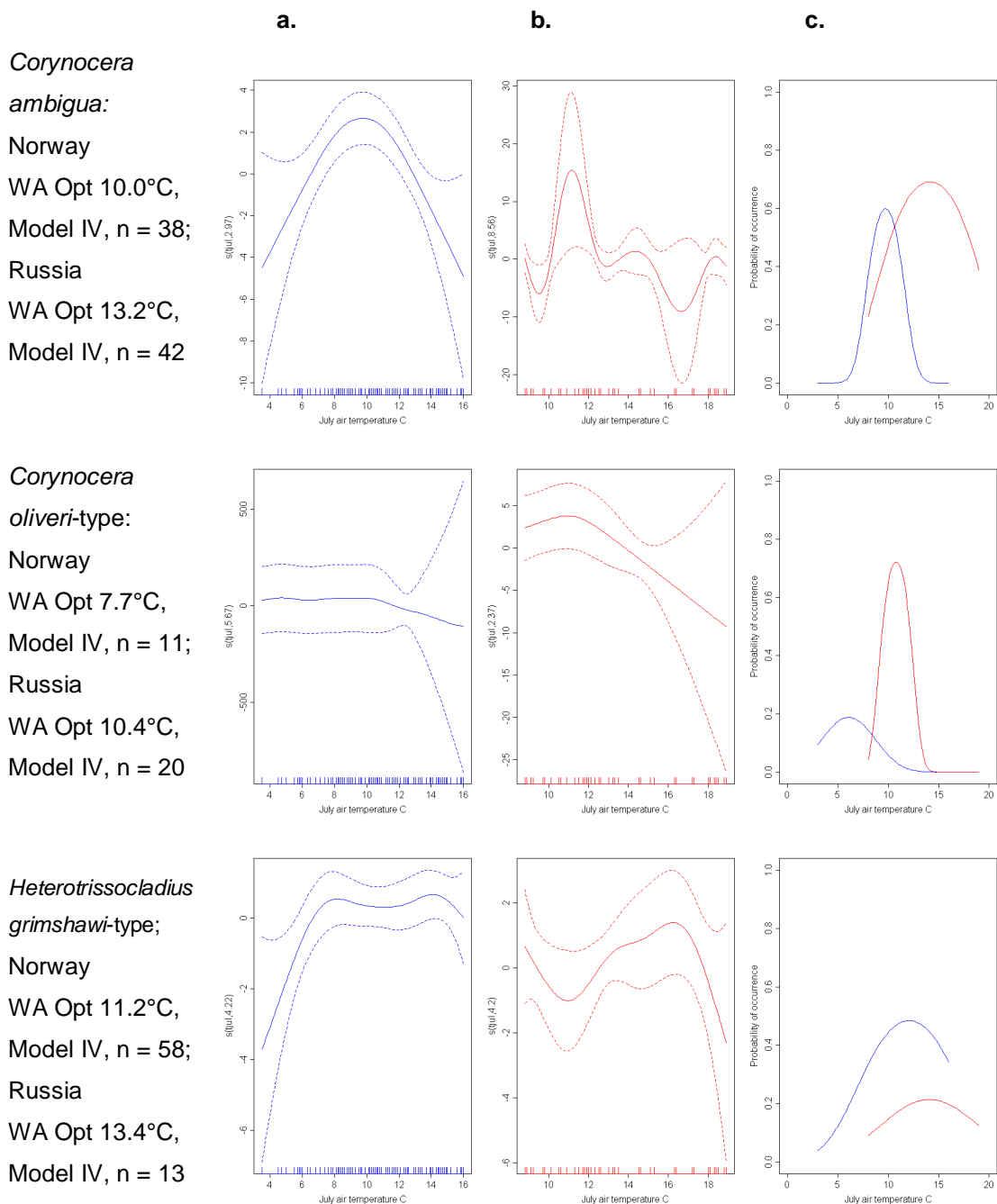


Figure 5.3. Taxon – July air temperature response curves continued.

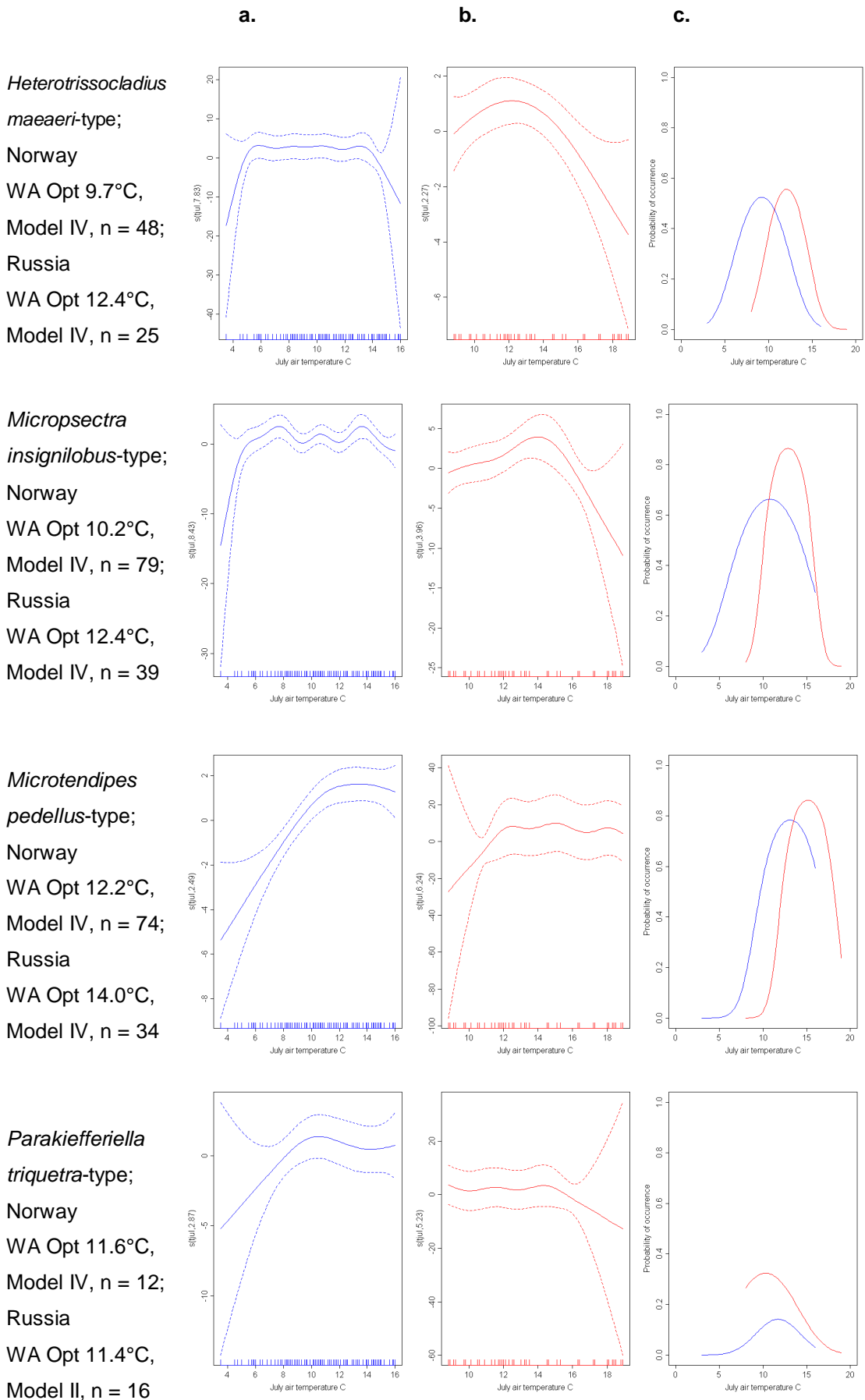


Figure 5.3. Taxon – July air temperature response curves continued.

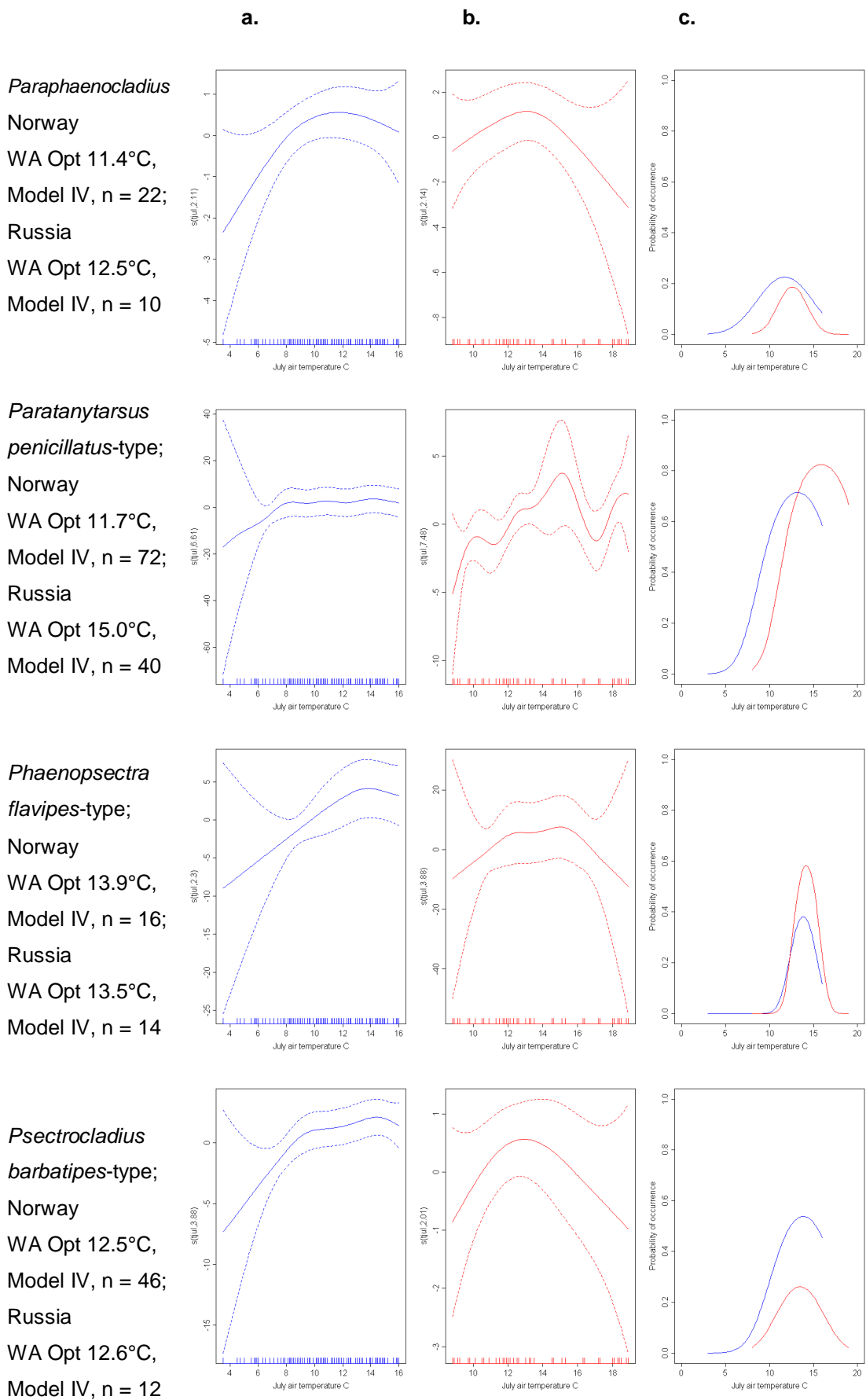


Figure 5.3. Taxon – July air temperature response curves continued.

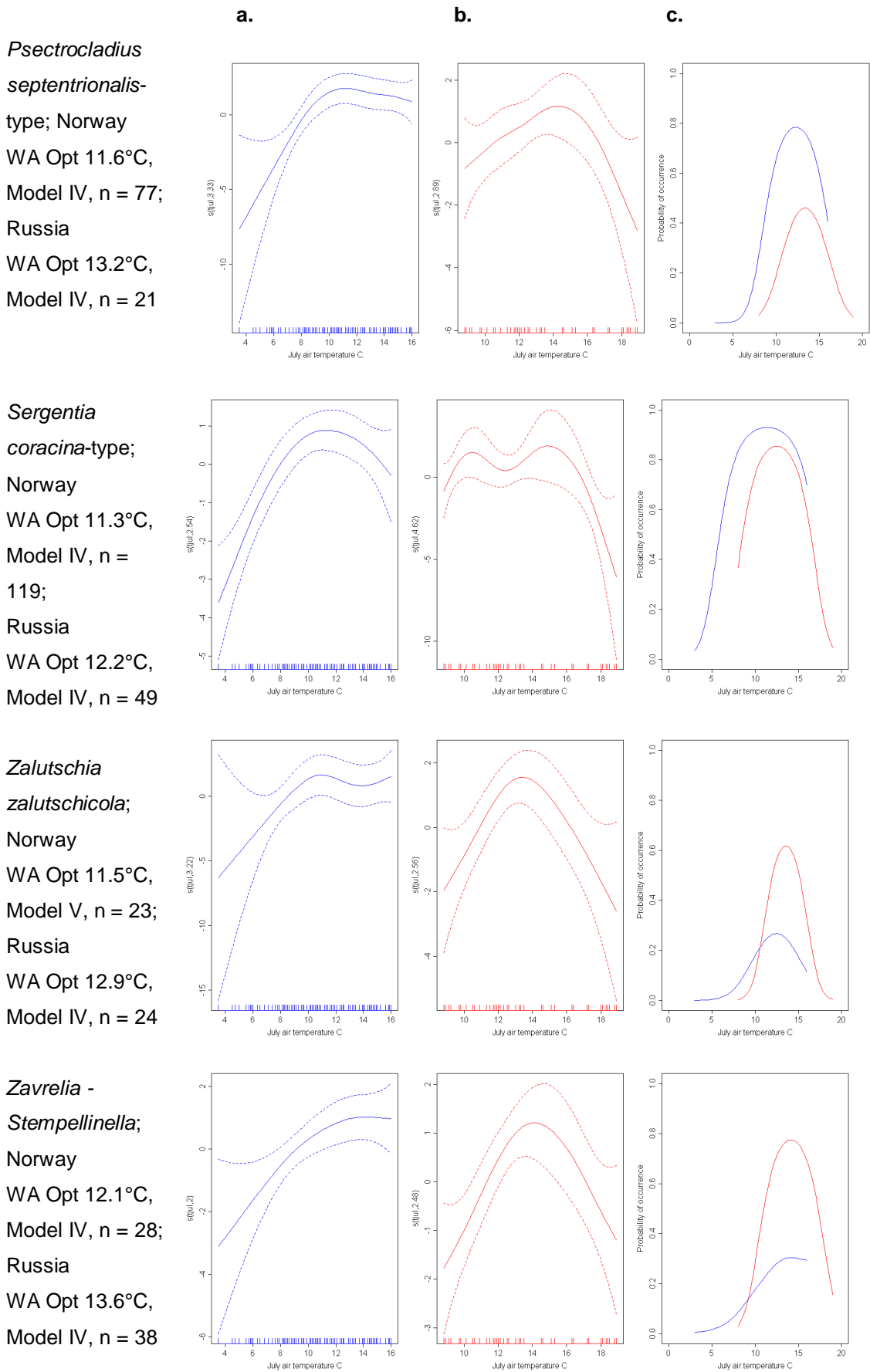


Figure 5.3. Taxon – July air temperature response curves continued.

Taxa with one or both datasets having a sigmoidal response

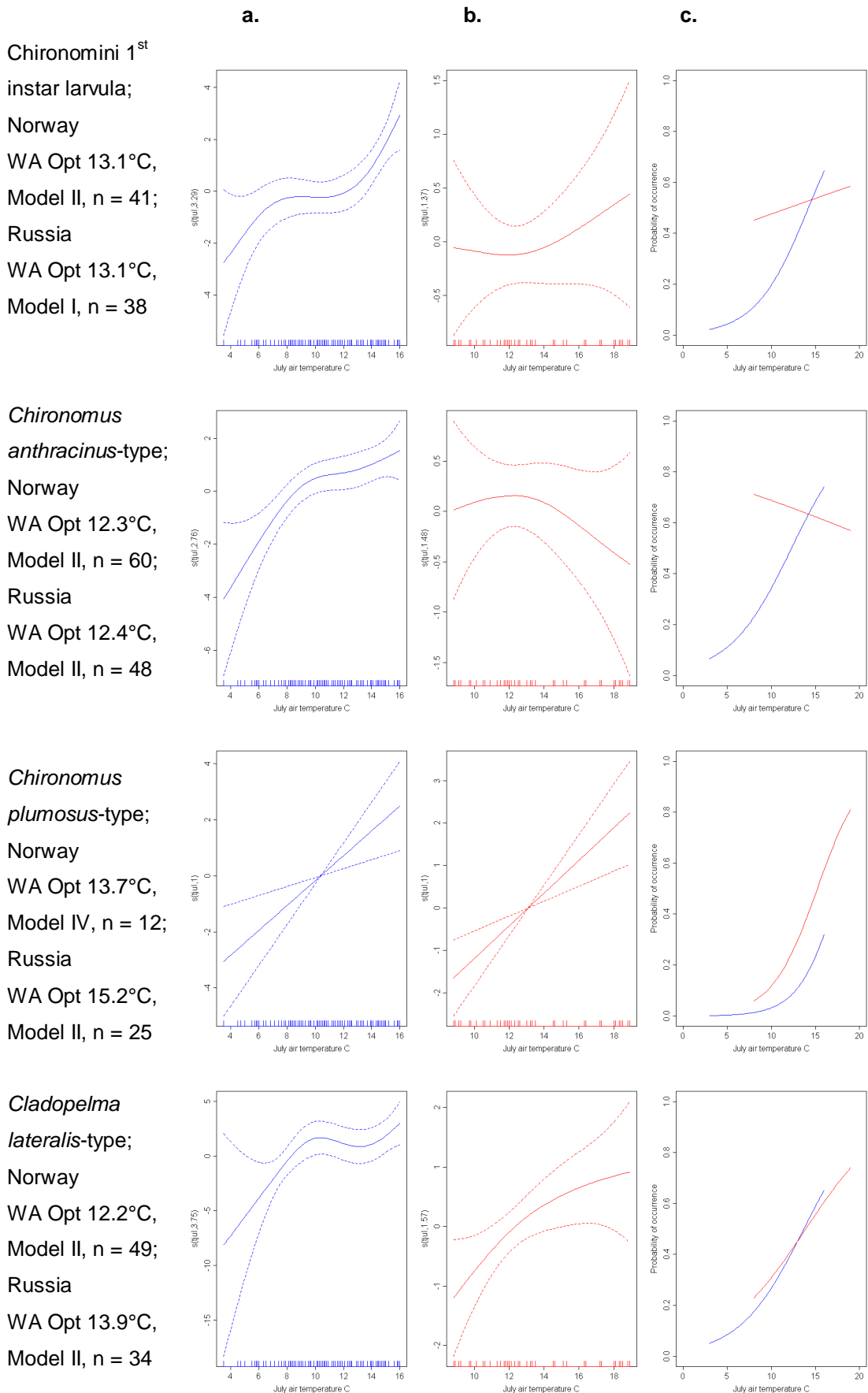


Figure 5.3. Taxon – July air temperature response curves continued.

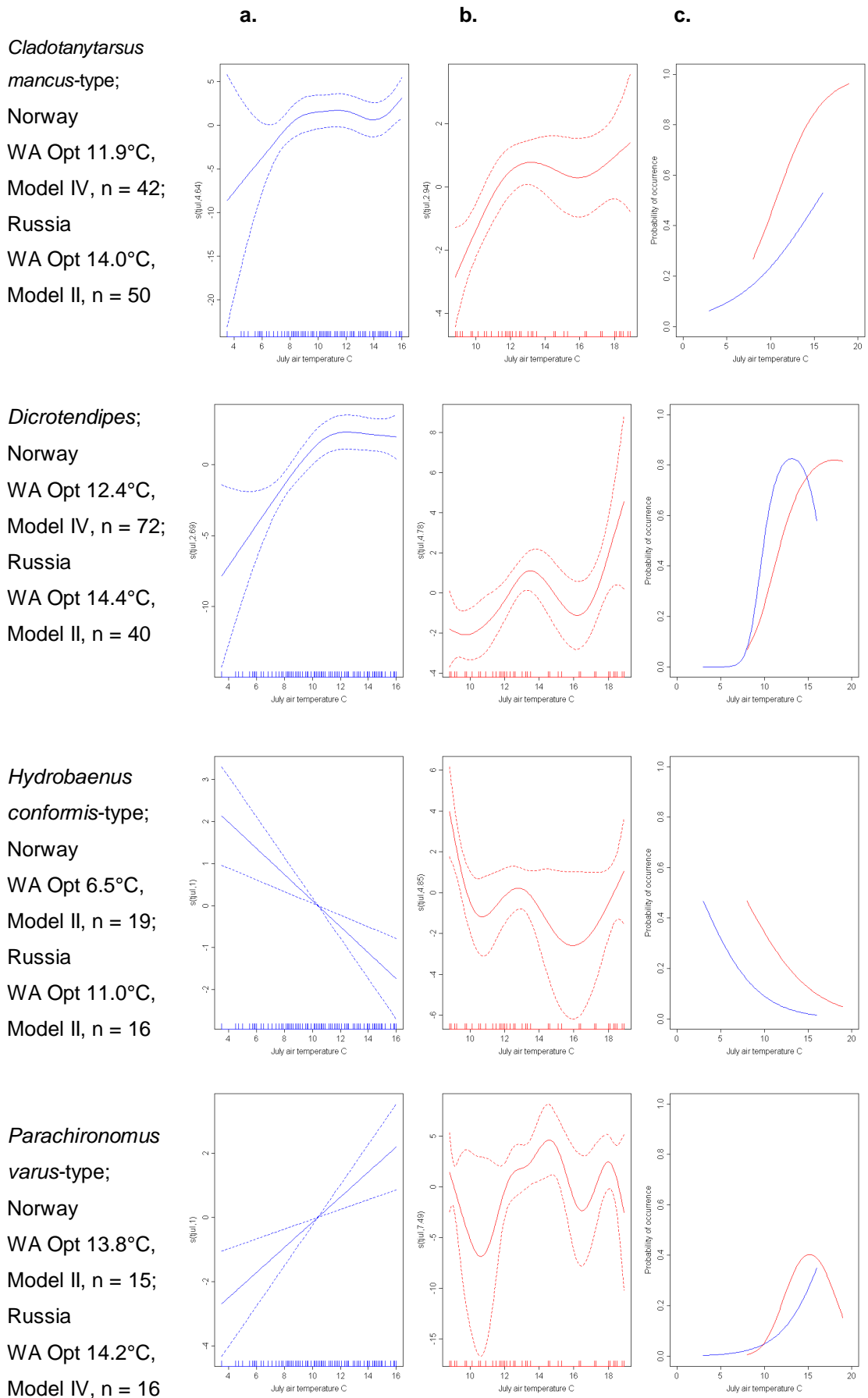


Figure 5.3. Taxon – July air temperature response curves continued.

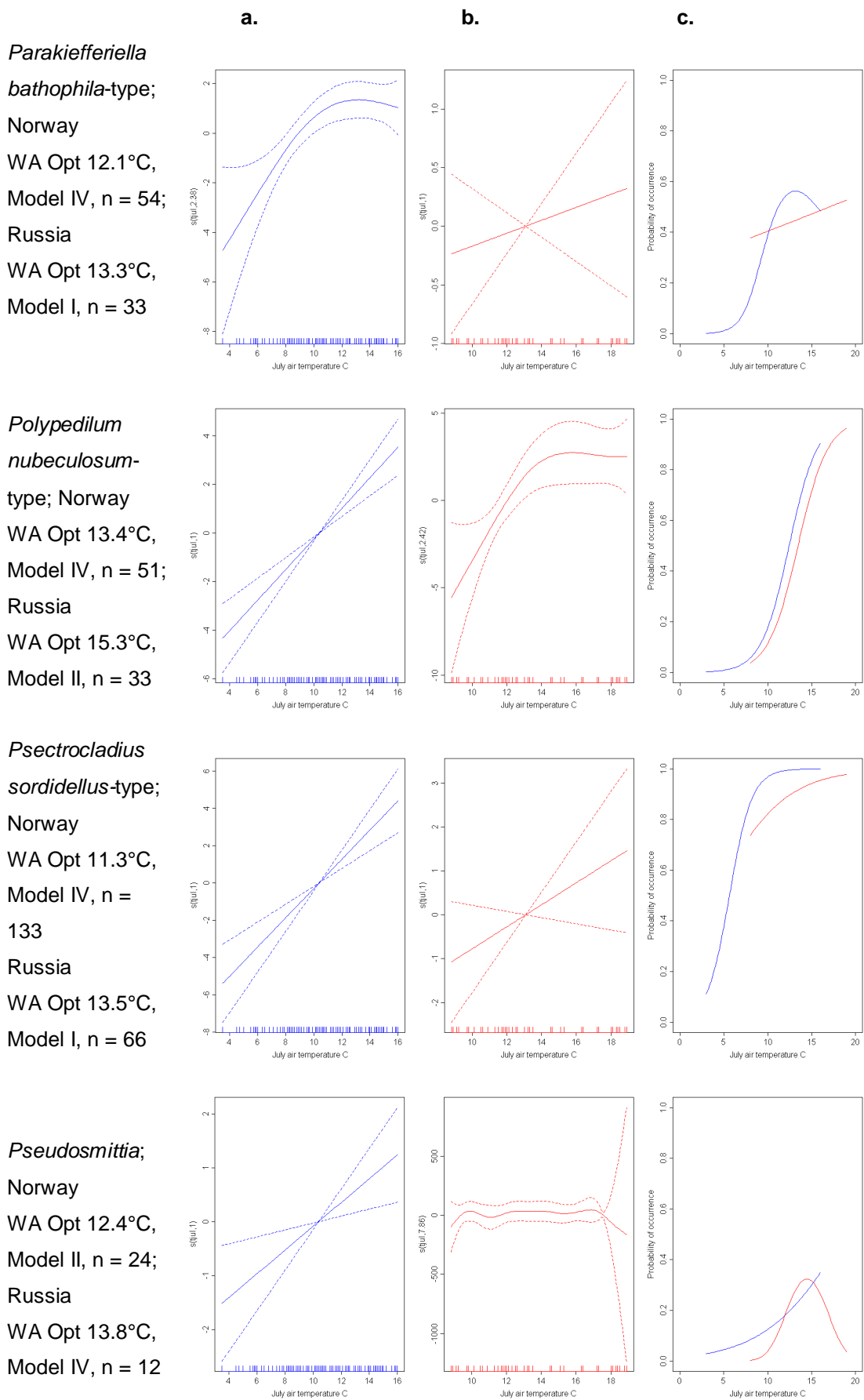


Figure 5.3. Taxon – July air temperature response curves continued.

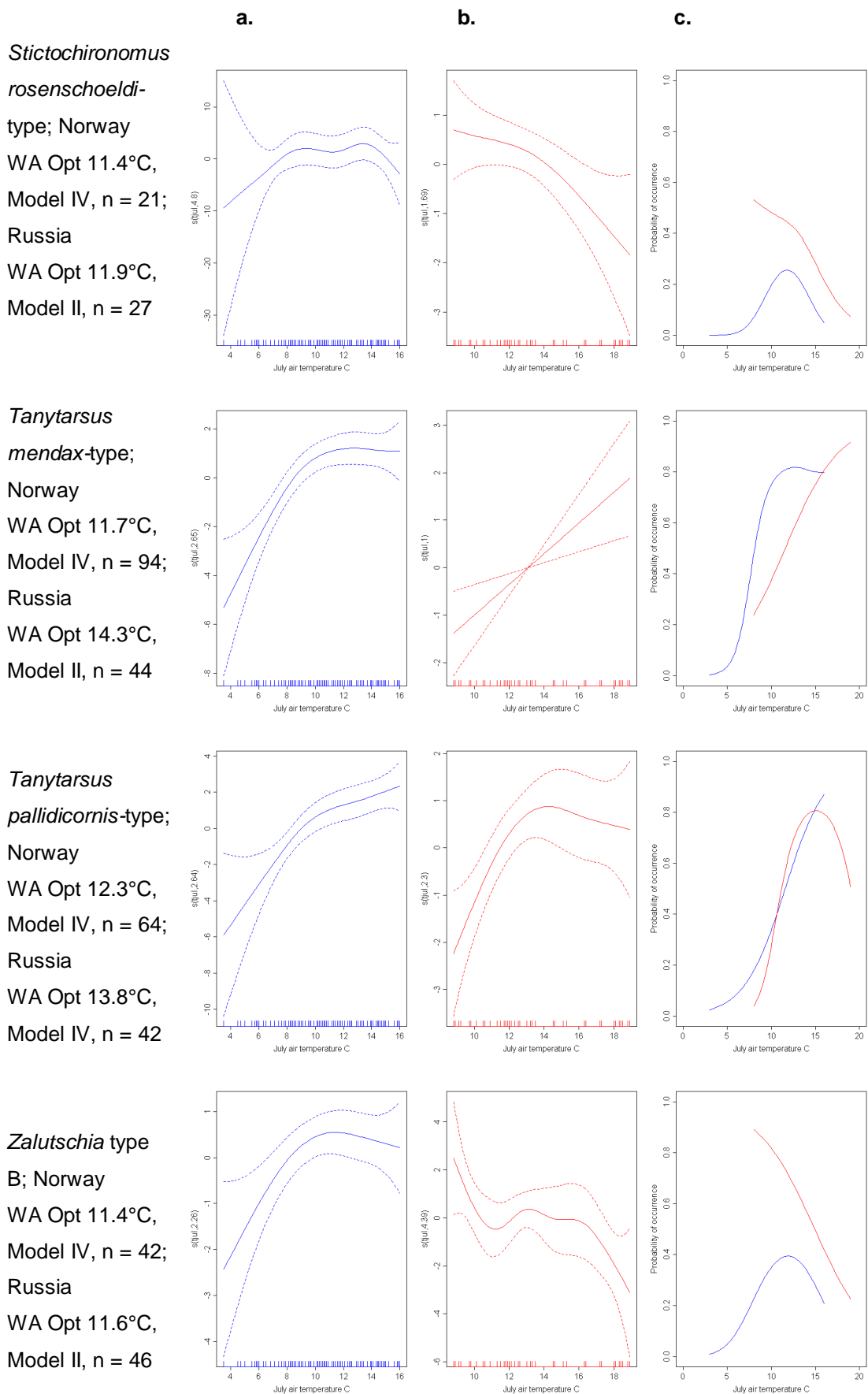
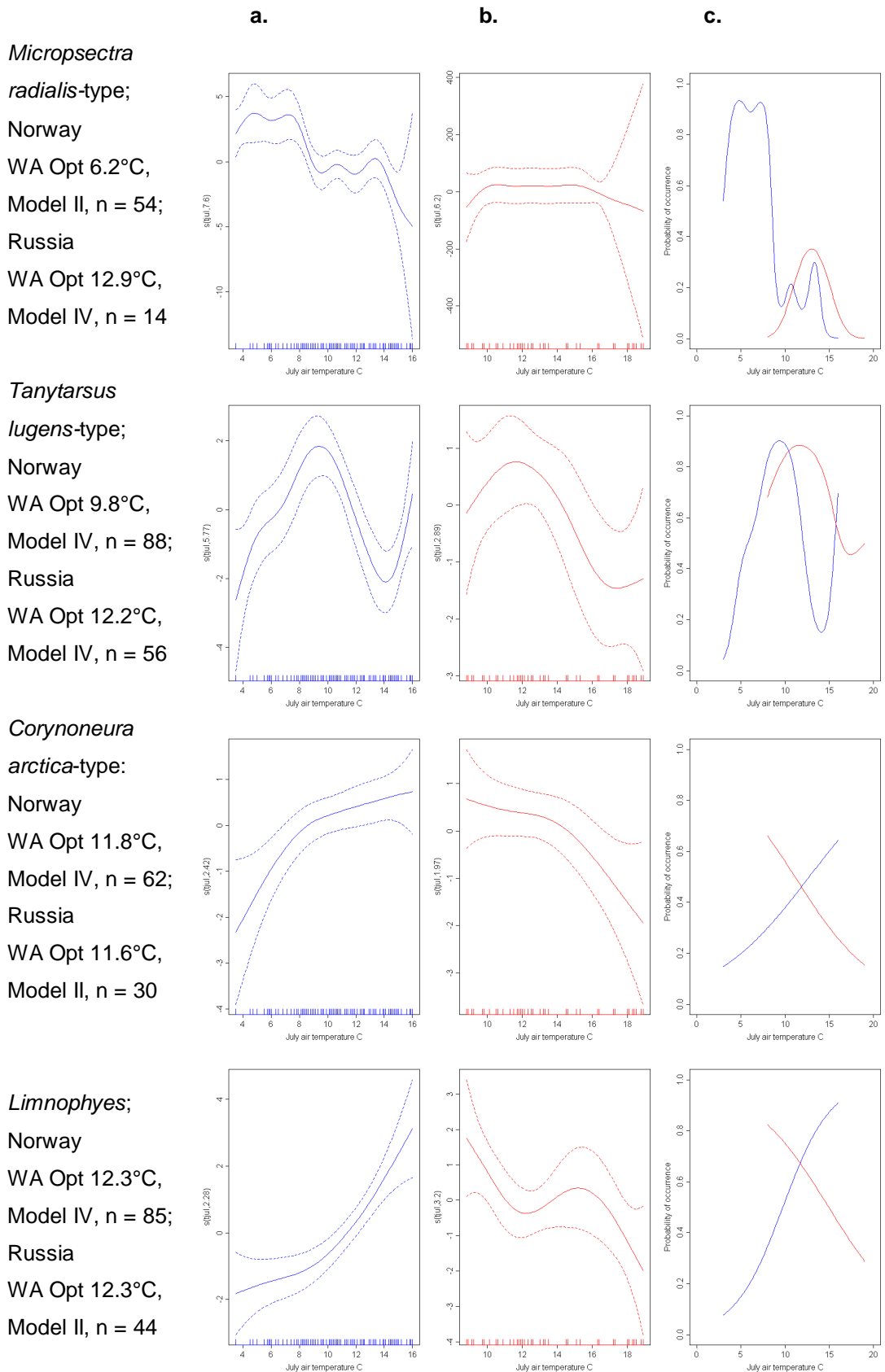


Figure 5.3. Taxon – July air temperature response curves continued.

Taxa with one or both datasets showing complex responses



Of the 42 taxa common to both Russia and Norway 16 have statistically significant unimodal responses to T_{july} in both datasets (*Corynocera ambigua*, *Corynocera oliveri*-type, *Cricotopus type P*, *Heterotrissocladius grimshawi*-type, *H. maeaeri*-type, *Micropsectra insignilobus*-type, *Microtendipes pedellus*-type, *Parakiefferiella triquetra*-type, *Paratanytarsus penicillatus*-type, *Paraphaenocladus*, *Phaenopsectra flavipes*-type, *Psectrocladius barbatipes*-type, *Ps. septentrionalis*-type, *Sergentia coracina*-type, *Zalutschia zalutschicola* and *Zavrelia*). Four taxa (*Chironomus plumosus*-type, *Cladopelma lateralis*-type, *Cladotanytarsus mancus*-type and *Polypedilum nubeculosum*-type) have sigmoidal increasing responses and temperature optima beyond the sampled range of warmest lakes (16.0°C for Norway and 19.0°C for Russia). *Hydrobaenus conformis*-type has sigmoidal decreasing responses and therefore temperature optima beyond the sampled ranges of the coolest lakes (3.5°C for Norway and 8.8°C for Russia). Where the optima are beyond the temperature range of the training sets, the WA optima of the taxa vary widely (for example 6.5°C for *H. conformis*-type from Norway and 11.0°C from Russia). This discrepancy reflects the limitations of WA estimation which results in distortions at the ends of the environmental gradient (ter Braak and Juggins 1993). Taxa with optima near the warmest temperatures of the Norwegian training set often show a sigmoidal increasing response to temperature whilst the Russian taxa have a unimodal response (for example *Parachironomus varus*-type, *Pseudosmittia* and *Tanytarsus pallidicornis*-type). The divergent confidence limits suggest this may result from better representation of the taxa in the central part of the environmental gradient than at the extremes. Five taxa, in the Russian data, have no statistically significant response to T_{july} (*Chironomini larvula*, *Chironomus anthracinus*-type, *Orthocladus oliveri*-type, *Parakiefferiella bathophila*-type and *Ps. sordidellus*-type). The modelled responses (Figure 5.3 and 5.4c) appear shallow sigmoidal but the high associated uncertainty (Figure 5.3 and 5.4b) means that although they may be responding to temperature the relationship can not be statistically established using the current dataset. The WA opt of *Micropsectra radialis*-type differs from 6.5°C in Norway to 12.9°C in the Russian data; the modelled response of the Norwegian data shows *M. radialis*-type has a bimodal response to T_{july} (Figure 5.3) with temperature optimum at 6°C and second, less well resolved optimum

between 10 - 15°C°. The Russian taxon response corresponds to the second optimum. As the two optima are so distinct the bimodal response may result from two morphologically similar species. *Tanytarsus lugens*-type has a unimodal response but the increasing probability of occurrence above 14°C suggests this morphotype may also have a bimodal response over a longer temperature gradient. *Limnophyes* and *Corynoneura arctica*-type have opposing responses to T_{july} ; sigmoidal increasing in the Norwegian samples and sigmoidal decreasing in the Russian. The larvae of *C. arctica*-type and some species of *Limnophyes* are associated with aquatic macrophytes (Brodin 1986), therefore the taxa may be responding, indirectly to temperature, through factors affecting the distribution of the plants.

The previous section showed *Procladius*, *Cricotopus/Orthocladius* and *Paratanytarsus* morphotypes were composed of a number of species in the Putorana lakes and the response of these taxa to T_{july} is illustrated in Figure 5.4. The Tanypodinae *Ablabesmyia* was included as this taxon is also species rich and undifferentiated in the training sets. *Cricotopus* type P has a unimodal response to T_{july} in both the Russian and Norwegian data and *C. cylindraceus*-type a unimodal response in the Norwegian data and sigmoidal increasing response in the Russian. This suggests these morphotypes are represented by a single species (or multiple species with identical responses), the Russian temperature optima are higher than the Norwegian. *C. laricomalis*-type and *Orthocladius oliveri*-type have bimodal responses in the Norwegian data. *C. laricomalis*-type has a sigmoidal response in the Russian data corresponding to the warmer Norwegian response and the Russian *O. oliveri*-type shows no relationship to T_{july} . The bimodal response suggests these morphotypes may be composed of more than one species or are responding to environmental factors other than temperature. *P. austriacus*- and *P. penicillatus*-types are distinguished by the number of inner teeth on the mandible. Mandibles are often absent in subfossil material; in these instances head capsules are identified as *Paratanytarsus* undifferentiated. This grouping has a complex response to temperature in the Russian and Norwegian data (Figure 5.4), having temperature optima at 8-11°C, 16°C and less well resolved peak at 13°C. The occurrence of *P. austriacus*-type is too low in the Russian data for

the temperature response to be modelled. One of the warmer optima probably corresponds to *P. penicillatus*-type; however the temperature optimum of the Norwegian taxon is 11.7°C and the Russian 15.0°C. Further distribution data are required to establish whether the *Paratanytarsus*-group is composed of taxa with 3 distinct optima and whether *P. penicillatus*-type are represented by different species in Norway and Russia. From a threshold of 5°C the occurrence of *Procladius* and *Ablabesmyia*, in the Norwegian data, increases until the taxa are present in all lakes with a T_{july} of 12 – 16°C (probability of occurrence = 1). This plateau suggests either several species are present and are successively replaced by species with higher temperature optima or the species have wide environmental tolerances. In the Russian data the response of *Ablabesmyia* is border-line between a sigmoidal and unimodal response. The GAM and HOF models are unimodal, however in the GLM the sigmoidal response is marginally more significant. Therefore from the GLM *Ablabesmyia* has a sigmoidal increasing response and temperature optimum beyond the range of the warmest lakes and *Procladius* a broad unimodal response. From these responses it is not possible to determine the composition of the Russian taxa.

In general, the modelled and WA temperature optima of the Russian taxa are higher than the Norwegian optima, even where taxonomic resolution is high and the errors showed by the confidence limits are low. Higher optima may be of adaptive value in the continental climate of Arctic Russia. Periods of sub-zero temperatures occur up to mid-July and the later onset of development may prevent the loss of vulnerable stages. Growth rate is temperature dependent (Danks and Oliver 1972a) so higher optima may facilitate completion of part of the life cycle within the short continental summer (see section 1.5). Damselflies (Odanata: Zygoptera) shorten their developmental time and increase their growth rate in response to time stress imposed by seasonality (Stoks et al. 2008). Changes in temperature optima may be due to phenotypic plasticity (as in the damselflies) or genotypic variation. Species, such as *C. ambigua* and *Z. zalutchicola*, could be represented by distinct genotypes and DNA analysis would be necessary to establish this. The implications for the development of a chironomid – temperature inference model are discussed in section 5.4.

Figure 5.4. Taxon – mean July air temperature response curves for species-rich taxa.
Explanation as per Figure 5.3.

Cricotopus/Orthocladius

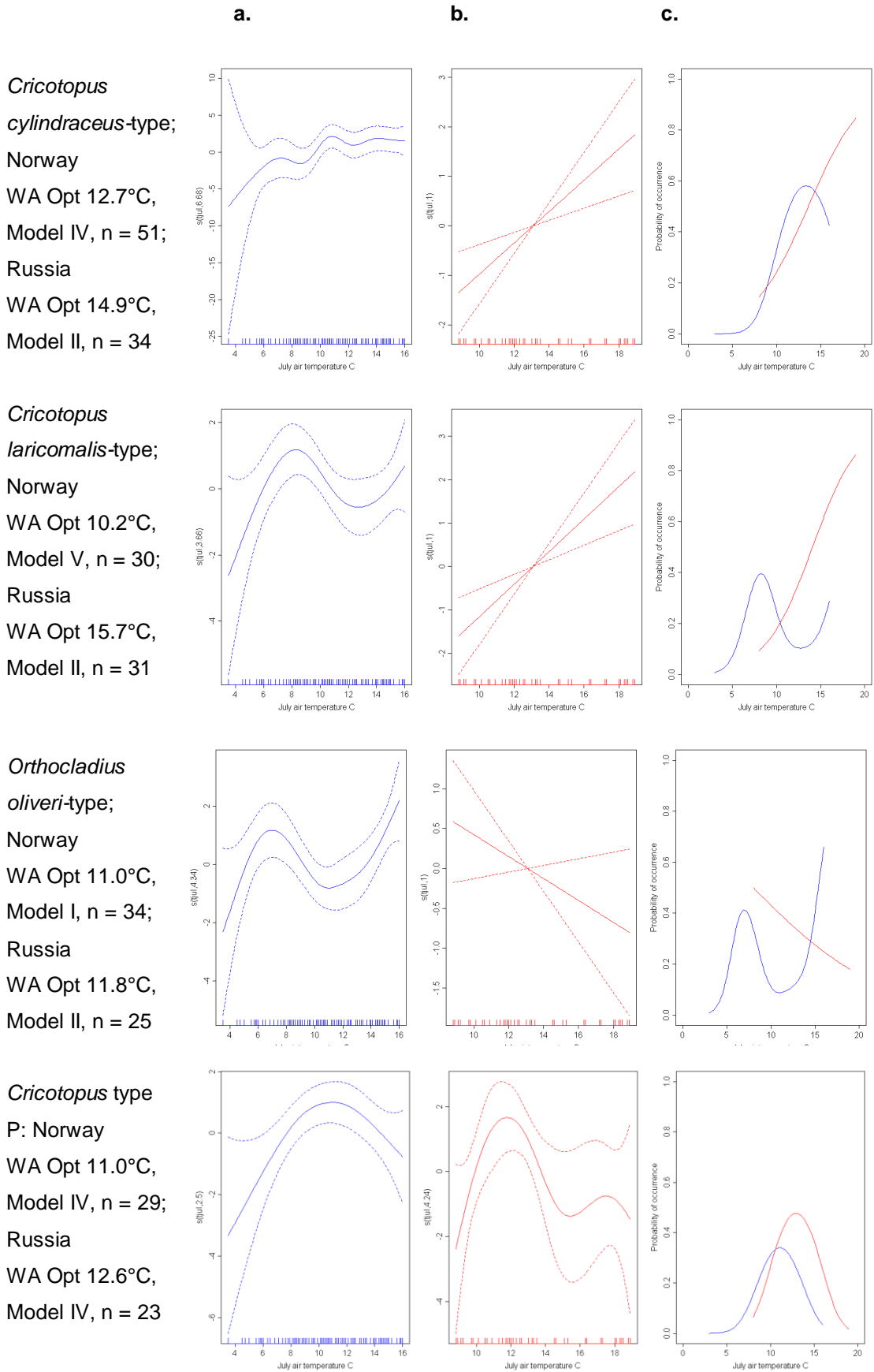


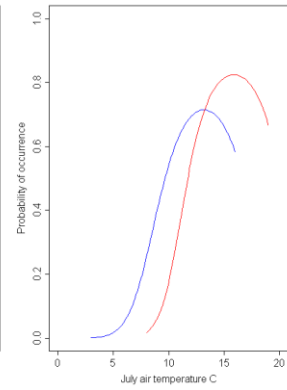
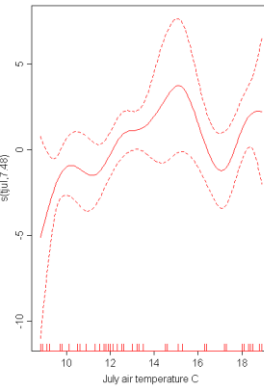
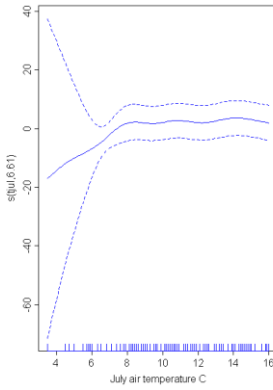
Figure 5.4. Taxon – mean July air temperature response curves continued.

***Paratanytarsus* and Tanypodinae: a.**

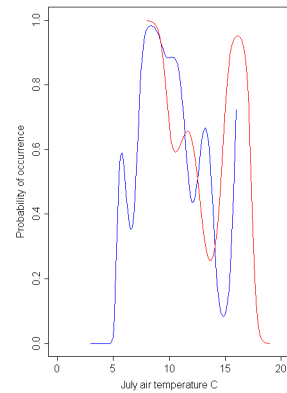
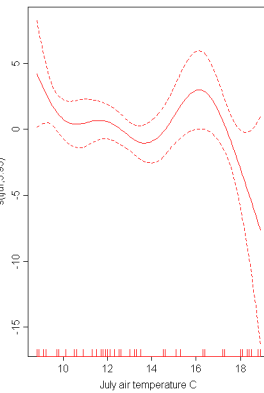
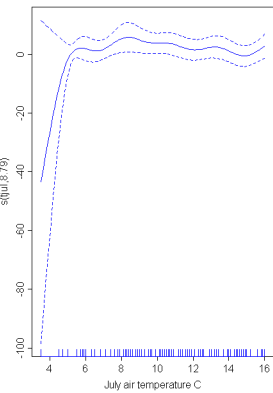
b.

c.

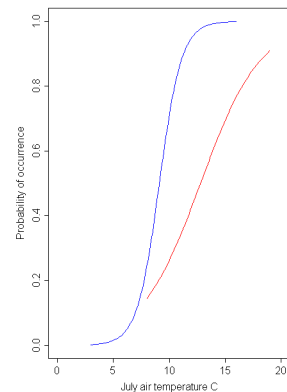
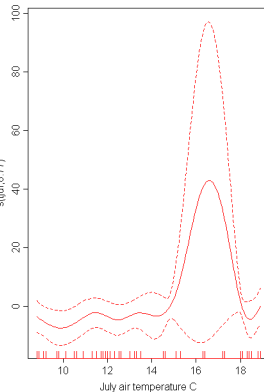
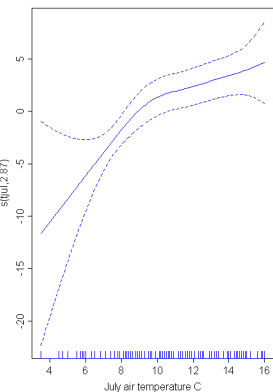
Paratanytarsus
penicillatus-type;
Norway
WA Opt 11.7°C,
Model IV, n = 72;
Russia
WA Opt 15.0°C,
Model IV, n = 40



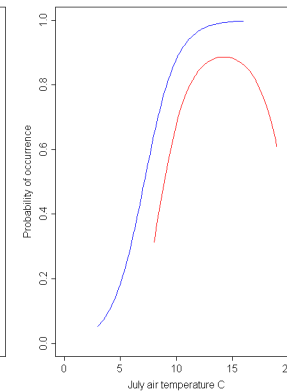
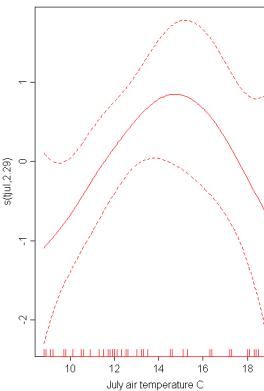
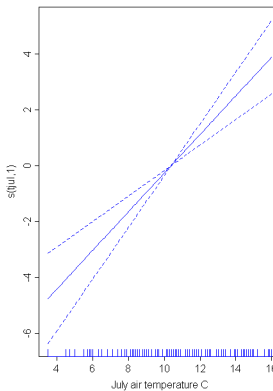
Paratanytarsus
undifferentiated;
Norway
WA Opt 9.8°C,
Model IV, n = 89;
Russia
WA Opt 11.4°C,
Model IV, n = 39



Ablabesmyia;
Norway
WA Opt 12.4°C,
Model IV, n = 98;
Russia
WA Opt 14.7°C,
Model V, n = 38



Procladius;
Norway
WA Opt 11.5°C,
Model IV, n = 118
Russia
WA Opt 13.4°C,
Model IV, n = 57



5.3.2. Species response to continentality (CI)

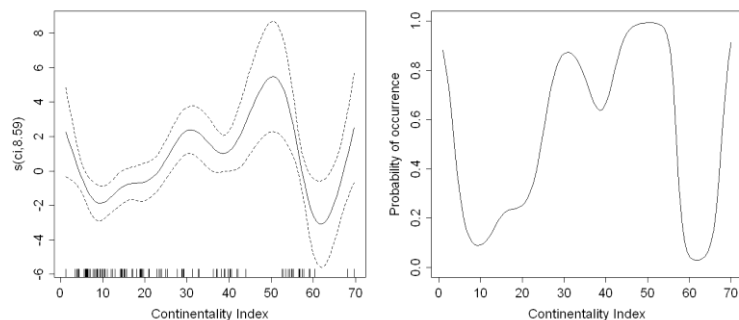
From the HOF models, of the training sets analysed in Chapter 4, 82% of the Russian taxa have a statistically significant response to the continentality index (CI) (Table 5.4). Fewer taxa (66%) have a significant response in the Norwegian lakes which may reflect the short CI gradient in Norway. The taxon – T_{july} response curves (Figures 5.3 and 5.4) show the temperature optima are generally higher for the Russian taxa and where optima are similar the probabilities of occurrence differ. Therefore the chironomid assemblages may also be expected to vary between Norwegian and Russian lakes with similar T_{july} . However the TWINSPAN analysis indicated the chironomid assemblages for the lakes (excluding Yakutia and Svalbard) were similar (Table 4.16). Chironomids may not be responding to continentality directly, i.e. the annual temperature range and latitude, but to variables that are co-linear with continentality, such as length of the summer, growing degree days or ice-free period. Taxon responses to continentality are modelled in this section to assess the feasibility of developing a chironomid-inferred continentality (CI-C) model.

Continentality is calculated from and therefore not independent of T_{july} . To minimise the risk of attributing a response to T_{july} instead of changes in continentality a subset of 149 lakes was selected covering a range of CI values for each 0.5°C temperature interval. This excluded samples from the extremities of the T_{july} gradient as all the coldest lakes (in Svalbard) have low CIs and all the warmest lakes (in Yakutia) have high CIs. When modelling species responses extrapolating responses beyond the sampled environmental gradient produces unreliable results (ter Braak and Juggins 1993) and excluding these extreme lakes enabled taxa responses to both continentality and T_{july} to be examined (section 5.3.3). Additional Norwegian samples were excluded to even the distribution of samples along the environmental gradient. The lakes included in the training set, and the criteria for their selection, are detailed in section 6.7.2. Taxon responses to CI were examined in the 149 lake data set by fitting response models to species abundance data, for taxa with 10 or more occurrences, using HOF, GLM and GAM models.

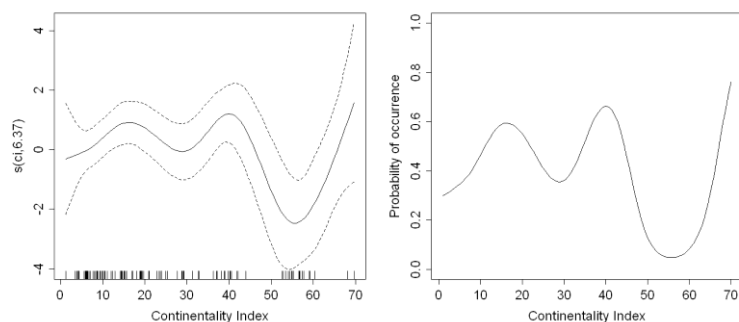
The fitted HOF models suggested 12 of the 82 taxa tested (14.6%) have no statistically significant relationship to continentality (Table 5.5). However the GAM models suggested the relationship was uncertain for an additional 25 taxa, examples of these are shown in Figure 5.5. The results vary as the taxon responses are more complex than the five specified HOF models; GAMs are data-driven and therefore not limited to an *a priori* model. The abrupt decreases in the probability of occurrence may result from the low number of occurrences for some rare taxa or the uneven distribution of samples along the CI gradient; there are no samples with indices of 24 – 28, 44 – 52 and 61 – 68. Expanding the training set by adding sites with these continentality indices would improve the assessment of the taxon response to continentality. The taxon responses, assessed by HOF and GLM/GAM models, show 54.9% have a statistically significant response to continentality (Table 5.5). In Figure 5.6 the minimal adequate model is compared to the fitted HOF model and CI optima (WA opt) calculated using Weighted Averaging regression (see methods 3.4.5).

Figure 5.5. Examples of taxon – continentality response curves for taxa identified as having a statistically significant response by HOF models but not supported by GAMs. Curve (a) is the GAM smoothers on the CI gradient plotted on the scale of the link function with 95% confidence limits and (b) the generalised additive (GAM) model on the scale of ‘probability of occurrence’.

Corynocera ambigua
HOF model II



Polypedilum nubeculosum-type
HOF model IV



Null response	Show HOF response: but insufficient data for GAM model	Sigmoidal decreasing response	Sigmoidal increasing response	Unimodal response
<i>Cricotopus cylindraceus</i> -type <i>Cricotopus sylvestris</i> -type <i>Cryptochironomus</i> <i>Dicrotendipes</i> <i>Heterotrissociadius maeaeeri</i> -type <i>Heterotrissociadius grimshawi</i> -type <i>Limnophyes</i> - <i>Paralimnophyes</i> <i>Orthocladus</i> type S <i>Pagastrella</i> <i>Paratanytarsus austriacus</i> -type <i>Parakiefferiella bathophila</i> -type <i>Phaenopsectra flavipes</i> -type <i>Zalutschia zalutschicola</i>	<i>Cladopelma lateralis</i> -type <i>Corynocera ambigua</i> <i>Corynoneura arcica</i> -type <i>Corynoneura edwardsi</i> -type <i>Corynoneura lobata</i> -type <i>Cricotopus</i> type C <i>Cricotopus</i> type P <i>Glyptotendipes pallens</i> -type <i>Macropelopia</i> <i>Mesocricotopus</i> <i>Microtendipes pedellus</i> -type <i>Micropsectra insignilobus</i> -type <i>Micropsectra radialis</i> -type <i>Monodiamesa</i> <i>Parakiefferiella nigra</i> -type <i>Paratanytarsus penicillatus</i> -type <i>Parachironomus varus</i> -type <i>Paracladius</i> <i>Paramerina</i> <i>Paratanytarsus</i> undiff. <i>Polypedilum nubeculosum</i> -type <i>Stictochironomus rosenschneideri</i> -type <i>Tanytarsus</i> 'no spur' <i>Zavrelia</i> - <i>Stempellinella</i>	<i>Abiabetesmyia</i> <i>Heterotanytarsus apicalis</i> -type <i>Orthocladus undiff.</i> <i>Paracladopelma</i> <i>Paraphaenocladus</i> <i>Protanypus</i> <i>Psectrocladius septentrionalis</i> -type <i>Psectrocladius sordidellus</i> -type <i>Pseudorthocladus</i> <i>Pseudosmittia</i> <i>Sergentia coracina</i> -type <i>Smittia</i> - <i>Parasmittia</i> <i>Synorthocladus</i> <i>Tanytarsus chinensis</i> -type <i>Thienemanniella clavicornis</i> -type <i>Thienemanniemyia</i> -group	<i>Abisomyia</i> <i>Chironomus anthracinus</i> -type <i>Chironomini</i> 1st instar larva <i>Chironomus plumosus</i> -type <i>Cricotopus intersectus</i> -type <i>Hydrobaenus conformis</i> -type <i>Orthocladus oliveri</i> -type <i>Tanytarsus lugens</i> -type <i>Zalutschia</i> type B Plateau response <i>Constempellina</i> - <i>Thienemanniola</i> <i>Corynocera oliveri</i> -type <i>Cricotopus laricomalis</i> -type <i>Procladius</i> <i>Tanytarsus mendax</i> -type	<i>Cladotanytarsus mancus</i> -type <i>Corynoneura</i> type A <i>Endochironomus albipennis</i> -type <i>Endochironomus impar</i> -type <i>Eukiefferiella claripennis</i> -type <i>Heterotrissociadius marcidus</i> -type <i>Lauterborniella</i> <i>Micropsectra pallidula</i> -type <i>Parakiefferiella triquetra</i> -type <i>Parakiefferiella</i> type A <i>Phaenopsectra</i> type A <i>Psectrocladius barbatipes</i> -type <i>Pseudochironomus</i> <i>Tanytarsus pallidicornis</i> -type <i>Zavrelimyia</i>

Table 5.5. Taxon responses to continentality, modelled using the HOF programme, GLM and GAMs, for species with more than 10 occurrences in the C-IC training set.

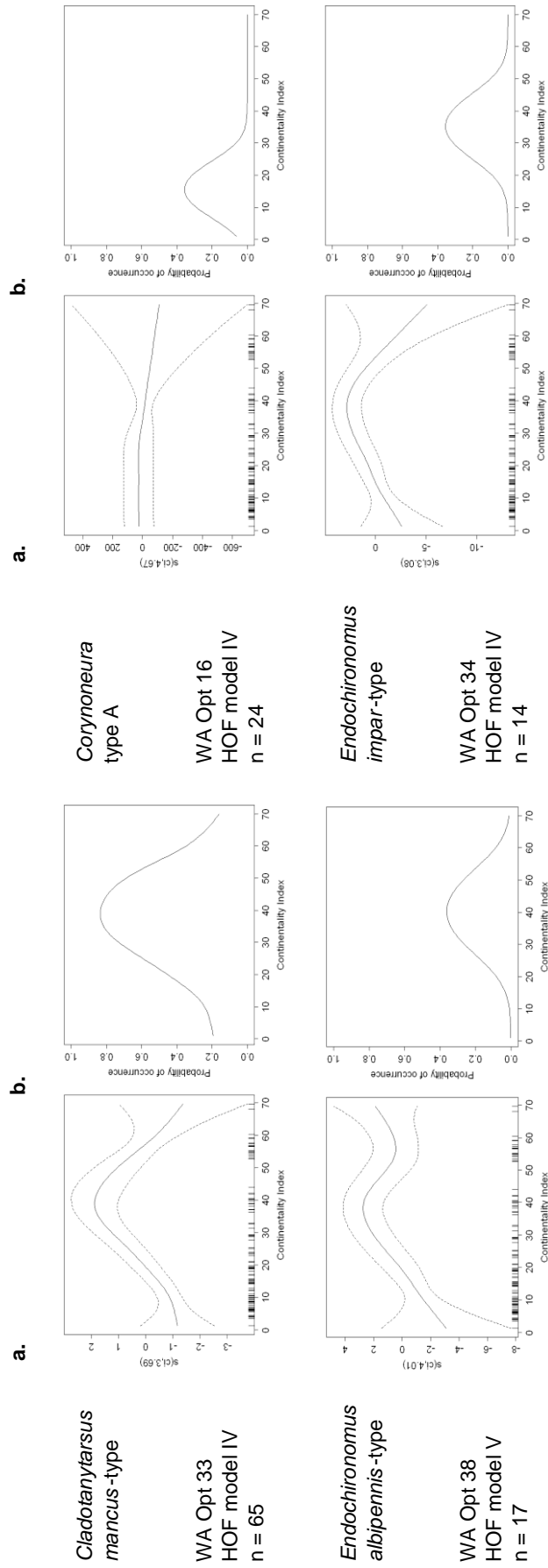


Figure 5.6. Taxon - continentality response curves for taxa common (10 or more occurrences) in the Ci-C training set. Curve (a) is the GAM smoothers on the Ci gradient plotted on the scale of the link function with 95% confidence limits and (b) the minimal adequate model plotted on the scale of 'probability of occurrence'. The HOF model, WA optima and number of occurrences (n) associated with each species are also illustrated.

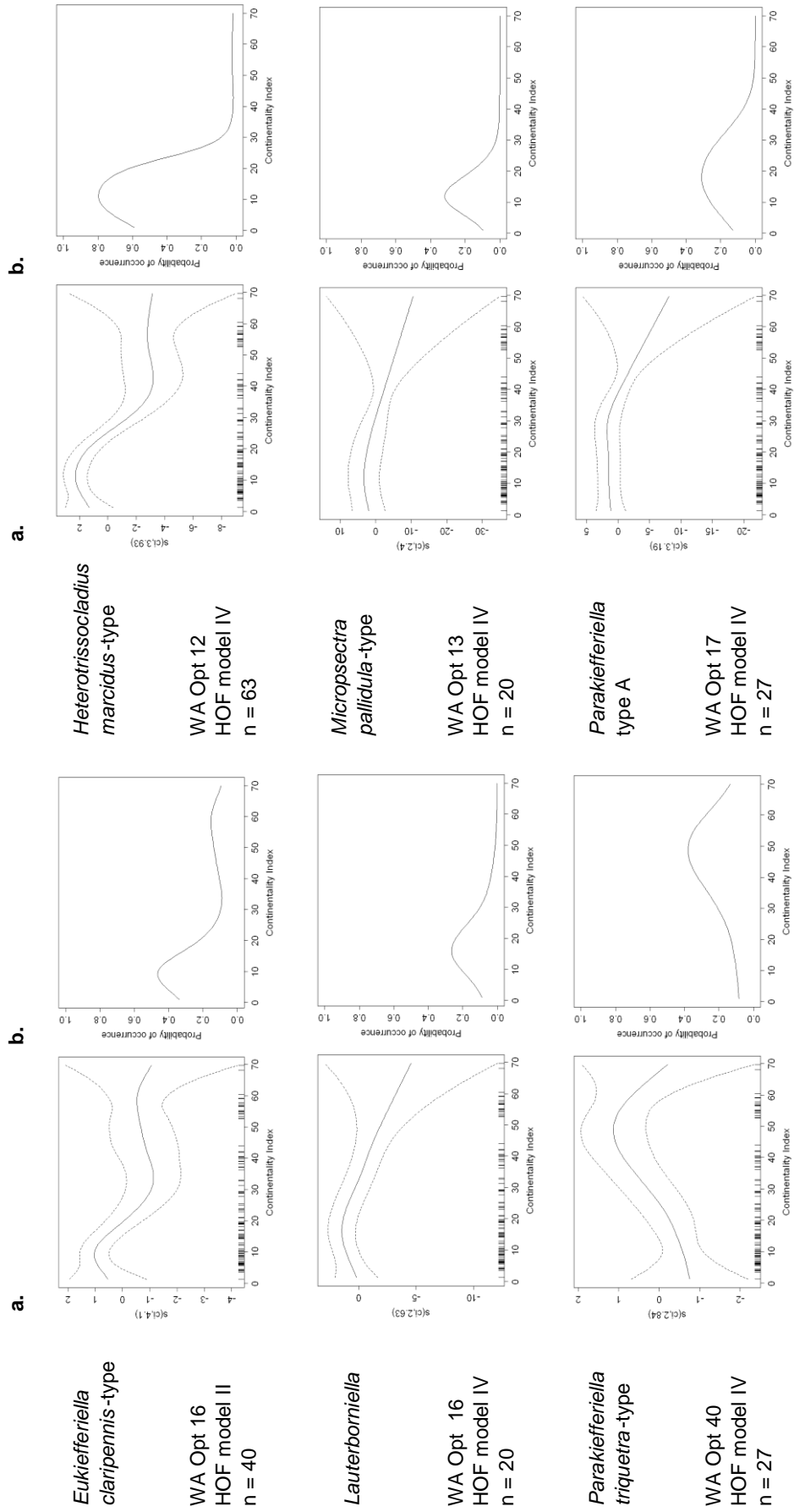


Figure 5.6. Taxon - continentality response curves continued. Species showing a unimodal response.

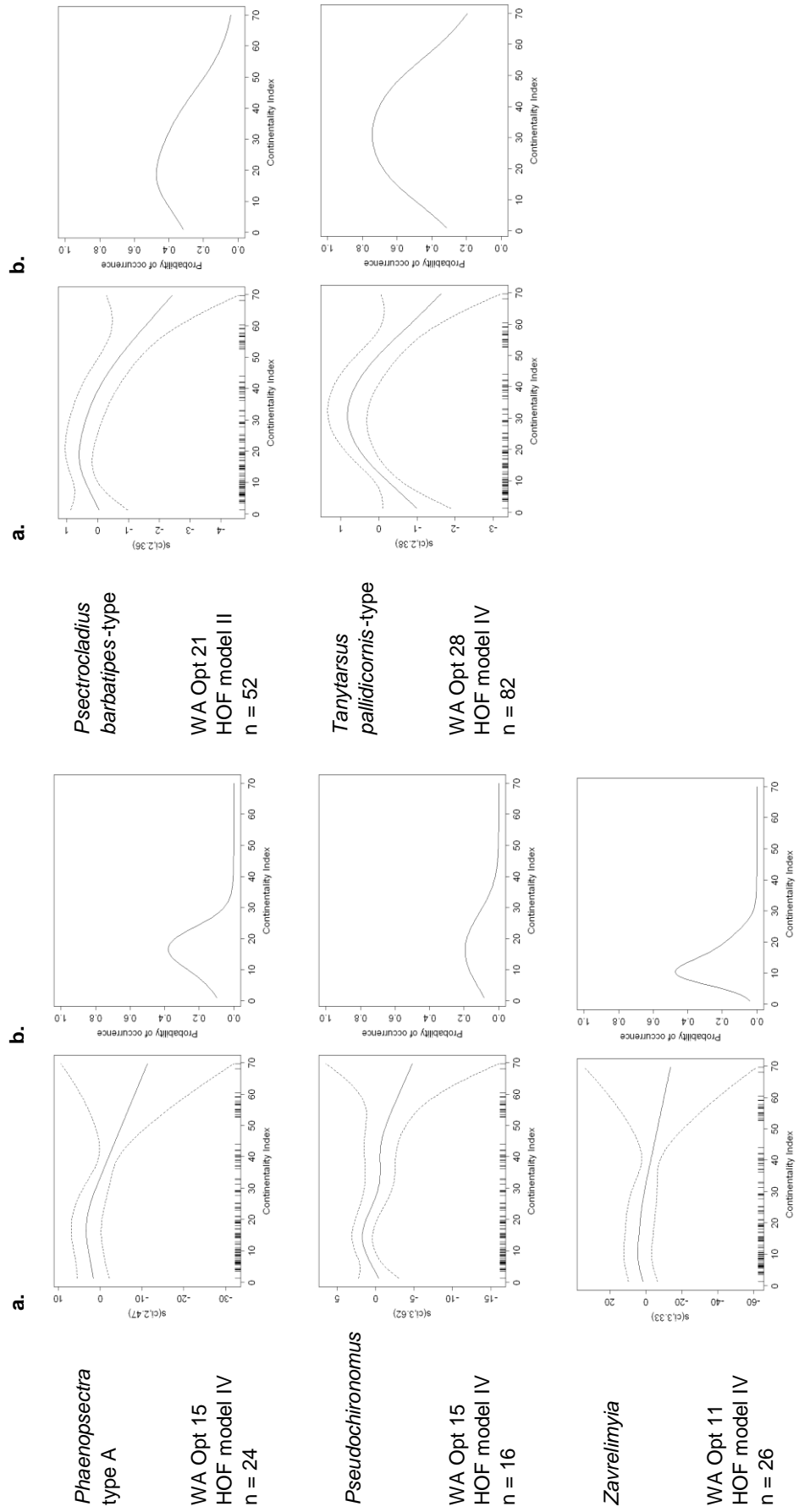


Figure 5.6. Taxon - continuity response curves continued. Species showing a unimodal response.

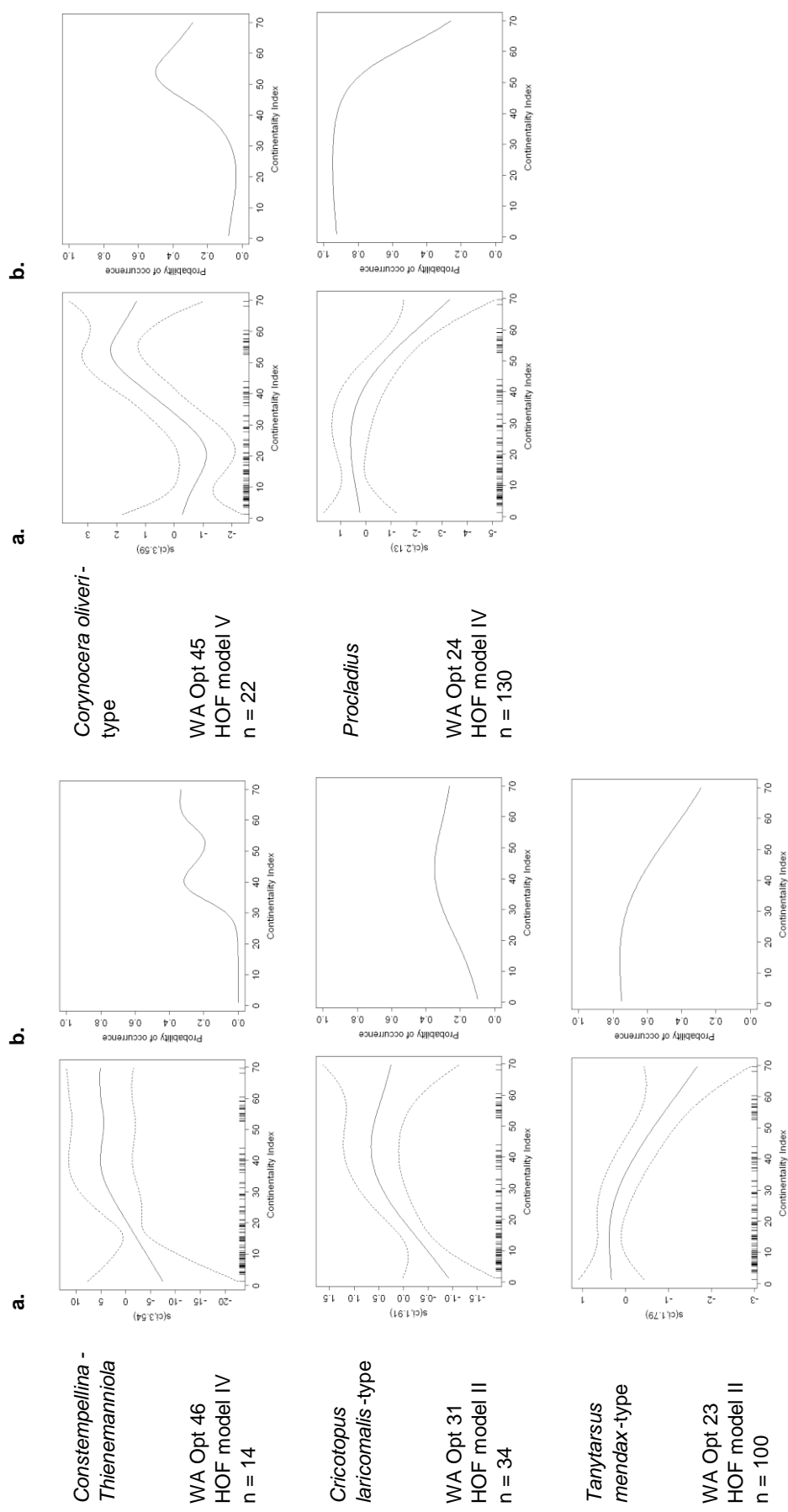


Figure 5.6. Taxon - continentiality response curves continued. Species where responses are unimodal or reach a plateau.

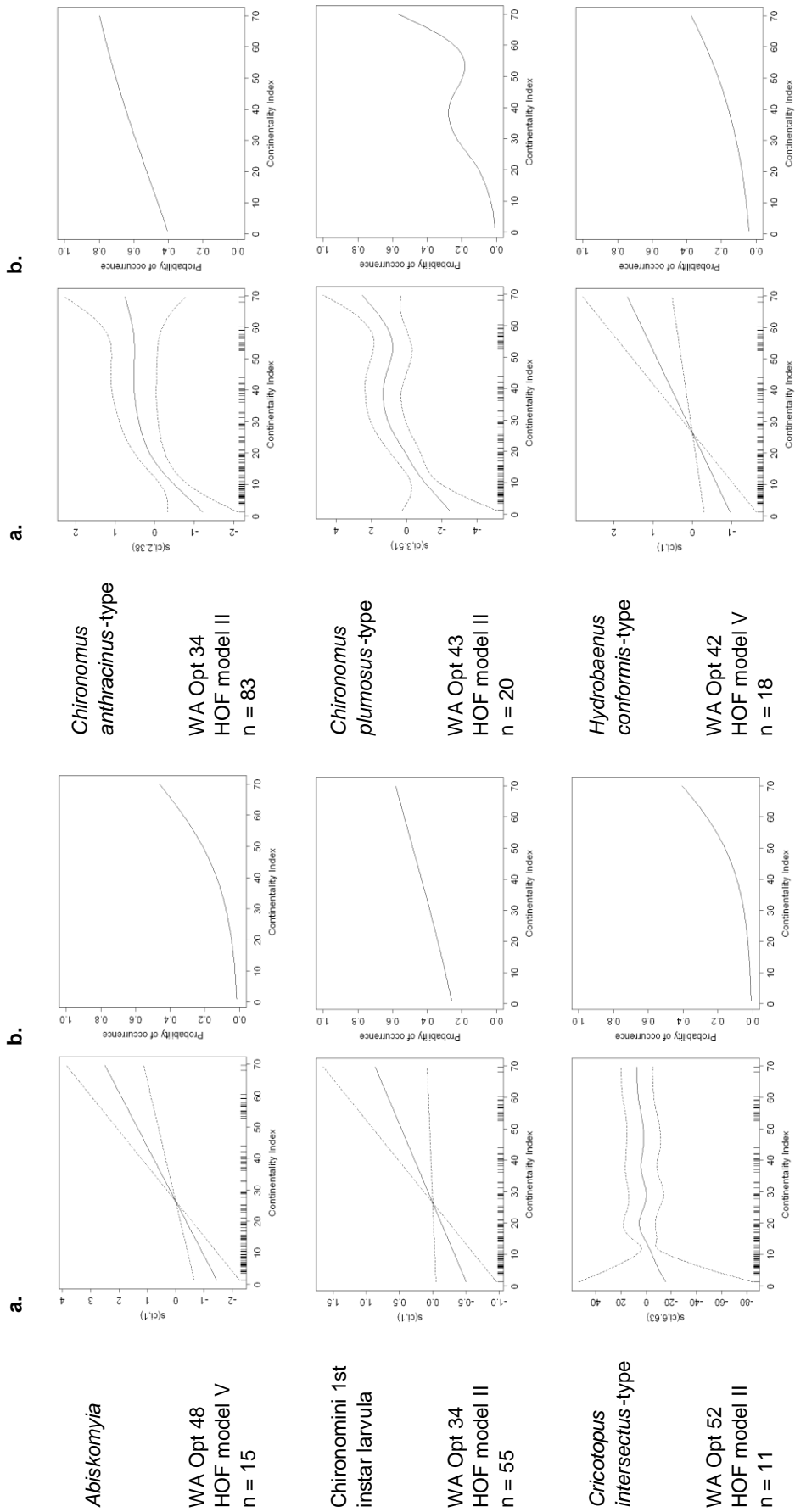


Figure 5.6. Taxon - continentality response curves continued. Species showing a sigmoidal or linear increasing response

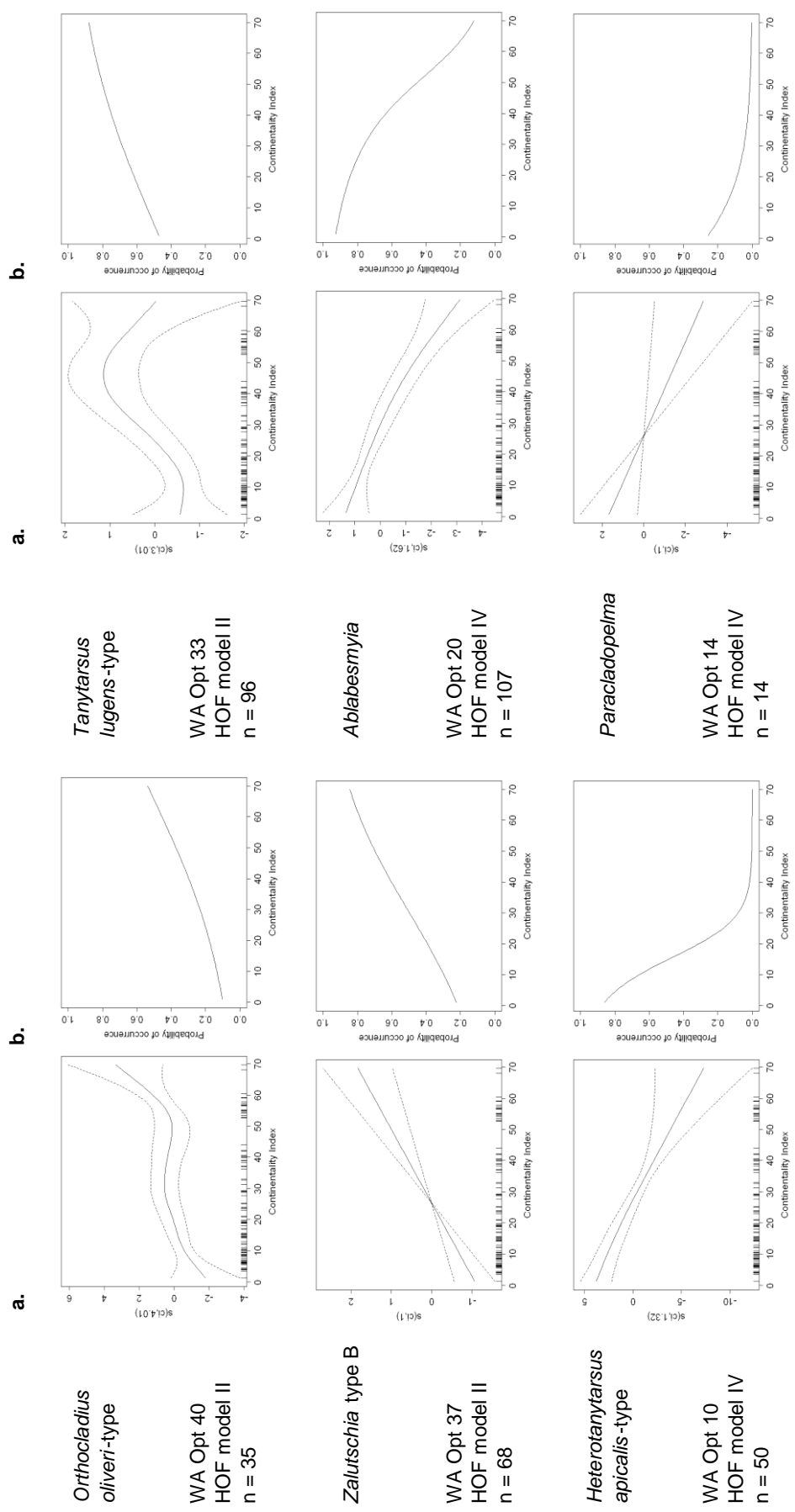


Figure 5.6. Taxon - continentiality response curves continued. Species showing a sigmoidal increasing or decreasing response

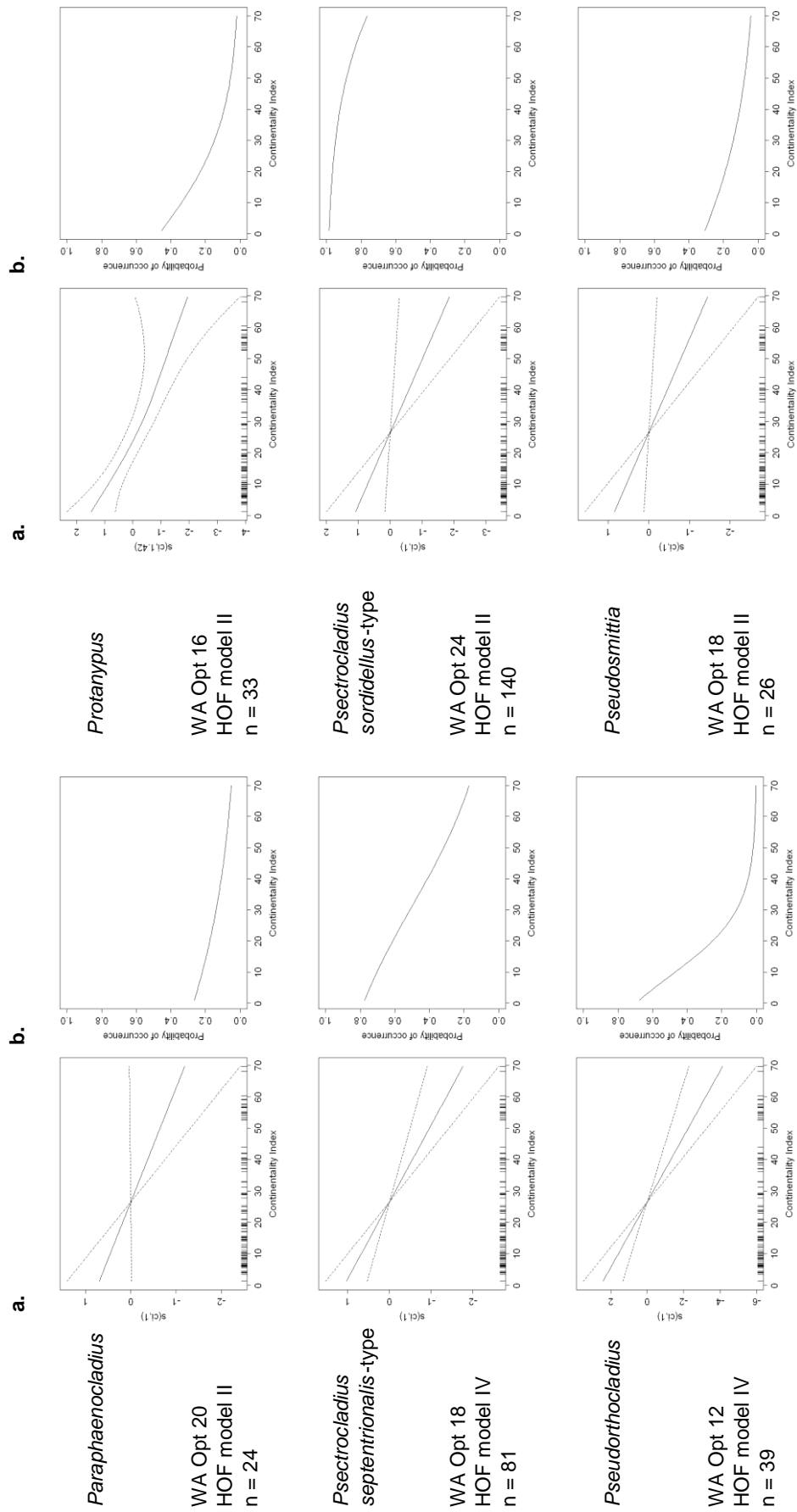


Figure 5.6. Taxon - continuity response curves continued. Species showing a sigmoidal decreasing response

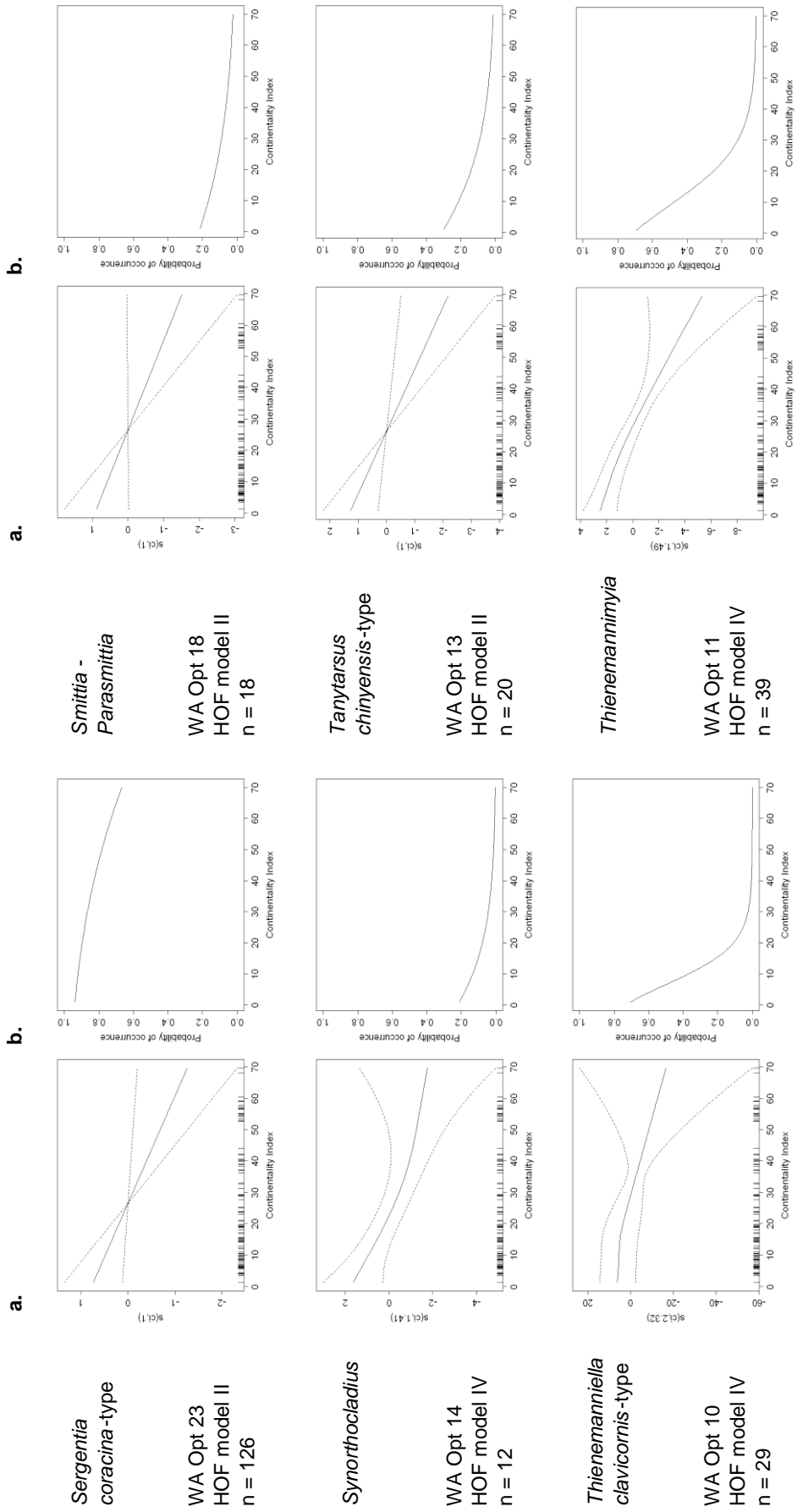


Figure 5.6. Taxon - continuity response curves continued. Species showing a sigmoidal decreasing response

Nine taxa have a statistically significant sigmoidal increasing response to continentality (*Abiskomyia*, *Chironomus anthracinus*-type, *Ch. plumosus*-type, Chironomini 1st instar larvula, *Cricotopus intersectus*-type, *Hydrobaenus conformis*-type, *Orthocladius oliveri*-type, *Tanytarsus lugens*-type and *Zalutschia* type B). *Constempellina* and *Corynocera oliveri*-type show an increase in the probability of occurrence between CI 20 - 40 and 20 - 50 respectively and the occurrence of *Cricotopus laricomalis*-type also increases up to CI of 40. Above these values the high associated uncertainty makes interpretation tentative but the occurrences appear to remain relatively constant (Figure 5.6). *Abiskomyia*, *H. conformis*-type, *T. lugens*-type and *C. oliveri*-type are cold stenothermic species (Brooks et al. 2007). Their increased occurrence in more continental climates (CI above 40) suggests these species are ecologically or behaviourally adapted to completing part of their life cycle within the short continental summers and surviving the long ice-covered winters. *Chironomus* spp. are typically thought to be indicative of warmer waters (Brooks and Birks 2000a; Walker 2001; Brooks et al. 2007), however they are adapted to the low dissolved oxygen concentrations which occur in lakes over extended periods of ice cover. Granados and Toro (2000) found that as temperatures increased the numbers of *Chironomus* spp. decreased due to the reduction in the length of ice covered period. The occurrence of *Chironomus* spp. increases with increased continentality; this could be in response to warmer summer temperatures or longer ice-covered periods.

Sixteen taxa have a statistically significant sigmoidal decreasing response to continentality (Table 5.5). Many species in these genera are terrestrial, semi-terrestrial or associated with the splash or very shallow littoral zone. Most species of *Smittia* and the larvae of many *Paraphaenocladius* species are terrestrial (Cranston et al. 1983). Many *Pseudosmittia* species are terrestrial or semi-terrestrial (Strenzlike 1950) and others occur in the littoral or splash zones (Cranston et al. 1983). *Psectrocladius* species are often associated with floating macrophytes (Brodersen et al. 2001) while *Pseudorthocladius* (Strenzlike 1950; Saether and Sublette 1983), *Synorthocladius* (Cranston et al. 1983), *Thienemanniella clavicornis*-type (Cranston et al. 1983) and *Thienemannimyia*-type (Fittkau and Roback 1983) occur in littoral, splash zones

or streams. Organisms in these environments are more vulnerable to cryogenic damage than those in the profundal zone. Once lake ice has formed the water body and surface sediment remains at 0-4°C until ice melt, the following spring. Although terrestrial habitats and the splash zone have thermal insulation from the snow layer this can melt and refreeze throughout the winter period or be removed by strong winds. Therefore the selective pressure is greater (Danks *et al.* 1994) and the decline in these species in more continental areas may reflect their inability to survive in these environments during the long cold winters rather than failure to complete part of their life cycle within the short summer. *Psectrocladius* spp. (Brodersen *et al.* 2001) and *Pseudosmittia* (Brodin 1986) are also associated with aquatic macrophytes, the more extensive ice-cover of continental zones may affect the distribution of these plants and therefore the occurrence of these taxa. Two taxa, *Procladius* and *Tanytarsus mendax*-type show a decrease in the probability of occurrence from indices of approximately 35 and 25 respectively. These taxa together with *Ablabesmyia* and *Heterotanytarsus* which show decreasing responses over the whole CI range are associated with warm lakes. The decrease in occurrence with increased continentality may reflect an inability to complete part of the life cycle within the summer or to survive the long winters. Two cold stenothermic taxa, *Paracladopelma* (Brundin 1956; Lindegaard 1992) and *Sergentia coracina*-type (Brundin 1956; Brodin 1986) also show a decrease in occurrence with increasing continentality. Cold stenotherms should be adapted to continental environments and therefore may be responding to other environmental factors, such as pH, independent of continentality.

Many of the taxa which have a statistically significant unimodal response to continentality are associated with the shallow littoral or surf zones of lakes. *Cladotanytarsus mancus*-type (Brundin 1949; Saether 1979; Brodin 1986), *Corynoneura*-type A (Brodin 1986; Moller Pillot and Buskens 1990), *Endochironomus albipennis*-type and *E. impar*-type (Pinder and Reiss 1983; Brodin 1986), *Lauterborniella* (Brooks *et al.* 2005), *Parakiefferiella triquetra*-type, *Parakiefferiella* type A (Brooks *et al.* 2007), *Psectrocladius barbatipes*-type (Lindegaard 1992), *Tanytarsus pallidicornis*-type (Brodin 1986) and *Zavrelimyia* (Fittkau and Roback 1983) are littoral and *Eukiefferiella claripennis*-type

(Cranston et al. 1983; Lindegaard 1992) occurs in the surf zone. As previously discussed these environments are susceptible to intense freezing and the CI optima (CI of 40 or lower) suggest these taxa are adapted to the maritime influenced climates of western Eurasia. *Heterotrissocladius marcidus*-type and *Micropsectra pallidula*-type are thermophilic taxa (Brooks et al. 2007) with CI optima of 12 and 13 respectively. As duration of the summer is unlikely to be the limiting factor in the life cycle at these CI, the occurrence of these taxa may reflect the ability of the species to survive the winter. Whereas increasing or decreasing sigmoidal responses reflect an adaptation to or tolerance of variations in the length of the summer or intensity of the winter; the concept of a continentality optimum is more difficult to explain in an ecologically meaningful way. Taxa with unimodal responses may have a competitive advantage under certain climate regimes but are out-competed by better adapted species in more maritime or continental climates. Alternatively the taxa may occur in a restricted biogeographic region for reasons unrelated to the present-day climate such as past dispersal patterns.

Many of the genera which show no statistically significant response to continentality have wide zoogeographical distributions. *Pagastiella*, *Zavrelia* (Pinder and Reiss 1983), *Paracladius* (Cranston et al. 1983) and *Monodiamesa* (Saether 1983) occur throughout the Holarctic, and *Limnophyes* (Cranston et al. 1983) and *Dicrotendipes* (Pinder and Reiss 1983) have worldwide distributions. Therefore the genus may be represented by different species along the continentality gradient. The fruit fly, *Drosophila subobscura*, has genetic variations that vary with latitude across continents (van Heerwaarden and Hoffmann 2006). Therefore even if the species remain unchanged their genotypes and adaptations to climate may vary. In taxa which show no response, the time stress imposed by continentality may lead to greater phenotypic plasticity, such as shortening development or increased growth rates. Taxa such as *Parakiefferiella nigra* (Tuiskunen 1986) and *Corynoneura arctica* (Danks and Oliver 1972a) develop rapidly and emerge soon after the lakes become ice-free, so may be unaffected by increased continentality. A number of the taxa are also found predominantly in the profundal zone, for example *Heterotrissocladius* spp. and *Zalutschia zalutschicola*, which would be

less exposed to the temperature extremes of continental climates. However other taxa, such as *Parachironomus varus*-type and *Polypedilum nubeculosum*-type are littoral (Pinder and Reiss 1983) so response is not solely environment-dependent.

Ordination (sections 4.2.4, 4.2.3 and 4.2.4) and taxon-response modelling techniques indicate that continentality is an important factor influencing the distribution and abundance of chironomids; 54.9% of taxa have a statistically significant response. This suggests it is feasible to develop a continentality inference model for the north-west Palaeartic. Many organisms are showing changes in phenology, in response to spring advance or delayed autumn (Walther *et al.* 2002; Hoye *et al.* 2007) caused by climate change, developing a continentality inference model would allow the amount and rate of seasonal change to be quantified. Present-day climate regimes could, also, be compared to past climates; to answer questions such as was the Younger Dryas more continental than present (as discussed in Chapter 1)? To assess inter-relationship between responses to continentality and July air temperature, and therefore the implications for the development of palaeotemperature inference models, the response of taxa to both T_{july} and continentality is examined in the next section.

5.3.3. Species response to continentality and July air temperature

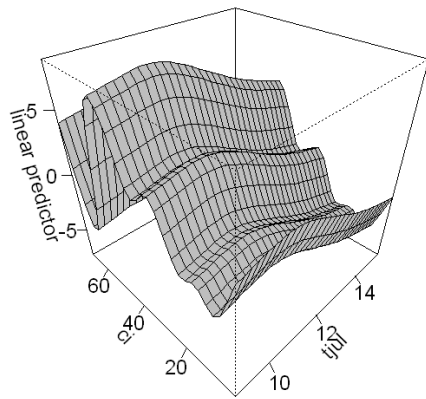
The quantitative relationships of the taxa, in the 149 lake dataset analysed in the previous section, to continentality and T_{july} were modelled by fitting multiple regression models. Details of the dataset are given in section 6.7.2. Linear and quadratic GLM were fitted and the significance of each variable evaluated using a chi-squared test. GAMs were generated for combinations of significant variables and fitted with a 3-dimensional response surface (see methods 3.4.3). Smoother functions are estimated from the data to give the maximum explanatory power; the response surface is expressed as the sum of the smoother functions for each variable. The smoother selected by the programme maximises the correlation coefficient (r^2) and the percentage deviance explained. The scattered distribution and low number of some samples results in a 'noisy' response surface (Figure 5.7). For example the

absence of samples with indices of 24 – 28, 44 – 52 and 61 – 68 frequently results in decreases at these intervals. Therefore to aid interpretation some response surfaces were smoothed using a lower dimensional smoother (k); this decreases the explanatory value of the model. In these instances the smoother is specified.

Figure 5.7. Examples of three-dimensional response surface plots of GAM models showing least-smooth surfaces. X axis is mean July air temperature (tjul), z-axis continentality index (ci) and y-axis is on the scale of the linear predictor.

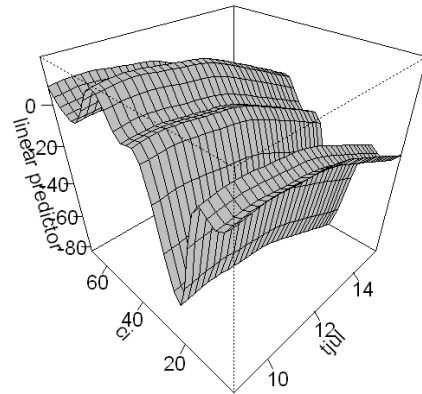
Corynocera ambigua

$R^2 = 0.458$ Deviance explained 44.4%
n = 60



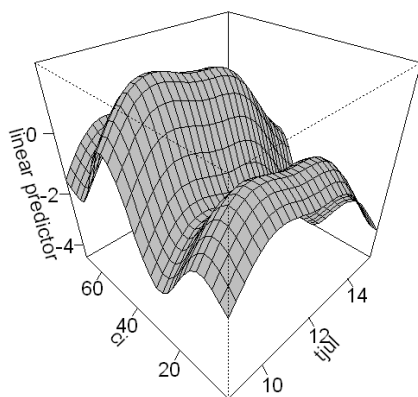
Corynocera oliveri-type

$R^2 = 0.459$ Deviance explained 54%
n = 22



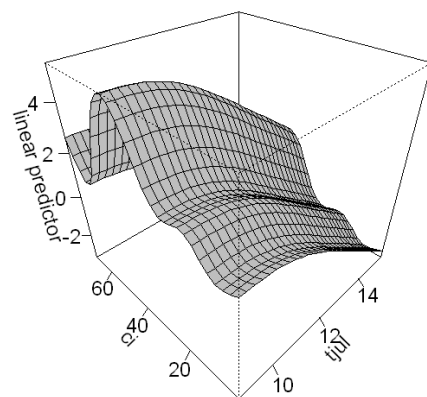
Heterotrissocladius maeeri-type

$R^2 = 0.148$ Deviance explained 18%
n = 55



Tanytarsus lugens-type

$R^2 = 0.371$ Deviance explained 33.1%
n = 96



The CI of the Norwegian samples ranges from 1 – 30 and the Russian samples from CI 31 – 71. Therefore if a taxon has different temperature optima in the two regions there should be a diagonal shift in the temperature optima with increasing CI. To examine the affect of CI on the temperature optima, 3-dimensional response surfaces were plotted for taxa common to both the Norwegian and Russian training sets which show a unimodal response to T_{july} (Figure 5.8). Fewer taxa showed a unimodal response to T_{july} than found in section 5.3.1 due to the shorter temperature gradient.

Figure 5.8. Response surface plots produced by the GAM models for selected taxa common to the Norwegian and Russian training sets which show a unimodal response to July air temperature. X axis (tjul) is mean July air temperature, z-axis (ci) continentality index and y-axis is plotted on the scale of the linear predictor. Plots also show the correlation coefficient (R^2), percentage deviance explained and the WA T_{july} optima for the Norwegian and Russian training sets (section 5.3.1, Figure 6.5).

***Chironomus plumosus*-type**

$R^2 = 0.184$ Deviance explained 25.2%
 Norway WA Opt 13.7°C,
 Russia WA Opt 15.2°C, n = 20

***Cladotanytarsus mancus*-type**

$R^2 = 0.227$ Deviance explained 20.1%
 Norway WA Opt 11.9°C,
 Russia WA Opt 14.0°C, n = 65

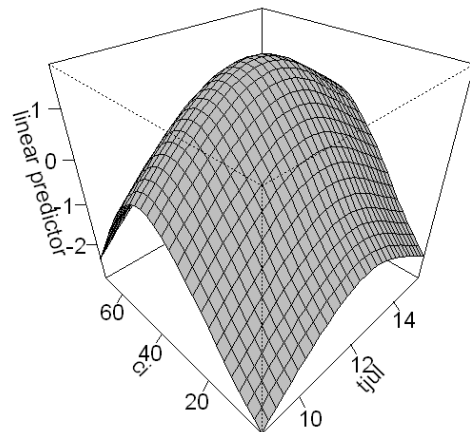
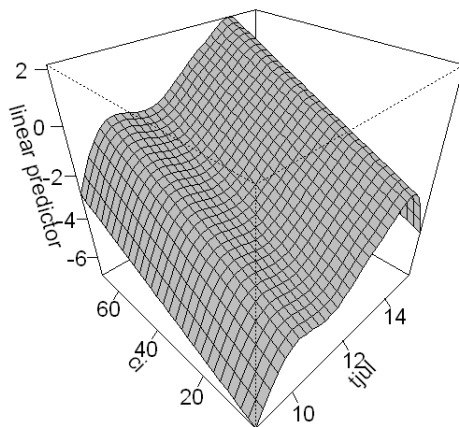


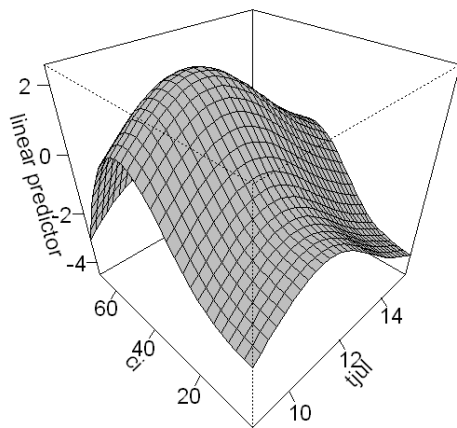
Figure 5.8. Response surface plots produced by the GAM models continued.

***Corynocera ambigua* (k = 4)**

$R^2 = 0.263$ Deviance explained 24.4%

Norway WA Opt 10.0°C,

Russia WA Opt 13.2°C, n = 60

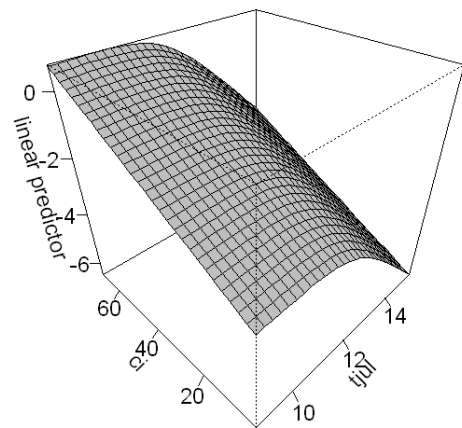


***Corynocera oliveri*-type (k = 9)**

$R^2 = 0.213$ Deviance explained 25.7%

Norway WA Opt 7.7°C,

Russia WA Opt 10.4°C, n = 22

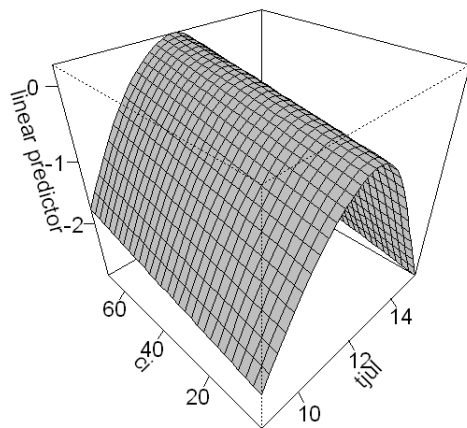


***Cricotopus* type P**

$R^2 = 0.101$ Deviance explained 10.7%

Norway WA Opt 11.0°C,

Russia WA Opt 12.6°C, n = 43



***Dicrotendipes* (k = 3)**

$R^2 = 0.164$ Deviance explained 13.8%

Norway WA Opt 12.4°C,

Russia WA Opt 14.4°C, n = 87

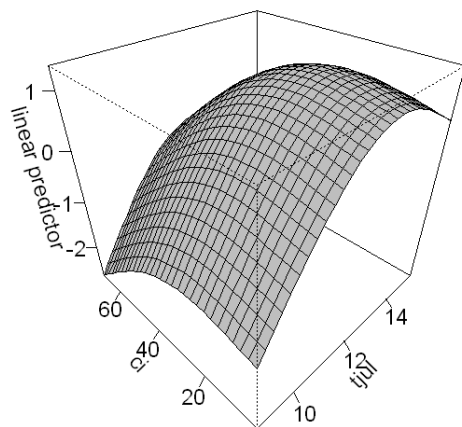


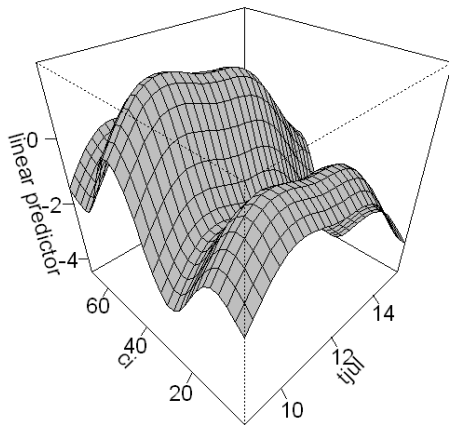
Figure 5.8. Response surface plots produced by the GAM models continued.

***Heterotrissocladius maeaeri*-type**

$R^2 = 0.148$ Deviance explained 18%

Norway WA Opt 9.7°C,

Russia WA Opt 12.4°C, n = 55

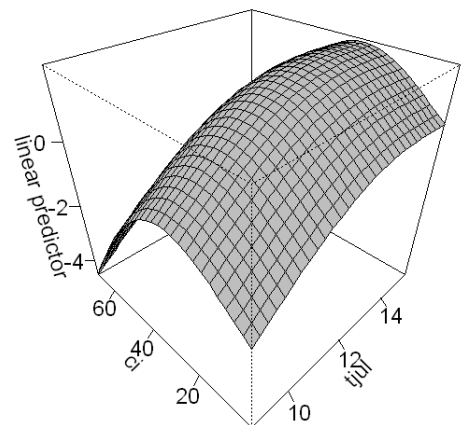


***Microtendipes pedellus*-type (k = 2)**

$R^2 = 0.279$ Deviance explained 23.6%

Norway WA Opt 12.2°C,

Russia WA Opt 14.0°C, n = 86

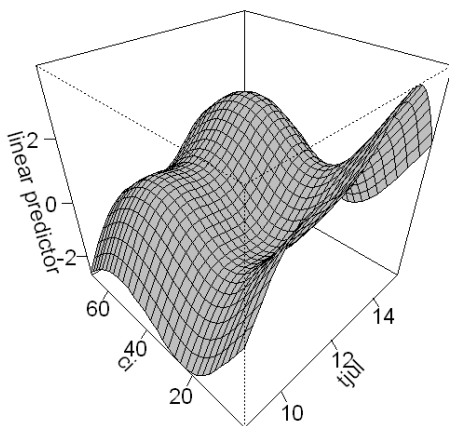


***Micropsectra insignilobus*-type (k = 5)**

$R^2 = 0.218$ Deviance explained 19.1%

Norway WA Opt 10.2°C,

Russia WA Opt 12.4°C, n = 89



***Phaenopsectra flavipes*-type**

$R^2 = 0.194$ Deviance explained 25.6%

Norway WA Opt 13.9°C,

Russia WA Opt 13.5°C, n = 27

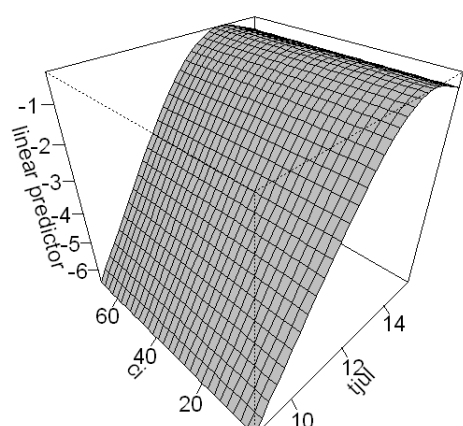


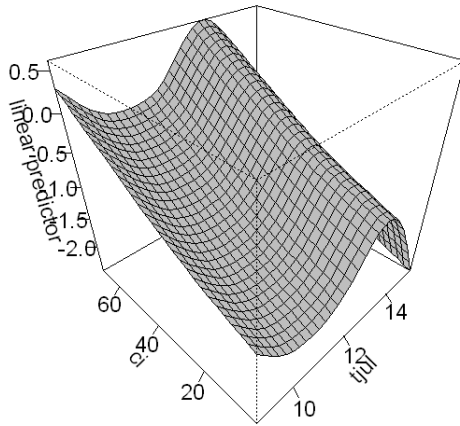
Figure 5.8. Response surface plots produced by the GAM models continued.

***Stictochironomus rosenschoeldi*-type**

$R^2 = 0.063$ Deviance explained 7.76%

Norway WA Opt 11.4°C,

Russia WA Opt 11.9°C, n = 27

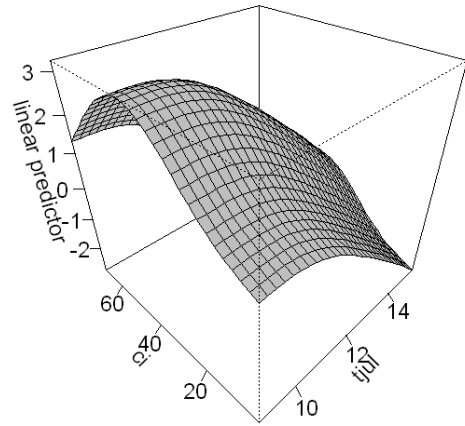


***Tanytarsus lugens*-type (k = 5)**

$R^2 = 0.327$ Deviance explained 27%

Norway WA Opt 9.8°C,

Russia WA Opt 12.2°C, n = 96

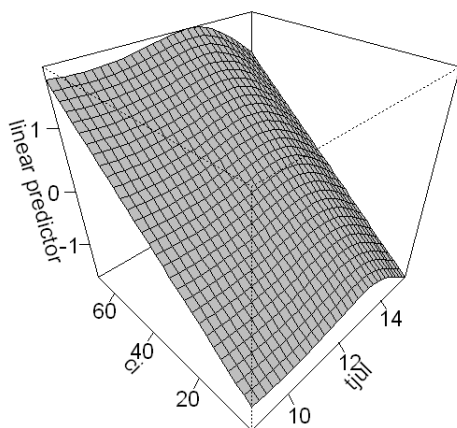


***Zalutschia* type B**

$R^2 = 0.130$ Deviance explained 11.3%

Norway WA Opt 11.4°C,

Russia WA Opt 11.6°C, n = 68

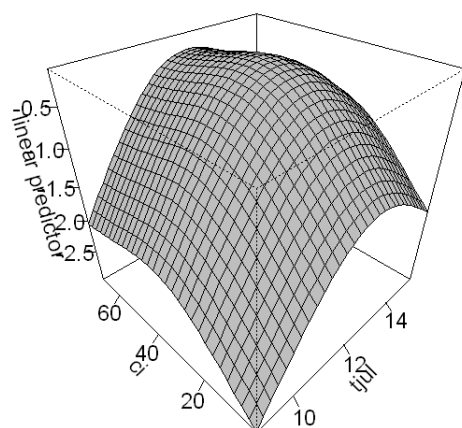


***Zalutschia zalutschicola* (k = 5)**

$R^2 = 0.074$ Deviance explained 8.3%

Norway WA Opt 11.5°C,

Russia WA Opt 12.9°C, n = 96



The taxon response curves to T_{july} are, generally, broader than the GLM/GAM responses (Figures 5.3 and 5.4) which suggest the smoothing functions may

have reduced the sensitivity of the model. However the temperature ranges are similar to the WA tolerances (Figure 6.5) and indicates the models are reliable. In all 14 taxa, the T_{july} optima remain the same even though the species abundance changes with increasing CI. For example, the WA optima for *Corynocera ambigua* was calculated as 10.0°C from the Norwegian data and 13.2°C from the Russian data but the model shows a single temperature optimum of approximately 12°C. The differences in WA optima, therefore, reflect the distribution of the samples within each dataset rather than changes in the optima of the population. To ensure an accurate optimum is obtained, the training set requires an even distribution of lakes along both the CI and T_{july} gradients otherwise, in a combined training set, higher abundances at suboptimal temperatures would result in incorrect optima. The distribution of *H. maeaeri*-type and *M. insignilobus*-type shows a bimodal response along the x-axis, with two relatively close T_{july} optima. This may reflect an absence of intermediate samples or the presence of more than one species within the morphotype. This bimodality is more pronounced in the GAM model produced by *Cricotopus cylindraceus*-type (Figure 5.9) where the sharp decline between the two optima suggests the presence of two distinct species. Inclusion of additional intermediate samples would be necessary to determine whether more than one species was present.

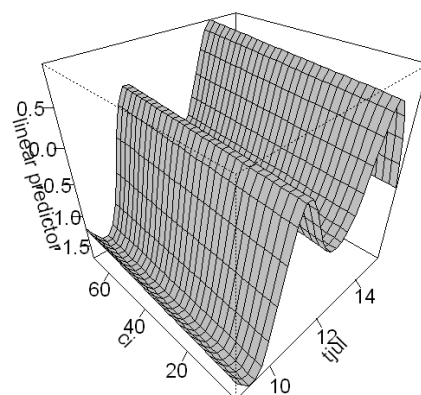
Figure 5.9. Response surface plots produced by the GAM models for *Cricotopus cylindraceus*-type showing bimodality along x-axis. X axis (tjul) is mean July air temperature, z-axis (ci) continentality index and y-axis is plotted on the scale of the linear predictor.

***Cricotopus cylindraceus*-type**

$R^2 = 0.0894$ Deviance explained 10.2%

Norway WA Opt 12.7°C,

Russia WA Opt 14.9°C, n = 62



5.4. Implications for the development of palaeoclimatic inference models

- Ordination and ecological modelling techniques show that July air temperature and continentality are important variables in determining the distribution of chironomids.
- July air temperature is the most important variable since over 90% of taxa showing a statistically significant response to it. The chironomid distribution data are, therefore, suitable for the development of a palaeotemperature inference model.
- WA and GLM/GAM response curves indicate that T_{july} optima for individual taxa are generally higher in Russia than Norway.
- In many taxa, the probability of occurrence also increases or decreases along the continentality gradient. Therefore to prevent temperature optima being derived from higher abundances at suboptimal temperatures the training set for the inference model must either:
 1. be limited to a narrow continentality range and not be applied to other geographical regions, *or*
 2. have an even and continuous distribution along both environmental gradients.
- Although fewer taxa have a statistically significant response to continentality (54%), many common taxa show a marked response and it should be feasible to develop a chironomid – continentality inference model.
- Analysis of pupal exuviae from the Putorana showed the genera *Procladius* and *Cricotopus/Orthocladius* include a number of different species which may or may not have similar environmental optima.
- Modelling taxon responses suggests that some morphotypes, such as *Cricotopus* type P, are represented by a single species with a single optimum. However, *Micropsectra radialis*-type and *Cricotopus cylindraceus*-type may be composites of two taxa with different optima.
- The occurrence of *Procladius* reaches a plateau and remains unaltered over a long temperature gradient. Therefore the species present may

either have wide environmental tolerances or are successively replaced by species with different optima.

- Many of these taxa from these speciose genera, such as *Procladius* and *Cricotopus/Orthocladius* where the taxonomy is poorly resolved at present, are rare in the training sets. Therefore inclusion of additional samples is necessary to determine whether the modelling or taxonomy needs refining. Their rarity also means they are unlikely to unduly affect palaeoenvironmental reconstructions in which rare species are downweighted.

Chapter 6

Development of the inference models

6.1. Introduction

The previous two chapters have demonstrated that July air temperature is a key environmental variable accounting for a significant proportion of the biological variance within the Russian training set and can, therefore, be considered suitable for the creation of a chironomid inferred-temperature (CI-T) model. This chapter describes the development of the inference models and evaluates their performance prior to application to down-core sequences in Chapters 7 and 8. The previous two chapters also indicated that continentality exerted a strong influence on chironomid distribution. The final section of this chapter explores the relationship between continentality and the ice-free period and describes the development of an exploratory chironomid inferred-continentality model.

Two models were developed from the Russian training sets. The first, CI-T model A (section 6.2.1), is based on the lakes detailed in Table 4.1 and analysed in the previous chapters. The temperature optima of the species were consistently higher than those derived from the Norwegian datasets; the reasons for these discrepancies are discussed in Chapter 5. Therefore a second Russian inference model, CI-T model K (section 6.2.2), was generated including lakes from the Komi Republic (prefixed K-). Inclusion of these lakes provided a more continuous July temperature gradient, however water chemistry data was unavailable to allow these lakes to be included in analysis of the factors influencing modern distribution (Chapter 4). Due to the economic and logistic constraints of working in remote areas of northern Russia, the Russian training set (100 lakes) had fewer lakes than the Norwegian training set (157 lakes). Combining the training sets would improve the representation of lake assemblages and individual taxon along the environmental gradients. But, as discussed in Chapter 1, use of a regional training set may be more appropriate if the species composition of morphotypes or the response of individual taxon to climate variables varies between the geographical regions.

Two combined Norwegian-Russian models were generated; model CI-T model C (section 6.4.1) excludes only outliers with extremely high environmental variables or restricted faunas. In CI-T model R (section 6.4.2) lakes were selected for inclusion to give an even distribution of lakes along both the continentality (CI) and July air temperature (T_{july}) gradients. The performance of the Russian and combined Norwegian-Russian inference models were compared to the performance of a Norwegian inference model (CI-T model N, developed in section 6.3 from the existing Brooks and Birks 2001 and unpublished data). Derived taxon-specific temperature optima, coefficients of determination (R^2), maximum bias and root-mean-square-errors of prediction (RMSEP) for the models were compared to determine whether a specific, Russian, regional model or a more generalised northern Eurasia model would give statistically the 'best' model. The models are then further evaluated in Chapter 7 by comparing reconstructed July air temperatures derived from all five models with instrumental data before final selection of the model which appeared most accurate, and therefore most appropriate, for T_{july} reconstructions in northern Russia.

6.2. Russian CI-T models

To generate a robust inference model the apparent and cross-validated predictive powers (RMSE/RMSEP ratio) must be similar. To achieve this the number of taxa should equal the number of lakes (Racca *et al.* 2003). The Russian training sets, for example, have more taxa than lakes, therefore the ratio of taxa:lakes was minimised in two ways. Firstly, only taxa with more than three occurrences were included in the inference models; fewer than 3 occurrences are insufficient to calculate accurate temperature optima for species showing a unimodal response. This criterion has been applied to existing inference models from Switzerland (Bigler *et al.* 2006) and Finland (Luoto 2008). Secondly, lakes identified as outliers due to their extreme environmental or physical variables were removed from the model. The lakes deleted are detailed in the appropriate sections.

6.2.1. CI-T model A

The original Russian training set (Table 4.1) has 119 taxa from 94 lakes; 6 lakes were identified as outliers due to their extreme environmental conditions (Table 6.1). Y1733 and Y1725 were identified as hypereutrophic and eutrophic respectively by Kumke *et al.* (2007). Fewer than 50 head capsules (total = 43) were isolated from Y1725, which is below the minimum count recommended for fossil chironomid analysis (Heiri and Lotter 2001; Larocque 2001). After exclusion of taxa with fewer than 3 occurrences the CI-T model A was developed based on 89 taxa from the remaining 88 lakes.

Table 6.1. Lakes identified as outliers in the CI-T model A. Values for the environmental variables are detailed in Table 4.1.

Lake	Reason for exclusion
Y1741	high conductivity
Y1740	high conductivity
Y1703	high pH
Y1718	high pH
Y1733	high conductivity – hypereutrophic
Y1725	eutrophic – low abundance

Models were generated by Weighted Averaging (WA or WA-TOL with classical and inverse deshrinking) and Weighted Averaging Partial Least Squares (WA-PLS) regression – training methods using C2 (Juggins 2005) as described in section 3.4.5. Additional models were generated using Modern Analogue (MAT) and MAT weighted by similarity (WMAT) techniques as described in section . The performance of the models were evaluated by comparing the coefficient of determination (R^2_{jack}), maximum bias and the errors associated with the model (root-mean-square-error of prediction - RMSEP) assessed by leave-one-out (jack-knifed) cross-validation (Table 6.2).

Table 6.2. Performance of the CI-T model A applied to the 88 sample chironomid-July air temperature dataset. All statistics are based on leave-one-out cross validation. Minimal adequate WA-PLS model highlighted in yellow.

Model	Component	r^2_{jack}	RMSEP _{jack}	Mean bias _{jack}	Max bias _{jack}	Reduction in prediction error (%)
MAT	4 closest analogues	0.95	0.82	0.15	2.74	...
WMAT	4 closest analogues	0.95	0.82	0.16	2.74	...
WA (inv)	...	0.86	1.29	-0.02	2.44	...
WA (cla)	...	0.86	1.33	-0.02	2.60	...
WA - TOL (inv)	...	0.81	1.54	-0.27	2.99	...
WA - TOL (cla)	...	0.81	1.62	-0.30	3.17	...
WA - PLS	1	0.86	1.29	-0.06	2.41	...
	2	0.91	1.04	-0.04	1.21	19.53
	3	0.90	1.09	-0.05	1.34	-5.47
	4	0.90	1.11	-0.05	1.10	-1.69
	5	0.89	1.16	-0.05	0.97	-4.07

The selection of the minimal adequate WA-PLS model was based on the combination of low RMSEP, low maximum bias (ter Braak and Juggins 1993) and high coefficient of determination (r^2) with the smallest number of ‘useful’ partial-least-squares components (Birks 1995). To be considered useful, inclusion of an additional component should give a reduction in the prediction error of 5% or more in the RMSEP (Birks 1998). Based on these criteria the 2-component WA-PLS model was selected as the minimal adequate model.

Plots of the predicted values against observed values (Figure 6.1a) and of residuals (predicted – observed) (Figure 6.1b) suggests the WA-PLS inference model is able to predict July temperatures reasonably well over the temperature range 9 – 19 °C. However the performance of model declines considerably between 14 – 18 °C due to the absence of samples.

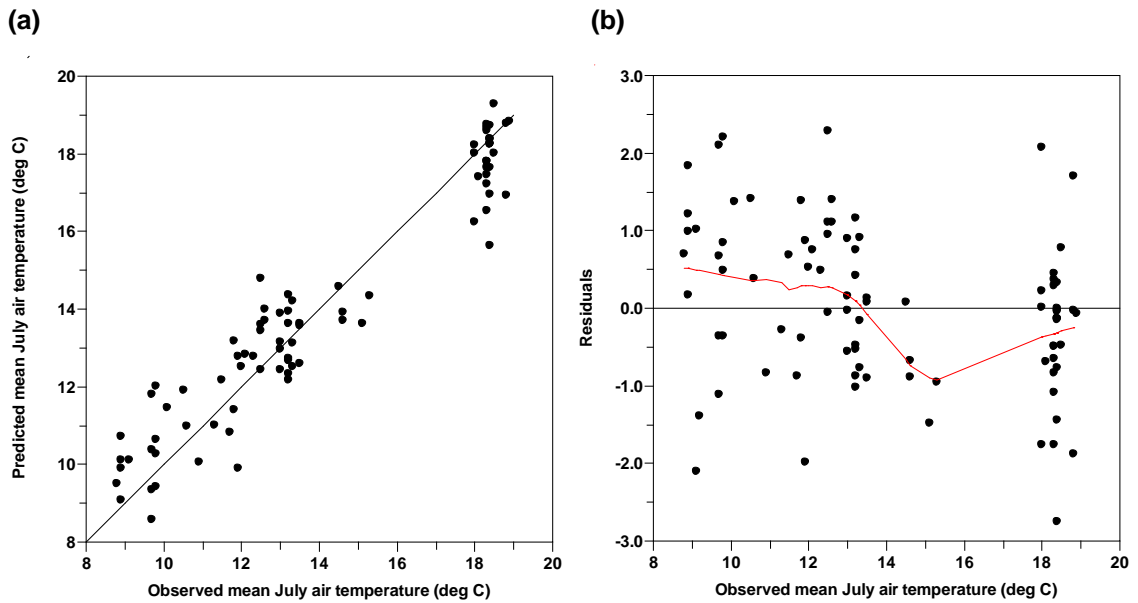


Figure 6.1. Relationship between (a) observed and predicted mean July air temperatures using a weighted averaging partial least squares (WA-PLS) 2 component CI-T model A. Solid line represents 1:1 relationship; (b) Residuals (predicted – observed) along the July air temperature gradient for the 2-component WA-PLS CI-T model A. The solid line is a LOESS scatterplot smoother (span = 0.45).

Comparison of the temperature optima of the 42 taxa with 10 or more occurrences in the training sets show the optima derived from the Russia CI-T model A are, generally, up to 7 °C higher than the optima from the Norwegian data (Figure 6.2). The exceptions are *Zalutschia* type B, *Parakiefferiella triquetra*-type, *Corynoneura arctica*-type, *Psectrocladius barbatipes*-type and *Phaeonopsectra flavipes*-type where the optima are similar between datasets. The discrepancies are particularly marked at the lower end of the temperature gradient (*Hydrobeanus conformis*-type and *Corynocera oliveri*-type). WA-based models overestimate optima at the low end of the environmental gradient (ter Braak and Juggins 1993); therefore the warmer temperature range of the Russian dataset (8 – 19 °C) compared to Norwegian lakes (3 – 16 °C) may result in overestimation of optima for cold stenothermic species. Therefore temperature optima were generated for the Norwegian dataset with the cold Svalbard lakes excluded to give a range of 6 – 16 °C. Although this increased the optima (Figure 6.2, open blue circles) the Norwegian values were still lower than the Russian optima. The optima of *Micropsectra radialis*-type differs from 6.5 °C in Norway to 12.9°C in CI-T model A. Modelling of the species-

temperature response (section 5.3.1) suggest this morphotype may be represented by two species.

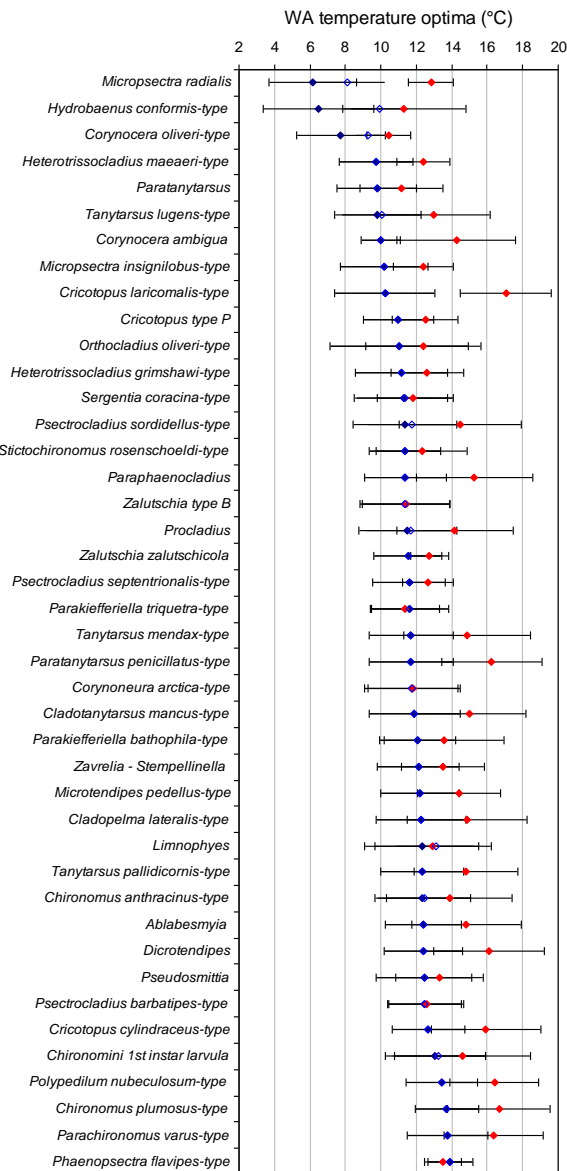


Figure 6.2. Comparison of the temperature optima of common taxa derived from the Norwegian CI-T model N (solid blue circle) and CI-T model A (solid red circle) training sets. Species selected have 10 or more occurrences in all datasets, optima calculated by weighted-averaging regression and training. Unfilled blue circles represent temperature optima derived from Norwegian dataset minus the Svalbard samples (mean July air temperatures 3-6 °C). Bars indicate species tolerances. Taxa are listed in order of increasing temperature optima derived from the Norwegian dataset.

Modelling taxon responses to temperature and continentality (CI) (Chapter 5) showed that species abundances vary along both environmental gradients. The taxon abundance at the temperature optima and low CI may be lower than the abundances at suboptimal temperatures and high CI resulting in the derivation of inaccurate optima. Therefore the discrepancies in optima may result from the bias towards high temperatures and high continentality in the Russian training set from inclusion of the Yakutia samples (29 Yakutian lakes from a total of 88 lakes). The lakes are also unevenly distributed along the temperature gradient

and the performance of the model declines between 14 – 18 °C due to absence of lakes. Therefore a second Russian training set (section 6.2.2) was compiled to rectify these shortcomings.

6.2.2. CI-T model K

Six lakes from the Komi Republic were included in the Russian training set to give a more continuous distribution along the July temperature gradient. In addition 19 lakes from Yakutia (Table 6.3) were excluded which provided a more even distribution along the temperature gradient (Figure 6.3). Lakes for exclusion were identified from their extreme environmental variables (Table 4.1); 8 lakes with conductivity greater than 367 $\mu\text{S}/\text{cm}$ (the maximum value in the Norwegian dataset), 3 identified as eutrophic (Kumke *et al.* 2007), 3 with pH greater than 9.5 and 2 with water depth less than 0.9m. Preliminary analysis of CI-T model K identified an additional 3 Yakutian lakes as outliers and these were also excluded from the final model. Their residual values (predicted – observed) were higher than the remaining Yakutian lakes ($\pm 0.06^\circ\text{C}$) and their removal improved the RMSEP from 1.14°C to 1.07°C . Kumke *et al.* (2007) classified the Yakutian lakes using cluster analysis of their vegetation, physico-chemical and geological characteristics. This reduced dataset contained a single representative from each tightly clustered pair of lakes with similar physical characteristics with the exception of paired lakes Y1709 - Y1713. Therefore Y1713 was also excluded as its residual value (predicted – observed) in the 2-component WA-PLS model was higher (-0.03°C) than that of Y1709 (-0.01°C). After exclusion of taxa with fewer than 3 occurrences the CI-T model K was developed based on 89 taxa from 81 lakes.

Table 6.3. Lakes identified as outliers in the CI-T model K. Values for the environmental variables are detailed in Table 4.1.

Lakes	Reason for exclusion
Y7111 Y1717 Y1727 Y1731 Y1733 Y1735 Y1740 Y1741	High conductivity
Y1703 Y1707	High pH
Y1700 Y1722 Y1725	Eutrophic
Y1718 Y1746	Shallow water depth
Y1716 Y1719 Y1737	Identified as outliers in preliminary runs of CI-T model K

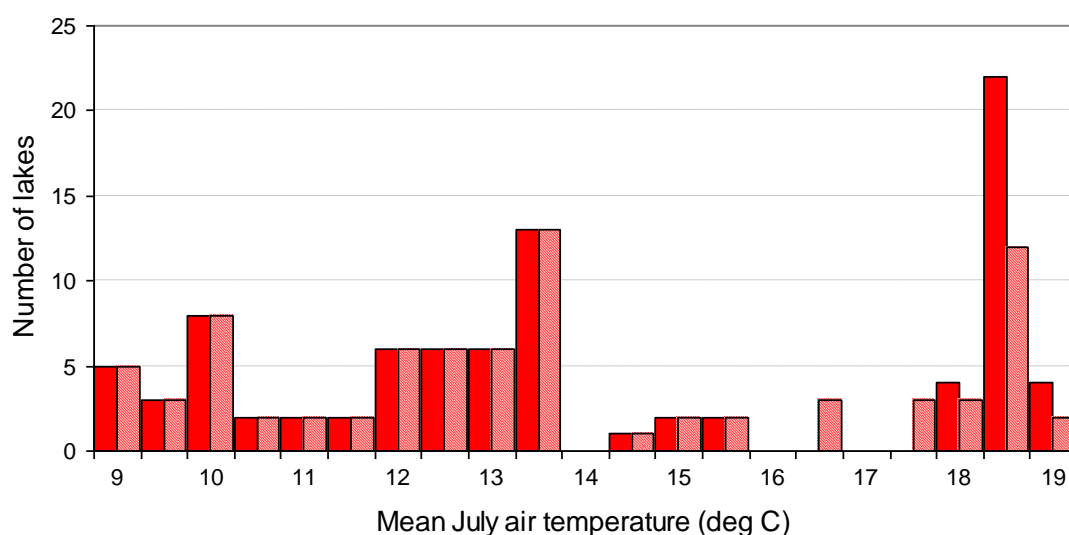


Figure 6.3. Frequency histogram showing the distribution of lakes along mean July air temperature gradient. (Solid red training set from section 6.2.1 used to generate CI-T model A, hatched red training set from this section used to generate CI-T model K).

Models were generated using WA, WA-TOL, WA-PLS, MAT and WMAT techniques; the performance of the models is summarised in Table 6.4. The 2-component WA-PLS model was selected as the minimal adequate model based on the combination of low RMSEP, low maximum bias and high coefficient of determination (r^2). Plots of the predicted values against observed values (Figure 6.4a) and of residuals (predicted – observed) (Figure 6.4b) suggests the inference model performs better than CI-T model A over the temperature range 13 – 18 °C (Figure 6.1). The model over-predicts temperatures below 13 °C and under-predicts above 13 °C, with a maximum bias of ± 1.28 °C.

Table 6.4. The performance of the CI-T inference model K applied to the 81 sample chironomid-July air temperature dataset. All statistics are based on leave-one-out cross validation. Minimal adequate WA-PLS model highlighted in yellow.

Model	Component	r_{jack}^2	RMSEP _{jack}	Mean bias _{jack}	Max bias _{jack}	Reduction in prediction error (%)
MAT	6 closest analogues	0.92	0.92	0.25	1.94	...
WMAT	6 closest analogues	0.92	0.92	0.25	1.95	...
WA (inv)	...	0.86	1.19	-0.02	2.02	...
WA (cla)	...	0.86	1.21	-0.02	2.06	...
WA - TOL (inv)	...	0.80	1.47	-0.16	2.56	...
WA - TOL (cla)	...	0.80	1.60	-0.19	2.68	...
WA - PLS	1	0.86	1.19	-0.05	2.05	...
	2	0.92	0.89	-0.02	1.28	24.73
	3	0.93	0.86	-0.02	0.82	3.31
	4	0.93	0.87	-0.02	0.74	-1.20
	5	0.92	0.90	-0.03	0.78	-3.06

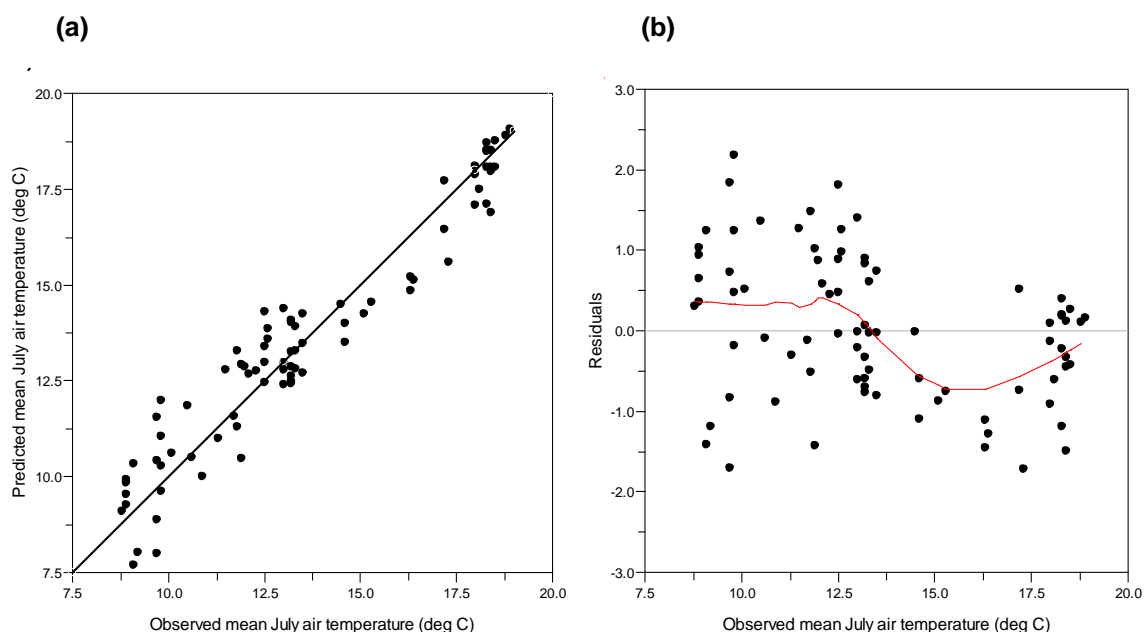


Figure 6.4. Relationship between (a) observed and predicted mean July air temperatures using a weighted averaging partial least squares (WA-PLS) 2 component CI-T model K. Solid line represents 1:1 relationship; (b) Residuals (predicted – observed) along the July air temperature gradient for the 2-component WA-PLS CI-T model K. The solid line is a LOESS scatterplot smoother (span = 0.45).

Comparison of the temperature optima of the 42 common taxa show the optima derived from the Russia CI-T model K are, generally, lower than those from CI-T model A. This trend is particularly marked for species with optima above 13.5 °C; 2 taxa, *Parakiefferiella bathophila*-type and *Ablabesmyia*, have identical optima in the two models whilst the remaining 18 taxa have temperature optima up to 1.0 °C lower in model K with the more even distribution of samples along the T_{july} gradient (Figure 6.5a). The temperature optima of 76% of the taxa, from CI-T model K, lie within 2.5°C of the optima from the Norwegian training set (analysed in section 6.3) minus the Svalbard samples (Figure 6.5b) and the optima of 86% of taxa lie within the tolerance range of the Russian CI-T model A dataset. The widest discrepancies occur with *Micropsectra radialis*-type (with a difference of 4.7 °C) and *Cricotopus laricomalis*-type (with difference of 6.3 °C). Modelling of the *Micropsectra radialis*-type - temperature response (section 5.3.1) suggests this morphotype may be represented by two species. Reasons for the discrepancy between *C. laricomalis*-type optima are unclear; they may represent 'real' differences due to differences in morphotype composition, problems with taxonomic resolution or regional differences in morpho-, pheno- or genotypic response. However, these taxa are absent from or form a minor component of the down-core samples and so are unlikely to have a strong influence on palaeoclimatic reconstructions (Chapters 7 and 8). In general the temperature optima derived from model K are closer to the optima derived from the Norwegian training set than model A (Figure 6.2). The remaining discrepancies may reflect the inherent bias within the two training sets, Norway for low CI and low temperatures and Russia for higher CI and temperatures. Combined Norwegian-Russian training sets were compiled (section 6.4) using the full temperature gradient and a gradient constrained by CI to examine the effects of these co-variables on palaeoenvironmental reconstructions.

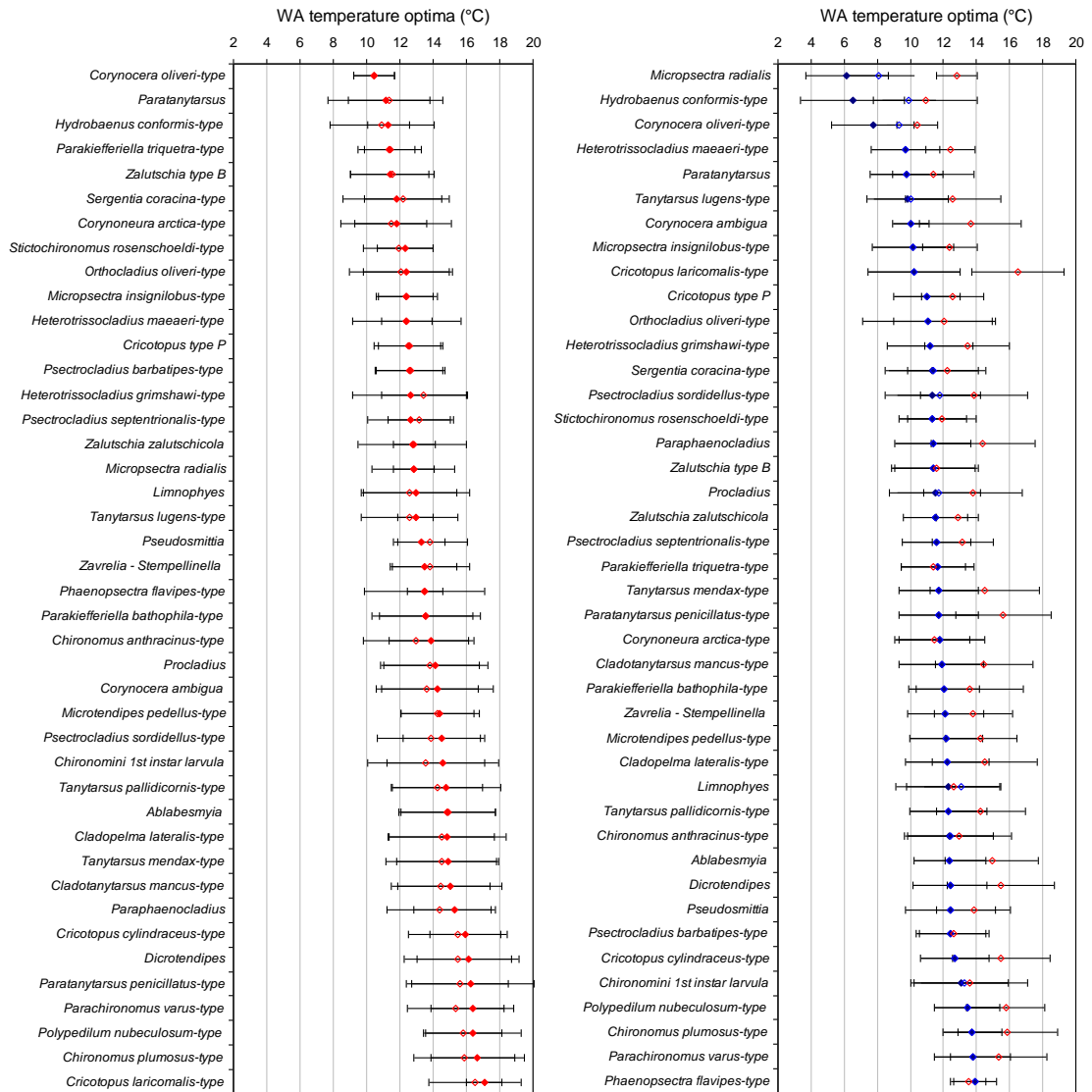
(a)**(b)**

Figure 6.5. Comparison of the temperature optima of common taxa derived from (a) the Russian CI-T model A (solid red circle) and CI-T model K (unfilled red circle) training sets and (b) the Norwegian CI-T model N (solid blue circle) and Russian CI-T model K (unfilled red circle). Species selected have 10 or more occurrences in all datasets, optima calculated by weighted-averaging regression and training. Unfilled blue circles represent temperature optima derived from Norwegian dataset (analysed in section 6.3) minus the Svalbard samples (mean July air temperatures 3 – 6 °C). Bars indicate temperature tolerances. Taxa are listed in order of increasing temperature optima derived from CI-T model A in (a) and the Norwegian dataset CI-T model N in (b).

6.3. Norwegian CI-T model (model N)

Surface sediments for the unpublished ‘Brooks-Birks’ Norwegian inference model were collected from mainland Norway and Svalbard between 1995 and 1999. In general, the lakes were selected on the following criteria: lake-area not more than 50 ha; simple shape and morphometry; water depth at least 4 m; minimal catchment disturbance with no arable farming or permanent residences; and acid bedrock geology with no limestone or other basic rock types (Brooks and Birks 2000a). Although, at high altitudes (above 1200 m) and on Svalbard some lakes shallower than 4 m had to be included because small deep lakes containing sediments are scarce in these areas. In total over 500 lakes were examined and surface sediments from 157 lakes were selected for chironomid analysis to maximise the temperature gradient whilst minimising variability within the other environmental variables (Birks, pers comm. 2007). The unpublished ‘Brooks-Birks’ inference model has been used to quantitatively reconstruct past climate change from sediment sequences in northern Eurasia with the inclusion of local material in Arctic Russia (for example Brooks and Birks 2000a, b; Solovieva *et al.* 2005). Therefore this inference model was included to compare the reconstructions and model performance with the Russian CI-T models A and K, and the combined Norwegian – Russian CI-T models C and R developed in this study.

Table 6.5. Lakes identified as outliers in the CI-T model N.

Lakes	Reason for exclusion
Lake Birgervatnet - Bir N98-1 99-23 N	Single taxon Fed by glacier meltwater / extensive snow-beds Identified as outlier in initial CI-T model N

The Norwegian training set (Table 4.8) has 142 taxa in 157 lakes; initial runs of the inference model with all 157 lakes identified 4 lakes as outliers (Table 6.5). Although there were biological or environmental justifications for the exclusion of Lake Birgervatnet, N98-1 and 99-23, possible reasons for the high residue value (4.5 °C) for lake N were not apparent from the known environmental data,

but as the residue was approximately 2°C warmer than the residues from all the other samples this lake was deleted from the training set. These 4 lakes were also deleted from the training set used for the ‘Brooks-Birks’ model (Brooks 2006b). Models were generated, based on 141 taxa from 153 lakes, in C2 using MAT, WMAT, WA, WA-TOL and WA-PLS techniques. Brooks (2006b) selected a 3-component WA-PLS model as the minimal adequate model based on the combination of low RMSEP (1.01 °C), low maximum bias (0.93 °C) and high coefficient of determination ($r^2 = 0.91$). These models were generated using CALIBRATE (Juggins and ter Braak 1994). In this analysis (Table 6.6) the 3-component WA-PLS model remained the best minimal adequate model although the performance was slightly poorer. The taxonomy of a number of species including *Cricotopus/Orthocladius* spp. have been revised in this study and this may account for the change in performance. The temperature optima of the 42 most common species derived from this model (CI-T model N) are shown in comparison with the optima from CI-T model A in Figure 6.2 and from CI-T model K in Figure 6.5.

Table 6.6. The performance of the CI-T inference model N applied to the 153 sample chironomid-July air temperature dataset. All statistics are based on leave-one-out cross validation. Minimal adequate WA-PLS model highlighted in yellow.

Model	Component	r^2_{jack}	RMSEP _{jack}	Mean bias _{jack}	Max bias _{jack}	Reduction in prediction error (%)
MAT	7 closest analogues	0.89	1.18	0.35	1.47	...
WMAT	7 closest analogues	0.89	1.18	0.35	1.47	...
WA (inv)		0.80	1.52	-0.01	2.29	...
WA (cla)		0.80	1.65	-0.01	2.62	...
WA - TOL (inv)	...	0.83	1.39	-0.02	1.81	...
WA - TOL (cla)	...	0.84	1.44	-0.02	1.39	...
WA - PLS	1	0.80	1.56	0.05	2.03	...
	2	0.89	1.14	-0.01	1.16	26.88
	3	0.90	1.10	0.03	1.05	3.95
	4	0.89	1.15	0.02	1.01	-4.95
	5	0.87	1.22	0.02	1.06	-6.00

6.4. Combined Norwegian – Russian CI-T models

Two inference models were developed from the combined Norwegian and Russian training sets. The first (CI-T model C) is based on a 232 lake training set which includes the majority of lakes from Norway and Russia selected to

minimise variation in environmental variables other than T_{july} and the second (CI-T model R) based on a subset of 188 lakes selected to minimise the effects of continentality on the temperature optima of the chironomids. The following sections (6.4.1 and 6.4.2) describe the criteria for omitting lakes from the respective training sets and details the omitted lakes. The performance of the two inference models are described and compared.

6.4.1. CI-T model C

The lakes in the Norwegian training set were specifically selected to minimise variation in environmental variables other than the variable of interest for palaeoenvironmental reconstruction, i.e. mean July air temperature (T_{july}) (Brooks and Birks 2000a also see section 6.3). Many of the environmental variables, such as pH, conductivity and water ion concentrations, are considerably higher in some of the Yakutian lakes than the maximum recorded in the Norwegian training set. For example, magnesium concentrations are 17300 $\mu\text{eq/l}$ in lake Y1741 compared with a maximum of 930 $\mu\text{eq/l}$ in the Norwegian lakes. TWINSPAN and multivariate analyses suggest the composition of the chironomid assemblages in the Yakutian lakes is distinct from either the Russian or Norwegian faunas (section 4.4). The high conductivity and ion concentrations of many of the Yakutian lakes suggest they, and their chironomid fauna, are strongly influenced by the aridity of the region and its associated moisture deficient (see section 2.5 and Figures 4.18 -4.19). Therefore 20 Yakutian lakes with pH, conductivity or water ion concentrations greater than the maximum in the Norwegian training set were omitted from the combined training set to give a training set with similar environmental conditions and enhance the performance of the inference model (Table 6.7). In addition, Lake Birgervatnet from the Norwegian training set whose chironomid fauna was composed of a single taxon and the three eutrophic lakes from Yakutia (Kumke *et al.* 2007) were excluded from the training set. After exclusion of the lakes, CI-T model C was developed based on 146 taxa from 233 lakes (157 Norwegian and 77 Russian lakes) using WA, WA-TOL, WA-PLS, MAT and WMAT techniques. The performance of the models are summarised in Table 6.8.

Table 6.7. Lakes identified as outliers in the CI-T model C. Values for the environmental variables for the Russian training sets are detailed in Table 4.1 and the maximum values of Norwegian lakes in Table 4.7. Some lakes are included in more than one category.

Lakes	Reason for exclusion
Y7111 Y1717 Y1727 Y1731 Y1733 Y1735 Y1740 Y1741	Above maximum conductivity of Norwegian training set
Y1700 Y1703 Y1707 Y1709 Y1711 Y1712 Y1716 Y1718 Y1720 Y1731 Y1732 Y1733 Y1737 Y1740 Y1741	Above maximum pH value of Norwegian training set
Y1741	Above maximum Cl concentration of Norwegian training set
Y1703 Y1707 Y1709 Y1711 Y1713 Y1717 Y1721 Y1727 Y1729 Y1731 Y1733 Y1735 Y1737 Y1740 Y1741 Y1746	Above maximum Mg concentration of Norwegian training set
Y1727 Y1731 Y1733 Y1740 Y1741	Above maximum Na concentration of Norwegian training set
Y1700 Y1722 Y1725	Eutrophic
Lake Birgervatnet - Bir	Single taxon

Table 6.8. The performance of the combined Norwegian – Russian CI-T model C, with 146 chironomid taxa in 233 lakes, based on leave-one-out cross validation. Minimal adequate WA-PLS model highlighted in yellow.

Model	Component	r^2_{jack}	RMSEP _{jack}	Mean bias _{jack}	Max bias _{jack}	Reduction in prediction error (%)
MAT	5 closest analogues	0.87	1.38	0.424	2.15	...
WMAT	5 closest analogues	0.87	1.38	0.423	2.15	...
WA (inv)	...	0.72	1.91	-0.009	3.69	...
WA (cla)	...	0.72	2.18	-0.009	4.27	...
WA - TOL (inv)	...	0.77	1.73	-0.029	2.40	...
WA - TOL (cla)	...	0.77	1.90	-0.035	2.90	...
WA - PLS	1	0.72	1.94	0.057	3.31	...
	2	0.84	1.44	-0.019	1.02	25.54
	3	0.86	1.36	0.019	1.02	5.93
	4	0.85	1.41	0.002	0.97	-3.58
	5	0.84	1.46	0.021	0.93	-3.60

The 3-component WA-PLS model was selected as the minimal adequate model based on the combination of low RMSEP (1.36 °C), low maximum bias (1.02 °C) and high coefficient of determination ($r^2 = 0.86$). Plots of the predicted values against observed values (Figure 6.6a) and of residuals (predicted – observed) (Figure 6.6b) suggests the WA-PLS model over-predicts

temperatures below 11.5 °C and under-predicts above 11.5 °C. There are a number of extreme outliers, 32 samples with residuals (predicted – observed values) greater than ± 2 °C and 3 samples with residuals greater than ± 4.2 °C.

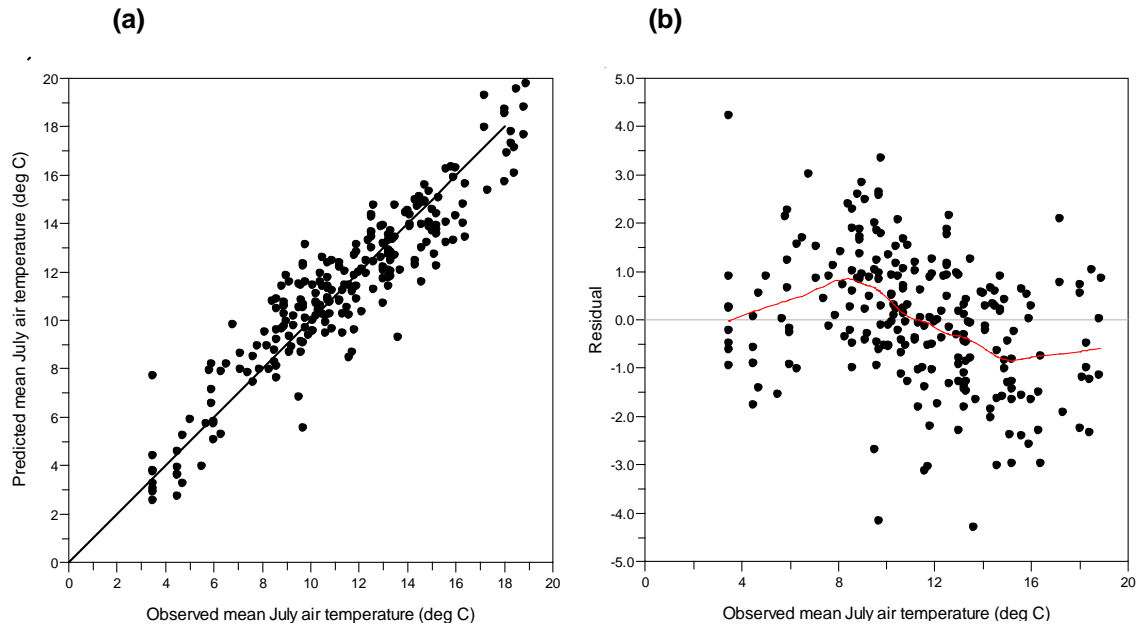


Figure 6.6. Relationship between (a) observed and predicted mean July air temperatures using a weighted averaging partial least squares (WA-PLS) 3-component CI-T model C. Solid line represents 1:1 relationship; (b) Residuals (predicted – observed) along the July air temperature gradient for the 3-component WA-PLS CI-T model C. The solid line is a LOESS scatterplot smoother (span = 0.45), scale on residuals = ± 5 °C.

6.4.2. CI-T model R

Modelling taxon responses to T_{july} and continentality (section 5.3.3) showed that although taxa in the combined Norwegian and Russian training sets had a single temperature optimum the species abundance also increased or decreased in response to continentality. For example, the abundance of a taxon can be higher at suboptimal T_{july} (see Figure 5.8) due to changes in continentality which would bias the WA temperature optimum derived in the inference model. To ensure accurate optima are obtained, the training set requires an even distribution along both the CI and T_{july} gradients. The combined Russian and Norwegian datasets, without deletions, comprise 257 lakes, with 0 – 24 lakes for each 0.5°C interval (Figure 6.7). For each 0.5°C interval the most extreme outliers were identified and deleted so that:

- (1) the number of Norwegian lakes, approximately, equalled the number of Russian lakes for each interval,
- (2) the widest range of CIs was retained in each temperature interval and
- (3) the total number of lakes in each 0.5°C interval did not exceed 10.

For example, there are 15 lakes with T_{july} of 8.6 – 9.0 °C; four (B98-15, 99-15, 99-19 and LS-8) were deleted as the residuals (predicted – observed) were greater than ± 1.90 °C. Five lakes (LS-3, -5, -6, -7 and -8) had CIs of 57 therefore LS-8 was deleted as it had the highest residual (1.79 °C). B98-13 was retained although the residual was higher than that of LS-8 (1.86 °C) as only one other lake B98-22 had a CI of 19. The limit of 10 lakes was selected as the Norwegian training set had a median value of 5 lakes for the temperature intervals; therefore the majority of intervals required only a small number of deletions. In the selected subset over 60% of the intervals between 5.5 - 16°C have 8 – 10 lakes. Lakes at either end of the temperature gradient were restricted to either Norway or Russia.

Table 6.9. Subset of 188 Norwegian – Russian lakes selected for CI-T model R.

Lake code								
F3-3	IGAR	LS-10	F	96-14	96-58	97-25	B98-18	99-20
F3-5	NERU	LS-11	G	96-15	96-60	97-26	B98-19	99-21
F3-6	VORK5	LS-13	H	96-20	96-61	97-27	B98-20	99-26
F4-4	Y1701	LS-15	I	96-21	96-63	97-28	B98-21	99-27
F4-5	Y1704	LS-16	J	96-24	96-65	97-31	B98-22	99-28
F7-4	Y1705	LS-19	K	96-25	96-67	97-32	B98-23	99-29
F8-4	Y1706	LS-24	M	96-26	96-70	97-33	99-2	99-30
TDRA2	Y1708	LS-25	O	96-29	96-71	B98-1	99-3	99-31
TDRC2	Y1724	LS-27	P	96-31	96-74	B98-2	99-4	99-32
TDRE1	Y1727	LS-30	Q	96-32	96-77	B98-3	99-5	99-33
TDRU11a	Y1730	K4	R	96-35	96-78	B98-4	99-6	99-34
TDRU42a	Y1735	K5	S	96-36	97-35	B98-5	99-7	99-35
Mitro	Y1739	K6	T	96-37	97-8	B98-6	99-8	99-37
Vanuk-ty	Y1743	K7	U	96-38	97-10	B98-7	99-9	99-38
AFOX	LS-1	K10	Scur	96-44	97-12	B98-8	99-10	99-40
WILD	LS-2	K11	Arsj	96-45	97-15	B98-9	99-12	99-42
ARTE	LS-3	A	96-1	96-47	97-16	B98-10	99-13	99-43
PTWO	LS-4	B	96-2	96-49	97-19	B98-12	99-14	99-45
PTHE	LS-5	C	96-7	96-51	97-21	B98-13	99-16	99-47
PFOR	LS-6	D	96-10	96-54	97-23	B98-14	99-17	99-50
PFIV	LS-7	E	96-13	96-56	97-24	B98-17	99-18	

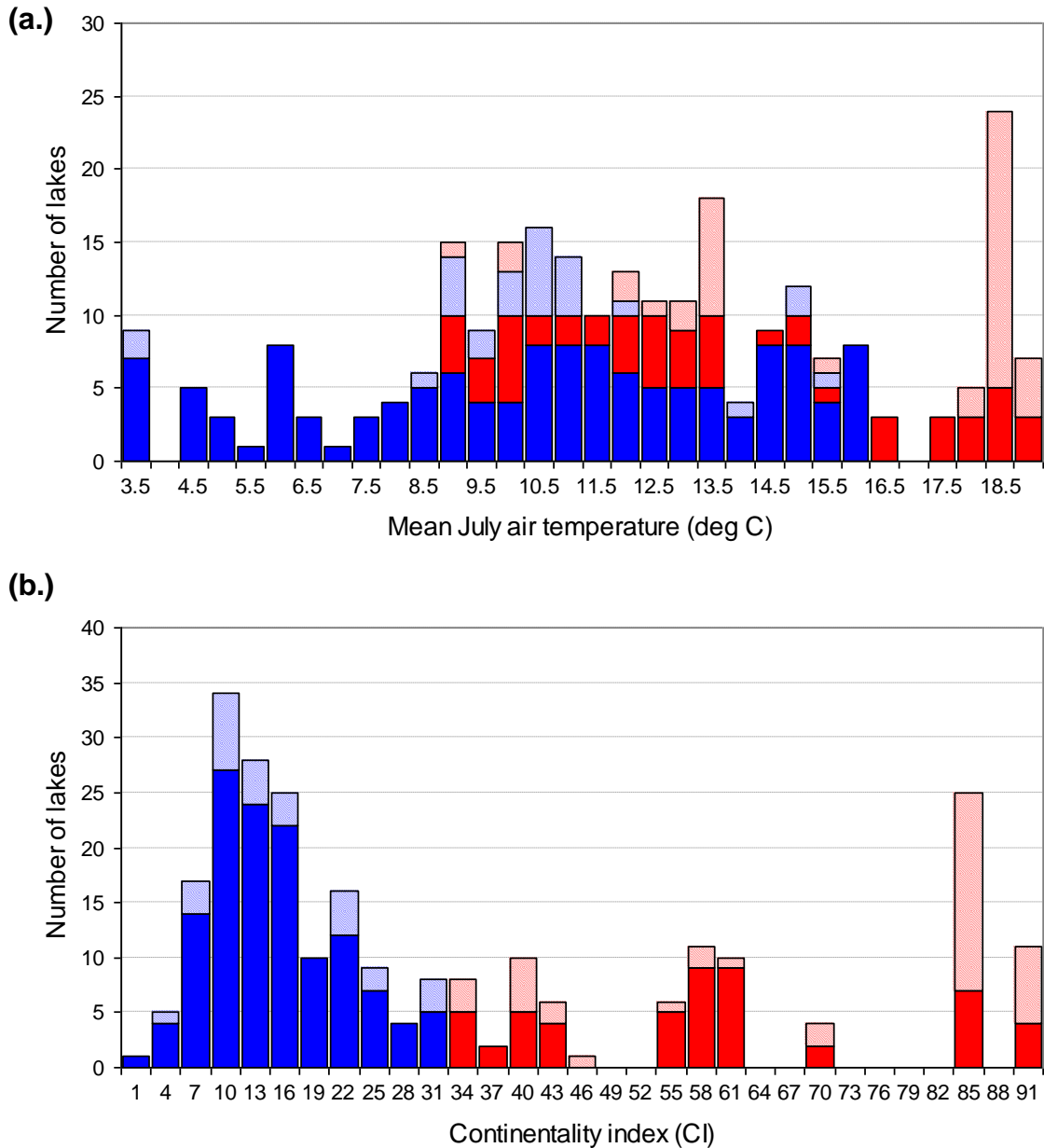


Figure 6.7. Frequency histograms showing the distribution of lakes along (a) the mean July air temperature and (b) the continentality index gradients. (Solid Blue: lakes from the Norwegian dataset included in the model, hashed blue: lakes from Norwegian dataset deleted from CI-T model R, solid red: lakes from Russian dataset included in the model and hashed red: lakes from Russian dataset deleted from the CI-T model R). Continentality indices for the Komi lakes are unavailable but are expected to be between 40 – 49.9).

A subset of 188 lakes, 58 Russian and 130 Norwegian, with 144 taxa (Table 6.9) was selected; the deletion process removed the 32 extreme outliers identified in model C. The distribution of lakes along the July air temperature and continentality gradients is shown in Figure 6.7. Models were generated

using WA, WA-TOL, WA-PLS, MAT and WMAT techniques using this restricted dataset (CI-T model R; 144 taxa in 188 lakes) and the performance of the model summarised in Table 6.10.

Table 6.10. The performance of the combined Norwegian - Russian CI-T model R, with 144 chironomid taxa in 188 lakes, based on leave-one-out cross validation. Minimal adequate WA-PLS model highlighted in yellow.

Model	Component	r^2_{jack}	RMSEP _{jack}	Mean bias _{jack}	Max bias _{jack}	Reduction in prediction error (%)
MAT	7 closest analogues	0.92	1.16	0.439	2.07	...
WMAT	7 closest analogues	0.92	1.16	0.437	2.06	...
WA (inv)	...	0.79	1.74	-0.010	3.41	...
WA (cla)	...	0.79	1.91	-0.010	3.56	...
WA - TOL (inv)	...	0.85	1.47	-0.061	2.09	...
WA - TOL (cla)	...	0.85	1.53	-0.067	1.75	...
WA - PLS	1	0.79	1.79	0.075	3.02	...
	2	0.91	1.16	-0.038	0.98	35.10
	3	0.93	0.99	-0.002	0.67	15.04
	4	0.93	0.98	-0.011	0.70	1.11
	5	0.93	1.01	0.001	0.61	-3.51

(a)

(b)

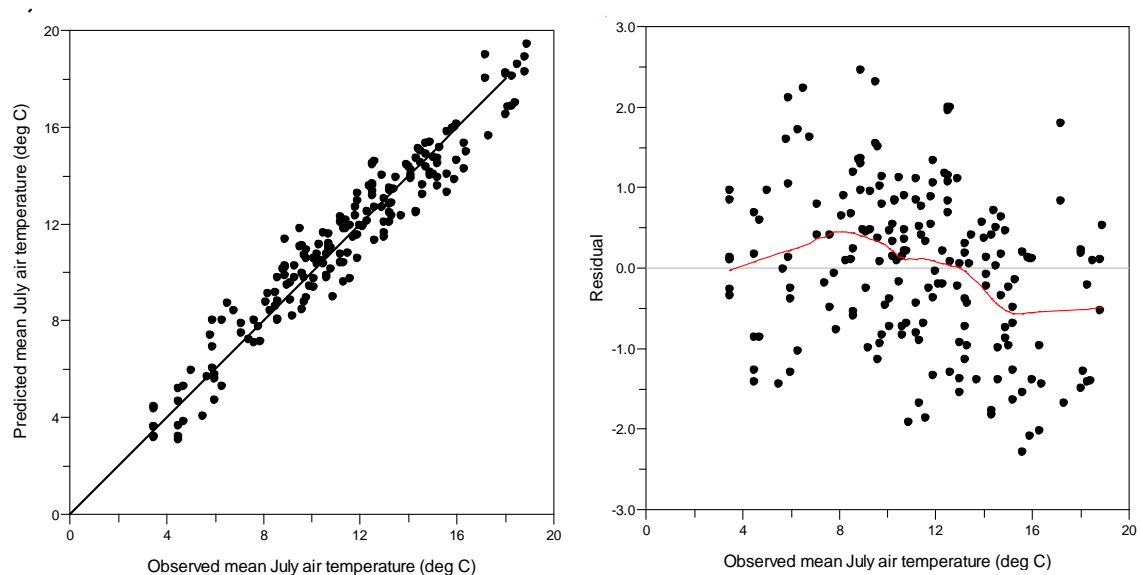


Figure 6.8. Relationship between (a) observed and predicted mean July air temperatures using a weighted averaging partial least squares (WA-PLS) 3-component CI-T model R. Solid line represents 1:1 relationship; (b) Residuals (predicted – observed) along the July air temperature gradient for the 3-component WA-PLS CI-T model R. The solid line is a LOESS scatterplot smoother (span = 0.45).

The 3-component WA-PLS model, for CI-T model R, was selected as the minimal adequate model based on the combination of low RMSEP (0.99 °C), low maximum bias (0.67 °C) and high coefficient of determination ($r^2 = 0.93$). Plots of the predicted values against observed values (Figure 6.8a) and of residuals (predicted – observed) (Figure 6.8b) suggests the inference model over-predicts temperatures below 13 °C and under-predicts above 13 °C. The RMSEP and maximum bias are lower and the coefficient of determination higher with CI-T model R selected to minimise the effect of continentality rather than CI-T model C selected to minimise environmental variation. The variation in residuals (predicted – observed values) is also reduced which suggests CI-T model R should perform better at reconstructing past T_{july} than the full CI-T model C.

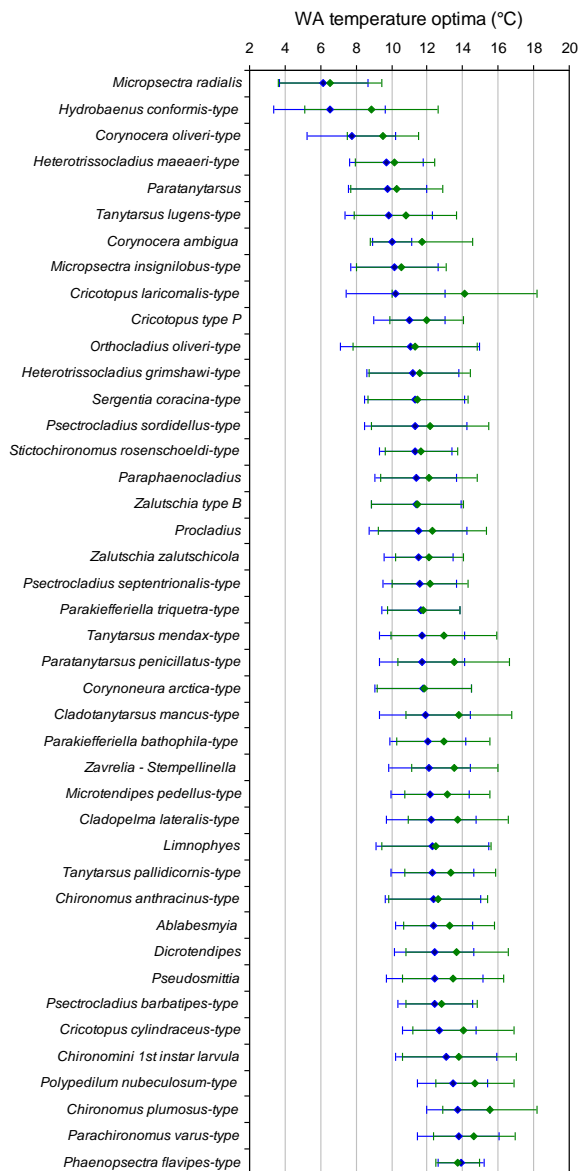


Figure 6.9. Comparison of the temperature optima of common taxa derived from the Norwegian CI-T model N (solid blue circle) and reduced Russian – Norwegian CI-T model R (solid green circle) training sets. Species selected have 10 or more occurrences in all datasets, optima calculated by weighted-averaging regression and training. Bars indicate species tolerances (blue – Norway; green combined dataset). Taxa are listed in order of increasing temperature optima derived from the Norwegian dataset.

The temperature optima of the 42 most common taxa are, in general, higher in the combined CI-T model R than the Norwegian CI-T model N (Figure 6.9), although the values are closer than those derived from the Russian CI-T models A and K. With the exception of *Hydrobaenus conformis*-type and *Cricotopus laricomalis*-type the optima lie within 1.8 °C and within the tolerances of the other dataset, which suggests the effects of continentality on the temperature optima have been minimised.

6.5. Comparison with published chironomid – July air temperature inference models

The majority of published Eurasian chironomid – July air temperature inference models have been generated using WA-PLS regression. The performance of the minimum adequate CI-T models A, K and N are comparable to published models, in terms of RMSEP, r^2 and maximum bias (Table 6.11). The combined CI-T model R performs better than the comparable Russian or Norwegian models. However this probably results from the removal of outliers in the selection process and may not equate to improved performance in the reconstruction.

Table 6.11. Comparison of the performance statistics of minimum adequate WA-PLS chironomid-mean July air temperature inference models from Finland (1) (Olander et al. 1999), Finland (2) (Luoto 2008), Norway (Brooks 2006b), Sweden (Larocque et al. 2001), Switzerland (Lotter et al. 1997) and this study.

Inference model	Finland (1)	Finland (2)	Brooks-Birks Norway	Sweden	Switzerland	Russia model A	Russia model K	Norway model N	Combined model C	Combined model R
No. lakes	53	77	153	100	50	88	81	153	232	188
No. taxa	38	84	140	48	58	89	89	141	146	144
Range (°C)	6.1 - 15.4	11.3 - 17.1	3.5 - 16.0	7.0 - 14.7	6.6 - 17.3	8.8 - 18.9	8.8 - 18.9	3.5 - 16.0	3.5 - 19.0	3.5 - 19.0
RMSEP (°C)	1.53	0.721	1.01	1.13	1.37	1.04	0.89	1.10	1.36	0.99
r^2_{jack}	0.37	0.78	0.91	0.65	0.85	0.91	0.92	0.90	0.86	0.93
Maximum bias (°C)	3.88	0.79	0.93	2.10	1.67	1.21	1.28	1.05	1.02	0.67
WA-PLS components	1	1	3	1	2	2	2	3	3	3

6.6. Summary and discussion of the temperature inference models

- Two Russian and two combined Norwegian – Russian training sets were compiled. These datasets were used to generate inference models using a range of statistical techniques. The performance of the Russian CI-T

models A and K and Norwegian-Russian models C and R, are compared to the existing Norwegian 'Brooks-Birks' model.

- Temperature optima of common taxa derived from the Russian and Norwegian – Russian models are consistently higher than those from Norway.
- The second Russian training set, CI-T model K, was compiled to even out the distribution along the T_{july} gradient by including lakes with only partial physico-chemical data and removing samples with extreme environmental variables. This decreased the temperature optima, but, in general, they remained higher than the Norwegian values.
- Modelling taxon responses (Chapter 5) suggests the temperature optimum of chironomid taxon vary between Norway and Russia. However the discrepancy in optima may also result from the uneven distribution of lakes along the T_{july} gradient or insufficient lakes in the training set.
- The higher temperature optima from the Russian datasets may also result from the warmer and narrower range of T_{july} in the training set truncating the species responses. The 'edge effect' inherent with WA and WA-PLS estimation results in distortion at the ends of the environmental gradient and the differences between optima are particularly marked at the cold end of the gradient. The warm-adapted taxa were restricted to Yakutia and therefore optima could not be compared with Norway.
- To generate a robust inference model the ratio of taxa : lakes must be decreased to a minimum (Racca *et al.* 2003). To achieve this, rare taxa were deleted from the Russian datasets. Rare taxa frequently have more specific ecological requirements and narrower tolerances, therefore may be particularly valuable in palaeoenvironmental reconstructions.
- From the performance statistics, the combined Norwegian-Russian inference models give the best performances in terms of low RMSEP, low bias and high correlation of determination. The training set, also, includes rare taxa which may improve the ability of the model to reconstruct past temperatures.

6.7. Chironomid – inferred continentality (CI-C) model

Changes in continentality or seasonality are of intrinsic interest as they contribute to a better understanding of the regional impacts of climatic warming (Hirschi *et al.* 2007). Analysis of satellite data and field observations (Walther *et al.* 2002; Comiso 2003; Hoyer *et al.* 2007) suggests climate warming has led to an extension of the ice-free season in the Arctic since the 1960s (Chapter 1). Changes in the length of the ice-free season has a profound influence on lake ecosystems (Schindler and Smol 2006; Smol and Douglas 2007). However production of a biotic – ice-free period inference model has been hampered by the difficulty in obtaining reliable estimates of the ice-free period in remote lakes (Clarke 2004). The results in section 5.3.2 showed that 54 – 82% of chironomid taxa have a statistically significant response to continentality. It should, therefore, be feasible to develop an inference model to reconstruct past continentality. As Figure 6.10 shows, there is an apparent relationship between continentality and ice-free season; the number of frost-free days decreases from western Europe to central Siberia as continentality increases.

(a.)

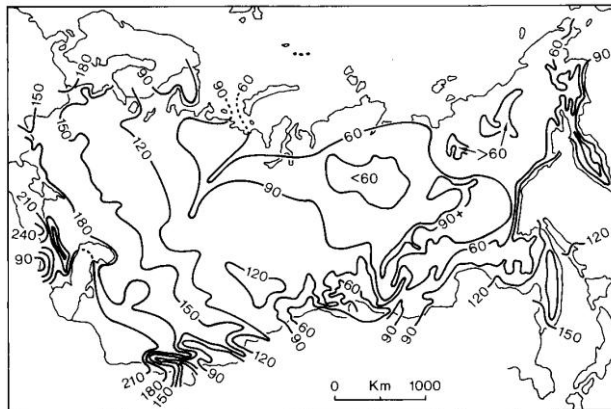
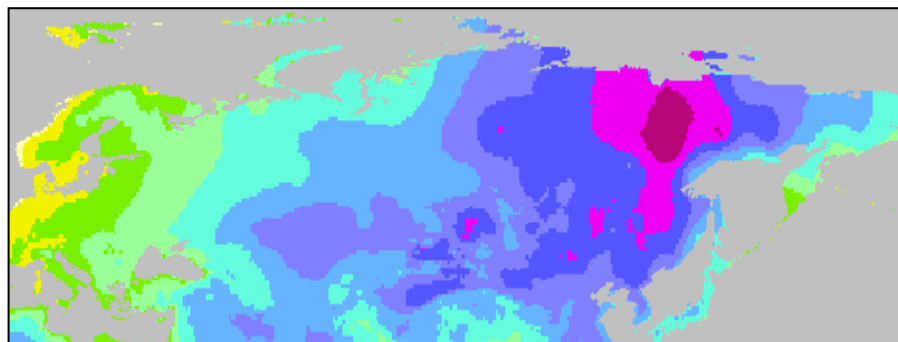
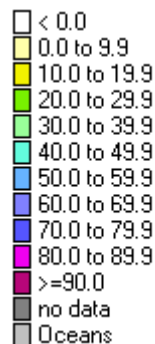


Figure 6.10. (a) Polar stereographic projection map showing the mean number of frost-free days per year in northern Eurasia (Dewdney 1982) and (b) equidistant cylindrical projection map showing the Gorchynski continentality indices (CI) (Grieser *et al.* 2006).

(b.) CI



The first part of this section examines the relationship between continentality, climate and the ice-free period to determine which climate variables most closely correlate to the length of the ice-free period and the strength of the relationship. The second part describes the development of the CI-C models.

6.7.1. The relationship between climate parameters and ice-free period

The total number of days per annum with air temperatures above 0°C and the longest continuous period above 0°C (in days) were determined using daily minimum air temperatures from 21 meteorological stations located between 60 - 72°N and 5 - 129°E for the period 1981-1990. This period was selected as it included positive, negative and neutral phases of the winter Arctic Oscillation - AO (Overland and Wang 2005). Variations in mean temperature and daily variance are associated with the state of the AO. In north-western Eurasia positive phases of the AO are associated with higher spring temperatures (Kryjov 2002). Meteorological records are often intermittent at high latitudes and the selected stations (Table 6.12) had complete daily minimum records for this period (for details of data source see Table 3.5).

Table 6.12. Meteorological station records used in the calculation of the climate parameters.

Meteorological station	WMO Station code	Latitude N	Longitude E	Altitude (m)
Bergen	NO000001317	60.38	5.33	12
Ona	NO000001212	62.53	6.53	15
Glomfjord	NO000001113	66.82	13.98	39
Bodo	NO000001152	67.27	14.43	11
Harnosand	SW000002361	62.63	17.95	0
Holmogadd	SW000002288	63.6	20.76	6
Helsinki	FI000000304	60.17	24.95	4
Kandalaksha	RS000022217	67.13	32.43	26
Kojnas	RS000022583	64.75	47.65	64
Narjan-Mar	RS000023205	67.65	53.02	4
Pecora	RS000023418	65.1	57.1	59
Hosedda-Hard	RS000023219	67.1	59.4	84
Hanty-Mansijsk	RS000023933	61	69	47
Aleksandrovskoe	RS000023955	60.4	77.9	48
Dudinka	RS000023074	69.4	86.17	19
Turukhansk	RS000023472	65.18	87.95	37
Bor	RS000023884	61.6	90.2	58
Yeniseysk	RS000029263	58.45	92.15	77
Khatanga	RS000020891	71.98	102.47	30
Olenyok	RS000024125	68.5	112.43	16
Tiksi	RS000021824	71.58	128.92	7

Total days and continuous period above 0°C were compared to mean May, mean July, summer (May – August and June - August) and mean annual temperatures (MeAT) calculated from mean monthly data. Continentality indices were calculated as described in section 3.3.5.

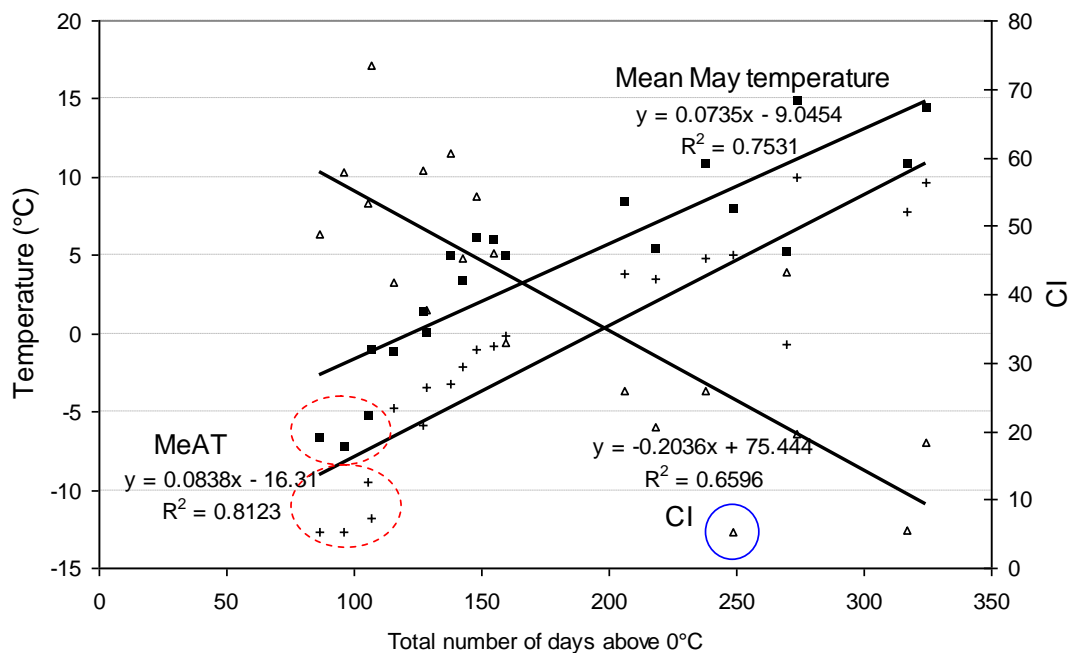
Table 6.13. Regression coefficients (r^2) showing the strength of the correlation between climate parameters and total days and continuous period above 0°C.

Climate parameter	Regression coefficient r^2	
	Total days above 0°C	Continuous days above 0°C
Mean May air temperature (°C)	0.75	0.62
Mean July air temperature (°C)	0.23	0.15
Mean May-August air temperature (°C)	0.56	0.44
Mean June-August air temperature (°C)	0.40	0.30
MeAT Mean annual temperature (°C)	0.81	0.69
CI Continentality Index	0.65	0.64

CI, MeAT and mean May temperatures are strongly correlated to total days and continuous period above 0°C (Table 6.13). The relationship between continuous period above 0°C and the climate parameters is weaker as the results are more susceptible to random variability i.e. a single cold day. Mean May temperature and MeAT are more strongly correlated to total days above 0°C than CI. However the strength of this relationship is derived from daily instrumental records and may not hold true when temperature records are extrapolated to remote locations. The atmospheric pressure systems affecting northern Eurasia are less stable in spring and autumn than winter and summer (Shahgedanova 2002). Air temperatures show considerable day-to-day and diurnal variation during this transition from polar night to polar day (Przybylak 2003). Localised factors, such as aspect, can determine whether air temperatures are above or below 0°C. It is, therefore, difficult to extrapolate spring and autumn temperatures from meteorological stations to remote lakes. Additionally MeAT and mean May temperatures consistently under-predict the total number of days above 0 °C at colder, arctic locations by up to 53 and 72 days respectively (Figure 6.11). Although CI performs poorly for some locations (for example Glomfjord: CI = 5, 248 days) the variation appears more random.

Therefore continentality was selected as a possible proxy for length of the ice-free season.

Figure 6.11. The relationship between the total number of days above 0°C per annum and mean May temperature, mean annual temperature (MeAT) and continentality (CI). (Squares represent mean May temperatures, crosses MeAT and triangles CI. Dashed red circles highlight locations where MeAT and May temperatures consistently underestimate the total number of days above 0°C and blue circle highlights results for Glomfjord, see text for details).



6.7.2. Chironomid – continentality inference model (CI-C)

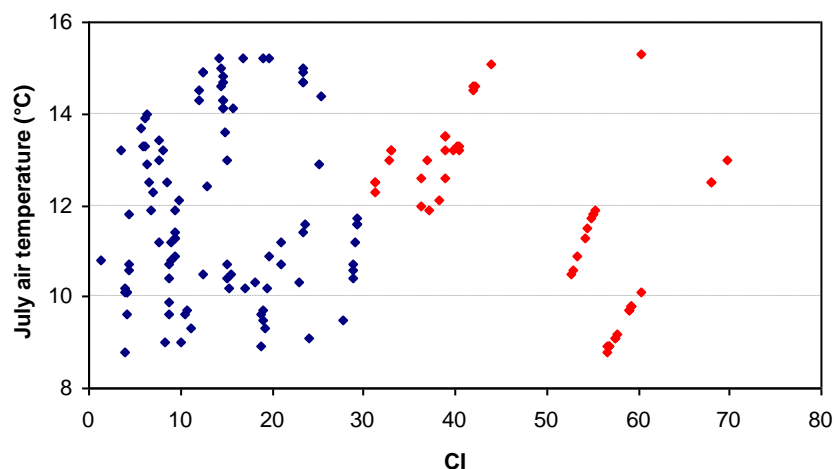
July air temperature is the main factor influencing the distribution of chironomids (section 5.3). The sites at the extremes of the T_{july} gradient are restricted to specific geographic locations. The warmest lakes are located in Yakutia with high CIs and the coldest lakes to Svalbard with low CIs. The chironomid assemblages found at these locations are probably responding primarily to T_{july} rather than continentality. Therefore to minimise the risk of wrongly attributing a temperature-driven response to continentality the lakes at both ends of the temperature gradient, from Svalbard and Yakutia, were excluded from the training set. A subset of 149 lakes was selected from the Norwegian – Russian datasets of lakes to ensure a range of CI values for each 0.5°C interval (Figure 6.12). Lakes for inclusion were selected by stratified sampling; lakes were

stratified by mean July air temperature (at 0.5°C intervals), then continentality (at 1 CI intervals) and finally by geographical location. If more than one lake from a single location had the same T_{july} and same CI, a single representative lake was chosen by random selection. The stratification process followed by selection of a single lake should minimise the risk of spatial autocorrelation. The selected lakes have CIs from 1 to 70 and July air temperatures of 8.8 – 15.3°C (Figure 6.12).

Table 6.14. Subset of Norwegian – Russian lakes selected for CI-C training set.

Lake codes							
96-1	96-39	96-77	B98-13	99-16	99-44	TDRE 1	LS-1
96-2	96-44	97-10	B98-14	99-17	99-45	TDRU11a	LS-2
96-7	96-45	97-12	B98-16	99-18	99-47	TDRU42a	LS-3
96-11	96-47	97-13	B98-17	99-20	99-50	Mitro	LS-4
96-13	96-49	97-15	B98-23	99-21	F3-2	Vanuk-ty	LS-5
96-15	96-51	97-16	N98-1	99-22	F3-5	GYXO	LS-6
96-20	96-52	97-17	99-1	99-24	F3-6	AFOX	LS-7
96-21	96-53	97-18	99-2	99-25	F4-2	WILD	LS-8
96-24	96-56	97-19	99-3	99-26	F4-4	ARTE	LS-10
96-25	96-58	97-21	99-4	99-32	F4-5	PONE	LS-11
96-26	96-60	97-23	99-5	99-33	F6-2	PTWO	LS-12
96-28	96-61	97-24	99-6	99-34	F7-3	PTHE	LS-13
96-29	96-63	97-25	99-7	99-35	F7-4	PFOR	LS-15
96-31	96-65	97-26	99-8	99-37	F7-5	PFIV	LS-17
96-32	96-67	97-27	99-9	99-38	F8-2	IGAR	LS-19
96-35	96-70	97-28	99-10	99-40	F8-4	NERU	LS-24
96-36	96-72	B98-11	99-11	99-41	TDRA 2	VORK3	LS-25
96-38	96-74	B98-12	99-13	99-42	TDRC 2	SAND	LS-27
			99-15	99-43	TDRD 2	VORK5	LS-30

Figure 6.12. The distribution of the selected lakes (see Table 6.14) along the July air temperature and CI gradients (Blue – Norwegian lakes, red – Russian lakes)



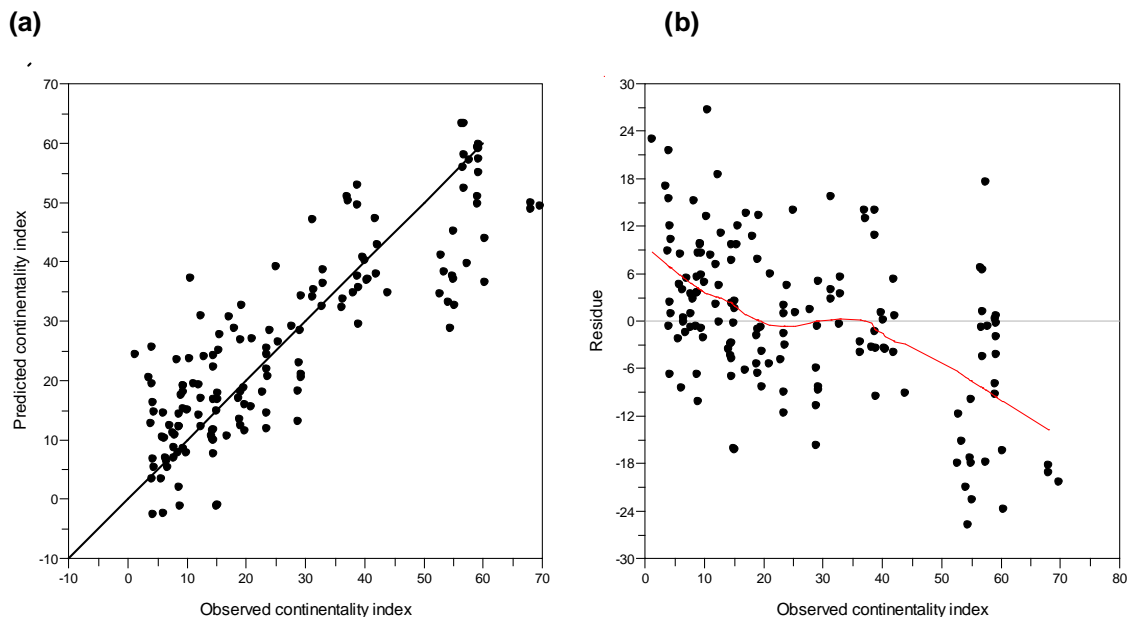
Models were created using WA and WA-PLS techniques with 149 lakes and 120 chironomid taxa using CI as the environmental parameter to be inferred. The results of the models tested are summarised in Table 6.15; model performance was assessed by $RMSEP_{jack}$, r^2_{jack} , mean and maximum biases. A 2-component WA-PLS model represents the minimal adequate model with a combination of high r^2_{jack} , low $RMSEP_{jack}$ and low mean and maximum bias with the fewest components. Additional components did not reduce the prediction error by 5% or more and were, therefore, not included (Birks 1998).

Model	Component	r^2_{jack}	$RMSEP_{jack}$	Ave. bias _{jack}	Max. bias _{jack}	Reduction in prediction error (%)
WA (inv)		0.65	11.16	0.06	25.39	...
WA (cla)		0.65	12.69	0.07	18.49	...
WA-TOL (inv)		0.57	12.50	0.06	20.72	...
WA-TOL (cla)		0.58	15.00	0.05	14.65	...
WA-PLS	1	0.65	11.16	-0.30	25.12	...
	2	0.73	9.88	0.08	19.26	11.53
	3	0.73	9.83	0.04	20.06	0.52
	4	0.71	10.23	0.03	19.97	-4.07
	5	0.69	10.69	0.07	18.79	-4.51

Table 6.15. Performance statistics of the continentality models created from subset of northern Eurasian lakes using WA and WA-PLS methods. Minimal adequate WA-PLS model highlighted in yellow.

Plots of predicted (jack-knifed) values against observed values (Figure 6.13a) and of residuals (predicted – observed) (Figure 6.13b) show the model predicts reasonably well over the CI range 10 – 40 but under-predicts above indices of 50.

Figure 6.13. (a) Predicted CI as a function of observed CI for 2-component WA-PLS model. The solid line is a 1 : 1 line; (b) Residuals (predicted – observed) of CI as a function of observed CI for the 2-component WA-PLS model. Solid line is a LOESS scatter plot smoother (span = 0.45)



As an independent test, CI was estimated for 6 lakes not included in the development of the CI-C model. The 2-component WA-PLS model underestimates the observed CI (Table 6.16) for the Norwegian samples (97-8 and 99-46) and gives differing estimates for the two Pechora lakes (F3-3 and F3-12) with identical observed values. However it does distinguish different regions of east and west Pechora and Norway and between the geographical regions.

Lakes	Estimated CI	Observed CI
97-8	8	20
99-46	19	29
F3-12	25	33
F3-3	36	33
KHAR	47	39
LS-16	55	59

Table 6.16. Comparison of the observed and estimated CI values from the independent test set. CI estimated from 2-component WA-PLS model; observed CI calculated from the meteorological data.

The weighted averaging CI optima show that many taxa found primarily in Norway (CI range 1 – 30) have narrow tolerances whereas those with higher optima, generally, have wider tolerances (Figure 6.14). The taxa may be restricted to Norway due to an inability to adapt to shorter summer or longer winters. It is difficult to generalise the characteristics of the taxa; for example *Heterotanytarsus* is thermophilic (Walker *et al.* 1991) and *Zavrelimyia* and *Thienemannimyia* are cold stenotherms (Fittkau and Roback 1983). These taxa may be restricted to habitats found only in Norway; possibly due to its metamorphic geology, high rainfall or the surrounding vegetation which is influenced by the distance to the coast (Giesecke *et al.* 2008). The CI optima for *Abiskomyia* is high (48.4) this taxon is found in the coldest oligotrophic lakes throughout the Holarctic (Cranston *et al.* 1983). Its distribution may therefore reflect an ability to survive long, cold winters rather than a requirement for the high summer temperature associated with continental climates. Freeze-tolerance is widespread in Chironomidae, with the exception of Tanypodinae (Danks 1971). The CI optima of *Ablabesmyia* and *Procladius* are low (19.5 and 23.6 respectively) and, even when their wide tolerances are taken into consideration, are less abundant in extremely continental environments. The wide tolerances of many taxa found in Russia means that the inference model may be insensitive to small changes in continentality.

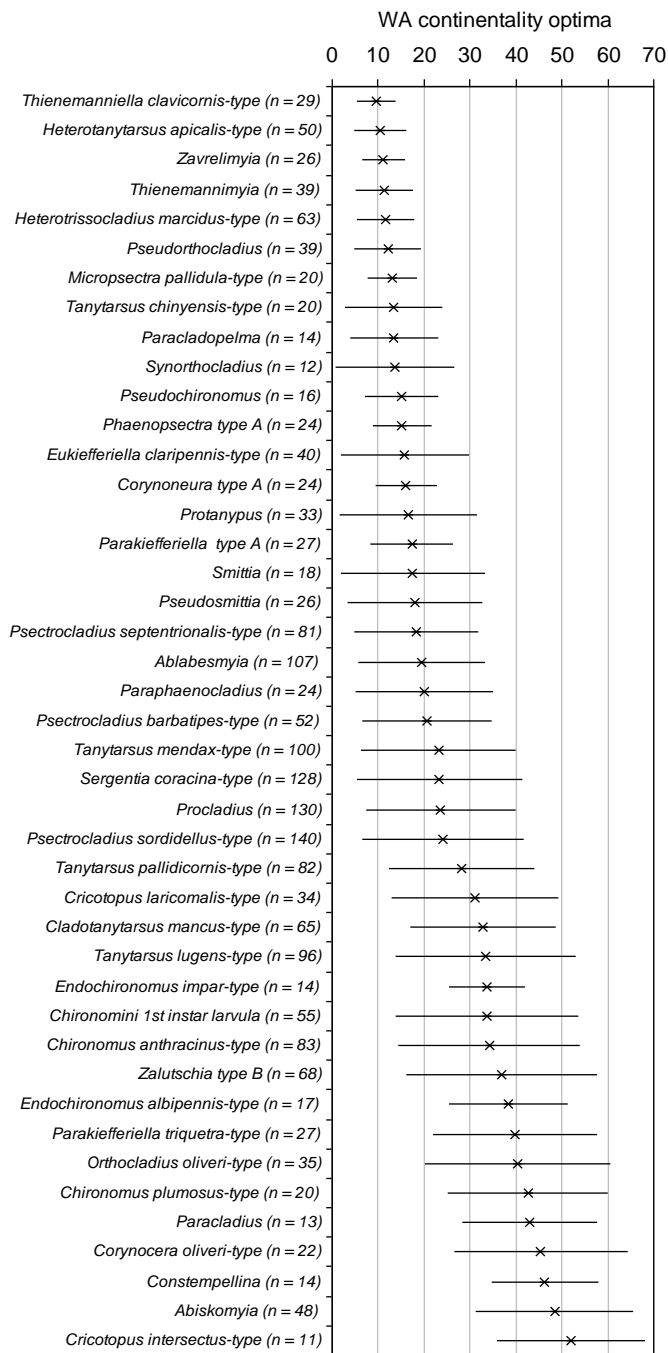


Figure 6.14. Continentality optima of taxa which showed a statistically significant response to continentality in Chapter 5. Bars indicate species tolerances. Taxa are listed in order of increasing continentality optima.

6.7.3. Summary and Conclusions for continentality inference model

- Although we may want to model the duration of the ice-free period, the environmental data are unavailable for developing an inference model. Continentality, expressed as Gorczynski Continentality Indices (CI), is strongly negatively correlated to total number of days and longest period above 0°C.

- There are a number of disadvantages to this approach;
 1. CI is calculated from, and therefore not independent of, T_{july} .
 2. Chironomid species respond primarily to summer temperature and some species show no response to continentality (section 5.3.2).
 3. Many taxa with optima within the continentality range of Russia (30 – 70) have wide tolerances so may be insensitive to small changes in continentality.
 4. Temperatures influence the initiation, rate of development and time to maturation of all stages in the life cycle of Chironomidae (section 1.5). During severe, cold summer chironomids may remain in ecdysis until the following summer. Therefore the chironomid assemblage may not reflect short-term fluctuations in weather.
 5. Additionally, the ice-free period of lakes, although primarily dependent on air temperature, is also dependent on localised or internal factors such as wind strength, lake topography, water depth and profile. These are not modelled by CI and variation may be poorly represented in the training set.
- The CI-C model has an r^2_{jack} of 0.73 and $\text{RMSEP}_{\text{jack}}$ of 9.9. To place this in context the predicted values could not reliably distinguish between different regions of eastern Norway but could distinguish the climate of Norway from eastern Europe.
- The WA-PLS model shows considerable noise; the gradient is discontinuous and unevenly distributed with a higher proportion of lower values and the model underpredicts CI above 50. However the model appears to capture an aspect of climate not represented by T_{july} and may therefore be useful in understanding palaeoenvironmental changes at the coring sites. The results should be interpreted as an indication of the trend rather than a precise value.

Chapter 7

Putorana Plateau

7.1. Introduction

This chapter presents and discusses the results of palaeoenvironmental analysis from lakes on the Putorana Plateau, Western Siberia. The physical and biological characteristics of the study area are described in Chapter 2. The present-day assemblages were included in the analysis of factors influencing chironomid distribution in northern Russia (Chapter 4). This chapter aims to examine localised and external factors which may have influenced changes in the chironomid assemblages within the Putorana lakes over, approximately, the past 750 years. Following preliminary analysis of the chironomid assemblages three lakes were selected for more detailed study. These lakes are described and the results from sedimentary, isotopic and chironomid analyses are presented. These results are then interpreted to produce a synthesis of recent palaeoenvironmental change on the Putorana Plateau.

7.2. Selection of lakes for palaeoenvironmental analysis

Short sediment cores were collected from nine lakes on the Putorana Plateau in July 2006. One of the initial objectives of the research (section 1.6) was to obtain representative Holocene sequences from two regions of northern Russia showing differing trends to recent, late 20th century, warming. However the long coring equipment was confiscated by customs officials at Moscow airport so only short cores, covering approximately the past 750 years, were obtained from the Putorana Plateau. The lakes on the Putorana Plateau were selected to represent differing habitat types based on the physical and vegetation characteristics of the catchments (see section 2.2.2). The locations of the coring sites are shown in Figure 2.4 and details of the core lengths and sampling resolution are given in Table 3.1. The coring procedures, laboratory methods, chironomid preparation and counting techniques are described in Chapter 3. The cores, measuring 28 – 35cm in length, were extruded in the field.

The chironomid assemblages were determined in sediment samples from the top 0.5 -1.0 cm and bottom 1 cm of each core. Estimations of contemporary chironomid-inferred July air temperatures were derived using an inference model based on the Norwegian and archived Pechora samples (Table 2.1). This analysis was undertaken before compilation of the Russian training set was completed; therefore data was only available from these lakes. Details of the species and environmental data used are given in Chapter 4. The cores had not been dated at this stage and were of varying lengths, therefore the age of the basal sediment probably differed between cores. Despite these restrictions this preliminary analysis enabled cores showing marked compositional changes to be, relatively quickly, selected for more detailed study.

Table 7.1. Temperature reconstructions based on chironomid assemblages in surface and basal sediments from short cores collected in the Putorana. Lakes selected for further analysis are shown in bold.

Altitude	Lake code	Temperature °C	
		Surface	Base
High 740 - 805m asl	PTHE	10.0	9.8
	PFOR	10.6	9.8
	PTWO	10.7	10.9
Intermediate 595 - 670m asl	ARTE	10.8	10.5
	PONE	8.7	11.8
	PFIV	9.3	8.9
Flood plain 555 - 575m asl	WILD	10.2	10.2
	AFOX	9.8	10.3
	GYXO	9.2	9.8

From the temperature estimates (Table 7.1) AFOX, PONE and PTHE were selected for further analysis. AFOX and PTHE were selected as they showed contrasting temperature trends; estimated air temperatures decreased by 0.5°C between the base and surface of the core at AFOX and increased by 0.2°C at PTHE. The reconstructed temperatures from PONE showed the greatest change of any lakes, decreasing by 3.1°C. Although temperature changes were greater in PFOR than the other high altitude lakes, only surface and basal sediments were available from this lake. PTWO also showed marked changes

in chironomid composition but was not selected due to the influence of a major inflow from a larger lake to the south. The inflow means it is possible that some larval subfossils or living larvae may be allochthonous rather than organisms which developed *in-situ* and therefore may not reflect local environmental conditions. The selected lakes are also representative of the altitudes sampled.

These selected cores were considered suitable for high resolution palaeolimnological analyses as they fulfilled the following criteria:

1. The cores were from undisturbed lake systems in order to maximise the climatic signal in the palaeolimnological record;
2. The abundance of the chironomid subfossils was high to enable the core to be sampled at high temporal resolution (0.5cm intervals) and;
3. The assemblage was taxon rich, having marked changes in faunal composition, indicating the assemblages are sensitive to environmental change.

The following sections 7.3.1 – 7.3.3 briefly describe the catchment characteristics of each lake with photographs and sketch maps (Figures 7.1, 7.2 and 7.3). Other environmental characteristics, such as water chemistry data, are detailed in Table 4.1.

7.3. Descriptions of selected lakes

7.3.1. Lake AFOX

AFOX is a small thermokarst lake on the valley flood plain between two larger lakes (lake 2 in Figure 2.4); the catchment is constrained by low clay ridges approximately 3-4 metres from the waters edge. Ridges to the south and east separate the lake from a river connecting the larger lakes. Emergent reed beds grow intermittently along the northern shore and raised sedge tussocks in gently shelving areas. Catchment vegetation is dominated by *Betula nana*, *Alnus* sp. and *Salix* spp. Axe-cut timbers and debris (glass bottles and tin cans), near the north-west shore suggest the area had been visited by fur trappers within the last 55 years. The 28cm core was taken at 4.1m water depth. The top 5cms were composed of slightly green – brown organic-rich gyttja, from 5 – 14 cm the sediment graded, gradually, to grey clay and the bottom 14 – 28 cm was grey clay.

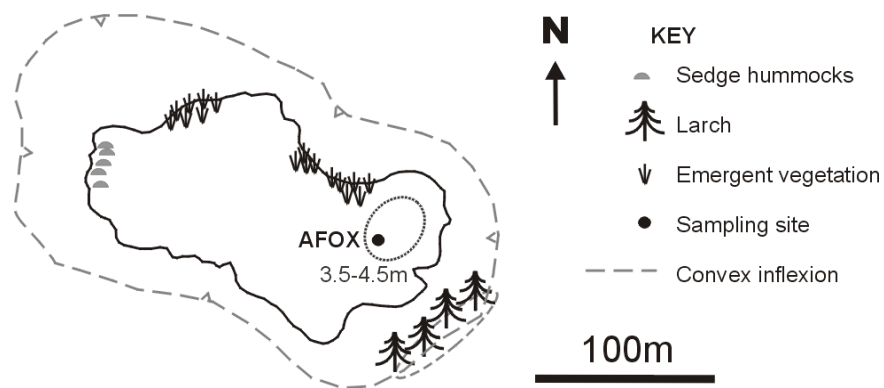
Figure 7.1. Unnamed lake, Code AFOX. (a) photograph by N. Solovieva, 2006 and (b) sketch map showing the simplified morphometry and location of the sampling site.

68.166390N, 92.228056E, Altitude 573m a.s.l., Area 1.5 ha, Depth 4.9 m, pH 7.28

(a)



(b)



7.3.2. Lake PONE

PONE is a small lake situated within the undulating topography of a hanging valley between two mountains (lake 5 in Figure 2.4). An outflow stream flows to the north-east, down the valley to other lakes. *Alnus* sp., *Salix* spp. and *B. nana* dominate the vegetation with occasional scattered larches on the higher ridges. The western shore is rocky and gently shelving with scattered sedge tussocks. The analysed core (PONE 1) was 28cm in length and collected at 5m water depth. Core PONE 2 comprised surface sediments (0 – 1 and 1 – 2 cm depth) only (Table 3.1) and was not analysed in this thesis. The top 0 – 2 cm of PONE 1 was composed of loose organic-rich sediment, from 2 – 10cm green – brown gyttja and below 10cm grey clay.

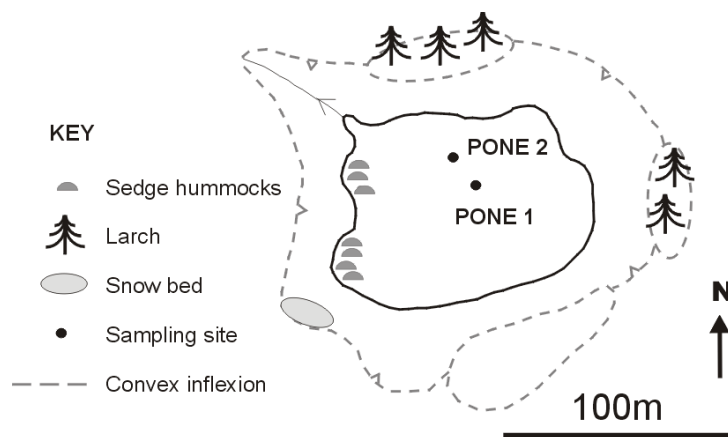
Figure 7.2. Unnamed lake, Code PONE. (a) photograph by N. Solovieva, 2006 and (b) sketch map showing the simplified morphometry and location of the sampling site.

68.142500N, 92.203056E, Altitude 596m a.s.l., Area 0.9 ha, Depth 5 m, pH 7.7

(a)



(b)



7.3.3. Lake PTHE

PTHE was the highest altitude lake sampled, at 805m and is located in a small rocky hollow below a 858m-summit on the plateau (lake 7 in Figure 2.4). Several small streams rise in the catchment and flow into the lake, these are probably fed by melt water from widespread snow beds on north and west-facing slopes and melt water from the active layer. The groundcover was predominately bare rock and talus slopes (20 – 80% by area) with sparse shrub-lichen tundra vegetation under 10cm in height. The 35cm core was collected at 3.7m water depth. The top 2cm was composed of loose algal

material, between 2 - 10cm the sediment graded, gradually, from gyttja to grey clay and the bottom 25cm comprised grey clay. Further analysis of the cores and details of the chironomid assemblages are discussed in the following sections.

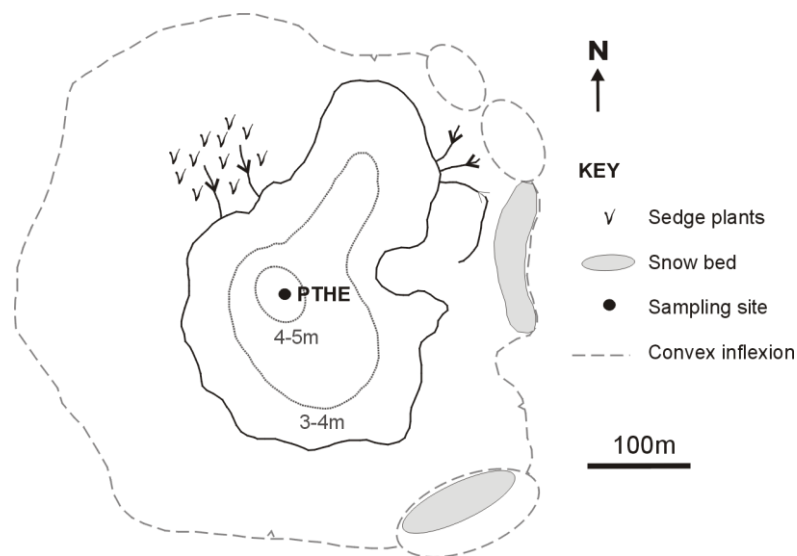
Figure 7.3. Unnamed lake, Code PTHE. (a) photograph and (b) sketch map showing the simplified morphometry and location of the sampling site.

68.203333N, 92.178889E, Altitude 805m a.s.l., Area 6.3 ha, Depth 3.9 m, pH 7.28

(a)



(b)



7.4. Radiometric chronologies

Age-depth models were developed for PONE and PTHE based on ^{210}Pb dating of sediments, constrained by ^{137}Cs and ^{241}Am . Analysis of the radionuclides was performed by H. Yang of UCL, as described in section 3.3.4.1, and development of the individual chronologies are described in the following

sections. AFOX was not dated as the wide fluctuations in dry weight suggest the lake material may contain allochthonous material and organisms, the data are presented in section 7.5.1.

7.4.1. PONE

Unsupported ^{210}Pb activities, calculated by subtracting supported ^{210}Pb activity from total ^{210}Pb activity, decline more or less exponentially with depth (Table 7.2, Figure 7.4a). This suggests there have not been significant changes in sediment accumulation rates and therefore ^{210}Pb chronological dates were calculated using CRS (Constant Rate of Supply) dating models (Appleby and Oldfield 1978).

Table 7.2. Summary table showing the ^{210}Pb and ^{137}Cs activity with respective errors, for the core PONE

Sample depth (cm)	^{210}Pb activity (Bq/kg)	Counting error (Bq/kg)	^{210}Pb unsupported activity (Bq/kg)	^{137}Cs activity (Bq/kg)	Counting error (Bq/kg)
0.5	221.63	25.86	203.3	36.78	3.83
1.75	240.35	18.34	224.76	37.91	2.81
2.75	150.57	11.02	135.56	52.1	1.92
3.25	95.65	12.31	83.73	52.6	2.52
3.75	121.95	17.89	114.38	56.96	3.31
4.75	86.37	11.67	72.77	53.23	2.15
6.25	39.13	8.43	25.28	5.55	0.98
7.75	35.8	8.9	22.25	1.35	0.93
9.25	13.1	5.91	2.3	0.96	0.64
12.25	7.74	4.85	-7.34	0.47	0.54
24.25	7.6	5.32	-5.46	0	0

The ^{137}Cs activity shows a relatively well-resolved peak at 3.75 cm (sample 4 – 3.5cm), recording the 1963 fallout maximum from the atmospheric testing of nuclear weapons (Figure 7.4b). This is in good agreement with the CRS model which places 1963 at 4 cm. The sediment accumulation rate declines from 79 years BP (6 cm) extrapolating the age – depth curve from this period gave an estimated age of 630 years BP for the base of the core (Figure 7.5). Dates, extrapolated beyond the age range of the dating technique, should be used with caution as variations in the sediment accumulation rate can significantly affect the estimated age. Present-day in these chronologies is 2006, the year of sampling.

Figure 7.4. Stratigraphy of (a) unsupported ^{210}Pb and total ^{210}Pb activity; and (b) the ^{137}Cs maximum; a stratigraphic marker for 1963 in PONE

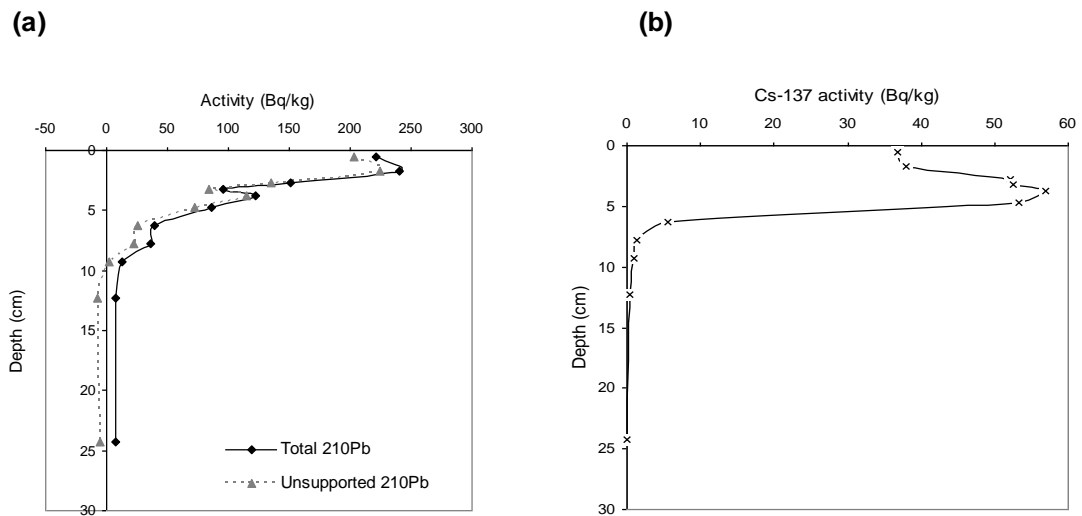
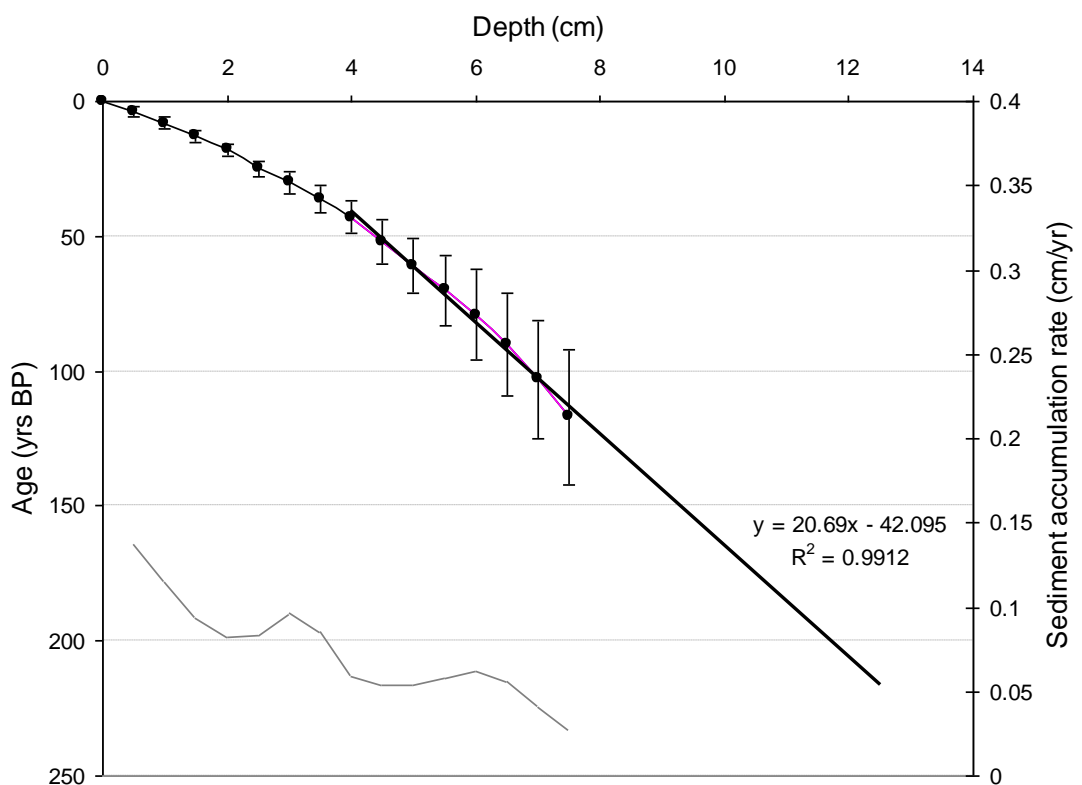


Figure 7.5. Age-depth model and sediment accumulation rates for core PONE. (Sediment accumulation rates are shown in grey and ages in black with 2 SD error). Regression coefficient (R^2) and linear equation of age-depth relationship extrapolated from the period 79 - 117 years BP are shown. The age of the sediments is calculated from the linear equation where $y = \text{age in years BP}$ and $x = \text{depth of sample, in cm, below sediment - water interface}$.



7.4.2. PTHE

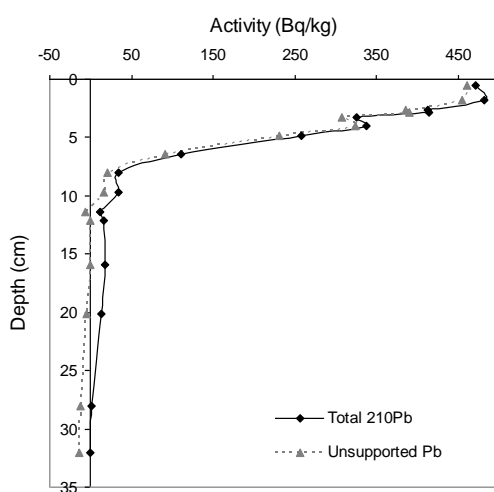
Unsupported ^{210}Pb activities decline more or less exponentially with depth between 4cm and 8cm which suggests a uniform sediment accumulation rate in this section of the core (Table 7.3, Figure 7.6a). However the relatively small change in unsupported ^{210}Pb activity in the top 4 cm indicates that this part of the core accumulated rapidly.

Table 7.3. Summary table showing the ^{210}Pb and ^{137}Cs activity with respective errors, for the core PTHE

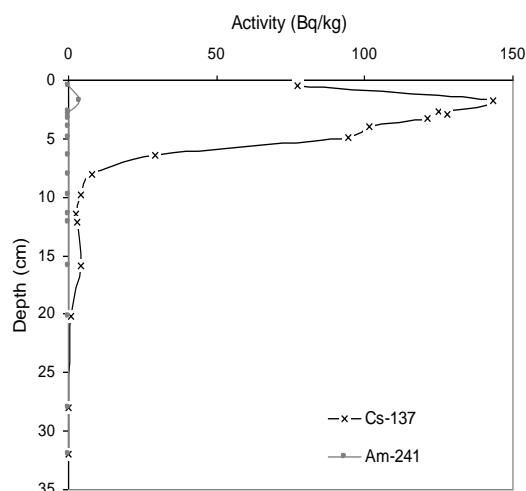
Sample depth (cm)	^{210}Pb activity (Bq/kg)	Counting error (Bq/kg)	^{210}Pb unsupported activity (Bq/kg)	^{137}Cs activity (Bq/kg)	Counting error (Bq/kg)
0.5	471.54	20.59	461.54	77.42	3.34
1.75	482.06	19.33	454.45	143.32	3.76
2.67	413.54	19.98	386.11	124.97	3.95
2.88	414.57	19.84	389.71	128.03	3.94
3.25	325.73	24.85	307.43	121.15	5.16
4	338.04	18.18	324.29	101.42	3.7
4.88	257.89	20.22	231.07	94.57	4.06
6.38	110.81	14.12	90.58	29.3	2.24
8	33.62	8.48	20.36	7.88	0.98
9.75	33.82	12.5	16.75	4.02	1.48
11.38	11.88	10.91	-6.75	2.67	1.27
12.13	16.25	6.7	-0.22	2.87	0.81
15.88	17.8	7.47	-0.95	4.24	0.86
20.13	12.67	7.48	-4.69	0.97	0.87
28	1.15	6.88	-11.84	0	0
32	0	0	-13.72	0	0

Figure 7.6. Stratigraphy of (a) unsupported ^{210}Pb and total ^{210}Pb activity; and (b) the maxima of the artificial fallout radionuclides ^{137}Cs and ^{241}Am , stratigraphic markers for 1963 in PTHE.

(a)



(b)



The ^{137}Cs and ^{241}Am activities show peaks at 1.75 cm depth (sample 2 – 1.5cm), recording the 1963 fallout maximum from the atmospheric testing of nuclear weapons (Figure 7.6b). ^{210}Pb chronological dates were calculated using the CRS (Constant Rate of Supply) and CIC (Constant Initial Concentration) dating models (Appleby 2001). The CRS method is used when sediment accumulation rates are uniform and continuous as demonstrated by the exponential decline in unsupported ^{210}Pb activity with depth, as shown in core PONE. However in areas with non-uniform accumulation the CIC (Constant Initial Concentration) model is widely used (Appleby 2004). This assumes that sediments have a constant initial ^{210}Pb concentration regardless of accumulation rates (Appleby 2001). The CRS and CIC models place the 1963 layer at 4.6 cm and 5.5 cm, respectively, which are below the 1963 layer suggested by the ^{137}Cs and ^{241}Am records. The CRS model places the 1963 layer closer to the artificial radionuclides marker than the CIC model which suggests that the CRS model is more valid. Due to the irregular nature of the ^{210}Pb record, the final chronology of the core was calculated by the CRS model and corrected using ^{137}Cs and ^{241}Am records. The corrected results show that post-1963 ^{210}Pb flux is $28.4 \text{ Bq m}^{-2} \text{ yr}^{-1}$, this is about 40% of that in pre-1963 section and suggests that part of the recent sedimentary sequence, i.e. above 1.75cm, is missing. Field observations and isotopic composition, presented in section 7.5.3, suggest a gelatinous algal or cyanobacterial growth is present at ca. 2 – 1.75cm depth, the growth of which may have altered the topography of the sediment surface causing a hiatus in sediment accumulation.

The sediment accumulation rates are relatively constant between 8 – 4 cm, with a mean at $0.00626 \text{ g cm}^{-2} \text{ yr}^{-1}$, then increases upwards, declining to a low level in the top 2 cm of the core due to the anomalous surface sediments. The chronology and sediment accumulation rates of the core are shown in Figure 7.7. As the sediment accumulation rate remained constant from 8 – 4 cm the linear relationship of age versus depth for this period was extrapolated to provide estimated ages for the remainder of the core (Figure 7.7). As with PONE, dates extrapolated beyond the age range of the dating technique should be used with caution and present-day in these chronologies is 2006, the year of sampling

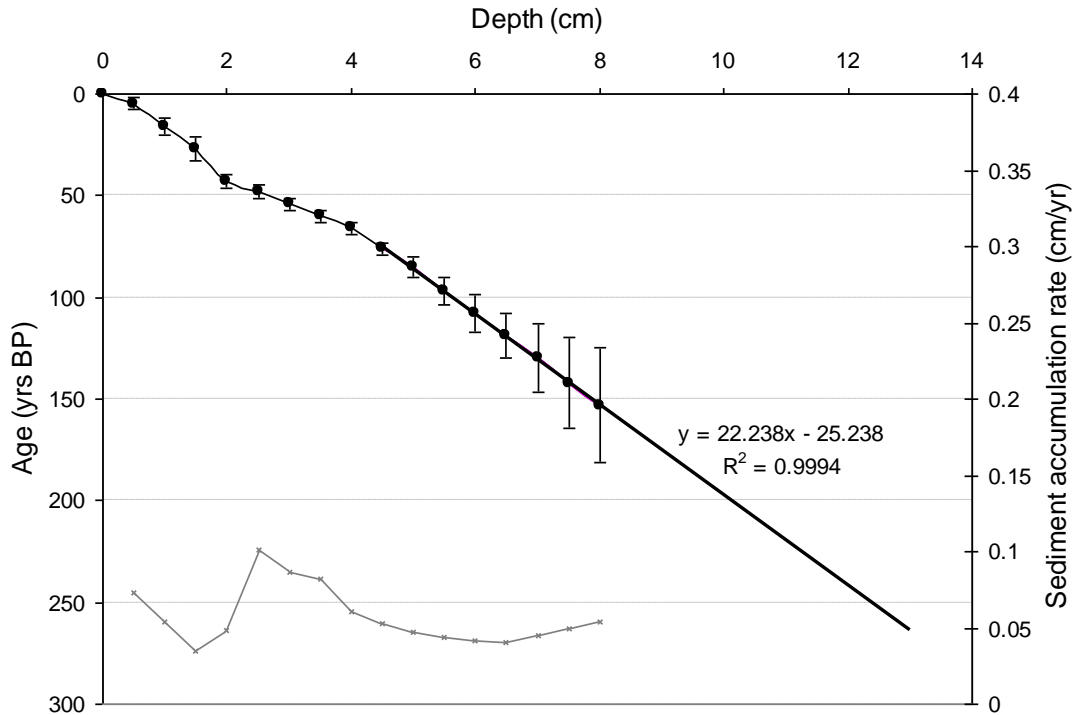


Figure 7.7. Age-depth model and sediment accumulation rates for core PTHE. (Sedimentation rates are shown in grey and ages in black with 2 SD error). Regression coefficient (R^2) and linear equation of age-depth relationship extrapolated from the period 66 – 153 years BP are shown. The age of the sediments is calculated from the linear equation where y = age in years BP and x = depth of sample, in cm, below sediment – water interface.

7.5. Sedimentary analysis

Dry weight and LOI were determined for AFOX, PONE and PTHE as described in section 3.3.2.1. Percentage loss-on-ignition (LOI) reflects the proportions of organic carbon and mineral matter in the sediment (for example Dean 1974; Birks and Birks 2006) and is used to summarise changes in the lake ecosystem including bioproductivity. The %TOC and carbon and nitrogen isotopic composition ($\delta^{13}\text{C}$ and $\delta^{15}\text{N}$) of the lake sediments were determined as described in section 3.3.2.2. Isotopic composition and C:N ratios were used to assess the relative importance of autochthonous and allochthonous sources of organic material to the lakes. The carbon isotopic composition ($\delta^{13}\text{C}$) of organic matter in the lake sediment is used to determine the dominant source of carbon in the lake (Meyers and Teranes 2001). However there is considerable overlap

in $\delta^{13}\text{C}$ values and C:N ratios are used to help distinguish between algal and vascular plant sources (Meyers and Teranes 2001). Similarly the nitrogen isotopic composition of sediment organic matter can help distinguish changes in the sources and availability of nitrogen to the lake (Meyers and Teranes 2001). The dynamics of the nitrogen biogeochemical cycle are more complicated than those of carbon so interpretation of sedimentary $\delta^{15}\text{N}$ records can be difficult (Talbot 2001). The results of the isotopic analysis only represent a preliminary interpretation as multi-proxy studies are required to fully interpret the results. For example, changes in pH would affect the carbonate:bicarbonate equilibrium of the water and, therefore, the $\delta^{13}\text{C}$ of the inorganic carbon. The chironomid subfossil assemblages do not show any major shifts from acidophilic to acidophobic taxa, or visa versa, however multi-proxy data such as diatom-inferred reconstructions are required to quantify past pH changes. In the absence of this quantitative data, and as no pH-related shifts in chironomid fauna were observed, the $\delta^{13}\text{C}$ of inorganic carbon is assumed to have remained constant through time. Further analysis, with multi-proxy data, will be the subject of future research. The cores, PONE and PTHE, were ^{210}Pb dated; approximate dates are based on the age-depth models developed in the previous section.

7.5.1. AFOX

The lake AFOX is situated on the valley flood plain and is separated from a river by low clay ridges (section 7.3.1). The percentage dry weight and LOI showed rapid, large variations of up to 25% in % dry weight (Figure 7.8). Fluctuations in the mineralogical fraction are associated with changes in the sedimentation rate and/or the sediment source. The fluctuations suggest the lake is prone to episodic flooding. It is, therefore, possible that some subfossil or living larvae may be allochthonous rather than organisms which have developed *in-situ* responding to local environmental conditions. Palaeoenvironmental reconstructions may be unreliable so apart from a preliminary analysis of the chironomid assemblages (section 7.6.1) this core was not analysed further.

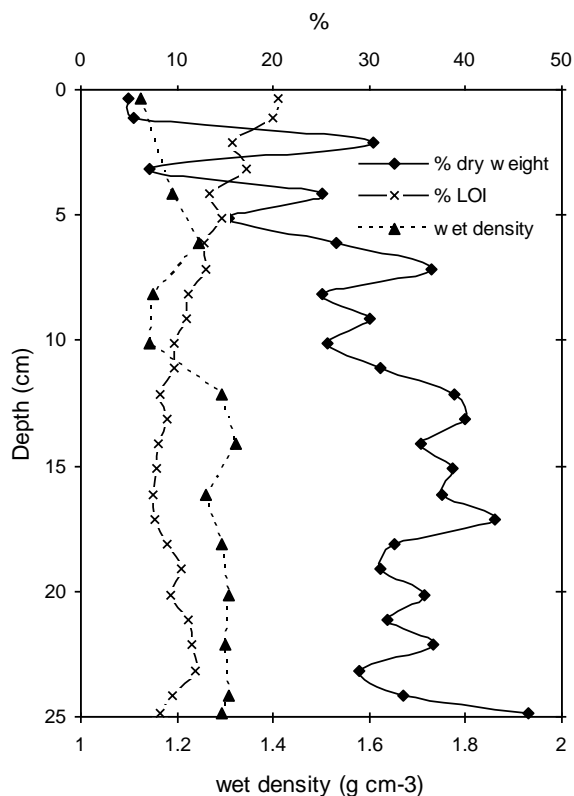


Figure 7.8. Wet density, percentage dry weight and loss-on-ignition in sediment core from AFOX

7.5.2. PONE

The percentage dry weight record from PONE shows differences of up to 11% between consecutive samples. These fluctuations are less than those observed in AFOX but suggest there are periodic variations in the rate and/or sources of sediment influxes to the lake, possibly associated with flooding or spring melt-out. In general, dry weight remains at 35 – 45% from the base of the core to approximately 350 years BP (17cm depth), decreases to 30 – 34% until 110 years BP (7cm depth) and gradually decreases to 24% at the top of the core (Figure 7.9). The decrease in dry weight over the past 100 years is accompanied by increases in LOI and TOC. LOI remains relatively stable at 9.6 – 11.9% from the base of the core until approximately 80 years BP (6 cm depth) then increases to 16.2% at the top of the core. TOC shows similar trends; values generally remaining stable at 3.0 – 4.0% until approximately 80 years BP (6 cm depth), then increase to 7.6% at the top of the core.

In general, C:N mass ratios for PONE remains between 9.5 – 15.5 mass ratio (11.0 – 18.2 atomic ratio) from the base of the core until ca. 20 years BP (2cm depth) (Figure 7.9) indicating a mixed aquatic – terrestrial carbon source,

dominated by submerged or floating macrophytes and/or aquatic algae (Meyers 1994; Tyson 1995). There are a number of peaks in the C:N ratio greater than 18 (21 in atomic ratio), for example at 22cm and 26cm depth. These excursions, particularly those associated with peaks in % LOI, %TOC and/or dry weight, may be associated with influxes of emergent or terrestrial vegetation into the lake.

The $\delta^{13}\text{C}$ and $\delta^{15}\text{N}$ records vary between -28 to -25 ‰ and +2.5 to +3.8 ‰, respectively, from the base of the core to 8cm depth, approximately 125 years BP. The $\delta^{13}\text{C}$ values are typical of lacustrine algae and C3 plants; the $\delta^{15}\text{N}$ of modern plankton is typically +2 to +14‰ (Talbot 2001), and the results indicate a predominantly algal source. The $\delta^{13}\text{C}$ and $\delta^{15}\text{N}$ records corroborate the C:N ratios that the carbon source is autochthonous (Meyers and Teranes 2001). The increase in $\delta^{13}\text{C}$ to less negative values (ca. -25‰) at 9.75 to 13.5 cm depth may indicate minor shifts in the plant community within the lake.

The gradual decrease in $\delta^{13}\text{C}$ and $\delta^{15}\text{N}$ between 8 – 2cm depth from -27.7 to -28.7‰ and +2.8 to +0.4‰ respectively, accompanied by increasing % LOI and TOC may reflect an increase in productivity. However the increases in LOI and TOC might also reflect a decrease in mineralogenic input and concomitant dilution of $\delta^{13}\text{C}$ and $\delta^{15}\text{N}$ values. Peaks in the % dry weight and C:N ratio, between 8 – 2cm depth, suggest periodic inwashing of material has occurred which may also affect the $\delta^{13}\text{C}$ and $\delta^{15}\text{N}$ records. The gradual decrease in $\delta^{15}\text{N}$ over this period might reflect a decreasing rate of soil organic matter degradation, reduced flux of soil nitrate from the catchment and/or an increase in the relative importance of atmospheric nitrogen as a source of nitrogen (Talbot 2001). In high altitude lakes in Colorado, USA a decrease of 2 – 3.5‰ in the $\delta^{15}\text{N}$ record, since 1900, has been attributed to changes in meltwater dynamics (Enders et al. 2008) and/or enhanced atmospheric deposition of fixed nitrogen from anthropogenic sources (Wolfe et al. 2001).

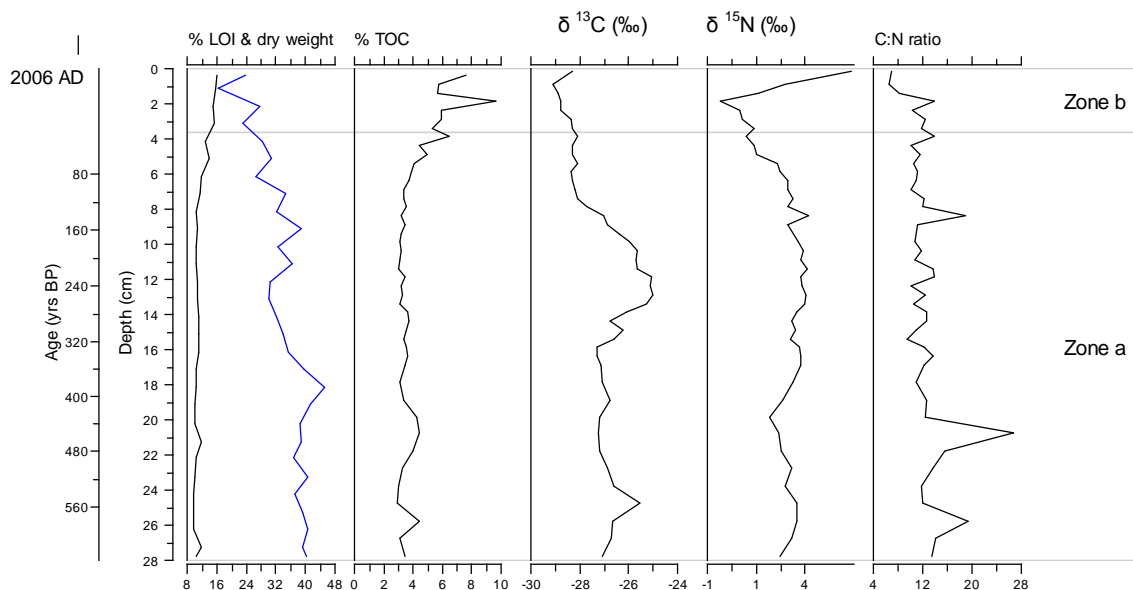


Figure 7.9. % LOI, % dry weight, % TOC, $\delta^{13}\text{C}$ (‰) and $\delta^{15}\text{N}$ (‰) from bulk sediment analysis of core PONE with C/N mass ratio. Zones displayed correspond to zones based on chironomid data (section 7.6.2). (%LOI shown as black line and % dry weight as blue line).

The increase in organic matter towards the top of the core, shown in the dry weight, LOI and TOC records, coincides with increases in $\delta^{15}\text{N}$ from +0.4‰ at 2cm depth to 5.9‰ at the surface and in $\delta^{13}\text{C}$ from -29.1‰ at 1cm depth to -28.3‰ at the surface. The direction and magnitude of the isotope alteration, particularly the decrease in $\delta^{15}\text{N}$ values with depth, is typical of degradation of organic material under anoxic condition which results in bacterial growth adding ^{15}N -depleted biomass to the residual material (Lehmann et al. 2002). The more pronounced decreases in the $\delta^{15}\text{N}$ record than the $\delta^{13}\text{C}$ probably also accounts for the decrease in C:N ratio towards the top of the core. These decreases are probably early diagenetic changes but suggest the decompositional environment changed ca. 1985 (2cm depth) (Enders *et al.* 2008). The shifts in the organic carbon and isotope records at 6-7cm depth, approximately 100 years BP, predate the major changes in the chironomid record indicated by the zone boundary (zonation of the core is discussed in section 7.6.2).

7.5.3. PTHE

Percentage dry weights are lower and show less variation (< 2%) between consecutive samples than PONE or AFOX. This suggests a lower and more constant mineralogical input from the catchment and may reflect the low relief and sparse vegetation of the plateau summit. With the exception of the surface sediment (0-1cm) and peaks at 34cm and 7cm depth percentage dry weights remain relatively constant at 10 – 14% throughout the core indicating there has been with little change in sediment source or in-wash of allochthonous material during deposition (Figure 7.10). LOI remains relatively stable at 19 - 22% from the base of the core (ca. 725 years BP) until approximately 150 years BP (8cm depth). LOI then increases steadily from 19% to 25% 40 years BP (2cm depth). TOC is initially high near the base of the core, 32 – 28cm depth, at ca. 8.5%. From approximately 600 years BP (28cm depth) the TOC decreases and stabilises at 7.5 to 8% between 600 and 150 years BP (18 – 8cm depth). TOC steadily increases from 8cm to 2cm depth suggesting organic carbon accumulation has increased from ca. 8% to 10%. The gradual increase in LOI and TOC over the past 150 years (from 8cm depth) probably reflects an increasing contribution of organic material to the sediment.

C:N mass ratios for PTHE remain relatively constant at 9.2 – 10.9 mass ratio (10.7 – 12.7 atomic ratio) from the base of the core until ca. 45 years BP (2cm depth) indicating a predominantly submerged or floating macrophytes and/or aquatic algal source for carbon (Meyers 1994; Tyson 1995). C:N ratios are similar to those from PONE however the $\delta^{13}\text{C}$ values are more positive; from the base of the cores to 2cm depth the $\delta^{13}\text{C}$ values in PTHE range from -19.5 to -18.5‰ compared to -28 to -25‰ in PONE. This would suggest that more carbon is derived from macrophytes in PTHE than PONE. The stepped changes in the $\delta^{15}\text{N}$ records between 34 – 6cm depth reflect changes in the sources of dissolved inorganic nitrogen which is subsequently incorporated into organic matter. As the C:N ratio remains relatively stable, suggesting little change in the vegetation composition, the stepwise positive increases may reflect an increasing contribution from rainfall, soil organic matter or terrestrial plants. The general decrease in $\delta^{15}\text{N}$ from 6 – 2.5 cm depth may reflect enhanced atmospheric deposition of nitrogen from anthropogenic sources

(Wolfe et al. 2001; Enders et al. 2008) as discussed for PONE. Both PONE and PTHE show a general trend of decreasing $\delta^{15}\text{N}$ values between ca. 300 and 50 years BP; this is consistent with an observed decrease in $\delta^{15}\text{N}$ values in the Greenland ice-core due to deposition of nitrate derived from fossil fuel emissions (Hastings *et al.* 2009). The deviation in trends over the last 50 years between the cores, and with the Greenland ice-core records, suggests that localised, within-lake processes have strongly influenced the recent record.

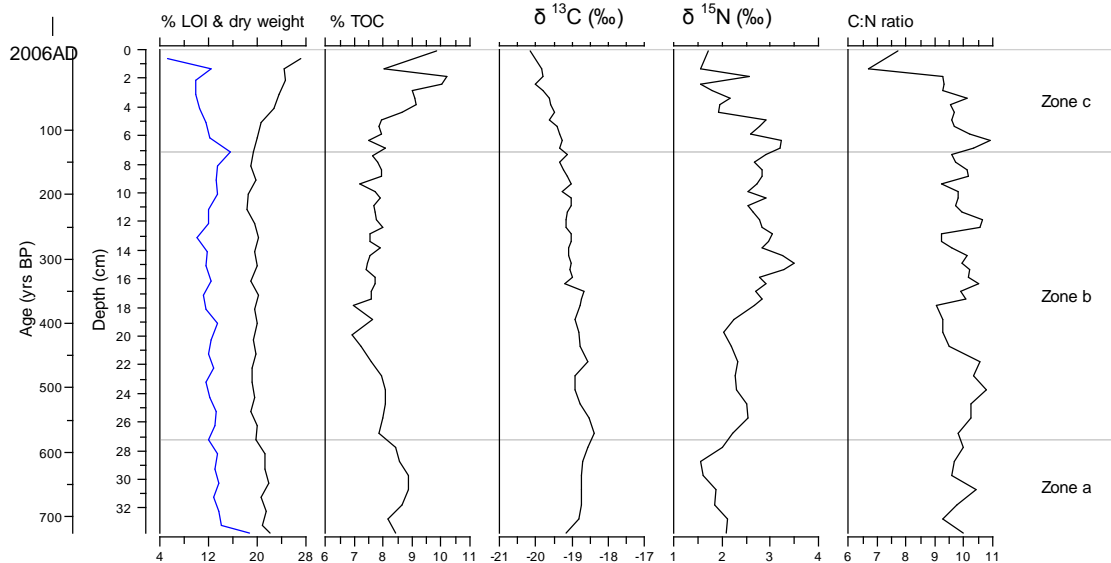


Figure 7.10. % LOI, % dry weight, % TOC, $\delta^{13}\text{C}$ (‰) and $\delta^{15}\text{N}$ (‰) from bulk sediment analysis of core PTHE with C/N mass ratio. Zones displayed correspond to zones based on chironomid data (section 7.6.3). (%LOI shown as black line and % dry weight in blue).

The $\delta^{13}\text{C}$ values show slight decreases over the past 30 years, from 1.5cm depth to the surface. This trend is not characteristic of microbial degradation under oxic or anoxic conditions (Lehmann et al. 2002) and suggests little or no biodegradation of organic matter is occurring in the surface sediments. Major shifts in the LOI, TOC, dry weight, $\delta^{15}\text{N}$ and C:N ratio occur at approximately 1.75 – 2.5 cm depth (Figure 7.10). The decline in C:N ratio from 9.2 to 6.7 suggests an increasing contribution from phytoplankton whilst the increase in $\delta^{15}\text{N}$ from +1.5‰ to +2.6‰ may indicate an increase in atmospheric nitrogen-fixing organisms such as cyanobacteria. Both TOC and LOI show concurrent decreases, the associated increase in dry weight probably reflects a change in percentage contribution rather than absolute value. The water content of the sediments from 2cm depth to the surface is high, ca. 95%. The isotopic data

supports the presence of *in-situ* algal growth at this depth, as noted in the field (section 7.3.3) which may have disrupted sediment accumulation rates in the core (as discussed in section 7.4.2).

7.6. Chironomid biostratigraphies

Chironomid larval head capsules were prepared and identified from subsamples of the AFOX, PONE and PTHE cores as described in section 3.3.2.3. Results of the down-core chironomid analysis are presented as percent abundance diagrams using the computer program C2 (Juggins 2005). Stratigraphic diagrams from PONE and PTHE were zoned by optimal sum-of-squares partitioning using the ZONE program, version 1.2 (Juggins 1991); the statistical significance of the zones was assessed using BSTICK (Bennett 1996).

7.6.1. AFOX

The wide fluctuations in sediment dry weight in the AFOX core (section 7.5.1) suggested the lake may have been periodically flooded by the neighbouring river system. The chironomid subfossils may, therefore, be allochthonous and unreliable for palaeoenvironmental reconstructions. The results are presented as a rough, undated stratigraphy (Figure 7.11), without further analytical or statistical analysis, for comparison with the other two cores. In total 53 taxa were identified in the AFOX core. Of these, 21 taxa were represented by one or two specimens only (Table 7.4) and include single occurrences of terrestrial taxa such as *Bryophaenocladus* (Cranston et al. 1983) and *Pseudosmittia* (Strenzke 1950).

Table 7.4. Chironomid fauna of AFOX core, with total number of occurrences (in 10 sub-samples), effective number of occurrences (Hill's N2) and minimum and maximum percent abundance.

Subfamily	Taxa	No. of occurrences	Hill's N2	Min % abundance	Max % abundance
Chironominae	Chironomini				
	<i>Chironomus anthracinus</i> -type	8	4.9	0	11.8
	Chironomini larvula	6	4.8	0	3.6
	<i>Chironomus plumosus</i> -type	2	2.0	0	1.3
	<i>Cladopelma</i>	3	3.0	0	1.4
	<i>Glyptotendipes pallens</i> -type	1	1.0	0	0.7
	<i>Phaenopsectra flavipes</i> -type	3	2.1	0	2.8
	<i>Sergentia coracina</i> -type	10	8.5	1.6	7.5
	<i>Stictochironomus rosenschoeldi</i> -type	1	1.0	0	0.9
	Pseudochironomini				
	<i>Pseudochironomus</i>	1	1.0	0	0.7
	Tanytarsini				
	<i>Cladotanytarsus mancus</i> -type	5	3.4	0	6.0
	<i>Corynocera ambigua</i>	10	8.9	9.2	50.7
	<i>Corynocera oliveri</i> -type	7	4.7	0	8.9
	<i>Micropsectra insignilobus</i> -type	10	7.1	1.3	28.6
	<i>Micropsectra radialis</i> -type	2	1.2	0	4.9
	<i>Paratanytarsus austriacus</i> -type	2	1.9	0	2.5
	<i>Paratanytarsus penicillatus</i> -type	3	1.9	0	4.8
	<i>Paratanytarsus undifferentiated</i>	6	5.6	0	2.8
	<i>Stempellinella - Zavrelia</i>	7	5.9	0	5.3
	<i>Tanytarsus lugens</i> -type	10	7.0	1.6	14.7
<i>Tanytarsus mendax</i> -type	6	5.1	0	4.8	
<i>Tanytarsus pallidicornis</i> -type	10	7.4	0.6	11.2	
<i>Tanytarsini undifferentiated</i>	9	8.1	0	7.2	
Orthoclaadiinae	<i>Abiskomyia</i>	5	4.2	0	5.0
	<i>Bryophaenocladus-Gymnometriocnemus</i>	1	1.0	0	1.6
	<i>Corynoneura arctica</i> -type	4	3.1	0	3.0
	<i>Corynoneura edwardsi</i> -type	2	1.8	0	2.6
	<i>Cricotopus bicinctus</i> -type	2	1.8	0	1.3
	<i>Cricotopus cylindraceus</i> -type	5	4.1	0	3.9
	<i>Cricotopus laricomalis</i> -type	5	3.9	0	3.4
	<i>Cricotopus sylvestris</i> -type	3	2.4	0	3.0
	<i>Cricotopus</i> type C	2	2.0	0	1.2
	<i>Cricotopus</i> type P	3	2.8	0	1.4
	<i>Orthocladus</i> type S	2	1.7	0	0.7
	<i>Orthocladus undifferentiated</i>	3	3.0	0	1.6
	<i>Heterotrissocladus grimshawi</i> -type	2	2.0	0	1.6
	<i>Heterotrissocladus maeaeri</i> -type	7	5.8	0	3.2
	<i>Hydrobaenus conformis</i> -type	2	2.0	0	1.3
	<i>Hydrobaenus johannseni</i> -type	1	1.0	0	1.5
	<i>Limnophyes - Paralimnophyes</i>	5	4.3	0	2.4
	<i>Mesocricotopus</i>	1	1.0	0	2.3
	<i>Paracladius</i>	3	2.4	0	1.7
	<i>Parakiefferiella bathophila</i> -type	3	2.6	0	1.4
	<i>Parakiefferiella nigra</i> -type	1	1.0	0	1.6
	<i>Parakiefferiella triquetra</i> -type	6	5.0	0	2.6
	<i>Psectrocladius septentrionalis</i> -type	1	1.0	0	0.9
	<i>Psectrocladius sordidellus</i> -type	9	7.3	0	5.3
	<i>Pseudosmittia</i>	2	1.9	0	2.6
	<i>Zalutschia</i> type B	8	6.6	0	7.7
	<i>Zalutschia zalutschicola</i>	2	1.9	0	1.5
Diamesinae	<i>Protanypus</i>	2	1.8	0	1.2
Prodiamesinae	<i>Monodiamesa</i>	1	1.0	0	1.5
Tanypodinae	<i>Ablabesmyia</i>	4	3.4	0	2.8
	<i>Procladius</i>	8	6.3	0	4.5

Sergentia coracina-type, *Corynocera ambigua*, *Micropsectra insignilobus*-type, *Tanytarsus lugens*-type and *Tanytarsus pallidicornis*-type occur throughout the core (Hill's N2 7.0-8.9). Of these taxa, *Corynocera ambigua* is the most abundant and occurs at 9 – 51% abundance. *S. coracina*-type, *M. insignilobus*-type, and *T. lugens*-type are cold stenotherms (Brundin 1956), but the temperature optima of *M. insignilobus*-type, for example, is higher than *M. radialis*-type which occurs only twice in the core at low abundance (Hill's N2 = 1.2). Similarly, the morphotaxa of *Heterotrissocladius* are valuable indicators of climate change in cold oligotrophic lakes (Brooks *et al.* 2007); the fauna includes *H. maeaeri*-type and *H. grimshawi*-type, but lacks *H. marcidus*-type found in the warmest lakes and *H. subpilosus*-type which occurs in the coldest lakes. The fauna is, therefore, typical of a relatively cold, oligotrophic lake.

The majority of rare taxa, including the terrestrial taxa *Bryophaenocladus* and *Pseudosmittia*, occur at 4cm and 22cm depth in the core. These intervals coincide with peaks in the mineralogical fraction (Figure 7.8) indicative of flood events suggesting terrestrial taxa may be washed into the lake during flooding. *Micropsectra insignilobus*-type, *Corynocera oliveri*-type, *Abiskomyia* and *Zalutschia* type B are common below 12cm depth (Figure 7.11). Above 12cm depth these taxa decline and are replaced by *Tanytarsus pallidicornis*-type, *Cladotanytarsus mancus*-type and *Zavrelia*. Cold-adapted taxa such as *Sergentia coracina*-type and *T. lugens*-type (Brundin 1956; Brodin 1986) are found throughout the core, but the presence of relatively warm taxa, including *C. mancus*-type (Brundin 1949; Brodin 1986), towards the top of the core may indicate a shift to warmer conditions.

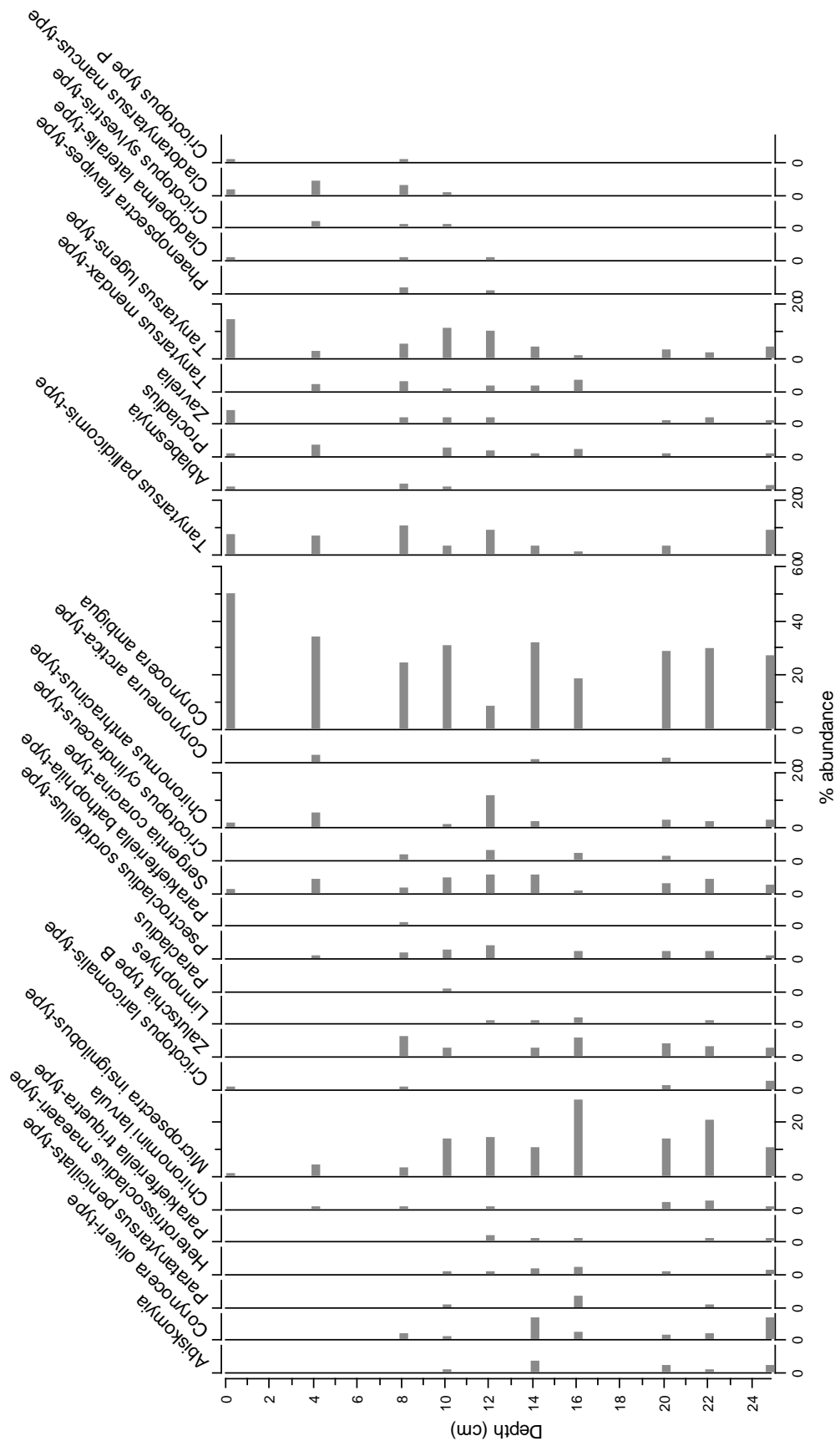
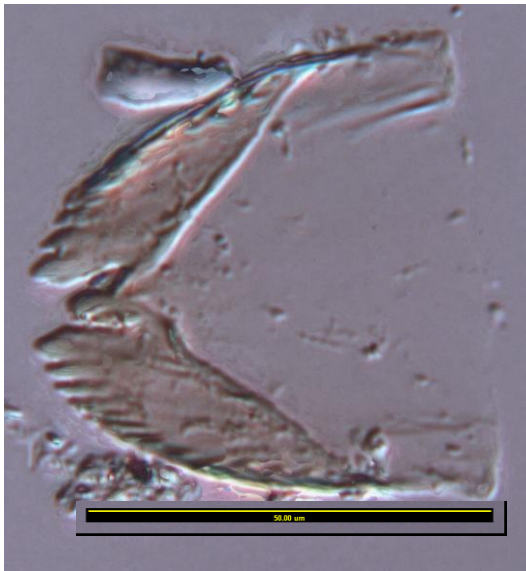


Figure 7.11. Chironomid stratigraphy, of taxa with more than 2 occurrences, from AFOX plotted against depth.

7.6.2. PONE

Sixty-two taxa were identified in the 17 samples analysed from core PONE; of these, 20 taxa were represented by one or two specimens only (Table 7.5). These rare taxa include *Thienemanniella clavicornis*-type and *Rheocrictopus* (at 27.75 cm depth) and *Rheotanytarsus* (at 12 – 8cm depths) which are typically found in flowing streams or rivers (Cranston *et al.* 1983; Pinder and Reiss 1983). Although there are no streams flowing into the lake at present the presence of these taxa suggests the hydrology of the lake may have changed over time. An unidentified Diamesinae and *Trichotanytus posticalis* form minor components of the assemblages (Figure 7.12). A single specimen of *T.posticalis* occurred in the basal sample (27.75cm) and the unidentified Diamesinae comprised 0.8 – 3% of the total fossil assemblage in a third of the down-core samples. *T. posticalis* is found among mosses in running or stagnant water across northern regions of the Holarctic (Brundin 1983). The mentum of the Diamesa sp. is similar to *D. aberrata*-type, but narrower with eight lateral teeth and five broad median teeth indented medially.

(a.)



(b.)

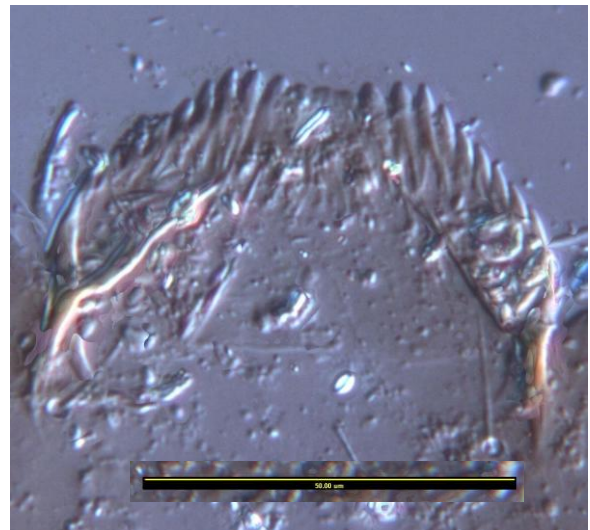


Figure 7.12. Larval mentum of (a) *Trichotanytus posticalis* and (b) unknown Diamesinae, at x400 magnification, scale bar = 50μm. (Photomontages by A. Polaszek, NHM).

Table 7.5. Chironomid fauna of PONE core, with total number of occurrences (in 17 subsamples), effective number of occurrences (Hill's N2) and minimum and maximum percent abundance.

Subfamily	Taxa	No. of occurrences	Hill's N2	Min % abundance	Max % abundance	
Chironominae	Chironomini					
	<i>Chironomus anthracinus</i> -type	10	8.0	0	6.0	
	Chironomini larvula	11	8.2	0	4.1	
	<i>Chironomus plumosus</i> -type	1	1.0	0	1.4	
	<i>Cladopelma lateralis</i> -type	4	2.8	0	2.8	
	<i>Dicrotendipes</i>	6	4.9	0	3.5	
	<i>Paracladopelma</i>	1	1.0	0	2.9	
	<i>Sergentia coracina</i> -type	11	9.5	0	3.5	
	<i>Stictochironomus rosenschoeldi</i> -type	12	9.4	0	8.2	
	Tanytarsini					
	<i>Cladotanytarsus mancus</i> -type	7	6.0	0	2.2	
	<i>Constempellina-Thienemanniola</i>	12	7.7	0	6.9	
	<i>Corynocera ambigua</i>	12	5.3	0	45.5	
	<i>Corynocera oliveri</i> -type	16	12.0	0	27.1	
	<i>Micropsectra insignilobus</i> -type	15	10.0	0	13.2	
	<i>Micropsectra radialis</i> -type	1	1.0	0	1.2	
	<i>Paratanytarsus austriacus</i> -type	9	6.8	0	5.3	
	<i>Paratanytarsus penicillatus</i> -type	3	2.6	0	4.9	
	<i>Paratanytarsus</i> undifferentiated	15	13.4	0	6.4	
	<i>Rheotanytarsus</i>	2	2.0	0	1.4	
	<i>Stempellinella - Zavrelia</i>	12	8.2	0	7.6	
	<i>Tanytarsus lugens</i> -type	17	14.9	5.2	22.8	
	<i>Tanytarsus mendax</i> -type	8	7.6	0	2.2	
	<i>Tanytarsus pallidicornis</i> -type	8	6.1	0	4.8	
	<i>Tanytarsini</i> undifferentiated	15	12.6	0	7.1	
	Orthoclaadiinae	<i>Abiskomyia</i>	13	7.8	0	13.0
		<i>Chaetocladius</i>	2	1.7	0	1.3
		<i>Corynoneura arctica</i> -type	13	8.5	0	8.2
		<i>Corynoneura edwardsi</i> -type	2	2.0	0	2.6
		<i>Cricotopus bicinctus</i> -type	3	2.7	0	2.6
		<i>Cricotopus cylindraceus</i> -type	2	1.7	0	2.2
		<i>Cricotopus laricomalis</i> -type	3	2.9	0	1.8
<i>Cricotopus</i> type C		2	2.0	0	1.2	
<i>Cricotopus</i> type P		2	1.3	0	1.4	
<i>Orthoclaadius oliveri</i> -type		2	1.9	0	2.5	
<i>Orthoclaadius trigonolabis</i> -type		1	1.0	0	1.4	
<i>Orthoclaadius</i> type S		4	3.6	0	2.7	
<i>Orthoclaadius</i> undifferentiated		10	9.2	0	3.2	
<i>Heterotrissocladius grimshawi</i> -type		5	4.6	0	2.5	
<i>Heterotrissocladius maeaeeri</i> -type		12	8.4	0	12.9	
<i>Hydrobaenus conformis</i> -type		5	3.5	0	5.5	
<i>Hydrobaenus johannseni</i> -type		2	2.0	0	1.3	
<i>Limnophyes - Paralimnophyes</i>		8	6.2	0	2.7	
<i>Mesocricotopus</i>		4	2.8	0	3.1	
<i>Paracladius</i>		15	11.0	0	19.5	
<i>Parakiefferiella bathophila</i> -type		2	1.6	0	3.5	
<i>Parakiefferiella triquetra</i> -type		15	11.3	0	5.2	
<i>Prosilocerus lacustris</i> -type		4	2.4	0	6.7	
<i>Psectrocladius barbatipes</i> -type		2	1.9	0	1.1	
<i>Psectrocladius septentrionalis</i> -type		3	2.2	0	1.2	
<i>Psectrocladius sordidellus</i> -type		9	6.2	0	4.8	
<i>Rheocricotopus effusus</i> -type		1	1.0	0	1.1	
<i>Smittia-Parasmittia</i>		1	1.0	0	1.1	
<i>Synorthoclaadius</i>		2	2.0	0	1.8	
<i>Thienemanniella clavicornis</i> -type		1	1.0	0	1.1	
<i>Zalutschia</i> type B		9	6.7	0	4.6	
<i>Zalutschia zalutschicola</i>	10	4.8	0	27.3		
Diamesinae	<i>Diamesa aberrata</i> -type	1	1.0	0	1.5	
	<i>Protanypus</i>	7	6.2	0	4.2	
	Unidentified Diamesinae	5	4.5	0	3.8	
Prodiamesinae	<i>Monodiamesa</i>	11	9.1	0	3.3	
Podonominae	<i>Trichotanypus</i>	1	1.0	0	1.1	
Tanypodinae	<i>Ablabesmyia</i>	3	2.5	0	1.8	
	<i>Procladius</i>	6	4.0	0	6.5	

As with AFOX, *Tanytarsus lugens*-type occurs throughout the core, at moderately high abundances (Hill's N2 = 14.9). Of the other taxa which occur throughout AFOX core, *Corynocera ambigua* and *Micropsectra insignilobus*-type occur in the majority of samples whereas *Sergentia coracina*-type and *Tanytarsus pallidicornis*-type occur in approximately half the samples at low abundance (less than 5%). *Micropsectra insignilobus*-type, *Paracladius*, *Parakiefferiella triquetra*-type and *Corynocera oliveri*-type occur in over 85% of the PONE samples. When present, *C. oliveri*-type can form a major component of the fauna (maximum abundance = 27%, Hill's N2 = 12.0) whereas *M. insignilobus*-type, *Paracladius* and *P. triquetra*-type occur more consistently at lower abundances (Hill's N2 10.0-12.0). *Paracladius* and *P. triquetra*-type are more abundant throughout the PONE core than AFOX. These taxa are present in the coldest lakes in the Norwegian and Russian training sets and their occurrence may reflect the slightly cooler, higher altitude at PONE. Of the 60 taxa present in the subfossil assemblages 58 occur in the training set. The assemblages should, therefore, give reliable palaeoenvironmental reconstructions. Two zones, in the PONE chironomid stratigraphy, were identified by optimal partitioning (Figure 7.13); these were designated zones a and b.

Zone a (28.0 – 3.75 cm; 630 – 39 years BP)

Paracladius, *Heterotrissocladius maeeri*-type and *M. insignilobus*-type are common in this zone, individually comprising up to 19% of the assemblages. These taxa are indicative of cold, oligotrophic conditions (Brundin 1956; Sæther 1979; Walker *et al.* 1991). They decline in abundance towards the top of the zone, together with other taxa associated with cold oligotrophic lakes such as *Protanypus* and *Paratanytarsus austriacus*-type which form minor components, at 3% and 5% abundance respectively.

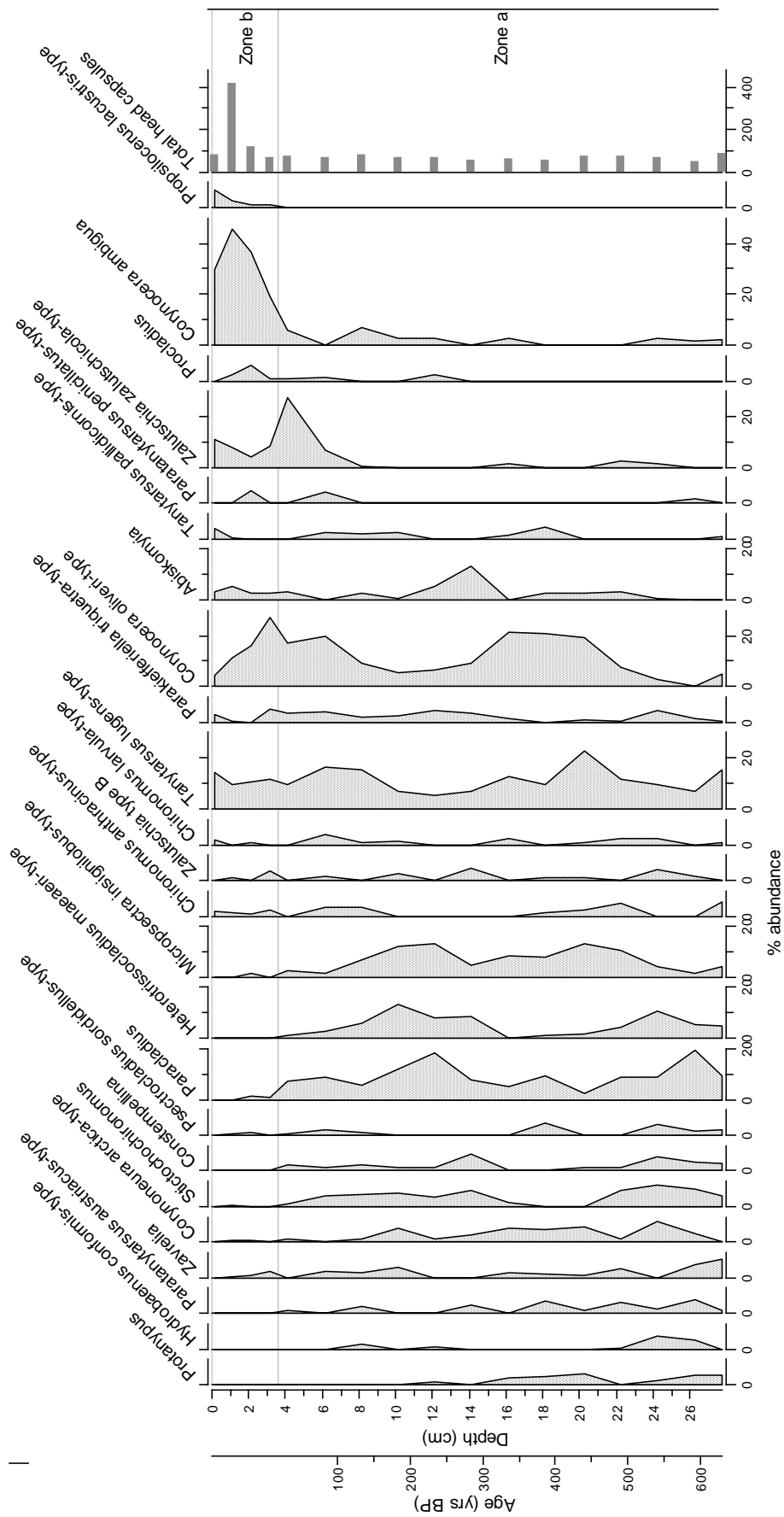


Figure 7.13. Chironomid stratigraphy, of taxa with greater than 4% abundance, from PONE.

Zone b (3.75 – 0.0 cm; 39 years BP – present)

This zone is characterised by large increases in *C. ambigua*, which dominates the assemblage (up to 45% abundance). This taxon is most abundant in last interstadial and early Holocene sediments from Scotland (Brooks et al. 1997) and Scandinavia (Velle et al. 2005a). However Brodersen and Lindegaard (1999b) found the taxon in surface sediments from warm, shallow, eutrophic lakes in Denmark. *Prosilocerus lacustris*-type, which is found in relatively warm lakes in England, southern Norway and Yakutia (Brooks et al. 2007), first appears in this zone. The abundance of the warm-adapted taxon *Zalutschia zalutschicola*-type is initially high but declines as *C. ambigua* increases.

The decline in cold stenotherms such as *Paratanytarsus austriacus*-type and *Paracladius* in zone b, together with the increases in *P. penicillatus*-type from 8cm depth and appearance of *Prosilocerus lacustris*-type at 3.75cm, may indicate a shift to warmer conditions. Additionally, many of the rare taxa, such as *Rheocricotopus* and *Rheotanytarsus*, and *Constempellina* associated with flowing water occur solely in zone a. Profundal taxa, including *Heterotrissocladius maeaeri*-type, decline towards the top of zone a and are absent from zone b. Therefore the boundary may, also, mark a transition from deeper, stream-fed lake to shallower, melt water-fed lake.

The assemblages were plotted passively on the CCA ordination diagram (see section 4.2.4.2) with significant chemical and environmental variables fitted by regression (Figure 7.14). The older samples plot near the upper part of axes 3 (Figure 7.14b) which suggests that the lake was deeper than present 630 years ago and has become gradually shallower over time. This trend is interrupted by a period of deeper water depth at ca. 10cm depth, with higher abundances of the profundal *H. maeaeri*-type. As with AFOX, cold-stenothermic taxa, including *T. lugens*-type, occur throughout the core and the samples plot along the lower part of axes 1 which suggests the lake was relatively cool throughout the period represented with a slightly increasing trend in T_{july} towards the top of the core.

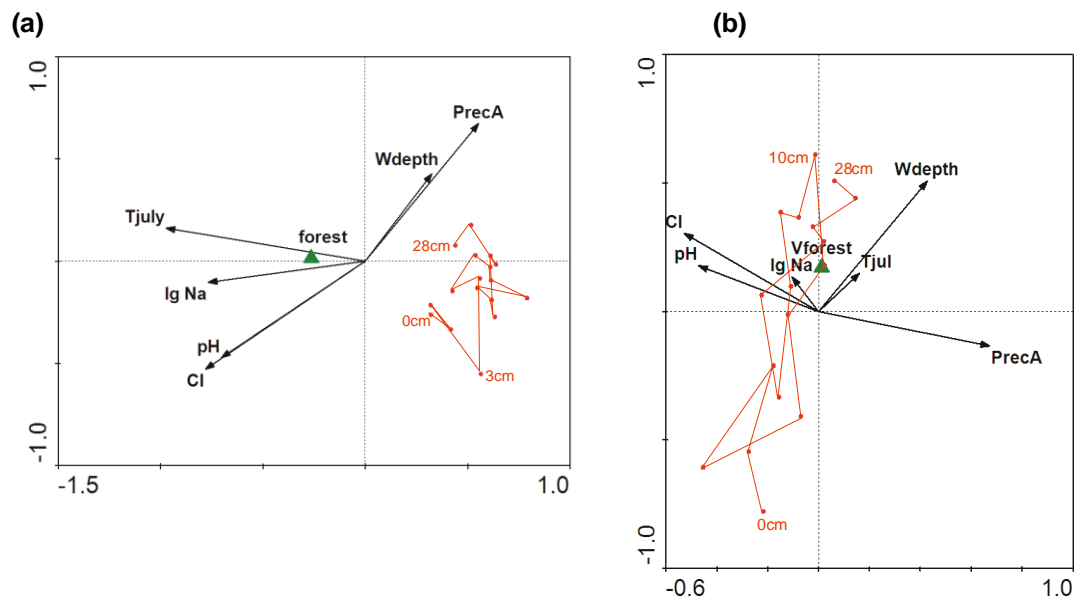


Figure 7.14. CCA plot of (a) axes 1 and 2 and (b) axes 2 and 3 with samples from PONE fitted passively and joined as a time-track to show the changes in chironomid assemblages in relation to lake chemical and physical variables over the last 630 years.

7.6.3. PTHE

The fauna of PTHE is taxonomically less diversity than PONE (Table 7.6), with 53 taxonomic groups identified in 19 samples from PTHE compared to 62 taxonomic groups in PONE, and lacks the taxa associated with flowing water such as *Rheocricotopus*, *Rheotanytarsus* and *Constempellina*. The fauna is similar in composition to AFOX with consistently high abundances of *Sergentia coracina*-type, *Corynocera ambigua*, *Micropsectra insignilobus*-type and *Tanytarsus lugens*-type throughout the majority of the samples (Hill's N2 9.4-14.7). The composition differs from either of the other cores in the presence of *Psectrocladius sordidellus*-type at 9-19% abundance (Hill's N2 = 17.1) throughout the core. Although present in AFOX and PONE, *Ps. sordidellus*-type forms a minor component with typically less than 6% abundance. *Ps. sordidellus*-type is acidophilic (Pinder and Morley 1995) but occurs at approximately 12% in the modern surface sediment where the pH is circum-neutral (Table 4.1). Therefore its occurrence in PTHE may be associated with the growth of macrophytes in the littoral zone (Brodersen *et al.* 2001; Brooks *et al.* 2007). *Corynocera ambigua* and *C. oliveri*-type, frequently, dominate the subfossil assemblages and occur at up to 27.3% and 36.5%

Table 7.6. Chironomid fauna of PTHE core, with total number of occurrences (in 19 sub-samples), effective number of occurrences (Hill's N2) and minimum and maximum percent abundance.

Subfamily	Taxa	No. of occurrences	Hill's N2	Min % abundance	Max % abundance	
Chironominae	Chironomini					
	<i>Chironomus anthracinus</i> -type	15	8.9	0	7.8	
	Chironomini larvula	11	7.5	0	6.6	
	<i>Chironomus plumosus</i> -type	4	3.5	0	2.5	
	<i>Cladopelma lateralis</i> -type	8	6.2	0	2.9	
	<i>Dicrotendipes</i>	7	5.5	0	3.5	
	<i>Microtendipes pedellus</i> -type	1	1.0	0	1.0	
	<i>Pagastiella</i>	2	1.4	0	1.4	
	<i>Sergentia coracina</i> -type	19	12.7	0.8	12.0	
	<i>Stictochironomus rosenschoeldi</i> -type	2	1.9	0	0.5	
	Tanytarsini					
	<i>Cladotanytarsus mancus</i> -type	9	7.3	0	5.4	
	<i>Corynocera ambigua</i>	18	13.0	0	27.3	
	<i>Corynocera oliveri</i> -type	18	14.0	0	36.5	
	<i>Micropsectra insignilobus</i> -type	16	9.4	0	20.8	
	<i>Micropsectra radialis</i> -type	2	1.3	0	1.1	
	<i>Paratanytarsus austriacus</i> -type	5	3.3	0	6.5	
	<i>Paratanytarsus penicillatus</i> -type	9	7.3	0	3.2	
	<i>Paratanytarsus</i> undifferentiated	16	13.0	0	4.5	
	<i>Stempellinella</i> - <i>Zavrelia</i>	1	1.0	0	1.3	
	<i>Tanytarsus glabrescens</i> -type	1	1.0	0	1.0	
	<i>Tanytarsus lugens</i> -type	19	14.7	1.3	24.6	
	<i>Tanytarsus mendax</i> -type	10	8.0	0	11.8	
	<i>Tanytarsus pallidicornis</i> -type	8	7.1	0	2.3	
	<i>Tanytarsini</i> undifferentiated	19	16.8	1.4	8.2	
	Orthoclaadiinae	<i>Abiskomyia</i>	4	2.3	0	3.3
		<i>Corynoneura arctica</i> -type	16	11.1	0	6.6
<i>Corynoneura edwardsi</i> -type		3	2.0	0	2.6	
<i>Corynoneura lobata</i> -type		1	1.0	0	0.9	
<i>Cricotopus bicinctus</i> -type		1	1.0	0	1.7	
<i>Cricotopus cylindraceus</i> -type		5	4.7	0	1.5	
<i>Cricotopus laricomalis</i> -type		12	10.2	0	2.9	
<i>Cricotopus sylvestris</i> -type		11	8.6	0	2.7	
<i>Cricotopus</i> type C		3	2.2	0	1.3	
<i>Cricotopus</i> type P		1	1.0	0	1.5	
<i>Orthocladus oliveri</i> -type		3	2.3	0	2.6	
<i>Orthocladus</i> undifferentiated		4	3.2	0	2.8	
<i>Heterotrissocladius maeaeri</i> -type		2	1.5	0	0.6	
<i>Hydrobaenus conformis</i> -type		3	2.7	0	2.0	
<i>Hydrobaenus lugubris</i> -type		3	2.5	0	3.0	
<i>Limnophyes</i> - <i>Paralimnophyes</i>		4	4.0	0	1.4	
<i>Mesocricotopus</i>		4	2.4	0	3.2	
<i>Paracladius</i>		3	2.3	0	1.6	
<i>Parakiefferiella bathophila</i> -type		4	2.9	0	3.2	
<i>Parakiefferiella triquetra</i> -type		10	6.2	0	7.0	
<i>Prosilocerus</i> type N		1	1.0	0	1.3	
<i>Psectrocladius septentrionalis</i> -type		11	9.0	0	2.3	
<i>Psectrocladius sordidellus</i> -type		19	17.1	0.9	19.9	
<i>Synorthocladus</i>		2	1.8	0	2.6	
<i>Thienemanniella clavicornis</i> -type		1	1.0	0	1.3	
<i>Zalutschia</i> type B		9	6.7	0	3.2	
Diamesinae		<i>Protanypus</i>	12	9.7	0	6.6
Prodiamesinae	<i>Monodiamesa</i>	4	3.6	0	1.3	
Tanypodinae	<i>Ablabesmyia</i>	4	3.5	0	1.8	
	<i>Procladius</i>	17	13.8	0	9.6	

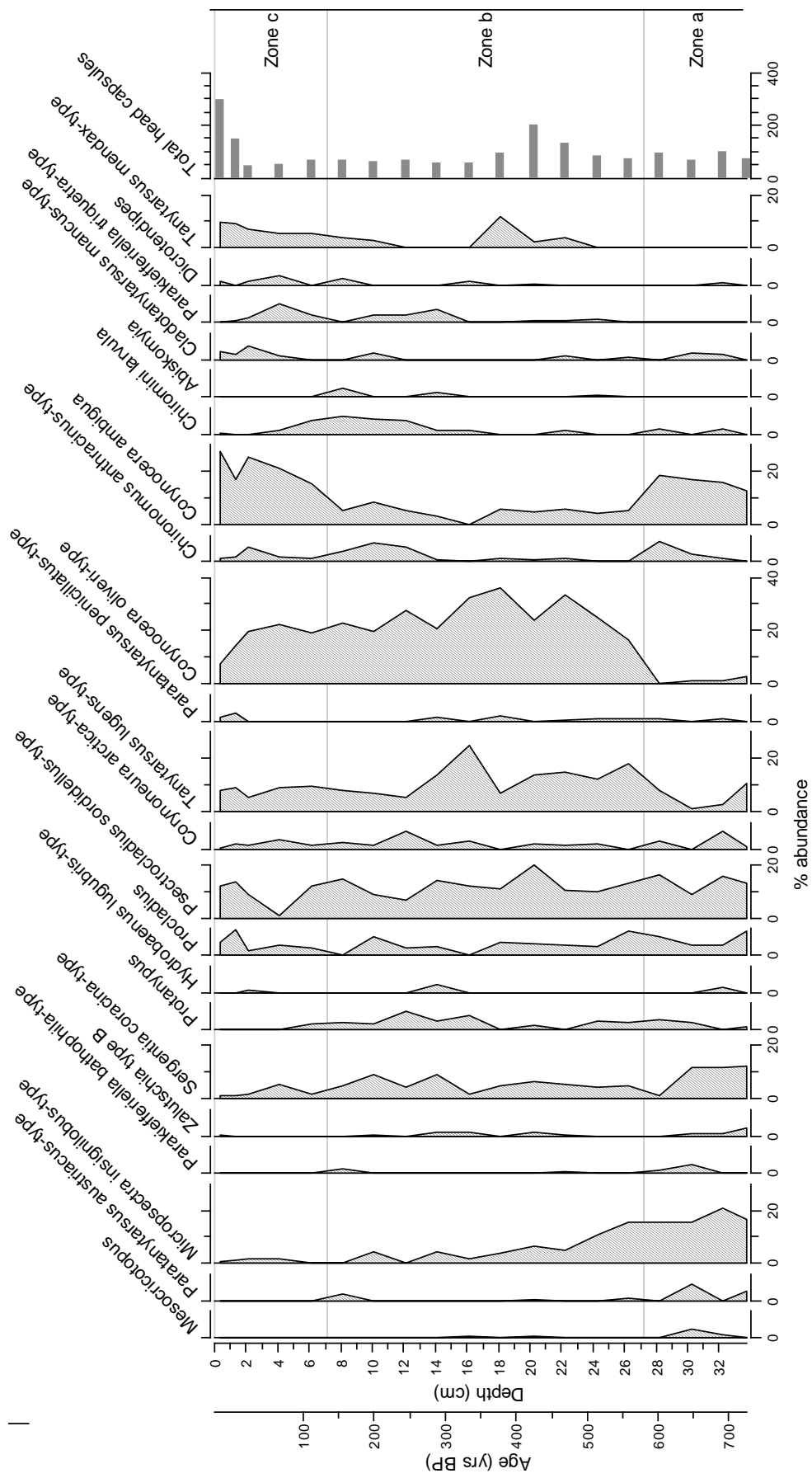


Figure 7.15. Chironomid stratigraphy, of taxa with greater than 4% abundance, in PTHE.

abundance respectively. *S. coracina*-type, *M. insignilobus*-type, and *T. lugens*-type are cold stenotherms (Brundin 1956), but as with AFOX, the coldest indicators such as *M. radialis*-type are rare so that the fauna is typical of a relatively cold, oligotrophic environment. Three zones were identified by optimal partitioning. These appear distinguished by variations in the relative abundance of taxa rather than their presence or absence (Figure 7.15).

Zone a (34 – 27 cm; 725 – 575 years BP)

This zone is dominated by *C. ambigua* and *M. insignilobus*-type with very low abundances of *C. oliveri*-type. Both *C. ambigua* and *C. oliveri*-type occur in cold, oligotrophic lakes, however *C. ambigua* is generally more abundant in early Holocene and *C. oliveri* in late-glacial sediments (Brooks and Birks 2000a; Hofmann 2001; Velle *et al.* 2005a). The dominance of *C. ambigua* may, therefore, be associated with slightly higher temperatures or productivity than zone b.

Zone b (27 – 7 cm; 575 – 130 years BP)

C. ambigua and *M. insignilobus*-type decline throughout this zone and are replaced by increases of *C. oliveri*-type to 20-36% and *T. lugens*-type to 5-25%. The cold stenotherms, *Abiskomyia* (3%) and *Parakiefferiella triquetra*-type (4%), first appear in this zone.

Zone c (7.0 – 0.0 cm; 130 years BP – present)

This zone is characterised by an increase of *C. ambigua* to ca. 25%, *C. oliveri*-type initially remains at 19-23% but declines to 8% between 0-2cm. *C. mancus*-type, *Dicrotendipes* and *T. mendax*-type which occur at low numbers in zone b increase to 5%, 3% and 9% respectively. *C. mancus*-type and *T. mendax*-type are typically found in the littoral of relatively warm, productive lakes (Brundin 1949; Brodin 1986) and *Dicrotendipes* occurs, predominantly, in the warmer lakes of the Russian and Norwegian training sets. The increases in these taxa may indicate a shift towards slightly warmer more productive conditions.

When the chironomid assemblages are plotted passively on the CCA ordination diagram (see section 4.2.4.2) the samples plot on the right of axes 1 which suggests the lake has remained relatively cool throughout the period represented (Figure 7.16a). However samples near the base of the core, at ca. 30cm depth, and the surface sediments appear to the left of the majority of the samples on axis 1 suggesting these periods may have been slightly warmer. The lowermost samples, 34 – 28 cm depth, plot near the centre of the water depth gradient then shift to the lower left of the biplot (Figure 7.16b). This suggests the water depth was deeper than present 725 years ago, gradually became shallower and has remained relatively stable over the last 500 years. Both PONE and PTHE show similar trends towards warmer, shallower conditions over the past 500 years and although undated AFOX shows a similar progression. This similarity suggests the lakes are responding to a regional climate signal rather than localised, within-lake processes.

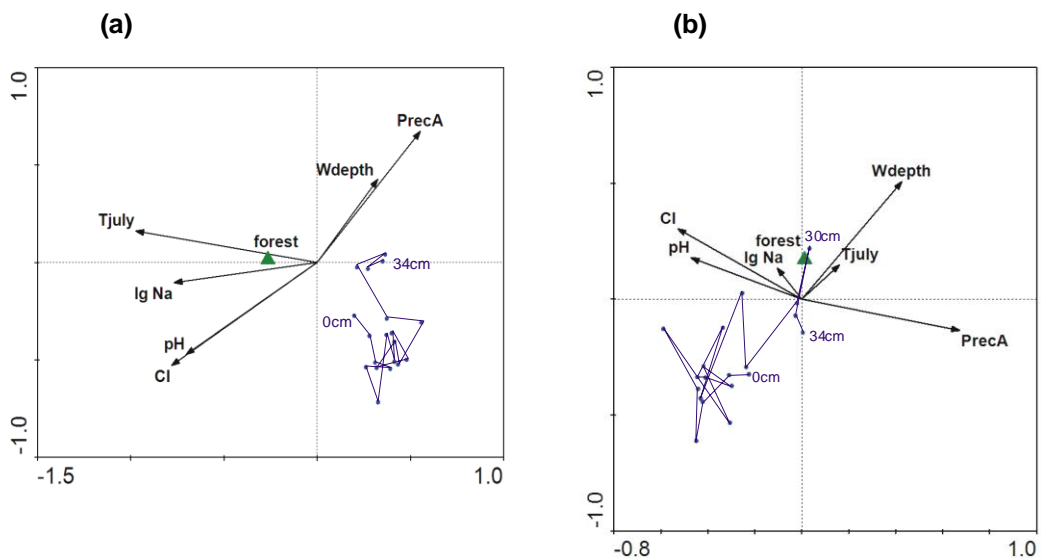


Figure 7.16. CCA plot of (a) axes 1 and 2 and (b) axes 2 and 3 with samples from PTHE fitted passively and joined as a time-track to show the changes in chironomid assemblages in relation to lake chemical and physical variables in the last 725 years.

7.7. Chironomid-inferred temperature (CI-T) reconstructions

The environmental and species training sets used in the development of the CI-T models are detailed in Chapter 6 (sections 6.2 – 6.4). WA-PLS, MAT and WMAT models were generated for each training set, together with WA and WA-TOL models with classical and inverse deshrinking regression. Sections 6.2 – 6.4 also give the performance statistics of each model (RMSEP, r^2 , mean and maximum bias) and the number of WA-PLS components and closest analogues in MAT selected to give the minimal adequate model. The key features of the models are summarised in Table 7.7. This section aims to examine the T_{july} reconstructions derived from these training sets to decide which regional model and statistical technique appears most appropriate for reconstructing past mean July air temperatures (T_{july}) at the Putorana lakes. Section 7.7.1 examines which regional training set and section 7.7.2 which statistical technique most accurately reconstructs recent instrumental T_{july} data, section 7.7.3 estimates the reliability and accuracy of the reconstructions and the T_{july} reconstructions from PONE and PTHE are compared in section 7.7.4.

Table 7.7. Summary of CI-T models developed in Chapter 6

Training set	Origins of material	No. of lakes	No. of taxa	No. of WA-PLS components	No. of closest analogues in MAT	Comments	Detailed in section
A	Russia	88	89	2	4	Absence of lakes with T_{july} of 14 – 18 °C	6.2.1
K	Russia	81	89	2	6	Includes Komi lakes with T_{july} 16.3 – 17.3 °C	6.2.2
N	Norway	153	141	3	7	Based on Brooks and Birks (2000 and unpublished data)	6.3
C	Russia - Norway	233	146	3	5	Minus extreme environmental outliers from Russian training set	6.4.1
R	Russia - Norway	188	144	3	7	Lakes selected to give even distribution along CI and T_{july} gradients	6.4.2

7.7.1. Selection of regional training set

Chironomid-inferred mean July air temperatures were estimated from the chironomid assemblage of the surface sediments from PONE (0.25 – 0cm depth, 2002 – 2005) using the inference models developed in Chapter 6. The present-day mean July air temperature at PONE was estimated at 11.7°C from the meteorological records. The T_{july} derived from the Russian CI-T training sets A and K are closest to the T_{july} estimated from the meteorological records

regardless of the statistical technique used (Table 7.8). The Norwegian training set N reconstructs T_{july} up to 2.3°C colder than the meteorological data. The Russian-Norwegian training sets C and R show up to 1.8 °C variation between statistical techniques. WA assumes that environmental variables other than the one of interest have a negligible influence on the biological assemblage whereas WA-PLS uses the additional structure to improve estimates of the taxa optima (Birks 2003). As the WA reconstructions (11.3 and 11.4°C respectively) for CI-T training sets C and R are closer to the instrumental data than the WA-PLS reconstruction (9.8 and 9.6°C), the additional components of the WA-PLS model may be over-fitting the PONE data by including variables or combinations of variables which, in reality, have a negligible effect on the PONE chironomid fauna.

Table 7.8. Reconstructions of mean July air temperatures for PONE estimated from the surface chironomid assemblage (2002 – 2005) using the inference models developed in Chapter 6. Present-day (2005) mean July temperatures estimated at 11.7°C from meteorological records.

Training set	July air temperature (°C)						
	WA-PLS	WA		WA-TOL		MAT	WMAT
		Inverse	Classical	Inverse	Classical		
A	11.1	11.7	11.4	11.7	11.5	11.1	11.1
K	11.2	11.5	11.2	11.6	11.3	11.2	11.2
N	9.4	10.5	10.6	9.9	9.9	10.0	10.0
C	9.8	11.3	11.2	10.9	10.8	11.0	11.1
R	9.6	11.4	11.4	10.8	10.7	10.9	10.9

The two Russian training sets, therefore, appear most accurate at reconstructing present-day T_{july} at PONE. Of these, the performance of the WA-PLS, WA and WA-TOL models derived from training set K were better, in terms of RMSEP and r^2 , than those from training set A. This suggests training set K would be most appropriate for reconstructing past T_{july} at PONE. However the CI-Ts estimated from the chironomid assemblage of the surface sediments from PTHE (0.5 – 0.25cm depth, 1997 – 2004) using the inference models developed in Chapter 6 do not indicate clearly which model is most appropriate (Table 7.9). The mean July air temperatures derived from the Russian CI-T training sets A and K are consistently higher (11.2 – 12.7°C) than the T_{july} estimated from the

meteorological records (10.5°C). The Norwegian training set N WA-PLS and MAT techniques reconstructs T_{july} up to 1.0°C colder than the meteorological data. The combined Russian-Norwegian training sets C and R show up to 1.7°C variation between the WA and WA-PLS techniques. The WA-PLS estimates (10.4°C) are closer to the instrumental value (10.5°C) than the WA estimates (11.8°C for training set C and 12.0°C for training set R) which suggests the chironomid assemblages in the surface sediments may be strongly influenced by other variables in addition to T_{july} .

Table 7.9. Reconstructions of mean July air temperatures for PTHE estimated from the surface chironomid assemblage (1977 – 2004) using the inference models developed in Chapter 6. Present-day (2005) mean July temperatures estimated at 10.5°C from meteorological records.

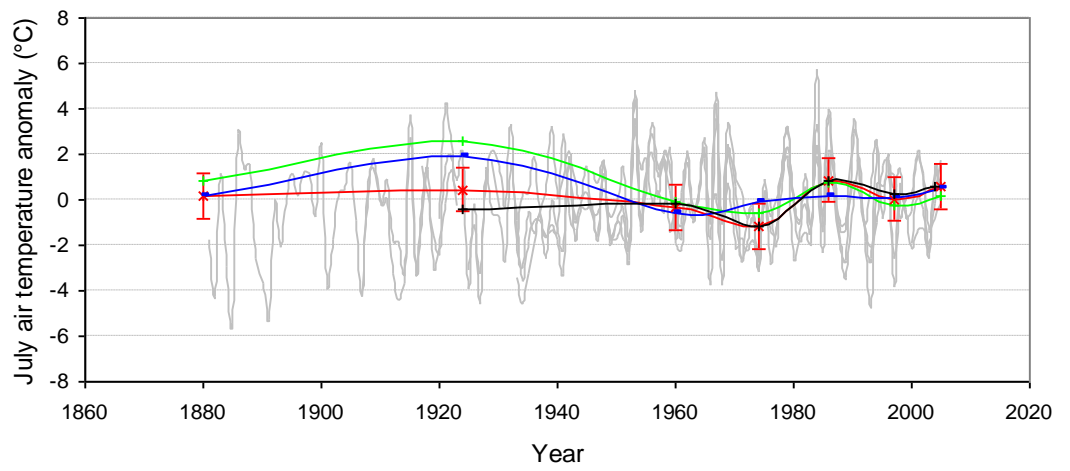
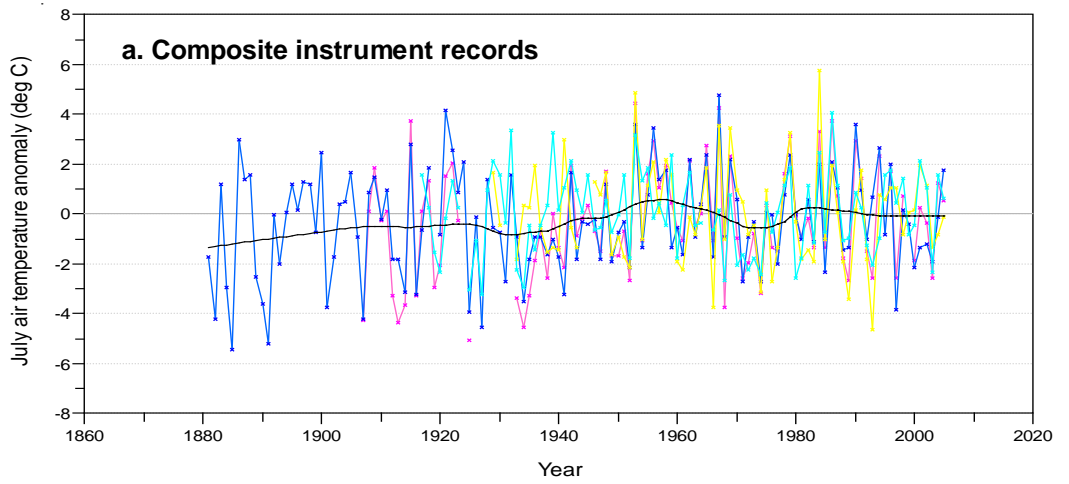
Training set	July air temperature (°C)						
	WA-PLS	WA		WA-TOL		MAT	WMAT
		Inverse	Classical	Inverse	Classical		
A	11.7	12.7	12.5	11.4	11.2	11.3	11.3
K	11.8	12.5	12.4	11.7	11.5	11.2	11.2
N	9.5	10.7	10.7	10.2	10.2	9.8	9.8
C	10.4	11.8	12.0	11.2	11.2	10.4	10.4
R	10.4	12.0	12.1	11.3	11.3	10.5	10.5

The comparisons of CI-Ts with present-day instrumental values in Tables 7.8 and 7.9 were based on analysis of the surface sediments. Part of the recent sediment record is absent from PTHE (section 7.4.2) with possible *in-situ* algal growth at ca. 2cm depth (section 7.5.3) which may have affected the chironomid assemblage of the surface sediments and the accuracy of the reconstruction. Therefore the WA-PLS T_{july} reconstructions from training sets K, N and R were compared to regional instrumental records dating back to 1880 (Figure 7.17), WA-PLS reconstructions were used as the T_{july} estimates for PTHE are, in general, closer to the instrumental value than the WA estimates. WA-PLS reconstructions for PONE based on training sets K, N and R are also presented in Figure 7.17.

A regional T_{july} anomaly record was constructed based on data from the four closest meteorological stations to the study area (68.17°N, 92.19°E), with

relatively complete and long duration records. Instrumental records were obtained from Dudinka (69.04°N, 86.17°E), Turuhansk (65.78°N, 87.93°E), Hatanga (71.98°N, 102.47°E) and Ostrov Dikson (73.50°N, 80.40°E). All records had missing data ranging from 1 – 7 years duration and only the Turuhansk record was complete for the period 1920 – 35. As these stations vary in their longitude, latitude and altitude to the studied lakes July air temperature anomalies were calculated as deviations from the 60 year monthly mean (for the period 1946 – 2005) rather than correct to a common reference point. The regional T_{july} anomaly record was calculated as deviations from the 60 year monthly mean (for the period 1946 – 2005). The 60 year period was selected as PONE had 5 temperature reconstructions within the last 50 years and PTHE 4 in the last 68 years. Therefore 60 years represented a compromise so that both lakes had sufficient reconstructions to calculate a mean. The regional anomaly record (Figure 7.17a) shows a general increasing trend in T_{july} of approximately 1°C over the twentieth century with periods of warmer than average T_{july} in the 1950s and 1980s and cooler periods in the 1970s and prior to 1940 (Figure 7.17a). Since 1980 T_{july} have remained static which confirms the satellite-derived trends discussed in Chapter 1.

The WA-PLS training set K CI-Ts from PONE show the 1980s warming and 1970s cooling. The 1950s warming and cooling prior to 1940 are not apparent but are within the sample specific errors of the T_{july} reconstructions (Figure 7.17b). Both the Norwegian training set N and combined Russian-Norwegian training set R give WA-PLS CI-Ts which are too warm in the early twentieth century. The CI-Ts from PTHE lack the resolution to reconstruct the fine-scale fluctuations in T_{july} observed in the instrumental record from 1950 - present (Figure 7.17c). The recent CI-Ts from 1982 and 2002 are higher than the composite trend from the instrumental record (as expected from the comparison of CI-Ts in Table 7.9). However the Russian training set K reconstructs the cooler than average period prior to the 1940s. The Norwegian training set N and combined Russian-Norwegian training set R fail to reconstruct any of the temperature fluctuations of the twentieth century. Therefore training set K would also appear most appropriate for T_{july} reconstructions for PTHE.



b. PONE CI-T anomalies

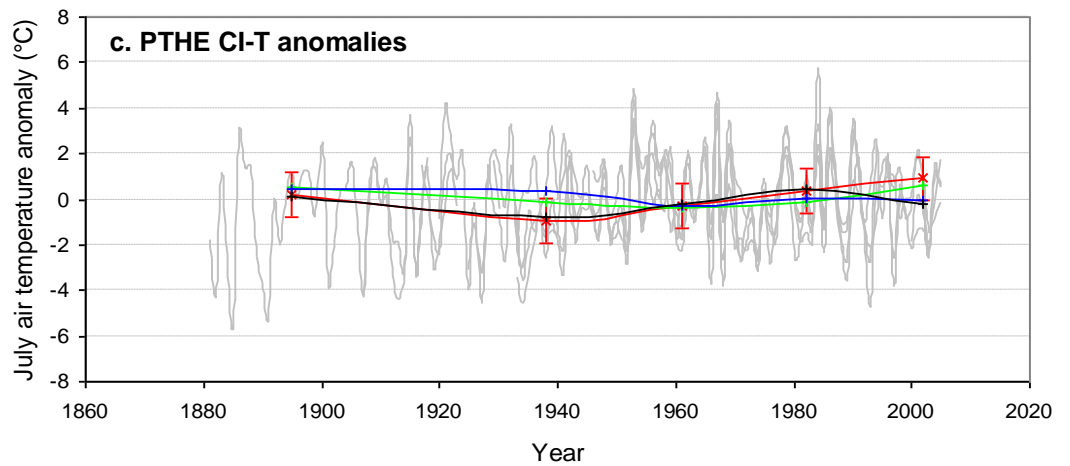


Figure 7.17. July air temperature anomalies (a) of instrumental records from Dudinka (pink), Turuhansk (blue), Hatanga (yellow) and Ostrov Dikson (cyan), based on deviation from a 60 year mean (1946 – 2005) fitted with LOWESS smoother (span 0.2). Comparison of anomalies from (b) PONE WA-PLS CI-T reconstructions, based on 50 year mean, and (c) PTHE WA-PLS CI-T reconstructions based on 68 year mean with instrumental record anomalies at the same sampling interval as the CI-T data in black and instrument record anomalies in grey. Results of Russian CI-T model K shown in red, with sample specific errors, Norwegian CI-T model N in blue and Russian-Norwegian CI-T model R in green.

7.7.2. Selection of statistical method

Mean July air temperatures for PONE and PTHE were reconstructed, from training set K, using WA-PLS, WA and MAT techniques and the trends compared to the regional T_{july} anomaly record (Figures 7.18 and 7.19).

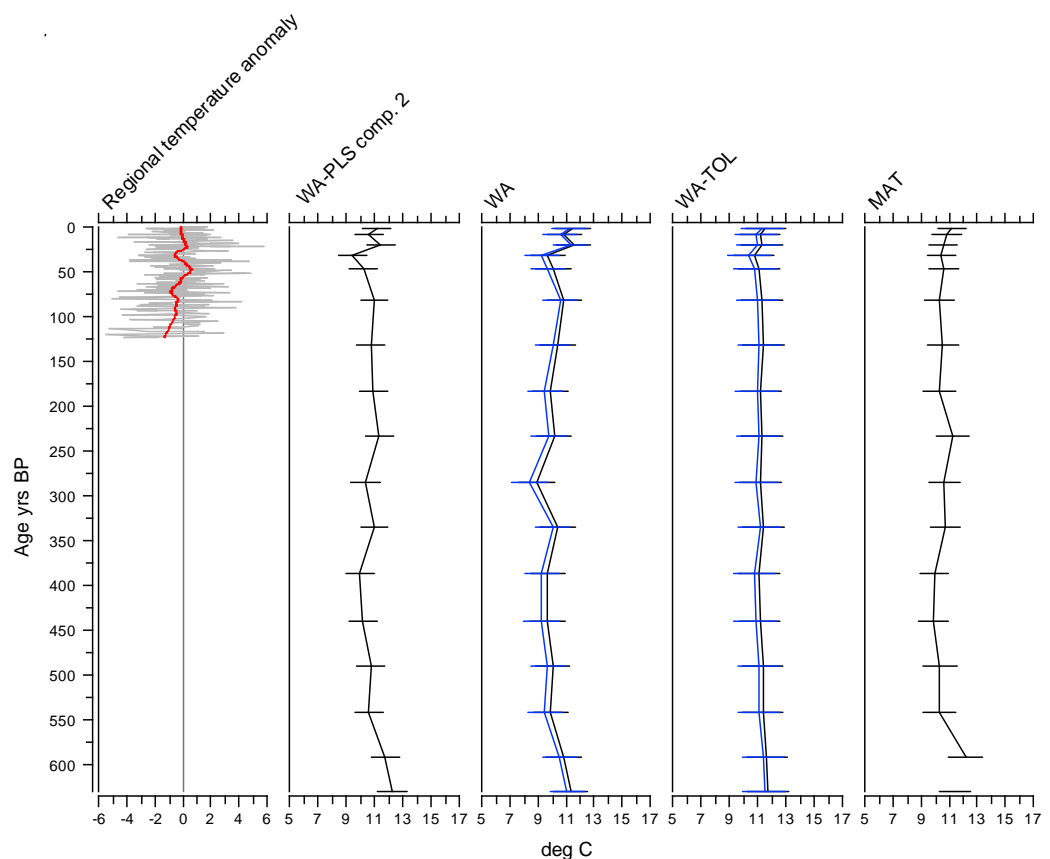


Figure 7.18. Reconstructions of mean July air temperature (°C) for PONE based on weighted-averaging partial least squares (WA-PLS, 2 component model), weighted averaging (WA), tolerance downweighted weighted averaging (WA-TOL) and modern analogue technique (MAT) using CI-T model K. WA and WA-TOL reconstructions with inverse deshrinking are shown in black and reconstructions with classical deshrinking in blue. Sample-specific errors of reconstruction are shown for all techniques. The left-hand plot shows regional T_{july} anomalies based on deviation from a 60 year mean and is fitted with a LOWESS smoother (span 0.2). Age presented as years before 2006.

WA and WA-PLS reconstructions for PONE (Figure 7.18) show similar trends to the regional temperature anomaly record. As discussed in the previous section WA-PLS, and WA, show the 1980s warming and 1970s cooling, but not the warming in the 1950s. Pre-twentieth century cooling is more pronounced with the WA than WA-PLS reconstruction and closer to the instrumental trend. At the base of the core the WA-PLS reconstruction is slightly warmer (12.3°C) than the WA (11.3°C) but within the range of the sample-specific errors. The WA-TOL reconstruction suggests there has been little change in T_{july} over the last 630 years. Tolerance down-weighting enables taxa with narrow tolerances to be given greater weight in the reconstruction than taxa with wide tolerances. *Corynocera oliveri* which occurs extensively throughout the core has a narrow tolerance (1.2°C) and is probably markedly influencing the temperature reconstruction. The ecological requirements of *C. oliveri* are poorly known and

its presence may be due to environmental variables other than T_{july} . There is little difference in reconstructed T_{july} using classical or inverse deshrinking. MAT reconstruction suggests a gradual increase in T_{july} over the last 50 years which is not seen in the temperature anomaly record. As discussed in following section (7.7.3), many of the fossil samples in PONE have no close analogue in the modern training set. They consistently select other Putorana lakes for the MAT reconstruction which appears to reflect localised environmental changes rather than a response to temperature. WA and WA-PLS perform better than direct analogue-matching techniques when there are no or few close analogues in the training set (ter Braak and Juggins 1993; ter Braak 1995; Birks 2003). Therefore WA or WA-PLS using CI-T model K would appear to be most appropriate for reconstructing past T_{july} in PONE.

The WA-PLS, WA and WA-TOL reconstructions for PTHE show the pre-1940s and pre-twentieth century cooling shown in the instrumental record, but fail to reconstruct any of the minor fluctuations in T_{july} over the twentieth century. WA-TOL shows wide sample-specific errors particularly at 380 years BP ($\pm 2.6^{\circ}\text{C}$). WA and WA-PLS, in general, show similar trends in T_{july} with the exception of specific samples such as the sample at 650 years BP which remains stable at 12.2°C in the WA-PLS reconstruction and declines by 0.5°C to 11.8°C in WA. MAT T_{july} for PTHE show little change over the past 725 years (Figure 7.19). As with PONE the other Putorana lakes are commonly selected for MAT reconstructions, these cover a narrow environmental range and so the reconstructions fail to accurately reconstruct past temperature fluctuations. Therefore as with PONE, WA or WA-PLS models would appear to be most appropriate for reconstructing past T_{july} in PTHE.

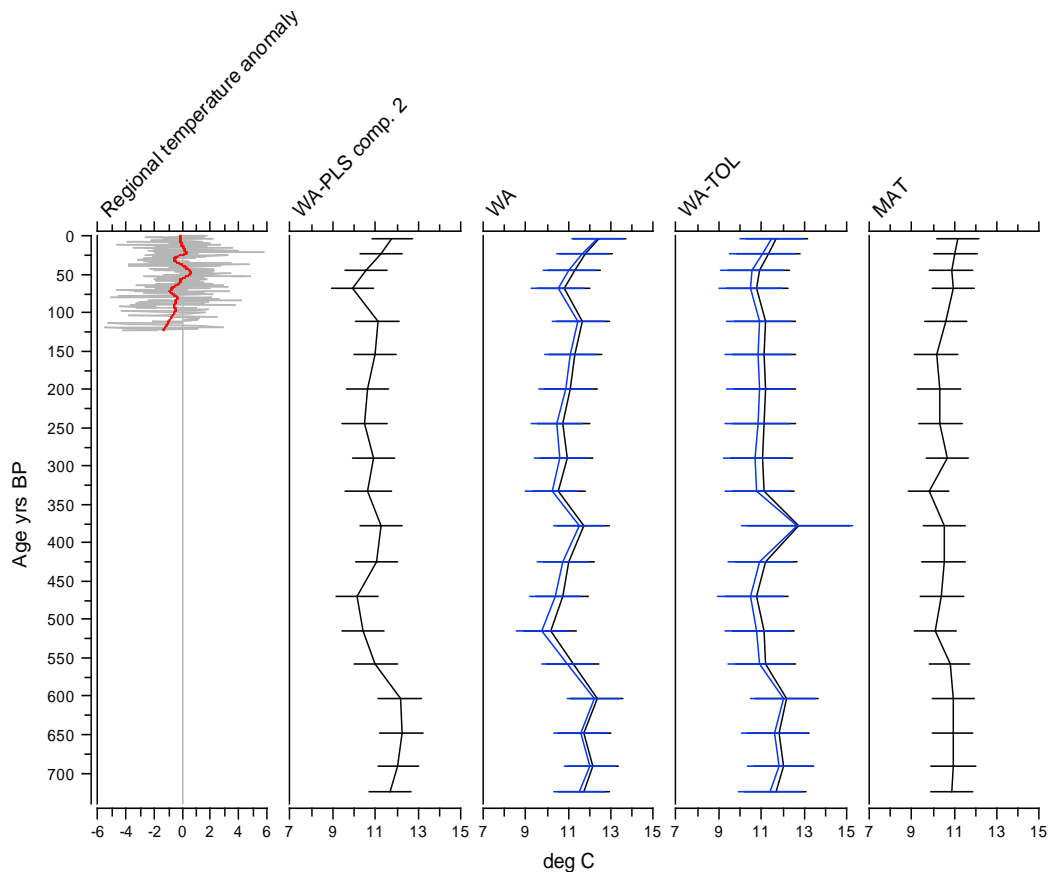


Figure 7.19. Reconstructions of mean July air temperature (°C) for PTHE based on WA-PLS (2 component model), WA, WA-TOL and MAT using CI-T model K. WA and WA-TOL reconstructions with inverse deshrinking are shown in black and reconstructions with classical deshrinking in blue. Sample-specific errors of reconstruction are shown for all techniques. The left-hand plot shows regional T_{july} anomalies based on deviation from a 60 year mean and is fitted with a LOWESS smoother (span 0.2). Age presented as years before 2006.

7.7.3. Comparison of July air temperature reconstructions for PONE and PTHE

The trends in the WA reconstructions, calculated as T_{july} anomalies or deviations for the long-term mean, are similar to trends in the WA-PLS reconstructions for both PONE and PTHE over the past 120 years (Figure 7.20), although the WA and WA-PLS reconstructions vary further down the core (see Figure 7.19). However the wide discrepancy between the present-day instrumental T_{july} (10.5°C) and WA T_{july} (12.7°C) for PTHE (Table 7.9) suggests WA-PLS regression is more appropriate for estimating past July temperatures

at the Putorana lakes. Reconstructions of mean July temperatures show differing trends between the two lakes over the past 120 years (Figure 7.20). For example, CI-T reconstructions from PONE show cooling in the 1970s and warming in the 1980s which are not evident in reconstructions from PTHE. However when the instrumental data anomalies are plotted for the same sampling intervals as the CI-T data (shown in black), both PONE and PTHE CI-T reconstructions show close similarity to the instrumental record. Therefore the CI-T record from PTHE may fail to reconstruct minor fluctuations in T_{july} over the late twentieth century due to the poor sampling resolution; sediment samples typically represent 2 -5 year periods at 20 year intervals.

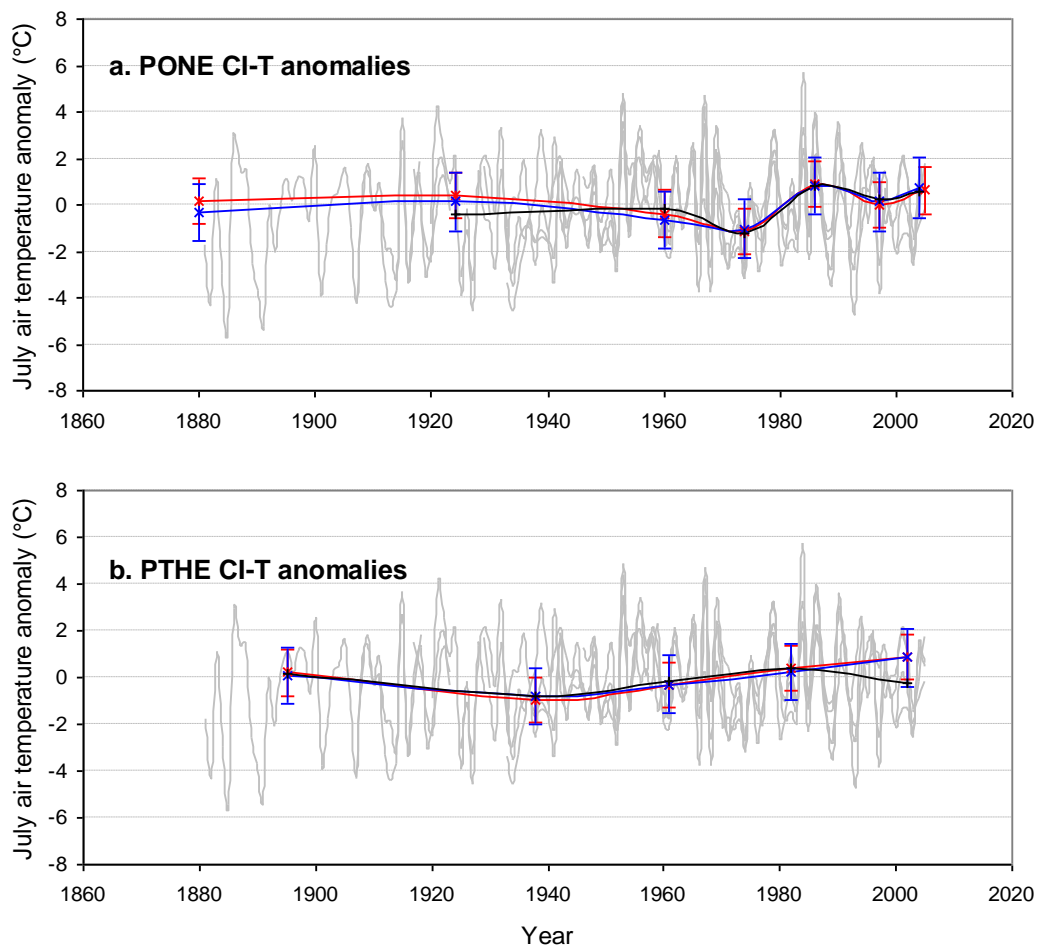


Figure 7.20. Comparison of July air temperature anomalies from CI-T WA-PLS (red) and WA (blue) reconstructions for (a) PONE, based on 50 year mean, and (b) PTHE, based on 68 year mean with instrumental record anomalies at the same sampling interval as the CI-T data in black and instrument record anomalies in grey. Reconstructions based on Russian training set K.

To overcome the poor sampling resolution and to highlight major trends in T_{july} CI-T records were combined from PONE and PTHE to produce a composite trend (Figure 7.21). Between 700 – 600 years BP chironomid-inferred T_{july} was approximately 12°C, which was 1°C warmer than present, but declined to 10.5°C by ca. 450 years BP. Although temperatures remained lower than present for the following 250 – 300 years, T_{july} show a gradual warming trend and reached present-day temperatures (ca. 11°C) 150-200 years BP.

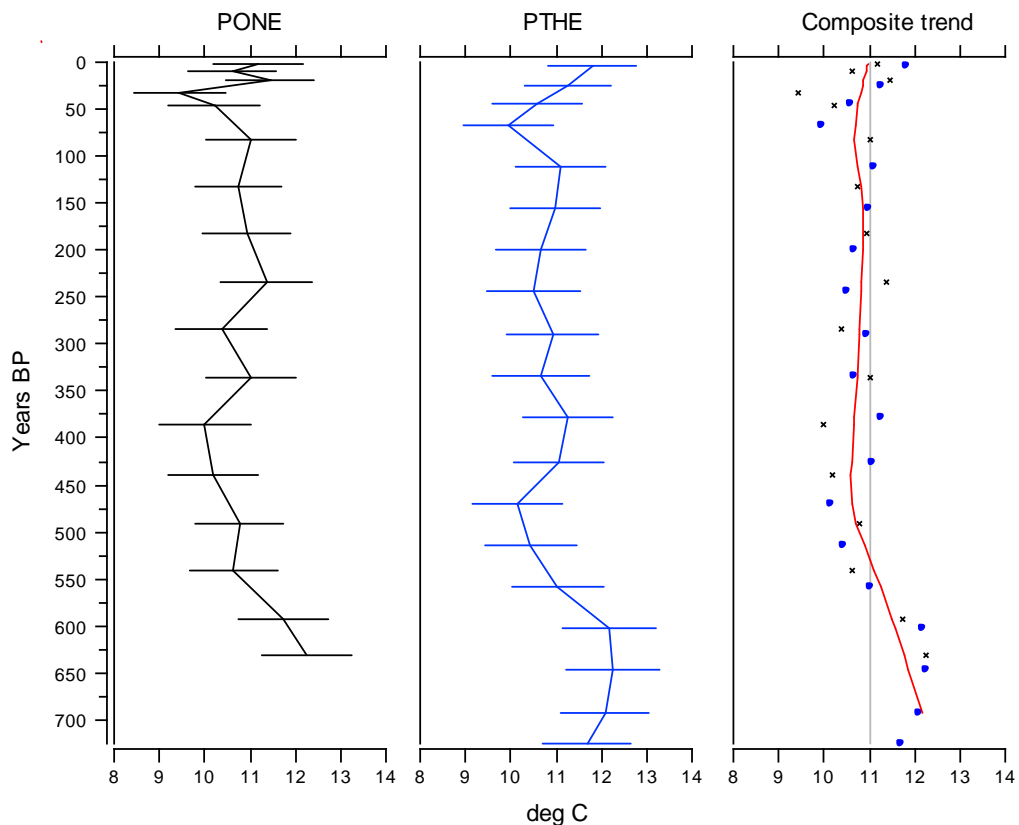


Figure 7.21. Reconstructions of mean July air temperature (°C) for PONE and PTHE based on weighted-averaging partial least squares (WA-PLS, 2 component model using training set K) and composite reconstruction fitted with LOWESS smoother (span 0.4). Sample-specific errors are shown for individual reconstructions. On composite reconstruction reference line indicates mean present-day temperature (present-day T_{july} for PONE is 11.7°C and 10.5°C for PTHE), black crosses PONE CI-T and blue circles PTHE CI-T. Age presented as years before 2006.

The instrumental record shows an increase of approximately 1°C over the past 100 years; the reconstructions for PONE and PTHE give increases of 0.4°C and 0.7°C respectively over approximately the same period. However the

instrumental record for 1880-1910 was compiled from a single station, Turuhansk, so may be less accurate than more recent records based on four stations. The instrumental records show cooler intervals prior to 1940 and in the 1970s. The reconstructions from PTHE show the pre-1940s cooling but not the later interval and the PONE reconstructions show the 1970s cool period but not the pre-1940s cooling. The records deviate markedly in their recent trends; after a slight increase ca. 1980 the instrumental record has remained stable near the 60 year mean. PONE shows a similar trend although the most recent sample (ca. 2004) shows a slight 0.5°C increase on the 1997 value. In general, the PONE reconstructions reflect the minor fluctuations in T_{july} since the 1960s whereas the PTHE reconstructions show a steady increase in T_{july} over the same period. However the accuracy of the reconstructions from PTHE between 1960 and 1990 would be affected by the possible algal growth and hiatus in sediment accumulation discussed in sections 7.4.2 and 7.5.3. The instrumental records show wide inter-annual variability and the sample specific errors of the reconstructions are within the inter-annual variation of the instrument record.

7.7.4. The reliability of down-core reconstructions

The reliability of the down-core CI-T WA-PLS reconstructions from PONE and PTHE, using the Russian training set K, was assessed by five criteria (Birks *et al.* 1990; Birks 1998; Heiri and Lotter 2001; Velle *et al.* 2005a; Engels *et al.* 2008). Less reliability is placed on CI-T reconstructions for fossil assemblages in which there are:

1. fewer than 50 chironomid head capsules,
2. more than 5% of taxa are not represented in the modern training set,
3. more than 5% rare taxa, where a rare taxon has a Hill's N_2 of 5 or less in the modern training set,
4. no close analogues for the fossil assemblages in the modern training set using squared chord distance as a measure of dissimilarity with a 5% cut level in the MAT reconstruction (Juggins 2005), and
5. no close analogues for the fossil assemblages in the modern training set based on a lack-of-fit between the fossil chironomid assemblages and T_{july} in a CCA of the modern training set with the fossil assemblages plotted passively. Lack-of-fit in the CCA was assigned to fossil

assemblages that had a squared residual distance to T_{july} greater than 10% of the extreme values in the modern training set.

Table 7.10. Assessment of the reliability of palaeoenvironmental reconstructions from PONE. Solid circle indicates more than 5% abundance of taxa that are rare or absent from training set in the subfossil assemblage, no close analogue in the modern training set and samples with a poor fit to temperature.

Sample	Sample depth (cm)	No. of HC	% taxa in training set	% rare taxa	WA-PLS sample-specific error	WA sample-specific error	Rare & non TS taxa	Non-analogue	CCA Fit-to-T
1	0 - 0.25	90	98.9	6.7	1.00	1.28	•		
2	1 - 1.25	422	100	2.6	0.98	1.26			
3	2 - 2.25	123.5	100	0.8	0.98	1.24			
4	3 - 3.25	77.5	100	2.6	1.01	1.25			
5	4 - 4.25	82.5	100	1.2	1.00	1.24			
6	6 - 6.25	73	98.6	0.0	0.97	1.24		•	
7	8 - 8.25	86.5	100	0.0	0.97	1.24			
8	10 - 10.25	73.5	94.6	0.0	0.98	1.24	•		
9	12 - 12.25	77	100	1.3	1.00	1.25		•	
10	14 - 14.25	65.5	95.4	0.0	1.01	1.26		•	•
11	16 - 16.25	70	97.1	2.9	0.99	1.24	•	•	
12	18 - 18.25	62.5	95.2	3.2	1.01	1.24	•		
13	20 - 20.5	83.5	100	4.2	1.00	1.24			
14	22 - 22.5	79.5	96.2	0.0	0.98	1.24		•	
15	24 - 24.5	73	100	1.4	0.98	1.24		•	
16	26 - 26.5	56.5	98.2	3.5	1.00	1.24	•	•	
17	27.5 - 28	92	95.7	3.8	1.00	1.24	•	•	

The percentages of non-training set taxa (100 - % taxa in training set) are high in a number of samples from PONE, up to 5.4%. During development of the Russian inference model K (section 6.2.2) taxa present in 3 or fewer lakes were omitted from the training set. Therefore a number of taxa which comprise frequent but minor components of the chironomid assemblages such as *Synorthocladius* and *Orthocladius trignolabis*-type are absent from the training set. High abundances of taxa absent from the training set and of rare taxa means the reconstructions from a number of samples from PONE may be unreliable, based on these criteria (Table 7.10). Many of the samples have no close analogue in the modern data, although in some instances (for example, sample 15, 24 cm depth) all the taxa are present in the training set and all the dominant taxa are well represented. In these instances the relative abundances of taxa in the fossil samples are probably not well represented in the individual

training set lakes (Engels et al. 2008). However WA-PLS, which was selected as the most appropriate statistical method in section 7.7.2, performs relatively well in poor analogue situations (Birks 1998). Only four samples have more than 5% rare taxa in PTHE and no samples were identified as unreliable in more than one criteria (Table 7.11). The increase in rare taxa between 16.25 – 12 cm depth is due to higher abundances of the cold stenotherms *Protanypus* and *Hydrobaenus lugubris*-type.

Table 7.11. Assessment of the reliability of palaeoenvironmental reconstructions from PTHE. Solid circle indicates more than 5% abundance of taxa that are rare or absent from training set in the subfossil assemblage, no close analogue in the modern training set and samples with a poor fit to temperature

Sample	Sample depth (cm)	No. of HC	% taxa in training set	% rare taxa	WA-PLS sample-specific error	WA sample-specific error	Rare & non TS taxa Non-analogue CCA Fit-to-T
1	0.25 - 0.5	304	100	0.0	0.969355	1.23296	
2	1.25-1.5	155.5	100	0.0	0.965808	1.22719	
3	2 - 2.25	55.5	100	0.9	0.985812	1.23375	
4	4 - 4.25	57.5	100	0.0	0.982909	1.23362	
5	6 - 6.25	73	100	2.1	1.00296	1.23645	
6	8 - 8.25	75.5	100	2.6	1.00108	1.23333	
7	10 - 10.25	71	100	2.1	0.996933	1.23513	
8	12 - 12.25	75.5	98.7	6.6	1.05063	1.23337	•
9	14 - 14.25	66.5	100	6.0	1.00494	1.22358	•
10	16 - 16.25	65	100	5.4	1.08664	1.23589	•
11	18 - 18.25	101.5	100	1.0	0.992637	1.22985	
12	20 - 20.5	209	100	1.4	0.983252	1.22132	
13	22 - 22.5	138	100	0.0	0.975853	1.22403	
14	24 - 24.5	92	100	3.3	1.01346	1.23233	
15	26 - 26.5	77.5	100	2.6	1.01337	1.22733	
16	28 - 28.5	102	100	3.9	1.03226	1.23533	
17	30 - 30.5	77	96.1	2.6	1.02118	1.23005	•
18	32 - 32.5	106	100	1.9	0.97689	1.21957	
19	33.5 - 34	79	98.7	1.3	0.982402	1.22389	

7.8. Chironomid-inferred continentality (CI-C) reconstruction

The environmental and species training set used in the development of the CI-C models are detailed in Chapter 6 (section 6.7.2). Section 6.7.2 also gives the performance statistics of each model (RMSEP, r^2 , mean and maximum bias) and the number of WA-PLS components selected to give the minimal adequate model. In this section the continentality reconstructions derived by WA-PLS, WA and WA-TOL are examined to determine which statistical technique

appears most appropriate for reconstructing past continentality in the Putorana. Trends in reconstructed CI are compared to instrumental-derived CI to examine the accuracy of the reconstructions.

7.8.1. Selection of the statistical technique for CI-C reconstructions

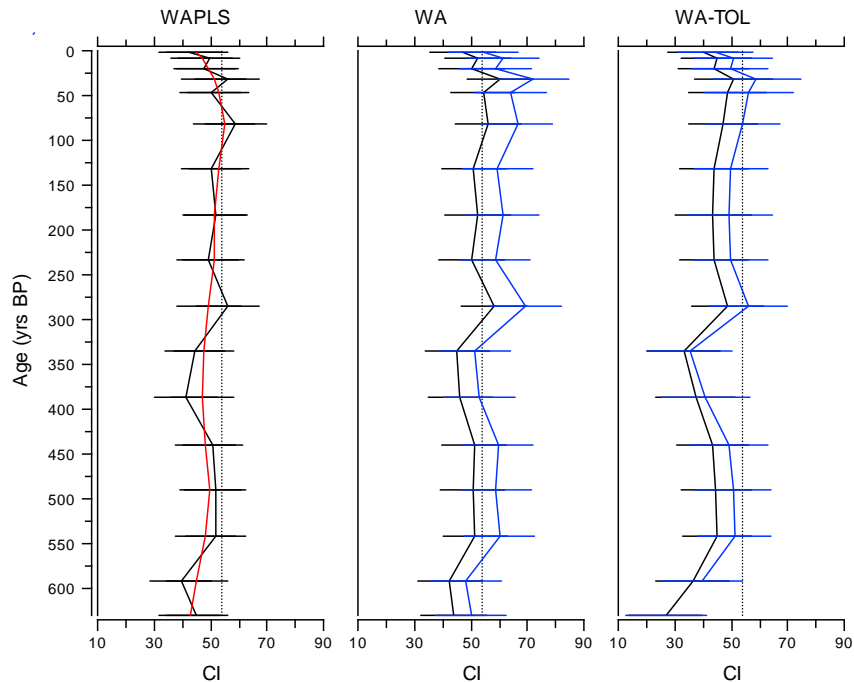


Figure 7.22. Reconstructions of continentality (CI) for PONE based on weighted-averaging partial least squares (WA-PLS, 2-component model, with LOWESS smoother span 0.45), weighted averaging (WA) and tolerance downweighted weighted averaging (WA-TOL). WA and WA-TOL reconstructions with inverse deshrinking are shown in black and reconstructions with classical deshrinking in blue. Vertical black dashed line indicates present-day CI of 54. Sample-specific errors of reconstruction are shown for all techniques. Age presented as years before 2006.

Both WA-PLS and WA-TOL appear to underestimate present-day continentality in the Putorana lakes. At PONE the reconstructed values are within the sample-specific errors (Figure 7.22) but at PTHE the reconstructed CI are 13 – 16 below present values (Figure 7.23). WA and WA-TOL reconstructions with classical deshrinking are closer to present-day values than those with inverse deshrinking and therefore classical deshrinking will be used for CI reconstructions. Before approximately 600 years BP the WA-TOL reconstructions show marked differences in CI trends from WA-PLS or WA. At the base of PONE WA and WA-PLS CI remained stable at 40 – 50 from 590 –

630 years BP but in the WA-TOL reconstruction declined to 27 at 630 years BP. The majority of taxa in these subfossil assemblages have broad tolerances with the exception of *Paracladius* (CI optima 42, tolerance 14). A decline in its relative abundance from 19% to 9% at 630 years BP may have resulted in the low CI WA-TOL reconstruction. However taxon richness was higher in the lower sample so the decline in relative abundance may not represent a decline in absolute values. The sensitivity of this technique to changes in species richness would preclude it from these reconstructions where the number of taxa varies from 18 – 30. The WA-PLS and WA trends also show minor variations; for example in PTHE, between 68 – 111 years BP, CI remained stable at 43 in WA-PLS but declined by 4 in WA with classical deshrinking.

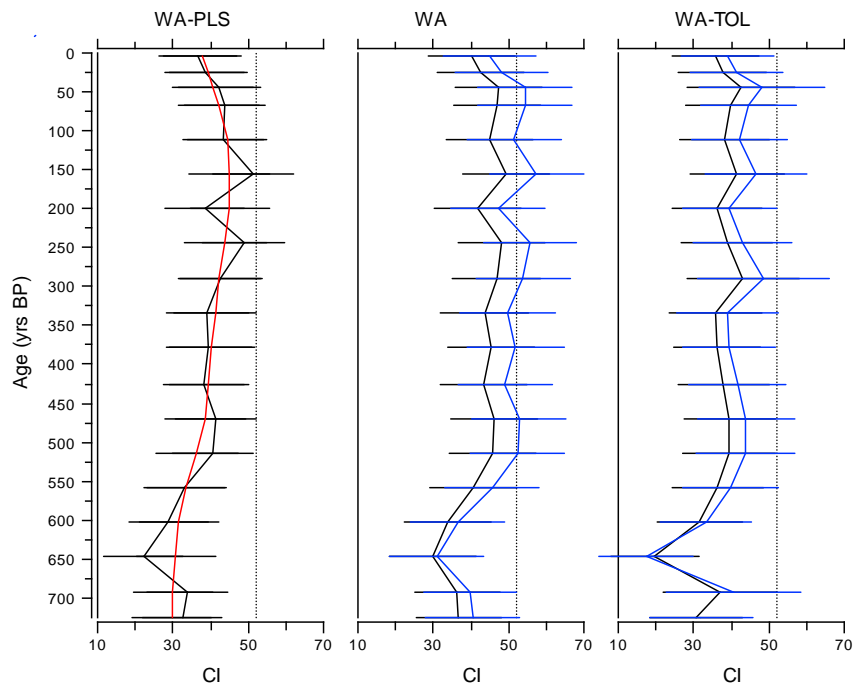


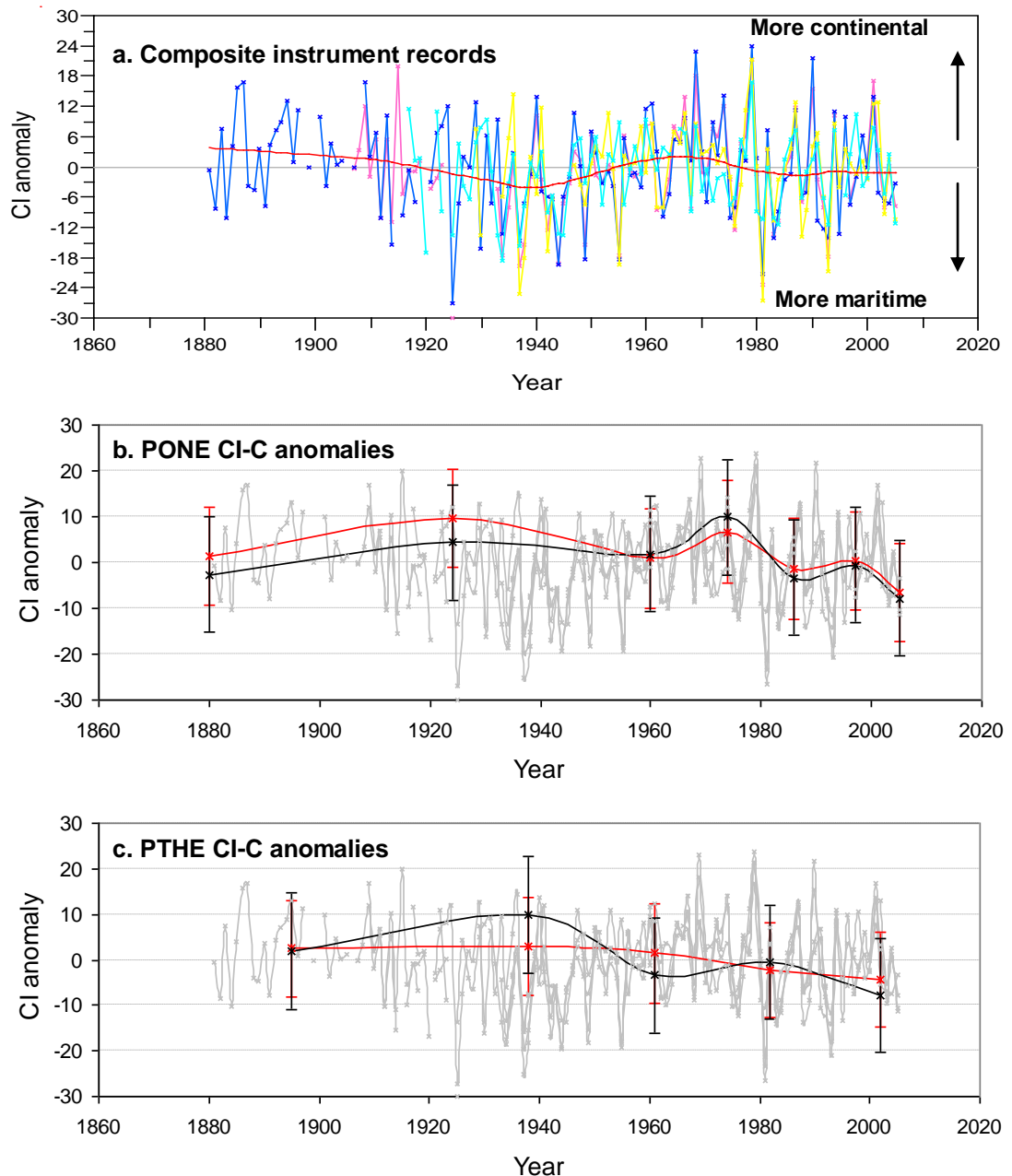
Figure 7.23. Reconstructions of continentality (CI) for PTHE based on weighted-averaging partial least squares (WA-PLS, 2-component model with LOWESS smoother span 0.45), weighted averaging (WA) and tolerance downweighted weighted averaging (WA-TOL). WA and WA-TOL reconstructions with inverse deshrinking are shown in black and reconstructions with classical deshrinking in blue. Vertical black dashed line indicates present-day CI of 52. Sample-specific errors of reconstruction are shown for all techniques. Age presented as years before 2006.

7.8.2. Comparison to instrumental records

WA with classical deshrinking and WA-PLS reconstructions were compared to CI derived from instrumental records from the four meteorological stations used to evaluate CI-T reconstructions (section 7.7.1). All the temperature records have missing data and records are particularly intermittent from 1919 – 1934. Continentality indices (CI) were calculated as described in section 3.3.5 and a regional CI anomaly record constructed as deviations from the 60 year mean (for the period 1946 – 2005). Reconstructions for PONE and PTHE were calculated as deviations from a 50 and 68 year mean respectively.

The LOWESS smoother fitted to the instrumental-derived CI record shows minor oscillations in the CI trend over the twentieth century (Figure 7.24a). However since 1880 the CI has decreased by approximately 0.25 decade^{-1} . The rate has accelerated over recent decades and CI has declined by 1.0 decade^{-1} since 1960. The instrumental anomalies record indicates the climate was more maritime (CI ca. 4 below mean) between 1920 - 1955 and more continental (CI 3 higher than mean) in the 1960s and 70s (Figure 7.24a). The WA-PLS and WA CI-C reconstructions from PONE and PTHE show a general decline in CI since 1900, however all reconstructions underestimate present-day CI anomaly (Figure 7.24b and c). WA CI-C from PONE and PTHE and WA-PLS reconstructions from PONE show a more continental interval in 1970-80 preceded by a less continental period. The CI-C from PONE in the 1970s is more continental (CI +10) than the instrumental anomaly but within the variation from the four meteorological stations. The CI-C reconstructions are also too continental for PONE in 1920 and PTHE in the 1940s, but also within the instrumental variation. WA with classical deshrinking more accurately estimates present-day CI for the Putorana lakes and reconstructs more of the minor trends in continentality over the twentieth century than WA-PLS. Previous evaluation of the WA-PLS model, in Chapter 6, showed it under-predicted continentality above indices of 50, i.e. on the Putorana (Figure 6.13) but performed well with an independent set of lakes from other areas of Russia (Table 6.16). Therefore it is necessary to assess whether the WA-PLS or the WA model is more appropriate for reconstructions in European Russia (section 8.9).

Figure 7.24. Continuity Indices anomalies (a) of instrumental records from Dudinka (pink), Turuhansk (blue), Hatanga (yellow) and Ostrov Dikson (cyan), based on deviation from a 60 year mean (1946 – 2005) fitted with Loess smoother (span 0.3). WA-PLS (red) and WA (black) CI-C anomalies from (b) PONE, based on 50 year mean, and (c) PTHE, based on 68 year mean. Instrument record anomalies are shown in grey.



7.8.3. Continuity Indices reconstructions

Figure 7.25 shows the reconstructed CI-C for PONE and PTHE and a composite trend based on both lakes. Reconstructed CIs were more maritime (CI ca. 10 lower than present) 700 years BP but increased to near or slightly above present-day values by ca. 530 years BP. CI-C increased steadily from

350 years BP to CI ca. 10 higher than present 80 -100 years BP. Over the last 100 years CI has declined with the rate of decline accelerating over the past 50 years. CI-C from PONE reconstruct more continental (i.e. have a shorter ice-free season) than PTHE, although the lake is at a lower altitude. This result emphasises the individualistic nature of ice-free season proxies which are greatly influenced by localised factors. PTHE is at higher altitude and experiences colder air temperatures, but has a more open aspect, than PONE which is situated in a SW-NE trending valley. The greater wind shear or more direct sunlight in early spring at PTHE may lead to earlier break up of lake ice.

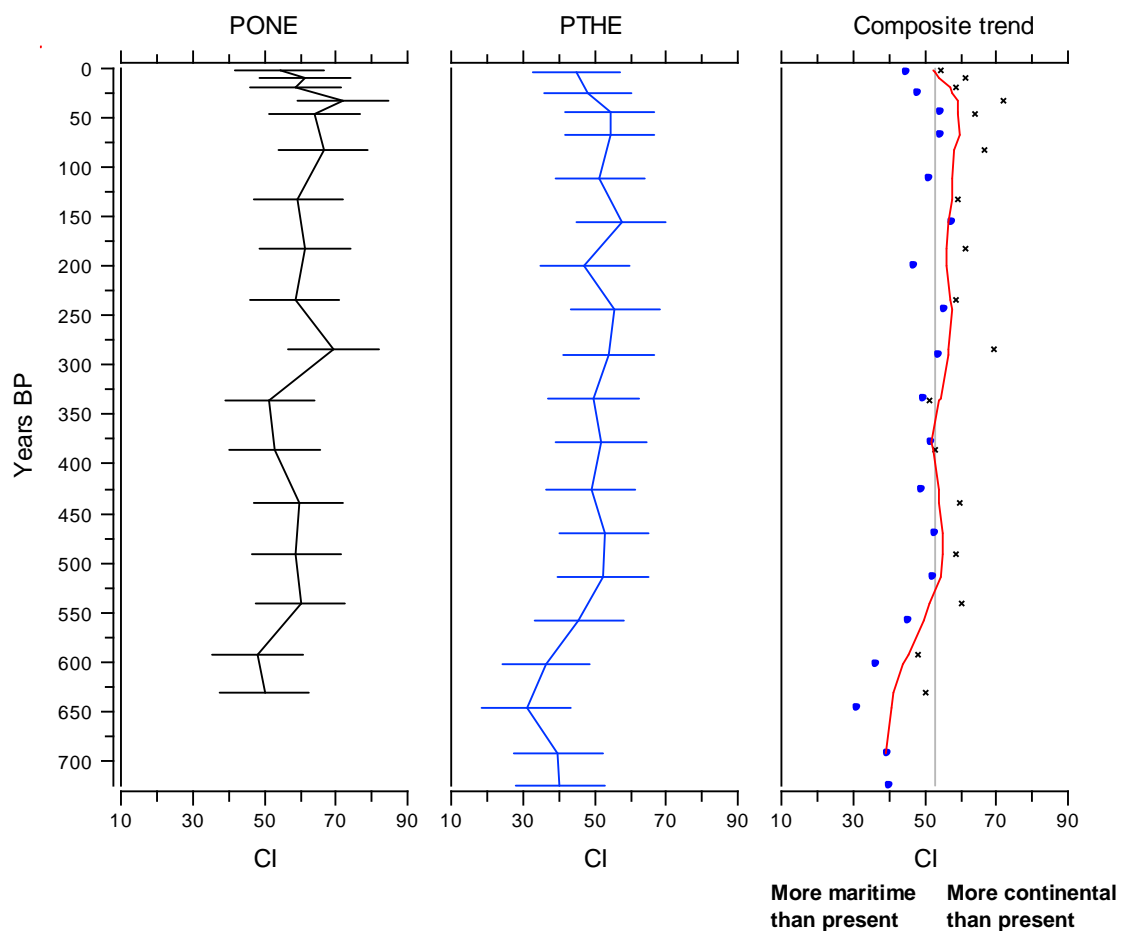


Figure 7.25. Reconstructions of CI-C for PONE and PTHE based on weighted-averaging (WA with classical deshrinking) and composite reconstruction fitted with LOWESS smoother (span 0.25). Sample-specific errors are shown for individual reconstructions. On composite reconstruction reference line indicates present-day CI, black crosses PONE CI-C and blue circles PTHE CI-C. Age presented as years before 2006.

7.9. Palaeoenvironmental interpretation

Chironomid biostratigraphy

The chironomid fauna, throughout the cores, which typically include *C. anthracinus*-type, *C. ambigua*, *Corynocera oliveri*-type, *S. coracina*-type, *Procladius*, *Micropsectra* spp., *T. lugens*-type and other abundant Tanytarsini spp., are similar in composition to early Holocene assemblages from northern Europe (Velle *et al.* 2005a). This similarity may be due to the cool climate and/or the oligotrophic status of the lakes, as many of these taxa, for example *T. lugens*, are found in the profundal of oligotrophic lakes or in the littoral of cold subarctic or subalpine lakes (Brundin 1956; Brodin 1986).

750 – 600 years BP

Chironomid-inferred reconstructions, and the absence of taxa with temperature optima below 11°C, in PTHE, indicate the climate was ca. 1°C warmer and more maritime than present 750 – 600 years BP (Figure 7.26). The timing and occurrence of the 'Medieval Warm Period' (MWP) is not uniform throughout the northern hemisphere (Crowley and Lowery 2000; Jones and Mann 2004). Analysis of tree-rings from Taymyr and Putorana identified a prolonged warm period during 1100 – 800 years BP as the MWP and short warm period 760 – 700 years BP (Naurzbaev and Vaganov 2000; Naurzbaev *et al.* 2002).

From 625 – 600 years BP chironomid-inferred continentality began to increase, T_{july} decreased and there was an influx of cool-water taxa with optima below 11°C in both PTHE and PONE (Figures 7.26 and 7.27). Major changes in atmospheric circulation, leading to a period of rapid climate change, started ca. 600 years BP (Meeker and Mayewski 2002; Mayewski *et al.* 2004). Strengthening atmospheric circulation led to a stronger Siberian High and deeper Icelandic Low pressure system. This intensified wind strength from the centre of the Siberian High towards Iceland, increasing the levels of potassium, derived from sea spray, which was deposited in the Greenland GISP2 ice-core (Mayewski *et al.* 2004). Changes in CI-C, particularly in PTHE, closely track K^+ concentrations in the ice-core over the last 700 years (Figure 7.28). In PTHE marked changes in CCA axes 1 and 2 sample scores occur during the period of climate change from 625 – 500 years BP. The CCA time-tracks (Figure 7.16)

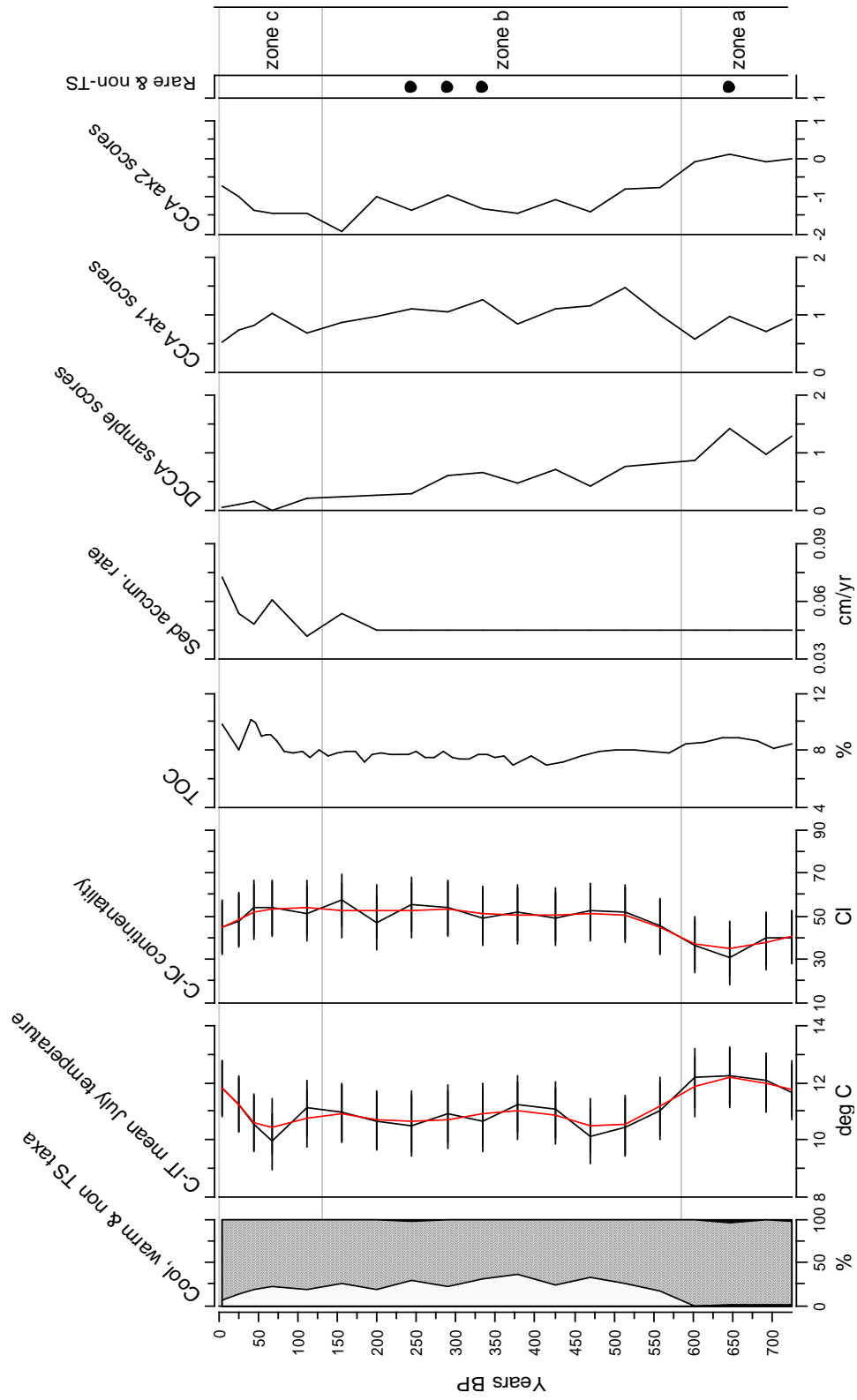


Figure 7.26. Summary diagram for PTHE showing the percentage of cool-water taxa (optima <11°C), warm-water taxa (optima >11°C) and non training set taxa, chironomid-inferred mean July air temperature and continentality, total organic carbon (TOC) of bulk sediment, sediment accumulation rate, DCCA scores, CCA axes 1 and 2 scores. C-IT and C-IC are shown with sample specific errors and LOWESS smoother (span 0.25). The solid circles indicate samples with more than 5% abundance of taxa that are rare or not included in training set. Age of samples are years before 2006.

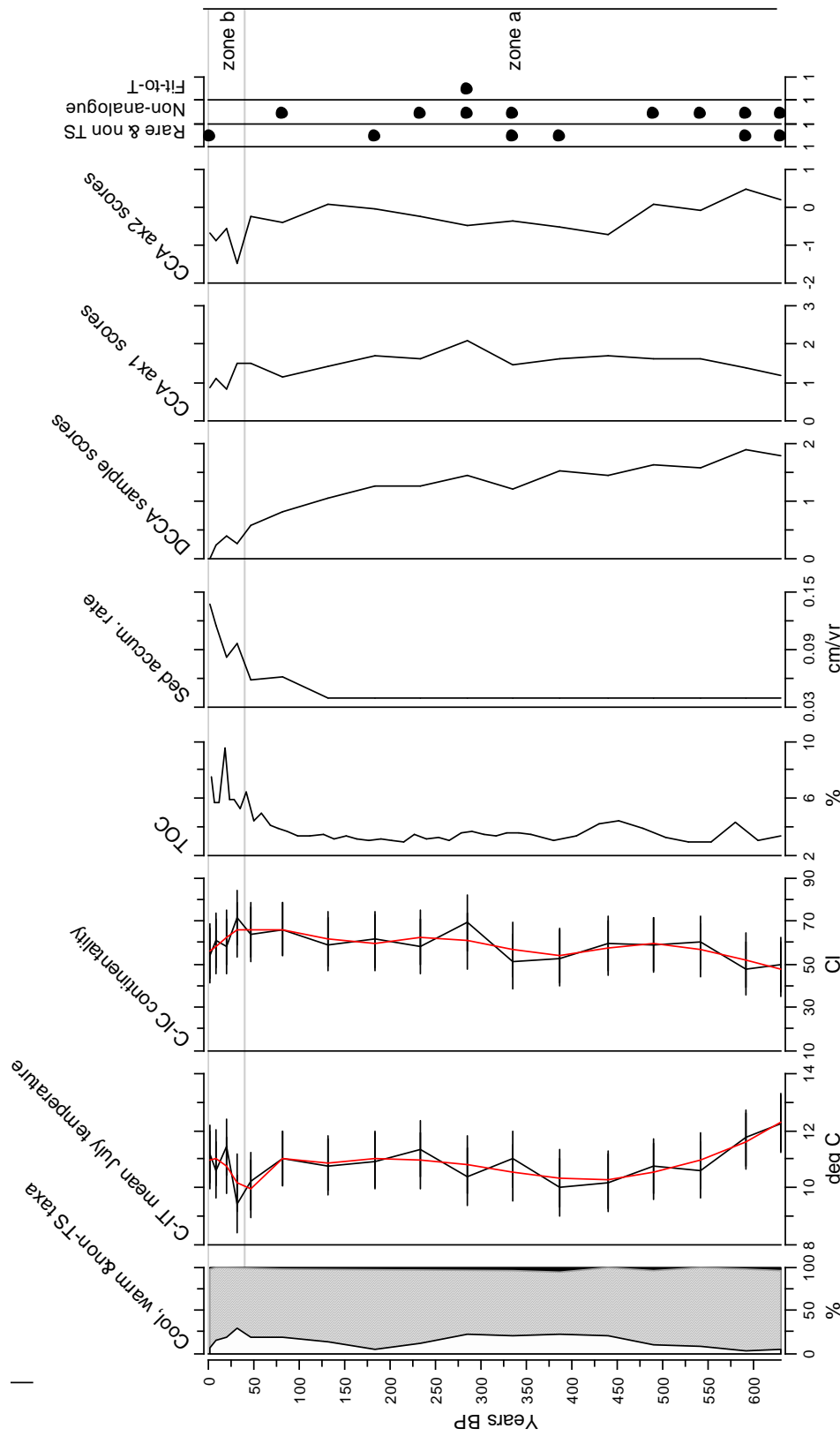


Figure 7.27. Summary diagram for PONE showing the percentage of cool-water taxa (optima <11°C), warm-water taxa (optima >11°C) and non training set taxa, chironomid-inferred mean July air temperature and continentality, total organic carbon (TOC) of bulk sediment, sediment accumulation rate, DCCA scores, CCA axes 1 and 2 scores. C-IT and C-IC are shown with sample specific errors and LOWESS smoother (span 0.25). The solid circles indicate samples with more than 5% abundance of taxa that are rare or not included in training set, have no close analogue and have a poor to temperature. Age of the samples presented as years before 2007.

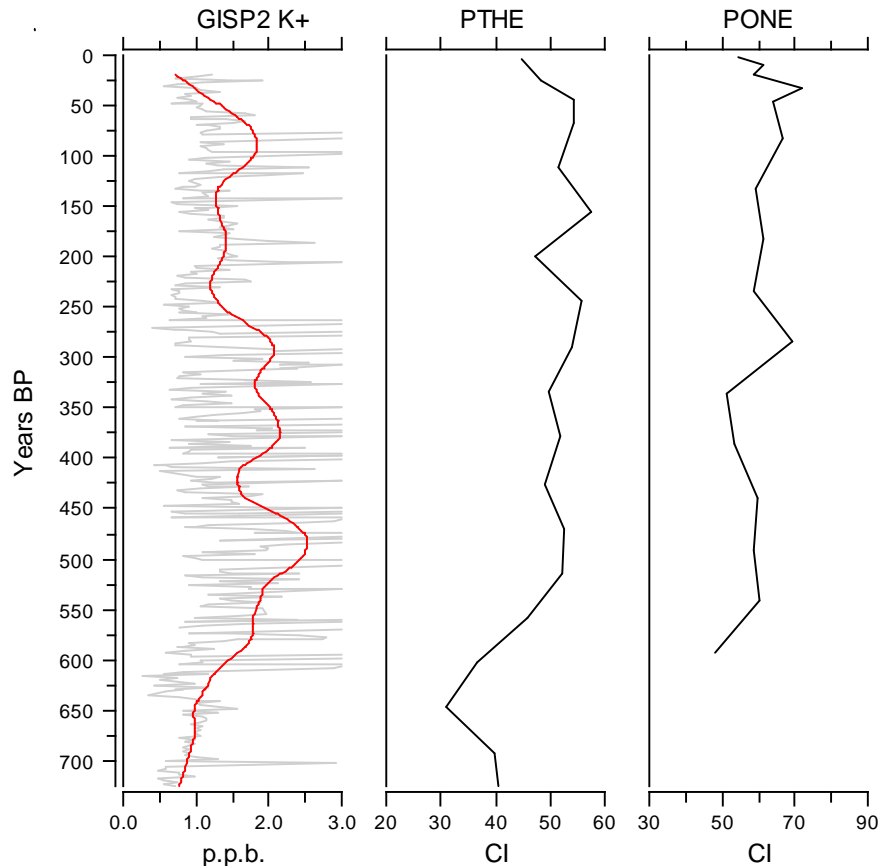


Figure 7.28. Comparison of chironomid-inferred continentality from PONE and PTHE with GISP2 K⁺ ice core record, proxy for the strength of the Siberian High (Meeker and Mayewski 2002; Mayewski et al. 2004). CI-C based on WA_{cl.a.}. Increased K⁺ indicates a stronger Siberian High. Age are years before 2006. GISP2 ion chemistry data obtained from: <ftp://ftp.ncdc.noaa.gov/pub/data/paleo/icecore/greenland/summit/gisp2/chem/ionb.txt>.

suggest this reflects changes in both T_{july} and water depth. The intensification of the Siberian High may have reduced precipitation and water availability on the Putorana Plateau. Increases or decreases in precipitation are typically associated with changes in sediment source or clastic influx which lead to changes in percentage dry weight. Percentage dry weight, in core PTHE, remains relative stable throughout the period of intensification of the Siberian High while TOC decline (Figure 7.10). Therefore the productivity of the lake and/or surrounding environment appears to have declined while sedimentation, in terms of sediment source and dry weight, remained largely unaffected. Together with the increase in the percentage of cool taxa (Figure 7.26) and the appearance of cold stenotherms in the sedimentary sequence (Figure 7.15),

this suggests the changes in the chironomid assemblages were primarily a response to declining temperatures. The results indicate that both climate and water depth exert a strong influence on chironomid faunal changes, however the assimilation of CCA axes 1 and 2 scores, changes in faunal composition and other proxy records allows the relative influence of the environmental variables to be assessed (see aims in Chapter 1). The DCCA scores, with age as the sole constraint (Birks 2007), show rapid compositional changes occurred in PTHE between 650 – 500 years BP. In the shorter core, PONE, these signals are more subdued.

500 – 150 years BP

Temperatures remained approximately 1.0 – 1.5 °C cooler than present-day and continentality relatively stable, with minor fluctuations, between 500 – 150 years BP. Occurrence of this cooler period is supported by pollen records from the Taymyr Lowlands (Andreev et al. 2002), tree-ring growth in northern Siberia (Jacoby *et al.* 2000; Naurzbaev and Vaganov 2000; Hantemirov and Shiyatov 2002; Naurzbaev et al. 2002) and glacier advances on Svalbard and Franz Josef Land (Tarussov 1992; Lubinski *et al.* 1999). However, the records show differences in the severity, timing and duration of the cold period. The pollen records suggest July temperatures were approximately 1°C cooler between 550 – 300 years BP (Andreev *et al.* 2002) whereas the tree-ring growth indicate June temperature were less than 0.5°C cooler from 600 – 300 years BP and again ca. 200 - 150 years BP (Naurzbaev and Vaganov 2000; Naurzbaev *et al.* 2002). This cooler period corresponds to the 'Little Ice Age' in European records (reviewed in Jones and Mann 2004), but the use of the term is disputed by Jones and Mann (2004) as the cooling trend is not global nor consistent in timing. Total organic carbon (TOC), remained low and stable, at 4% in PONE and 8% in PTHE. C:N ratios suggest organic matter is derived primarily from aquatic algae or macrophytes throughout the core so low TOC may reflect a period of low productivity (section 7.4). Tree-ring records from northern Siberia show a colder interval ca. 200 - 150 years BP (for example Jacoby et al. 2000) which is not evident in the CI-T reconstructions where T_{july} are similar to present-day values.

150 years BP – present day

From 150 – 100 years BP TOC and sediment accumulation rates start to increase; these changes occur concurrently with declines in $\delta^{15}\text{N}$ (sections 7.5.2 and 7.5.3). The decline in $\delta^{15}\text{N}$, at least partially, may reflect enhanced deposition of fixed nitrogen from fossil fuel burning and other anthropogenic sources (Wolfe *et al.* 2001; Hastings *et al.* 2009). These changes precede changes in CI-T and CI-C in PONE (Figure 7.27) but the timing is less certain in PTHE where the sedimentation rate is more erratic (Figure 7.26). Over the last 100 years CI-C has declined and the rate of decline has accelerated over the past 50 years, the magnitude and rate of decline is consistent with data from instrumental records for the Arctic (Hirschi *et al.* 2007). The GISP2 record also shows a major decline in K^+ concentrations over this period indicating a change in atmospheric circulation and weakening of the Siberian High (Figure 7.27). The Siberian High is responsible for the severity of winter across Siberia and remains influential until the end of April (Przybylak 2003). Weakening of the Siberian High would increase spring temperature and therefore the length of the ice-free period. After a cold interval in the early – mid twentieth century, T_{july} increased to present-day levels. The evidence for recent warming is ambivalent; instrumental records and CI-T from PONE suggest T_{july} temperatures remained relatively stable over the past 30 years whereas CI-T from PTHE increased (section 7.7.1). However the reconstructions from the surface sediments of PTHE may be unreliable due to uncertainties associated with the age-depth model for this part of the core. The ^{210}Pb dating identified a hiatus in recent sediment accumulation (section 7.4.2). The DCCA scores from PONE, with age as the sole constraint (Birks 2007), shows enhanced levels of compositional turnover particularly over the last 20 years. The recent rates of compositional change are unprecedented compared to the previous 600 years and are comparable to the increases in beta-diversity (expressed as SD units), over the last 150 years, observed in biological communities from other arctic lakes in Canada, Fennoscandia and north-east European Russia (Smol *et al.* 2005). The CI-T has remained stable over this period, whilst CI-C has decreased, which suggests the chironomid fauna may be responding to changes in the length of the ice-free season and enhanced productivity.

The relationship between air temperatures and continentality

Prior to 100 years BP CI and T_{july} demonstrate an inverse relationship which has become decoupled over the last century. Hirschi *et al.* (2007) suggested the stable summer temperature, with decreasing continentality, could be a consequence of increased melting of Arctic sea ice which extracts heat from the atmosphere (the standard enthalpy of fusion). This is the heat needed to be added to a system to create the disordered atomic structure of a liquid from the ordered crystalline structure of solid ice, and is absorbed without raising the temperature of the solid. The most rapid decrease in sea-ice coverage occurs in June and July, so that these are the months when most heat is extracted from the air for ice melting (Hirschi *et al.* 2007). The application of inference models for both July air temperature and continentality to subfossil assemblages enhances the explanatory power of the reconstructions and, as the link between sea-ice and continentality demonstrates, enables possible mechanisms to be suggested for the observed climate change. The relationship between continentality and the strength of the Siberian High also contributes to a better understanding of the regional impacts of climate change.

7.10. Summary

- Sediment cores were collected and analysed from three lakes on the Putorana Plateau, Western Siberia. These were selected as representative of the altitudinal-based habitats on the Plateau.
- The chironomid assemblages from these lakes, over the past 750 years, are typical of cold and/or oligotrophic lakes from northern Eurasia. They are distinguished from other Russian and Norwegian lakes by the high abundances of *Corynocera ambigua* and *C. oliveri*-type.
- CCA sample scores and the occurrence of taxa associated with streams or flowing water suggest many of the lakes have been subject to periodic flooding and/or changes in catchment hydrology over time.
- For one lake, AFOX, the high frequency of flooding made palaeoenvironmental reconstructions unreliable. Further analysis suggests there has been *in situ* algal or cyanobacterial growth and/or a hiatus in

sediment accumulation at PTHE which means recent reconstructions (over the last 50 years) might also be unreliable.

- Testing of the regional training sets and statistical methods indicated that a 2-component WA-PLS inference model using Russian training set K most accurately reconstructed the regional instrumental records for July air temperature over the past 120 years.
- A WA inference model, with classical deshrinking, most accurately reconstructed continentality at the Putorana lakes. However, previous evaluation (in Chapter 6) suggests a WA-PLS model may be more appropriate for European Russia.
- Chironomid-inferred reconstructions indicate the climate was approximately 1°C warmer than present between 750 – 600 years BP. This may correspond to the ‘Medieval Warm Period’ in European records, but is slightly later than a warm period identified from tree-rings (760 – 700 years BP) from the Taymyr-Putorana region.
- Between 625 – 500 years BP there was a period of rapid climate change marked by decreases in T_{july} and increasing continentality which may be linked to hemispheric-scale changes in atmospheric circulation. This is accompanied by rapid compositional changes in the chironomid fauna at PTHE, although the response is more muted at PONE.
- The climate remained stable, in this cooler phase, until approximately 150 years BP. This interval shows close agreement with the timing and duration of the ‘Little Ice Age’ in European and other northern Russian records.
- From approximately 150 years BP to present-day, TOC and sediment accumulation rates have increased, this is associated with a decrease in $\delta^{15}\text{N}$ which may originate from increased deposition of atmospheric nitrogen derived from the burning of fossil fuels.
- CI-C has declined over the past 100 years with the rate of decline accelerating over the last 50 years. This may result from a weakening of the Siberian High pressure system and would lead to increasing spring temperatures and lengthening of the ice-free period.

- After a cool period in early – mid twentieth century, T_{july} increased to present-day values. Instrumental records and CI-T from PONE indicate T_{july} have remained relative stable over the last 50 years. CI-T from PTHE increased over this period, but these reconstructions may be unreliable.
- The chironomid fauna at PONE shows enhanced levels of compositional turnover over the past 150 years. The changes are unprecedented over the last 600 years and are comparable in magnitude to changes in biological communities observed in other lakes throughout the Arctic.

Chapter 8

North-east European Russia

8.1. Introduction

This chapter presents and discusses the results of palaeoenvironmental analyses on lake sediment cores from north-east European Russia (NEER). The physical and biological characteristics of the study area are described in Chapter 2. The present-day assemblages were included in the analysis of variables influencing chironomid distribution in northern Russia (Chapter 4). This chapter aims to examine factors which have influenced changes in the past chironomid assemblages within these lakes. Sediment cores were collected from four lakes which are described in section 8.2. Following preliminary range-finder radiocarbon dating, two lakes were selected for more detailed study. The results from sedimentary, isotopic and chironomid analyses are presented in sections 8.6 – 8.9. These results are then interpreted to produce a synthesis of palaeoenvironmental change in NEER over the late Quaternary.

8.2. Description of coring sites

Coring sites were selected on the Putorana Plateau as this area had experienced a decline in temperature between 1981 and 2001. The palaeoenvironmental analyses from the Putorana are presented and discussed in Chapter 7. The NEER was selected as this area, by contrast, had experienced a positive trend over this period (see Chapter 1). The warming had occurred throughout European Russia (Comiso 2003) but lakes were selected within the Arctic as these are remote from most anthropogenic inputs and sensitive to environmental change.

Sediment cores were collected from four lakes in NEER in April 2007; these included one forested and three tundra lakes (section 2.2.1.2). The coring procedures, extrusion process, laboratory methods, chironomid preparation and counting are described in Chapter 3. The locations of the coring sites are shown in Figure 2.3 and details of the core lengths and sampling resolution given in Table 3.2. The cores taken with the Russian corer were extruded in the field

and sub-sampled later at 1cm intervals, cores from the Renberg corer were extruded in the field at 0.5cm intervals for the first 5cm, then at 1cm intervals for the remaining core. Changes in the colour and texture of the sediment were recorded in the field.

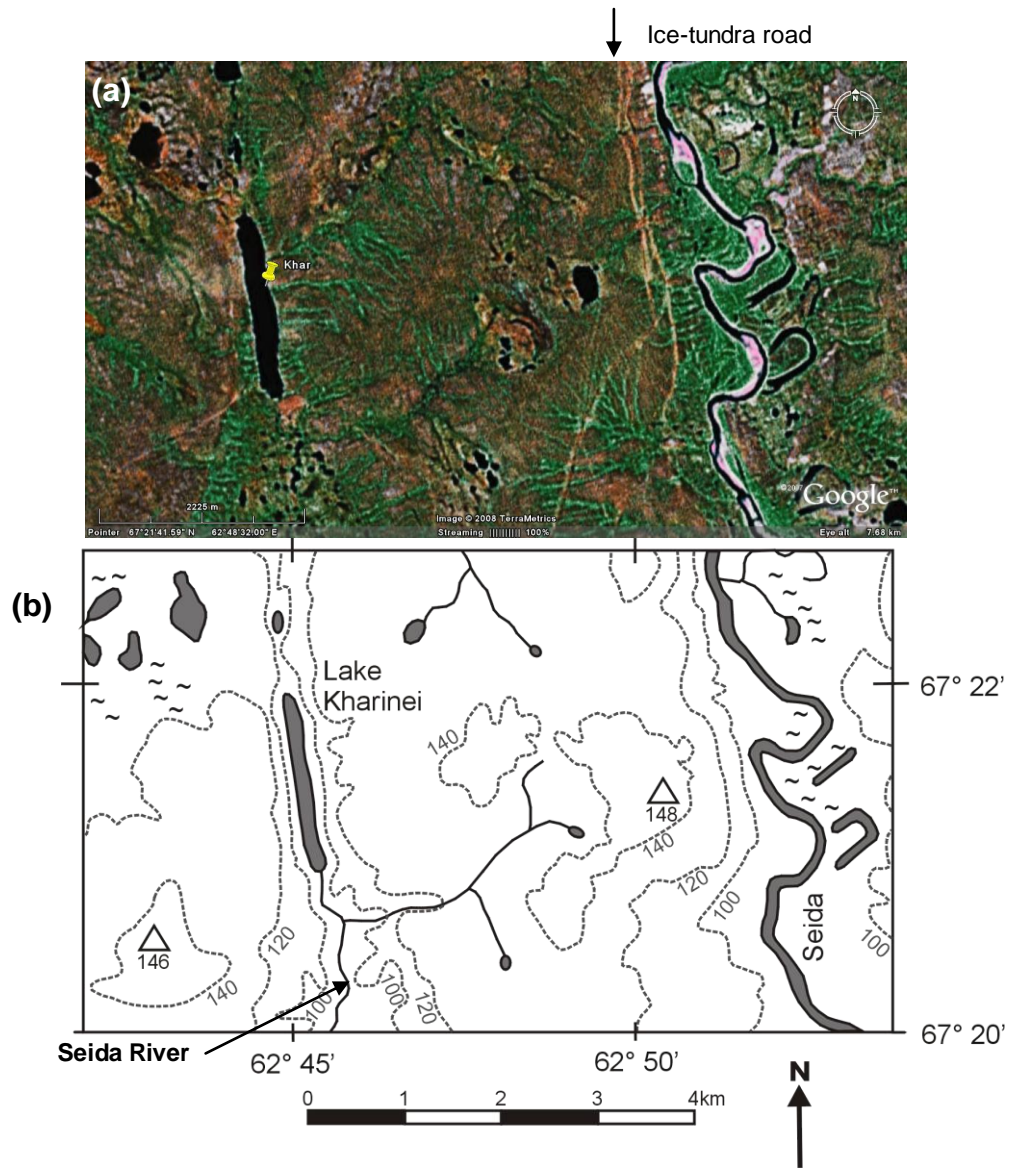
Note - Unless specified otherwise, all sample depths from sedimentary cores collected in NEER and presented in this chapter refer to depth below the water surface (i.e. the water-air interface).

The following sections provide brief descriptions of the catchment of each lake with sketch maps and/or GoogleEarth™ images. The catchments were snow-covered throughout the fieldwork; details of the vegetation are therefore based on descriptions from secondary sources.

8.2.1. Lake Kharinei, code KHAR

Lake Kharinei is a narrow, elongated lake situated between low ridges within undulating tundra (Figure 8.1a). The lake is approximately 50 km southwest of Vorkuta and a tundra-ice road, from Vorkuta, runs parallel to the lake and the Seida River (Figure 8.1b). The catchment has typical tundra shrub and dwarf-shrub vegetation (V. Ponomarev, pers. com., 2007), although taller *Salix* trees (1-3m) were seen within the Seida river valley. Water flows south from the lake into a tributary of the Seida river system. The centre of the lake was between 10 -16m deep and the core was taken from adjacent ice holes at 7.8m water depth in the northern part of the lake. The overlapping Russian cores gave a total length of 3.18m. The base of the two deepest cores varied in texture; KHAR-4 had a basal layer of sand at 1074 – 1078cm below the water surface whereas KHAR-5 was clay-gyttja sediment to 1096cm depth. A more detailed stratigraphy is presented in section 8.6.

Figure 8.1. Lake Kharinei, Code KHAR. (a) GoogleEarth™ image (accessed 20.05.2007) and (b) topographic map of Kharinei (based on Russian map, 1981, scale 1:200 000).
 67.362806N, 62.750722E, Altitude 108m a.s.l., Area 50 ha, Depth 16 m, pH 7.25



8.2.2. Lake Nerusaveito code NERU.

Lake Nerusaveito is a large, irregular shaped (ca. 100 ha) lake approximately 50 km west of Vorkuta which is part of a series of lakes and streams that flow towards the south-west. The lake was cored in the south-eastern basin at 5.85m water depth (Figure 8.2), although the maximum depth of the lake is probably much deeper. The catchment of the lake was gently undulating tundra with typical tundra shrub vegetation (V. Ponomarev, pers. com., 2007). The overlapping Russian cores gave a total length of 2.40m of clay-gyttja sediment.

Preliminary radiocarbon dating (section 5.3) indicated sediment accumulation at the lake was discontinuous with a hiatus in the mid-late Holocene and the core was not analysed further.

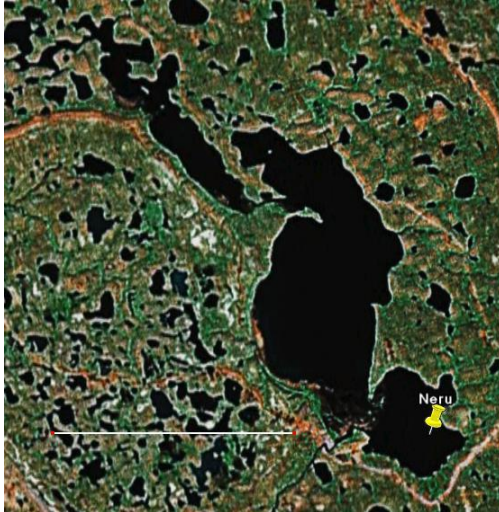


Figure 8.2. GoogleEarth™ image of Lake Nerusaveito. (Scale bar = 3km, accessed 20.05.2007)

67.525500N, 62.757611E, Altitude 121m a.s.l., lake area ca. 98 ha, sampling depth 5.85 m (lake depth unknown), pH 7.23

8.2.3. Sandivei Lake, code SAND.

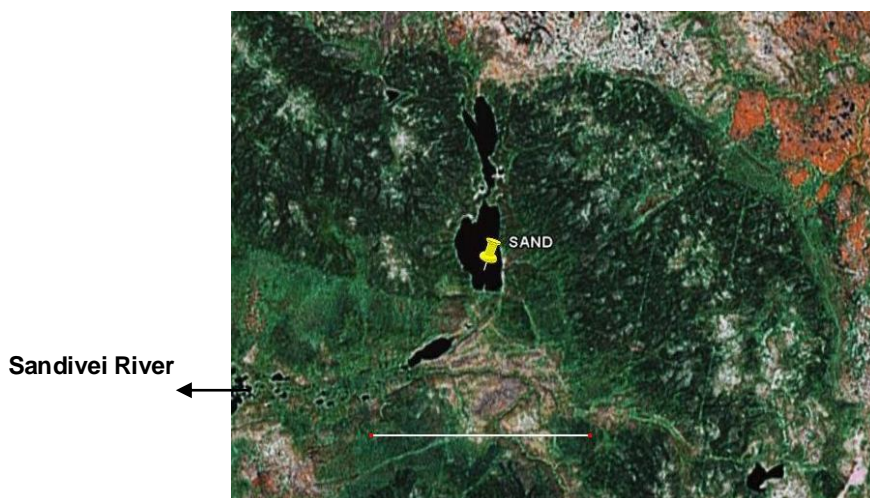


Figure 8.3. GoogleEarth™ image of Sandivei Lake. (Scale bar = 3km, accessed 20.05.2007)). Areas of peat bog are shown in white-pink and areas of spruce-birch forest in dark green.

66.921833N, 58.77925E, Altitude 86m a.s.l., lake area ca. 50 ha, Lake depth over 15m, pH 7.25

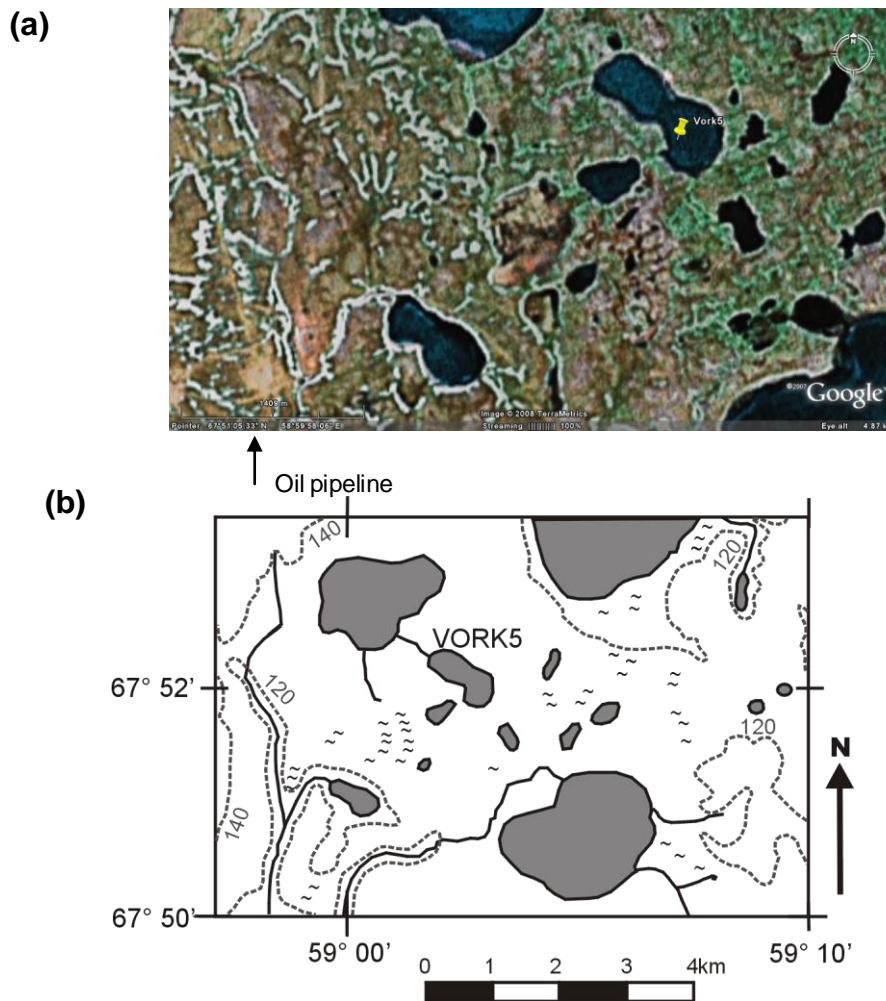
Sandivei Lake is located approximately 240km west south-west of Vorkuta. The lake was selected for coring, prior to the fieldwork, as a representative forest lake. However the sediment became peaty ca. 60cm below the sediment

surface, the peat content increased below this depth and became difficult to core with the Russian corer. A deeper core, 5.2 – 5.7m, below the sediment surface also contained peat and the base of the peat was not reached. The lake is surrounded by spruce-birch forest with areas of peat bog or mire to the north-east, east and west of the lake. Vertical growth of the peat beds around Lake Sandivei, earlier in the Holocene, may have resulted in changes in topography and/or hydrology which caused localised flooding to form the lake. Water flows into the lake from a smaller lake to the north and flows out to the south-west into the Sandivei River (Figure 8.3).

8.2.4. Unnamed tundra lake, code VORK5

Figure 8.4. Unnamed lake, Code VORK5. (a) GoogleEarth™ image (accessed 20.05.2007) and (b) topographic map (based on Russian map, 1981, scale 1:200 000).

67.856972N, 59.025722E, Altitude 123m a.s.l., Area 42 ha, Depth 2.5 m, pH 7.16



VORK5 is remote from human habitation and lies approximately 215km west north-west of Vorkuta. The lake is surrounded by low mounds, in the gently undulating landscape of the Bol'shezemel'skaya Tundra. The vegetation is typical scrub-lichen tundra dominated by *Betula nana*, with some *Empetrum nigrum* and *Vaccinium vitis-idaea* (Solovieva et al. 2005). The water was shallow, typically 1.5 – 2m deep, with a maximum depth of 2.5m. An oil pipeline with intermittently spaced drilling or exploration rigs runs to the south-west of the lake, the impact on the lake is unknown (Figure 8.4). The total length collected by the Russian corer was 1.85m. The sediment was grey clay with intermittent sandier layers; these were particularly prevalent between 136cm and 165cm below the sediment surface. A more detailed stratigraphy is presented in section 8.6.

8.3. Selection of lakes for palaeoenvironmental analysis

Of the four sediment cores collected, two were selected for detailed analysis. The following section details the rationale behind the selection of these two cores. The sediment core from the forested lake (SAND) became peaty ca. 60cm below the water-sediment interface, the peat content increased below this depth and became difficult to core. To prevent damage to the coring equipment, cores were only collected from 0-160cm and 520-570cm depth below the water-sediment interface. Sub-sampling was also problematic due to the presence of large fragments of wood. Due to discontinuous nature of the cores and imprecise sub-sampling this core was not analysed further. Four sediment samples from the remaining three lakes (KHAR, NERU and VORK5) were radiocarbon dated (as described in section 3.3.4.2) to provide a preliminary chronology. The duration and integrity of the core, together with the abundance and richness of the chironomid fauna, were used to select lakes for further analysis.

Chironomid assemblages were examined in surface sediment samples (0 – 0.5cm) from KHAR, NERU and VORK5 as described in section 3.3.2.3. Abundances and the number of taxa identified, for all cores (Table 8.1), are similar to faunas identified in other Russian arctic lakes (for example Andreev *et al.* 2004b; Solovieva *et al.* 2005). Chironomid abundance and diversity are

lowest at VORK5. This lake is situated at higher latitude than NERU and KHAR and the more restricted fauna may reflect cooler summer temperatures.

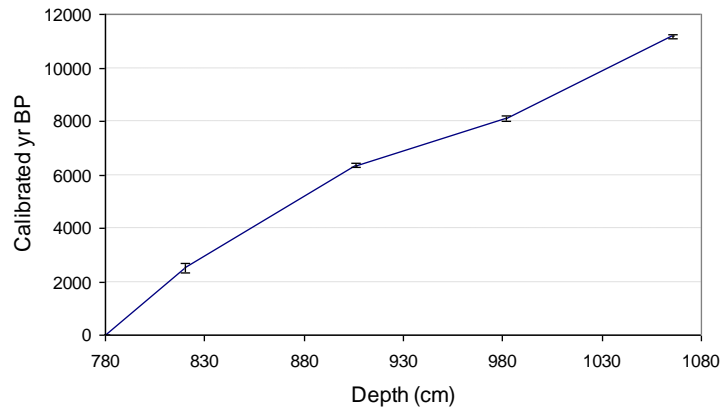
Table 8.1. The abundance and diversity of the chironomid fauna in surface samples from the NEER lakes.

Lake code	Number of taxa identified	Abundance of head capsules (HC g ⁻¹ dry wt)
KHAR	27	81.9
NERU	38	94.6
VORK5	18	53

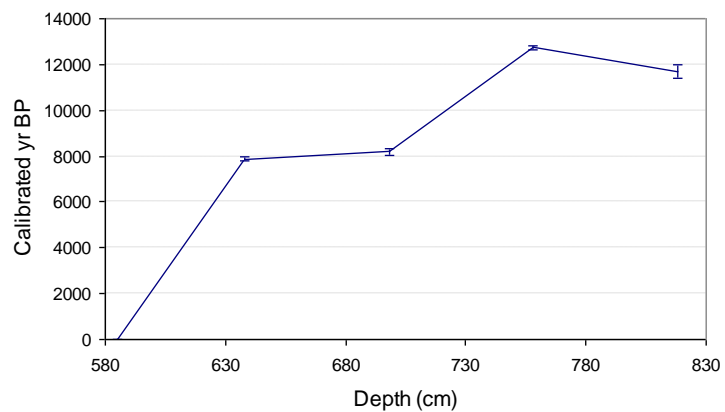
Four bulk sediment samples, at approximately equal intervals, from the three cores were radiocarbon dated by Accelerator Mass Spectrometry (AMS) at the SUERC AMS laboratory, East Kilbride (as described in section 3.3.4.2). The radiocarbon dates were calibrated using the OxCal v.4 program (Table 8.2) (Bronk Ramsey 1995, 2001) based on the IntCal04: Northern Hemisphere calibration curve (Reimer et al. 2004). Calibrated dates were plotted against depth to provide a preliminary chronology (Figure 8.5).

From the preliminary rangefinder results KHAR appears to have a complete Holocene sequence, with a basal date older than 10905-11242 yrs BP and a date towards the top of the core of 2346-2699 yrs BP (Figure 8.5a). Sediment accumulation rates (Table 8.2) are low, but generally constant, throughout the core except for a period of slightly higher accumulation between c. 6350-8100 yrs BP. The preliminary dates suggest only the early Holocene sequence is present at NERU (Table 8.2), although sedimentation began slightly earlier at this site than KHAR (Figure 8.5b). The date at 758cm is older than the date at 818cm which indicates that the basal date may be contaminated with younger material or that the date above may have older material incorporated.

(a) KHAR



(b) NERU



(c) VORK5

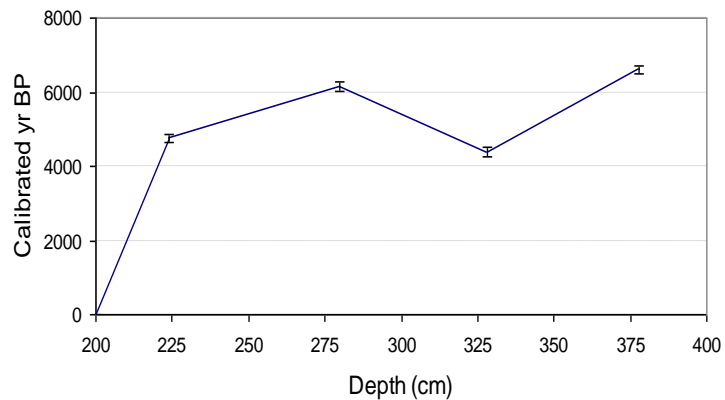


Figure 8.5. Preliminary age-depth models for the northeast European lakes based on calibrated ^{14}C dates (a) Lake Kharinei, code KHAR, (b) Lake Nerusaveito, code NERU and unnamed lake VORK5.

The dates from VORK5 suggest that only a mid-Holocene sequence is present (Table 8.2 and Figure 8.5c) having a basal date of 6495-6716 BP and an upper date of 4648-4870 BP. The date at 328 cm (4258-4520 BP) (Figure 8.1c) appears too young and is assumed to be unreliable due to possible contamination by younger material. The sediment accumulation rate is very

variable with high rates at the base of the core (Table 8.2) declining to 0.04 cm yr⁻¹ at the top of the sequence which is similar to rates at Kharinei (KHAR). The very low sediment accumulation rate at the top of the core probably indicates a hiatus. Analysis of the core would give a high resolution record for the mid-Holocene period between approximately 6500 – 4800 cal yrs BP.

Table 8.2. Radiocarbon rangefinder dates for the NEER sediment cores

Lab No	Core & sample depth (cm)	$\delta^{13}\text{C}_{\text{VPDB}}\text{‰}$	Conventional Radiocarbon Age (years BP $\pm 1\sigma$)	Calendar years BP (95.4% probability)	Approx. sediment acc. rate cm/yr
SUERC-17505	KHAR 820	-29.9	2411 +/- 37	2520 (2699 - 2346)	0.0158
SUERC-17506	KHAR 906	-31.6	5555 +/- 38	6350 (6406 - 6290)	0.0224
SUERC-17509	KHAR 982	-30.7	7304 +/- 37	8100 (8180 - 8023)	0.0433
SUERC-17510	KHAR 1066	-29	9738 +/- 43	11170 (11242 - 11094)	0.0274
SUERC-17511	NERU 638	-26.4	7041 +/- 39	7880 (7953 - 7793)	0.0067
SUERC-17512	NERU 698	-26.3	7389 +/- 40	8200 (8339 - 8054)	0.1854
SUERC-17513	NERU 758	-25.9	10683 +/- 45	12750 (12829 - 12662)	ND
SUERC-17514	NERU 818	-26.1	10106 +/- 46	11700 (11975 - 11404)	0.0343
SUERC-17515	VORK5 224	-28.6	4249 +/- 36	4750 (4870 - 4648)	0.0039
SUERC-17516	VORK5 280	-27.7	5387 +/- 35	6150 (6285 - 6019)	0.0402
SUERC-17519	VORK5 328	-28.1	3950 +/- 37	4390 (4520 - 4258)	ND
SUERC-17520	VORK5 378	-28.6	5802 +/- 38	6600 (6716 - 6495)	0.216

Lake Kharinei (KHAR) and VORK5 were selected for detailed palaeolimnological analyses as:

1. the cores were from undisturbed lake systems with a long record of continuous sedimentation in order to maximise the climatic signal in the palaeolimnological record;
2. the abundance of the chironomid subfossils was high enough to enable the core to be sampled at reasonable temporal resolution (0.5cm intervals) and;
3. the assemblages were taxon rich to maximise its potential sensitivity to environmental change.

The age – depth relationship for KHAR and VORK5 are modelled in sections 8.4 and 8.5 respectively, with additional radiocarbon and radiometric dates, to provide a more detailed chronology.

8.4. Chronology of Lake Kharinei

8.4.1. Correlation of Russian cores

Russian cores of 1 or 0.5m length were collected, alternately, from two adjacent holes in the lake ice as described in section 3.2.2. Two-metre rods were added, as required, to the corer before it was driven into the sediment. The depth of the cored section was determined by measuring the height of the rods remaining above the water surface and subtracting this from the overall length of the corer and rods. Details of the length and depth of the extracted cores are given in Table 3.2. Due to the extreme environmental conditions in the field, errors occur in the accuracy of field measurements and calculations. Therefore consecutive cores were correlated by comparing the values and trends in dry weight and LOI (Figure 8.6). Figure 8.6 shows the percent dry weights and LOI values for a 12-20cm section at the base of the shallower core and the top of the underlying core. The depth of the deeper core was adjusted (± 2 cm depth), if necessary, to provide a closer visual match in trends and values. The correlation between KHAR-1 and KHAR-2 was hampered by the absence of a sample at 844cm depth. This sample contained a large plant macrofossil with little sediment. The sample was sent to Helsinki for identification; therefore this correlation remains tentative.

Ideally consecutive cores should overlap by 10 – 20cm, however due to a miscalculation in the field KHAR-3 (930 – 1029cm depth) did not overlap with KHAR-4 (1030 – 1079cm). As the problem in calculating the required depth was confined to KHAR-4, the depth of KHAR-5 was assumed to be more accurate and KHAR-4 was correlated to KHAR-5 (Figure 8.4). This suggested a continuous sequence was retrieved from KHAR-3 and KHAR-4. Measured depths and adjusted depths on the master chronology are summarised in Table 8.3.

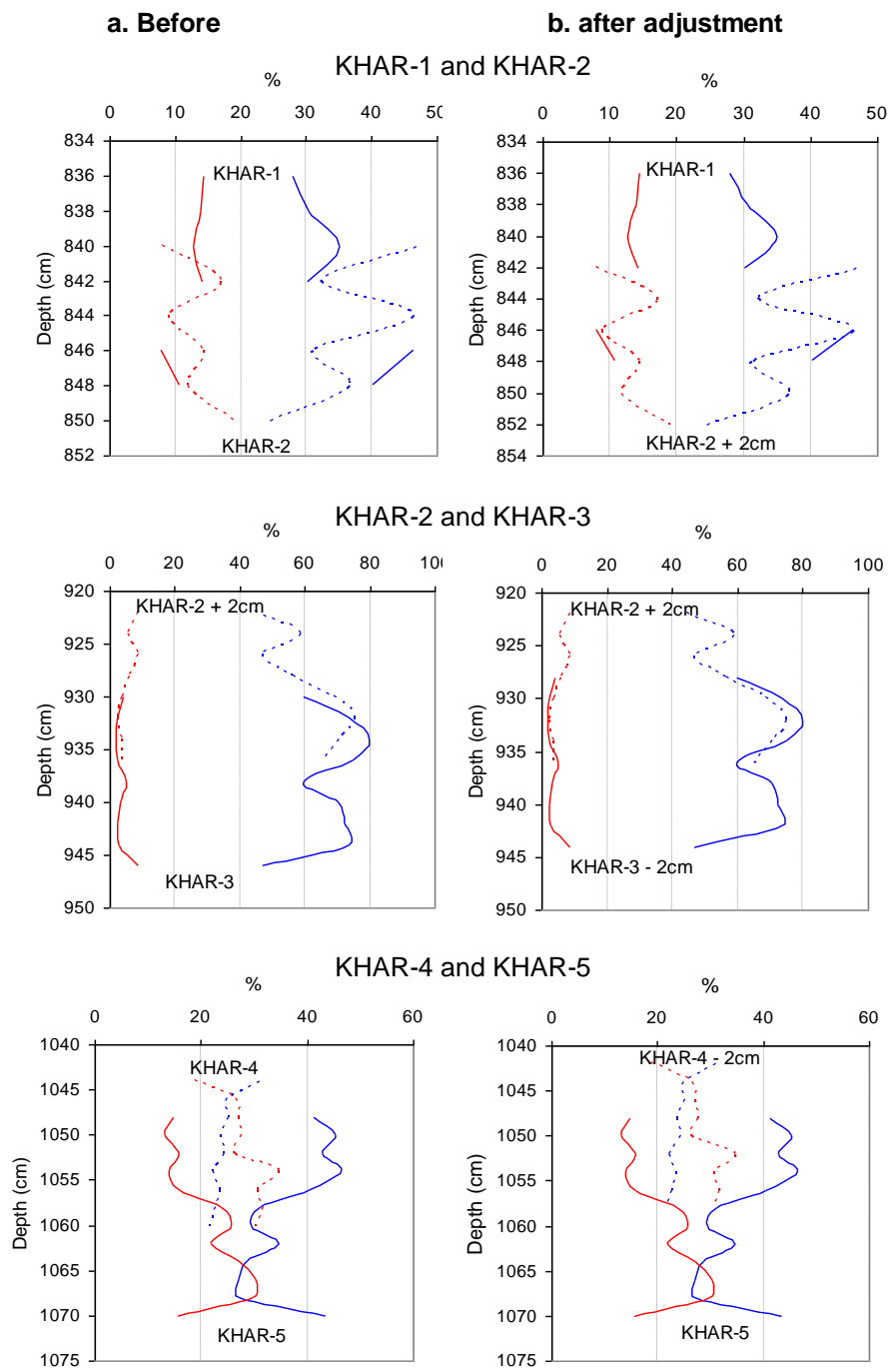


Figure 8.6. Comparison of percentage dry weight (red) and LOI (blue) in consecutive KHAR cores (a) before and (b) after adjustment of estimated depths to correlate cores. Consecutive cores are shown in solid or dashed lines.

Table 8.3. Summary of measured and adjusted depths for Russian cores from Lake Kharinei.

Core	Core depth measured in field (cm)	Depth on master chronology (cm)
KHAR-1	780 - 849	780 - 849
KHAR-2	840 - 939	842 - 941
KHAR-3	930 - 1029	928 - 1027
KHAR-4	1030 - 1079	1028 - 1077
KHAR-5	1048 - 1097	1048 - 1097

8.4.2. Dating and development of age – depth model

The sediment sequence from 780 – 800 cm depth was dated by ^{210}Pb to provide a high resolution chronology for recent sediments (0 – 150 years) (Appleby 2001). The remaining sequence, from 800 – 1056 cm depth, was radiocarbon dated. Age – depth models were developed for each sequence individually. The age – depth relationship was then interpolated between the sequences to provide a continuous chronology for the whole core.

8.4.2.1. ^{210}Pb dating and chronology

The radionuclides were analysed by H. Yang of UCL, as described in section 3.3.4.1 who developed an age-depth model based on ^{210}Pb dating of the sediments, constrained by ^{137}Cs and ^{241}Am . The total ^{210}Pb activity in sediments has two components; supported ^{210}Pb which derives from the *in situ* decay of the parent radionuclide ^{226}Ra and unsupported ^{210}Pb which derives from the atmospheric flux (Appleby 2001). The supported component is usually in radioactive equilibrium with ^{226}Ra and the unsupported ^{210}Pb is determined by subtracting the supported activity from total activity. ^{210}Pb decays to stable ^{206}Pb with a half-life of 22.3 years therefore the age of the sediment can be determined, assuming the atmospheric flux of ^{210}Pb has remained constant. With the exception of the surface sediment from KHAR, the unsupported ^{210}Pb activities (i.e. the component derived from the atmosphere) decline more or less exponentially with depth between 780.75 and 790.5 cm. This indicates sediment accumulation rates were relatively uniform in this section of the core (Table 8.4, Figure 8.7). However the relatively low level of unsupported ^{210}Pb

activity in the surface sample suggests a recent increase in sedimentation. The unsupported ^{210}Pb inventory in the core was 1085 Bq m^{-2} . This corresponds to a mean ^{210}Pb supply of $33 \text{ Bq m}^{-2} \text{ yr}^{-1}$, which is much less than the estimated flux in this region. The low ^{210}Pb supply implies that the coring location has been subject to significant sediment focusing i.e. water turbulence has re-suspended and moved deposited material from this area of the lake to deeper zones. However this appears to have only affected the most recent sediments.

Table 8.4. Summary table showing the ^{210}Pb and ^{137}Cs activity with respective errors, for Lake Kharinei

Sample depth (cm)	^{210}Pb activity (Bq/kg)	Counting error (Bq/kg)	^{210}Pb unsupported activity (Bq/kg)	^{137}Cs activity (Bq/kg)	Counting error (Bq/kg)
780.25	209.05	27.36	157.5	93.86	6.11
780.75	240.0	20.08	199.94	173.51	5.31
781.25	181.01	23.19	139.99	203.21	7.19
781.75	145.58	17.09	111.45	146.07	4.32
782.25	117.0	11.67	76.74	102.36	3.05
782.75	72.58	12.15	34.74	47.7	2.59
783.25	39.15	10.55	-4.36	36.39	2.22
783.75	52.42	12.13	21.51	18.58	2.08
784.25	30.94	6.52	-4.41	18.36	1.23
785.5	27.9	9.03	-7.99	4.11	1.27
787.5	35.92	8.84	5.05	0	0
790.5	31	8	-0.62	0	0

(a)

(b)

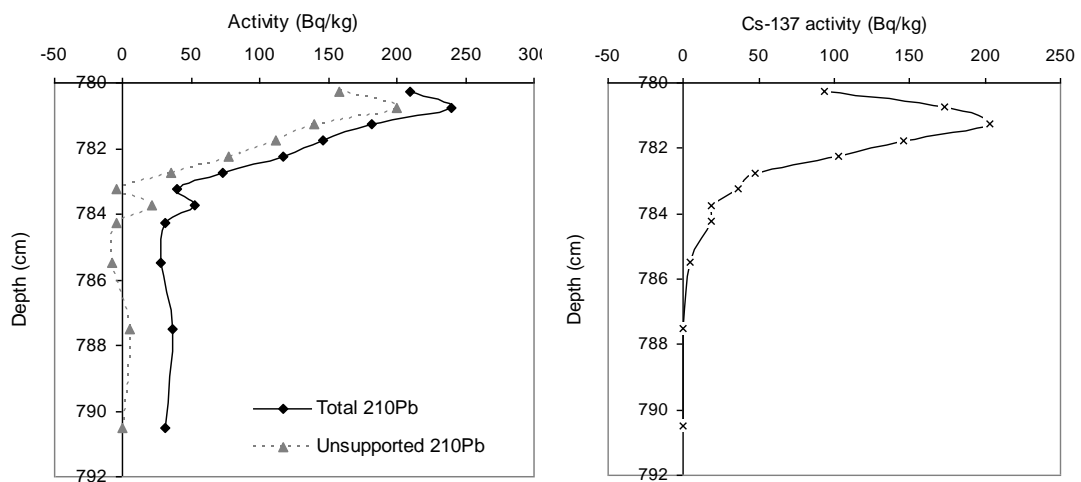
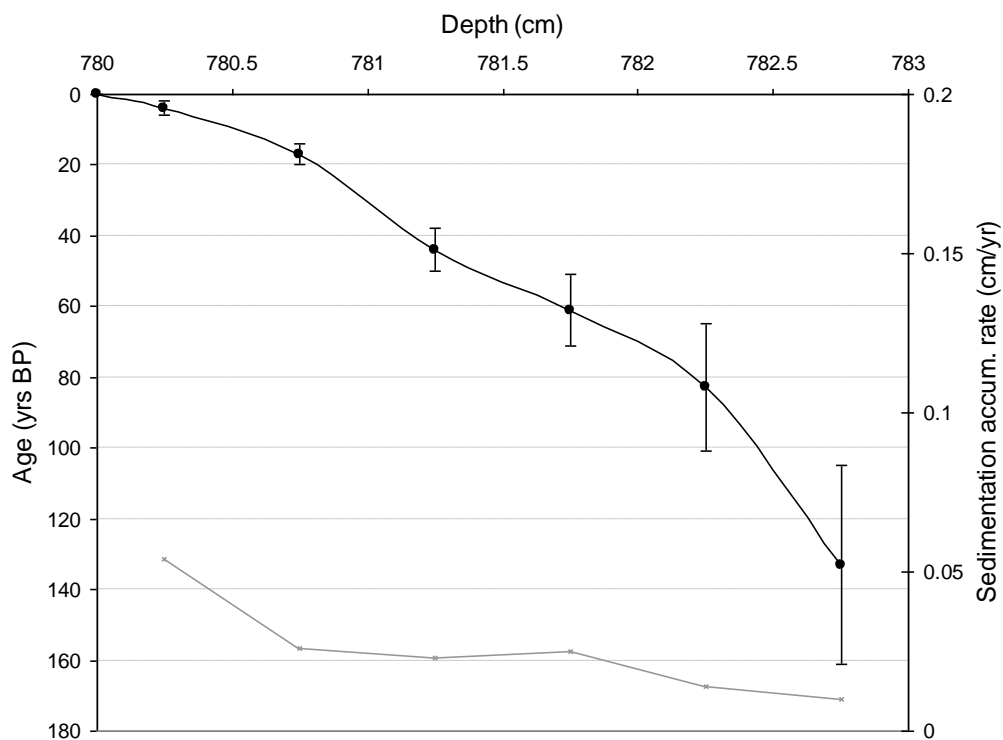


Figure 8.7. Stratigraphy of (a) unsupported ^{210}Pb and total ^{210}Pb activity; and (b) the ^{137}Cs maximum, as a stratigraphic marker for 1963, in Lake Kharinei.

The ^{137}Cs activity shows a relatively well-resolved peak at 781.25 cm, recording the 1963 fallout maximum from the atmospheric testing of nuclear weapons

(Figure 8.7). ^{210}Pb chronologies were calculated using the Constant Rate of Supply (CRS) dating model (Appleby and Oldfield 1978). The CRS model assumes there is a constant rate of sediment accumulation in the lake and that each layer of sediment has the same initial unsupported ^{210}Pb activity. Therefore it is used when the unsupported ^{210}Pb activity shows a close approximation to an exponential relationship to depth, indicating uniform sediment accumulation (Appleby 2001). With the exception of the unsupported ^{210}Pb concentrations in the surface sediments and at 783.5cm depth, unsupported ^{210}Pb shows an exponential decline with depth validating the use of the CRS model. The raw CRS dating model places the 1963 layer at 781.8 cm, slightly below the 1963 layer suggested by the ^{137}Cs record. The final dates were calculated using the CRS model and corrected by the $^{137}\text{Cs}/^{210}\text{Pb}$ records (Figure 8.8). Present-day in the ^{210}Pb chronologies is 2007, the year of sampling.

Figure 8.8. Age-depth model and sedimentation rates for Lake Kharinei. (Sediment accumulation rates are shown in grey and ages in black with 2 SD error). Depth shown as distance (in cm) below water surface.



8.4.2.2. Radiocarbon dating and chronology

Fourteen bulk sediment samples were radiocarbon dated by Accelerator Mass Spectrometry (AMS) at the SUERC AMS laboratory, East Kilbride, i.e. an additional ten samples to the rangefinder dates in section 8.3. Pre-treatment of the raw samples and the analytical procedures are described in section 3.3.4.2. The results are reported as conventional radiocarbon years BP, relative to AD 1950 (Table 8.5). The dates were calibrated with the OxCal version 4.0 program (Bronk Ramsey 1995, 2001) based on the IntCal04: Northern Hemisphere calibration curve (Reimer et al. 2004).

Table 8.5. Radiocarbon dates from Lake Kharinei (KHAR) sediment core. Ages given as years before 1950. Sample depths given as depth below water surface.

Lab No	Sample depth (cm)	Depth on master chronology (cm)	$\delta^{13}\text{C}_{\text{VPDB}}\text{‰}$	Conventional Radiocarbon Age (years BP $\pm 1\sigma$)	Calendar years BP (95.4% probability)
SUERC-21513	800 – 801	800	-29.1	2663 +/- 37	2795 (2848 – 2742)
SUERC-21516	810 – 811	810	-29.5	2256 +/- 37	2250 (2345 – 2155)
SUERC-17505	820 – 821	820	-29.9	2411 +/- 37	2524 (2699 – 2349)
SUERC-21517	850 – 851	852	-31.3	4640 +/- 38	5387 (5467 – 5307)
SUERC-21518	878 – 879	880	-29.8	3571 +/- 40	3851 (3979 – 3723)
SUERC-17506	906 – 907	908	-31.6	5555 +/- 38	6348 (6406 – 6290)
SUERC-21519	930 – 931	932	-29.8	6878 +/- 39	7707 (7794 – 7620)
SUERC-21520	954 – 955	952	-30.4	7039 +/- 39	7873 (7954 – 7791)
SUERC-17509	982 – 983	980	-30.7	7304 +/- 37	8102 (8180 – 8023)
SUERC-21521	1010 – 1011	1008	-30.6	8661 +/- 44	9635 (9733 – 9536)
SUERC-21522	1036 – 1037	1034	-32	10212 +/- 45	11923 (12093 – 11752)
SUERC-17510	1066 – 1067	1064	-29	9738 +/- 43	11168 (11242 – 11094)
SUERC-21523	1080 – 1081	1080	-31.7	10213 +/- 45	11923 (12092 – 11754)
SUERC-21526	1092 – 1095	1094	-31.5	10610 +/- 44	12604 (12805 – 12402)

The preliminary age-depth graph (Figure 8.9) shows a relatively steady accumulation rate over the past 12,500 years with the exception of a period of more rapid accumulation from ca. 8100 – 7700 cal. yrs BP (980 – 932 cm). The majority of AMS ages provide a reliable age – depth relationship for the chronology. However two dates from 800 and 1034 cm (2795 \pm 53 and 11923 \pm 171 cal. yrs BP) show reversals with older ages than deeper samples. These dates are assumed to be unreliable due to possible contamination of the sediments by inwashed older carbon at the time of deposition or contamination during the coring and sub-sampling procedures. These dates were excluded from the final age – depth model.

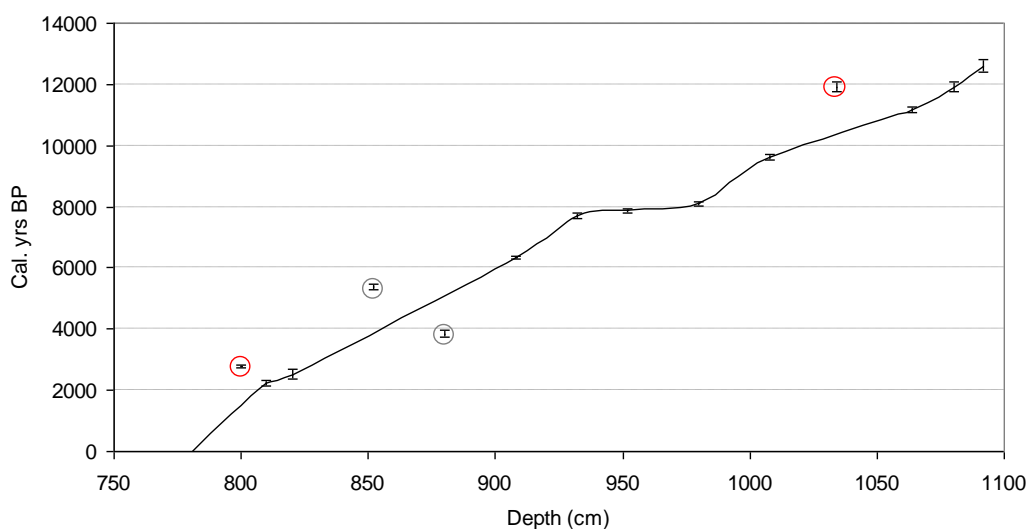


Figure 8.9. Preliminary age – depth relationship of Lake Kharinei (KHAR) based on 14 calibrated radiocarbon dates (Table 8.5). The model assumes a modern age (-57 years before 1950) for the sediment surface at 780 cm depth. Unreliable dates with ages which are too old are highlighted by red circles and uncertain dates are highlighted by grey circles.

Additionally, one of the dates from either 852 or 880 cm depth (5387 ± 80 or 3851 ± 128 cal. yrs BP) must be unreliable as the deeper sample appears younger. From the preliminary age-depth model either date could theoretically be correct, therefore the age-depth relationship was initially modelled without either date then with each date included individually to see which date is more likely to be correct. The age-depth relationship was modelled using OxCal v. 4.0 program (Bronk Ramsey 1995, 2001) based on a Bayesian approach to the analysis of radiocarbon chronologies. The use of a Bayesian approach to radiocarbon dating of sedimentary sequences allows prior information such as the order of deposition and depth to be incorporated into the calibration process (Bronk Ramsey 2008). Data were modelled using a deposition model (p – Sequence) which assumes random variation from an approximately constant deposition rate where the variation has a Poisson distribution. Analysis was performed without boundaries. Models were assessed using agreement indices (A) and the convergence integral. The probability distribution of each radiocarbon age measurement is treated independently in the analysis, so that the expected age is not based on knowledge of the other radiocarbon dates in

the sequence (unconstrained distribution). However, the analysis also can be constrained by Bayesian methods to recognise the stratigraphical order of the samples from which the radiocarbon dates were obtained (constrained distribution). The differences between the prior (unconstrained) and posterior (constrained) probability distributions are expressed as an agreement index (A) and should be over 60% (Blockley et al. 2004). The convergence integral tests the ability of the Markov Chain Monte Carlo (MCMC) algorithm to provide a representative set of posterior probability distributions and should be over 95% (Bronk Ramsey 2001, 2008). The 'k' parameter, which is the number of increments per unit length, determines the rigidity of the model. For some sediments, such as varves, this can be determined mathematically, however for homogeneous sediment, such as gyttja, this is determined by progressively increasing k to find the highest value which gives satisfactory agreement with the actual dating information using the agreement indices i.e. indices over 60%.

When the dates at 852 and 880 cm depth were excluded from the Bayesian model (Figure 8.8a) the k-parameter 0.5 depth^{-1} gave an overall agreement index (A_{overall}) of 72.6% and convergence indices (C) greater than 97.5%. However the sample at 980 cm (8180 – 8023 cal. yrs BP) showed poorer agreement, individual agreement index (A) of 51.8%. This suggests there was a marked change in the deposition rate at this time i.e. the change in rate is at the extremes of the values predicted by the Poisson distribution. Including the date at 852 cm depth (Figure 8.8b) reduced the performance of the model ($A_{\text{overall}} = 58\%$, $C < 97.5\%$) with poor agreement for the dates at 980 and 852 cm ($A = 59.5\%$ and 49.8% respectively). Including the date at 880 cm depth only (Figure 8.8c) improved the performance of the model ($A_{\text{overall}} = 77.8\%$, $C > 97.5\%$) with reasonable agreement for the date at 980 cm ($A = 59.8\%$). This suggests that the date at 880 cm should be included in the age-depth model and the date at 852 cm excluded along with the dates at 800 and 1034 cm. The final age-depth model, to give a complete chronology for the core, also used the ^{210}Pb dating to constrain the age of the surface sediments.

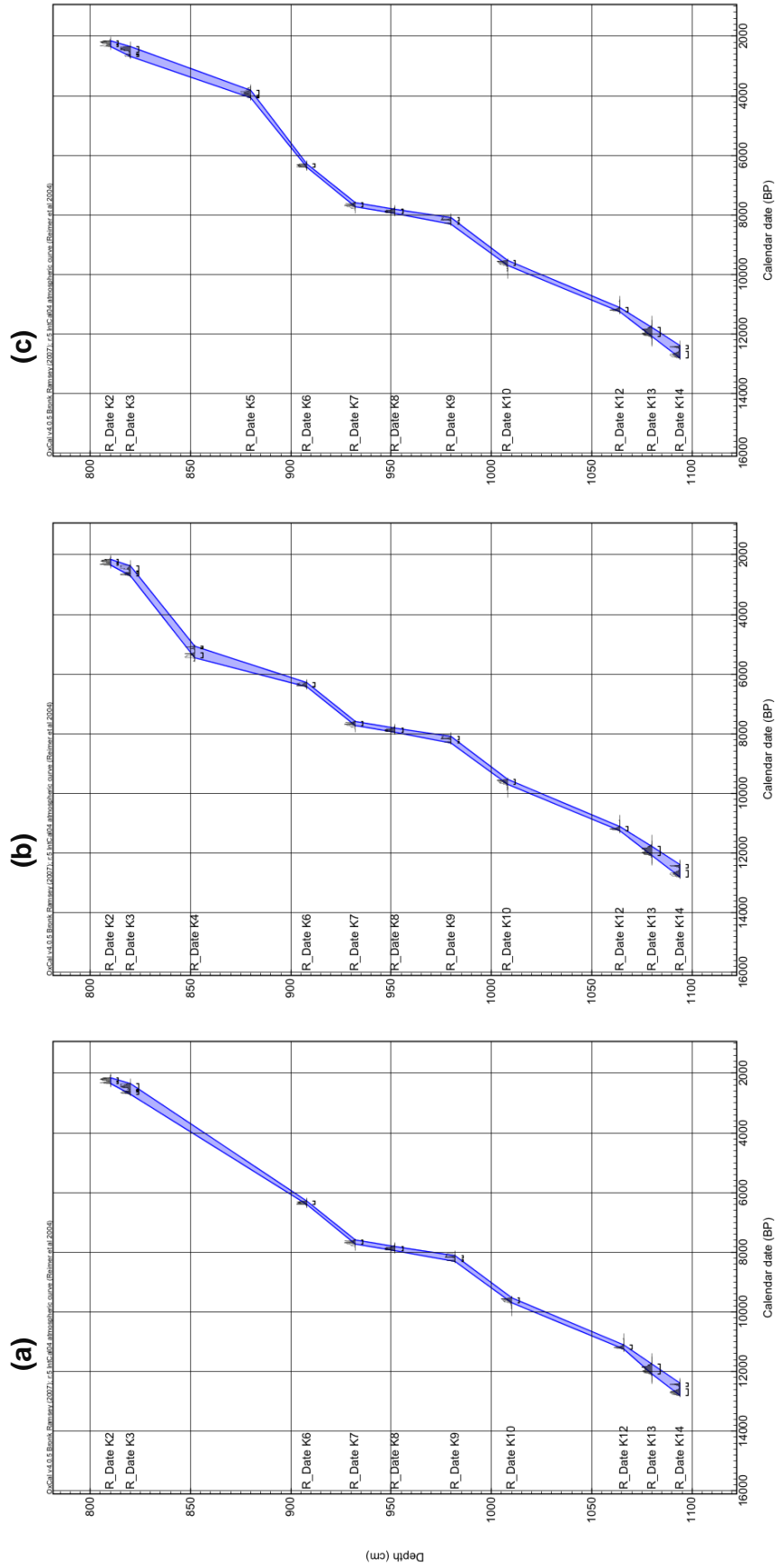


Figure 8.10. Age-depth models for Lake Kharinei, (a) excluding dates at 852 and 880 cm depth; (b) excluding dates at 800 and 1034 cm depth; (c) excluding date at 880 cm depth only and (c) excluding date at 852cm depth only. Unreliable dates from 800 and 1034 cm depth were excluded from all models. Probability distributions for the radiocarbon dates were calibrated in OXCAL v4 program (Bronk Ramsey 1995, 2001) based on IntCal04 (Reimer et al. 2004), depth model curves are envelopes for the 95% highest probability density (HPD) range.

8.4.2.3. Compiled ^{210}Pb and radiocarbon chronology

Constraining the top of the KHAR radiocarbon chronology with a ^{210}Pb date of 133 years before 2007 at 782.75cm depth improved the performance of the model (A_{overall} increased from 77.8% to 79.9%). The individual agreement index of the sample at 810cm depth (2345 – 2155 cal. yrs BP) declined from 95.3 to 93.6%, although the convergence index (C) remained at approximately 99%. The improvement in the Bayesian model suggests sedimentation accumulation was continuous between the two dated sequences. The calendar and modelled age of dated samples, with approximate sediment accumulation rates, are summarised in Table 8.6.

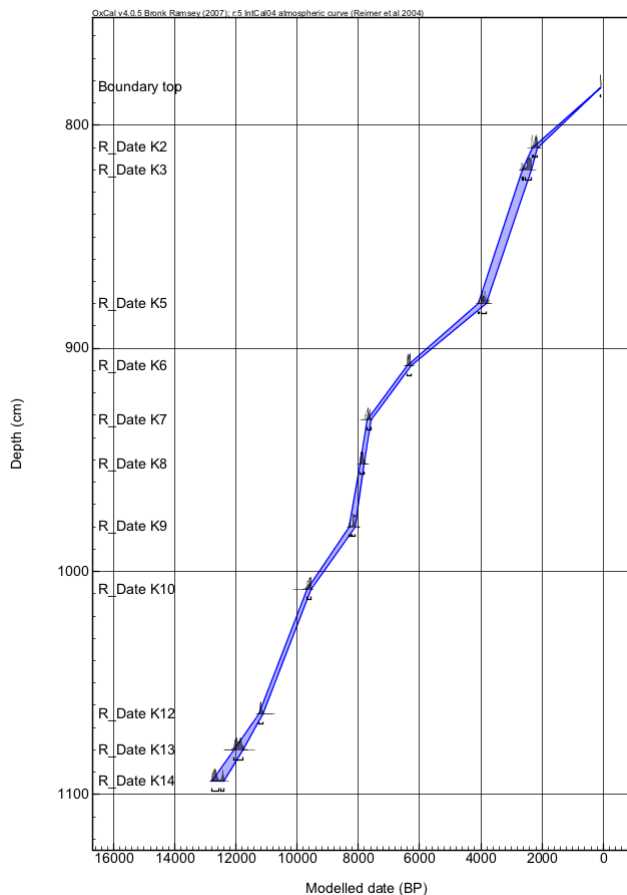
Table 8.6. Age and depth of samples dated by ^{210}Pb and radiocarbon determinations. Ages are given as years before 2007, the year of sampling. Calendar years BP are based on range derived from calibrated ^{14}C dates and the modelled dates represent the part of this range used in the Bayesian age-depth model. Sample depths given as depth below water surface.

Lab No	Sample depth (cm)	Depth on master chronology (cm)	Modelled age cal years BP	Approx. sediment acc. rate cm/yr
^{210}Pb dating, UCL		780	0	
		780.25	4 (6 - 2)	0.054
		780.75	17 (20 - 14)	0.026
		781.25	44 (50 - 38)	0.023
		781.75	61 (71 - 51)	0.025
		782.25	83 (101 - 65)	0.014
		782.75	133 (161 - 105)	0.010
SUERC-21516	810 – 811	810	2300(2400 - 2210)	0.013
SUERC-17505	820 – 821	820	2560 (2720 - 2400)	0.038
SUERC-21518	878 – 879	880	4010 (4140 - 3880)	0.041
SUERC-17506	906 – 907	908	6400 (6460 - 6350)	0.012
SUERC-21519	930 – 931	932	7760 (7850 - 7680)	0.018
SUERC-21520	954 – 955	952	7930 (8000 - 7860)	0.119
SUERC-17509	982 – 983	980	8160 (8240 - 8080)	0.122
SUERC-21521	1010 – 1011	1008	9670 (9740 - 9590)	0.019
SUERC-17510	1066 – 1067	1064	11240 (11300 - 11180)	0.036
SUERC-21523	1080 – 1081	1080	11980 (12140 - 11820)	0.022
SUERC-21526	1092 – 1095	1094	12660 (12860 - 12460)	0.021

The age-depth model produced by the Bayesian analysis (Figure 8.11) shows relatively uniform sediment accumulation rates throughout most of the core, with a period of enhanced rates of sediment accumulation from ca. 8100 –

7700 cal. yrs BP (980 – 932 cm). From 932cm (ca. 7700 yrs BP) the sequence shows a gradual return to the former sediment accumulation rates. However the rates have started to increase over the last 100 years. (782 to 780cm depth).

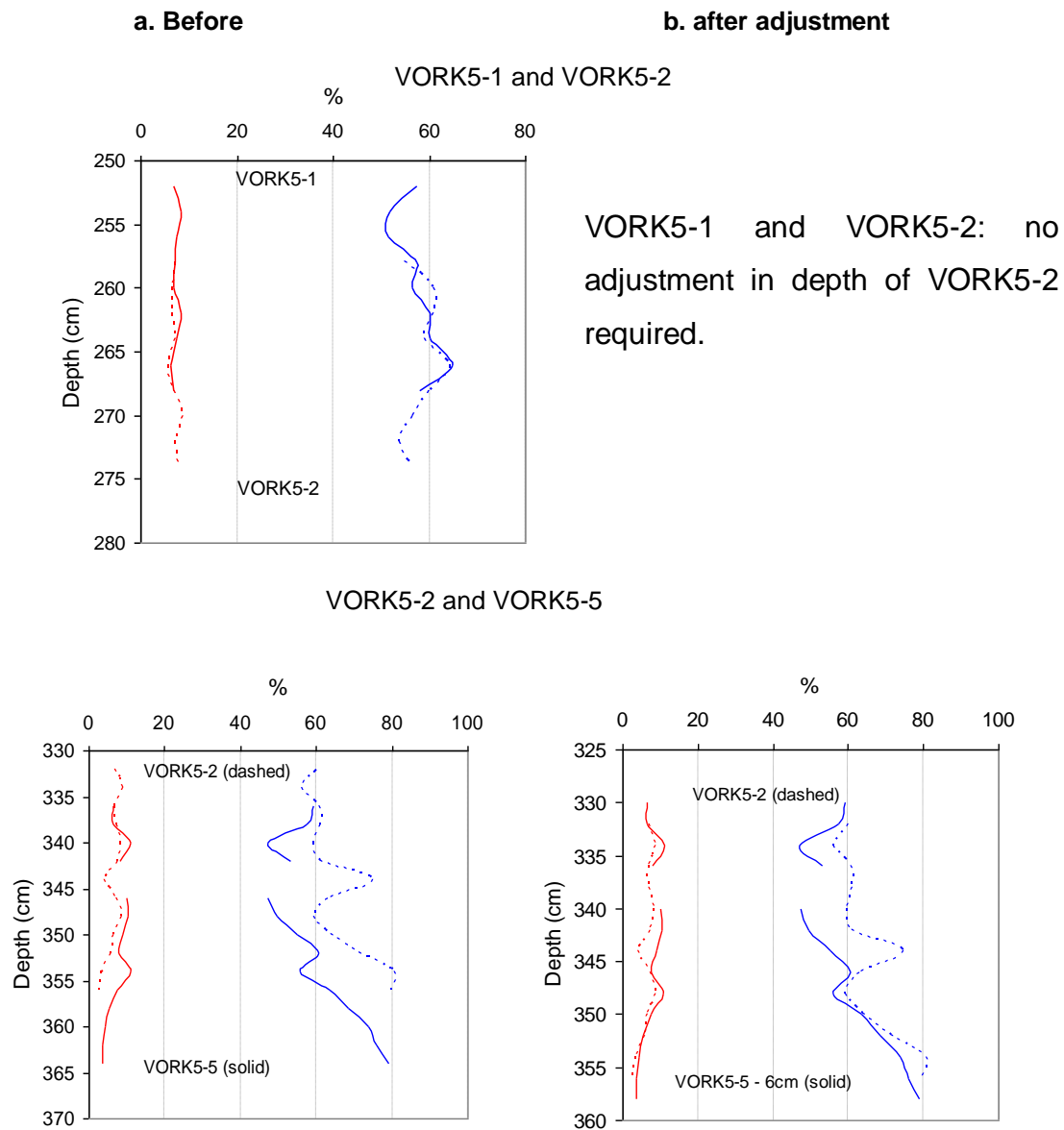
Figure 8.11. Age-depth models for Lake Kharinei with top of core constrained by ^{210}Pb date. Probability distributions for the radiocarbon dates were calibrated in OXCAL v4 program (Bronk Ramsey 1995, 2001) based on IntCal04 (Reimer et al. 2004), depth model curves are envelopes for the 95% highest probability density (HPD) range.



8.5. Chronology of VORK5

8.5.1. Correlation of Russian cores

Consecutive Russian cores from VORK5 were correlated by comparing the values and trends in dry weight and LOI, as described in section 8.4.1. Details of the length and depth of the extracted cores are given in Table 3.2. Cores 3 and 4 are replicates of cores 1 and 2, respectively, and were not analysed in this study. Core VORK5-1 correlated well with VORK5-2, without adjusting the estimated depth of the core (Figure 8.12). To correlate VORK5-5 with VORK5-2 (Figure 8.12) the depth of samples from VORK5-5 needed to be decreased by 6cm towards the surface. This seems a large error in measurements, weather conditions were extremely poor in the field, but the results should be interpreted with caution. Measured depths and adjusted depths on the master chronology are summarised in Table 8.7.



VORK5-1 and VORK5-2: no adjustment in depth of VORK5-2 required.

Figure 8.12. Comparison of percentage dry weight (red) and LOI (blue) in consecutive cores (a) before and (b) after adjustment of estimated depths to correlate cores. Consecutive cores are shown in solid or dashed lines.

Table 8.7. Summary of measured and adjusted depths for Russian cores from VORK5

Core	Core depth measured in field (cm)	Depth on master chronology (cm)
VORK5-1	206 - 269	206 - 269
VORK5-2	258 - 357	258 - 357
VORK5-5	286 - 383	280 - 377

8.5.2. Dating and development of age – depth model

The sediment sequence from 205 – 217 cm depth was ^{210}Pb dated (Appleby 2001) and the remaining sequence, from 224 - 373 cm depth, radiocarbon dated. Age – depth models were developed for each sequence individually. Comparison of the age – depth relationship between the sequences suggested there was a possible hiatus preventing the development of a continuous chronology for the whole core.

8.5.2.1. ^{210}Pb dating and chronology

The radionuclides were analysed by H. Yang of UCL, as described in section 3.3.4.1 who developed an age-depth model based on the ^{210}Pb dates, constrained by ^{137}Cs and ^{241}Am . Unsupported ^{210}Pb activity declines irregularly with depth (Table 8.8, Figure 8.13a), which suggests sediment accumulation rates have varied during deposition of the core. The ^{137}Cs activity versus depth profile (Figure 8.13b) has a well-resolved peak at 213.5 cm, with detectable levels of ^{241}Am . These peaks represent the fallout maxima from the atmospheric testing of nuclear weapons in 1963.

Table 8.8. Summary table showing the ^{210}Pb , ^{137}Cs and ^{241}Am activity, with respective errors, for VORK5. Sample depths given as depth below water surface.

Sample depth (cm)	^{210}Pb activity (Bq/kg)	Counting error (Bq/kg)	^{210}Pb unsupported activity (Bq/kg)	^{137}Cs activity (Bq/kg)	Counting error (Bq/kg)	^{241}Am activity (Bq/kg)	Counting error (Bq/kg)
205.25	223.54	32.85	175.1	18.83	4.3	0	0
206.25	155.93	17.47	118.98	17.29	2.48	0	0
207.75	167.67	19.84	137.76	15.16	2.71	0	0
209.25	134.57	21.38	105.28	26.53	3.31	0	0
210.50	115.76	13.79	85.71	38.61	2.41	0	0
211.50	84.47	14.08	43.58	45.52	2.64	0	0
212.50	70.03	13.67	37.17	65.5	2.68	0	0
213.50	60.72	12.23	19.93	82.67	2.83	2.14	1.17
214.50	47.51	10.9	20.66	58.37	2.05	0	0
215.50	54.11	12.78	23.22	24.23	2.02	0	0
216.50	47.82	10.87	13.23	6.56	1.52	0	0
217.50	43.07	11.17	10.62	0	0	0	0
218.50	23.17	10.43	-3.43

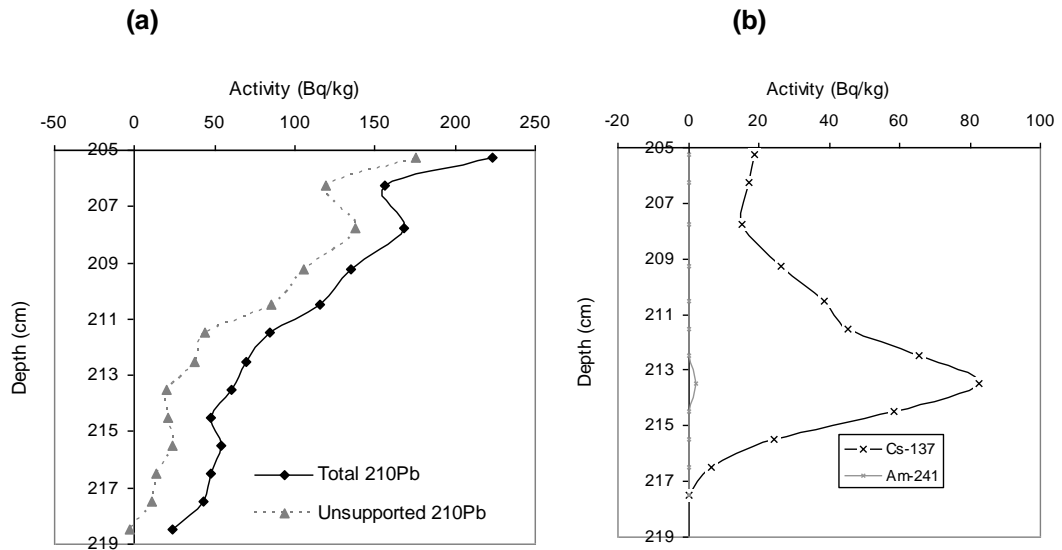


Figure 8.13. Stratigraphy of (a) unsupported ^{210}Pb and total ^{210}Pb activity; and (b) the ^{137}Cs and ^{241}Am maxima, as stratigraphic markers for 1963, in VORK5.

The unsupported ^{210}Pb activities show a non-monotonic relationship to depth (i.e. unsupported ^{210}Pb activities do not consistently decrease with depth). This indicates changes have occurred in the initial ^{210}Pb concentrations supplied to the sediment over time and so precludes the use of the Constant Initial Concentration (CIC) model which assumes the sediments have a constant initial ^{210}Pb concentration regardless of accumulation rates (Appleby 2001). Therefore ^{210}Pb chronologies were calculated using the Constant Rate of Supply (CRS) dating model (Appleby and Oldfield 1978). The raw CRS dating model places the 1963 layer at 211 cm, slightly below the 1963 layer suggested by the ^{137}Cs record. The final dates were calculated using the CRS model and corrected by the $^{137}\text{Cs}/^{210}\text{Pb}$ records (Figure 8.14). Present-day in the ^{210}Pb chronologies is 2007, the year of sampling.

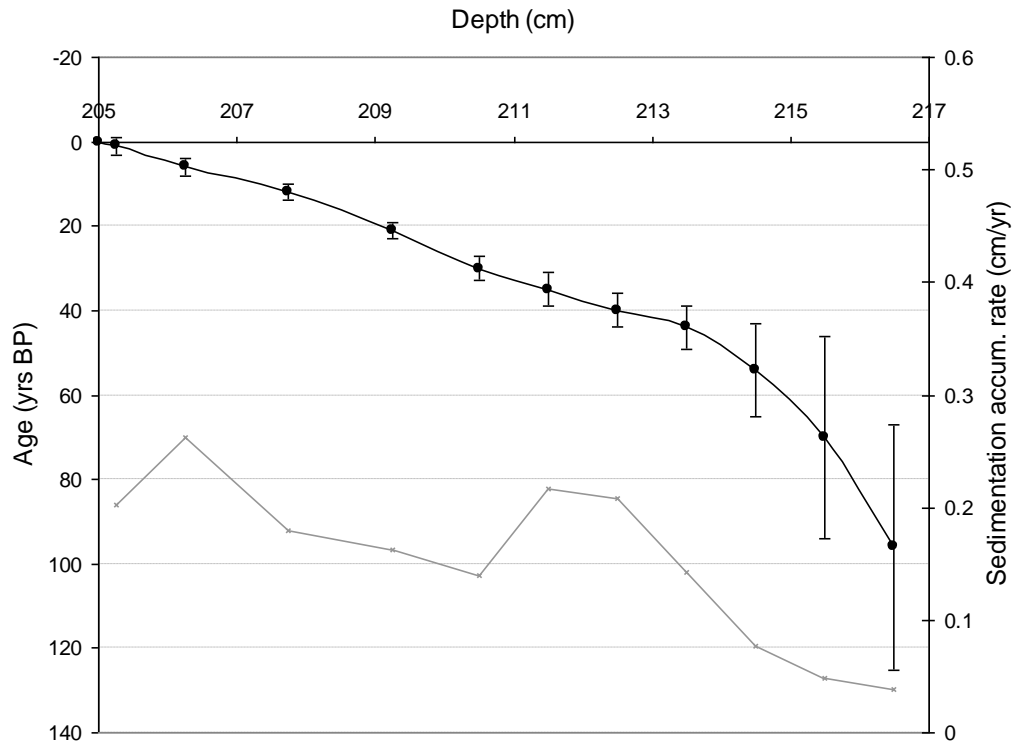


Figure 8.14. Age-depth model and sediment accumulation rates for VORK5. (Sediment accumulation rates are shown in grey and ages in black with 2 SD error). Depth measured from water surface.

8.5.2.2. Radiocarbon dating and chronology

Two bulk sediment samples, in addition to the four preliminary results in section 8.2, were radiocarbon dated at the SUERC AMS laboratory, East Kilbride as described in section 3.3.4.2. *Chara* oospores were observed in the sediment which may indicate relatively hard water conditions and Kultti *et al.* (2003) found a hard water effect of c. 1800 years at Mezhgornoe lake in the Polar Urals. So a series of paired macrofossil – sediment samples were also dated to determine whether there was a hard water effect in the lake. The results are reported as conventional radiocarbon years BP, relative to AD 1950 (Table 8.9). The dates were calibrated with the OxCal version 4.0 program (Bronk Ramsey 1995, 2001) based on the IntCal04: Northern Hemisphere calibration curve (Reimer et al. 2004).

Table 8.9. Radiocarbon dates from VORK5 sediment cores. Ages given as years before 1950 and sample depths as depth below water surface.

Lab No	Sample depth (cm)	Depth on master chronology (cm)	Sample type	$\delta^{13}\text{C}_{\text{VPDB}}\text{‰}$	Conventional Radiocarbon Age (years BP $\pm 1\sigma$)	Calendar years BP (95.4% probability)
SUERC-17515	224 - 225	224	bulk sediment	-28.6	4249 +/- 36	4760 (4870 - 4648)
SUERC-21934	240 - 241	240	bulk sediment	-28.2	5506 +/- 37	6310 (6399 - 6216)
SUERC-17516	280 - 281	280	bulk sediment	-27.7	5387 +/- 35	6150 (6285 - 6019)
SUERC-17519	328 - 329	328	bulk sediment	-28.1	3950 +/- 37	4390 (4520 - 4258)
SUERC-21935	344 - 345	344	bulk sediment	-27.6	4914 +/- 39	5660 (5721 - 5590)
SUERC-17520	378 - 379	372	bulk sediment	-28.6	5802 +/- 38	6600 (6716 - 6495)
SUERC-21937	240 - 241	240	Wood - macrofossil	-26.9	6598 +/- 37	7500 (7566 - 7432)
SUERC-21939	280 - 281	280	Wood - macrofossil	-26.6	7057 +/- 40	7880 (7963 - 7795)
SUERC-21938	344 - 345	344	Wood - macrofossil	-27.7	7579 +/- 41	8390 (8446 - 8331)

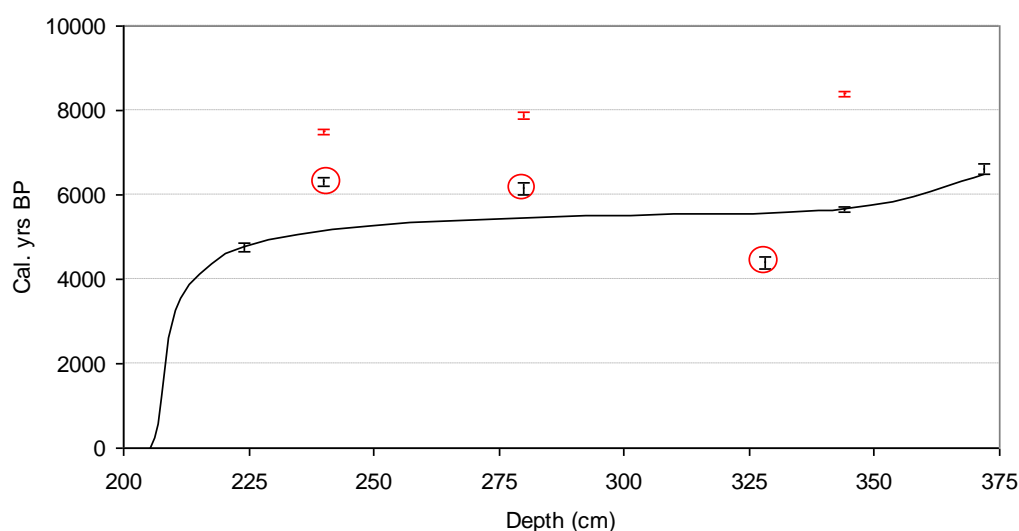


Figure 8.15. Age – depth relationship for the lake VORK5, based on 6 bulk sediment (black) and 3 macrofossil (red) calibrated radiocarbon dates (Table 8.9). The model assumes a modern age (-57 years before 1950) for the sediment surface at 205 cm depth. Unreliable dates, see text, are highlighted in red circles.

The radiocarbon dates show a poor relationship between age and depth for the VORK5 core (Table 8.9; Figure 8.15). The wood macrofossils are typically 1000 – 3000 years older than the associated sediments. With hard water error sub-aquatic photosynthesis and carbonate secretion by freshwater organisms dilutes the ^{14}C levels within the lake causing the age of material within the lake to be overestimated (Peglar *et al.* 1989). Terrestrial material, such as wood, is unaffected by the hardwater effect, therefore if the lake were subject to hard water errors the wood macrofossils would have appeared younger than the

associated sediment. Whilst the older dates for the macrofossils discounts hard water error, it suggests that dead trees are lying within the catchment for up to 3000 years before being washed into the lake. 'Old' allochthonous carbon from the wood may then be incorporated into the sediment during deposition, contaminating the sediment and introducing errors in the radiocarbon dates. The sediments at 240 and 280 cm depth are similar in age to basal material at 372cm (6700 – 6000 cal. yrs BP), so too old for their stratigraphic context. As macrofossils were found at these levels the bulk sediment dates from 240 and 280cm depth are probably unreliable due to contamination by old carbon from the wood. By comparison, the date of 4390 yrs BP at 328cm is younger than all other determinations and is, therefore, probably unreliable due to contamination by younger material.

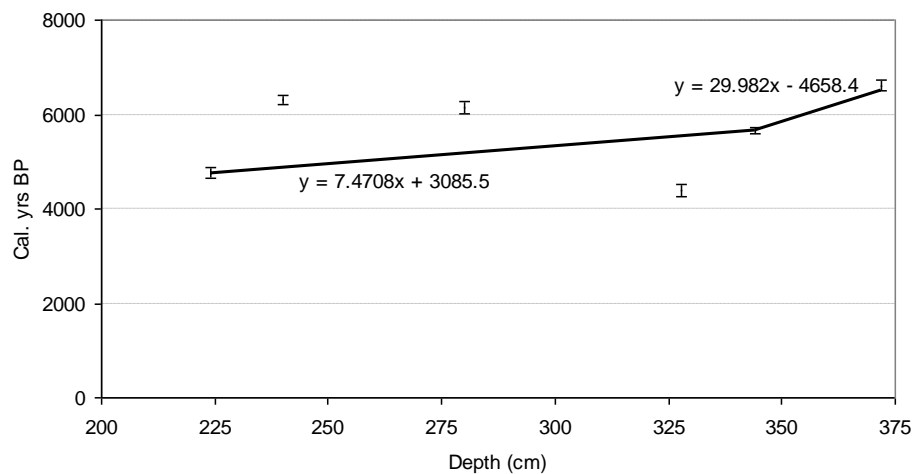


Figure 8.16. Age – depth profile for VORK5 with linear regression lines fitted to 'reliable' dates. Sample age estimated from equations where $y = \text{age in cal. yrs BP}$ and $x = \text{depth in cm}$.

The relationship between age and depth is too poor to model using the Bayesian approach. Therefore approximate estimates of age were derived from linear interpolation between the more 'reliable' bulk sediment dates at 224, 344 and 372 cm depth (Figure 8.16). Although older than the bulk sediment dates, the ages of wood macrofossil show an approximately linear, positive relationship between age and depth from 344 to 240cm depth which suggests sediment accumulation was, probably, relatively uniform during this period. Linear interpolation of the bulk sediment dates can, therefore, be justified but the estimated dates should be used with caution.

8.5.2.3. Combined ^{210}Pb and radiocarbon chronology

The ^{210}Pb dating gave an age of 96 yrs BP (before 2007) at 216.5 cm depth and the radiocarbon analysis an age of 4820 cal yrs BP at 224 cm depth. This equates to a sediment accumulation rate of 0.002 cm yr^{-1} between the two sequences. This is considerably less than the average rate in the ^{210}Pb dated sequence (0.120 cm yr^{-1}) and suggests either a hiatus or a period of reduced deposition between 4820 and 96 cal yrs BP. A hiatus could result in subaerial exposure, erosion and reworking of deposited material. Therefore the core should be treated as two separate sequences, a modern sequence from 217 to 205 cm depth and a period of rapid deposition between 6800 – 4700 cal. yrs BP (at 372 – 224 cm depth). Sediment accumulation rates have increased over the last 50 years (Table 8.10) but have varied considerably throughout deposition of the core.

Table 8.10. Age and depth of samples dated by ^{210}Pb and radiocarbon determinations. Ages are given as years before 2007, the year of sampling and sample depths as depth below water surface.

Lab No	Sample depth (cm)	Depth on master chronology (cm)	Modelled age cal years BP	Approx. sediment acc. rate cm/yr
^{210}Pb dating, UCL		205	0	
		205.25	2 (3 - 1)	0.203
		206.25	6 (8 - 4)	0.262
		207.75	12 (14 - 10)	0.180
		209.25	21 (23 - 19)	0.163
		210.5	30 (33 - 27)	0.139
		211.5	35 (39 - 31)	0.216
		212.5	40 (44 - 36)	0.208
		213.5	44 (49 - 39)	0.143
		214.5	54 (65 - 43)	0.077
		215.5	70 (94 - 46)	0.048
		216.5	96 (125 - 67)	0.038
SUERC-17515	224 - 225	224	4820 (4930 - 4710)	0.002
SUERC-21935	344 - 345	344	5720 (5780 - 5650)	0.133
SUERC-17520	378 - 379	372	6660 (6770 - 6550)	0.030

8.6. Sedimentary analysis

Dry weight and loss-on-ignition (LOI) were determined on sediment samples from KHAR and VORK5 as described in section 3.3.2.1. LOI is used to summarise changes, such as productivity, in the lake ecosystem (Dean 1974; Birks and Birks 2006). The %TOC and carbon and nitrogen isotopic composition ($\delta^{13}\text{C}$ and $\delta^{15}\text{N}$) of the KHAR sediments were determined as described in section 3.3.2.2 to determine the dominant sources of carbon and nitrogen in the lake (Meyers and Teranes 2001). The results of the isotopic analysis represent a preliminary interpretation as multi-proxy studies, including diatoms and pollen analysis, for example, are required to fully interpret the results and this will be the subject of future research. For example, as discussed in section 7.5, changes in pH would affect the carbonate:bicarbonate equilibrium of the water and, therefore, the $\delta^{13}\text{C}$ of inorganic carbon. Diatom-inferred reconstructions would quantitatively show any pH changes, to determine when pH might be affecting the $\delta^{13}\text{C}$ record.

8.6.1. Lake Kharinei (KHAR)

To facilitate palaeoenvironmental reconstruction, interpretation of the sedimentary data (Figure 8.17) is based on the zones identified by optimal partitioning of the chironomid biostratigraphy in section 8.7.1.

Zone K-I (1097 – 1024 cm; 13000 – 10000 cal yrs BP)

Throughout the zone $\delta^{13}\text{C}$ remains relatively stable at -32 to -30‰ which is typical of terrestrial C3 plants (Meyers and Teranes 2001). At ca. 1090cm (12500 cal yrs BP) the C:N ratio of 21 indicates a significant input from terrestrial plants, but from 1082cm (12000 cal yrs BP) the C:N ratio stabilises at 10 – 20 which suggests organic matter is derived from mixed terrestrial – aquatic sources or predominately submerged and floating aquatic macrophytes (Tyson 1995). Peaks in carbonate (18%) occur at 1040 cm (10500 cal yrs BP) and 1092 cm depth (12500 cal yr BP). *Chara* oospores were found in this section of the core, inclusion of oospores may be responsible for the increased carbonate levels. Peaks in percentage carbonate are associated with a decrease in $\delta^{15}\text{N}$ by 2‰ to 0.5‰ which suggests alterations in water chemistry have occurred. Changes in water chemistry may

either result from summer carbonate precipitation in warm stratified lakes or a change in water source with an increase in nutrient supply. In Sky Pond, an oligotrophic, alpine lake in Colorado, USA, a decline of 2 – 3.5‰ in the $\delta^{15}\text{N}$ record, since 1900, has been attributed to changes in meltwater dynamics. Increased snowmelt increases the supply of biologically available nitrogenous compounds to the lake which stimulates phytoplankton growth (Enders et al. 2008). Peaks in TOC (25 – 30%) lag these changes and may result from an increase in lake productivity.

Zone K-II (1024 – 856 cm; 10000 – 3300 cal yrs BP)

In this, and zone K-III, $\delta^{13}\text{C}$ increases from -31.5‰ to -30 – -28‰ while the C:N ratio remains at 10 -20 which suggests that organic matter is increasingly derived from aquatic macrophytes (Meyers 1994; Tyson 1995). Percentage dry weight is high between 10000 – 8000 cal yrs BP indicating an increase in mineral content. This may reflect a change in sediment source, enhanced sediment supply or a reduction in the relative proportion of organic matter (Birks and Birks 2006). TOC is initially low during this period suggesting low productivity but increases from ca. 8000 cal yrs together with $\delta^{15}\text{N}$ which increases from 2 to 3‰. As the C:N ratio remains relatively stable the increase in $\delta^{15}\text{N}$ may reflect an increasing contribution of nitrogenous compounds from rainfall or soil organic matter leading to slightly enhanced productivity. Peaks in the C:N ratio greater than 18, particularly those associated with peaks in % LOI or dry weight may be associated with influxes of sediment with terrestrial vegetation into the lake.

Zone K-III (856 – 800 cm; 3300 – 1500 cal yrs BP)

C:N ratio and $\delta^{15}\text{N}$ remain relatively stable throughout the zone, at 10 – 11 and 3.1 – 3.7‰ respectively. TOC decreases rapidly from 14 to 8% between 3500 – 3000 cal yrs BP whilst $\delta^{13}\text{C}$ increases from -31.5 to -29.5‰. After these initial rapid changes the divergent trends in TOC and $\delta^{13}\text{C}$ continue throughout the zone. As the low C:N ratio indicates there is little input of terrestrial carbon the trends in TOC and $\delta^{13}\text{C}$ suggest productivity is declining (Leng 2003).

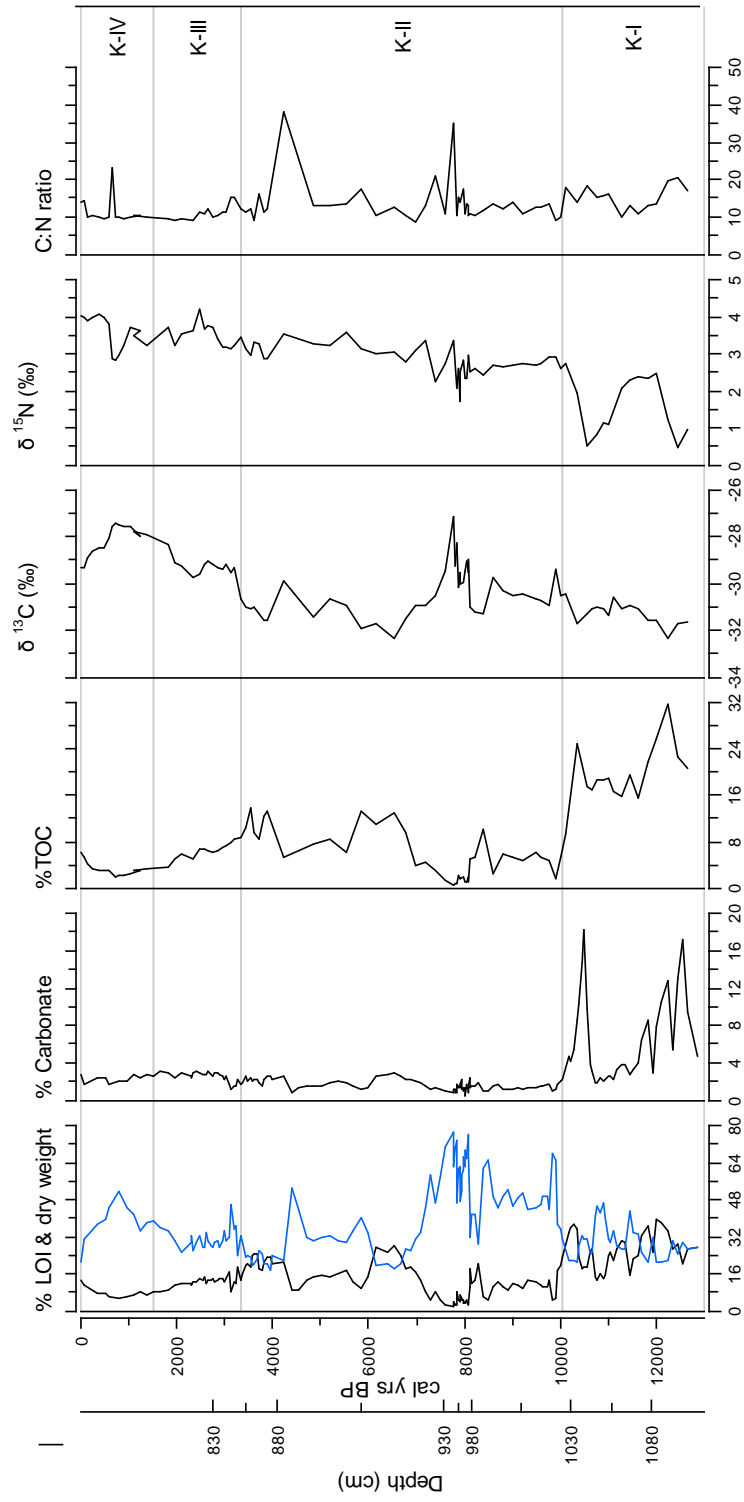


Figure 8.17. % LOI, % dry weight, % carbonate, % TOC, $\delta^{13}\text{C}$ (‰) and $\delta^{15}\text{N}$ (‰) of sediments from KHAR, with C/N mass ratio. Zones displayed based on chironomid biostratigraphy (section 8.7.1). (%LOI shown as black line and % dry weight as blue line).

Zone K-IV (800 – 780 cm; 1500 cal yrs BP – present day)

Initially the trends in zone K-III continue until approximately 600 years ago. Between 900 – 500 cal yrs BP dry weight increases to 50% associated with a short-lived decrease in $\delta^{15}\text{N}$, suggesting a change in nutrient source and an influx of sediment. Over the last 600 years dry weight and $\delta^{13}\text{C}$ have decreased whilst TOC has increased which may indicate a gradual increase in productivity.

8.6.2. VORK5

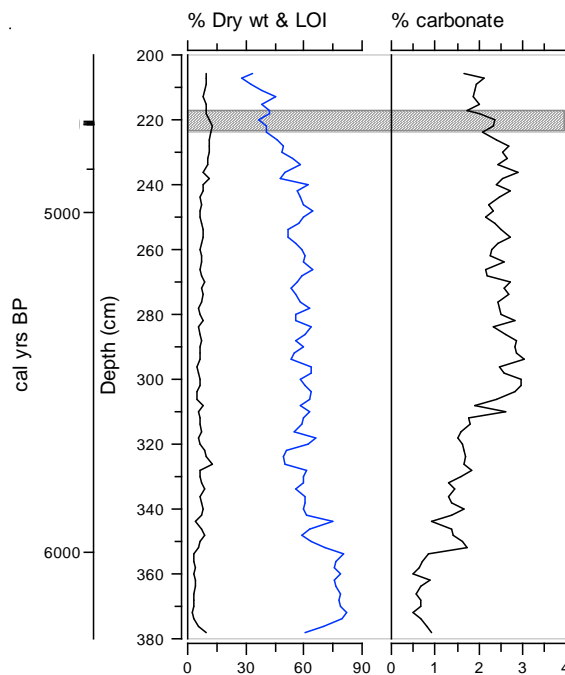


Figure 8.18. % LOI, % dry weight and % carbonate in sediments from VORK5. LOI are shown as black line and % dry weight as blue line, hashed area indicates a hiatus or period of low deposition.

Carbonate increases from 0.5 – 3% between 380 – 310 cm depth but remains low throughout the core (Figure 8.18). LOI also remains low at 5 – 8%. Prior to the hiatus dry weight decreases from 82% at 372cm to 40% at 224cm. Consecutive samples vary by up to 10% dry weight suggesting the sediment source may vary over time and/or the rate of sediment influx to the lake were highly variable. The variability in sediment source and/or rate of sediment influx continues after the hiatus. After the hiatus, percent carbonate and LOI remain stable at 1.9% and 9.7% respectively from 218 – 205cm depth whereas percentage dry weight shows a general decline from 42% at 218cm depth to 33% at 205cm depth. The results of the sedimentary analysis of KHAR and VORK5 are discussed, within the context of the other palaeoenvironmental analyses, in section 8.10.

8.7. Chironomid biostratigraphy

Chironomid larval head capsules were prepared and identified from subsamples of the KHAR and VORK5 as described in section 3.3.2.3. Results of the down-core chironomid analysis are presented as a percentage abundance diagrams using the computer program C2 (Juggins 2005). Stratigraphic diagrams were zoned by optimal sum-of-squares partitioning using the ZONE program, version 1.2 (Juggins 1991) and the statistical significance of the zones assessed using BSTICK (Bennett 1996).

8.7.1. Lake Kharinei (KHAR)

Of the 83 taxa present in the subfossil assemblages only 27 have a maximum abundance greater than 5% (Table 8.11). No taxa occur consistently throughout the core. *Procladius*, *Tanytarsus lugens*-type, *Tanytarsus mendax*-type and *Micropsectra insignilobus*-type occur in more than 35 of the 39 subsamples analysed, but the percentage abundances in the sub-samples vary considerably (Hill's $N_2 = 22 - 29$). The subfossil assemblages are taxon-rich and vary considerably down the core. This suggests the chironomid fauna were sensitive to, and responded to, environmental change over the late Quaternary. An unidentified Chironomini comprised 0.8 – 1.9% of the total fossil assemblage in three down-core samples at 874, 1006 and 1038cm depth. The mentum of the Chironomini sp. has a single broad, apically flattened median tooth which is distinctly longer than the lateral teeth (Figure 8.19). The six lateral teeth decrease in size from the second to the sixth lateral

tooth. The first lateral tooth is reduced and partially fused to the median tooth.

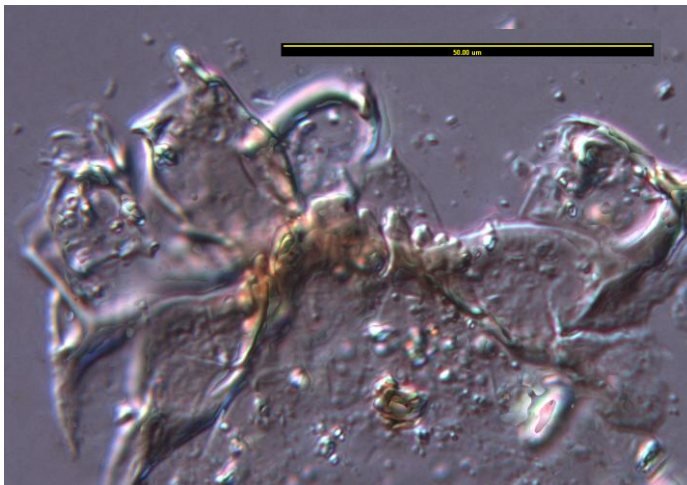


Figure 8.19. Larval mentum of unknown Chironomini, at x400 magnification, scale bar = 50µm. (Photomontage by A. Polaszek, NHM)

Subfamily	Taxa	No. of occurrences	Hill's N2	Min % abundance	Max % abundance	Subfamily	Taxa	No. of occurrences	Hill's N2	Min % abundance	Max % abundance
Chironominae						Orthoclaidiinae					
	<i>Chironomus anthracinus</i> -type	26	12.6	0	15.5		<i>Abiskomyia</i>	8	5.7	0	5.8
	<i>Chironomini</i> larva	12	9.7	0	2.7		<i>Chaetocladus</i>	7	5.8	0	2.8
	<i>Chironomus plumosus</i> -type	21	13.6	0	9.2		<i>Corynoneura arctica</i> -type	10	6.8	0	4.0
	<i>Cladopalma lateralis</i> -type	6	4.4	0	3.0		<i>Cricotopus bicinctus</i> -type	4	3.5	0	2.0
	<i>Cryptochironomus</i>	1	1.0	0	0.8		<i>Cricotopus cylindraceus</i> -type	12	10.8	0	2.7
	<i>Dicortendipes</i>	25	16.3	0	14.1		<i>Cricotopus laricornalis</i> -type	17	13.3	0	3.3
	<i>Endochironomus albipennis</i> -type	20	11.2	0	11.7		<i>Cricotopus sylvestris</i> -type	1	1.0	0	2.8
	<i>Endochironomus impar</i> -type	2	1.7	0	2.8		<i>Cricotopus trifaciatus</i> -type	2	1.4	0	3.0
	<i>Endochironomus tendens</i> -type	2	1.4	0	2.8		<i>Cricotopus</i> type C	4	3.3	0	1.9
	<i>Glyptotendipes barbipes</i> -type	6	4.0	0	6.5		<i>Cricotopus</i> type P	4	3.9	0	1.0
	<i>Glyptotendipes pallens</i> -type	21	14.9	0	8.9		Orthoclaidiinae indeterminate	6	5.2	0	2.0
	<i>Glyptotendipes severini</i> -type	1	1.0	0	2.8		<i>Orthocladus consobrinus</i> -type	11	9.7	0	3.0
	<i>Microtendipes pedellus</i> -type	20	14.3	0	6.9		<i>Orthocladus oliveri</i> -type	12	9.2	0	4.0
	<i>Microtendipes rydalsensis</i> -type	1	1.0	0	1.4		<i>Orthocladus trigonoblabis</i> -type	1	1.0	0	1.5
	<i>Parachironomus varus</i> -type	2	1.8	0	1.5		<i>Orthocladus undifferentiated</i>	3	2.6	0	1.0
	<i>Paratendipes albianus</i> -type	1	1.0	0	1.6		Heterotrissocladus indeterminate	11	8.7	0	34.0
	<i>Phaenopspectra flavipes</i> -type	3	2.4	0	4.4		<i>Heterotrissocladus maeaeeri</i> -type	3	2.9	0	1.5
	<i>Phaenopspectra</i> type A	8	5.3	0	4.1		<i>Hydrobaenus conformis</i> -type	2	2.0	0	1.1
	<i>Polypedium nubeculosum</i> -type	32	22.7	0	8.2		<i>Krenosmittia</i>	1	1.0	0	2.0
	<i>Polypedium sordens</i> -type	1	1.0	0	0.7		<i>Limnophyes - Paralimnophyes</i>	13	9.5	0	4.1
	<i>Sergentia coracina</i> -type	32	18.6	0	47.0		<i>Mesocricotopus</i>	1	1.0	0	1.8
	<i>Sitochironomus rosenchoeldi</i> -type	27	20.5	0	7.9		<i>Metriceremus eurynotus</i> -type	2	1.7	0	1.8
	Unidentified Chironomini	3	2.6	0	1.9		<i>Nanocladus brachicollis</i> -type	1	1.0	0	1.3
	Pseudochironomini						<i>Nanocladus rectinervis</i> -type	1	1.0	0	1.0
	<i>Pseudochironomus</i>	1	1.0	0	1.5		<i>Paraccladius</i>	17	9.5	0	11.6
	Tanytarsini						<i>Parakiefferiella bathophila</i> -type	13	11.3	0	2.5
	<i>Cladotanytarsus mancus</i> -type	32	16.6	0	15.4		<i>Parakiefferiella triquetra</i> -type	2	1.5	0	4.0
	<i>Constempellina-Thienemanniola</i>	15	9.4	0	14.1		<i>Psectrocladius septentrionalis</i> -type	1	1.0	0	0.6
	<i>Corynocera ambigua</i>	20	10.1	0	26.4		<i>Psectrocladius sordidellus</i> -type	33	23.9	0	8.9
	<i>Corynocera oliveri</i> -type	9	6.8	0	3.1		<i>Pseudosmittia</i>	4	3.9	0	1.0
	<i>Micropspectra insignilobus</i> -type	38	29.3	0	38.1		<i>Rheocricotopus effusus</i> -type	1	1.0	0	1.4
	<i>Micropspectra radialis</i> -type	1	1.0	0	1.5		<i>Smittia foliacea</i> -type	1	1.0	0	0.9
	<i>Paratanytarsus austriacus</i> -type	3	2.1	0	3.0		<i>Zalutschia mucronata</i> -type	1	1.0	0	1.4
	<i>Paratanytarsus penicillatus</i> -type	17	6.6	0	17.4		<i>Zalutschia zalutschicola</i> -type	10	9.4	0	1.8
	<i>Paratanytarsus undifferentiated</i>	31	25.0	0	7.9		<i>Zalutschia</i> type B	10	6.1	0	5.3
	<i>Stempellinaella - Zavrelia</i>	14	9.9	0	4.4	Diamesinae	<i>Diamesa zerrifficinerella</i> -type	1	1.0	0	0.8
	<i>Tanytarsus lugens</i> -type	38	28.4	0	13.6		<i>Protanytus</i>	2	2.0	0	1.1
	<i>Tanytarsus mendax</i> -type	12	8.0	0	7.2	Prodiamesinae	<i>Monodiamesa</i>	18	15.5	0	2.7
	<i>Tanytarsus pallidicornis</i> -type	33	26.5	0	7.4	Podonominae	<i>Lasiodiamesa</i>	5	4.8	0	1.5
	<i>Tanytarsini</i> undifferentiated					Tanytopodinae	<i>Ablabesmyia</i>	30	18.6	0	8.4
							<i>Monopelopia</i>	1	1.0	0	0.7
							<i>Procladius</i>	36	29.4	0	7.7
							<i>Tanytus</i>	2	1.6	0	2.7
							Undifferentiated Pentaneurini	1	1.0	0	0.8

Table 8.11. Chironomid fauna of KHAR core, with total number of occurrences (in 39 sub-samples), effective number of occurrences (Hill's N2) and minimum and maximum percent abundance.

The total number and abundances of Chironomini taxa are higher in the Kharinei core than in the faunal assemblages from the Putorana cores (section 7.6). Chironomini taxa, typically, have warmer temperature optima in the training set than other taxa suggesting that Lake Kharinei has probably been warmer and/or more productive than the high altitude lakes of the Putorana throughout the late Quaternary.

17 taxa are not represented in the Russian training set. The unrepresented taxa typically form minor components of the assemblages (1 or 2 occurrences at less than 2%), although *Glyptotendipes barbipes*-type, *Paracladopelma* and *Lasiodiamesa* occur 5 – 7 times at up to 4.5% abundance. Four zones (K-I to K-IV) were identified by optimal partitioning (Figure 8.20);

Zone K-I (1097 – 1024 cm; 13000 – 10000 cal yrs BP)

Tanytarsus pallidicornis-type, *T. mendax*-type, *Dicrotendipes* and *Chironomus plumosus*-type are common in this zone, individually comprising up to 10% of the assemblages. These taxa, which are indicative of relatively warm, productive lakes (Brodin 1986), decline in abundance towards the top of the zone. *Corynocera ambigua* initially occurs at 20-26%, but its abundance fluctuates widely throughout the zone. In palaeolimnological sequences *C. ambigua* is typically found in interstadial and early Holocene sequences (Brooks *et al.* 1997; Velle *et al.* 2005a) and is commonly associated with *Chironomus* spp. which are also early colonisers after significant environmental disturbance (Brooks *et al.* 1997).

Zone K-II (1024 – 856 cm; 10000 – 3300 cal yrs BP)

This zone is dominated by the cold stenotherms *Sergentia coracina*-type and *Micropsectra insignilobus*-type (Brundin 1956; Brodin 1986) which each occur at approximately 30% abundance. Taxa indicative of warm, productive lakes in zone K-I continue to decline and are absent or rare throughout the zone. *Sergentia* declines towards the top of the zone but is replaced by other cold stenotherms such as *Stictochironomus rosenschoeldi*-type and *Paracladius*.

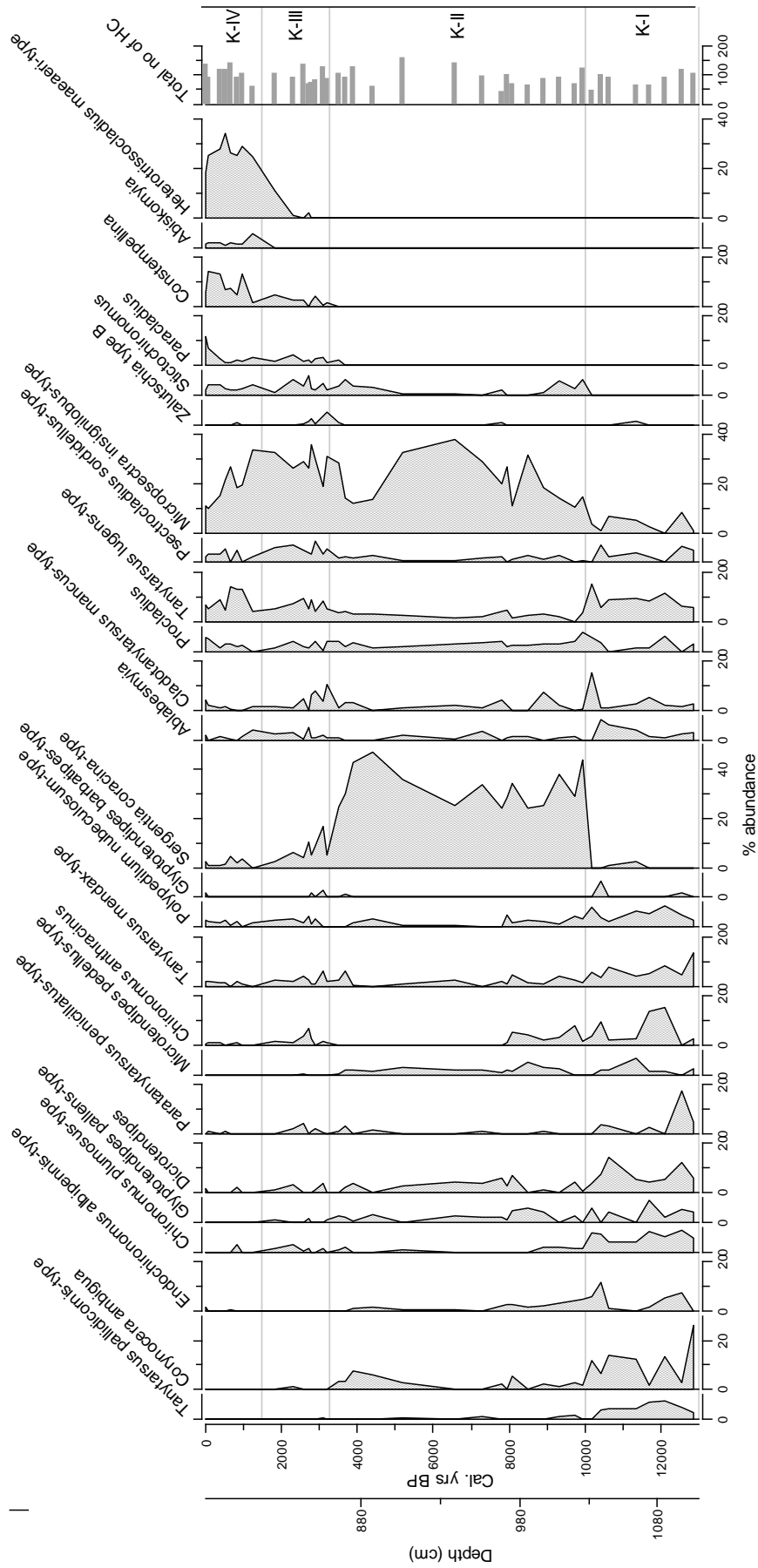


Figure 8.20. Lake Kharinei chironomid stratigraphy. Taxa shown have abundances greater than 5% and are ordered, by abundance, from bottom left to top right (oldest – youngest). Bars represent total number of head capsules examined. Zonation based on optimal partitioning with significant zones identified by the broken-stick model.

Zone K-III (856 – 800 cm; 3300 – 1500 cal yrs BP)

Sergentia declines steadily throughout the zone although *M. insignilobus*-type remains abundant at ca. 26-35%. The zone also marks the first appearance of *Constempellina*, *Abiskomyia* and *Heterotrissocladius maeaeri*-type.

Zone K-IV (800 – 780 cm; 1500 cal yrs BP – present day)

This zone is characterised by a decline in *M. insignilobus*-type and increased abundances of *Constempellina*, *Abiskomyia* and *H. maeaeri*-type. All these taxa are associated with cold oligotrophic lakes and the replacement of the acidophobic *M. insignilobus*-type by acidophilic *H. maeaeri*-type (Brodin 1986) may represent a decline in pH due to changes in the catchment.

The subfossil assemblages were plotted passively on the CCA ordination diagram (see section 4.2.4.2) with significant chemical and environmental variables fitted by regression (Figure 8.21). The older samples plot to the left on axis 1 and the lower part of axes 3 (Figure 8.21b) suggesting the lake was warmer and shallower than present 13000 – 10000 cal yrs BP and has become gradually colder and deeper over time. The most recent samples, from 788 cm depth, 600 years BP show a reversal in this trend with a return to slightly warmer, shallower conditions.

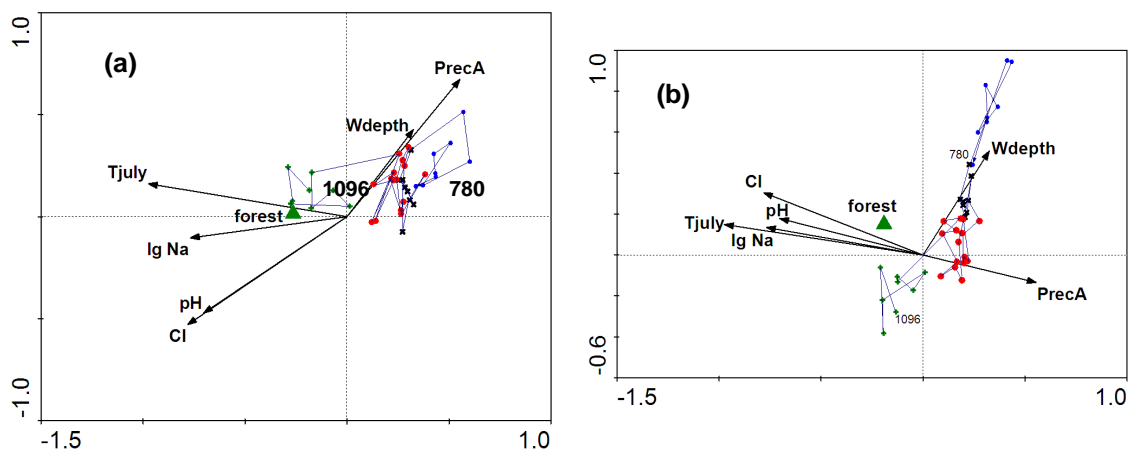


Figure 8.21. CCA plot of (a) axes 1 and 2 and (b) axes 1 and 3 with samples from Lake Kharinei fitted passively and joined as a time-track to show the changes in chironomid assemblages in relation to lake chemical and physical variables in the last 13000 years. Zones K-I – green crosses, K-II – red circles, K-III – black crosses and K-IV blue circles.

8.7.2. VORK5

Of the 82 taxa present in the subfossil assemblages, 29 occur once or twice in the subfossil assemblages (Table 8.12). Many of the rare taxa, for example *Georthocladius* (Cranston et al. 1983) and *Parachaetocladus* (Wülker 1959) are associated with streams and others, such as *Smittia* and *Metriocnemus terrester*-type (Cranston et al. 1983) are terrestrial or semi-terrestrial. The presence of these taxa may indicate that the lake has been subject to rapid changes in water depth or flooding events. No taxa occur throughout the core, *T. lugens*-type, *T. mendax*-type, *Psectrocladius sordidellus*-type and *Sergentia coracina*-type occur in 18 – 20 of the 21 samples analysed. Although *Sergentia* and *T. lugens*-type are cold stenotherms other taxa such as *Ps. sordidellus* are associated with warmer lakes (Brundin 1949). Therefore their presence may be a response to pH rather than temperature as these taxa are acidophilic or tolerate acidic conditions (Brodin 1986; Pinder and Morley 1995).

In total, 15 taxa are not represented in the Russian training set. The unrepresented taxa typically form minor components of the assemblages (1 or 2 occurrences at less than 2%) and are unlikely to affect the palaeoclimate reconstructions. No significant zones were identified by optimal partitioning (Figure 8.22). However *T. lugens*-type which was relatively abundant before the hiatus is less abundant after the hiatus and *Corynocera ambigua* and *Corynocera oliveri*-type which were rare before the hiatus are more abundant after the hiatus. The exact timing of the hiatus is imprecise, but occurred between the end of the radiocarbon dated sequence (4760 cal. yrs BP, 224cm depth) and the beginning of the ²¹⁰Pb dated sequence (ca. 100 yrs BP, 216.5cm). The hiatus probably resulted from changes in hydrology within the catchment causing lake levels to decline. This may have been accompanied by a period of subaerial exposure during which sediments may have been eroded and/or reworked before deposition within the undated section of the core. Therefore all results from the undated sequence between 216.5 and 224cm depth should be treated as unreliable and interpreted with caution.

Subfamily	Taxa	No. of occurrences	Hill's N2	Min % abundance	Max % abundance	Subfamily	Taxa	No. of occurrences	Hill's N2	Min % abundance	Max % abundance
Chironominae	Chironomini					Orthoclaidiinae	Abiskomyia				
	<i>Chironomus anthracinus</i> -type	14	10.4	0	9.7		<i>Chaetocladius</i>	1	1.0	0	1.9
	<i>Chironomini</i> larva	15	9.7	0	9.8		<i>Coynoneura arctica</i> -type	6	4.9	0	2.9
	<i>Chironomus plumosus</i> -type	7	4.9	0	5.8		<i>Coynoneura edwardsi</i> -type	2	2.0	0	1.2
	<i>Cladopeima lateralis</i> -type	2	1.5	0	2.4		<i>Cricotopus binctus</i> -type	1	1.0	0	1.7
	<i>Cryptochironomus</i>	1	1.0	0	1.9		<i>Cricotopus cylindraceus</i> -type	5	4.5	0	3.2
	<i>Cryptotendipes</i>	1	1.0	0	1.9		<i>Cricotopus intersectus</i> -type	9	7.8	0	3.0
	<i>Dicrotendipes</i>	5	4.6	0	5.4		<i>Cricotopus laricomalis</i> -type	3	2.7	0	1.2
	<i>Endochironomus albipennis</i> -type	4	3.1	0	3.2		<i>Cricotopus trifacatus</i> -type	4	3.9	0	2.0
	<i>Endochironomus impar</i> -type	5	2.8	0	7.4		<i>Cricotopus</i> type C	1	1.0	0	2.0
	<i>Glyptotendipes barbipes</i> -type	3	2.5	0	4.7		Orthoclaidiinae indeterminate	2	2.0	0	1.0
	<i>Glyptotendipes pallens</i> -type	2	2.0	0	1.4		<i>Orthoclaadius oliveri</i> -type	7	5.9	0	3.9
	<i>Lauterborniella</i>	1	1.0	0	2.1		<i>Orthoclaadius</i> undifferentiated	7	6.2	0	2.1
	<i>Lipniella</i>	2	1.8	0	2.0		<i>Eukiefferiella devonica</i> -type	3	2.9	0	2.4
	<i>Microchironomus</i>	1	1.0	0	0.9		<i>Georhtoclaadius</i>	2	1.3	0	1.9
	<i>Microtendipes pedellus</i> -type	13	8.2	0	7.8		<i>Tvetenia bavarica</i> -type	1	1.0	0	1.4
	<i>Parachironomus varus</i> -type	1	1.0	0	1.2		<i>Heterotrissocladius maeaeeri</i> -type	5	4.0	0	4.7
	<i>Phaenopsectra flavipes</i> -type	4	3.9	0	2.0		<i>Heterotrissocladius grimshawi</i> -type	4	1.3	0	22.4
	<i>Phaenopsectra</i> type A	7	5.1	0	5.9		<i>Hydrobaenus coniformis</i> -type	2	2.0	0	1.0
	<i>Polypedium nubeculosum</i> -type	7	5.4	0	5.0		<i>Hydrobaenus lugubris</i> -type	12	7.5	0	10.8
	<i>Polypedium sordens</i> -type	2	1.5	0	3.6		<i>Limnophyes</i> - <i>Paralimnophyes</i>	9	6.6	0	5.4
	<i>Sergentia coracina</i> -type	20	14.9	0	30.8		<i>Mesocricotopus</i>	17	11.4	0	6.9
	<i>Stictochironomus rosenchoeldi</i> -type	4	3.6	0	2.0		<i>Metricrocnemus eurynotus</i> -type	3	2.5	0	2.9
	Tanytarsini						<i>Metricrocnemus fusipes</i> -type	4	3.4	0	1.9
	<i>Cladotanytarsus mancus</i> -type	19	14.0	0	13.2		<i>Metricrocnemus terrester</i> -type	4	3.8	0	2.9
	<i>Constempellina-Thienemanniella</i>	19	15.7	0	11.1		<i>Oliveridia</i>	2	1.9	0	2.1
	<i>Corynocera ambigua</i>	11	3.1	0	38.2		<i>Parachaetoclaadius</i>	1	1.0	0	0.9
	<i>Corynocera oliveri</i> -type	9	3.9	0	19.6		<i>Nanoclaadius rectinervis</i> -type	1	1.0	0	1.2
	<i>Micropsectra insignibbus</i> -type	8	4.7	0	9.4		<i>Paraccladius</i>	4	2.0	0	11.8
	<i>Paratanytarsus austriacus</i> -type	3	2.7	0	3.8		<i>Parakiefferiella bathophila</i> -type	9	8.4	0	2.4
	<i>Paratanytarsus penicillatus</i> -type	6	4.9	0	5.8		<i>Parakiefferiella nigra</i> -type	1	1.0	0	2.4
	<i>Paratanytarsus</i> undifferentiated	15	8.9	0	7.8		<i>Parakiefferiella triquetra</i> -type	3	2.9	0	1.9
	<i>Stempellina</i>	1	1.0	0	2.4		<i>Parakiefferiella</i> type A	1	1.0	0	1.9
	<i>Stempellinella</i> - <i>Zavrelia</i>	14	10.5	0	7.8		<i>Proplosocerus lectustris</i> -type	1	1.0	0	2.0
	<i>Tanytarsus lugens</i> -type	18	11.3	0	38.9		<i>Psectrocladius septentrionalis</i> -type	1	1.0	0	1.2
	<i>Tanytarsus mendax</i> -type	19	13.5	0	19.3		<i>Psectrocladius sordidellus</i> -type	18	12.2	0	13.1
	<i>Tanytarsus pallidicornis</i> -type	7	5.0	0	4.2		<i>Pseudosmittia</i>	4	3.8	0	1.6
	<i>Tanytarsini</i> undifferentiated	20	15.0	0	13.6		<i>Smittia foliacea</i> -type	3	2.9	0	1.7
	<i>Ablebesmyia</i>	4	3.5	0	4.4		<i>Zalutschia zalutschicola</i> -type	3	1.9	0	19.3
Tanypodinae	<i>Procladius</i>	17	13.1	0	9.8		<i>Zalutschia</i> type A	1	1.0	0	0.8
	Undifferentiated Pentaneurini	1	1.0	0	1.4		<i>Zalutschia</i> type B	16	10.8	0	7.5
						Diamesinae	<i>Protanytus</i>	7	5.4	0	5.7
						Prodiamesinae	<i>Morodiamesa</i>	3	3.0	0	2.0

Table 8.12. Chironomid fauna of VORK5 core, with total number of occurrences (in 21 sub-samples), effective number of occurrences (Hill's N2) and minimum and maximum percent abundance.

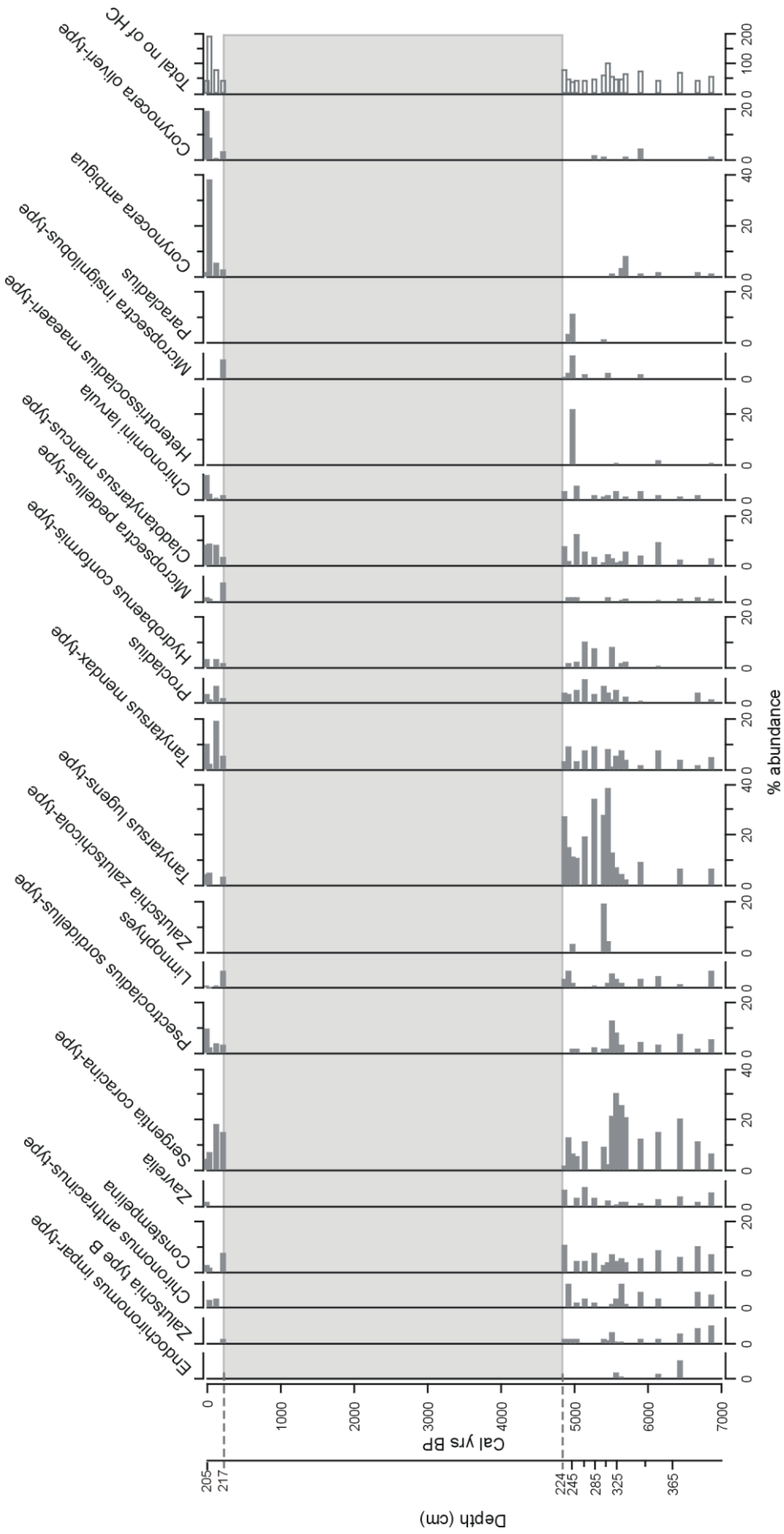


Figure 8.22. VORK5 chironomid stratigraphy. Taxa shown have abundances greater than 6% and are ordered, by abundance top right (oldest – youngest). Unfilled bars represent total number of head capsules examined and shaded area duration of t low deposition.

When the chironomid assemblages are plotted passively on the CCA ordination diagram (see section 4.2.4.2) the samples plot on the right of axes 1 which suggests the lake has remained cool throughout the period represented (Figure 8.23a). The samples show wide variations along the water depth gradient suggesting water depths have fluctuated considerably during deposition of the sequence. From Figure 8.23b the lake was probably at its deepest ca. 5000 years BP (246cm depth), faunal assemblages from 246 and 238cm depth suggest this was followed by a marked decrease in water depth. Water depth then remained relatively stable or the sediments were exposed, eroded and homogenised as the samples cluster closely together. The time-track suggests water depth decreased again from 221cm depth. The CCA time-track plots and the occurrence of terrestrial taxa and taxa associated with flowing water suggests the gently undulating catchment of VORK5 (see site description in section 8.2.4) may be highly sensitive to changes in catchment hydrology and water depth.

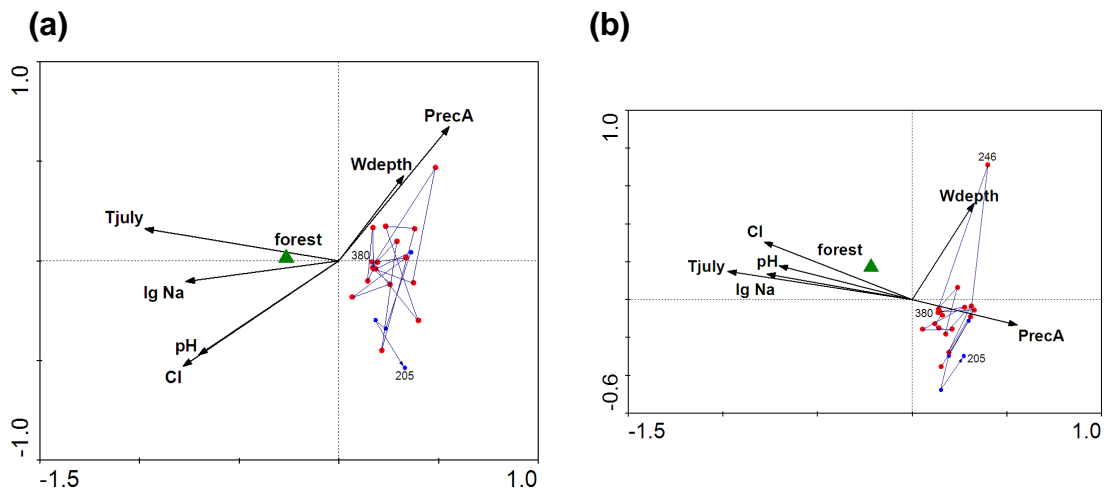


Figure 8.23. CCA plot of (a) axes 1 and 2 and (b) axes 1 and 3 with samples from VORK5 fitted passively and joined as a time-track to show the changes in chironomid assemblages in relation to lake chemical and physical variables. Red circles indicate pre-hiatus samples and blue circles from post-hiatus samples.

8.8. Chironomid-inferred temperature (CI-T) reconstructions

CI-T reconstructions from the Putorana lakes (section 7.7) suggested the 2-component WA-PLS model using the Russian K training set more accurately and reliably reconstructed the instrumental T_{july} record than estimates derived

from other training sets or statistical techniques. However to compare reconstructions using a number of statistical techniques over a longer time-scale, with greater variations in July air temperatures, than was possible with the Putorana samples T_{july} were reconstructed for KHAR and VORK5 using WA, WA-PLS and MAT methods and Russian training set K. The reliability of the down-core CI-T reconstructions is assessed using the criteria described in section 7.7.3.

8.8.1. Lake Kharinei (KHAR)

Applying the CI-T models to the surface sediments suggests the mean July air temperature derived from the WA-PLS 2-component model (13.3°C) is closer to the present-day T_{july} of 13.3°C than the WA (12.1°C) or MAT (12.0°C) reconstructions (Figure 8.24). The WA-PLS CI-T are consistently higher than the WA or MAT estimates from 10000 cal yrs BP to present. Although the statistical techniques show similar temperature trends major differences occur between the MAT and WA-PLS/WA reconstructions. For example, between 13000 – 10000 cal yrs BP the MAT reconstruction varies by approximately 4°C , between 13.3 and 17.5°C , compared with $2 - 2.5^{\circ}\text{C}$ in the WA and WA-PLS reconstructions. The discrepancies may arise from the availability and environmental characteristics of close analogues in the training set. The 6 closest analogues are used in the MAT reconstructions (section 6.2.2) and similarity is measured using squared chord distance. Between 13000 – 10000 cal yrs BP the lowest MAT CI-T (13.3°C) occurs at 1070cm depth (ca. 11400 cal yrs BP), all 6 of the closest analogues are derived from NEER with a maximum squared chord distance of 37. The highest MAT CI-T of 17.5°C occurs at 1092cm depth (ca. 12600 cal yrs BP), 5 of the 6 closest analogues are from Yakutia with a maximum squared chord distance of 29. The Yakutian lakes are characterised by high conductivity, pH and salinity (section 4.2), although the most extreme outliers have been removed from the training set. Therefore the subfossil assemblages which select Yakutian lakes as their closest analogue may be reflecting these environmental characteristics rather than T_{july} directly. The use of MAT may be unsuitable with the Russian training set k where the lakes with the highest T_{july} temperatures are so strongly correlated to other environmental variables and there are no analogues for

warm temperature, neutral pH lakes. WA and WA-PLS tends to perform better in 'no-analogue' situations than MAT and these statistical techniques would therefore be more appropriate for CI-T reconstructions for KHAR (ter Braak and Juggins 1993; Birks 2003). Birks (2003) uses consensus plots from pollen-inferred temperature reconstructions in Fennoscandia to highlight major climate trends. However MAT, and therefore the consensus approach, may be unreliable in this analysis given the poor analogues in the Russian chironomid training set. Subsequent interpretation of the Lake Kharinei record is based on the WA-PLS model.

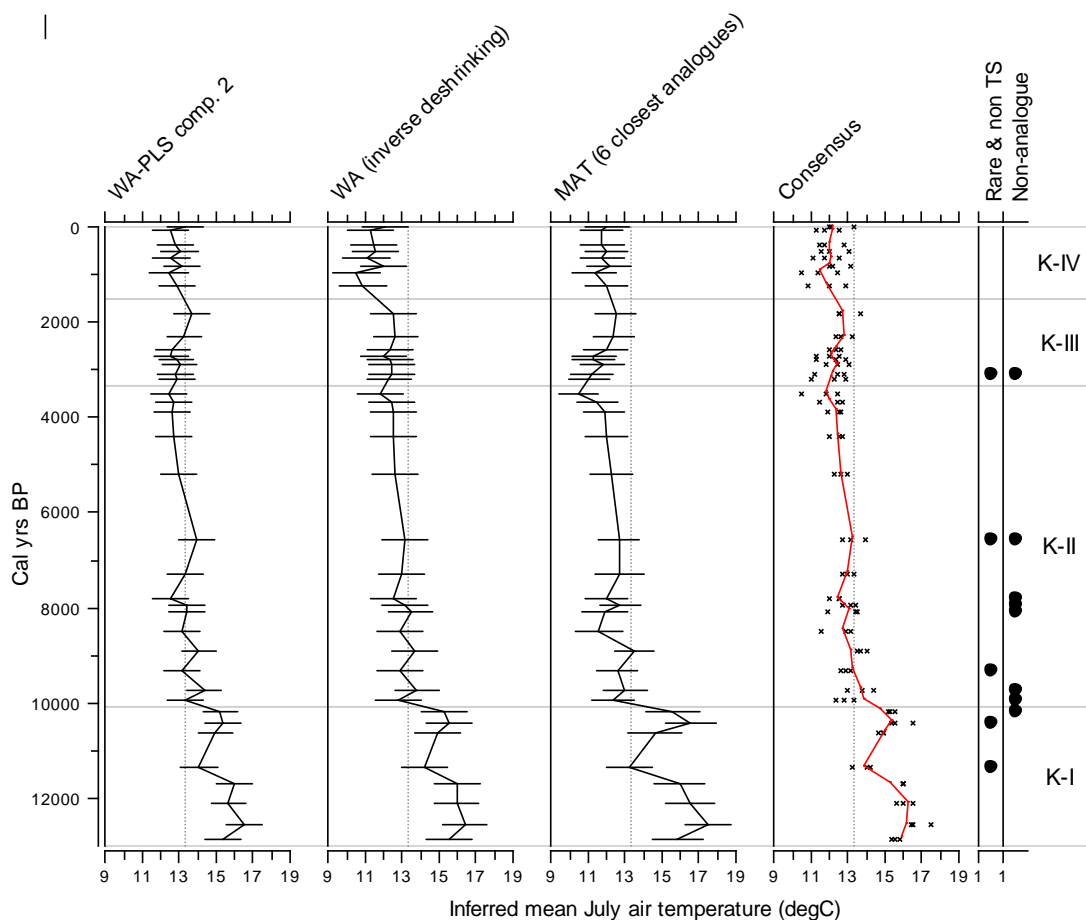


Figure 8.24. Reconstructions of mean July air temperature (°C) for Lake Kharinei (KHAR) based on WA-PLS (2 component model), WA with inverse deshrinking, MAT and consensus reconstruction derived by fitting LOWESS smoother (span 0.1) through all reconstructed values. Sample-specific errors of reconstruction are shown for individual techniques. Vertical dashed line indicates present-day T_{july} . Solid circles indicate samples with more than 5% abundance of taxa that are rare or not included in training set or have no close analogue in training set.

T_{july} were approximately 3°C warmer than present (16.5°C) ca. 12000 cal yrs BP (Figure 8.24) but declined by 2.5°C to 14°C at 11300 cal yrs BP. Temperatures then increased gradually to 15.3°C at 10300 cal yrs BP before decreasing sharply by 2°C at ca. 10000 cal yrs BP. T_{july} fluctuated between 13.3 – 14.0 °C but remained warmer than present until approximately 6000 cal yrs BP with the exception of a cooler period ca 7900 cal yrs BP. From 6000 cal yrs BP temperatures declined to present-day temperatures, this cool phase was interrupted by warmer interval at approximately 2000 cal yrs BP.

8.8.2. VORK5

Due to the long hiatus CI-T reconstructions are presented for the surface and base sequences separately (Figure 8.25); time scales for the two sequences vary. As with the Lake Kharinei, the MAT reconstructions fluctuate more widely and show different trends from the WA and WA-PLS CI-T. Many of these samples have high abundances of rare or non-training set taxa or have no close analogues in the modern training set and support the use of WA and WA-PLS techniques for reconstruction. All techniques underestimate present-day T_{july} (11.9°C), although the WA CI-T (11.3°C) is closer than the WA-PLS value (10.8°C).

As with Lake Kharinei CI-T T_{july} declines by approximately 1°C between 6800 – 4800 cal yrs BP. In KHAR CI-T decline, steadily, to below present-day values ca 6000 cal yrs BP. The higher resolution of the VORK5 reconstructions suggest this was a period of climate instability with temperatures fluctuating by $\pm 1^\circ\text{C}$ between 6000 – 5300 cal yrs BP. Temperatures increase by 1.5°C to 13°C ca 5000 cal yrs BP but decline again before the apparent hiatus. The recent sequence lacks the resolution for detailed CI-T reconstructions, however, T_{july} shows no apparent increase over the past 50 years.

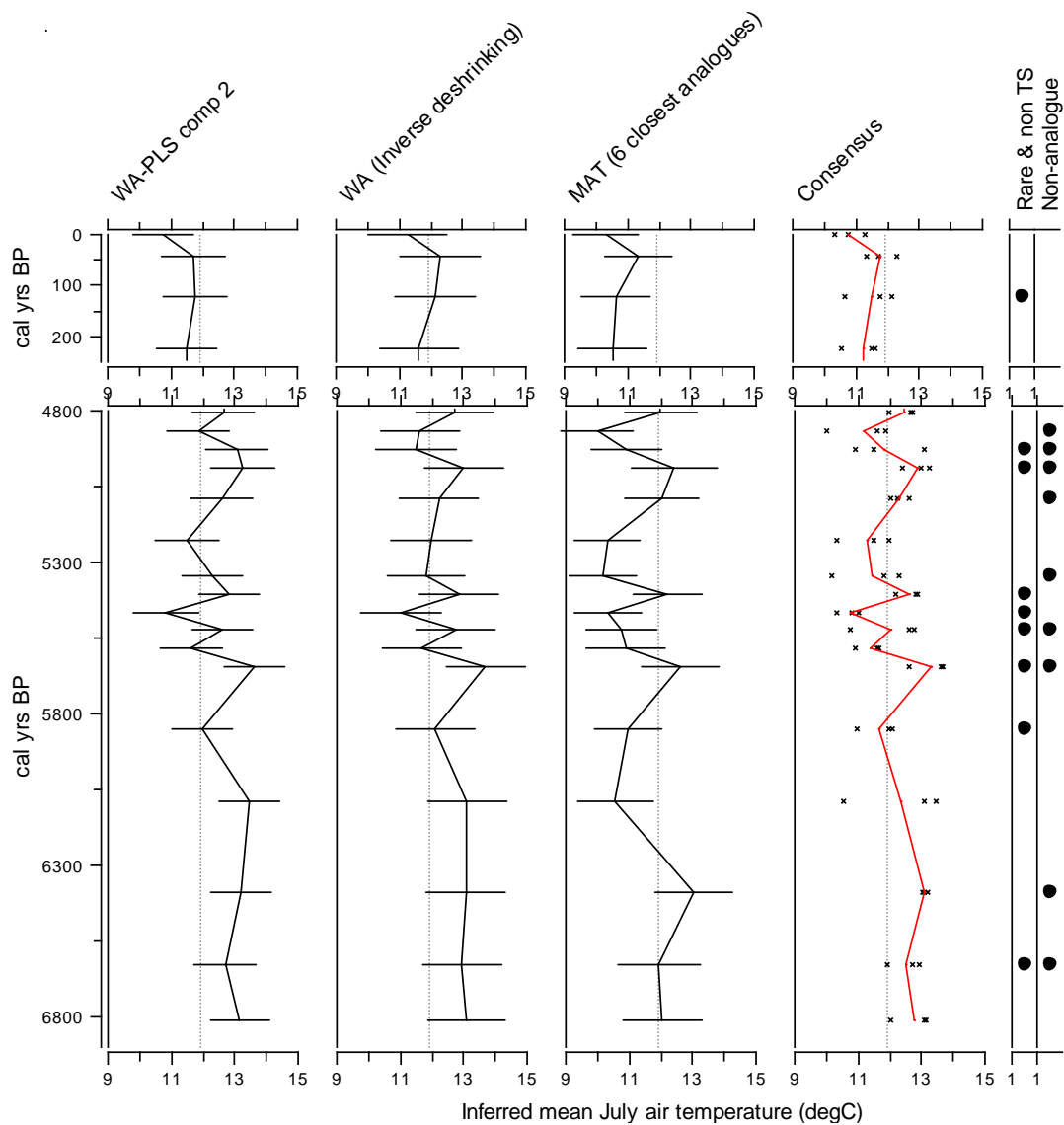


Figure 8.25. Reconstructions of mean July air temperature (°C) for VORK5 based on WA-PLS (2 component model), WA with inverse deshrinking, MAT and consensus reconstruction derived by fitting LOWESS smoother (span 0.1) through all reconstructed values. Sample-specific errors of reconstruction are shown for individual techniques. Vertical dashed line indicates present-day T_{July} . Solid circles indicate samples with more than 5% abundance of taxa that are rare or not included in training set or have no close analogue in training set.

8.9. Chironomid-inferred continentality (CI-C) reconstructions

CI-C reconstructions from the Putorana lakes (section 7.8) suggested the WA model with classical deshrinking more accurately estimates present-day values and recent trends in continentality than WA-PLS 2-component model. However evaluation of the WA-PLS model, in Chapter 6, showed it under-predicted continentality above indices of 50, i.e. on the Putorana (Figure 6.13)

but performed well in other areas of Russia (Table 6.16). Therefore CI-C was reconstructed for KHAR and VORK5 by WA and WA-PLS.

8.9.1. Lake Kharinei (KHAR)

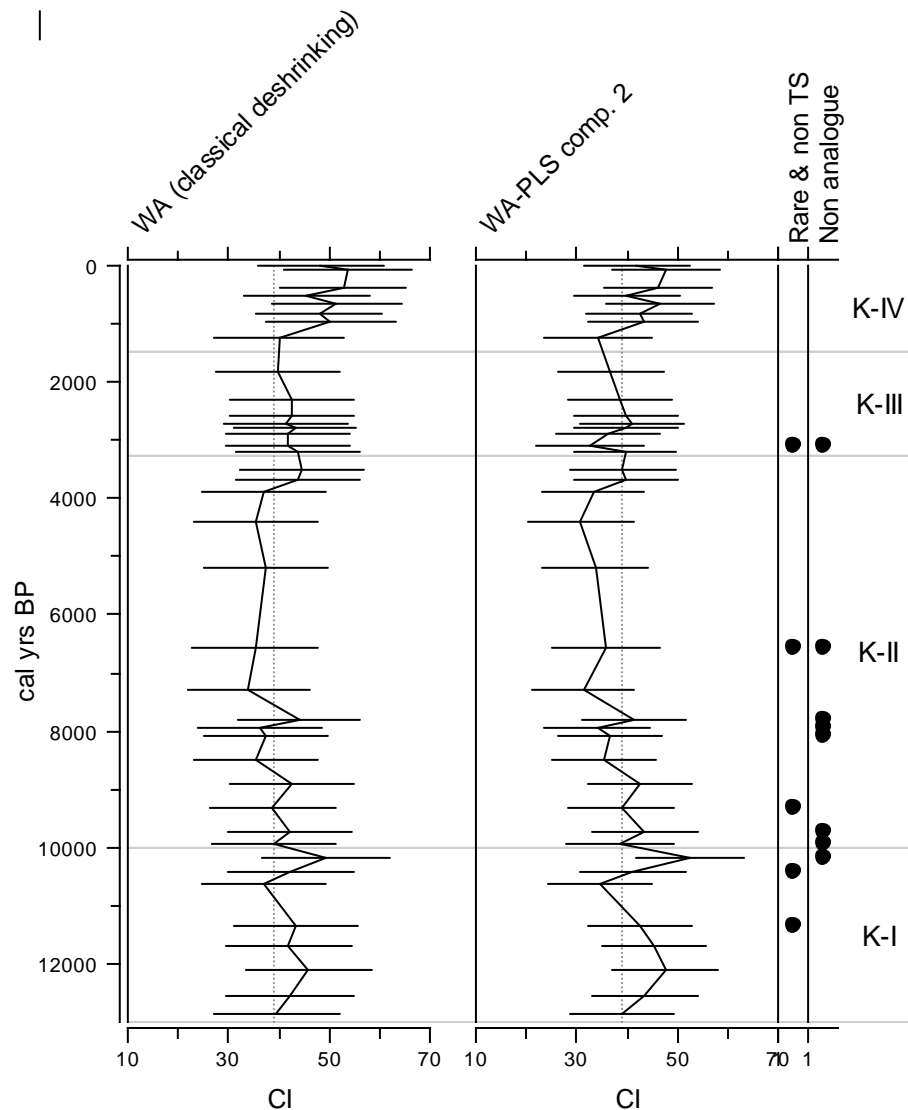


Figure 8.26. Reconstructions of CI, continentality index, for Lake Kharinei (KHAR) based on WA-PLS (2 component model) and WA with classical deshrinking. Sample-specific errors of reconstruction are shown for individual techniques. Vertical dashed line indicates present-day CI. Solid circles indicate samples with more than 5% abundance of taxa that are rare or not included in training set or have no close analogue in training set.

The estimated present-day continentality index of 42, derived from the WA-PLS 2-component model, is closer to the instrumental CI of 39 than the WA CI-

C reconstruction of 48 (Figure 8.26). Although the statistical techniques show similar trends occasional differences occur between the WA and WA-PLS reconstructions. For example, WA-PLS CI-C decreases by 8 to a continentality index of 33 at approximately 3000 cal yrs whereas the WA CI-C remains stable at 42.

The CI-C reconstructions suggest the climate was more continental (CI up to 10 higher) than present between 12500 - 10000 cal yrs BP. This period was interrupted by a more maritime interval ca 10500 cal yrs BP, before continentality returned, briefly, to more continental conditions. From 10000 cal yrs BP continentality declined to present-day levels until 8500 cal yrs BP when the climate became more maritime for approximately 600 years. Between 7800 - 3900 cal yrs BP CI-C declined to give the most maritime phase in the reconstruction. The climate became more continental, but below present-day values, ca 3500 cal yrs BP then declined steadily until 1200 cal yrs BP. The present-day continentality was established approximately 1000 cal yrs BP. CI has declined by 6 over the past 75 years which is similar to the decrease calculated from instrumental records for the Arctic (Hirschi et al. 2007).

8.9.2. VORK5

As with KHAR, the estimated present-day CI of 44, derived from the WA-PLS 2-component model, is closer to the instrumental CI of 37 than the WA CI-C reconstruction of 57 and within the sample specific error (Figure 8.27). CI-C reconstructions are presented for the basal and surface sequences separately and with different time scales due to the long hiatus. CIs from VORK5 are more continental than those from KHAR suggesting a shorter ice-free season. In general CI-C was lower between 6800 – 4800 cal yrs BP than the present-day CI-C. But whereas the reconstructions from KHAR suggest a stable maritime climate, the higher resolution of VORK5 indicates greater climate instability with major fluctuations in CI of ± 4 between 5600 – 5300 cal yrs BP. The recent sequence lacks the resolution for detailed reconstructions however WA-PLS CI shows a decrease of 5 over the past 50 years which is similar to the decreases calculated by Hirschi *et al.* (2007).

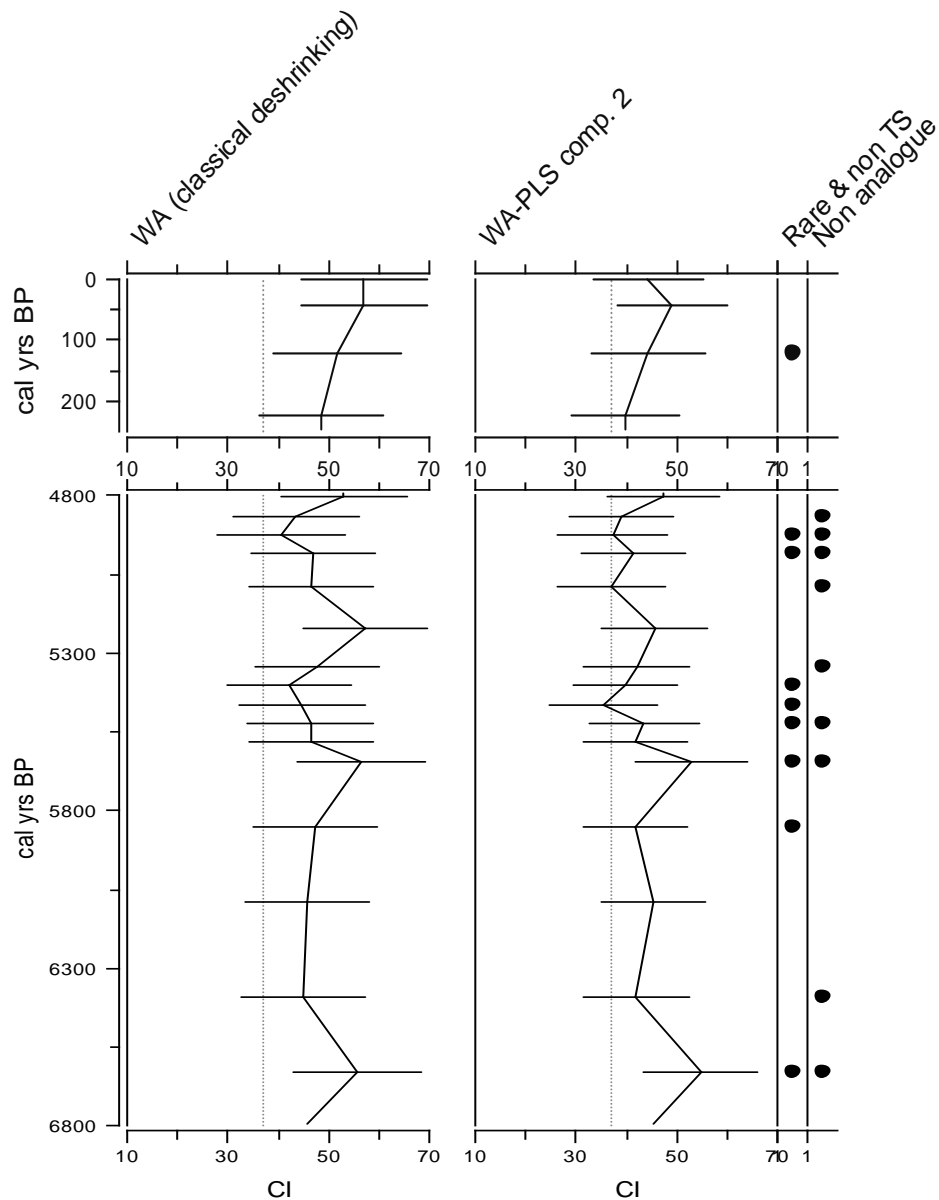


Figure 8.27. Reconstructions of CI, continentality index, for VORK5 based on WA-PLS (2 component model) and WA with classical deshrinking with sample-specific errors. Vertical dashed line indicates present-day CI. Solid circles indicate samples with more than 5% abundance of taxa that are rare or not included in training set or have no close analogue in training set.

8.10. Palaeoenvironmental interpretation

13000 – 10000 cal yrs BP

The initiation of sedimentation at Lake Kharinei (KHAR) after 13000 cal yrs BP coincides with enhanced melting of the permafrost (Henriksen et al. 2001; Sidorchuk et al. 2001) and formation of other lakes in NEER (for example Väiliranta et al. 2006). The reconstructions from Kharinei (Figure 8.28) suggest

the climate was approximately 3°C warmer and more continental than present between 12500 – 10000 cal yrs BP. CI-T reconstructions from Lake Lyadhej-To, in the Polar Urals also suggest T_{july} was ca. 2 - 4°C warmer than present between 10700 – 10550 cal yrs BP (Andreev *et al.* 2005) and up to 2 - 3°C warmer between 10300 – 9200 cal yrs BP at Nikolay Lake, in the Lena Delta (Andreev *et al.* 2004b). The isotopic analyses from Kharinei (section 8.6.1) also suggest a productive environment with a significant input of organic material from terrestrial plants.

Glacial, marine and terrestrial records show pronounced cooling in the North Atlantic region during the period from 12900 – 11700 cal yrs BP, the Younger Dryas (YD) (Alley 2000; Overpeck and Cole 2006) with mean annual temperatures approximately 5 – 15°C lower than present-day (Severinghaus *et al.* 1998; Alley 2000). CI-T reconstructions from Kråkenes, Norway (Brooks and Birks 2001) and the Swiss Alps (Ilyashuk *et al.* 2009) indicate July air temperatures were ca. 6°C and 2.5°C cooler, respectively, than present-day in Europe during the YD whereas the CI-T reconstructions from Kharinei and other arctic lakes in continental Russia (Andreev *et al.* 2004b; Andreev *et al.* 2005) were ca. 3°C warmer than present. Similar spatially-complex regional patterns, during the YD, are observed in other parts of the Arctic. The YD was characterised by (1) cooler-than-present summer temperatures in Southern Alaska and Eastern Siberia and (2) uniform to warmer-than-present conditions through most of Central Alaska and North-eastern Siberia (Kokorowski *et al.* 2008). Kokorowski *et al.* (2008) suggested the spatial heterogeneity, in Beringia, reflected the localised moderating influence of topography on climate change driven by changes in sea surface temperatures (SST), atmospheric circulation and insolation. In climate simulations of the LGM, the jet stream over western Eurasia is partially blocked by the Fennoscandian Ice Sheet and so westerlies over the continental interior to the east of the ice sheet are weaker than present (Bush 2004). The blocking of cold westerlies and resulting increased influence of more continental air masses may have resulted in the warm summer temperature seen in NEER in the YD.

Winters in Europe, during the YD, were drastically colder resulting in increases in the annual temperature range of 10 – 20°C and enhanced seasonality (Renssen *et al.* 2001; Lie and Paasche 2006). The Kharinei reconstructions suggest T_{july} were 3°C warmer than present during the YD, to derive the observed increase in continentality (CI) winter temperatures would have been approximately 3° colder than present. Therefore the increase in annual temperature range was less than in Europe (Renssen *et al.* 2001; Lie and Paasche 2006) and mean annual temperatures probably remained similar to present-day.

The early Holocene at Kharinei, 11500 – 10000 cal yrs BP, shows high variability in July temperature with CI-T varying between 14 – 15.3°C. CI-C declines to a CI of 7 below present-day value at ca. 10600 cal yrs BP. Solar insolation ca 10000 years ago, at 60°N, was approximately 10% higher in summer and 20% lower in winter due to orbital forcing of the Milankovitch cycles (Berger and Loutre 1991). Therefore this period (12000 – 8000 yrs BP) should have been more continental, as the CI-C record from Kharinei for this period, in general, shows. However vegetation composition to the west, in Fennoscandia, indicates the Younger Dryas – early Holocene transition was, primarily, a change in winter temperature and, consequently, a shift to a more maritime climate (Seppä *et al.* 2005; Giesecke *et al.* 2008; Heikkila *et al.* 2009). As the insolation record indicates the global climate should be more continental than present in the early Holocene, Giesecke *et al.* (2008) suggested the changes in western Europe mark a change in atmospheric circulation allowing oceanic air masses to dominate over Fennoscandia. The short duration changes in CI-T and CI-C at Kharinei may be a regional expression of the synoptic changes in atmospheric circulation and/or the increased frequency of cyclones entering Europe.

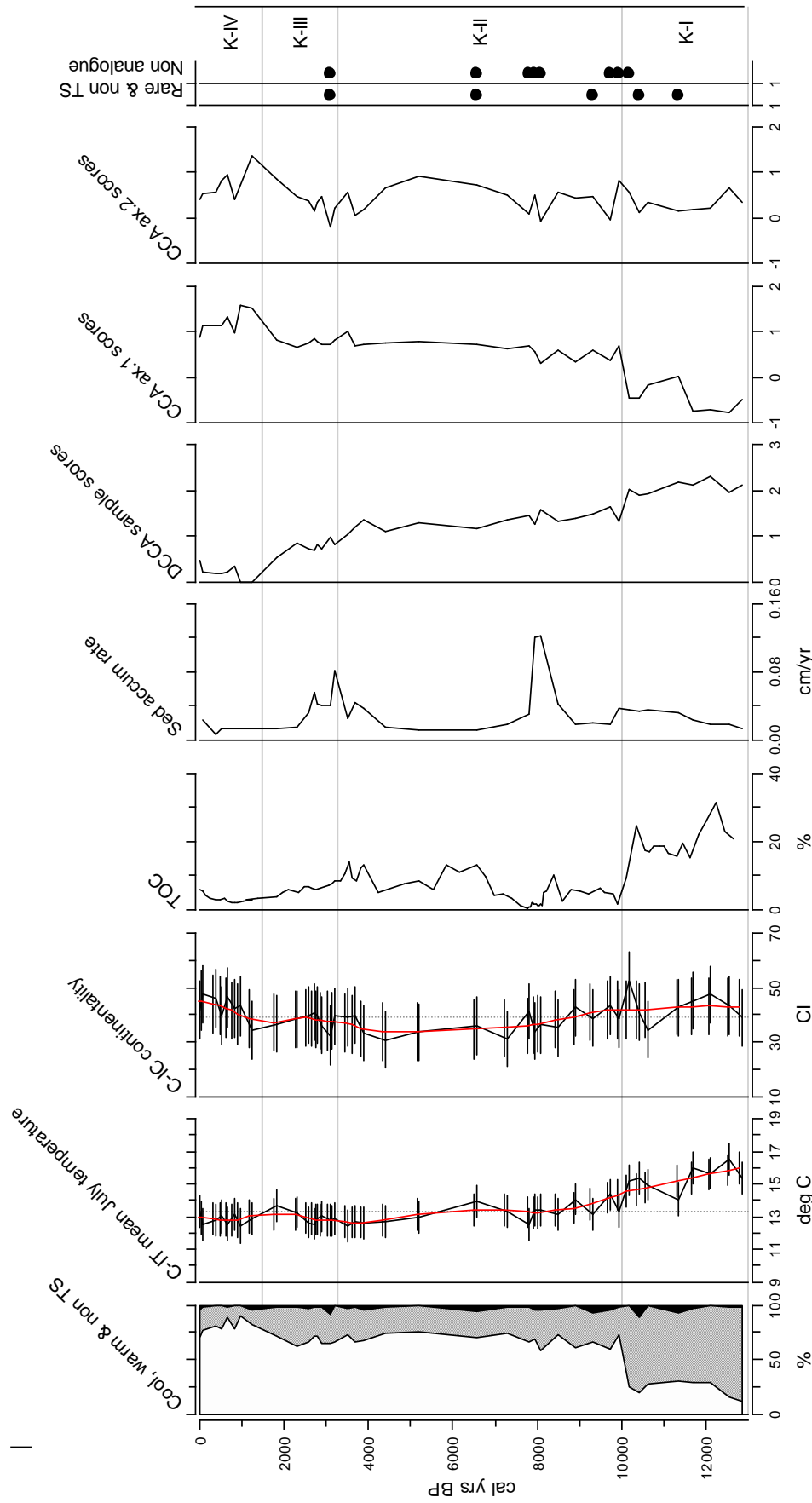


Figure 8.28. Summary diagram for Lake Kharinei (KHAR) showing the percentage of cool-water taxa (optima <13°C), warm-water taxa (optima >13°C) and non training set taxa, chironomid-inferred mean July air temperature and continentality, total organic carbon (TOC) of bulk sediment, sediment accumulation rate, DCCA scores, CCA axes 1 and 2 scores. C-IT and C-IC are shown with sample specific errors and LOWESS smoother (span 0.25). The solid circles indicate samples with more than 5% abundance of rare or non training set taxa that are rare or have no analogue in modern training set. Age of samples are presented as years before 2007.

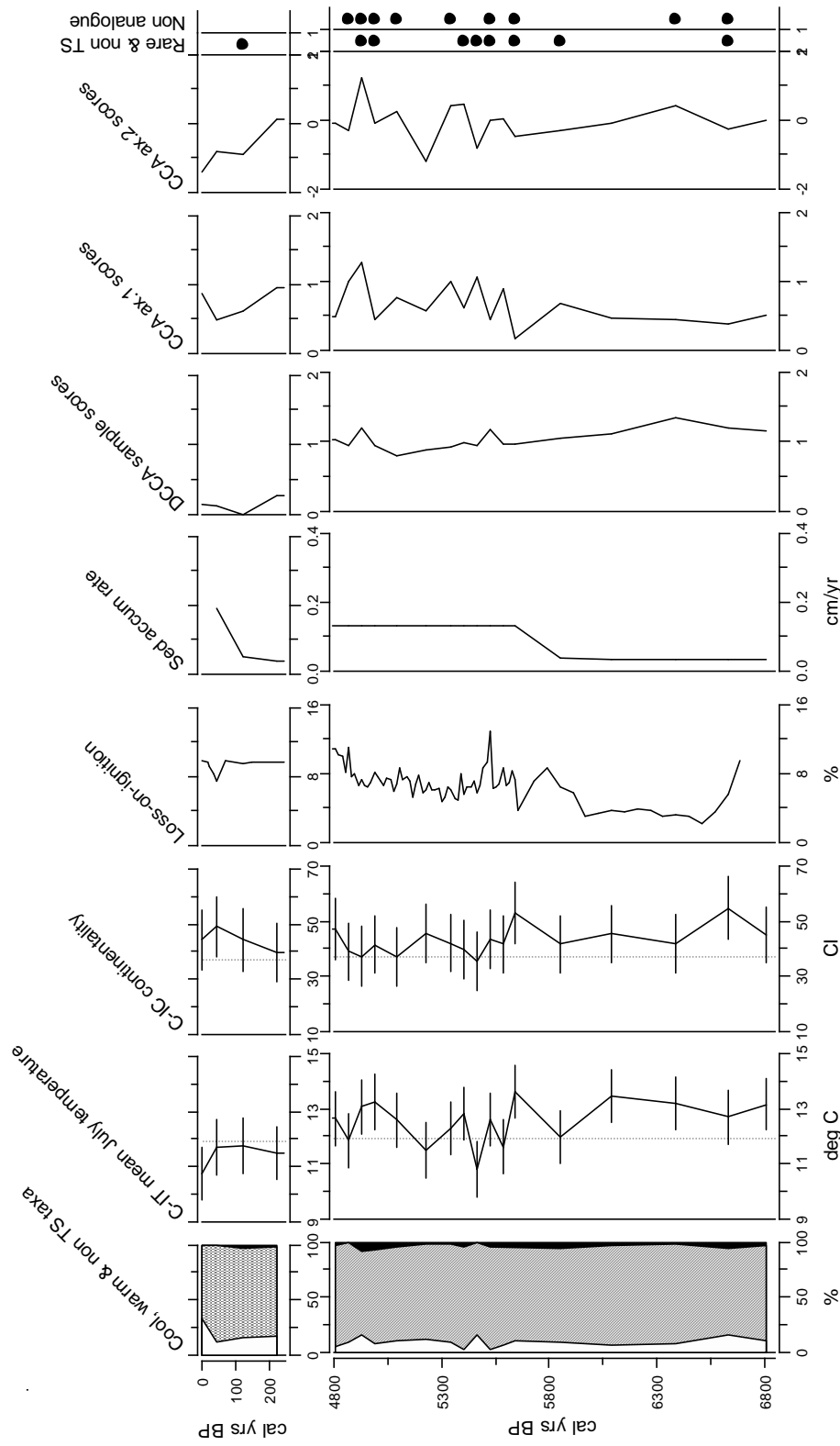


Figure 8.29. Summary diagram for VORK5 showing the percentage of cool-water taxa (optima <11°C), warm-water taxa (optima >11°C) and non training set taxa, chironomid-inferred mean July air temperature and continentality, total organic carbon (TOC) of bulk sediment, sediment accumulation rate, DCCA scores, CCA axes 1 and 2 scores. C-IT and C-IC are shown with sample specific errors. The solid circles indicate samples with more than 5% abundance of rare or non training set taxa that are rare or have no analogue in modern training set. Age of samples presented as years before 2007.

Although T_{july} remained 1.5 - 2°C higher than present at Kharinei ca. 10000 cal yrs BP, the proportion of cool to warm taxa and CCA axis 1 scores suggest a change to cold-adapted assemblages possibly in response to the temperature variability. Giesecke (2008) suggested the high variability in climate, due to the increased frequency of cyclones, resulted in frequent freeze-thaw cycles in winter and spring. These severe cold spells limited the early Holocene expansion of *Quercus* and *Picea abies* and may also have resulted in the change to cold-adapted chironomid fauna.

10000 – 4000 cal yrs BP

From 10000 cal yrs BP until approximately 6000 cal yrs BP, although cooler than the preceding Pleistocene – early Holocene interval, T_{july} remained slightly warmer (up to 1°C) than present. Occurrence of a warmer period in the early Holocene is supported by studies of pollen (Andreev *et al.* 2004b; Andreev *et al.* 2005; Väiliranta *et al.* 2006), diatoms (Westover *et al.* 2006), chironomids (Porinchu and Cwynar 2002; Westover *et al.* 2006) and tree-line dynamics (Kremenetski *et al.* 1998; MacDonald *et al.* 2000) from northern Russia. CI-T and pollen reconstructions suggest the warmest interval of the Holocene (the Holocene Thermal Maximum – HTM) occurred prior to 8000 yrs BP in northern Fennoscandia (for example Larocque and Hall 2004; Velle *et al.* 2005b) and in the Polar Urals (Andreev *et al.* 2005) and the Lena Delta (Andreev *et al.* 2004b) in Russia. However CI-T reconstructions from lakes in the southern boreal zones of central Sweden suggest maximum T_{july} were reached after 7000 cal yrs BP (Antonsson *et al.* 2006) and pollen analyses from lakes in southern Fennoscandia (Giesecke *et al.* 2008) and the Kola Peninsula, western Russia (Seppä *et al.* 2008) place the HTM at 7500–6500 cal yr BP. This spatial heterogeneity may reflect the track of cool, moist oceanic air flow during the more maritime climate of the early Holocene.

Several early Holocene reconstructions from Russia (for example MacDonald *et al.* 2000; Andreev *et al.* 2004b) based on plant macrofossils and pollen suggest the HTM was up to 2.5°C warmer than present, however the CI-T reconstructions from Kharinei estimate the early Holocene was less than 1°C warmer than present. The discrepancy may result from;

1. unreliable T_{july} reconstructions due to the high abundances of taxa not included in the training set,
2. the chironomid model may be underestimating T_{july} during this period or
3. a loss of thermal response in the chironomid fauna.

Time-tracks plotted passively on the CCA (Figure 8.21) suggest Lake Kharinei was shallower than present 13000 – 10000 cal yrs BP and became deeper over the early – mid Holocene. CCA sample scores, from ca. 10000 cal yrs BP to 6000 cal yrs BP, show a slight steady increase on axis 1, inversely associated with temperature, and greater fluctuations on axis 2 associated with water depth. Records from the European Lake Level database show generally wet conditions in Europe from ca. 9520 – 6295 cal yrs BP (Yu and Harrison 1995; Verschuren and Charman 2008). Therefore the chironomids at Kharinei may be responding to increasing water depth which is dampening the climate response.

The warm early - mid Holocene period, at Kharinei, was interrupted by a cooler, more maritime-influenced period ca 7900 cal yrs BP which lasted approximately 600 years. T_{july} declined by 1°C to 12.5°C. This cool period may be the regional expression of the 8200 cal yrs BP event which resulted in a cold interval in the North Atlantic region. Analysis of the Greenland ice cores suggest an abrupt cooling of 2 - 6°C (Alley *et al.* 1997; Alley and Agustsdottir 2005). Decreases in atmospheric CH₄ composition (Spahni *et al.* 2003) and large-scale changes in atmospheric circulation (Stager and Mayewski 1997) indicate the impact was widespread, however this view has been challenged by Seppå *et al.* (2007) who found no response at sites in the North-European tree-line region. In the Kharinei record, the increase in sediment accumulation rate associated with the cold interval appears to predate this period, but this apparent discrepancy may result from the sampling resolution. Sediment accumulation rates were 0.04 cm yr⁻¹ at 8400 cal yrs BP and 0.12 cm yr⁻¹ at 8000 cal yrs BP so sedimentation may have increased at any time within this 400 year interval. Further analysis of this section of the sequence, at higher resolution, may clarify the timing and duration of the cooling event.

The period from 6000 – 4000 cal yrs BP shows the beginnings of a deterioration in climate; T_{july} declined to recent temperatures (12.5 – 13.0 °C) and Cl-C

decreased to a CI of 8 below present-day values, to give the most maritime phase of the Kharinei record. CI-T and CI-C reconstructions from VORK5 show similar trends (Figure 8.29). A transition to cooler temperatures at 6000 cal yrs BP is seen in diatom (Westover et al. 2006) and chironomid (Porinchu and Cwynar 2002) records from Siberia and pollen records from the Polar Urals (Andreev et al. 2005). Time-tracks plotted passively on the CCA (Figure 8.21) and CCA axis 2 scores suggest a marked decline in water depth at Lake Kharinei. This trend is supported by declining lake levels, culminating in drought, ca. 5070 – 4485 years BP in the European record (Yu and Harrison 1995; Verschuren and Charman 2008). The higher resolution of the VORK5 core (Figure 8.29) indicates a period of climate instability between 5600 – 5300 cal yrs BP, with fluctuations in both CI-T and CI-C. A period of global climate change between 6000 – 5000 cal yrs BP has been attributed to a decline in solar output (Mayewski et al. 2004). A decline in solar output should result in decreased T_{july} and increased continentality. However reconstructions from many of the VORK5 samples from this period may be unreliable due to the lack of modern analogues or high percentage of non-training set or rare taxa, but the reconstructions suggest the climate was unstable.

4000 cal yrs BP – present day

From ca. 4000 cal yrs BP T_{july} , at Kharinei, remained stable but continentality increased from CI 33 to 45, therefore the ice-free period would have become considerably shorter. Based on the modern relationships (section 6.7.1) the increase in CI would have reduced the total number of days per year with air temperatures above 0°C by approximately 60 days to 150 days. However, the differences in atmospheric circulation and insolation between 4000 cal yrs BP and the present-day mean the relationship between CI and total number of days per year above 0°C has probably changed over time, so these figures may be unreliable. Stable isotope analysis indicates low input of terrestrial carbon into the lake at this time and declining within-lake productivity (Figure 8.17). The continuing deterioration in climate is evident in a number of records; tree-lines retreated to their present positions, in NEER, between 4000 and 3000 yrs BP (Kremenetski et al. 1998; MacDonald et al. 2000). Permafrost aggradation recommenced in the region ca 4500 yrs BP (Kultti et al. 2004) and glaciers

expanded on Franz Josef Land to reach their present margins between 3200 – 2000 yrs BP (Lubinski et al. 1999). Between 4000 – 1200 cal yrs BP DCCA scores constrained against age, from Kharinei, show a decreasing trend indicating a period of pronounced compositional change in the chironomid subfossil assemblages.

CI-T and CI-C reconstructions indicate a relatively warm period ca. 1800 cal yrs BP. T_{july} was 0.4°C warmer and the continentality index higher than present which would have resulted in a warmer, longer summer. The timing of the warm interval at Kharinei is earlier than the Medieval Warm Period (MWP) in Europe (1100 – 800 cal yrs BP) (Bradley *et al.* 2003) but consistent in date with a warm interval observed in CI-T reconstructions from the Lena River delta (Andreev *et al.* 2004b) and pollen (Andreev *et al.* 2002) and tree-ring records (Naurzbaev and Vaganov 2000) from the Taymyr-Putorana region of northern Siberia. Between 1100 – 800 cal yrs BP T_{july} at Kharinei were similar to present-day values. The dating of this section of the sequence lies between the ^{210}Pb - and radiocarbon-dated sequences and may be unreliable. Therefore, the warm period at Kharinei may be the 'Medieval Warm Period' or an earlier warm period with no evidence of the MWP. The expression of the MWP shows considerable spatial heterogeneity with differences in the magnitude and even in the direction of climate change (Bradley *et al.* 2003; Jones and Mann 2004). However a second warm period is apparent in tree-rings from northern Siberia (Naurzbaev and Vaganov 2000; Briffa *et al.* 2002a) ca. 1000 yrs BP which is not apparent at Kharinei.

The intervals of analysed samples in the VORK5 core and sediment focusing in the Lake Kharinei cores means the recent sequences lack the resolution for detailed palaeoenvironmental reconstructions. The most recent samples, from Kharinei (KHAR) and VORK5, show a return to slightly more maritime conditions (CI decreased by -5 to -6) over the last 50 years. The magnitude and rate of decline is consistent with reconstructions from the Putorana (section 7.9) and instrumental records for the Arctic (Hirschi et al. 2007). The stable isotope and sedimentary analyses, from Kharinei, show a decrease in dry

weight and $\delta^{13}\text{C}$, over the past 600 years, whilst TOC increased which may indicate an increase in productivity.

Comparison of CI-C reconstructions and GISP2 K^+ record

The GISP2 K^+ record and CI-C reconstructions from NEER indicate a period of instability between 11000 – 7500 cal yrs BP. Some, but not all, periods with a strong Siberian High coincide with more continental reconstructions (Figure 8.30). The discrepancies may partially result from the wide errors associated with dating material ($\pm 200 - 300$ years, Table 8.6). The increased strength of the Siberian High at ca. 5500 cal yrs BP is suggested by fluctuations in CI-T and CI-C in VORK5. Its apparent absence from the Kharinei record may reflect the low sampling resolution in this section of the sequence. CI-C reconstructions are more continental ca. 3000 cal yrs BP during a period of strong Siberian High, although the strong phase is longer in the CI-C record. The brief positive excursion at 3000 cal yrs in the WA-PLS values is not present in the WA reconstruction (Figure 8.26). The phase of strong Siberian High over the last 1000 years with recent decline is apparent in both the KHAR and VORK5 records. The coherence of CI-C with the GISP2 record and other records of continentality previously discussed suggests CI-C is able to reconstruct trends in continentality but is less sensitive in NEER than the Putorana. CI-C reconstructions from the Putorana track decadal-scale fluctuations in the GISP K^+ record (Figure 7.28). The Putorana sites lie close to the boundary between maritime, Atlantic-influenced and continental, Siberian-High influenced climate zones while the NEER lakes are centrally located in the Atlantic-influenced zone and continentality is relatively stable over vast distances (see Chapter 2).

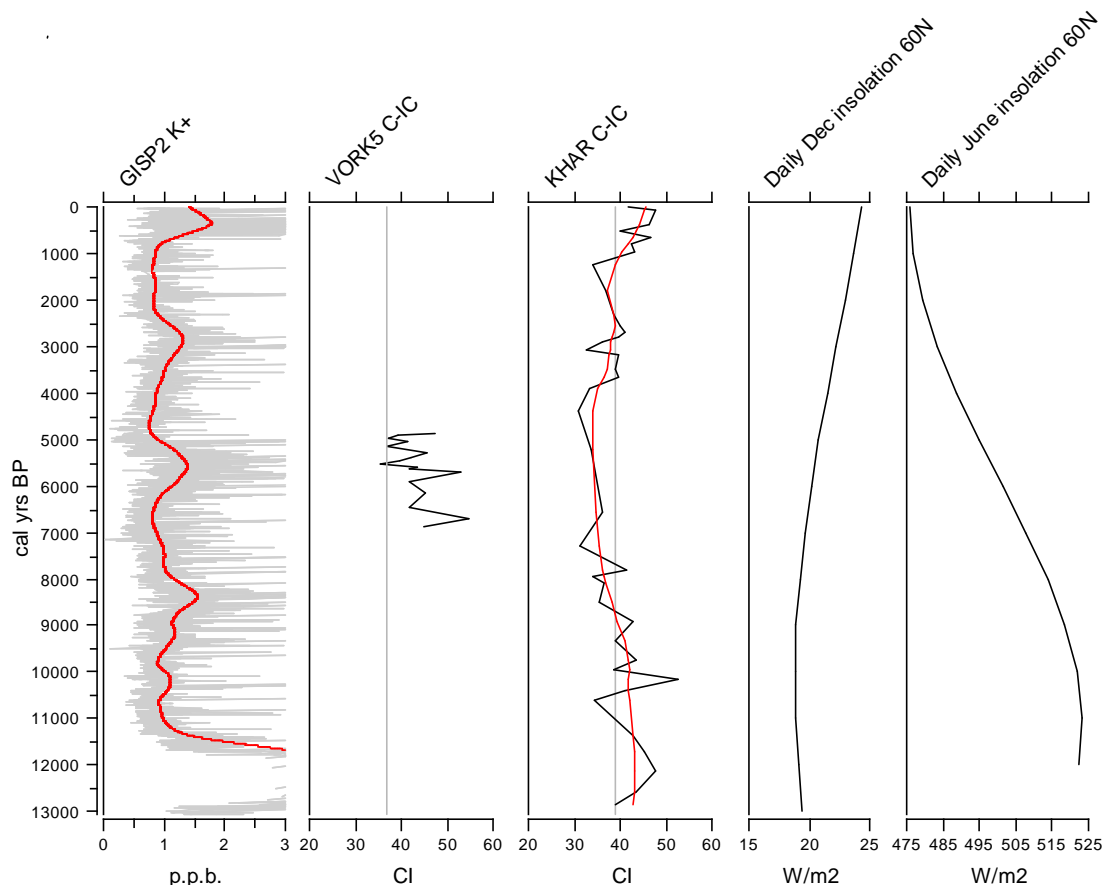


Figure 8.30. Comparison of chironomid-inferred continentality from KHAR and VORK5 with GISP2 K^+ record and solar insolation at 60°N (Berger and Loutre 1991) over the past 13000 years. K^+ is a proxy for the strength of the Siberian High with increased values indicating a stronger Siberian High (Meeker and Mayewski 2002; Mayewski *et al.* 2004). CI-C based on WA-PLS 2 component model, Kharinei record fitted with 0.25 span LOWESS smoother. GISP2 record fitted with LOWESS smoother (span 0.075), ion chemistry data obtained from:

<ftp://ftp.ncdc.noaa.gov/pub/data/paleo/icecore/greenland/summit/gisp2/chem/ionb.txt>

Comparison of CI-C reconstructions and solar insolation at 60°N

CI-C reconstructions, from Kharinei, also appear to be sensitive to solar insolation. Insolation is a measure of the intensity of incoming solar radiation at the top of Earth's atmosphere which is determined by total amount of radiation emitted by the sun and variations in the eccentricity, axial tilt and precession of Earth's orbit (the Milankovitch cycles) (see section 1.2). CI-C reconstructions are most continental from 12000 – 8000 years ago (Figure 8.30), when northern summers occurred at the perihelion resulting in warmer summers and colder winters than present (Berger and Loutre 1991). Between 12000 – 6000 yrs BP

CI-C, at Kharinei, gradually declines as expected from the decreasing June insolation and increasing December insolation trends at 60°N (Berger and Loutre 1991). However from the mid-Holocene CI-C at Kharinei increases whilst the difference between the June and December insolation records continues to decline. Reconstructed T_{july} at Kharinei start to decline from 6000 cal yrs BP and reach the lowest Holocene values ca. 4500 cal yrs BP. The discrepancy between trends predicted by the solar insolation records and CI-C from 6000 cal yrs BP may reflect positive feedback from increasing sea ice, snow/ice-albedo or vegetation changes. During the early Holocene and HTM, when sea ice volume is low and declining, changes in CI-C and CI-T occur concurrently as T_{july} decreases, continentality decreases, and visa versa. But in the late Holocene, as Arctic sea-ice cover increases, (Koç and Jansen 1994) this synchronicity breaks down and T_{july} remains relatively stable while continentality increases. This supports the role of a positive feedback, possibly via the melting enthalpy mechanism proposed by Hirschi, however higher resolution studies would be needed to establish a direct causal relationship.

8.11. Summary

- Sediment cores, or partial sequences, were collected from four lakes in north-east European Russia (NEER); three lakes were located within the tundra vegetation zone and one in the forest – taiga zone.
- The sequence from the forest lake (Lake Sandivei, SAND) showed that significant changes in hydrology had occurred within the catchment; the lake had formerly been a peat bog and, so, was unsuitable for palaeolimnological analysis.
- Cores from Lake Kharinei (KHAR) and an un-named lake (code VORK5) were selected for detailed analysis. Lake Kharinei had a complete Late Quaternary – Holocene sequence and VORK5 a mid-Holocene sequence with higher temporal resolution than KHAR for this period.
- The chironomid subfossil assemblages from these lakes (KHAR and VORK5) are taxon-rich and show marked changes in faunal composition over the sequence suggesting the chironomids are responding to environmental change.

- The initiation of sediment accumulation at Lake Kharinei ca. 13000 cal yrs BP coincides with enhanced melting of the permafrost and formation of other lakes within NEER.
- CI-T and CI-C reconstructions suggest the climate in NEER during the Younger Dryas (YD) was ca. 3°C warmer and more continental than present. Although viewed as a cold interval from European records, the inferred warm climate is consistent with other areas of the Arctic which show considerable spatial heterogeneity in climate at this time.
- The early Holocene sequence (11500 – 10000 cal yrs BP), at Kharinei, is characterised by variability in T_{july} and continentality and a shift to cold-adapted chironomid species although T_{july} , in general, remained higher than present. The climate variability may be associated with changes in atmospheric circulation.
- T_{july} remained higher than present-day between 10000 – 6000 cal yrs BP, however the reconstructions do not show a distinct thermal maximum, the Holocene Thermal Maximum, and the magnitude of the T_{july} increase is less than that observed in European or other northern Russian records.
- Changes in the faunal assemblages at Kharinei suggest the lake became deeper between 10000 – 6000 cal yrs BP. The apparent insensitivity of the CI-T reconstruction at this time may reflect the high abundances of taxa not included in the training set, underestimation by the chironomid model or a reduction in thermal response as the chironomids responded to increasing water depth.
- Between 6000 – 4000 cal yrs BP T_{july} declined to present-day values and the climate became more maritime at Kharinei and VORK5. The decline in T_{july} is consistent with other proxy records from northern Russia. Changes in the faunal assemblages at Kharinei suggest water depth was declining.
- From ca. 4000 cal yrs BP T_{july} remained stable, but continentality increased so reducing the length of the ice-free period. The inflow of terrestrial carbon to Lake Kharinei was low, lake productivity declined and the chironomid assemblages show an increase in the rate of compositional change. The cool phase was interrupted by a warm interval ca. 1800 yrs BP.

- The sequences lack the resolution for detailed reconstructions of recent climate variability. However both KHAR and VORK5 show a decrease in continentality over the past 50 years.
- The GISP2 K⁺ record is a proxy for the strength of the Siberian High pressure system, a component of atmospheric circulation. In general, periods of a strong Siberian High, during the Holocene, show a positive relationship to CI-C.
- CI-C trends track change in insolation over the late Quaternary – mid Holocene. From the mid Holocene CI-C increases whilst insolation records suggest it should have become more maritime. The discrepancy may reflect positive feedback from increasing ice and snow or vegetation changes.

Chapter 9

Conclusions

9.1. Introduction

The main aims of the research (as detailed in section 1.6) were firstly to investigate the environmental variables influencing the modern distribution of chironomids in lakes from northern Russia and assess the suitability of the key climate variables for the development of inference models. Then secondly to apply the inference models to provide high resolution, quantitative reconstructions of climate, over the Holocene, from two sites in northern Russia showing differing trends in recent warming and so, enable the relative influence of hemispheric versus local climate drivers to be assessed. Additionally, the role of climate and other environmental variables on chironomid faunal changes could also be assessed by examining the biotic response of chironomids to environmental change over the Holocene.

The aim of this chapter is to evaluate the research in this thesis, to examine the performance of the inference models and summarise the main findings of the research within the context of current palaeoenvironmental research. Further work is then suggested designed to address issues or answer questions that have arisen from the research undertaken in this thesis.

9.2. Evaluation of the inference models

Chapters 4 and 5 examined the modern chironomid assemblages in northern Eurasia and the factors influencing their distribution. Multivariate analysis showed July air temperature was the principal environmental variable determining the occurrence and abundance of chironomids. Modelling responses to July air temperature and continentality, using HOF models, indicated that 90.6% of taxa had a statistically significant response to July air temperature and 82% to continentality, quantified as the Gorczynski continentality index (CI) (Gorczynski 1920).

The relationship between the occurrence and abundance of chironomids and mean July air temperature, and between the occurrence and abundance of chironomids and continentality, enabled inference models to be developed to reconstruct these variables (Chapter 6). The use of chironomid-inferred temperature (CI-T) models is well established (Brooks 2006a; Heiri 2006) and the performance of the CI-T model developed in this thesis is comparable to published models, in terms of RMSEP, r^2 and maximum bias (Table 6.11). However the development of the chironomid-inferred continentality (CI-C) model represents a novel approach to palaeoenvironmental reconstructions. Inferred values from the CI-T and CI-C models show close agreement with present-day values and instrumental records (sections 7.7.2 and 7.8.2) and the inferred values are consistent with published reconstructions using chironomids and other climate proxies (sections 7.9 and 8.10).

In previous reconstructions of chironomid-inferred temperatures from lakes in arctic Russia, mean July air temperatures were inferred using either a Swedish inference model (Larocque *et al.* 2001) or a Norwegian inference model (Brooks and Birks 2001) with the training set supplemented by data from additional lakes in the Pechora region (Solovieva *et al.* 2005). A number of taxa which frequently occur in subfossil assemblages, from arctic Russian lakes, are absent from the training sets. For example, *Constempellina* is absent from both training sets and *Paracladius* from the Swedish training set. *Constempellina* was originally recorded in the Swedish data (Larocque *et al.* 2001) but was later revised to *Stempellinella/Zavrelia* (Andreev *et al.* 2005). *Constempellina* was recorded in subfossil assemblages from both lakes in NEER (maximum abundance 14%) and PONE from the Putorana Plateau (maximum abundance 5.5%) and *Paracladius* was ubiquitous (maximum abundance 19.5%). These are cold-adapted taxa and therefore their absence from the training sets could lead to overestimations of July temperatures in samples where these taxa form a major component (for example see Andreev *et al.* 2005). The training sets compiled in this thesis also improve the representation of taxa, such as *Corynocera oliveri*-type, which often form a major component of the Russian subfossil assemblages. *Corynocera oliveri*-type occurred in approximately 95% of the subfossil assemblages from the Putorana lakes. In the training sets C.

oliveri-type occurred in 10 of the 153 Norwegian lakes, where it was rare in all but one lake, and 20 of the 81 Russian lakes. Therefore, the temperature optima derived for the taxon based on the Russian data, and hence the inferred temperatures, are likely to be more accurate than those estimated from the Norwegian data.

WA-PLS derived temperature optima (Chapter 6) and GLM/GAM response curves (Chapter 5) indicate that the T_{july} optimum for individual taxa is generally higher in the Russian training set than the Norwegian. In many taxa, the probability of occurrence, for a given July temperature, also increases or decreases along the continentality gradient (section 5.3.3). This suggests that, in general, inference models may be specific to a narrow continentality range and should not be applied in other geographical regions which have markedly different continentality or climate regimes. Similarly, combining the datasets to form a Norwegian-Russian training set would result in the derivation of erroneous temperature optima and inaccurate T_{july} reconstructions (section 7.7.1). Therefore, the application of the Russian inference model would be more appropriate than the Norwegian model or a combined Norwegian-Russian model for chironomid sequences from Russian lakes. The inclusion of taxa common in Russian subfossil assemblages and the revision of the temperature optima suggest the inference models developed in this thesis represent a significant improvement over existing models for the reconstruction of mean July air temperatures from high-latitude Russian lakes.

The degree of continentality, a quantification of its seasonality, is a fundamental property of climate but is less easy to interpret than a simple temperature value. CI is strongly, negatively, correlated to total number of days per year with air temperatures above 0°C and to the longest continuous period per year with air temperatures above 0°C (section 6.7). Reconstructions from the Putorana and NEER show a coherent relationship between CI and the strength of the Siberian High, based on the GISP2 K^+ record, and between CI and solar insolation (sections 7.9 and 8.10). Although the duration of the ice-free period is primarily dependent on air temperatures, and therefore the period above 0°C, the relationship with CI needs to be established by validation with field data. The

ice-free period of individual lakes is also influenced by localised or internal factors such as wind strength, lake area, lake aspect, catchment topography, water depth and profile. Some of these environmental variables have been used to produce simple models of the duration of the lake ice cover (for example Håkanson and Boulion 2001) and application of these models could be used to validate the chironomid inferences.

Chironomid-inferred continentality values are generally higher (i.e. more continental) from PONE than PTHE (Figure 7.22) which suggests that PONE may have a shorter ice-free season. PTHE is at higher altitude and experiences colder air temperatures, but has a more open aspect than PONE which is situated in a SW-NE trending valley. The greater wind shear or more direct sunlight in early spring at PTHE may lead to earlier break up of lake ice. However the influence of the local physical environment on CI-C suggests trends in inferred continentality, compared to the present-day, are probably more reliable than absolute values. Although calculated from T_{july} , trends in CI-T and CI-C have diverged, particularly over the last 100 years (section 7.9), suggesting the inferred continentality is, at least partially, independent of T_{july} .

The CI-C reconstructions (Chapter 7 and 8) suggest the Putorana lakes may be more sensitive to changes in continentality than those in NEER. Approximately 550 – 500 cal yrs BP the CI declined by 15 at PTHE, in the Putorana Plateau, and by 2 at Lake Kharinei, in NEER, although the lower resolution of the Kharinei records means the CI minima may have been missed as the rates and magnitude of continentality changes over the last 50 years are similar. The Putorana sites lie close to the boundary between maritime-influenced Atlantic subarctic and the continental Siberian subarctic, while the NEER lakes are centrally located within the Atlantic-influenced zone (see Chapter 2). Therefore, the Putorana Plateau may be more sensitive to changes in atmospheric or oceanic circulation affecting the relative strength of the Icelandic Low and Siberian pressure systems and amelioration by warm oceanic currents. To establish its sensitivity, the CI-C inference model needs to be applied to additional subfossil sequences from cores collected close to the boundaries of

climate zones, to compare with the magnitude of the response estimated from lakes positioned centrally within climate zones.

The performance statistics, in terms of r^2 , RMSEP and bias, of the CI-C model are poorer than the CI-T model (Chapter 6). Fewer taxa showed a statistically significant response to continentality than T_{july} (section 5.3) and the continentality tolerances of many taxa are wide (Figure 6.13). The distribution of lakes along the continentality gradient is uneven as the lakes were selected primarily for the T_{july} gradient. Inclusion of additional lakes, particularly with CI greater than 30, would improve the estimation of optima and tolerances and so improve the performance of the model.

Using inference models to reconstruct both T_{july} and continentality enhances the explanatory power of the palaeoenvironmental reconstruction and contributes to reconciling apparent differences with other proxy records. For example, chironomid-inferred temperatures from Lake Kharinei, in NEER, suggest July air temperatures in the early Holocene were higher than present-day whereas pollen-inferred summer temperature reconstructions from the same lake estimate summer temperatures (i.e. May – August) as similar to present values (Sakari, unpublished data). However, the CI-C reconstructions indicate the climate was extremely continental at this time. Therefore summers would be relatively short with high maximal temperatures. Based on the modern relationships (section 6.7.1) the higher CI would have reduced the total number of days per year with air temperatures above 0°C by approximately 40 days to 140 days. Therefore T_{july} could be higher than present whilst reconstructions of May – August temperatures remain similar to present values. At other periods, such as 4000 cal yrs BP to present-day, chironomid-inferred temperatures, at Lake Kharinei have remained relatively stable whilst continentality has increased. An increase in continentality would reduce the length of the summer, and consequently increase the duration of lake ice cover. The increase in continentality had a pronounced effect on the lake ecosystem as shown by the CCA axis scores and rates of compositional change (section 8.10). The use of CI-T alone would make interpretation of these trends difficult.

Comparing trends in CI-T and CI-C may help to identify possible driving mechanisms underlying climate change. During the period 1996 to 2005, monthly instrumental temperatures for the Arctic region have been at least 0.5°C warmer than the long-term average (1948-2005) for every month except June, July and August. Over the same period continentality declined by 8% compared to the long-term mean (Hirschi *et al.* 2007). Hirschi *et al.* (2007) suggested the stable summer temperatures with decreasing continentality could be a consequence of increased melting of Arctic sea ice during summer. The melting enthalpy of ice means that large amounts of heat would be extracted from the atmosphere above the sea ice and therefore summer winds from the Arctic Ocean would remain cool, dampening the warming that is seen in other seasons.

9.3. Application of the inference models

Chironomid-inferred temperatures have previously been reconstructed from a number of areas of northern Russia. Due to the absence of a regional training set these reconstructions have either been qualitative (for example Porinchu and Cwynar 2002) or based on the Norwegian or Swedish training sets, in some instances supplemented with local data (see Andreev *et al.* 2005; Solovieva *et al.* 2005). Although a CI-T model has been developed by Nazavora for central Eurasia (Nazarova, unpublished data), the results presented in this thesis represent the first palaeoenvironmental reconstructions using a Russian-based CI-T model and the first attempts to reconstruct continentality using the chironomid fauna.

There has been little published work on the biology or past and present environment of the Putorana Plateau. This research represents the first description of the modern chironomid fauna from this region. Although past temperatures have been reconstructed using diatoms and pollen from lakes on the northern Putorana Plateau (Pavlov *et al.* 2002; Kumke *et al.* 2004), the palaeoenvironmental reconstructions in this study are the first chironomid-inferred reconstructions and extend our knowledge of the temporal and spatial extent of the climate fluctuations, such as the 'Little Ice Age' in this region. Smol *et al.* (2005) compiled data from arctic lakes in Canada, Svalbard,

Fennoscandia and European Russia showing the increases in beta-diversity, the rate of compositional change, of algae and invertebrate communities over the past 150 years. This study extends the coverage of recent trends into central Siberia and shows that the changes in beta-diversity in the Putorana are similar to rates observed in Fennoscandia, Svalbard, Labrador and Quebec. Due to the shortness of the cores collected, complete Holocene sequences were not sampled and the palaeoenvironment reconstructions only extend to the past 650 – 750 years.

Although the palaeoenvironmental history of north-east European Russia has been studied in greater detail (for example Kultti *et al.* 2003; Andreev *et al.* 2005; Solovieva *et al.* 2005) and is better understood than that of the Putorana Plateau, the duration of the sedimentary sequence from Lake Kharinei provided a rare opportunity to study the late glacial – Holocene transition in northern Russia and, in particular, the spatial extent of the Younger Dryas cooling and mid-Holocene warming (HTM) observed in western European records. The combination of chironomid-inferred July temperature and continentality reconstructions demonstrated that changes in continentality, independent of July temperature, may cause rapid and profound changes in faunal composition. As instrumental records show continentality has decreased at high northern latitudes over the last 100 years at an accelerating rate (Hirschi *et al.* 2007), this trend could lead to profound changes in arctic ecosystems.

9.4. Evaluation of the Research

There were a number of difficulties encountered during the research that limited the ability to fulfil the aims and answer the questions detailed in Chapter 1. One of initial aims of the project was to compare palaeoclimatic reconstructions from two areas which showed different trends in climate change over the past 30 years, to allow the extent and persistence of the spatial heterogeneity to be examined. However during the research it proved impossible to obtain complete Holocene sequences from the two locations in arctic Russia. The coring equipment was impounded by customs officials at Moscow airport, during the 2006 fieldtrip, so only short cores could be collected from lakes on the Putorana Plateau. Four long cores were collected from NEER in 2007. However, of the

three radiocarbon-dated cores, only one, from Lake Kharinei, had a complete late Pleistocene – Holocene sequence.

The cores were primarily dated using bulk sediment samples. The radiocarbon dates showed a number of reversals or dates which appeared 'too young' so establishing chronologies was problematic. The ^{210}Pb dating of the Kharinei core showed sediment focusing had reduced the temporal resolution of the recent sequence. The ^{210}Pb dates from the NEER lakes only became available after the chironomid subfossils assemblages had been prepared and analysed. Samples from the Kharinei core, which had poor temporal resolution, were analysed at 1cm intervals whereas samples from VORK5, which ^{210}Pb dating showed had a continuous, high resolution sequence, were analysed at 8cm intervals. The Putorana lakes, therefore, gave a high resolution, 650 – 750 year climate record and the NEER lakes a 13000 year record with the last 650 – 750 years at low temporal resolution. The incompatibility in the resolution of the two palaeoclimate records meant it was not possible to compare recent or Holocene climate changes between the two study sites. Dating of the cores prior to analysing the subfossil assemblages would enable resources to be targeted more effectively, but was not possible within the timescale of the research programme.

Difficulties in establishing reliable chronological frameworks appear to be a common feature of palaeolimnological studies in northern Russia (for example Porinchu and Cwynar 2002; Andreev *et al.* 2005). Dating of bulk sediment may be unreliable due to the contamination by old carbon (Kultti *et al.* 2003). Many of the lowland lakes are underlain by Quaternary deposits derived from Ordovician sedimentary rocks which may act as a source of old carbon (Väliranta *et al.* 2006). Dating of terrestrial macrofossils, in this thesis, gave dates which were typically 1000 – 3000 years older than the associated sediments (section 8.5.2.2) and there were no large fragments of other macrofossils to improve the dating. Therefore, sediment cores from the Putorana lakes, underlain by igneous rocks, may give more reliable chronologies than lakes on poorly consolidated Quaternary deposits.

9.5. Conclusions

The main conclusions of the research are:

1. Mean July air temperature is the most important environmental variable driving the distribution of chironomids on a regional scale, however other factors, such as water depth, influence their occurrence and abundance at a local or site-specific scale. At the macro-scale, continentality (i.e. the difference between summer and winter temperatures) appears to be a significant determinant over wider geographical areas.
2. Chironomids are sensitive enough to reconstruct changes in mean July air temperature and continentality. The reconstructed values and trends for both variables from the Putorana Plateau show close coherence with instrumental records over the past 120 years. For the majority of subfossil assemblages the availability of close analogues within the training sets suggests the ecology of the chironomids has remained constant over the late Quaternary. Therefore the use of the inference models over this time-scale is appropriate.
3. At present, the best choice of statistical method for continentality reconstructions is uncertain. The WA-PLS model underpredicts continentality for lakes with continentality indices above 50. At Lake Kharinei and VORK5, in NEER, the WA-PLS derived continentality indices are closer to the present-day instrumental CI of 37 – 39 than the WA estimates. Whereas in the Putorana lakes, where present-day continentality indices are 52 – 54, reconstructions derived from the WA model showed closer agreement with the instrumental record than the WA-PLS model. The chironomid-inferred continentality records provide reliable trends of past climate change, but not necessarily accurate absolute values which tend to be under-estimated
4. The Russian training set includes a number of taxa which are common in Russian subfossil assemblages but absent or poorly represented in the Norwegian training set. In addition, the temperature optima of individual taxa derived from the Russian training set are generally higher than those from the Norwegian training set so that the Norwegian inference model underestimates T_{july} from Russian assemblages. Therefore the Russian training set K and inference model appears most appropriate for

palaeoclimate reconstructions from subfossil assemblages from north east European Russia - central Siberia.

5. The reconstructions from Lake Kharinei suggest the cooling during the Younger Dryas was probably restricted to the North Atlantic region. In NEER, mean July air temperature appeared approximately 3°C warmer than present but the climate was considerably more continental. The increased continentality may have resulted from the influence of the Fennoscandian Ice Sheet on atmospheric circulation (Bush 2004). A more continental climate would result in more severe winters and supports the suggestion by Giesecke *et al.* (2008) that cooling in Europe, during the Younger Dryas, was restricted primarily to the winter.
6. A cool period, ca. 7900 cal yrs BP, and lasting approximately 600 years may be the regional expression of the 8200 cal yrs BP event which resulted in a cold interval in the North Atlantic region. Higher resolution analysis and improved dating of this section of the core would be required to clarify the timing and duration of the cool period at Lake Kharinei. However this cool interval at Kharinei is evident in CI-T, CI-C and sediment accumulation records which suggest cooling occurred throughout the year. The differing spatial and seasonal response between this cool interval and the Younger Dryas probably reflects the decline of the Fennoscandian Ice Sheets and the reduction of their influence on atmospheric circulation.
7. Climate deterioration from ca. 4000 cal yrs BP, also evident from proxy records from other Russian sites (Kremenetski *et al.* 1998; Lubinski *et al.* 1999; MacDonald *et al.* 2000; Kultti *et al.* 2004), reflects a response to a shorter ice-free or growing season as T_{july} inferred from chironomids remained stable but continentality increased.
8. CI-T reconstructions show a cool period between 600 – 150 years ago, at the Putorana lakes, which is probably equivalent to the 'Little Ice Age' seen in European records (reviewed in Jones and Mann 2004).
9. After a cold interval in the early – mid twentieth century, July air temperatures increased to present-day levels at the Putorana lakes approximately 50 years ago. CI-C declined over the past 100 years with the rate of decline accelerating over the last 50 years.

10. The evidence for recent warming is equivocal; instrumental records and CI-T from PONE on the Putorana Plateau suggest T_{july} temperatures remained relatively stable over the past 30 years whereas CI-T from PTHE increased (section 7.7). In the NEER lakes, the sampling resolution and changes in sedimentation mean only 2 intervals were sampled from the twentieth century. At Kharinei chironomid-inferred July air temperatures increased by 0.9°C over the past 80 years and decreased by 0.9°C at VORK5. However the lakes show a consistent response in the timing and magnitude of decreasing continentality over 50 years for the Putorana lakes and 100-120 years for the NEER lakes (sections 7.9 and 8.10). The decrease in continentality is consistent with instrumental records and may be mediated by the removal of heat from the atmosphere by the melting Arctic sea-ice as proposed by Hirschi *et al.* (2007).
11. During the early Holocene and Holocene Thermal Maximum, when sea ice volumes were low, changes in CI-C and CI-T occurred concurrently but in the late Holocene as Arctic sea-ice cover increases (Koç and Jansen 1994) this synchronicity breaks down. This result supports the melting enthalpy mechanism proposed by Hirschi *et al.* (2007), however higher resolution studies would be needed to establish a direct causal relationship.

9.6. Suggestions for future work

Evaluating the performance of the inference models and the palaeoenvironmental reconstructions, in this thesis, has highlighted a number of issues which require further work.

9.6.1. Expanding the Russian training sets

The collection of additional surface samples and integration of these into the current training sets would enhance the climatic information derived from the application of the inference models to late Quaternary sequences. In particular, the inclusion of data from lakes with present-day mean July air temperatures between $14 - 18^{\circ}\text{C}$ and from lakes with T_{july} of 18°C or higher, from regions other than Yakutia so the effects of continentality and the negative water

balance are reduced, would improve the representation of chironomid taxa and assemblages, and therefore, the reconstruction of temperatures from warm lakes. Above CI of 30, the lakes are clustered in groups with similar T_{july} , for example between CI of 30 – 50 there are no lakes with T_{july} of 8 – 11°C. Improving the distribution of lakes along both gradients may reduce the errors associated with the reconstruction of continentality.

9.6.2. Improving the climate reconstructions for NEER

As discussed in section 9.4, delays in establishing chronologies for the lakes in NEER meant the recent climate record was reconstructed at low temporal resolution (2-3 samples per core for the past 150 years). From the ^{210}Pb dating, the top of VORK5 appears to have a complete recent sequence at high temporal resolution. Analysis of this sequence would enable recent trends in NEER and the Putorana to be compared. These sampling areas were selected as satellite records showed different trends in climate change over the past 30 years (Comiso 2003). Comparing the records between the two areas would allow the extent and persistence of the spatial heterogeneity to be examined, so that the relative influence of hemispheric versus local climate drivers could be assessed (Chapter 1). At present, some of the initial research questions from Chapter 1 cannot be answered; comparison of recent climate records from NEER and the Putorana would help answer these questions. Higher sampling resolution of the Kharinei sequence would also produce a more detailed palaeoclimate record. This would help constrain the timing and duration of major climate fluctuations detected in the current record, such as the 8200 yrs BP event and the Holocene Thermal Maximum.

9.6.3. Testing the sensitivity of the chironomid-inferred continentality (CI-C) model

As the application of a chironomid-inferred continentality transfer function represents a novel approach, the sensitivity and limitations of the method need to be assessed to determine whether the results are reliable and accurate, if the model can be applied to locations throughout north-west Eurasia and whether the reconstructions are of value in understanding the mechanisms driving compositional changes in the chironomid subfossil records. In the CI-C

reconstruction from Lake Kharinej, all the fluctuations in continentality lie within the range of the sample specific errors of the individual samples (Figure 9.28). This is probably due to the broad tolerances of the individual taxon (Figure 6.14) which may result from poor representation in the training set or a lack of sensitivity by the chironomids i.e. most taxa tolerate a wide range of continentality indices. Expanding the training set (section 9.7.1) would address the former issue. The sensitivity of the chironomids to continentality could be assessed by comparing CI-C reconstructions from cores at multiple sites within a limited geographic region, over the same time frame.

The magnitude of the CI changes from the Putorana Plateau over the past 750 years (section 7.8) appears greater than the changes from Lake Kharinej, in NEER, over the Holocene (section 8.9). The apparent greater sensitivity of the Putorana fauna may result from the proximity of the Plateau to the boundary between climate zones (section 2.5). To assess the affect of geographic location on CI-C reconstructions, continentality should be reconstructed from sequences collected from lakes in regions where continentality changes rapidly with longitude and in regions where continentality is stable over long distances. For example, continentality changes rapidly with longitude in western Europe so subfossil assemblages, from this region, should be sensitive to changes in continentality. Applying the CI-C model to reconstruct continentality in late Pleistocene - Holocene sequences from western Europe may show a greater magnitude of continentality change than chironomid-inferred continentality reconstructions from late Pleistocene – Holocene sequences from arctic Siberia where continentality is stable over long distances. Although the magnitude, timing and spatial expression of continentality may be heterogeneous between the regions, major trends such as insolation-driven declines in continentality over the early to mid-Holocene should be consistent between locations of similar latitude.

9.6.4. Modelling chironomid responses to variation in the length of the ice-free period

The results presented in this thesis (Chapters 4 and 5) suggest chironomid distribution is strongly influenced by continentality. Chironomids in arctic

environments generally overwinter in diapause or a dormant state in frozen lakes where water temperatures remain at or above 0°C. Therefore it is unlikely they directly respond to the difference between summer and winter temperatures, used in the continentality indices. It is more likely they are responding to variations in the length of the ice-free period which is negatively correlated to continentality. Therefore it should be possible to develop a chironomid-lake ice cover inference model. Observational data of the duration of lake ice-free period is available for some of the Norwegian lakes used in the training set (Clarke 2004) although not for the Russian lakes. However the use of simple mathematical models (Håkanson and Boulion 2001) could allow the ice-free period to be quantified for the training set lakes. A chironomid-inferred lake ice cover model is probably ecologically more appropriate and easier to understand than the CI-C model. And, if the chironomid taxa have a stronger relationship to the length of the ice-free period than the difference between summer and winter temperatures, this should enhance the performance of the model and the accuracy of the palaeoenvironmental reconstructions.

9.6.5. Integration into multiproxy studies

The results presented in this thesis are part of wider multiproxy studies undertaken by colleagues in the EU-funded project Carbo-North. Diatoms have been identified and counted in sediment samples from the Putorana lakes PONE and PTHE and pollen, plant macrofossils, diatoms and plant pigments in sediment samples from Lake Kharinei and VORK5 in NEER. Integrating the results presented in this thesis with data from the various proxies should give a clearer understanding of the internal and external factors driving compositional change within the lakes but is beyond the scope of this thesis. For example, the decline in ^{15}N over the past 250 years, in the Putorana lakes (section 7.5) suggests nitrogen is primarily derived from atmospheric sources. The diatom assemblages suggest pH has not changed significantly over this period. Therefore the major compositional changes observed in chironomids and diatoms assemblages from the Putorana lakes over the past 150 years are not mediated by lake acidification. This lends support to the conclusions presented in this thesis that the chironomids are responding to changes in climate.

References

- Aagaard K. 1982. Profundal chironomid populations during a fertilization experiment in Langvatn, Norway. *Holarctic Ecology* 5: 325-313.
- ACIA 2004. Impacts of a warming Arctic: Arctic Climate Impact Assessment. Cambridge University Press, Cambridge, 140 pp.
- ACIA 2005. Arctic Climate Impact Assessment. Cambridge University Press, Cambridge, 1042 pp.
- Aleksandrova V.D. 1980. Arctic and Antarctic: Their division into geobotanical areas. Cambridge University Press, Cambridge, 247 pp.
- Alisov B.P. 1956. *Klimat SSSR (Climate of the USSR)*. Moscow State University Press, Moscow, 127 pp.
- Alley R., Mayewski P.A., Sowers T., Stuiver M., Taylor K.C. and Clark P.U. 1997. Holocene climate instability: a prominent widespread event 8200 yr ago. *Geology* 25: 483-486.
- Alley R. 2000. Younger Dryas cold interval as viewed from central Greenland. *Quaternary Science Reviews* 19: 213-226.
- Alley R.B. and Agustsdottir A.M. 2005. The 8k event: cause and consequences of a major Holocene abrupt climate change. *Quaternary Science Reviews* 24: 1123-1149.
- Andersen F.S. 1938. Späglaziale Chironomiden. *Meddelelser Dansk Geologisk Forening* 9: 320-326.
- Andreev A., Siegert C., Klimanov V., Derevyagin A., Shilova G.N. and Melles M. 2002. Late Pleistocene and Holocene vegetation and climate on the Taymyr Lowland, Northern Siberia. *Quaternary Research* 57: 138-150.
- Andreev A., Tarasov P., Klimanov V., Melles M., Lisitsyna O.M. and Hubberten H.-W. 2004a. Vegetation and climate change around the Lama Lake, Taymyr Peninsula, Russia during the Late Pleistocene and Holocene. *Quaternary International* 122: 69-84.
- Andreev A., Tarasov P., Schwamborn G., Ilyashuk B., Ilyashuk E., Bobrov A., Klimanov V., Rachold V. and Hubberten H.-W. 2004b. Holocene paleoenvironmental records from Nikolay Lake, Lena River Delta, Arctic Russia. *Palaeogeography, Palaeoclimatology, Palaeoecology* 209: 197-217.

- Andreev A., Tarasov P., Ilyashuk B., Ilyashuk E., Cremer H., Hermichen W.-D., Wischer F. and Hubberten H.-W. 2005. Holocene environmental history recorded in Lake Lyadhej-To sediments, Polar Urals, Russia. *Palaeogeography, Palaeoclimatology, Palaeoecology* 223: 181-203.
- Andres R.J., Marland G., Boden T. and Bischof S. 2000. Carbon dioxide emissions from fossil fuel consumption and cement manufacture, 1751-1991, and an estimate of their isotopic composition and latitudinal distribution. In: T. M. L. Wigley and D. S. Schimel (eds.), *The Carbon Cycle*. Cambridge University Press, Cambridge, pp. 53-62.
- Anon 1955. Vorkuta., *Time Magazine*,
<http://www.time.com/time/magazine/article/0,9171,861142,00.html>.
- Antonsson K., Brooks S.J., Seppä H., Telford R.J. and Birks H.J.B. 2006. Quantitative palaeotemperature records inferred from fossil pollen and chironomid assemblages from Lake Giltjärnen, northern central Sweden. *Journal of Quaternary Science* 21: 831-841.
- Appleby P. and Oldfield F. 1978. The calculation of ^{210}Pb dates assuming a constant rate of supply of unsupported ^{210}Pb to the sediment. *Catena* 5: 1-8.
- Appleby P.G. 2001. Chronostratigraphic techniques in recent sediments. In: W. M. Last and J. P. Smol (eds.), *Tracking environmental change using lake sediments*. Kluwer Academic Publishers, Dordrecht, The Netherlands, pp. 171-203.
- Appleby P.G. 2004. Environmental change and atmospheric contamination on Svalbard: sediment chronology. *Journal of Paleolimnology* 31: 433-443.
- Are F. and Reimnitz E. 2000. An overview of the Lena River Delta setting: Geology, tectonics, geomorphology and hydrology. *Journal of Coastal Research* 16: 1083-1093.
- Armitage P., Cranston P.S. and Pinder L.C.V. 1995. *The Chironomidae: the biology and ecology of non-biting midges*. Chapman and Hall, London, 572 pp.
- Arnell N.W. 2005. Implications of climate change for freshwater inflows to the Arctic Ocean. *Journal of Geophysical Research - atmospheres* 110: D07105.

- Bakke J., Dahl S.O., Paasche Ø., Løvlie R. and Nesje A. 2005. Glacier fluctuations, equilibrium-line altitudes and palaeoclimate in Lyngen, northern Norway, during the Late glacial and Holocene. *The Holocene* 15: 518-540.
- Barber K.E. and Charman D.J. 2003. Holocene palaeoclimate records from peatlands. In: A. MacKay, R. W. Battarbee, H. J. B. Birks and F. Oldfield (eds.), *Global change in the Holocene*. Hodder Arnold, London, pp. 210-226.
- Battarbee R.W., Jones V.J., Flower R.J., Cameron N.G., Bennion H., Carvalho L. and Juggins S. 2001. *Diatoms*. Kluwer Academic Publishers, Dordrecht, 155-202 pp.
- Battarbee R.W. and Binney H.A. 2008. *Natural climate variability and global warming: a Holocene perspective*. Wiley-Blackwell Chichester, West Sussex, 276 pp.
- Beer J. and Van Geel B. 2008. Holocene climate change and the evidence for solar and other forcing. In: R. W. Battarbee and H. A. Binney (eds.), *Natural climate variability and global warming: A Holocene perspective*. Wiley-Blackwell, Chichester, West Sussex, pp. 138-162.
- Bennett K.D. 1996. Determination of the number of zones in a biostratigraphical sequence. *New Phytologist* 132: 155-170.
- Bennion H. 1994. A diatom-phosphorus transfer function for shallow, eutrophic ponds in southeast England. *Hydrobiologia* 275/276: 391-410.
- Berger A. and Loutre M.F. 1991. Insolation values for the climate of the last 10 Ma. *Quaternary Science Reviews* 10: 297-317.
- Bezmaternyh D.M. 2001. List of chironomid species of two rivers of Upper Ob River basin (Barnaulka and Bolshaya Cheremshanka). In: E. A. Makarchenko (ed.), *The Russian chironomid home page*. <http://www.biosoil.ru/tendipes/catalog.htm>, p. Catalogues and checklists.
- Bezmaternyh D.M. and Nazarova L. 2006. Catalogues and checklists. In: E. A. Makarchenko and A. Voronkov (eds.), *The Russian chironomid home page*. <http://www.biosoil.ru/tendipes/catalog.htm>.
- Bianchi G.G. and McCave I.N. 1999. Holocene periodicity in North Atlantic climate and deep-ocean flow south of Iceland. *Nature* 397: 515-518.

- Bigler C. and Hall R.I. 2003. Diatoms as quantitative indicators of July temperature: a validation attempt at century-scale with meteorological data from northern Sweden. *Palaeogeography Palaeoclimatology Palaeoecology* 189: 147-160.
- Bigler C., Heiri O., Krskova R., Lotter A.F. and Sturm M. 2006. Distribution of diatoms, chironomids and cladocera in surface sediments of thirty mountain lakes in south-eastern Switzerland. *Aquatic Science* 68: 154-171.
- Birks H.H. and Ammann B. 2000. Two terrestrial records of rapid climatic change during the glacial–Holocene transition (14,000–9,000 calendar years B.P.) from Europe. *Proceedings of the National Academy of Sciences of the United States of America* 97: 1390-1394.
- Birks H.H. and Birks H.J.B. 2003. Reconstructing Holocene climates from pollen and plant macrofossils. In: A. MacKay, R. W. Battarbee, H. J. B. Birks and F. Oldfield (eds.), *Global change in the Holocene*. Hodder Arnold, London, pp. 342-357.
- Birks H.J.B. 1981. The use of pollen analysis in the reconstruction of past climates: a review. In: T. M. L. Wigley, M. J. Ingram and G. Farmer (eds.), *Climate and history*. Cambridge University Press, Cambridge pp. 111-138.
- Birks H.J.B. and Gordon A.D. 1985. *Numerical methods in Quaternary pollen analysis*. Academic Press, London, 289 pp.
- Birks H.J.B., Line J.M., Juggins S., Stevenson A.C. and ter Braak C.J.F. 1990. Diatoms and pH reconstruction. *Philosophical Transactions of the Royal Society of London: B* 327: 263-2788.
- Birks H.J.B. 1995. Quantitative palaeoenvironmental reconstructions. In: D. Maddy and J. S. Brew (eds.), *Statistical Modelling of Quaternary Science Data*. Quaternary Research association., Cambridge, pp. 161-254.
- Birks H.J.B. 1998. Numerical tools in palaeolimnology - progress, potentialities and problems. *Journal of Paleolimnology* 20: 307-332.
- Birks H.J.B. 2003. Quantitative palaeoenvironmental reconstructions from Holocene biological data. In: A. MacKay, R. W. Battarbee, H. J. B. Birks and F. Oldfield (eds.), *Global change in the Holocene*. Hodder Arnold, London, pp. 107-123.

- Birks H.J.B. and Birks H.H. 2004. Quaternary palaeoecology. The Blackburn Press, Caldwell, New Jersey, 289 pp.
- Birks H.J.B., Monteith D.T., Rose N.L., Jones V.J. and Peglar S.M. 2004. Recent environmental change and atmospheric contamination on Svalbard as recorded in lake sediments - modern limnology, vegetation and deposition. *Journal of Paleolimnology* 31: 411-431.
- Birks H.J.B. and Birks H.H. 2006. Multi-proxy studies in palaeolimnology. *Vegetation History and Archaeobotany* 15: 235-251.
- Birks H.J.B. and Simpson G.L. 2006. Numerical analyses of biological and environmental data., Short course. Environmental Change Research Centre, UCL.
- Birks H.J.B. 2007. Estimating the amount of compositional change in late-Quaternary pollen-stratigraphical data. *Vegetation History and Archaeobotany* 16: 197-202.
- Blockley S.P.E., Lowe J.J., Walker J.C., Asioli A., Trincardi F., Coope G.R., Donahue R.E. and Pollard A.M. 2004. Bayesian analysis of radiocarbon chronologies: examples from the European Late-glacial. *Journal of Quaternary Science* 19: 159-175.
- Boyle J.F. 2001. Inorganic geochemical methods in palaeolimnology. In: W. Last and J. P. Smol (eds.), *Tracking environmental change using lake sediments*. Kluwer Academic Publishers, Dordrecht, the Netherlands, pp. 83-143.
- Bradley R.S., Hughes M.K. and Diaz H.F. 2003. Climate in Medieval time. *Science* 302: 404-405.
- Bradshaw W.E. 1976. Geography of photoperiod response in a diapausing mosquito. *Nature* 262: 384-385.
- Bradshaw W.E. and Holzapfel C.M. 2001. Genetic shift in photoperiodic response correlated with global warming. *Proceedings of the National Academy of Sciences of the United States of America* 98: 14509-14511.
- Briffa K.R., Osborn T., Schweingruber F.H., Jones P.D., Shiyatov S. and Vaganov E.A. 2002a. Tree-ring width and density data around the Northern Hemisphere: Part 2, spatio-temporal variability and associated climate patterns. *The Holocene* 12: 759-789.

- Briffa K.R., Osborn T., Schweingruber F.H., Jones P.D., Shiyatov S. and Vaganov E.A. 2002b. Tree-ring width and density data around the Northern Hemisphere: Part 1, local and regional climate signals. *The Holocene* 12: 737-757.
- Brodersen K.A. and Lindegaard C. 1999a. Classification, assessment and trophic reconstruction of Danish lakes using chironomids. *Freshwater Biology* 42: 143-157.
- Brodersen K.P. and Lindegaard C. 1999b. Mass occurrence and sporadic distribution of *Corynocera ambigua* Zetterstedt (Diptera, Chironomidae) in Danish lakes. Neo- and palaeolimnological records. *Journal of Paleolimnology* 22: 41-52.
- Brodersen K.P. and Anderson N.J. 2000. Subfossil insect remains (Chironomidae) and lake-water temperature inference in the Sisimuit-Kangerlussuaq region, southern West Greenland. *Geology of Greenland Survey Bulletin* 186: 78-82.
- Brodersen K.P., Odgaard B.V., Vestergaard O. and Anderson N.J. 2001. Chironomid stratigraphy in the shallow and eutrophic Lake Sobygaard, Denmark: chironomid-macrophyte co-occurrence. *Freshwater Biology* 46: 253-267.
- Brodersen K.P., Pedersen O., Lindegaard C. and Hamburger K. 2004. Chironomids (Diptera) and oxy-regulatory capacity: An experimental approach to paleolimnological interpretation. *Limnology and Oceanography* 49: 1549-1559.
- Brodersen K.P. and Quinlan R. 2006. Midges as palaeoindicators of lake productivity, eutrophication and hypolimnetic oxygen. *Quaternary Science Reviews* 25: 1995-2012.
- Brodin Y.W. 1986. The postglacial history of Lake Flarken, southern Sweden, interpreted from subfossil insect remains. *Internationale Revue der Gesamten Hydrobiologie* 71: 371-432.
- Broecker W. and Denton G.H. 1989. The role of ocean-atmosphere reorganisations in glacial cycles. *Geochimica et Cosmochimica Acta* 53: 2465-2501.
- Broecker W.S. 1987. Unpleasant surprises in the greenhouse? *Nature* 328: 123-126.

- Bronk Ramsey C. 1995. Radiocarbon calibration and analysis of stratigraphy: The OxCal program. *Radiocarbon* 37: 425-430.
- Bronk Ramsey C. 2001. Development of the radiocarbon calibration program OxCal. *Radiocarbon* 43: 355-363.
- Bronk Ramsey C. 2008. Deposition models for chronological records. *Quaternary Science Reviews* 27: 42-60.
- Brooks S.J., Mayle F.E. and Lowe J.J. 1997. Chironomid-based Late-glacial climatic reconstruction for southeast Scotland. *Journal of Quaternary Science* 12: 161-167.
- Brooks S.J. and Birks H.J.B. 2000a. Chironomid-inferred late-glacial and early-Holocene mean July air temperatures for Kråkenes Lake, western Norway. *Journal of Paleolimnology*: 23: 77-89.
- Brooks S.J. and Birks H.J.B. 2000b. Chironomid-inferred late-glacial air temperatures at Whitrig Bog, southeast Scotland. *Journal of Quaternary Science* 15: 759-764.
- Brooks S.J., Bennion H. and Birks H.J.B. 2001. Tracing lake trophic history with a chironomid-total phosphorus inference model. *Freshwater Biology* 46: 513-533.
- Brooks S.J. and Birks H.J.B. 2001. Chironomid-inferred air temperatures from Late-glacial and Holocene sites in north-west Europe: progress and problems. *Quaternary Science Reviews* 20: 1723-1741.
- Brooks S.J. and Birks H.J.B. 2004. The dynamics of Chironomidae (Insecta: Diptera) assemblages in response to environmental change during the past 700 years on Svalbard. *Journal of Paleolimnology* 31: 483-498.
- Brooks S.J., Udachin V. and Williamson B.J. 2005. Impact of copper smelting on lakes in the southern Ural Mountains, Russia, inferred from chironomids. *Journal of Paleolimnology* 33: 229-241.
- Brooks S.J. 2006a. Chironomid records: Late Pleistocene of Europe. In: S. A. Elias (ed.), *Encyclopedia of Quaternary Science*. Elsevier Science, pp. 377-390.
- Brooks S.J. 2006b. Fossil midges (Diptera: Chironomidae) as palaeoclimatic indicators for the Eurasian region. *Quaternary Science Reviews* 25: 1894-1910.

- Brooks S.J., Langdon P.G. and Heiri O. 2007. The identification and use of Palaeartic Chironomidae larvae in palaeoecology. Quaternary Research Association, London, 276 pp.
- Brundin L. 1949. Chironomiden und andere Bodentiere der südschwedischen Urgebirgseen. Ein Beitrag zur Kenntnis der bodenfaunistischen Charakterzüge schwedischer oligotropher Seen. Report of the Institute of Freshwater Research, Drottningholm, pp. 1-914.
- Brundin L. 1956. Zur Systematik der Orthoclaadiinae (Dipt., Chironomidae). Report of the Institute of Freshwater Research, Drottningholm, pp. 5-185.
- Brundin L. 1958. The bottom faunistic lake type system and its application to the southern hemisphere. Moreover a theory of glacial erosion as a factor of productivity in lakes and oceans. Verhandlungen der Internationalen Vereinigung für Theoretische und Angewandte Limnologie 13: 288-297.
- Brundin L. 1983. The larvae of Podonominae (Diptera: Chironomidae) of the Holarctic region - keys and diagnoses. In: T. Wiederholm (ed.), Chironomidae of the Holarctic region. Keys and diagnoses. Part 1 - Larvae. Entomologica Scandinavica Supplement No. 19, Lund, Sweden, pp. 23-31.
- Bryce D. 1962. Chironomidae (Diptera) from freshwater sediments, with special reference to Malham Tarn (Yorks). Transactions of the Society for British Entomology 15: 41-45.
- Bush A.B.G. 2004. Modelling of late Quaternary climate over Asia: a synthesis. Boreas 33: 155-163.
- Butler M.G. 1982. A 7-year life cycle for two *Chironomus* species in arctic Alaskan tundra ponds (Diptera: Chironomidae). Canadian Journal of Zoology 60: 58-70.
- Butler M.G. 2000. *Tanytarsus aquavolans*, spec. nov. and *Tanytarsus nearcticus*, spec. nov., two surface-swarming midges from arctic tundra ponds (Insecta, Diptera, Chironomidae). Spixiana 23: 211-218.
- C.I.A 1984. Permafrost regions in the Soviet Region. In: U. Government (ed.), Perry - Castaneda Library map collection. The University of Texas at Austin, www.lib.utexas.edu/maps/commonwealth.html.

- Camp C.D. and Tung K.K. 2007. Surface warming by the solar cycle as revealed by the composite mean difference projection. *Geophysical Research Letters* 34: L14703.
- Capra L. 2006. Abrupt climatic changes as triggering mechanisms of massive volcanic collapses. *Journal of Volcanology and Geothermal Research* 155: 329-333.
- Carter C.E. 1980. The life cycle of *Chironomus anthracinus* in Lough Neagh. *Holarctic Ecology* 3: 214-217.
- Castellano E., Becagli S., Hansson M., Hutterli M., Petit J.R., Rampino M.R., Severi M., Steffensen J.P., Traversi R. and Udisti R. 2005. Holocene volcanic history as recorded in the sulfate stratigraphy of the European Project for Ice Coring in Antarctica Dome C (EDC96) ice core. *Journal of Geophysical Research* 110: D06114.
- Chapin F.S., Sturm M., Serreze M.C., McFadden J.P., Key J.R., Lloyd A.H., McGuire A.D., Rupp T.S., Lynch A.H., Schimel J.P., Beringer J., Chapman W.L., Epstein H.E., Euskirchen E.S., Hinzman L.D., Jia G., Ping C.L., Tape K.D., Thompson C.D.C., Walker D.A. and Welker J.M. 2005. Role of land-surface changes in Arctic summer warming. *Science* 310: 657-660.
- Clarke G.H. 2004. The relationship between diatoms and climate in a European mountain lake training set: implications for detecting the little ice age in lake sediments from central Norway. Ph.D thesis, Dept. of Geography. University of London, London, UK, p. 433.
- Clarke G.K.C., Leverington D.W., Teller J.T. and Dyke A.S. 2004. Paleohydraulics of the last outburst flood from glacial Lake Agassiz and the 8200 BP cold event. *Quaternary Science Reviews* 23: 389-407.
- Clement A.C., Seager R. and Cane M.A. 2000. Suppression of El Niño during the mid-Holocene by changes in Earth's orbit. *Paleoceanography* 15: 731-737.
- Coffman W.P. 1973. Energy flow in a woodland stream ecosystem II. The taxonomic composition and phenology of the Chironomidae as determined by the collection of pupal exuviae. *Archiv für Hydrobiologie* 71: 281-322.

- Comiso J.C. 2001. Satellite-observed variability and trends in sea-ice extent, surface temperature, albedo and clouds in the Arctic. *Annals of Glaciology* 33: 457-473.
- Comiso J.C. 2003. Warming trends in the Arctic from clear sky satellite observations. *Journal of Climate* 16: 3498-3509.
- Coope G.R., Lemdahl G., Lowe J.J. and Walking A. 1998. Temperature gradients in northern Europe during the last glacial–Holocene transition (14–9 14C kyr BP) interpreted from coleopteran assemblages. *Journal of Quaternary Science* 13: 419-433.
- Corbet P.S. and Danks H.V. 1975. Egg-laying habits of mosquitoes in the high arctic. *Mosquito News* 35: 8-14.
- Cranston P.S., Oliver D.R. and Sæther O.A. 1983. The larvae of the Orthocladiinae (Diptera: Chironomidae) of the Holarctic region: Keys and diagnoses. In: T. Wiederholm (ed.), *Chironomidae of the Holarctic region. Keys and diagnoses. Part 1 - Larvae*. *Entomologica Scandinavica Supplement No. 19*, Lund, Sweden, pp. 149-291.
- Cranston P.S. 1995. Introduction. In: P. Armitage, P. S. Cranston and L. C. V. Pinder (eds.), *The Chironomidae. The biology and ecology of non-biting midges*. Chapman and Hall, London, pp. 1-7.
- Crowley T.J. 2000. Causes of climate change over the past 1000 years. *Science* 289: 270-277.
- Crowley T.J. and Lowery T.S. 2000. How warm was Medieval Warm Period? *Ambio* 29: 51-54.
- Danks H.V. 1971. Overwintering of some north temperate and arctic Chironomidae. II. Chironomid biology. *Canadian Entomologist* 103: 1875-1910.
- Danks H.V. and Oliver D.R. 1972a. Seasonal emergence of some high Arctic Chironomidae (Diptera). *Canadian Entomologist*: 104: 661-686.
- Danks H.V. and Oliver D.R. 1972b. Diel periodicities of emergence of some high Arctic Chironomidae (Diptera). *Canadian Entomologist* 104: 903-916.
- Danks H.V. 1981. *Arctic arthropods: a review of systematics and ecology with particular reference to the North American fauna*. Entomological Society of Canada, Ottawa, 608 pp.

- Danks H.V. 1992. Long life cycles in insects. *Canadian Entomologist* 124: 167-187.
- Danks H.V., Kukal O. and Ring R.A. 1994. Insect cold-hardiness: Insights from the Arctic. *Arctic* 47: 391-404.
- Danks H.V. 2004. Seasonal Adaptations in Arctic Insects. *Intergrative and comparative biology* 44: 85-94.
- Dansgaard W., White J.W.C. and Johnsen S.J. 1989. The abrupt termination of the Younger Dryas climatic event. *Nature* 339: 532-534.
- Dansgaard W., Johnsen S.J., Clausen H.B., Dahl-Jensen D., Gundestrup N.S., Hammer C.U., Hvidberg C.S., Steffensen J.P., Sveinbjornsdottir A.E., Jouzel J. and Bond G. 1993. Evidence for general instability of past climate from a 250-kyr ice-core record. *Nature* 364: 218-220.
- Dean W.E. 1974. Determination of carbonate and organic matter in calcareous sediments and sedimentary rocks by loss on ignition. *Journal of Sedimentary Petrology* 44: 242-248.
- Delettre Y.R. and Morvan N. 2000. Dispersal of adult aquatic chironomidae (Diptera) in agricultural landscapes. *Freshwater Biology* 44: 391-411.
- Dewdney J.C. 1982. *USSR in maps*. Hodder and Stoughton, London, 117 pp.
- Downes J.A. 1965. Adaptations of insects in the arctic. *Annual Review of Entomology* 10: 257-274.
- Duff K., Laing T.E., Smol J.P. and Lean D.R.S. 1998. Limnological characteristics of lakes located across arctic tree-line in northern Russia. *Hydrobiologia* 391: 205-222.
- Dzyuba O.F. 2006. Pollen from Surface Samples as an Environmental Indicator. *Paleontological Journal* 40: S584-S589.
- Edwards D.H.D. 1986. Chironomidae (Diptera) of Australia. In: P. De Deckker and W. D. Williams (eds.), *Limnology in Australia*. CSIRO, Dordrecht, Melbourne, pp. 159-173.
- Eggermont H., Heiri O. and Verschuren D. 2006. Fossil Chironomidae (Insecta : Diptera) as quantitative indicators of past salinity in African lakes. *Quaternary Science Reviews* 25: 1966-1994.
- Elias S.A. 2006. *Encyclopedia of Quaternary Science*. Elsevier, Amsterdam, 3576 pp.

- Ellis J.M. and Calkin P.E. 1984. Chronology of Holocene glaciation, central Brooks Range, Alaska. *Geological Society of America Bulletin* 95: 897-912.
- Enders S.K., Pagani M., Pantoja S., Baron J.S., Wolfe A.P., Pedentchouk N. and Nun˜ez L. 2008. Compound-specific stable isotopes of organic compounds from lake sediments track recent environmental changes in an alpine ecosystem, Rocky Mountain National Park, Colorado. *Limnology and Oceanography* 53: 1468-1478.
- Engels S., Bohncke S.J.P., Bos J.A.A., Brooks S.J., Heiri O. and Helmens K.F. 2008. Chironomid-based palaeotemperature estimates for northeast Finland during Oxygen Isotope Stage 3. *Journal of Paleolimnology* 40: 49-61.
- EPICA community members 2004. Eight glacial cycles from an Antarctic ice core. *Nature* 429: 623-628.
- Fittkau E.J. and Roback S.S. 1983. The larvae of the Tanypodinae (Diptera: Chironomidae) of the Holarctic region - keys and diagnoses. In: T. Wiederholm (ed.), *Chironomidae of the Holarctic region. Keys and diagnoses. Part 1 - Larvae*. *Entomologica Scandinavica Supplement No. 19*, Lund, Sweden, pp. 33-112.
- Flanner M.G., Zender C.S., Randerson J.T. and Rasch P.J. 2007. Present-day climate forcing and response from black carbon in snow. *Journal of Geophysical Research - atmospheres* 112: D11202.
- Formozov N.A. and Yakhontov E.L. 2003. Sympatry zone of Alpine (*Ochotona alpina*) and Northern (*O. hyperborea*) pikas on the Putorana Plateau with description of a new subspecies (*Ochotona hyperborea naumovi ssp. n.*). *Zoologicheskyy Zhurnal* 82: 485-496.
- Forster P., V. Ramaswamy, P. Artaxo, T. Berntsen, R. Betts, D.W. Fahey, J. Haywood, J. Lean, D.C. Lowe, G. Myhre, J. Nganga, R. Prinn, G. Raga, Schulz M. and R. Van Dorland 2007. Changes in Atmospheric Constituents and in Radiative Forcing. In: S. Solomon, D. Qin, M. Manning, Z. Chen, M. Marquis, K.B. Averyt, M. Tignor and H. L. Miller (eds.), *Climate Change 2007: The Physical Science Basis. Contribution of Working Group I to the Fourth Assessment Report of the*

- Intergovernmental Panel on Climate Change. Cambridge University Press, Cambridge, UK and New York, NY, USA., pp. 131-234.
- Frauenfeld O.W., T. Zhang, R.G. Barry and Gilichinsky. D. 2004. Interdecadal changes in seasonal freeze and thaw depths in Russia. *Journal of Geophysical Research* 109: D5101.
- Fritz S.C. 2003. Lacustrine perspectives on Holocene climate. In: A. MacKay, R. W. Battarbee, H. J. B. Birks and F. Oldfield (eds.), *Global change in the Holocene*. Hodder Arnold, London, pp. 227-241.
- Generoso S., Bey I., Attie J.L. and Breon F.M. 2007. A satellite- and model-based assessment of the 2003 Russian fires: Impact on the Arctic region. *Journal of Geophysical Research - atmospheres* 112: D15302.
- Giesecke T., A.E. B., Chiverrell R.C., Seppä H., Ojala A.E.K. and Birks H.J.B. 2008. Exploring Holocene continentality changes in Fennoscandia using present and past tree distributions. *Quaternary Science Reviews* 27: 1296-1308.
- Google-Earth™ v4.2 2007. Images © TerraMetrics and Geocentre Consulting.
- Gorczyński W. 1920. Sur le calcul du degré de continentalisme et son application dans la climatologie. *Geografiska Annaler* 2: 324-331.
- Gordon A.D. 1999. *Classification*. Chapman & Hall/CRC, 272 pp.
- Goulden C.E. 1964. The history of the cladoceran fauna of Esthwaite Water (England) and its limnological significance. *Archiv für Hydrobiologie* 60: 1-52.
- Granados I. and Toro M. 2000. Recent warming in a high mountain lake (Laguna Cimera, Central Spain) inferred by means of fossil chironomids. *Journal of Limnology* 59: 109-119.
- Green A.J. and Sánchez M.I. 2006. Passive internal dispersal of insect larvae by migratory birds. *Biology Letters* 2: 55-57.
- Grieser J., Gommers R., Cofield S. and Bernardi M. 2006. Data sources for FAO worldmaps of Koeppen climatologies and climatic net primary production. The Agromet Group, SDRN, Food and agriculture organization of the United Nations, Rome, Italy.
- Groisman P.Y., Sherstyukov B.G., Razuvaev V.N., Knight R.W., Enloe J.G., Stroumentova N.S., Whitfield P.H., Forland E., Hannsen-Bauer I., Tuomenvirta H., Aleksandersson H., Mescherskaya A.V. and Karl T.R.

2007. Potential forest fire danger over Northern Eurasia: Changes during the 20th century. *Global and planetary change* 56: 371-386.
- Grove J.M. 1988. *The Little Ice Age*. Routledge, London, 500 pp.
- Gruzdev A.D. 1996. Kariofondy chironomid kriolitozony Yakutii: triba Chironomini (Cariofonds of chironomids of the Cryolithozone of Yakutia: tribe Chirinomini). Nauka, Siberian Publishing House of the RAS, Novosibirsk, 237 pp.
- Haigh J. and Blackburn M. 2006. Solar influences on dynamical coupling between the stratosphere and troposphere. *Space Science Reviews* 125: 331-344.
- Hairston N.G. and Kearns C.M. 1995. The Interaction of Photoperiod and Temperature in Diapause Timing: A Copepod Example. *Biological Bulletin* 189: 42-48.
- Håkanson L. and Boulion V.V. 2001. A practical approach to predict the duration of the growing season for European lakes. *Ecological Modelling* 140: 235-245.
- Hantemirov R. and Shiyatov S. 2002. A continuous multimillennial ring-width chronology in Yamal, northwestern Siberia. *The Holocene* 12: 717-726.
- Hastings M.G., Jarvis J.C. and Steig E.J. 2009. Anthropogenic impacts on nitrogen isotopes of ice-core nitrate. *Science* 324: 1288.
- Hauer F.R. and Benke A.C. 1991. Rapid growth of snag-dwelling chironomids in a blackwater river: the influence of temperature and discharge. *Journal of the North American Benthological Society* 10: 154-164.
- Heikkila M., Fontana S.L. and Seppa H. 2009. Rapid Lateglacial tree population dynamics and ecosystem changes in the eastern Baltic region. *Journal of Quaternary Science* DOI: 10.1002/jqs.
- Heiri O. 2001. Holocene palaeolimnology of Swiss mountain lakes reconstructed using chironomid remains: past climate and prehistoric human impact on lake ecosystems. Ph.D. thesis, University of Bern, Bern, Switzerland, p. 113.
- Heiri O. and Lotter A.F. 2001. Effects of low count sums on quantitative environmental reconstructions: an example using subfossil chironomids. *Journal of Paleolimnology* 26: 343-350.

- Heiri O., Lotter A.F. and Lemcke G. 2001. Loss on ignition as a method for estimating organic and carbonate content in sediments: reproducibility and comparability of results. *Journal of Paleolimnology* 25: 101-110.
- Heiri O. 2006. Chironomid records: Postglacial Europe. In: S. A. Elias (ed.), *Encyclopedia of Quaternary Science*. Elsevier, Amsterdam, pp. 390-398.
- Henderson K.A. 2002. An ice core paleoclimate study of Windy Dome, Franz Josef Land, Russia: Development of a recent climate history for the Barents Sea. Ph.D. thesis, Ohio State University, Columbus, Ohio, USA.
- Henriksen M., Mangerud J., Maslenikova O., Matiouchkov A. and Tveranger J. 2001. Weichselian stratigraphy and glaciotectonic deformation along the lower Pechora River, Arctic Russia. *Global and planetary change* 31: 297-319.
- Hill M.O. 1979. TWINSpan - a FORTRAN program for arranging multivariate data in an ordered two-way table by classification of the individuals and attributes. Cornell University, Ithaca, New York.
- Hill M.O. and Šmilauer P. 2005. TWINSpan for Windows version 2.3. Centre for Ecology and Hydrology & University of South Bohemia, Huntingdon & České Budějovice.
- Hirschi J.J.-M., Sinha B. and Josey S.A. 2007. Global warming and changes in continentality since 1948. *Weather* 62: 215-221.
- Hofmann W. 1988. The significance of chironomid analysis for paleolimnological research. *Palaeogeography, Palaeoclimatology, Palaeoecology* 62: 501-509.
- Hofmann W. 2001. Late-Glacial/Holocene succession of the chironomid and cladoceran fauna of the Soppensee (Central Switzerland). *Journal of Paleolimnology* 25: 411-420.
- Holmes N. 2006. Evaluating the use of subfossil chironomids for the reconstruction of Holocene climate in N and NW Iceland., Ph.D. thesis, Dept. of Geography. University of Exeter, Exeter, UK, p. 374.
- Hoye T.T., Post E., Meltofte H., Schmidt N.M. and Forchhammer M.C. 2007. Rapid advancement of spring in the High Arctic. *Current Biology* 17: R449-R451.
- Huisman J., Olff H. and Fresco L.F.M. 1993. A hierarchical set of models for species response analysis. *Journal of Vegetation Science* 4: 37-46.

- Ilyashuk B., Gobet E., Heiri O., Lotter A.F., van Leeuwen J.F.N., van der Knaap W.O., Ilyashuk E., Oberli F. and Ammann B. 2009. Lateglacial environmental and climatic changes at the Maloja Pass, Central Swiss Alps, as recorded by chironomids and pollen. *Quaternary Science Reviews* 28: 1340-1353.
- IPCC 2007. Summary for Policymakers. In: S. Solomon, D. Qin, M. Manning, Z. Chen, M. Marquis, K.B. Averyt, M. Tignor and H. L. Miller (eds.), *Climate Change 2007: The Physical Science Basis. Contribution of Working Group I to the Fourth Assessment Report of the Intergovernmental Panel on Climate Change*. Cambridge University Press, Cambridge, UK and New York, NY, USA.
- Ivanova M.M. 1976. Sources of development for the Putoran flora. In: L. N. Malyshev (ed.), *Flora Putorana: Report on features in the composition and genesis of an alpine subarctic mountain flora of Siberia* Nauka, Novosibirsk, pp. 187-216.
- Iwakuma T. 1986. Ecology and production of *Tokunagayusurika akamusi* (Tokunga) and *Chironomus plumosus* (L.) (Diptera: Chironomidae) in a shallow eutrophic lake. Ph. D. thesis, Kyushu University, Kyushu, Japan.
- Jacoby G.C., Lovelius N.V., Shumilov O.I., Paspopov O.M., Karbainov J.M. and Frank D.C. 2000. Long-term temperature trends and tree growth in the Taymir region of northern Siberia. *Quaternary Research* 53: 312-318.
- Jansen E., J. Overpeck, K.R. Briffa, J.-C. Duplessy, F. Joos, V. Masson-Delmotte, D. Olago, B. Otto-Bliesner, W.R. Peltier, S. Rahmstorf, R. Ramesh, D. Raynaud, D. Rind, O. Solomina, Villalba R. and D. Zhang 2007. Palaeoclimate. . In: S. Solomon, D. Qin, M. Manning, Z. Chen, M. Marquis, K.B. Averyt, M. Tignor and H. L. Miller (eds.), *Climate Change 2007: The Physical Science Basis. Contribution of Working Group I to the Fourth Assessment Report of the Intergovernmental Panel on Climate Change*. Cambridge University Press., Cambridge, United Kingdom and New York, NY, USA, pp. 435-497.
- Jennings A.E., Knudsen K.I., Hald M., Hansen C.V. and Andrews J.T. 2002. A Mid-Holocene shift in Arctic sea ice variability on the East Greenland shelf. *The Holocene* 6: 179-191.

- Johannsson O.E. 1980. Energy dynamics of the eutrophic chironomid *Chironomus plumosus* f. *semireductus* from the Bay of Qunite, Lake Ontario. *Canadian Journal of Fisheries and Aquatic Sciences* 37: 1254-1265.
- Johnsen S., Dahl-Jensen D., Gundestrup N.S., Steffensen J.P., Clausen H.B., Miller H., Masson-Delmotte V., Sveinbjornsdottir A.E. and White J.W.C. 2001. Oxygen isotope and palaeotemperature records from six Greenland ice core stations: Camp Century, Dye-3, GRIP, GISP2, Renland and NorthGRIP. *Journal of Quaternary Science* 16: 299-307.
- Jones P.D. and Mann M. 2004. Climate over past millennia. *Reviews of Geophysics* 42: RG2002.
- Jowsey P.C. 1966. An improved peat sampler. *New Phytologist* 65: 245-248.
- Juggins S. 1991. ZONE, version 1.2. University of Newcastle, Newcastle Upon Tyne, UK.
- Juggins S. and ter Braak C.J.F. 1994. CALIBRATE version 0.81. Unpublished computer program. Department of Geography, University of Newcastle-upon-Tyne.
- Juggins S. 2005. C2 Version 1.4.3. Software for ecological and palaeoecological data analysis and visualisation. Newcastle University, Newcastle upon Tyne, UK. .
- Kaplan M.R. and Wolfe A.P. 2006. Spatial and temporal variability of Holocene temperature in the North Atlantic region. *Quaternary Research* 65: 223-231.
- Kaufman D.S., Ager T.A., Anderson N.J., Anderson P.M., Andrews J.T., Bartlein P.J., Brubake L.B., Coats L.L., Cwynar L.C., Duvall M.L., Dyke A.S., Edwards M.E., Eisner W.R., Gajewski K., Geirsdóttir A., Hu F.S., Jennings A.E., Kaplan M.R., Kerwin M.W., Lozhkin A.V., MacDonald G.M., Miller G.H., Mock C.J., Oswald W.W., Otto-Bliesner B.L., Porinchu D.F., Rühland K., Smol J.P., Steig E.J. and Wolfe B.B. 2004. Holocene thermal maximum in the western Arctic (0-180°W). *Quaternary Science Reviews* 23: 529-560.
- Keeling R.F., Piper S.C., Bollenbacher A.F. and Walker S.J. 2009. Atmospheric CO₂ values (ppmv) derived from in situ air samples collected at Mauna Loa, Hawaii, USA. <http://cdiac.ornl.gov/ftp/trends/co2/maunaloa.co2>,

Carbon Dioxide Research Group, Scripps Institution of Oceanography (SIO), University of California, California, USA.

- Kim J.H., Rimbu N., Lorenz S.J., Lohmann G., Nam S.-I., Schouten S., Rühlemann C. and Schneider R.R. 2004. North Pacific and North Atlantic sea-surface temperature variability during the Holocene. *Quaternary Science Reviews* 23: 2141-2154.
- Koç N. and Jansen E. 1994. Response of the high-latitude Northern-Hemisphere to orbital climate forcing - Evidence from the Nordic Seas. *Geology* 22: 523-526.
- Kokorowski H.D., Anderson P.M., Mock C.J. and Lozhkin A.V. 2008. A re-evaluation and spatial analysis of evidence for a Younger Dryas climatic reversal in Beringia. *Quaternary Science Reviews* 27: 1710-1722.
- Korhola A., Olander H. and Blom T. 2000. Cladoceran and chironomid assemblages as quantitative indicators of water depth in subarctic Fennoscandian lakes. *Journal of Paleolimnology* 24: 43-53.
- Koronkevich N. 2002. Rivers, lakes, inland seas and wetlands. In: M. Shahgedanova (ed.), *The physical geography of northern Eurasia*. Oxford University Press, Oxford, pp. 122-148.
- Koronovsky N. 2002. Tectonics and geology. In: M. Shahgedanova (ed.), *The physical geography of northern Eurasia*. Oxford University Press, Oxford, pp. 1-35.
- Kotlyakov V. and Khromova T. 2001. Maps of permafrost and ground ice. In: V. Stolbovoi and I. McCallum (eds.), *CD-ROM Land Resources of Russia*. Institute of Applied Systems Analysis and the Russian Academy of Science, Laxenburg, Austria.
- Kremenetski C.V., Sulerzhitsky L.D. and Hantemirov R. 1998. Holocene History of the Northern Range Limits of Some Trees and Shrubs in Russia. *Arctic and Alpine Research* 30: 317-333.
- Kryjov V.N. 2002. The influence of the winter Arctic Oscillation on the Northern Russia spring temperature. *International Journal of Climatology* 22: 779-785.
- Kultti S., Väliiranta M., Sarmaja-Korjonen K., Solovieva N., Virtanen T., Kauppila T. and Eronen M. 2003. Palaeoecological evidence of changes in

- vegetation and climate during the Holocene in the pre-Urals, northeast European Russia. *Journal of Quaternary Science* 16: 503-520.
- Kultti S., Oksanen J. and Valiranta M. 2004. Multiproxy record of Holocene environmental change in the Nenets region, East-European Russian arctic. *Journal of Canadian Earth Science* 41: 1141-1158.
- Kumke T., Kienel U., Weckström J., Korhola A. and Hubberten H.-W. 2004. Inferred Holocene Paleotemperatures from diatoms at Lake Lama, Central Siberia. *Arctic, Antarctic and Alpine Research* 36: 624-634.
- Kumke T., Ksenofontova M., Pestryakova L., Nazarova L. and Hubberten H.-W. 2007. Limnological characteristics of lakes in the lowlands of Central Yakutia, Russia. *Journal of Limnology* 66: 40-53.
- Kureck A. 1979. Two circadian eclosion times in *Chironomus thummi* (Diptera: Chironomidae), alternately selected with different temperatures. *Oecologia (Berlin)* 40: 311-323.
- Kureck A. 1980. Circadian eclosion rhythm in *Chironomus thummi*; ecological adjustment to different temperature levels and the role of temperature cycles, in Chironomidae. In: D. A. Murray (ed.), *Chironomidae. Ecology, systematics, cytology and physiology*. Pergamon Press, New York, pp. 73-80.
- Laaksonen K. 1976. The dependence of mean air temperatures upon latitude and altitude in Fennoscandia (1921-1950). *Annales Academiae Scientiarum Fennicae A III*: 1-19.
- Langdon P.G., Ruiz Z., Brodersen K.P. and Foster I.D.I. 2006. Assessing lake eutrophication using chironomids: understanding the nature of community response in different lake types. *Freshwater Biology* 51: 562-577.
- Langdon P.G., Holmes N. and Caseldine C.J. 2008. Environmental controls on modern chironomid faunas from NW Iceland and implications for reconstructing climate change. *Journal of Paleolimnology* 40: 273-293.
- Langdon P.H. 1991. A key to pupal exuviae of West Palaearctic Chironomidae. Private publication available from 5 Kylebeg Avenue, Coleraine BT52 1JN, N. Ireland.

- Langton P.H. and Visser H. 2003. Chironomid exuviae: a key to pupal exuviae of the West Palaearctic region World Biodiversity Database, Expert Centre for Taxonomic Identification, University of Amsterdam.
- Larocque I. 2001. How many chironomid head capsules are enough? A statistical approach to determine sample size for palaeoclimatic reconstructions. *Palaeogeography, Palaeoclimatology, Palaeoecology* 172: 133-142.
- Larocque I., Hall R.I. and Grahn E. 2001. Chironomids as indicators of climate change: a 100-lake training set from a subarctic region of northern Sweden (Lapland). *Journal of Paleolimnology* 26: 307-322.
- Larocque I. and Hall R.I. 2003. Chironomids as quantitative indicators of mean July air temperature, validation by comparison with century-long meteorological records from northern Sweden. *Journal of Paleolimnology* 29: 475-493.
- Larocque I. and Hall R.I. 2004. Holocene temperature estimates and chironomid community composition in the Abisko Valley, northern Sweden. *Quaternary Science Reviews* 23: 2453-2465.
- Larocque I., Pienitz R. and Rolland N. 2006. Factors affecting the distribution of chironomids in lakes distributed along a latitudinal gradient in northwestern Quebec. *Canadian Journal of Fisheries and Aquatic Sciences* 63: 1286-1297.
- Lauritzen S.-E. 2003. Reconstructing Holocen climate records from speleothems. In: A. MacKay, R. W. Battarbee, H. J. B. Birks and F. Oldfield (eds.), *Global change in the Holocene*. Hodder Arnold, London, pp. 242-262.
- Lee R.E. and Denlinger D.L. 1991. *Insects at low temperatures*. Chapman and Hall, New York and London, 513 pp.
- Lehmann M.F., Bernasconi S.M., Barbieri A. and McKenzie J.A. 2002. Preservation of organic matter and alteration of its carbon and nitrogen isotope composition during simulated and in situ early sedimentary diagenesis. *Geochimica et Cosmochimica Acta* 66: 3573-3584.
- Lemdahl G. 2000. Late-glacial and early Holocene Coleoptera assemblages as indicators of local environment and climate at Krakenes Lake, western Norway. *Journal of Paleolimnology* 23: 57-66.

- Lemke P., J. Ren, R.B. Alley, I. Allison, J. Carrasco, G. Flato, Y. Fujii, G. Kaser, P. Mote, Thomas R.H. and Zhang. T. 2007. Observations: Changes in Snow, Ice and Frozen Ground. In: S. Solomon, D. Qin, M. Manning, Z. Chen, M. Marquis, K.B. Averyt, M. Tignor and H. L. Miller. (eds.), *Climate Change 2007: The Physical Science Basis. Contribution of Working Group I to the Fourth Assessment Report of the Intergovernmental Panel on Climate Change*. Cambridge University Press, Cambridge, United Kingdom and New York, NY, USA.
- Leng M.L. 2003. Stable isotopes in lakes and lake sediment archives. In: A. MacKay, R. W. Battarbee, H. J. B. Birks and F. Oldfield (eds.), *Global change in the Holocene*. Hodder Arnold, London, pp. 124-139.
- Leonova G.A. 2004. Biogeochemical Indicators of Aquatic Ecosystem Pollution by Heavy Metals. *Water Resources* 31: 195-202.
- Lie Ø., Dahl S.O., Nesje A., Matthews J.A. and Sandvold S. 2004. Holocene fluctuations of a polythermal glacier in highalpine eastern Jotunheimen, central-southern Norway. *Quaternary Science Reviews* 23: 1925-1945.
- Lie Ø. and Paasche Ø. 2006. How extreme was northern hemisphere seasonality during the Younger Dryas? . *Quaternary Science Reviews* 25: 404-407.
- Lindegaard C. 1992. Zoobenthos ecology of Thingvallavatn: vertical distribution, abundance, population, dynamics and production. *Oikos* 64: 257-304.
- Lindegaard C. 1995. Classification of water-bodies and pollution. In: P. Armitage, P. S. Cranston and L. C. V. Pinder (eds.), *The Chironomidae: the Biology and Ecology of Non-biting Midges*. Chapman and Hall, London, pp. 385–404.
- Lindquist S.J. 1999. The Timan-Pechora Basin Province of Northwest Arctic Russia: Domanik – Paleozoic Petroleum System: USGS Open File Report 99-50G Timan-Pechora:
<http://greenwood.cr.usgs.gov/energy/WorldEnergy/OF99-50G/abstract.html>.
- Livingstone D.M. and Lotter A.F. 1998. The relationship between air and water temperatures in lakes of the Swiss Plateau: a case with palaeolimnological implications. *Journal of Paleolimnology* 19: 181-198.

- Livingstone D.M., Lotter A.F. and Walker I.R. 1999. The decrease in summer surface water temperature with altitude in Swiss Alpine lakes: a comparison with air temperature lapse rates. *Arctic, Antarctic and Alpine Research* 31: 341-352.
- Lopez C.M.L., Brouchkov A., Nakayama H., Takakai F., Fedorov A.N. and Fukuda M. 2007. Epigenetic salt accumulation and water movement in the active layer of central Yakutia in eastern Siberia. *Hydrological Processes* 1. Institute of Low Temperature Science, Hokkaido University. 21: 103-109.
- Lotter A.F., Birks H.J.B., Hofmann W. and Marchetto A. 1997. Modern diatom, cladocera, chironomid, and chrysophyte cyst assemblages as quantitative indicators for the reconstruction of past environmental conditions in the Alps. I. Climate. *Journal of Paleolimnology* 18: 395-420.
- Lotter A.F., Birks H.J.B., Hofmann W. and Marchetto A. 1998. Modern diatom, cladocera, chironomid, and chrysophyte cyst assemblages as quantitative indicators for the reconstruction of past environmental conditions in the Alps. II. *Journal of Paleolimnology* 19: 443-463.
- Lotter A.F. 2003. Multi-proxy climatic reconstructions. In: A. MacKay, R. W. Battarbee, H. J. B. Birks and F. Oldfield (eds.), *Global change in the Holocene*. Hodder-Arnold, London, pp. 373-383.
- Lubinski D., Forman S.L. and Miller G.H. 1999. Holocene glacier and climate fluctuations on Franz Josef Land, Arctic Russia, 80°N. *Quaternary Science Reviews* 18: 85-108.
- Luoto T.P. 2008. Subfossil Chironomidae (Insecta: Diptera) along a latitudinal gradient in Finland: development of a new temperature inference model. *Journal of Quaternary Science* 24: 150-158.
- MacDonald G.M., Kremenetski C.V., Velichko A.A., Cwynar L.C., Riding R.T., Goleva A.A., Andreev A., Borisova O.K., Edwards T.W.D., Hammarlund D., Szeicz J.M., Forman S.L. and Gataullin V. 2000. Holocene treeline history and climate change across northern Eurasia. *Quaternary Research* 53: 302-311.
- Mackey A.P. 1977. Trophic dependencies of some larval Chironomidae (Diptera) and fish species in the River Thames. *Hydrobiologia* 62: 241-247.

- Magnuson J.J., D.M. Robertson, B. J. Benson, R. H. Wynne, D. M. Livingstone, T. Arai, R.A. Assel, R.G. Barry, V. Card, E. Kuusisto, N.G. Granin, T.D. Prowse, K.M. Stewart and Vuglinski. V.S. 2000. Historical trends in lake and river ice cover in the Northern Hemisphere. *Science* 289: 1743-1746.
- Major J. 1980. Review of Flora Putorana. *Arctic and Alpine Research* 12: 583-584.
- Makarchenko E.A. and Makarchenko M.A. 1999. Chironomidae. In: S. J. Tsalolikhin (ed.), *Key to Freshwater Invertebrates of Russia and adjacent lands*. Zoological Institute RAS, St. Petersburg, pp. 210-295.
- Malyshev L.N. 1976. *Flora Putorana (Flora Putorana: Materials to Elucidate the Singularities of Composition and Genesis of a Siberian Subarctic Mountain Flora)*. Nauka, Novosibirsk, 246 pp.
- Manley G. 1974. Central England temperatures: monthly means 1659 to 1973. *Quarterly Journal of the Royal Meteorological Society* 100: 389-405.
- Marcus N.H. 1982. Photoperiodic and temperature regulation of diapause in *Labidocera aestiva*. *Biological Bulletin* 162: 45-52.
- Marshall J.D., Jones R.T., Crowley S.F., Oldfield F., Nash S. and Bedford A. 2002. A high resolution Late-Glacial isotopic record from Hawes Water, Northwest England Climatic oscillations: calibration and comparison of palaeotemperature proxies. *Palaeogeography, Palaeoclimatology, Palaeoecology* 185: 24-40.
- Mayewski P.A., Meeker L.D., Twickler M.S., Whitlow S.I., Yang Q., Berry Lyons W. and Prentice I.C. 1997. Major features and forcing of high-latitude northern hemisphere atmospheric circulation using a 110,000 year long glaciochemical series. *Journal of Geophysical Research* 102: 26345-26366.
- Mayewski P.A., Rohling E.E., Stager J.C., Karlen W., Maasch K.A., Meeker L.D., Meyerson E.A., Gasse F., van Kreveld S., Holmgren K., Lee-Thorp J., Rosqvist G., Rack F., Staubwasser M., Schneider R.R. and Steig E.J. 2004. Holocene climate variability. *Quaternary Research* 62: 243-255.
- McClelland J., Holmes R.M., Peterson B.J. and Stieglitz M. 2004. Increasing river discharge in the Eurasia Arctic: consideration of dams, permafrost thaw and fires as potential agents of change. *Journal of Geophysical Research - atmospheres* 109: D18102.

- McDermott F., Matthey D.P. and Hawkesworth C. 2001. Centennial-scale Holocene climate variability revealed by a high-resolution speleotherm delta 18O record from SW Ireland. *Science* 294: 1328-1331.
- McGill J.D. 1980. The distribution of Chironomidae (Diptera) throughout the River Chew drainage system, Avon, England. Ph.D. thesis, Department of Zoology. University of Bristol, Bristol. UK.
- Meeker L.D. and Mayewski P.A. 2002. A 1400-year high-resolution record of atmospheric circulation over the North Atlantic and Asia. *The Holocene* 12: 257-266.
- Meltser N., Kashi Y. and Broza M. 2008. Does polarised light guide chironomids to navigate towards water surfaces? *Boletim do Museu Municipal do Funchal Suplemento No. 13*: 141-149.
- Meshkova V. 2002. Dependency of outbreaks distribution from insects-defoliators' seasonal development. In: M. L. McManus and A. M. Liebhold (eds.), *Proceedings of the Ecology, Survey and Management of Forest Insects*. USDA Forest Service, Kraków, Poland, pp. 52-60.
- Meyers P.A. 1994. Preservation of source identification of sedimentary of sedimentary organic matter during and after deposition. *Chemical Geology* 144: 289-302.
- Meyers P.A. and Teranes J.L. 2001. Sediment organic matter. In: W. Last and J. P. Smol (eds.), *Tracking environmental change using lake sediments* Kluwer Academic Publishers, Dordrecht, The Netherlands, pp. 239-271.
- Mikhailov V.N. 1997. The river mouths of Russia and contiguous countries: past, present and future. GEOS, Leningrad, 413 pp.
- Mol D., Tikkonov A., van der Plicht J., Kahlke R.-D., Debruyne R., van Geel B., van Reenen G., Pals J.P., de Marliave C. and Reumer J.W.F. 2006. Results of the CERPOLEX/Mammuthus Expeditions on the Taimyr Peninsula, Arctic Siberia, Russian Federation. *Quaternary International* 142-143: 186-202.
- Moller Pillot H.K.M. and Buskens R.F.M. 1990. De larven der Nederlandse Chironomidae. Autoecologie en verspreiding. *Nederlandse Faunistische Medelelingen* 1c: 1-87.
- Moss B. 1998. *Ecology of fresh waters: man and medium, past to future*. Blackwell Publishing, Oxford, 557 pp.

- Mudelsee M. 2001. The phase relations among atmospheric CO₂ content, temperature and global ice volume over the past 420 ka. *Quaternary Science Reviews* 20: 583-589.
- Murdmaa I., Polyak L., Ivanova E. and Khromova N. 2003. Paleoenvironments in Russkaya Gavan' Fjord (NW Novaya Zemlya, Barents Sea) during the last millennium. *Palaeogeography Palaeoclimatology Palaeoecology* 209: 141-155.
- Murphy J. and Riley J. 1962. A modified single solution for the determination of phosphate in natural waters. *Analytica Chimica Acta* 27: 31-39.
- Nalvikin D.V. 1973. *The geology of the U.S.S.R.* Translated from the Russian by N. Rast. Oliver and Boyd, Edinburgh, UK, 855 pp.
- Naurzbaev M.M. and Vaganov E.A. 2000. Variation of early summer and annual temperatures in east Taymyr and Putoran (Siberia) over the last two millenia inferred from tree rings. *Journal of Geophysical Research* 105 D6: 7317-7326.
- Naurzbaev M.M., Vaganov E.A., Sidorova O.V. and Schweingruber F.H. 2002. Summer temperatures in eastern Taimyr inferred from a 2427-year late-Holocene tree-ring chronology and earlier floating series. *The Holocene* 12: 727-736.
- Nazarova L.B., Pestryakova L.A., Ushnitskaya L.A. and Hubberten H.-W. 2008. Chironomids (Diptera: Chironomidae) in Lakes of Central Yakutia and Their Indicative Potential for Paleoclimatic Research. *Contemporary Problems of Ecology*. 15: 141-150.
- Neff U., Burns S.J., Mangini A., Mudelsee M., Fleitmann D. and Matter A. 2001. Strong coherence between solar variability and the monsoon in Oman between 9 and 6 kyr ago. *Nature* 411: 290-293.
- Nesje A. and Dahl S.O. 2003. Glaciers as indicators of Holocene climate change. In: A. MacKay, R. W. Battarbee, H. J. B. Birks and F. Oldfield (eds.), *Global change in the Holocene*. Hodder-Arnold, London, pp. 264-280.
- Nyman M., Korhola A. and Brooks S.J. 2005. The distribution and diversity of Chironomidae (Insecta: Diptera) in western Finnish Lapland, with special emphasis on shallow lakes. *Global Ecology and Biogeography*. 14: 137-153.

- O'Brien S.R., Mayewski P.A., Meeker L.D., Meese D.A., Twickler M.S. and Whitlow S.I. 1996. Complexity of the Holocene climate as reconstructed from a Greenland ice core. *Science* 270: 1962-1964.
- Oberman N.G. and Mazhitova G.G. 2001. Permafrost dynamics in the north-east of European Russia at the end of the 20th century. *Norwegian Journal of Geography* 55: 241-244.
- Oksanen J. and Minchin P.R. 1997. Instability of Ordination Results under Changes in Input Data Order: Explanations and Remedies. *Journal of Vegetation Science* 8: 447-454.
- Oksanen J. and Minchin P.R. 2002. Continuum theory revisited: what shape are species responses along ecological gradients? . *Ecological Modelling* 157: 119-129.
- Olafsson J.S., Adalsteinsson H., Gislason G.M., Hansen I. and Hrafnisdottir T. 2002. Spatial heterogeneity in lotic chironomids and simuliids in relation to catchment characteristics in Iceland. *Verhandlungen der Internationalen Vereinigung für Theoretische und Angewandte Limnologie* 28: 157-163.
- Olander H., Birks H.J.B., Korhola A. and Blom T. 1999. An expanded calibration model for inferring lakewater and air temperatures from fossil chironomid assemblages in northern Fennoscandia. *The Holocene* 9: 279-294.
- Oldfield F. 2003. Introduction: the Holocene, a special time. In: A. MacKay, R. W. Battarbee, H. J. B. Birks and F. Oldfield (eds.), *Global change in the Holocene*. Hodder Arnold, London, pp. 1-9.
- Oliver D.R. 1968. Adaptations of arctic Chironomidae. *Annales Zoologici Fennici* 5: 111-118.
- Oliver D.R. 1971. Life history of the Chironomidae. *Annual Review of Entomology* 16: 211-230.
- Olsson I. 1986. Radiometric dating. In: B. E. Berglund (ed.), *Handbook of Holocene Palaeoecology and Palaeohydrology*. John Wiley, Chichester pp. 273-312.
- Orloci L. 1967. An agglomerative method for the classification of plant communities. *Journal of Ecology* 55: 193-206.

- Overland J. and Wang M. 2005. The Arctic climate paradox: The recent decrease of the Arctic Oscillation. *Geophysical Research Letters* 32: L06701.
- Overpeck J.T. and Cole J.E. 2006. Abrupt change in Earth's climate system. *Annual Review of Environment and Resources* 31: 1-31.
- Overpeck J.T. 2007. Paleoclimate perspectives on climate change., *The science of climate change: A Royal Society showcase of the IPCC 4th Assessment Working Group 1 report*. The Royal Society, London.
- Pavlov A.V. 1996. Permafrost-climate monitoring of Russia: analysis of field data and forecast. *Polar Geography* 20: 44-64.
- Pavlov A.V., Razina V.V. and Bolshiyarov D.Y. 2002. Climate changes of the last millennium and reconstruction of the Little Ice Age from Arctic lake sediments. *PAGES Meeting on High Latitude Paleoenvironments*, Moscow.
- Peglar S.M., Fritz S.C. and Birks H.J.B. 1989. Vegetation and land-use history at Diss, Norfolk. *Journal of Ecology* 77: 203-222.
- Peteet D. 1995. Global Younger Dryas. *Quaternary International* 28: 93-104.
- Peterson B.J., Holmes R.M., McClelland J., Vorosmarty C.J., Lammers R.B., Shiklomanov A.I., Shiklomanov I.A. and Rahstorf S. 2002. Increasing river discharge to the Arctic Ocean. *Science* 298: 2171-2173.
- Petridis D. and Sinis A. 1993. Benthic macrofauna of Tavropos reservoir (Central Greece). *Hydrobiologia* 262: 1-12.
- Peyron O., Be'geot C., Brewer S., Heiri O., Magny M., Millet L., Ruffaldi P., Van Campo E. and Yu G. 2005. Late-Glacial climatic changes in Eastern France (Lake Lautrey) from pollen, lake-levels, and chironomids. *Quaternary Research* 64: 197-211.
- Pinder L.C.V. and Reiss F. 1983. The larvae of Chironominae (Diptera: Chironomidae) of the Holarctic region - keys and diagnoses. In: T. Wiederholm (ed.), *Chironomidae of the Holarctic region. Keys and diagnoses. Part 1 - Larvae*. *Entomologica Scandinavica Supplement No. 19*, Lund, Sweden, pp. 149-292.
- Pinder L.C.V. 1986. Biology of freshwater Chironomidae. *Annual Review of Entomology* 31: 1-23.

- Pinder L.C.V. 1995. The habitats of chironomid larvae. In: P. Armitage, P. S. Cranston and L. C. V. Pinder (eds.), *The Chironomidae: Biology and ecology of non-biting midges*. Chapman and Hall, London, pp. 107-135.
- Pinder L.C.V. and Morley D.J. 1995. Chironomidae as indicators of water quality - with a comparison of the chironomid faunas of a series of contrasting Cumbrian Tarns. In: R. Harrington and N. E. Stork (eds.), *Insects in a changing environment*. Academic Press, London, pp. 272-293.
- Pisaric M.F.J., MacDonald G.M., Cwynar L.C. and Velichko A.A. 2001a. Modern pollen and conifer stomates from north-central Siberian lake sediments: their use in interpreting late Quaternary fossil assemblages. *Arctic, Antarctic and Alpine Research* 33: 18-27.
- Pisaric M.F.J., MacDonald G.M., Velichko A.A. and Cwynar L.C. 2001b. The Lateglacial and Postglacial vegetation history of the northwestern limits of Beringia, based on pollen, stomate and tree stump evidence. *Quaternary Science Reviews* 20: 235-245.
- Pitul'ko V. 2001. Terminal Pleistocene – Early Holocene occupation in northeast Asia and the Zhokhov assemblage. *Quaternary Science Reviews* 20: 267-275.
- Porinchi D.F. and Cwynar L.C. 2000. The distribution of freshwater Chironomidae (Insecta: Diptera) across the treeline near the lower Lena River, northeast Siberia. *Arctic, Antarctic and Alpine Research* 32: 429-437.
- Porinchi D.F. and Cwynar L.C. 2002. Late-Quaternary history of midge communities and climate from a tundra site near the lower Lena River, northeast Siberia. *Journal of Paleolimnology* 27: 59-69.
- Porinchi D.F., Rolland N. and Moser K. 2009. Development of a chironomid-based air temperature inference model for the central Canadian Arctic. *Journal of Paleolimnology* 41: 349-368.
- Przybylak R. 2003. *The climate of the Arctic*. Kluwer Academic Publishers, The Netherlands, 270 pp.
- Quinlan R., Smol J.P. and Hall R.I. 1998. Quantitative inferences of past hypolimnetic anoxia in south-central Ontario lakes using fossil midges (Diptera : Chironomidae). *Canadian Journal of Fisheries and Aquatic Science* 55: 587-596.

- Quinlan R. and Smol J.P. 2001. Setting minimum head capsule abundance and taxa deletion criteria in chironomid-based inference models. *Journal of Paleolimnology* 26: 327-342.
- Racca J.M.J., Wild M., Birks H.J.B. and Prairie Y.T. 2003. Separating wheat from chaff: Diatom taxon selection using an artificial neural network pruning algorithm. *Journal of Paleolimnology* 29: 123-133.
- Rahmstorf S. and Schellnhuber H.J. 2006. *Der Klimawandel*. Beck Verlag, Munich, 144 pp.
- Rasmussen S.O. 1984. The life-history, distribution and production of *Chironomus riparius* and *Glyptotendipes paripes* in a prairie pond. . *Canadian Journal of Fisheries and Aquatic Sciences* 42: 1418-1422.
- Rawlins M.A. and Willmott C.J. 2003. Winter air temperature change over the Terrestrial Arctic, 1961-1990. *Arctic, Antarctic and Alpine Research* 35: 530-537.
- Raymo M.E. and Ruddiman W.F. 1992. Tectonic forcing of late Cenozoic climate. *Nature* 359: 117-122.
- Reimer P.J., Baillie M.G.L., Bard E., Bayliss A., Beck J.W., Bertrand C.J.H., Blackwell P.G., Buck C.E., Burr G.S., Cutler K.B., Damon P.E., Edwards R.L., Fairbanks R.G., Friedrich M., Guilderson T.P., Hogg A.G., Hughen K.A., Kromer B., McCormac G., Manning S., Bronk Ramsey C., Reimer R.W., Remmele S., Southon J.R., Stuiver M., Talamo S., Taylor F.W., van der Plicht J. and Weyhenmeyer C.E. 2004. IntCal04 terrestrial radiocarbon age calibration, 0-26 cal kyr BP. *Radiocarbon* 46: 1029-1058.
- Renberg I. 1991. The HON-Kajak sediment corer. *Journal of Paleolimnology* 6: 167-170.
- Renssen H., Isarin R.F.B., Jacob D., Podzun R. and Vandenberghe J. 2001. Simulation of the Younger Dryas climate in Europe using a regional climate model nested in an AGCM: preliminary results. *Global and Planetary Change* 30: 41-57.
- Renssen H., Goosse H., Fichefet T., Brovkin V., Driesschaert E. and Wolk F. 2005. Simulating the Holocene climate evolution at northern high latitudes using a coupled atmosphere-sea ice-ocean-vegetation model. *Climate Dynamics* 24: 23-43.

- Renssen H., Seppä H., Heiri O., Roche D.M., Goosse H. and Fichet T. 2009. The spatial and temporal complexity of the Holocene thermal maximum. *Nature Geoscience* DOI: 10.1038/NGEO513.
- Richter-Menge J., Overland J., Proshutinsky A., Romanovsky V., Bengtsson L., Brigham L., Dyurgerov M., Gascard J.C., Gerland S., Graversen R., Haas C., Karcher M., Kuhry P., Maslanik J., Melling H., Maslowski W., Morison J., Perovich D., Przybylak R., Rachold V., Rigor I., Shiklomanov A., Stroeve J., Walker D. and (2006) J.W. 2006. State of the Arctic Report., NOAA OAR Special Report. NOAA/OAR/PMEL, Seattle, WA, p. 36.
- Rieradevall M. and Brooks S.J. 2001. An identification guide to subfossil Tanypodinae larvae (Insecta: Diptera: Chironomidae) based on cephalic setation. *Journal of Paleolimnology* 25: 81-99.
- Rigor I.G., Colony R.L. and Martin S. 2000. Variations in surface air temperature observations in the Arctic, 1979-1997. *Journal of Climate* 13: 896-914.
- Rind D. and Overpeck J. 1993. Hypothesised causes of decade-to-century-scale climate variability: climate model results. *Quaternary Science Reviews* 12: 357-374.
- Robock A. 2000. Volcanic eruptions and climate. *Reviews of Geophysics* 38: 191-219.
- Rozenbaum G.E. and Shpolyanskaya N.A. 1998. Late Cenozoic permafrost history of the Russian Arctic. *Permafrost and periglacial processes* 9: 247-273.
- Ruddiman W.F. 2003. The anthropogenic greenhouse era began thousands of years ago. *Climatic change* 61: 261-293.
- Rudolf B., H. Hauschild, Rueth W. and Schneider U. 1994. Terrestrial Precipitation Analysis: Operational Method and Required Density of Point Measurements. In: M. Desbois and F. Desalmond (eds.), *Global Precipitations and Climate Change*. Springer-Verlag, pp. 173-186.
- Rudolf B., Fuchs T., Schneider U. and Meyer-Christoffer A. 2003. Introduction of the Global Precipitation Climatology Centre (GPCC). *Deutscher Wetterdienst, Offenbach a.M*, 16 pp.

- Ruiz Z., Brown A.G. and Langdon P.G. 2006. The potential of chironomid (Insecta: Diptera) larvae in archaeological investigations of floodplain and lake settlements. *Journal of Archaeological Science* 33: 14-33.
- Sæther O.A. 1976. Revision of *Hydrobaenus*, *Trissocladius*, *Zalutschia*, *Paratrissocladius* and some related genera (Diptera: Chironomidae). *Bulletin of the Fisheries Research Board of Canada* 195: 1-287.
- Sæther O.A. 1979. Chironomid communities as water quality indicators. *Holarctic Ecology* 2: 65-74.
- Sæther O.A., Spies M. and de Jong H. 2007. Fauna Europaea: Chironomidae. . Fauna Europaea version 1.1, <http://www.faunaeur.org>.
- Sæther O.A. 1979. Chironomid communities as water quality indicators. *Holarctic Ecology* 2: 65-74.
- Sæther O.A. 1983. The larvae of Prodiamesinae (Diptera: Chironomidae) of the Holarctic region - keys and diagnoses. In: T. Wiederholm (ed.), *Chironomidae of the Holarctic region. Keys and diagnoses. Part 1 - Larvae*. Entomologica Scandinavica, Lund, Sweden, pp. 141-147.
- Sæther O.A. and Sublette J.E. 1983. A review of the genera *Doithrix* n. gen., *Georthocladius* Strenzke, *Parachaetocladius* Wülker, and *Pseudorthocladius* Goetghebuer (Diptera: Chironomidae: Orthoclaadiinae). *Entomologica Scandinavica Supplement* 20: 1-100.
- Sarmaja-Korjonen K., Kultti S., Valiranta M. and Solovieva N. 2003. Mid-Holocene palaeoclimatic and palaeohydrological conditions in northeastern European Russia: a multi-proxy study of Lake Vankavad. *Journal of Paleolimnology* 30: 415-426.
- Schindler D.W. and Smol J.P. 2006. Cumulative effects of climate warming and other human activities on freshwaters of Arctic and subarctic North America. *Ambio* 35: 160-168.
- Schmid P.E. 1993. A key to the larval Chironomidae and their instars from Austrian Danube Region streams and rivers. Part 1. Diamesinae, Prodiamesinae and Orthoclaadiniinae. Federal Institute for Water Quality, Wien.
- Schnell O.A. and Willassen E. 1996. The chironomid (Diptera) communities in two sediment cores from Store Hovvatn, S. Norway, an acidified lake. *Annales De Limnologie-International Journal of Limnology* 32: 45-61.

- Self S. 2006. The effects and consequences of very large explosive volcanic eruptions. *Philosophical Transactions of the Royal Society a-Mathematical Physical and Engineering Sciences* 364: 2073-2097.
- Seppä H. and Birks H.J.B. 2001. July mean air temperature and annual precipitation trends during the Holocene in the Fennoscandian tree-line area: pollen-based climate reconstructions. *The Holocene* 11: 527-539.
- Seppä H., Hammarlund D. and Antonsson K. 2005. Low-frequency and high-frequency changes in temperature and effective humidity during the Holocene in south-central Sweden: implications for atmospheric and oceanic forcings of climate. *Climate Dynamics* 25: 285-297.
- Seppä H., Birks H.J.B., Giesecke T., Hammarlund D., Alenius T., Antonsson K., Bjune A.E., Heikkilä M., MacDonald G.M., Ojala A.E.K., Telford R.J. and Veski S. 2007. Spatial structure of the 8200 cal yr BP event in northern Europe. *Climate of the Past* 3: 225-236.
- Seppä H., MacDonald G.M., Birks H.J.B., Gervais B.R. and Snyder J.A. 2008. Late-Quaternary summer temperature changes in the northern-European tree-line region. *Quaternary Research* 69: 404-412.
- Serreze M.C., Holland M.M. and Stroeve J. 2007. Perspectives on the Arctic's shrinking sea-ice cover. *Science* 315: 1533-1536.
- Severinghaus J.P., Sowers T., Brook E.J., Alley R.B. and Bender M.L. 1998. Timing of abrupt climate change at the end of the Younger Dryas interval from thermally fractionated gases in polar ice. *Nature* 391: 141-146.
- Shahgedanova M. 2002. Climate at present and in the historical past. In: M. Shahgedanova (ed.), *The physical geography of northern Eurasia*. Oxford University Press, Oxford, pp. 70-102.
- Shahgedanova M. and Kuznetsov M. 2002. The Arctic Environments. In: M. Shahgedanova (ed.), *The physical geography of northern Eurasia*. Oxford University Press, Oxford, UK, pp. 191-215.
- Shahgedanova M., Perov V. and Mudrov Y. 2002. The mountains of Northern Russia. In: M. Shahgedanova (ed.), *The physical geography of Northern Eurasia*. Oxford University Press, Oxford, pp. 284-313.
- Sharp Z. 2005. *Principles of Stable Isotope Geochemistry*. Prentice Hall, New Jersey, USA, 360 pp.

- Shuman B., W. Thompson, P. Bartlein and J.W. Williams 2002. The anatomy of a climatic oscillation: vegetation change in eastern North America during the Younger Dryas chronozone. *Quaternary Science Reviews* 21: 1777-1791.
- Sidorchuk A., Borisova O. and Panin A. 2001. Fluvial response to the Late Valdair Holocene environmental change on the East European Plain. *Global and Planetary Change* 28: 303-318.
- Sidorova O.V., Vaganov E.A., Naurzbaev M.M., Shishov V.V. and Hughes M.K. 2007. Regional Features of the Radial Growth of Larch in North Central Siberia According to Millennial Tree-Ring Chronologies
Original Russian Text © O.V. Sidorova, E.A. Vaganov, M.M. Naurzbaev, V.V. Shishov, M.K. Hughes, 2007, published in *Ekologiya*, 2007, Vol. 38, No. 2, pp. 99–103. 38: 90-93.
- Siegenthaler U., Stocker T., Monnin E., Lüthi D., Schwander J., Stauffer B., Raynaud D., Barnola J.-M., Fischer H., Masson-Delmotte V. and Jouzel J. 2005. Stable carbon cycle-climate relationship during the late Pleistocene. *Science* 310: 1313-1317.
- Smith L.C. 2000. Trends in Russian Arctic river-ice formation and breakup, 1917-1994. *Physical Geographer* 21: 46-56.
- Smith L.C., Sheng Y., MacDonald G.M. and Hinzman L.D. 2005. Disappearing Arctic lakes. *Science* 308: 1429.
- Smol J.P., Wolfe A.P., Birks H.J.B., Douglas M.S.V., Jones V.J., Korhola A., Pienitz R., Ruhland K., Sorvari S., Antoniades D., Brooks S.J., Fallu M.-A., Hughes M., Keatley B.E., Laing T.E., Michelutti N., Nazarova L., Nyman M., Paterson A., Perren B., Quinlan R., Rautio M., Saulnier-Talbot E., Siitonen S., Solovieva N. and Weckstrom J. 2005. Climate-driven regime shifts in the biological communities of arctic lakes. *PNAS* 102: 4397-4402.
- Smol J.P. and Douglas M.S.V. 2007. From controversy to consensus: making the case for recent climate change in the Arctic using lake sediments. *Frontiers in Ecology* 5: 466-474.
- Soja A.J., Tchebakova N.M., French N.H.F., Flannigan M.D., Shugat H.H., Stocks B.J., Sukhinin A.I., Varfenova E.I., Chapin F.S. and Stackhouse

- P.W. 2007. Climate-induced boreal forest change: Predictions versus current observations. *Global and planetary change* 56: 274-296.
- Solomina O. 2000. Retreat of mountain glaciers of northern Eurasia since the Little Ice Age maximum. *Annals of Glaciology* 31: 26-30.
- Solomina O. and Alverson K. 2004. High latitude Eurasian palaeoenvironments: introduction and synthesis. *Palaeogeography Palaeoclimatology Palaeoecology* 209: 1-18.
- Solomon S., D. Qin, M. Manning, R.B. Alley, T. Berntsen, N.L. Bindoff, Z. Chen, A. Chidthaisong, J.M. Gregory, G.C. Hegerl, M. Heimann, B. Hewitson, B.J. Hoskins, F. Joos, J. Jouzel, V. Kattsov, U. Lohmann, T. Matsuno, M. Molina, N. Nicholls, J. Overpeck, G. Raga, V. Ramaswamy, J. Ren, M. Rusticucci, R. Somerville, T.F. Stocker, P. Whetton, Wood R.A. and D. Wratt 2007. Technical Summary. In: S. Solomon, D. Qin, M. Manning, Z. Chen, M. Marquis, K.B. Averyt, M. Tignor and H. L. Miller (eds.), *Climate Change 2007: The Physical Science Basis. Contribution of Working Group I to the Fourth Assessment Report of the Intergovernmental Panel on Climate Change*. Cambridge University Press, Cambridge, United Kingdom and New York, NY, USA.
- Solovieva N., Jones V.J., Appleby P.G. and Kondratenok B.M. 2002. Extent, environmental impact and long-term trends in atmospheric contamination in the Usa basin of east-European Russian Arctic. *Water, Air and Soil Pollution* 139: 237-260.
- Solovieva N., Jones V.J., Nazarova L., Brooks S.J., Birks H.J.B., Grytnes J.-A., Appleby P.G., Kauppila T., Kondratenok B., Renberg I. and Ponomarev V. 2005. Palaeolimnological evidence for recent climatic change in lakes from the northern Urals, arctic Russia. *Journal of Paleolimnology* 33: 463-482.
- Sømme L. and Block W. 1991. Adaptations to alpine and polar environments in insects and other terrestrial arthropods. In: R. E. Lee and D. L. Denlinger (eds.), *Insects at low temperatures*. Chapman and Hall, New York and London pp. 318-359.
- Spahni R., Schwander J., Flückiger J., Stauffer B., Chappellaz J. and Raynaud D. 2003. The attenuation of fast atmospheric CH₄ variations recorded in polar ice cores. *Geophysical Research Letters* 30: GL017093.

- Spies M. and Sæther O.A. 2004. Fauna Europaea: Zalutschia. In: H. de Jong (ed.), Fauna Europaea: Diptera: Nematocera. Fauna Europaea version 1.3, <http://www.faunaeur.org>.
- Spurk M., Leuschner H.H., Baillie M.G.L., Briffa K.R. and Friedrich M. 2002. Depositiona; frequency of German subfossil oaks: climatically and non-climatically induced fluctuations in the Holocene. *The Holocene* 12: 707-715.
- Stager J.C., Cumming B. and Meeker L.D. 1997. A high-resolution 11,400-yr diatom record from Lake Victoria, East Africa. *Quaternary Research* 47: 81-89.
- Stager J.C. and Mayewski P.A. 1997. Abrupt early to Mid-Holocene climatic transition registered at the equator and the poles. *Science* 276: 1834-1836.
- Staubwasser M., Sirocko F., Grootes P.M. and Zielinski G.A. 2002. South Asian monsoon climate change and radiocarbon in the Arabian Sea during early and middle Holocene. *Paleoceanography* 17: art. no. 1063.
- Stenina A.S., Khokhlova L.G., Patova E.N. and Lytkina Z.A. 2004. Environmental Condition of Water Bodies in the Territory of an Oil–Gas Condensate Field (the Pechora Delta). *Water Resources* 31: 545-552.
- Stoks R., Johansson F. and De Block M. 2008. Life-history plasticity under time stress in damselfly larvae. In: A. Córdoba-Aguilar (ed.), *Dragonflies and damselflies: model organisms for ecological and evolutionary research*. Oxford University Press, Oxford, pp. 39-50.
- Storey A.W. 1987. Influence of temperature and food quality on the life history of an epiphytic chironomid. *Entomologica Scandinavica Supplement* 29: 339-347.
- Strenzke K. 1950. Systematik, Morphologie und Ökologie der terrestrischen Chironomiden. *Archiv für Hydrobiologie Supplement* 18: 207-414.
- Strenzke K. 1950. Systematik, Morphologie und Ökologie der terrestrischen Chironomiden. *Archiv für Hydrobiologie Supplement* 18: 207-414.
- Stuiver M. and Braziunas T.F. 1993. Sun, ocean, climate and atmospheric ^{14}C : an evaluation of causal and spectral relationships. *The Holocene* 3: 289-205.

- Talbot M.R. and Laerdal T. 2000. The late Pleistocene-Holocene palaeolimnology of Lake Victoria, East Africa, based upon elemental and isotopic analyses of sedimentary organic matter. *Journal of Paleolimnology* 23: 141-164.
- Talbot M.R. 2001. Nitrogen isotopes in palaeolimnology. In: W. Last and J. P. Smol (eds.), *Tracking environmental change using lake sediment*. Kluwer Academic Publishers, Dordrecht, The Netherlands, pp. 401-440.
- Tarasov L. and Peltier W.R. 2005. Arctic freshwater forcing of the Younger Dryas cold reversal. *Nature* 435: 662-665.
- Tarussov A. 1992. The Arctic: from Svalbard to Severnaya Zemlya climate reconstructions from ice-cores. In: R. S. Bradley and P. D. Jones (eds.), *Climate since 1550*. Routledge, London, pp. 505-516.
- Tauber M.J., Tauber C.A., Obrycki J.J., Gallands B. and Wright R.J. 1988a. Voltinism and the induction of aestival diapause in the Colorado potato beetle, *Leptinotarsa decemlineata* (Coleoptera: Chrysomelidae). *Annals of the Entomological Society of America* 81: 748-754.
- Tauber M.J., Tauber C.A., Obrycki J.J., Gallands B. and Wright R.J. 1988b. Geographical variation in responses to photoperiod and temperature by *Leptinotarsa decemlineata* (Coleoptera: Chrysomelidae). *Annals of the Entomological Society of America* 81: 764-773.
- ter Braak C.J.F. and Looman C.W.N. 1986. Weighted averaging, logistic regression and the Gaussian response model. *Vegetatio* 65: 3-11.
- ter Braak C.J.F. 1987. Ordination. In: R. H. G. Jongman, C. J. F. ter Braak and O. F. R. Tongeren (eds.), *Data Analysis in Community and Landscape Ecology*. Backhuys Publishers Leiden, Netherlands, pp. 91-169.
- ter Braak C.J.F. and Prentice I.C. 1988. A theory of gradient analysis. *Advances in ecological research* 18: 271-317.
- ter Braak C.J.F. and Juggins S. 1993. Weighted averaging partial least squares regression (WA-PLS): an improved method for reconstructing environmental variables from species assemblages. *Hydrobiologia* 269: 485-502.
- ter Braak C.J.F. 1994. Canonical community ordination. Part i: Basic theory and linear methods. *Ecoscience* 1: 127-140.

- ter Braak C.J.F. 1995. Non-linear models for multivariate statistical calibration and their use in palaeoecology: a comparison of inverse k -nearest neighbours, partial least squares and weighted averaging partial least squares, and classical approaches. *Chemometrics and Intelligent Laboratory Systems* 28: 165-180.
- ter Braak C.J.F. and Smilauer P. 2002. CANOCO reference manual and user's guide to CANOCO for Windows: Software for Canonical Community Ordination version 4.5. Microcomputer Power, Ithaca, New York.
- Tinner W. and Lotter A.F. 2001. Central European vegetation response to abrupt climate change at 8.2 ka. *Geology*. 29: 551-554.
- Tishkov A. 2002. Boreal forests. In: M. Shahgedanova (ed.), *The physical geography of Northern Eurasia*. Oxford University Press, Oxford, pp. 216-233.
- Tokeshi M. 1985. Life cycles and population dynamics. In: P. Armitage, P. S. Cranston and L. C. V. Pinder (eds.), *The Chironomidae: Biology and ecology of non-biting midges*. Chapman and Hall, London, pp. 225-268.
- Trenberth K.E., P.D. Jones, P. Ambenje, R. Bojariu, D. Easterling, A. Klein Tank, D. Parker, F. Rahimzadeh, J.A. Renwick, M. Rusticucci, Soden B. and P. Zhai 2007. Observations: Surface and Atmospheric Climate Change. In: S. Solomon, D. Qin, M. Manning, Z. Chen, M. Marquis, K.B. Averyt, M. Tignor and H. L. Miller (eds.), *Climate Change 2007: The Physical Science Basis. Contribution of Working Group I to the Fourth Assessment Report of the Intergovernmental Panel on Climate Change*. Cambridge University Press, Cambridge, United Kingdom and New York, NY, USA., pp. 237-336.
- Tuiskunen J. 1986. The Fennoscandian species of *Parakiefferiella* Thienemann (Diptera, Chironomidae, Orthocladiinae). *Annales Zoologici Fennici* 23: 175-196.
- Tyson R.V. 1995. *Sedimentary organic matter: Organic Facies and Palynofacies*. Chapman and Hall, London, 615 pp.
- Ulmishek G.F. 2003. Petroleum Geology and Resources of the West Siberian Basin, Russia. Bulletin 2201-G, U.S. . Department of the Interior and U.S. Geological Survey, <http://pubs.usgs.gov/bul/2201/G/B2201-G.pdf>, p. 53.

- Vaganov E.A., Hughes M.K., Kirilyanov A.V., Schweingruber F.H. and Silkin P.P. 1999. Influence of snowfall and melt timing on tree growth in subarctic Eurasia. *Nature* 400: 149-151.
- Väliranta M., Kultti S. and Seppä H. 2006. Vegetation dynamics during the Younger Dryas - Holocene transition in the extreme northern taiga zone, northeastern European Russia. *Boreas* 35: 202-212.
- van den Wollenberg A.L. 1977. Redundancy Analysis: An Alternative For Canonical Correlation Analysis. *Psychometrika* 42: 207-219.
- van Heerwaarden B. and Hoffmann A.A. 2006. Global warming: Fly populations are responding rapidly to climate change. *Current Biology* 17: R16-R18.
- Vaughan R. 1994. *The Arctic: a history*. Alan Sutton Publishing Limited, Stroud, Gloucestershire, 340 pp.
- Velle G., Brooks S.J., Birks H.J.B. and Willassen E. 2005a. Chironomids as a tool for inferring Holocene climate: an assessment based on six sites in southern Scandinavia. *Quaternary Science Reviews* 24: 1429-1462.
- Velle G., Larsen J., Eide W., Peglar S.M. and Birks H.J.B. 2005b. Holocene environmental history and climate of Råtåsjøen, a low-alpine lake in south-central Norway. *Journal of Paleolimnology* 33: 129-153.
- Venables W.N. and Ripley B.D. 2003. *Modern Applied Statistics with S*. Springer-Verlag, New York, 512 pp.
- Verschuren D., Cumming B.F. and Laird K.R. 2004. Quantitative reconstruction of past salinity variations in African lakes: assessment of chironomid-based inference models (Insecta : Diptera) in space and time. *Canadian Journal of Fisheries and Aquatic Sciences* 61: 986-998.
- Verschuren D. and Charman D.J. 2008. Latitudinal linkages in late Holocene moisture-balance variation In: R. W. Battarbee and H. A. Binney (eds.), *Natural climate variability and global warming: A Holocene perspective*. Wiley-Blackwell, Chichester, West Sussex, pp. 189-231.
- Veski S., Seppä H. and Ojala A.E.K. 2004. Cold event at 8200 yr BP recorded in annually laminated lake sediments in eastern Europe. *Geology* 32: 681-684.
- Walker D. and MacDonald G.M. 1995. Distributions of Chironomidae (Insect: Diptera) and other freshwater midges with respect to treeline, Northwest Territories, Canada. *Arctic, Antarctic and Alpine Research* 27: 258-263.

- Walker I.R. and Mathewes R.W. 1987. Chironomidae (Diptera) and postglacial climate at Larion Lake, British Columbia, Canada. *Quaternary Research* 27: 89-102.
- Walker I.R. and Mathewes R.W. 1989. Early postglacial chironomid succession in British Columbia, Canada and its paleoenvironmental significance. *Journal of Paleolimnology* 2: 1-14.
- Walker I.R., Smol J.P., Engstrom D.R. and Birks H.J.H. 1991. An assessment of Chironomidae as quantitative indicators of past climatic change. *Canadian Journal of Fisheries and Aquatic Science* 48: 975-987.
- Walker I.R., Wilson S.E. and Smol J.P. 1995. Chironomidae (Diptera): quantitative paleosalinity indicators for lakes of western Canada. *Canadian Journal of Fisheries and Aquatic Science* 52: 950-960.
- Walker I.R., Levesque A.J., Cwynar L.C. and Lotter A.F. 1997. An expanded surface-water paleotemperature inference model for use with fossil midges from eastern Canada. *Journal of Paleolimnology* 18: 165-178.
- Walker I.R. 2001. Midges: Chironomidae and related diptera. In: J. P. Smol, H. J. B. Birks and W. Last (eds.), *Tracking Environmental Change Using Lake Sediments*. Kluwer, Dordrecht, pp. 43-66.
- Walker I.R., Levesque A.J., Pienitz R. and Smol J.P. 2003. Freshwater midges of the Yukon and adjacent Northwest Territories: a new tool for reconstructing Beringia palaeoenvironments? *Journal of North American Benthological Society* 22: 323-337.
- Walsh J., O. Anisimov, J.O.M H., T. Jakobsson, J. Oerlemans, T.D. Prowse, V. Romanovsky, N. Savelieva, M. Serreze, A. Shiklomanov, I. Shiklomanov and S. Solomon 2005. Cryosphere and hydrology. In: ACIA. (ed.), *Arctic Climate Impact Assessment*. Cambridge University Press, Cambridge, United kingdom and New York, NY, USA. , pp. 183-242.
- Walter K.M., Zimov S.A., Chanton J.P., Verbyla D. and Chapin F.S. 2006. Methane bubbling from Siberian thaw lakes as a positive feedback to climate warming. *Nature* 443: 71-75.
- Walther G.-R., Post E., Convey P., Menzel A., Parmesan C., Beebee T.J.C., Fromentin J.-M., Hoegh-Guldberg O. and Bairlein F. 2002. Ecological responses to recent climate change. *Nature* 416: 389-395.

- Wang X. and Sæther O.A. 2001. The larvae of *Prosilocerus sinicus* Sæther et Wang and *P. paradoxus* (Lundström) (Diptera: Chironomidae). Aquatic Insects 23: 141-145.
- Ward G.M. and Cummins K.W. 1979. Effects of food quality on growth of a stream detritivore, *Paratendipes albimanus*, (Meigen) (Diptera: Chironomidae). Ecology 60: 57-64.
- Webber J.P. and Klein D.R. 1977. Geobotanical and ecological observations at two locations in the west-central Siberian Arctic. Arctic and Alpine Research 9: 305-315.
- Weiderholm T. 1983. Chironomidae of the Holarctic. Keys and diagnoses. Part 1. Larvae Entomologica Scandinavica Supplement No. 19, Lund, Sweden, 457 pp.
- Welch H.E. 1976. Ecology of Chironomidae (Diptera) in a polar pond. Journal of the Fisheries Research Board of Canada 33: 227-247.
- Westover K.S., Fritz S.C., Blyakharchuk T.A. and Wright H.E. 2006. Diatom paleolimnological record of Holocene climatic and environmental change in the Altai Mountains, Siberia. Journal of Paleolimnology 35: 519-541.
- Wiederholm T. 1983. Chironomidae of the Holarctic. Keys and diagnoses. Part 1. Larvae Entomologica Scandinavica Supplement No. 19, Lund, Sweden, 457 pp.
- Wiederholm T. 1984. Responses of aquatic insects to environmental pollution. In: V. H. Resh and D. M. Rosenberg (eds.), The ecology of aquatic insects. Praeger Publishers, New York, pp. 508-557.
- Williams G.E. 1975. Possible relation between periodic glaciation and the flexure of the Galaxy. Earth and Planetary Science Letters. 26: 361-369.
- Wilson R.S. and Ruse L.P. 2005. A guide to the identification of genera of chironomid pupal exuviae occurring in Britain and Ireland (including common genera from Northern Ireland) and their use in monitoring lotic and lentic fresh waters. Freshwater Biological Association, Ambleside, Cumbria, 177 pp.
- Wipking W. and Neumann D. 1986. Polymorphism in the larval hibernation strategy of the burnet moth, *Zygaena trifolii*. In: F. Taylor and R. Karban (eds.), Evolution of insect life cycles. Springer-Verlag, New York, pp. 125-134.

- Wolfe A.P., Baron J.S. and Cornett J. 2001. Anthropogenic nitrogen deposition induces rapid ecological changes in alpine lakes of the Colorado Front Range (USA). *Journal of Paleolimnology* 25: 1-7.
- Wood R. 2007a. Climate models and their evaluation., The science of climate change: A Royal Society showcase of the IPCC 4th Assessment Working Group 1 report. The Royal Society, London.
- Wood S. 2007b. GAMs with GCV smoothness estimation and GAMMs by REML/PQL. The mgcv package. simon.wood@r-project.org.
- Wülker W.F. 1959. Drei neue Chironomiden-Arten (Dipt.) und ihre Bedeutung für das Konvergenzproblem bei Imagines und Puppen. *Archiv für Hydrobiologie Supplement* 25: 44-64.
- Yu G. and Harrison S.P. 1995. Lake status records from Europe, Database documentation: IGBP PAGES/World Data Center - A for Paleoclimatology Data Contribution Series 95-009: . NOAA/NGDC Paleoclimatology Program, Boulder, CO.
- Zaitsev A.S. and Wolters V. 2006. Geographic determinants of oribatid mite communities structure and diversity across Europe: a longitudinal perspective. *European Journal of Soil Biology* 42: S358-S361.
- Zhang E., Jones R., Bedford A., Langdon P. and Tang H. 2007. A chironomid-based salinity inference model from lakes on the Tibetan Plateau. . *Journal of Paleolimnology* 38: 477-491.
- Zhang T., R.G. Barry, Knowles K., Ling F. and Armstrong R. 2003. Distribution of seasonally and perennially frozen ground in the Northern Hemisphere. In: M. Phillips, S.M. Springman and L. U. Arenson. (eds.), *Proceedings of the 8th International Conference on Permafrost, 21-25 July 2003, . A.A. Balkema, Lisse, the Netherlands., Zurich, Switzerland., pp. 1289-1294.*
- Zielinski G.A., Mayewski P.A., Meeker L.D., Whitlow S.I., Twickler M.S., Morrison M., Meese D.A., Gow A.J. and Alley R. 1994. Record of volcanism since 7000 B.C. from the GISP2 Greenland ice core and implications for the volcano-climate system. *Science* 264: 948-952.
- Zielinski G.A. 2000. Use of paleo-records in determining variability within the volcano-climate system. *Quaternary Science Reviews* 19: 417-438.

- Zlotin R. 2002. Biodiversity and productivity of ecosystems. In: M. Shahgedanova (ed.), *The physical geography of northern Eurasia*. Oxford University Press, Oxford, pp. 167-190.
- Zolotukhin V.V. and Almukhamedov A.I. 1988. Traps of the Siberian Platform. In: J. D. MacDougall (ed.), *Continental Flood Basalts* Kluwer Academic Publishers, Dordrecht, pp. 273-310.
- Zwiers F. 2007. Understanding and attributing climate change., *The science of climate change: A Royal Society showcase of the IPCC 4th Assessment Working Group 1 report*. The Royal Society, London.